Synthesis and *in vitro* anticancer activity of 1,3,4-thiadiazole and 1,3-thiazolidine-4-one scaffold-based heterocyclic molecules

THESIS SUBMITTED BY

AVIK MAJI

DOCTOR OF PHILOSOPHY (PHARMACY)

DEPARTMENT OF PHARMACEUTICAL TECHNOLOGY

FACULTY COUNCIL OF ENGINEERING & TECHNOLOGY

JADAVPUR UNIVERSITY

KOLKATA-700032, INDIA

2025

Dedicated
To
My Beloved
Parents

JADAVPUR UNIVERSITY
KOLKATA-700032, INDIA
INDEX NO.: 280/19/Ph

Index No: 280/19/Ph

1. **Title of the Thesis:** Synthesis and *in vitro* anticancer activity of 1,3,4-thiadiazole and 1,3-thiazolidine-4-one scaffold-based heterocyclic molecules.

2. **Name, Designation & Institution of the Supervisor:**

   Prof. (Dr.) Tapan Kumar Maity
   Professor of Pharmaceutical Chemistry,
   Department of Pharmaceutical Technology,
   Jadavpur University, Kolkata-700032, India

3. **List of Publications:**

   Research and Review articles:

   Maji A, Himaja A, Nikhitha S, Rana S, Paul A, Samanta A, Shee U, Mukhopadhyay C, Ghosh B, Maity TK. Synthesis and antiproliferative potency of 1,3,4-thiadiazole and 1,3-thiazolidine-4-one based new binary heterocyclic molecules: *in vitro* cell-based anticancer studies. *RSC Med Chem*. 2024 Jul 31; 15(9): 3057-3069.

   A. Maji, D. Begum, S. Regula, S. Rana, A. Paul, U. Shee, A. Samanta, R.P. Bhagat, C. Mukhopadhyay, B. Ghosh, T.K. Maity, Synthesis, XRD-sc study and antiproliferative, apoptotic & anti-angiogenic potency of 1,3,4-thiadiazole and 1,3-thiazolidine-4-one scaffold-based hybrid compounds (Part-II): *in vitro* cell-based anticancer studies, *J. Mol. Struct.* 1350 (2026) 143999.

   Maji A, Paul A, Sarkar A, Nahar S, Bhowmik R, Samanta A, Nahata P, Ghosh B, Karmakar S, Kumar Maity T. Significance of TRAIL/Apo-2 ligand and its death receptors in apoptosis and necroptosis signalling: Implications for cancer-targeted therapeutics. *Biochem Pharmacol*. 2024 Mar; 221: 116041.

   A. Samanta, **A. Maji**, A. Paul, S.S. Mishra, S. Nahar, T.K. Maity, 1,3,4-Oxadiazole-based EGFR inhibitors as anticancer therapeutics: SAR study and binding mode of interaction analysis, *Eur. J. Med. Chem. Reports* 14 (2025) 100265.

   A. Paul, S.S. Mishra, A. Sarkar, R. Bhowmik, A. De, **A. Maji**, U. Shee, A. Samanta, S. Karmakar, T.K. Maity, Synthesis, single crystal XRD, in vitro evaluation, molecular docking and ADMET studies of cuminaldehyde-thiazolidine-2,4-dione hybrids as potential α-glucosidase inhibitors, *J. Mol. Struct.* 1331 (2025): 141510.

   A. Paul, S.S. Mishra, **A. Maji**, A. Samanta, S. Nahar, T.K. Maity, Exploring the therapeutic potentials of cuminaldehyde: a comprehensive review of biological activities, mechanisms, and novel delivery systems, *Phytochem. Rev.* (2025).

A. Paul, S. Nahar, P. Nahata, A. Sarkar, A. **Maji, A**. Samanta, S. Karmakar, T.K. Maity, Synthetic GPR40/FFAR1 agonists: An exhaustive survey on the most recent chemical classes and their structure-activity relationships, *Eur. J. Med. Chem.* 264 (2024) 115990.

A. Sarkar, A. Paul, T. Banerjee, **A. Maji**, S. Saha, A. Bishayee, T.K. Maity, Therapeutic advancements in targeting BCL-2 family proteins by epigenetic regulators, natural, and synthetic agents in cancer, *Eur. J. Pharmacol.* 944 (2023) 175588.

A. Paul, A. **Maji, A**. Sarkar, S. Saha, P. Janah, T.K. Maity, Recent Approaches in the Synthesis of 5-Arylidene-2,4-thiazolidinedione Derivatives Using Knoevenagel Condensation, *Mini. Rev. Org. Chem*. 20 (2023) 5–34.

A. Sarkar, R. Saha, S. Saha, R. Bhowmik, A. Chatterjee, A. Paul, **A. Maji**, M.A. Shaharyar, S. Karmakar, B. Sarkar, T.K. Maity, Transesterification, GC-MS profiling, and in vitro antimicrobial potential of oil obtained from seeds of Citrus maxima (Burm.) Merr, *Ind. Crops Prod*. 189 (2022) 115764.

Paul A, Sarkar A, Saha S, **Maji A**, Janah P, Kumar Maity T. Synthetic and computational efforts towards the development of peptidomimetics and small-molecule SARS-CoV 3CLpro inhibitors. *Bioorg Med Chem*. 2021 Sep 15; 46: 116301.

Sarkar A, Saha S, Paul A, **Maji A**, Roy P, Maity TK. Understanding stem cells and its pivotal role in regenerative medicine. *Life Sci*. 2021 May 15; 273: 119270.

4. List of Patents:

None

5. Book Chapters:

Arnab Sarkar, Abhik Paul, **Avik Maji**, Shrabanti Sarkar, Puspita Roy, Tanmoy Banerjee, Tanmoy Guria, Citrus and its Fight against Cancer, *Bentham Science Publishers*, 2024, Oct 17 (pp: 228).

Arnab Sarkar, Tanmoy Banerjee, **Avik Maji**, Abhik Paul, Tanmoy Guria. Mikania Species: Revealing Phytochemicals from the Pandora's Box, *Bentham Science Publishers*, 2023 Aug 1 (pp: 149-167).

6. List of National/International Conferences/Workshops:

- Presented poster in "INTERNATIONAL SEMINAR ON MODERN MEDICINE AND RATIONAL USE OF MEDICINE-A CHALLENGE" held on Triguna Sen Memorial Hall, Jadavpur University, Kolkata, India on 17th January, 2025.
- Secured 2nd position for poster presentation in "INTERNATIONAL SEMINAR ON MODERN MEDICINE AND RATIONAL USE OF MEDICINE-A CHALLENGE" held on Triguna Sen Memorial Hall, Jadavpur University, Kolkata, India on 17th January, 2025.

- Participated in conducting the Two-Day hands-on Workshop on "Polymerase Chain Reaction Technique" held on 21st & 22nd January, 2025, organized by DBT-Builder facility, University of Calcutta.
- Presented poster in 14th International Conference on "NAVIGATING THE FUTURE OF HEALTHCARE: Trends, Challenges and Innovations" Organised by NSHM Institute of Health Sciences, NSHM Knowledge Campus, Kolkata on 27th and 28th September, 2024.
- Participated in International Online Conference on "DRUG DISCOVERY, DEVELOPMENT AND LEAD OPTIMIZATION, Organised by School of Pharmacy and Emerging Sciences, Baddi University of Emerging Sciences & Technology, Baddi, Himachal Pradesh, India, 05-06 April, 2024.
- Participated in an online international webinar "Pharmacological Mutation of Oxidative Stress" organised by the seminar committee & Internal Quality Assurance Cell of Eminent College of Pharmaceutical Technology. Barasat, Kolkata-700126, India.
- Attended National Seminar on "Role of Medicinal plants to combat metabolic disorders and associated pathological complications" held at School of Natural Product studies, Jadavpur University, Kolkata, India, June 30-July 01, 2023.
- Participated in the National Workshop on 'Unravelling the Path from Protein Targets to Drug Development: Exploring Computational Biology' held on 28th Sep to 1st October, 2023, organized by the Department of Pharmaceutical Technology, School of Health and Medical Sciences, Adamas University, Kolkata.
- Participated in 2nd International Conference On "Transforming Ripples in Healthcare Research: Obstacles Sustenance & Cutting-edge Innovations" Organized by School of Medical Sciences, Adamas University, Kolkata, India on 10th – 11th February, 2022.

STATEMENT OF ORIGINALITY

I, Avik Maji, registered on 03/06/2019, do hereby declare that this thesis entitled **"Synthesis and *in vitro* anticancer activity of 1,3,4-thiadiazole and 1,3-thiazolidine-4-one scaffold-based heterocyclic molecules"** contains literature survey and original research work done by me as part of my Doctoral studies.

All information in this thesis has been obtained and presented in accordance with existing academic rules and ethical conduct. I declare that, as required by these rules and conduct, I have fully cited and referred all materials and results that are not original to this work.

I also declare that I have checked this thesis in accordance with the "Policy on Anti-Plagiarism, Jadavpur University, 2019", and the level of similarity, as determined by the iThenticate software, is 8%.

Avik Maji 07.07.2025

Signature of the Candidate:

Date:

TMaity 07.07.2025

Certified by Supervisor:

(Signature with date, seal)

Dr. Tapan Kr. Maity
M. Pharm., Ph.D.
Professor
Dept. of Pharmaceutical Technology
Jadavpur University, Kolkata - 700 032

CERTIFICATE FROM THE SUPERVISOR

This is to certify that the thesis entitled "**Synthesis and *in vitro* anticancer activity of 1,3,4-thiadiazole and 1,3-thiazolidine-4-one scaffold-based heterocyclic molecules,**" submitted by **Mr. Avik Maji**, who got his name registered on 03/06/2019, Registration No:1021913005 for the award of Ph.D (Pharmacy) degree of Jadavpur University, is absolutely based upon his work under the supervision of **Prof. Tapan Kumar Maity** and that neither his thesis nor any part of the thesis has been submitted for any degree/diploma or any other academic award anywhere before.

TKMaity 07/07/25

Prof. (Dr.) Tapan Kumar Maity (Supervisor)
Professor of Pharmaceutical Chemistry,
Dept. of Pharmaceutical Technology,
Jadavpur University, Kolkata 700032, India

Dr. Tapan Kr. Maity
M. Pharm., Ph.D.
Professor
Dept. of Pharmaceutical Technology
Jadavpur University, Kolkata - 700 032

ACKNOWLEDGEMENT

My path to successfully finishing my thesis has been enhanced by the priceless advice, encouragement, and support of several people. I would like to thank them from the core of my heart for helping me achieve this academic milestone.

First and foremost, I would like to express my sincere gratitude and heartfelt thanks to my Ph.D. supervisor, Prof. Tapan Kumar Maity, for providing me with the opportunity to undertake this research. His mentorship has not only guided my research but has also greatly influenced my intellectual development. The wisdom contained in even a few minutes of his advice has provided me with clarity and direction during moments of doubt. Without his encouragement, constructive feedback, and ongoing inspiration, this thesis would not have been possible. I am genuinely grateful for his invaluable contributions to my academic journey.

I am also deeply grateful to Prof. Amalesh Samanta, Head of the Department, for his invaluable support during my pre-submission phase. His insightful advice and encouragement were crucial in refining and finalising my work. My sincere thanks also go to Prof. Pulok K. Mukherjee, under whose tenure I was registered for my PhD. His guidance and motivation played a pivotal role in shaping my research endeavours. Additionally, I would like to express my gratitude to Prof. Pallab Kanti Haldar, whose assistance during my PhD selection process was instrumental in enabling me to embark on this academic path. I extend my sincere thanks to Prof. Sanmoy Karmakar and his laboratory for their invaluable assistance with various experiments. Their expertise and resources were instrumental in enabling me to conduct my research successfully.

I am also extremely grateful to Prof. Balaram Ghosh and his lab members for their extensive collaboration during the research work, which contributed to the successful completion of the project, and for their continued support throughout the publication process. Their scientific knowledge and skills inspire me to perform successful and good research.

I would like to thank Dr. Birendra Nath Karan for his valuable suggestions and guidance during the early period of my Ph.D. work. He was also my teacher at the Institute of Pharmacy, Kalyani, Nadia. His wisdom, patience, and unwavering support have greatly influenced my PhD research. My heartfelt thanks also go to the late Dr. Jayanta Kumar Das and Dr. Sudipta Saha for encouraging me to pursue higher studies.

I wish to acknowledge my dear companions, Mr. Soumitra Rana, Mr. Sudeep Ranjan Jana, Mr. Uday Shee, Mr. Abhik Paul, Mr. Arnab Sarkar, Mr. Pratik Chakraborty, Mrs. Ajeya Samanta, Dr. Sanjib Das, Dr. Rudranil Bhowmik, Mr. Md. Adil Shaharyar, for their unwavering support and association through the ups and downs.

I also thank my lab junior, Ms. Shrabanti Sarkar, Ms. Sourin Nahar, Mr. Pankaj Nahata, Mr. Sai Satyarakash Mishra, Mr. Rajesh Khan, Mr. Sourav Mondal, Mr. Abdul Qadir, and Ms. Nikki Gupta for their help and support in the laboratory.

I extend my sincere gratitude to the office staff of the Department of Pharmaceutical Technology, including Mr. Umesh Kumar and others, for their unwavering administrative support. A special thank you to Mr. Umesh Kumar for his assistance in the laboratory, providing solvents and chemicals during my Ph.D. tenure.

I would like to express my sincere gratitude to the funding agencies, including UGC-UPE and RUSA 2.0, for their generous financial support. Additionally, I am grateful to the SVMCM Scholarship scheme of the Government of West Bengal for the financial support it provided during my Ph.D. tenure.

I am also grateful to the Department of Biotechnology, New Delhi, for providing a fellowship at Ballygunge Science College, University of Calcutta.

I am very grateful to the Almighty, whose graces have enabled me to do this task. I couldn't have finished my voyage without the help of heavenly grace. I will always be appreciative of my family's unwavering support, tolerance, and love. My most significant source of strength has come from their unshakeable trust in me. I would like to extend my sincere appreciation to my parents, Mr. Dipak Kumar Maji and Mrs. Minati Maji, whose unwavering support and belief in me have been the cornerstones of my academic career.

Lastly, I extend my gratitude to all those who contributed, directly or indirectly, to my research but may not be mentioned by name. Your support and contributions have not gone unnoticed, and I am deeply appreciative of your help.

This thesis is the culmination of a collective effort, and I am deeply grateful to each and every person who has contributed to this journey.

Kolkata, July, 2025

Avik Maji 07.07.2025

Avik Maji

PREFACE

This research work is carried out in partial fulfilment of the Doctor of Philosophy degree (Pharmacy). The current research work, entitled **"Synthesis and *in vitro* anticancer activity of 1,3,4-thiadiazole and 1,3-thiazolidine-4-one scaffold-based heterocyclic molecules,"** demonstrates the anticancer effect of novel binary heterocyclic molecules.

Among illnesses, cancer ranks second in terms of mortality, whereas heart disease is the leading cause of death worldwide in terms of disease-related mortality incidence. Cancer develops as a result of unchecked cell division and a lack of cellular apoptotic activity, which significantly increases the number of malignant cells. Approximately one in four deaths (22.8%) from noncommunicable diseases (NCDs) and one in six deaths (16.8%) worldwide are caused by cancer. In the twenty-first century, it is an important social, public health, and economic concern. The disease is responsible for three out of ten premature deaths globally from NCDs (30.3%), and it is among the top three causes of death for those aged 30 to 69 in 177 out of 183 countries. Depending on the kind, location, and gender of the cancer, there are varying degrees of significant social and macroeconomic costs associated with the disease. Additionally, it presents a significant barrier to increasing life expectancy.

A recent study showed the substantial impact of disproportionate cancer mortality in women, estimating that one million children became maternal orphans in 2020 due to their mother's cancer-related death, with nearly half of these orphans resulting from maternal deaths from either female breast or cervical cancer. An estimated one in nine men and one in twelve women will die from cancer, while one in five men and women may get the illness at some time in their lives. Lung cancer was the most frequently diagnosed cancer in 2022, accounting for around 2.5 million new cases, or one in eight cancers globally (12.4% of all cancers). Prostate (7.3%), colorectal (9.6%), stomach (4.9%), and female breast (11.6%) cancers came next. Lung cancer was also the leading cause of cancer-related death, with an estimated 1.8 million deaths (18.7%). The subsequent most frequent malignancies were colorectal (9.3%), liver (7.8%), female breast (6.9%), and stomach (6.8%). Lung cancer and breast cancer were the most prevalent cancers in men and women, respectively, in terms of both cases and deaths.

Current cancer treatments rely on processes that cause genetic damage, imbalances in kinase and phosphatase activity, spindle issues, and variations in cell cycle checkpoints. Since most treatment methods aim to stop the proliferation of cancer cells, they are often unable to

eradicate them completely. Apoptosis of cancer cells often leads to complete remission of the disease, thereby improving outcomes and reducing the likelihood of recurrence. However, breast cancer cannot be cured entirely by the various systemic medicines that have lately been devised. Furthermore, adverse effects might include cardiovascular problems, osteoporosis, and drug resistance. Therefore, continuous progress in identifying and developing new, potent lead compounds for long-term cancer therapy with fewer side effects is urgently needed.

Over the last several decades, heterocyclic compounds, their numerous derivatives, and their applications in the chemical and pharmaceutical sectors have garnered the attention of chemists. The synthesis and use of a broad range of heterocyclic compounds, including pyrazole, tetrahydroquinolines, benzotriazole, 1,2,3,4-tetrazine, thiazole, 2-thiazoline, pyrimidine, and others, have been extensively covered in recent research papers. A common and necessary five-membered heterocyclic system with two nitrogen atoms and one sulfur atom is 1,3,4-thiadiazole. 1,3,4-Thiadiazole has recently been the subject of numerous research studies for the synthesis of biologically active compounds, as indicated by a brief analysis of reputed research publications. The literature has documented several intriguing compounds, suggesting that 1,3,4-thiadiazoles have been intensively studied for their potential as anticancer agents.

The research on 1,3-thiazolidin-4-ones, which are heterocycles featuring a carbonyl function at the fourth position and sulfur and nitrogen at the first and third positions, respectively, has expanded significantly in recent years. A crucial component in drug development, the thiazolidine-4-one molecule features a thiazolidine ring with a carbonyl group and exhibits a range of biological effects. This moiety makes a distinct contribution to a range of pharmacological substances that support the development of several anticancer drugs.

A helpful approach in medication design is molecular hybridisation, which enables the creation of pharmacological agents for various illnesses and promotes the development of new treatments with improved efficacy and fewer side effects. In this context, several hybrid compounds combining 1,3,4-thiadiazole and 1,3-thiazolidine-4-one were synthesised, and their *in vitro* anticancer activity was evaluated. The newly developed compounds showed notable anticancer effects against cancer cells through different mechanisms, including apoptosis, cell cycle arrest, and the production of intracellular reactive oxygen species (ROS), as well as chromosomal condensation and the upregulation of proapoptotic protein biomarkers and

downregulation of antiapoptotic protein biomarkers and also inhibit angiogenesis in tube formation assay.

The primary objective of this work is to develop new, potent anticancer compounds by synthesising hybrid molecules using these extensively studied heterocycles. Ultimately, the research justifies further development of a promising lead molecule, which may advance through a drug discovery process to develop potential anticancer medicines.

Kolkata, July, 2025

Avik Maji 07.07.2025

Avik Maji

CONTENTS

LIST OF TABLES

LIST OF FIGURES

LIST OF ABBREVIATIONS

Abbreviation	Full Form
5-FU	5-fluoro uracil
ADME	Absorption, Distribution, Metabolism and Excretion
AKT	Protein kinase B
AML	Myeloid Leukemia
ANOVA	Analysis of variance
AO	Acridine orange
BCL-2	B-cell lymphoma 2
BCL-XL	BCL extra-large
CAM	Chorioallantoic membrane
CARD	Caspase activation and recruitment domains
CCDC	Cambridge Crystallographic Data Centre
CDK2	Cyclin-dependent kinase-2
cDNA	Complementary DNA
CLL	Chronic lymphocytic leukaemia
COSMIC	Catalogue of Somatic Mutations in Cancer
COX	Cyclooxygenase
COX-2	Cyclooxygenase-2
cyt-C	Cytochrome-c
DAPI	4′,6-diamidino-2-phenylindole
DCC	*N*, N′-Dicyclohexylcarbodiimide
DCFDA	2′,7′-Dichlorodihydrofluorescein diacetate
DEAD	Diethyl acetylenedicarboxylate
DLBCL	Diffuse large B-cell lymphoma
DMAD	Dimethyl acetylenedicarboxylate
DMEM	Dulbecco’s modified Eagle medium
DMF	Dimethylformamide
DMSO	Dimethyl sulfoxide
EDCI	1-Ethyl-3-(3-dimethylaminopropyl) carbodiimide
EGFR	Epidermal growth factor receptor
EMA	European Medicines Agency

Abbreviation	Full Form
ESI	Electrospray ionization
FDA	U.S. Food and Drug Administration
FISH	Fluorescence *in situ* hybridisation
FITC	fluorescein isothiocyanate
FLT3	Fms-like tyrosine kinase 3
GAA	Glacial acetic acid
GBM	Glioblastoma
GWAS	Genome-wide association studies
HDAC	Histone deacetylase
HDI	Human development indices
HL	Hodgkin's lymphoma
HPV	Human papillomavirus
HRMS	High-resolution mass spectrometry
HTS	High-throughput screening
IARC	International Agency for Research on Cancer
IL-8	Interleukin-8
JAK 2	Janus kinase 2
KC	Knoevenagel condensation
LR	Lawesson's reagent
LSCM	Laser Scanning Confocal Microscope
MCP-1	Monocyte chemoattractant protein 1
MCR	Multi-component reaction
MDS	Myelodysplastic syndrome
miRNA	microRNA
MMP	Matrix metalloproteinase
MNK	MAP kinase-interacting serine/threonine-protein kinases
MTT	3-(4,5-dimethylthiazol-2-yl)-2,5-diphenyltetrazolium bromide
NCDs	Noncommunicable diseases
NFκB	Nuclear factor kappa B
NHL	non-Hodgkin lymphoma
NMR	Nuclear magnetic resonance
NSCLC	Non-Small Cell Lung Cancer

Abbreviation	Full Form
PBS	Phosphate buffer saline
PCl_5	Phosphorous pentachloride
PDGF	Platelet-derived growth factor
PI	Propidium iodide
PPA	Phenylpropanolamine
PPA	Phenylpropanolamine
PPh_3	Triphenylphosphine
PTSA	Paratolune sulphonic acid
PVDF	Polyvinylidene fluoride
ROS	Reactive oxygen species
RPMI	Roswell Park Memorial Institute
SAR	Structure-activity relationship
SDS-PAGE	Sodium dodecyl sulfate-polyacrylamide gel electrophoresis
shRNAs	Short hairpin RNAs
$SOCl_2$	Thionyl chloride
SOLiDTM	Sequencing by oligonucleotide ligation and detection
STB	sulfinyl-bis((2,4-dihydroxyphenyl) methanethione)
TCNE	Ethylenetetracarbonitrile
TEA	Triethylamine
TGFβ2	Transforming growth factor-β2
THF	Tetrahydrofuran
TLR4	Toll-like receptor-4
TMSCl	Trimethylsilyl chloride
TNBC	Triple-negative breast cancer
TNF-α	Tumour necrosis factor-α
TOF	Time of flight
TsCl	*p*-toluenesulfonyl chloride
VEGFR-2	Vascular endothelial growth factor receptor-2
VEGFR2	Vascular endothelial growth factor receptor 2
WHO	World Health Organisation
XRD	X-ray diffraction

CHAPTER-I

INTRODUCTION

1. Introduction:

1.1. Drug Discovery and Development:

The process of identifying potential novel therapeutic entities through a combination of computational, experimental, translational, and clinical models is known as drug discovery [1,2]. Drug development remains a drawn-out, expensive, challenging, and ineffective process, with a high attrition rate of novel therapeutic discoveries, despite advancements in biotechnology and increased knowledge of biological systems. The creative process of developing novel drugs based on an understanding of a biological target is known as drug design. In its most basic form, drug design is the process of creating molecules that complement the molecular target they interact and bind to in terms of shape and charge. In the big data age, computer modelling and bioinformatics methodologies are often, but not always, used in drug design. Along with small molecules, biopharmaceuticals, particularly therapeutic antibodies, are a growing class of medications. Computational techniques for enhancing the stability, selectivity, and affinity of these protein-based treatments have also advanced significantly [3]. Preclinical studies using animal and cell-based models, human clinical trials, and ultimately securing regulatory approval to bring the medicine to market are all part of the drug development and discovery process. Identifying screening hits, medicinal chemistry, and optimising those hits to improve their affinity, selectivity (to lower the risk of adverse effects), efficacy/potency, metabolic stability (to lengthen the half-life), and oral bioavailability are all part of modern drug research. The process of medication development begins before clinical trials are conducted, after a molecule that satisfies all of these parameters has been identified.

1.2. Steps of Drug Discovery and Development:

1.2.1. Identification of the Target:

- The first step in the drug development process is target identification. A biological target is a component or mechanism that contributes to the development of a specific disease.

- The illness may be caused by any biological process that is necessary for its development, including genes, proteins, enzymes, and others.
- Several genetic and biochemical methods are used to identify and characterise the molecular pathways linked to a given illness.

Scientists identify potential targets using a range of techniques, including clinical observations, epidemiological studies, and genetic and biochemical procedures.

- To achieve this, scientists may identify the proteins and enzymes that play a significant role in the onset of the illness, as well as the genes that are overexpressed or altered in the condition.
- To identify compounds that interact with the target, researchers may also search through large chemical databases. Large datasets are examined in epidemiological studies to determine characteristics, such as genetic risk factors or environmental exposures, that are associated with a specific illness.
- Disease association, bioactive substances, cell-based models, protein interactions, signalling pathway analysis, functional analysis of genes, in vitro genetic manipulation, antibodies, and chemical genomics are some of the state-of-the-art tools and techniques that researchers use to validate targets.

1.2.2. Finding Leads:

Once a possible target has been identified, the next phase of drug development is lead identification. A lead compound is a substance that interacts with the target and exhibits a favourable pharmacological effect. Numerous techniques, including high-throughput screening, the Hit to Lead (H2L) approach, virtual screening, and natural product screening, can be employed to identify leads.

- Finding compounds that interact with the target involves sifting through enormous chemical libraries as part of **high-throughput screening**.

- This is accomplished using robotic systems that can test tens of thousands of compounds per day. Small chemical hits from an HTS are evaluated and optimised into lead compounds under strict guidelines using the **Hit to Lead (H2L) process**.
- These compounds are subsequently subjected to the lead optimisation process. Using computer simulations, **virtual screening** is the process of identifying compounds that are most likely to interact with the target based on its structure and characteristics.
- Searching for compounds that interact with the target in natural products, including plant extracts or microbial cultures, is known as **natural product screening**.

1.2.3. Optimisation of Leads:

Following the discovery of a lead molecule, the next stage of therapeutic development is lead optimisation. The structure needs to be modified to enhance the pharmacological activity, selectivity, and safety of the lead compound. Numerous techniques, including pharmacology, structural biology, and medicinal chemistry, may be used to optimise leads.

- Novel compounds with structural similarities to the lead chemical are created and evaluated in medicinal chemistry. To improve potency and selectivity, the lead compound's chemical structure may need to be slightly changed.
- X-ray crystallography and other techniques are used in structural biology to determine the target's three-dimensional structure and its interactions with the lead molecule. This information can be used to design new compounds that target the desired modification more effectively.
- Pharmacology is the study of the pharmacokinetic, pharmacodynamic, and safety properties of lead compounds in preclinical studies.

1.2.4. Preclinical Examination:

- Before a lead chemical is tested on people, preclinical testing is required.
- Examining the drug's pharmacokinetics, efficacy, and safety in animal models is known as preclinical testing.
- Preclinical testing aims to determine the optimal dosage and dosing schedule for the drug in question, as well as to identify any potential safety concerns.
- The development of new drugs using animal models, including mice, rats, and canines, is an example of in vivo preclinical research. Lab-based research is known as *in vitro* research.
- Animal tissues or cells from an inanimate animal are used in *ex vivo* procedures. Finding efficient cancer therapies, assessing the physical, thermal, electrical, and optical characteristics of tissue, and developing precise models for cutting-edge surgical methods are all examples of *ex vivo* research studies. An *ex vivo* test typically begins with a cell for small explant cultures, which provide a dynamic, controlled, and sterile environment.

1.2.5. Clinical Trials in Drug Development:

- A crucial step in developing new medications is conducting clinical trials.
- They are designed to assess the pharmacokinetics, efficacy, and safety of a potential novel drug in human test subjects.
- Clinical trials are conducted in phases, each of which aims to answer specific queries about the medication's efficacy and safety.

1.2.6. Healthy Volunteer Study/Phase I Clinical Trials:

- The first stage of clinical testing for a potential new medication is phase I clinical trials.
- To evaluate the pharmacokinetics, safety, and tolerability of the medication, these tests are often performed on healthy volunteers.

- The primary objectives of Phase I clinical studies are to determine the highest acceptable dosage of the medication and identify any adverse effects or side effects.
- Phase I clinical investigations are conducted with small volunteer groups, typically comprising 20 to 80 individuals.
- These studies may last for many weeks or months, depending on the medication's pharmacokinetics and the number of doses being assessed.
- Phase I clinical trial participants undergo routine blood and urine testing to evaluate the medication's pharmacokinetics and are continuously monitored for adverse effects.

1.2.7. Phase II Clinical Trials/Patient Population Research:

- The second phase of clinical testing for a potential new medication is known as a Phase II clinical study.
- These studies often include a small number of individuals with the target illness or condition.
- The primary objective of Phase II clinical studies is to evaluate the safety and efficacy of the drug in human participants.
- Phase II clinical trials are often larger than Phase I trials and may involve several hundred participants.
- These studies may last anywhere from a few months to a few years, depending on the treatment's efficacy and the number of doses being assessed.
- Participants in phase II clinical trials undergo routine imaging and blood tests to assess the efficacy of the medication, and they are continuously monitored for adverse effects.

1.2.8. Clinical Trials in Phase III:

- The last stage of clinical testing for a potential new medication is phase III clinical trials.
- These studies often screen a large number of individuals for the target disease or condition.

- The primary objectives of Phase III clinical studies are to identify any uncommon or persistent adverse effects and to demonstrate the drug's efficacy and safety in a larger patient population.
- Phase III clinical trials are often significantly larger than Phase II trials and may include hundreds of participants.
- These studies often span several years and are conducted at multiple sites to ensure a large patient population.
- Phase III clinical trial participants undergo frequent imaging scans, blood tests, and other assessments to ascertain the medication's efficacy and safety, as well as close monitoring for adverse effects.

1.2.9. Regulatory Acceptance in Drug Development:

- Once a medication has completed Phase III clinical trials, the data are transmitted to regulatory agencies, such as the U.S. Food and Drug Administration (FDA) or the European Medicines Agency (EMA).
- These groups review the data to determine if the medication is safe, effective, and whether the benefits outweigh the risks.

1.2.10. Post-Marketing Surveillance:

- Even after a medicine has been approved and released to the market, ongoing monitoring is necessary to ensure its effectiveness and safety.
- This is known as pharmacovigilance or post-marketing monitoring. Post-marketing monitoring involves closely monitoring for any uncommon or persistent adverse effects that may have been missed in clinical trials, in order to assess the drug's safety and efficacy in a larger patient population.

Clinical trials are a significant component of drug development and discovery. They are designed to evaluate the pharmacokinetics, efficacy, and safety of a potential novel medication

in human volunteers. Every stage of clinical trials aims to answer a specific question about the medication's effectiveness and safety. Clinical study findings are used to evaluate a medication's safety and efficacy, as well as whether it is suitable for patient use. Continuous monitoring is required to ensure the safety and effectiveness of a medication even after it has been approved.

1.3. Cancer:

Cancer accounts for about one in six fatalities (16.8%) and one in four deaths (22.8%) from noncommunicable diseases (NCDs) globally. It is a significant social, public health, and economic issue in the twenty-first century. The illness is one of the top three causes of mortality for those aged 30 to 69 in 177 out of 183 nations, and it accounts for three out of ten premature deaths worldwide from NCDs (30.3%) [4]. Cancer is linked to significant social and macroeconomic expenses, which vary in degree depending on the kind of cancer, location, and gender. It also poses a substantial obstacle to extending life expectancy [5]. An estimated one million children became maternal orphans in 2020 as a result of their mother's cancer-related death, with nearly half of these orphans resulting from maternal deaths from either female breast or cervical cancer, according to a recent study that demonstrated the significant effects of disproportionate cancer mortality in women [6]. According to estimates, one in five men and women will have cancer at some point in their lives, while one in nine men and one in twelve women will pass away from the disease. With about 2.5 million new cases, or one in eight cancers worldwide (12.4% of all cancers), lung cancer was the most commonly diagnosed cancer in 2022. It was followed by stomach (4.9%), colorectal (9.6%), prostate (7.3%), and female breast (11.6%) cancers. With an anticipated 1.8 million fatalities (18.7%), lung cancer was also the most common cause of cancer-related mortality. Colorectal (9.3%), liver (7.8%), female breast (6.9%), and stomach (6.8%) cancers were the next most common [7]. In terms

of both cases and fatalities, breast cancer and lung cancer were the most common cancers in women and men, respectively.

The care of cancer patients is undergoing a significant paradigm shift, which may be completed by 2020, when standard diagnosis will include molecular-based patient profiles. New medications that target specific pathways have been made possible by the molecular study of human cancers; examples include the monoclonal antibody trastuzumab and the tyrosine kinase inhibitor imatinib. The understanding of the genetic abnormalities underlying the malignant transformation of normal cells is being significantly enhanced by the molecular tools that have emerged in the last five years, particularly next-generation DNA sequencing. These alterations include chromosomal translocations, insertions and deletions in DNA, copy number variations, coding mutations, and modifications in the sequence of enhancers and promoters. In an effort to determine which tumours would respond to specific therapies, pharmaceutical companies are developing medications that target the alterations that promote the growth and survival of cancer cells.

Specific genetic alterations that characterise each tumour in terms of the molecular pathways involved are present in cancers that arise inside a particular tissue. The activation of one oncogene is crucial for the development and survival of a few cancer cells; this phenomenon has been termed oncogene addiction [8]. A novel method of tumour classification based on molecular biology is being made possible by the growing understanding of the genetic abnormalities that cause cancer [9]. The more subjective, observable methods that pathologists have historically used, such as tissue staining with haematoxylin and immunohistochemistry, are supplemented with more objective molecular classifications, such as fluorescence *in situ* hybridisation (FISH). Additionally, these more recent methods are simplifying the process of standardising molecular testing so that different labs may get similar findings [10].

1.4. Causes of Cancer:

In a multi-stage process that often advances from a precancerous lesion to a malignant tumour, cancer develops when normal cells change into tumour cells. These modifications are the outcome of the interplay between an individual's genetic makeup and three types of outside influences, such as:

- Biological carcinogens, such as infections from specific viruses, bacteria, or parasites;
- Chemical carcinogens, such as asbestos, tobacco smoke components, alcohol, aflatoxin (a food contaminant), and arsenic (a drinking water contaminant).
- Physical carcinogens, such as ultraviolet and ionising radiation.

WHO maintains a categorisation of chemicals that cause cancer via the International Agency for Research on Cancer (IARC), its cancer research agency. Age-related increases in the risk of some malignancies are probably the cause of the sharp rise in cancer incidence. The propensity for cellular repair systems to become less efficient with age is coupled with an increase in overall risk.

1.5. Risk Factors:

Risk factors for cancer and other noncommunicable illnesses include air pollution, bad eating habits, alcohol usage, tobacco use, and physical inactivity.

Certain chronic infections increase the likelihood of developing cancer; this is especially problematic in low- and middle-income nations. Carcinogenic diseases, such as Helicobacter pylori, human papillomavirus (HPV), hepatitis B, hepatitis C, and Epstein-Barr viruses, were responsible for around 13% of cancer diagnoses worldwide in 2018.

Specific forms of HPV and the hepatitis B and C viruses raise the risk of cervical and liver cancer, respectively. HIV infection significantly raises the chance of acquiring some other malignancies, such as Kaposi sarcoma, and increases the risk of developing cervical cancer by six times.

1.6. Prevention:

Cancer risk can be reduced by:

- not using tobacco;
- maintaining a healthy body weight;
- eating a healthy diet, including fruit and vegetables;
- doing physical activity on a regular basis;
- avoiding or reducing consumption of alcohol;
- getting vaccinated against HPV and hepatitis B if you belong to a group for which vaccination is recommended;
- avoiding ultraviolet radiation exposure (which primarily results from exposure to the sun and artificial tanning devices) and/or using sun protection measures;
- ensuring safe and appropriate use of radiation in health care (for diagnostic and therapeutic purposes);
- minimising occupational exposure to ionising radiation; and
- reducing exposure to outdoor air pollution and indoor air pollution, including radon (a radioactive gas produced from the natural decay of uranium, which can accumulate in buildings — homes, schools and workplaces).

1.7. Cancer Epidemiology:

One in six fatalities today is attributable to cancer, making it the second leading cause of mortality globally. In 2020, there were around 19.3 million new cases of cancer and 10 million deaths from the illness, according to the International Agency for Research on Cancer (IARC). By 2030, there are expected to be 23.8 million cases and 13.0 million deaths from cancer [11,12]. In this sense, it is evident that environmental elements, such as processed foods and environmental toxins, are becoming more and more important as causes and promoters of

cancer [13]. In **Table 1**, the types of cancer that cause the most cases and fatalities globally are listed.

Table 1: Total Numbers of Cancer Cases and Deaths Worldwide in 2020 by Cancer Type (According to the Global Cancer Observatory, IARC).

Cases		
Both Sexes	**Women**	**Men**
Breast (2.26 million)	Breast (2.26 million)	Lung (1.43 million)
Lung (2.20 million)	Colorectal (865,000)	Prostate (1.41 million)
Colorectal (1.93 million)	Lung (770,000)	Colorectal (1.06 million)
Prostate (1.41 million)	Cervical (604,000)	Stomach (719,000)
Stomach (1.08 million)	Thyroid (448,000)	Liver (632,000)

According to **Figure 1**, the most prevalent cancers worldwide are lung, breast, prostate, and colorectal, and they are primarily found in nations with high to very high human development indices (HDI). Despite having a high incidence, colon, prostate, and breast cancers cause very few fatalities, which is due mainly to the significant progress gained in controlling them. These statistics also highlight the types of cancer that require more attention in terms of prevention, accurate early detection to prevent overdiagnosis, and effective treatment. In the instances of pancreatic, liver, lung, and oesophageal cancer, the gap between the number of cases and fatalities is less pronounced (**Figure 1B**). In several nations, social and economic changes have led to a decline in the prevalence of infection-related neoplasms, while also increasing the incidence of those linked to nutritional, hormonal, and reproductive factors [14]. Except for pancreatic cancer and lung cancer in women, cancer death rates have decreased in high HDI nations during the last three decades.

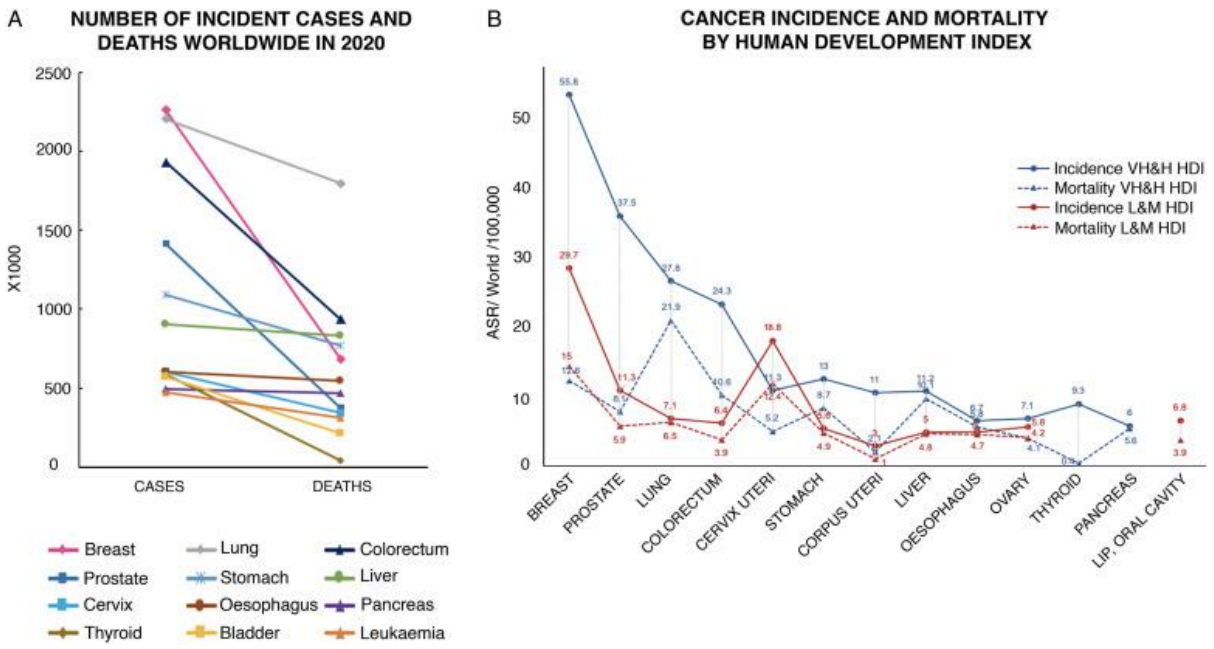

Figure 1: Incidence and mortality for some types of cancer in the world. (A) Estimated number of cases and deaths in 2020 for the most frequent cancer types worldwide. (B) Incidence and mortality rates, normalised according to age, for the most frequent cancer types in countries with very high/& high (VH&H; blue) and/low and middle (L&M; red) Human Development Index (HDI). Data includes both genders and all ages. Data as of June 10, 2021, according to https://gco.iarc.fr/today as of June 2021.

However, variations in cancer incidence do not exhibit the same consistency, which factors like genetic predisposition, exposure to risk factors, or the potential for early identification may cause [15,16]. The incidence and mortality of stomach, colon, lung, and ovarian cancer have decreased, and survival rates have increased, according to reports from nations including Australia, Canada, Denmark, Ireland, New Zealand, Norway, and the United Kingdom [17]. Changes have significantly aided prevention in modifiable risk factors, such as tobacco use. In this regard, it has been calculated that a decrease in tobacco usage accounts for between 35 and 45 per cent of the drop-in cancer death rates. In contrast, the reduction in stomach cancer incidence and mortality may be partially ascribed to the management of Helicobacter pylori infection [18,19]. The rise in early diagnosis, brought about by screening programs, has also played a significant role in the decline in death rates in industrialised nations. For example, the mortality rates for breast and prostate cancer have significantly dropped despite an increase in their incidence [15].

The rise in survival rates, particularly in high Human Development Index (HDI) nations, is another significant improvement observed in recent decades. In the United States, for instance, the five-year survival rates for patients with prostate cancer were 28% in 1947–1951; 69% in 1975–1977; and 100% in 2003–2009. Similarly, the 5-year survival rate for breast cancer was 54% in 1947–1951; 75% in 1975–1977; and 90% in 2003–2009 [20]. Age-standardised 5-year survival rates for patients with breast cancer and prostate cancer in the United States from 2010 to 2014 were 90% and 97%, respectively, according to the CONCORD 3 edition [21]. Crucially, there are notable variations in survival rates even across high HDI countries. The primary determinants of survival in these countries are comorbidities, the time it takes to receive adequate therapy, and the stage of the illness at diagnosis [17]. Unfortunately, a number of variables, such as inadequate screening and early detection programs, restricted access to treatment, inadequate cancer registration, and a lack of knowledge, contribute to the much poorer survival rates in low HDI nations [21]. It should be mentioned that the most common neoplasms in low- to middle-HDI countries are those that affect women, such as breast and cervical cancer. This indicates a serious inequality problem that involves social, cultural, and even religious barriers, in addition to a problem with access to healthcare [22].

In the United States, potentially modifiable risk factors, including tobacco use, physical activity, nutrition, and infection, account for up to 42% of incident cases and 47% of cancer-related deaths [23]. It has been estimated that tobacco use is responsible for 2.4 million cancer-related deaths, mostly from lung cancer [12]. Lung cancer incidence rates in 2020 were 2.2 in Western Africa and 37.3 and 34.4 in Polynesia and Eastern Asia, respectively [11]. In comparison, the worldwide burden of infection-related cancer was 15.4%, while it was 30% in Sub-Saharan Africa [24]. Similarly, the incidence of cervical cancer in Eastern Africa was 40.1, compared to 6.2 in the United States and Canada. This demonstrates that lowering the risk

factors associated with specific cancer types that may be modifiable is one of the challenges we face.

Another significant concern is the improvement of survival rates and the variations in them worldwide. For instance, the United States had a 90% five-year survival rate for breast cancer diagnosed between 2010 and 2014, but South Africa had a 40% five-year survival rate [21]. The 5-year survival rate for childhood leukaemia is 90% in the United States and some European nations, compared to 50–76% in Latin American countries [25]. It's interesting to note that survival rates for certain neoplasms, including pancreatic cancer, have not increased much and are still poor (5–15%) in both wealthy and developing nations [22].

Global incidence and death statistics provide a broad picture of the epidemiology of cancer, but it's crucial to remember that cancer registries' coverage varies significantly around the globe. Only one out of every three nations now provides high-quality data on cancer incidence [26]. The IARC has supported population-based cancer registries for the past 50 years; however, almost one-third of WHO member nations, primarily low- and middle-income countries (LMICs), lack data on more than half of the 18 Sustainable Development Goal indicators [27]. Only 4% of people in Africa, 8% in Asia, and 7% in Latin America are covered by high-quality cancer registries. In comparison, 83% of people in the USA and Canada, and 33% of people in Europe, are covered [28]. The Global Initiative for Cancer Registry Development was established in 2012 in response to this circumstance, with the goal of developing a stronger infrastructure that would enable more comprehensive coverage and higher-quality registries, particularly in nations with low and intermediate Human Development Index (HDI) [27].

Initiatives of this kind are anticipated to provide more and better data to improve cancer control policies globally, particularly in lower-income nations, in the years to come. This will enable the monitoring of survival over more extended periods (10, 15, or 20 years), providing an effective way to manage cancer. In order to achieve the WHO's 2025 target of reducing deaths

from cancer and other non-transmissible diseases by 25% among people aged 30 to 69, more effective prevention strategies are needed to lower incidence, and more effective health systems are required in order to reduce mortality and boost survival. The COVID-19 pandemic has had a detrimental influence on cancer prevention and health services, making it an even bigger issue at present [29].

1.8. Classification of Cancer:

Cancer kinds can be classified into major categories. The significant types of cancer include:

- **Carcinoma** is a type of cancer that develops in the skin or tissues surrounding internal organs.
- **Sarcoma** is a cancer that can develop in bone, cartilage, fat, muscle, blood vessels, or other connective or supporting tissue.
- **Leukaemia** is a cancer that begins in blood-forming tissue, such as bone marrow, resulting in the production of abnormal blood cells that enter the bloodstream.
- **Lymphoma** and **myeloma** are cancers that originate in immunological cells.
- **Germ cell tumours** are derived from totipotent cells. In adults, it is most commonly seen in the testicle and ovary; in foetuses, newborns, and early toddlers, it is most frequently located on the midline of the body, particularly at the tip of the tailbone.
- **Blastic tumour or blastoma - A tumour** (usually malignant) which resembles an immature or embryonic tissue. Many of these tumours are most common in children.
- **Central nervous system cancers** – Cancers that begin in the tissues of the brain and spinal cord.

1.9. Differences between a benign tumour and a malignant tumour:

Benign tumours are not cancerous. They can often be removed, and in most cases, they do not come back. Cells in benign tumours do not spread to other parts of the body.

Malignant tumours are cancerous. Cells in these tumours can invade nearby tissues and spread to other parts of the body. The spread of cancer from one part of the body to another is called metastasis.

1.10. Characteristics of cancer cells:

Cancer cells exhibit distinct properties compared to normal cells. They do not stop growing and dividing, ignore signals from other cells, and don't stick together. Cancer cells can lose the molecules on their surface that maintain normal cells in the correct position, enabling them to become detached from their neighbours. Cancer cells don't specialise, repair themselves, or die. They look different.

1. Cancer cells develop self-sufficiency in growth signals through the activation of oncogenes, leading to abnormal mitosis (autonomous proliferation).
2. Cancer cells deactivate tumour suppressor genes, such as Rb, which typically restrict growth, making them insensitive to antigrowth signals.
3. Cancer cells prevent planned cell death (apoptosis) by suppressing and deactivating genes and pathways.
4. Cancer cells possess an unlimited reproductive ability by activating specific gene pathways, rendering them immortal even after multiple generations.
5. Sustained angiogenesis occurs when cancer cells develop the ability to create their blood supply and form new arteries, a process known as tumour angiogenesis.
6. Cancer cells can travel and invade other organs and tissues, leading to metastasis.

1.11. The hallmarks of cancer:

- **Growth signal autonomy:**

(a) Normal cells need external signals from growth factors to divide.

(b) Cancer cells are not dependent on normal growth factor signalling.

(c) Acquired mutations short-circuit growth factor pathways, leading to unregulated growth.

- **Evasion of growth inhibitory signals:**

a) Normal cells respond to inhibitory signals to maintain homeostasis (most cells of the body are not actively dividing)

b) Cancer cells do not respond to growth inhibitory signals.

- **Avoiding immune destruction (emerging hallmark):**

(a) There is evidence to support the theory of immune surveillance that states the immune system can recognize and eliminate cancer cells.

(b) Successful cancer cells may be those that do not stimulate an immune response or can interfere with the immune response so as to avoid immune destruction.

- **Unlimited replicative potential:**

(c) Normal cells have an autonomous counting device to define a finite number of cell doublings after which they become senescent. This cellular counting device measures the shortening of chromosomal ends, known as telomeres, that occurs during every round of DNA replication.

(d) Cancer cells maintain the length of their telomeres.

(e) Altered regulation of telomere maintenance results in unlimited replicative potential.

- **Genome instability and mutation (an enabling characteristic):**

(a) Acquiring the core hallmarks of cancer usually depends on genomic alterations.

(b) Faulty DNA repair pathways can contribute to genomic instability.

(c) Normal cells are removed by apoptosis, often in response to DNA damage.

(d) Cancer cells evade apoptotic signals.

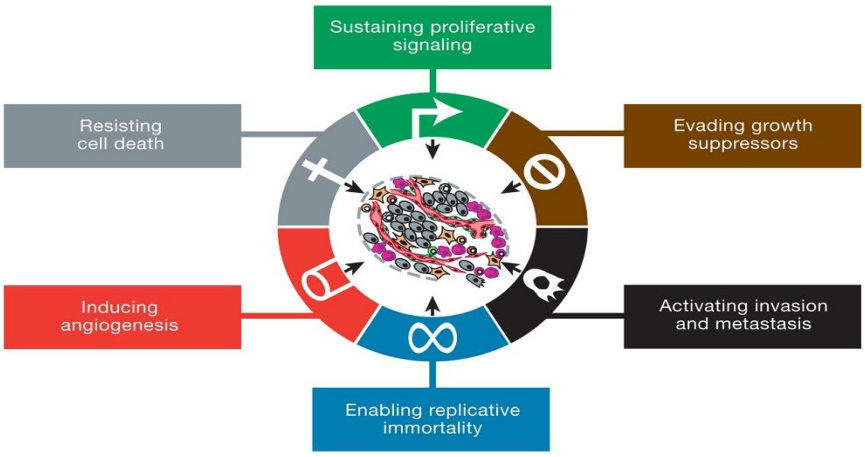

Figure 2: Hallmark of cancer

1.12. Technology drivers of cancer diagnosis:

DNA sequencing, specifically next-generation sequencing, is the technology currently driving the development of molecular diagnostics in cancer. Examples of such technologies include the Life Technologies SOLiDTM (sequencing by oligonucleotide ligation and detection) platforms (Foster City, CA, USA), the Genome AnalyzerTM by Illumina (San Diego, CA, USA), and the 454 Genome SequencerTM FLX system from Roche (Branford, CT, USA) [30]. However, the results of these studies and others, such as The Cancer Genome Atlas project sponsored by the National Cancer Institute and the National Human Genome Research Institute, and the COSMIC (Catalogue of Somatic Mutations in Cancer) project supported by the Wellcome Trust, are indicative of what will be accomplished on a very large scale in the coming years through comprehensive genome sequencing. These technologies are currently being utilised to detect alterations to genes and their expression in tumours. Cancers with mutations in mismatch repair genes will complicate this kind of test due to their higher mutation rates [31].

Older methods, such as transcriptional profiling, which employs oligonucleotide arrays to analyse gene expression, and the use of large-scale single-nucleotide polymorphism arrays to identify deletions and amplifications in malignancies, will inevitably be replaced by DNA sequencing as its cost decreases. The "$1,000 genome," a technological challenge for publicly funded labs and businesses to provide technologies that enable the human genome to be

sequenced for $1,000, is contributing to this momentum in sequencing. To create a comprehensive database of all typical genome variations, the "1,000 Genomes" initiative aims to sequence 1,000 genomes as cost-effectively as possible [32]. Although all of these initiatives have a technological emphasis, turning raw sequence data into meaningful information comes with an extra (often disregarded) significant cost, particularly if the data will be utilised to assist clinical decision-making. Placing genetic information in its appropriate biological context is becoming increasingly important. There aren't many published complete tumour genome sequences produced by second-generation DNA sequencing [33].

Clinical utility is evidently being considered in the development of third-generation systems, including the HeliScopeTM platform (Helicos, Cambridge, MA, USA), SMRTTM DNA sequencing (Pacific Biosciences, Menlo Park, CA, USA), sequencing from Complete Genomics (Mountain View, CA, USA), and nanopore sequencing (Oxford Nanopore Technologies, Oxford, UK) [34]. It's critical to assess if such sequencing is appropriate for diagnostic purposes. One of the most common questions is whether to sequence a patient's and tumour’s genomic DNA and separate the relevant information from the vast amount of data, or only the areas of interest [31]. Several selection systems are already available for separating specific genomic regions, such as those from Agilent (Santa Clara, CA, USA) and Roche NimbleGen (Madison, WI, USA), with more being developed [35,36]. Exons, areas of genetic association, and other RNA types, such as transcribed regions via complementary DNA (cDNA), microRNA (miRNA), and other short RNAs of interest, may all be chosen for study by these methods. To uncover frequent and uncommon variations in the genome, including a gene implicated in a dominant hereditary disease, targeted capture by hybridisation of 12 human exomes (the entire set of exons) has been used to produce over 300 megabases of coding regions. Uncommon mutations that contribute to cancer are also being found using this method [37].

Genome-wide association studies (GWAS) are another critical technological driver for cancer screening. Numerous GWAS in cancer and other diseases have been published as a result of the development of the HapMap project, which compares the genetic sequences of various individuals to identify chromosomal areas where genetic variations are shared, and the availability of reasonably priced chip-based methods to analyse single-nucleotide polymorphisms across the human genome [38]. Since only a tiny percentage of the total genetic risk is being investigated in this research, some have questioned its usefulness. However, when it comes to cancer, GWAS have provided new insights into the biology of the disease [39,40]. However, since the connections are in common alleles and each one alone carries a negligible increased risk of illness, they have not yet shown any usefulness for cancer screening [41]. Analysis of cancer susceptibility genes in mice suggests that combinations of low-risk alleles may have a considerably bigger effect, but it will be challenging to find and test these combinations. On the other hand, nobody would contest the value of checking at-risk people for gene changes that are known to raise their relative chance of developing cancer [42]. Analysing BRCA1 and BRCA2 mutations is one of the most significant examples of this strategy. Women who have mutations in one or both of these genes are much more likely to develop breast and ovarian cancer, and various alleles of BRCA1 and BRCA2 have distinct predisposing effects [43]. The GWAS-identified common alleles that confer low risk do not fully explain the genetic risk of the malignancies in question, and they have not yet been linked to outcome (only susceptibility) [44]. Therefore, it is believed that the extra risk is caused by mutations in uncommon alleles of specific genes that have not yet been found. It is intriguing to consider the possibility of employing next-generation sequencing to search for rare mutant alleles in DNA, which may lead to the discovery of genes with diagnostic value [37].

At the same time, GWAS may identify more prevalent genes that impose even less extra risks in populations with varied allele frequencies and larger patient cohorts [38].

The use of miRNAs and short hairpin RNAs (shRNAs) is a related technology that is advancing our understanding of cancer at the molecular level and has potential therapeutic applications. Although the development of miRNAs as therapeutic or diagnostic agents may hold significant promise for the future, their effectiveness in identifying cancer-related genes has already been demonstrated [45]. Genes implicated in the growth and survival of cancer cells have been identified through several loss-of-function RNA interference screens. ShRNAs are introduced into tumour cells by retroviral vectors. Following a series of cell replications, shRNAs that knock down a gene necessary for ongoing cell development are removed from the total shRNA population; these RNAs (and therefore their targets) may then be identified by looking for a barcode tag attached to each individual shRNA. This type of screen identified CARD11, a gene associated with nuclear factor kappa B (NFκB) signalling, in diffuse large B-cell lymphoma (DLBCL) [46]. Since then, this method has been used to examine the processes behind DLBCL cells' resistance to small-molecule inhibitors that block IκB (inhibitor of NFκB kinase subunit) [47]. A scaled-up version of this method has also been used on patient leukemic cells. In addition to recognised genes like JAK2 and KRAS, mutations were discovered in several previously unidentified genes associated with this condition [48].

RNA interference-driven synthetic lethal screening has also been utilised to identify pathways not previously linked to KRAS [49–52]. The findings suggest several new areas for intervention, focusing on genes that are crucial to the malignant process but do not always undergo alterations to promote growth.

1.13. 'Conventional cancer therapies:

The most often advised traditional cancer treatment methods include removing the tumours surgically, followed by chemotherapy and/or radiation [53]. Surgery is the most successful of these treatments while the illness is still in its early stages. Radiation treatment has the potential to harm healthy tissues, organs, and cells. Almost all chemotherapeutic drugs harm healthy

cells, remarkably quickly proliferating and developing cells, even though chemotherapy has decreased morbidity and death [54]. One of the main issues with chemotherapy is drug resistance, which is the development of drug resistance in cancer cells that were first reduced by an anti-cancer medication. The leading causes of this are increased drug efflux and decreased drug absorption [55]. The traditional chemotherapeutic modality's drawbacks include its inability to determine the correct dose, lack of selectivity, rapid drug metabolism, and predominantly adverse side effects [56].

1.13.1. Anticancer Chemotherapy:

To prevent invasion and metastasis, chemotherapy aims to suppress tumour growth and cell division. However, since chemotherapy affects normal cells, it leads to harmful consequences. The cell and its surroundings may inhibit tumour development on multiple levels. By interfering with the production of DNA, RNA, or proteins, or by altering the proper functioning of preformed molecules, traditional chemotherapy drugs primarily impact the macromolecular synthesis and function of neoplastic cells. Apoptosis, or the direct effects of the chemotherapeutic drug, causes cell death when there is sufficient disruption in macromolecular production or function. Since many cells die as a result of a particular therapy, cell death may be postponed using standard medications. Therefore, it may be necessary to repeat the medication to elicit a reaction. Since the S phase of the cell cycle is when DNA is synthesized, this is the time when cytotoxic medicines are most harmful. Taxanes and vinca alkaloids inhibit the production of mitotic spindles during the M phase.

Combination chemotherapy is often used to get satisfactory results as well. By inducing cytotoxicity in both resting and dividing cells, they appear to prevent the formation of resistant clones [57]. Numerous genes, receptors, and signal transduction are involved in the complex cellular processes that either stimulate or inhibit cell division and proliferation. Significant new insights into the processes underlying apoptosis, angiogenesis, metastasis, cell signalling,

differentiation, and growth factor regulation have emerged from studies in cancer cell biology [58]. On these routes, scientists are developing molecularly targeted therapies that specifically inhibit growth by blocking protein breakdown, angiogenesis, or cell signalling, for example. Chemotherapy may be used in various situations, including metastatic, adjuvant, neoadjuvant, and combination therapies. A treatment administered before the main course of treatment is known as neoadjuvant therapy. To inhibit or eradicate the proliferation of occult cancer cells, adjuvant therapy is administered in conjunction with the primary treatment. Nowadays, the accepted treatment for ovarian, colorectal, lung, and breast cancers is adjuvant therapy, for malignancies such as head and neck, lung, and anal, combined modalities including chemotherapy and radiation are utilized to reduce the tumor before surgery or for curative purposes.

Combining chemotherapeutic agents is delivered cyclically based on the 3 basic principles.

1. Fraction kills hypothesis: A uniform drug dose kills a constant fraction of tumour cells rather than a constant number, regardless of tumour burden.
2. Neoplastic tumour cells exhibit a linear relationship between dose and efficacy.
3. Goldie-Coldman hypothesis: Cancer cells acquire spontaneous mutations that cause drug resistance.

For the majority of cancer therapies, multitargeted or combination therapies are now considered superior to single-agent therapies. To further reduce resistance and toxicities, combination chemotherapeutic drugs with distinct modes of action and nonoverlapping toxicities might be used. Combination chemotherapy includes treatment regimens such as bleomycin/vinblastine/cisplatin for testicular malignancies. Combination chemotherapy is often used to get satisfactory results as well. By encouraging cytotoxicity in both resting and dividing cells, they seem to stop the formation of resistant clones.

1.13.2. Chemotherapeutic agents can be classified according to the mechanism of action:

a) Alkylating Agents:

Examples of alkylating agents are as follows:

- **Nitrogen mustard**- Bendamustine, cyclophosphamide, ifosfamide
- **Nitrosoureas**– Carmustine, lomustine
- **Platinum analogues**– Carboplatin, cisplatin, oxaliplatin
- **Triazenes**- Dacarbazine, procarbazine, temozolamide
- **Alkyl sulfonate**- Busulfan
- **Ethyleneimine**- Thiotepa

Mechanism of action (MOA): These drugs yield an unstable alkyl group, R-CH2+, reacting with nucleophilic centres on proteins and nucleic acids. Inhibit DNA replication and transcription.

Toxicity: Dose-limiting toxicity: myelosuppression (neutropenia nadir: 6 to 10 days with recovery in 14 to 21 days). Mucositis, nausea, vomiting, neurotoxicity, and alopecia. Long-term toxicities: pulmonary fibrosis, infertility, secondary malignancies

b) Antimetabolites:

Mechanism of Action: Inhibits the replication of DNA

Examples of antimetabolites are as follows

1. Cytidine analogues – Azacitidine, decitabine, cytarabine, gemcitabine

MOA: Directly incorporates into DNA and inhibits DNA methyltransferase (azacitidine, decitabine) or DNA polymerase (cytarabine, gemcitabine)

Indications: Azacitidine and decitabine for MDS, AML, cytarabine for MDS, AML, and gemcitabine for breast, NSCLC, ovarian, pancreatic, bladder, sarcoma, HL, NHL

Toxicity: Myelosuppression in general. Cytarabine high dose causes neurotoxicity and conjunctivitis. Gemcitabine causes liver enzyme elevations and interstitial pneumonitis.

2. Folate antagonists – Methotrexate, pemetrexed

MOA: reduces folate, which is essential in the synthesis of purine nucleotides and thymidylate

Indications: Methotrexate for ALL, NHL, CNS, sarcoma, and pemetrexed for malignant pleural mesothelioma, NSCLC (non-squamous)

Toxicity: Myelosuppression, mucositis, hepatotoxicity, nephrotoxicity, cutaneous reactions

Toxicity prevention: Hydration and alkalization of the urine, leucovorin rescue

3. Purine analogues – Cladribine, clofarabine, nelarabine

MOA: structural analogues of guanine and act as false metabolites

Indications: Cladribine for hairy cell leukaemia, AML, CLL, NHL. Clofarabine for ALL, AML. Fludarabine for CLL, AML, NHL, and BMT conditioning agents. Nelarabine for T-ALL, lymphoma. Pentostatin is used to treat hairy-cell leukaemia, cutaneous T-cell lymphoma (CTCL), and chronic lymphocytic leukaemia (CLL).

Toxicities: Myelosuppression and immunosuppression (suppress CD4+ cells) put patients at risk for opportunistic infections

4. Pyrimidine analogues – 5-fluorouracil (5-FU), capecitabine (prodrug of 5-FU).

MOA: Active metabolite (F-dUMP) forms a stable covalent complex with thymidine synthetase in the presence of reduced folate, interfering with DNA synthesis and repair.

Indications: 5-FU for colorectal cancer, anal cancer, pancreatic cancer, gastric cancer. Capecitabine for colorectal cancer and breast cancer.

Toxicity: Dose-limiting hand-foot, mucositis, diarrhoea. Dose-limiting myelosuppression [59]. Toxic levels of 5FU can occur in patients with Dihydropyrimidine Dehydrogenase deficiency or drug overdose. This can lead to cardiac dysfunction, colitis, neutropenia, and encephalopathy. Uridine triacetate is approved for the treatment of these patients.

c) Antimicrotubular Agents

Examples of antimicrotubular agents are as follows:

1. **Topoisomerase II inhibitors:** Anthracyclines (doxorubicin, daunorubicin, idarubicin, and mitoxantrone) inhibit RNA and DNA synthesis. Additionally, it inhibits topoisomerase II, leading to the inhibition of DNA repair and a subsequent blockade of DNA and RNA synthesis.

- **Indications:** Daunorubicin for ALL, AML, APL. Doxorubicin is used for the treatment of acute lymphoblastic leukaemia (ALL), acute myeloid leukaemia (AML), Wilms' tumour, neuroblastoma, sarcomas, breast cancer, ovarian cancer, bladder cancer, thyroid cancer, Hodgkin's lymphoma (HL), and non-Hodgkin lymphoma (NHL). Liposomal doxorubicin has a longer half-life and is less cardiotoxic.
- **Toxicity:** Myelosuppression, cardiotoxicity (cumulative), mucositis. The lifetime cumulative dose of adriamycin is 550 mg/m^2. Secondary malignancies like treatment-related MDS/AML(t-MDS/t-AML) are rare complications with poor prognosis and have often been reported from alkylating agents and topoisomerase II inhibitors. These patients usually present 5 to 7 years after the drug exposure.
- **Epipodophyllotoxins (Etoposide and Teniposide) Indications:** Testicular, SCLC, ALL, AML, Breast, CNS, Sarcoma, HL, NHL, Merkel cell, NSCLC, BMT conditioning agent. Dose-limiting myelosuppression – primary leukopenia

2. **Topoisomerase I inhibitors:** Irinotecan, Topotecan

- **MOA:** Prevents relegation by blocking the release of Top I from the cleavable complex & forming a ternary complex
- **Indications:** Irinotecan for colorectal, cervical, oesophageal, sarcoma, pancreatic, and lung. Topotecan for cervical, ovarian, and SCLC
- **Toxicity:** Irinotecan causes dose-limiting diarrhoea. Topotecan causes dose-limiting neutropenia and thrombocytopenia.

3. **Taxanes** – Paclitaxel, docetaxel, cabazitaxel

- **MOA:** Disruption in the equilibrium of polymerisation and depolymerisation of microtubules, causing abnormal cellular function and disruption of replication, leading to apoptosis. Inhibit assembly of microtubules—M phase-specific.
- **Indications:** Docetaxel for breast, lung, prostate, ovarian, cervical, and sarcoma; paclitaxel for breast, lung, and ovarian; and cazazitaxel for prostate cancer.
- **Toxicity:** Hypersensitivity reactions, myelosuppression, peripheral neuropathy

4. Vinca alkaloids: Vinblastine, vincristine, vinorelbine

- **MOA:** Binds to tubulin, inhibits microtubule formation, and arrests cells in metaphase. M-phase specific.
- **Indication:** Vincristine for ALL, HL, NHL, Neuroblastoma, SCLC
- **Toxicity:** Peripheral neuropathy (both motor and sensory function affected), myelosuppression.

d) Antibiotics:

Examples of antibiotics used as chemotherapy agents include actinomycin D, bleomycin, and daunomycin.

- **MOA:** Inhibits RNA and DNA synthesis
- Bleomycin binds to DNA, producing single and double-strand DNA breaks.
- **Indications:** Testicular, HL, Head, and neck cancers
- **Toxicity:** Cumulative pulmonary toxicity, hyperpigmentation

e) Miscellaneous

1. Hydroxyurea: MOA: inhibits ribonucleoside diphosphate reductase; S-phase specific

- **Indications:** AML, CML, sickle cell disease
- **Toxicity:** Myelosuppression, dermatologic reactions

2. Tretinoin:

- **MOA:** Vitamin A derivative; targets RAR-α promoting cell differentiation

- **Indication:** APL
- **Toxicity:** APL differentiation syndrome – fevers, cardiopulmonary symptoms

3. Arsenic trioxide:

- **MOA:** Induces cell differentiation
- **Indication:** APL
- **Toxicity:** QT prolongation – baseline and serial EKG monitoring, replace K, Mg. APL differentiation syndrome

4. Proteasome inhibitors:

- **Indication:** Bortezomib is used in the treatment of multiple myeloma.
- **Toxicity:** Peripheral neuropathy

1.14. Overview of 1,3,4-thiadiazole and its chemical and biological significance:

Heterocyclic compounds, their several derivatives, and their importance in both the pharmaceutical and chemical sectors have garnered chemists' attention over the past several decades. A number of recent research investigations have focused on a wide range of heterocyclic compounds, including pyrazole, tetrahydroquinolines, benzotriazole, 1,2,3,4-tetrazine, thiazole, 2-thiazoline, pyrimidine, and so on. A common and vital five-membered heterocyclic system, thiadiazole is made up of two nitrogen atoms and one sulfur atom. 1,2,3-thiadiazole, 1,2,4-thiadiazole, 1,2,5-thiadiazole, and 1,3,4-thiadiazole are among the several isomers of thiadiazole (***Figure 1***) [60].

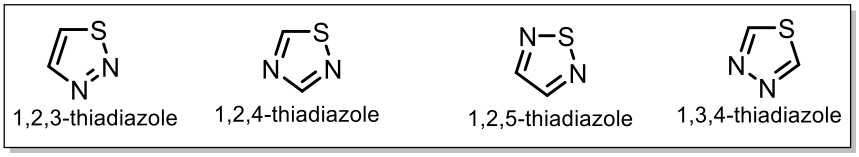

Figure 3: Various isomers of thiadiazole.

Thiadiazoles are substances that belong to the azole class. They are five-membered heterocyclic molecules having one sulphur atom and two nitrogen atoms. The word Thiadiazole came into light after the Hantzsch-Widman nomenclature, which indicates an aromatic ring

because of the presence of two double bonds. Freud and Kuhn established the presence of the ring system in 1890, although Fischer had first reported the thiadiazole in 1882. Thiadiazole and its structurally similar chemical compounds are referred to as 1, 3, 4-thiadiazole (a five-membered cyclic ring with two heteroatoms of nitrogen and one of sulfur). 1,3,4-thiadiazole is one of the most effective isomeric forms due to its numerous biological effects within the body. For instance, compounds with the 1,3,4-thiadiazole framework have been shown to possess unique anti-inflammatory and antibacterial properties in the body. A range of therapeutic attributes, such as analgesic, antibacterial, antitubercular, anticonvulsant, and anti-hepatitis B viral activities, have also been found in structurally substituted derivatives of 1,3,4-thiadiazole [61]. Thiadiazoles are nitrogen-sulfur heterocycles that are widely used as useful intermediates in pharmaceutical chemistry and as structural components of physiologically active compounds. Due to their diverse range of pharmacological properties, substituted 1,3,4-thiadiazole products have garnered considerable interest and have been the subject of extensive research in recent years. It is supposed that 1,3,4-thiadiazole derivatives exhibit various biological activities due to the presence of the =N-C-S- moiety [62]. Some authors believe that the strong aromaticity of the ring, which also confers excellent in vivo stability and minimal toxicity to higher vertebrates, including humans, is the feature that endows 1,3,4-thiadiazole derivatives with their biological activity [63]. Some studies showed the importance of isosterism for the pharmacological profile of a compound. According to these studies, 1,3,4-thiadiazole is the bioisostere of pyrimidine, while 1,3,4-thiadiazole is the bioisostere of pyridazine through the substitution of -CH=CH- by -S- [64,65]. The thiadiazole ring is also a bioisostere of oxadiazole, oxazole, thiazole, and benzene ring [60,64]. Compounds with enhanced lipophilicity and improved biological properties may result from the bioisosteric substitution of one ring for another. Because of the sulphur atoms that give them great liposolubility, the thiadiazole compounds exhibit strong cell permeability, oral absorption, and

good bioavailability. Furthermore, the synthesis of other analogues that interact more strongly with the receptors is made feasible by replacing a heterocycle with a homocyclic ring [65–67]. Moreover, 1,3,4-thiadiazole derivatives can produce mesoionic salts (**Figure 2**). A pentatomic heterocyclic ring with a sextet of p and π electrons and a positive charge balanced by a formal negative charge is present in the mesoionic system. The mesoionic molecules are neutral and capable of passing across cellular membranes despite their internal charges, which helps explain why 1,3,4-thiadiazole derivatives have high cell permeability. The mesoionic nature of 1,3,4-thiadiazoles enables these compounds to interact strongly with biomolecules (e.g., DNA and proteins) (***Figure 2)*** [64,68].

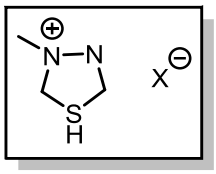

Figure 4: Chemical structure of the mesoionic salt derivatives formed by 1,3,4-thiadiazole compounds.

The inductive effect of the sulfur atom makes the 1,3,4-thiadiazole ring a very weak base, and it has a comparatively high aromaticity [69]. Although it can experience ring cleavage with an aqueous base, it is relatively stable in aqueous acid solutions. Furthermore, the electron-withdrawing effect of the nitrogen atoms makes the ring highly electron-deficient and relatively inert to electrophilic substitution, although it is vulnerable to nucleophilic attack. In contrast, the ring would be highly activated and react readily to produce a variety of derivatives if substitutions were made into the 2′ or 5′ positions. Due to these characteristics, 1,3,4-thiadiazole derivatives are widely utilised in materials chemistry, pharmaceuticals, and agriculture. Additionally, 1,3,4-Thiadiazoles show great promise as insecticides, fungicides, herbicides, bactericides, and even regulators of plant growth. Some agrochemicals developed from thiadiazole were prohibited, but others are commercially available. Thiadiazoles are also commonly used in optics and electrochemistry due to the electron-deficient character of the

1,3,4-thiadiazole core, its strong electron-withdrawing capacity, and its thermal and chemical stability. Applications are also heavily centred on their ability to carry charges, photoluminescence, photoconductivity, and the mesomorphic properties that create liquid crystals, as well as the metal's anticorrosive properties, etc [70].

Medicinal chemists have extensively studied the 1,3,4-thiadiazole moiety to investigate its biological activities, as reported in numerous recent publications. Recent years have seen the synthesis and investigation of a large variety of compounds containing thiadiazole residue, many of which are known to exhibit exceptional and advantageous pharmacological activities, including antibacterial, antitubercular, antihelicobacter pylori, antiinflammatory, antiepileptic, antihypertensive, antioxidant, anticancer, antifungal, and antileishmanial activity [71,72]. Among the various 1,3,4-thiadiazole-based marketed drugs, Filanesib (a Kinesin spindle protein, KIF11 inhibitor), Litronesib (an Inhibitor of the kinesin-related motor protein, Eg5), and Azatepa (an Anticancer alkylating agent) are the drugs employed in cancer therapy [73,74].

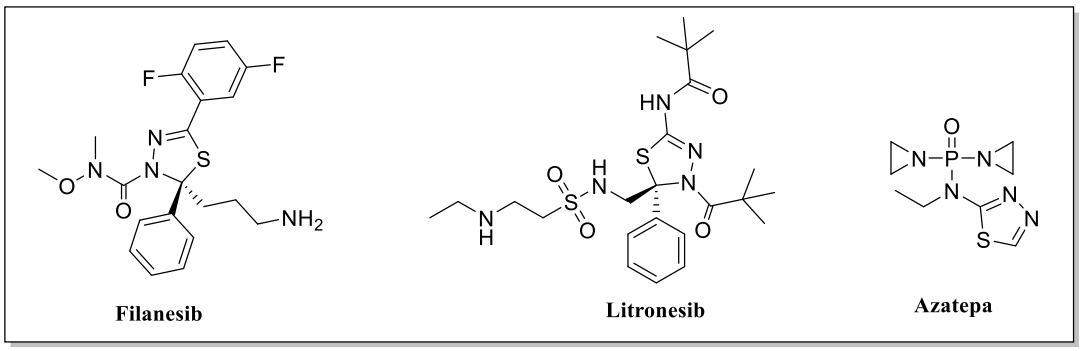

Figure 5: 1,3,4-thiadiazole-based anticancer drugs.

The other well-known commercial medications that contain a 1,3,4-thiadiazole scaffold include methazolamide and acetazolamide (diuretics and carbonic anhydrase inhibitors), megazol (an antiprotozoal agent and inhibitor of protein and DNA synthesis), and cefazolin and cefazedone (antibiotics and cell wall synthesis inhibitors) [74]. As a result, the 1,3,4-thiadiazole scaffold has drawn the attention of researchers seeking to understand the molecular processes underlying its diverse therapeutic activities against various illnesses.

1.15. Overview of 1,3-thiazolidine-4-one scaffold and its chemical and biological significance:

In recent years, there has been a significant expansion in the study of 1,3-thiazolidine-4-ones, which are heterocycles containing sulfur and nitrogen at the 1st and 3rd positions, respectively, and a carbonyl function at the 4th position [75]. Numerous precise diagnostic and therapeutic compounds have utilised the flexible and agile thiazolidinone scaffold [76]. The thiazolidinone molecules, which consist of a thiazolidine ring with a carbonyl group, are known to exhibit a variety of biological effects and are an essential moiety in drug discovery. This moiety contributes uniquely to a variety of pharmacological compounds that aid in the creation and development of several anticancer medications [77]. It is possible to alter the thiazolidin-4-one ring at Positions **2**, **3**, and **5**. These changes enable the discovery of novel molecules with the desired activity. According to published research, thiazolidin-4-one is one of the significant scaffolds with therapeutic value. It has a broad spectrum of biological activity when modified with different substituents, including antiglycemic [78], antioxidant [79], antitubercular [80], antibacterial [81–84], anticonvulsant [85], anticancer [86–88], antiprotozoal [89,90], and anti-inflammatory [91,92] properties. Furthermore, thiazolidine-2,4-diones are a well-known class of antidiabetic medications that have affinity for PPARγ, including pioglitazone and rosiglitazone [93,94].

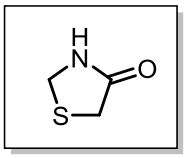

Figure 6: Structure of 1,3-thiazolidine-4-one scaffold.

Natural compounds used to treat cancer also include thiazolidin-4-one ring structures [95–98]. DNA-interacting agents, molecular targeting agents, anti-tubulin agents, antimetabolites, monoclonal antibodies, hormones, and other biological agents are all considered anticancer

agents. These biological agents have been shown to be a valuable foundation for investigating more recent anticancer drugs [99,100]. Most chemotherapeutic anticancer medications on the market currently work by either directly interacting with DNA or by preventing DNA from relaxing [101,102]. With the aim of creating more structurally varied compounds of this class with the intended biological effects, techniques based on quantitative structure–activity relationships have been established for thiazolidin-4-ones [103–105].

Numerous researchers are interested in examining this skeletal structure for its diverse biological roles due to the vast variety of pharmacological activity shown by thiazolidinones and variations in the biological response profile.

References:

[1] W.-Z. Zhong, S.-F. Zhou, Molecular Science for Drug Development and Biomedicine, Int J Mol Sci 15 (2014) 20072–20078. https://doi.org/10.3390/ijms151120072.

[2] X. Xiao, J.-L. Min, W.-Z. Lin, Z. Liu, X. Cheng, K.-C. Chou, iDrug-Target: predicting the interactions between drug compounds and target proteins in cellular networking via benchmark dataset optimization approach, J Biomol Struct Dyn 33 (2015) 2221–2233. https://doi.org/10.1080/07391102.2014.998710.

[3] K.T. Luu, E. Kraynov, B. Kuang, P. Vicini, W.-Z. Zhong, Modeling, Simulation, and Translation Framework for the Preclinical Development of Monoclonal Antibodies, AAPS J 15 (2013) 551–558. https://doi.org/10.1208/s12248-013-9464-8.

[4] F. Bray, M. Laversanne, E. Weiderpass, I. Soerjomataram, The ever-increasing importance of cancer as a leading cause of premature death worldwide, Cancer 127 (2021) 3029–3030. https://doi.org/10.1002/cncr.33587.

[5] S. Chen, Z. Cao, K. Prettner, M. Kuhn, J. Yang, L. Jiao, Z. Wang, W. Li, P. Geldsetzer, T. Bärnighausen, D.E. Bloom, C. Wang, Estimates and Projections of the Global Economic Cost of 29 Cancers in 204 Countries and Territories From 2020 to 2050, JAMA Oncol 9 (2023) 465. https://doi.org/10.1001/jamaoncol.2022.7826.

[6] F. Guida, R. Kidman, J. Ferlay, J. Schüz, I. Soerjomataram, B. Kithaka, O. Ginsburg, R.B. Mailhot Vega, M. Galukande, G. Parham, S. Vaccarella, K. Canfell, A.M. Ilbawi, B.O. Anderson, F. Bray, I. dos-Santos-Silva, V. McCormack, Global and regional estimates of orphans attributed to maternal cancer mortality in 2020, Nat Med 28 (2022) 2563–2572. https://doi.org/10.1038/s41591-022-02109-2.

[7] F. Bray, M. Laversanne, H. Sung, J. Ferlay, R.L. Siegel, I. Soerjomataram, A. Jemal, Global cancer statistics 2022: GLOBOCAN estimates of incidence and mortality worldwide for 36 cancers in 185 countries, CA Cancer J Clin 74 (2024) 229–263. https://doi.org/10.3322/caac.21834.

[8] I.B. Weinstein, A. Joe, Oncogene Addiction, Cancer Res 68 (2008) 3077–3080. https://doi.org/10.1158/0008-5472.CAN-07-3293.

[9] L.D. Wood, D.W. Parsons, S. Jones, J. Lin, T. Sjöblom, R.J. Leary, D. Shen, S.M. Boca, T. Barber, J. Ptak, N. Silliman, S. Szabo, Z. Dezso, V. Ustyanksky, T. Nikolskaya, Y. Nikolsky, R. Karchin, P.A. Wilson, J.S. Kaminker, Z. Zhang, R. Croshaw, J. Willis, D. Dawson, M. Shipitsin, J.K. V. Willson, S. Sukumar, K. Polyak, B.H. Park, C.L. Pethiyagoda, P.V.K. Pant, D.G. Ballinger, A.B. Sparks, J. Hartigan, D.R. Smith, E. Suh, N. Papadopoulos, P. Buckhaults, S.D. Markowitz, G. Parmigiani, K.W. Kinzler, V.E. Velculescu, B. Vogelstein, The Genomic Landscapes of Human Breast and Colorectal Cancers, Science (1979) 318 (2007) 1108–1113. https://doi.org/10.1126/science.1145720.

[10] N. Papadopoulos, K.W. Kinzler, B. Vogelstein, The role of companion diagnostics in the development and use of mutation-targeted cancer therapies, Nat Biotechnol 24 (2006) 985–995. https://doi.org/10.1038/nbt1234.

[11] H. Sung, J. Ferlay, R.L. Siegel, M. Laversanne, I. Soerjomataram, A. Jemal, F. Bray, Global Cancer Statistics 2020: GLOBOCAN Estimates of Incidence and Mortality Worldwide for 36 Cancers in 185 Countries, CA Cancer J Clin 71 (2021) 209–249. https://doi.org/10.3322/caac.21660.

[12] J., E.M., L.F., C.M., M.L., P.M., . . . & B.F. Ferlay, Global cancer observatory: cancer today, Lyon: International Agency for Research on Cancer (2020) 20182020.

[13] M.C. Turner, Z.J. Andersen, A. Baccarelli, W.R. Diver, S.M. Gapstur, C.A. Pope, D. Prada, J. Samet, G. Thurston, A. Cohen, Outdoor air pollution and cancer: An overview of the current evidence and public health recommendations, CA Cancer J Clin 70 (2020) 460–479. https://doi.org/10.3322/caac.21632.

[14] F. Bray, A. Jemal, N. Grey, J. Ferlay, D. Forman, Global cancer transitions according to the Human Development Index (2008–2030): a population-based study, Lancet Oncol 13 (2012) 790–801. https://doi.org/10.1016/S1470-2045(12)70211-5.

[15] C. Santucci, G. Carioli, P. Bertuccio, M. Malvezzi, U. Pastorino, P. Boffetta, E. Negri, C. Bosetti, C. La Vecchia, Progress in cancer mortality, incidence, and survival: a global overview, European Journal of Cancer Prevention 29 (2020) 367–381. https://doi.org/10.1097/CEJ.0000000000000594.

[16] S.A. Frank, Genetic predisposition to cancer — insights from population genetics, Nat Rev Genet 5 (2004) 764–772. https://doi.org/10.1038/nrg1450.

[17] M. Arnold, M.J. Rutherford, A. Bardot, J. Ferlay, T.M.-L. Andersson, T.Å. Myklebust, H. Tervonen, V. Thursfield, D. Ransom, L. Shack, R.R. Woods, D. Turner, S. Leonfellner, S. Ryan, N. Saint-Jacques, P. De, C. McClure, A. V Ramanakumar, H. Stuart-Panko, G. Engholm, P.M. Walsh, C. Jackson, S. Vernon, E. Morgan, A. Gavin, D.S. Morrison, D.W. Huws, G. Porter, J. Butler, H. Bryant, D.C. Currow, S. Hiom, D.M. Parkin, P. Sasieni, P.C. Lambert, B. Møller, I. Soerjomataram, F. Bray, Progress in cancer survival, mortality, and incidence in seven high-income countries 1995–2014 (ICBP SURVMARK-2): a population-based study, Lancet Oncol 20 (2019) 1493–1505. https://doi.org/10.1016/S1470-2045(19)30456-5.

[18] M.B. Reitsma, N. Fullman, M. Ng, J.S. Salama et al. Smoking prevalence and attributable disease burden in 195 countries and territories, 1990–2015: a systematic analysis from the Global Burden of Disease Study 2015, The Lancet 389 (2017) 1885–1906. https://doi.org/10.1016/S0140-6736(17)30819-X.

[19] Y.-C. Lee, T.-H. Chiang, C.-K. Chou, Y.-K. Tu, W.-C. Liao, M.-S. Wu, D.Y. Graham, Association Between Helicobacter pylori Eradication and Gastric Cancer Incidence: A Systematic Review and Meta-analysis, Gastroenterology 150 (2016) 1113-1124.e5. https://doi.org/10.1053/j.gastro.2016.01.028.

[20] P. Piña-Sánchez, A. Chávez-González, M. Ruiz-Tachiquín, E. Vadillo, A. Monroy-García, J.J. Montesinos, R. Grajales, M. Gutiérrez de la Barrera, H. Mayani, Cancer Biology, Epidemiology, and Treatment in the 21st Century: Current Status and Future Challenges From a Biomedical Perspective, Cancer Control 28 (2021). https://doi.org/10.1177/10732748211038735.

[21] C. Allemani, T. Matsuda, V. Di Carlo et al. Global surveillance of trends in cancer survival 2000–14 (CONCORD-3): analysis of individual records for 37 513 025 patients diagnosed with one of 18 cancers from 322 population-based registries in 71 countries, The Lancet 391 (2018) 1023–1075. https://doi.org/10.1016/S0140-6736(17)33326-3.

[22] O. Ginsburg, R. Badwe, P. Boyle, G. Derricks, A. Dare, T. Evans, A. Eniu, J. Jimenez, T. Kutluk, G. Lopes, S.I. Mohammed, Y.-L. Qiao, S.F. Rashid, D. Summers, D. Sarfati, M. Temmerman, E.L. Trimble, A.I. Padela, A. Aggarwal, R. Sullivan, Changing global policy to deliver safe, equitable, and affordable care for women's cancers, The Lancet 389 (2017) 871–880. https://doi.org/10.1016/S0140-6736(16)31393-9.

[23] F. Islami, A. Goding Sauer, K.D. Miller, R.L. Siegel, S.A. Fedewa, E.J. Jacobs, M.L. McCullough, A. V. Patel, J. Ma, I. Soerjomataram, W.D. Flanders, O.W. Brawley, S.M. Gapstur, A. Jemal, Proportion and number of cancer cases and deaths attributable to potentially modifiable risk factors in the United States, CA Cancer J Clin 68 (2018) 31–54. https://doi.org/10.3322/caac.21440.

[24] D.M. Parkin, L. Hämmerl, J. Ferlay, E.J. Kantelhardt, Cancer in Africa 2018: The role of infections, Int J Cancer 146 (2020) 2089–2103. https://doi.org/10.1002/ijc.32538.

[25] R.D. Kehm, L.G. Spector, J.N. Poynter, D.M. Vock, S.F. Altekruse, T.L. Osypuk, Does socioeconomic status account for racial and ethnic disparities in childhood cancer survival?, Cancer 124 (2018) 4090–4097. https://doi.org/10.1002/cncr.31560.

[26] IARC. The value of cancer data, (n.d.). https://gicr.iarc.fr/about-the-gicr/value-of-cancer- (accessed July 2, 2025).

[27] L. Mery, F. Bray, Population-based cancer registries: a gateway to improved surveillance of non-communicable diseases, Ecancermedicalscience 14 (2020). https://doi.org/10.3332/ecancer.2020.ed95.

[28] M. Piñeros, M.G. Abriata, L. Mery, F. Bray, Cancer registration for cancer control in Latin America: a status and progress report., Rev Panam Salud Publica 41 (2017) e2. https://doi.org/10.26633/RPSP.2017.2.

[29] E. Raymond, C. Thieblemont, S. Alran, S. Faivre, Impact of the COVID-19 Outbreak on the Management of Patients with Cancer, Target Oncol 15 (2020) 249–259. https://doi.org/10.1007/s11523-020-00721-1.

[30] E.R. Mardis, The impact of next-generation sequencing technology on genetics, Trends in Genetics 24 (2008) 133–141. https://doi.org/10.1016/j.tig.2007.12.007.

[31] M.R. Stratton, P.J. Campbell, P.A. Futreal, The cancer genome, Nature 458 (2009) 719–724. https://doi.org/10.1038/nature07943.

[32] N. Siva, 1000 Genomes project, Nat Biotechnol 26 (2008) 256–256. https://doi.org/10.1038/nbt0308-256b.

[33] M.L. Metzker, Sequencing technologies — the next generation, Nat Rev Genet 11 (2010) 31–46. https://doi.org/10.1038/nrg2626.

[34] D. Pushkarev, N.F. Neff, S.R. Quake, Single-molecule sequencing of an individual human genome, Nat Biotechnol 27 (2009) 847–850. https://doi.org/10.1038/nbt.1561.

[35] M. Stratton, Genome resequencing and genetic variation, Nat Biotechnol 26 (2008) 65–66. https://doi.org/10.1038/nbt0108-65.

[36] N. Blow, Genomics: catch me if you can, Nat Methods 6 (2009) 539–544. https://doi.org/10.1038/nmeth0709-539.

[37] S.B. Ng, E.H. Turner, P.D. Robertson, S.D. Flygare, A.W. Bigham, C. Lee, T. Shaffer, M. Wong, A. Bhattacharjee, E.E. Eichler, M. Bamshad, D.A. Nickerson, J. Shendure, Targeted capture and massively parallel sequencing of 12 human exomes, Nature 461 (2009) 272–276. https://doi.org/10.1038/nature08250.

[38] T.A. Manolio, L.D. Brooks, F.S. Collins, A HapMap harvest of insights into the genetics of common disease, Journal of Clinical Investigation 118 (2008) 1590–1605. https://doi.org/10.1172/JCI34772.

[39] D.B. Goldstein, Common Genetic Variation and Human Traits, New England Journal of Medicine 360 (2009) 1696–1698. https://doi.org/10.1056/NEJMp0806284.

[40] J.N. Hirschhorn, Genomewide Association Studies — Illuminating Biologic Pathways, New England Journal of Medicine 360 (2009) 1699–1701. https://doi.org/10.1056/NEJMp0808934.

[41] P. Kraft, D.J. Hunter, Genetic Risk Prediction — Are We There Yet?, New England Journal of Medicine 360 (2009) 1701–1703. https://doi.org/10.1056/NEJMp0810107.

[42] W.D. Foulkes, Inherited Susceptibility to Common Cancers, New England Journal of Medicine 359 (2008) 2143–2153. https://doi.org/10.1056/NEJMra0802968.

[43] BRCA Gene Changes: Cancer Risk and Genetic Testing, (2009). https://www.cancer.gov/about-cancer/causes-prevention/genetics/brca-fact-sheet (accessed July 2, 2025).

[44] D. Altshuler, M.J. Daly, E.S. Lander, Genetic Mapping in Human Disease, Science (1979) 322 (2008) 881–888. https://doi.org/10.1126/science.1156409.

[45] J. Couzin, MicroRNAs Make Big Impression in Disease After Disease, Science (1979) 319 (2008) 1782–1784. https://doi.org/10.1126/science.319.5871.1782.

[46] V.N. Ngo, R.E. Davis, L. Lamy, X. Yu, H. Zhao, G. Lenz, L.T. Lam, S. Dave, L. Yang, J. Powell, L.M. Staudt, A loss-of-function RNA interference screen for molecular targets in cancer, Nature 441 (2006) 106–110. https://doi.org/10.1038/nature04687.

[47] L.T. Lam, R.E. Davis, V.N. Ngo, G. Lenz, G. Wright, W. Xu, H. Zhao, X. Yu, L. Dang, L.M. Staudt, Compensatory IKKα activation of classical NF-κB signaling during IKKβ inhibition identified by an RNA interference sensitization screen, Proceedings of the National Academy of Sciences 105 (2008) 20798–20803. https://doi.org/10.1073/pnas.0806491106.

[48] J.W. Tyner, M.W. Deininger, M.M. Loriaux, B.H. Chang, J.R. Gotlib, S.G. Willis, H. Erickson, T. Kovacsovics, T. O'Hare, M.C. Heinrich, B.J. Druker, RNAi screen for rapid therapeutic target identification in leukemia patients, Proceedings of the National Academy of Sciences 106 (2009) 8695–8700. https://doi.org/10.1073/pnas.0903233106.

[49] J. Luo, M.J. Emanuele, D. Li, C.J. Creighton, M.R. Schlabach, T.F. Westbrook, K.-K. Wong, S.J. Elledge, A Genome-wide RNAi Screen Identifies Multiple Synthetic Lethal Interactions with the Ras Oncogene, Cell 137 (2009) 835–848. https://doi.org/10.1016/j.cell.2009.05.006.

[50] D.A. Barbie, P. Tamayo, J.S. Boehm, S.Y. Kim, S.E. Moody, I.F. Dunn, A.C. Schinzel, P. Sandy, E. Meylan, C. Scholl, S. Fröhling, E.M. Chan, M.L. Sos, K. Michel, C. Mermel, S.J. Silver, B.A. Weir, J.H. Reiling, Q. Sheng, P.B. Gupta, R.C. Wadlow, H. Le, S. Hoersch, B.S. Wittner, S. Ramaswamy, D.M. Livingston, D.M. Sabatini, M. Meyerson, R.K. Thomas, E.S. Lander, J.P. Mesirov, D.E. Root, D.G. Gilliland, T. Jacks, W.C. Hahn, Systematic RNA interference reveals that oncogenic KRAS-driven cancers require TBK1, Nature 462 (2009) 108–112. https://doi.org/10.1038/nature08460.

[51] C. Scholl, S. Fröhling, I.F. Dunn, A.C. Schinzel, D.A. Barbie, S.Y. Kim, S.J. Silver, P. Tamayo, R.C. Wadlow, S. Ramaswamy, K. Döhner, L. Bullinger, P. Sandy, J.S. Boehm, D.E. Root, T. Jacks, W.C. Hahn, D.G. Gilliland, Synthetic Lethal Interaction between Oncogenic KRAS Dependency and STK33 Suppression in Human Cancer Cells, Cell 137 (2009) 821–834. https://doi.org/10.1016/j.cell.2009.03.017.

[52] A. Singh, P. Greninger, D. Rhodes, L. Koopman, S. Violette, N. Bardeesy, J. Settleman, A Gene Expression Signature Associated with "K-Ras Addiction" Reveals Regulators of EMT and Tumor Cell Survival, Cancer Cell 15 (2009) 489–500. https://doi.org/10.1016/j.ccr.2009.03.022.

[53] M. Arruebo, N. Vilaboa, B. Sáez-Gutierrez, J. Lambea, A. Tres, M. Valladares, Á. González-Fernández, Assessment of the Evolution of Cancer Treatment Therapies, Cancers (Basel) 3 (2011) 3279–3330. https://doi.org/10.3390/cancers3033279.

[54] M.A. Moses, H. Brem, R. Langer, Advancing the field of drug delivery, Cancer Cell 4 (2003) 337–341. https://doi.org/10.1016/S1535-6108(03)00276-9.

[55] A. Shapira, Y.D. Livney, H.J. Broxterman, Y.G. Assaraf, Nanomedicine for targeted cancer therapy: Towards the overcoming of drug resistance, Drug Resistance Updates 14 (2011) 150–163. https://doi.org/10.1016/j.drup.2011.01.003.

[56] Mondal J, Panigrahi AK, Khuda-Bukhsh, Conventional Chemotherapy: Problems and Scope for Combined Therapies with Certain Herbal Products and Dietary Supplements, Austin Journal of Molecular and Cell Biology 1 (2014) 10.

[57] R. Baserga, The Cell Cycle, New England Journal of Medicine 304 (1981) 453–459. https://doi.org/10.1056/NEJM198102193040803.

[58] A.A. Adjei, M. Hidalgo, Intracellular Signal Transduction Pathway Proteins As Targets for Cancer Therapy, Journal of Clinical Oncology 23 (2005) 5386–5403. https://doi.org/10.1200/JCO.2005.23.648.

[59] A. Chidharla, T. Kanderi, A. Kasi, Chemotherapy Acral Erythema, 2025.

[60] Y. Hu, C.-Y. Li, X.-M. Wang, Y.-H. Yang, H.-L. Zhu, 1,3,4-Thiadiazole: Synthesis, Reactions, and Applications in Medicinal, Agricultural, and Materials Chemistry, Chem Rev 114 (2014) 5572–5610. https://doi.org/10.1021/cr400131u.

[61] S. Sahu, T. Sahu, G. Kalyani, B. Gidwani, Synthesis and Evaluation of Antimicrobial Activity of 1, 3, 4-Thiadiazole Analogues for Potential Scaffold, J Pharmacopuncture 24 (2021) 32–40. https://doi.org/10.3831/KPI.2021.24.1.32.

[62] B. Shivarama Holla, K. Narayana Poojary, B. Sooryanarayana Rao, M.K. Shivananda, New bis-aminomercaptotriazoles and bis-triazolothiadiazoles as possible anticancer agents, Eur J Med Chem 37 (2002) 511–517. https://doi.org/10.1016/S0223-5234(02)01358-2.

[63] E. Yousif, A. Majeed, K. Al-Sammarrae, N. Salih, J. Salimon, B. Abdullah, Metal complexes of Schiff base: Preparation, characterization and antibacterial activity, Arabian Journal of Chemistry 10 (2017) S1639–S1644. https://doi.org/10.1016/j.arabjc.2013.06.006.

[64] Y. Li, J. Geng, Y. Liu, S. Yu, G. Zhao, Thiadiazole—a Promising Structure in Medicinal Chemistry, ChemMedChem 8 (2013) 27–41. https://doi.org/10.1002/cmdc.201200355.

[65] Wermuth CG, Aldous D, Raboisson P, Rognan D, The Practice of Medicinal Chemistry, n.d.

[66] Brown N, Bioisosteres in Medicinal Chemistry, n.d.

[67] R. Tripathy, A. Ghose, J. Singh, E.R. Bacon, T.S. Angeles, S.X. Yang, M.S. Albom, L.D. Aimone, J.L. Herman, J.P. Mallamo, 1,2,3-Thiadiazole substituted pyrazolones as potent KDR/VEGFR-2 kinase inhibitors, Bioorg Med Chem Lett 17 (2007) 1793–1798. https://doi.org/10.1016/j.bmcl.2006.12.054.

[68] A. Senff-Ribeiro, A. Echevarria, E.F. Silva, C.R.C. Franco, S.S. Veiga, M.B.M. Oliveira, Cytotoxic effect of a new 1,3,4-thiadiazolium mesoionic compound (MI-D) on cell lines of human melanoma, Br J Cancer 91 (2004) 297–304. https://doi.org/10.1038/sj.bjc.6601946.

[69] A.T. Balaban, D.C. Oniciu, A.R. Katritzky, Aromaticity as a Cornerstone of Heterocyclic Chemistry, Chem Rev 104 (2004) 2777–2812. https://doi.org/10.1021/cr0306790.

[70] Y. Hu, C.-Y. Li, X.-M. Wang, Y.-H. Yang, H.-L. Zhu, 1,3,4-Thiadiazole: Synthesis, Reactions, and Applications in Medicinal, Agricultural, and Materials Chemistry, Chem Rev 114 (2014) 5572–5610. https://doi.org/10.1021/cr400131u.

[71] A. Aliabadi, 1,3,4-Thiadiazole Based Anticancer Agents, Anticancer Agents Med Chem 16 (2016) 1301–1314. https://doi.org/10.2174/1871520616666160628100936.

[72] S. Haider, M.S. Alam, H. Hamid, 1,3,4-Thiadiazoles: A potent multi targeted pharmacological scaffold, Eur J Med Chem 92 (2015) 156–177. https://doi.org/10.1016/j.ejmech.2014.12.035.

[73] V.A. Obakachi, B. Kushwaha, N.D. Kushwaha, S. Mokoena, A.M. Ganai, T.K. Pathan, W.E. van Zyl, R. Karpoormath, Synthetic and anti-cancer activity aspects of 1, 3, 4-thiadiazole containing bioactive molecules: A concise review, Journal of Sulfur Chemistry 42 (2021) 670–691. https://doi.org/10.1080/17415993.2021.1963441.

[74] D. Kumar, H. Kumar, V. Kumar, A. Deep, A. Sharma, M.G. Marwaha, R.K. Marwaha, Mechanism-based approaches of 1,3,4 thiadiazole scaffolds as potent enzyme inhibitors for cytotoxicity and antiviral activity, Med Drug Discov 17 (2023) 100150. https://doi.org/10.1016/j.medidd.2022.100150.

[75] A. Ayati, S. Emami, A. Asadipour, A. Shafiee, A. Foroumadi, Recent applications of 1,3-thiazole core structure in the identification of new lead compounds and drug discovery, Eur J Med Chem 97 (2015) 699–718. https://doi.org/10.1016/j.ejmech.2015.04.015.

[76] A.M. Isloor, D. Sunil, P. Shetty, S. Malladi, K.S.R. Pai, N. Maliyakkl, Synthesis, characterization, anticancer, and antioxidant activity of some new thiazolidin-4-ones in MCF-7 cells, Medicinal Chemistry Research 22 (2013) 758–767. https://doi.org/10.1007/s00044-012-0071-5.

[77] S. D Shankara, A.M. Isloor, P.K. Jayaswamy, P. Shetty, D. Chakraborty, P.P. Venugopal, Vetting of New 2,5-Bis (2,2,2-trifluoroethoxy) Phenyl-Linked 1,3-Thiazolidine-4-one Derivatives as AURKA and VEGFR-2 Inhibitor Antiglioma Agents Assisted with In Vitro and In Silico Studies, ACS Omega 8 (2023) 43596–43609. https://doi.org/10.1021/acsomega.3c04662.

[78] A. Kumar, A. Chawla, S. Jain, P. Kumar, S. Kumar, 3-Aryl-2-{4-[4-(2,4-dioxothiazolidin-5-ylmethyl)phenoxy]-phenyl}-acrylic acid alkyl ester: synthesis and antihyperglycemic evaluation, Medicinal Chemistry Research 20 (2011) 678–686. https://doi.org/10.1007/s00044-010-9369-3.

[79] M. Djukic, M. Fesatidou, I. Xenikakis, A. Geronikaki, V.T. Angelova, V. Savic, M. Pasic, B. Krilovic, D. Djukic, B. Gobeljic, M. Pavlica, A. Djuric, I. Stanojevic, D. Vojvodic, L. Saso, In vitro antioxidant activity of thiazolidinone derivatives of 1,3-thiazole and 1,3,4-thiadiazole, Chem Biol Interact 286 (2018) 119–131. https://doi.org/10.1016/j.cbi.2018.03.013.

[80] N. Trotsko, Antitubercular properties of thiazolidin-4-ones – A review, Eur J Med Chem 215 (2021) 113266. https://doi.org/10.1016/j.ejmech.2021.113266.

[81] N. Trotsko, U. Kosikowska, A. Paneth, M. Wujec, A. Malm, Synthesis and antibacterial activity of new (2,4-dioxothiazolidin-5-yl/ylidene)acetic acid derivatives with thiazolidine-2,4-dione, rhodanine and 2-thiohydantoin moieties, Saudi Pharmaceutical Journal 26 (2018) 568–577. https://doi.org/10.1016/j.jsps.2018.01.016.

[82] GABRIEL MARC, IOANA IONUȚ, ADRIAN PÎRNĂU, LAURIAN VLASE, DAN CRISTIAN VODNAR, MIHAELA DUMA, BRÎNDUȘA TIPERCIUC, OVIDIU ONIGA, MICROWAVE ASSISTED SYNTHESIS OF 3,5-DISUBSTITUTED THIAZOLIDINE-2,4-DIONES WITH ANTIFUNGAL ACTIVITY. DESIGN, SYNTHESIS, VIRTUAL AND IN VITRO ANTIFUNGAL SCREENING, Journal of the Romanian Society for Pharmaceutical Science 65 (2017). https://farmaciajournal.com/issue-articles/microwave-assisted-synthesis-of-35-disubstituted-thiazolidine-24-diones-with-antifungal-activity-design-synthesis-virtual-and-in-vitro-antifungal-screening/ (accessed July 2, 2025).

[83] D.K. Aneja, P. Lohan, S. Arora, C. Sharma, K.R. Aneja, O. Prakash, Synthesis of new pyrazolyl-2, 4-thiazolidinediones as antibacterial and antifungal agents, Org Med Chem Lett 1 (2011) 15. https://doi.org/10.1186/2191-2858-1-15.

[84] N. Trotsko, U. Kosikowska, A. Paneth, T. Plech, A. Malm, M. Wujec, Synthesis and Antibacterial Activity of New Thiazolidine-2,4-dione-Based Chlorophenylthiosemicarbazone Hybrids, Molecules 23 (2018) 1023. https://doi.org/10.3390/molecules23051023.

[85] S. Saini, Synthesis and Anticonvulsant Studies of Thiazolidinone and Azetidinone Derivatives from Indole Moiety, Drug Res 69 (2019) 445–450. https://doi.org/10.1055/a-0809-5098.

[86] V. Asati, D.K. Mahapatra, S.K. Bharti, Thiazolidine-2,4-diones as multi-targeted scaffold in medicinal chemistry: Potential anticancer agents, Eur J Med Chem 87 (2014) 814–833. https://doi.org/10.1016/j.ejmech.2014.10.025.

[87] V. Asati, S.K. Bharti, Design, synthesis and molecular modeling studies of novel thiazolidine-2,4-dione derivatives as potential anti-cancer agents, J Mol Struct 1154 (2018) 406–417. https://doi.org/10.1016/j.molstruc.2017.10.077.

[88] N. Trotsko, A. Przekora, J. Zalewska, G. Ginalska, A. Paneth, M. Wujec, Synthesis and *in vitro* antiproliferative and antibacterial activity of new thiazolidine-2,4-dione derivatives, J Enzyme Inhib Med Chem 33 (2018) 17–24. https://doi.org/10.1080/14756366.2017.1387543.

[89] N. Trotsko, A. Bekier, A. Paneth, M. Wujec, K. Dzitko, Synthesis and In Vitro Anti-Toxoplasma gondii Activity of Novel Thiazolidin-4-one Derivatives, Molecules 24 (2019) 3029. https://doi.org/10.3390/molecules24173029.

[90] A. Kryshchyshyn, D. Kaminskyy, O. Karpenko, A. Gzella, P. Grellier, R. Lesyk, Thiazolidinone/thiazole based hybrids – New class of antitrypanosomal agents, Eur J Med Chem 174 (2019) 292–308. https://doi.org/10.1016/j.ejmech.2019.04.052.

[91] C.D. Barros, A.A. Amato, T.B. de Oliveira, K.B.R. Iannini, A.L. da Silva, T.G. da Silva, E.S. Leite, M.Z. Hernandes, M. do C.A. de Lima, S.L. Galdino, F. de A.R. Neves, I. da R. Pitta, Synthesis and anti-inflammatory activity of new arylidene-thiazolidine-2,4-diones as PPARγ ligands, Bioorg Med Chem 18 (2010) 3805–3811. https://doi.org/10.1016/j.bmc.2010.04.045.

[92] H. Ghafoori, M. Rezaei, A. Mohammadi, Anti-inflammatory Effects of Novel Thiazolidinone Derivatives as Bioactive Heterocycles on RAW264.7 Cells., Iran J Allergy Asthma Immunol 16 (2017) 28–38.

[93] S. Nazreen, M.S. Alam, H. Hamid, M.S. Yar, A. Dhulap, P. Alam, M.A.Q. Pasha, S. Bano, M.M. Alam, S. Haider, C. Kharbanda, Y. Ali, K.K. Pillai, Thiazolidine-2,4-diones derivatives as PPAR-γ agonists: Synthesis, molecular docking, in vitro and in vivo antidiabetic activity with hepatotoxicity risk evaluation and effect on PPAR-γ gene expression, Bioorg Med Chem Lett 24 (2014) 3034–3042. https://doi.org/10.1016/j.bmcl.2014.05.034.

[94] P.R. Devchand, T. Liu, R.B. Altman, G.A. FitzGerald, E.E. Schadt, The Pioglitazone Trek via Human PPAR Gamma: From Discovery to a Medicine at the FDA and Beyond, Front Pharmacol 9 (2018). https://doi.org/10.3389/fphar.2018.01093.

[95] Q. Zhang, H. Zhou, S. Zhai, B. Yan, Natural Product-Inspired Synthesis of Thiazolidine and Thiazolidinone Compounds and their Anticancer Activities, Curr Pharm Des 16 (2010) 1826–1842. https://doi.org/10.2174/138161210791208983.

[96] A.K. Jain, A. Vaidya, V. Ravichandran, S.K. Kashaw, R.K. Agrawal, Recent developments and biological activities of thiazolidinone derivatives: A review, Bioorg Med Chem 20 (2012) 3378–3395. https://doi.org/10.1016/j.bmc.2012.03.069.

[97] A. Saeed, N. Abbas, U. Flörke, Synthesis and antibacterial activity of some novel 2-Aroylimino-3-aryl-thiazolidin-4-ones, J Braz Chem Soc 18 (2007) 559–565. https://doi.org/10.1590/S0103-50532007000300010.

[98] S. Nobili, D. Lippi, E. Witort, M. Donnini, L. Bausi, E. Mini, S. Capaccioli, Natural compounds for cancer treatment and prevention, Pharmacol Res 59 (2009) 365–378. https://doi.org/10.1016/j.phrs.2009.01.017.

[99] S. Nussbaumer, P. Bonnabry, J.-L. Veuthey, S. Fleury-Souverain, Analysis of anticancer drugs: A review, Talanta 85 (2011) 2265–2289. https://doi.org/10.1016/j.talanta.2011.08.034.

[100] P. Chander Sharma, D. Sharma, A. Sharma, K.K. Bansal, H. Rajak, S. Sharma, V.K. Thakur, New horizons in benzothiazole scaffold for cancer therapy: Advances in bioactivity, functionality, and chemistry, Appl Mater Today 20 (2020) 100783. https://doi.org/10.1016/j.apmt.2020.100783.

[101] R. Palchaudhuri, P.J. Hergenrother, DNA as a target for anticancer compounds: methods to determine the mode of binding and the mechanism of action, Curr Opin Biotechnol 18 (2007) 497–503. https://doi.org/10.1016/j.copbio.2007.09.006.

[102] M.A. Jordan, L. Wilson, Microtubules as a target for anticancer drugs, Nat Rev Cancer 4 (2004) 253–265. https://doi.org/10.1038/nrc1317.

[103] A. Deep, P. Kumar, B. Narasimhan, K. Ramasamy, V. Mani, R. Mishra, A. Majeed, Synthesis, Antimicrobial, Anticancer Evaluation of 2-(aryl)-4- Thiazolidinone Derivatives and their QSAR Studies, Curr Top Med Chem 15 (2015) 990–1002. https://doi.org/10.2174/1568026615666150317221849.

[104] K. Jayalakshmi, M. Mahendra, Basappa, B.H. Doreswamy, M.A. Sridhar, J.S. Prasad, K.S. Rangappa, Synthesis and X-ray structure of 3-(4-methyl phenyl)-2-(4-biphenyl)-1,3-thiazolidin-4-one, J Chem Crystallogr 35 (2005) 67–70. https://doi.org/10.1007/s10870-005-1156-5.

[105] O. Devinyak, B. Zimenkovsky, R. Lesyk, Biologically Active 4-Thiazolidinones: A Review of QSAR Studies and QSAR Modeling of Antitumor Activity, Curr Top Med Chem 12 (2013) 2763–2784. https://doi.org/10.2174/1568026611212240006.

CHAPTER II

LITERATURE REVIEW

1. Synthetic Procedures of 1,3,4-Thiadiazole and its derivatives:

The late 19th-century discovery of phenylhydrazines and hydrazine is linked to the development of 1,3,4-thiadiazole chemistry. **Figure 1** illustrates the numbering of the 1,3,4-thiadiazole ring system. Generally, 1,3,4-thiadiazoles can be derived through transformations from 1,3,4-oxadiazoles or by the cyclisation of acylhydrazines, such as N, N′-diacylhydrazines and monoacylhydrazines (**Scheme 1**). Additionally, thiohydrazines, including thiosemicarbazides, thiocarbazides, dithiocarbazates, thioacylhydrazines, and bithioureas, can be converted into 1,3,4-thiadiazole. It is believed that this classification may assist scientists in their preparations. Some current methods for synthesising 1,3,4-thiadiazole derivatives are compiled below [1].

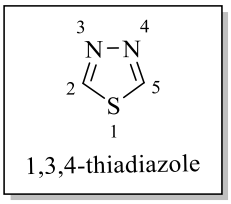

Figure 1: Numbering of 1,3,4-thiadiazole scaffold.

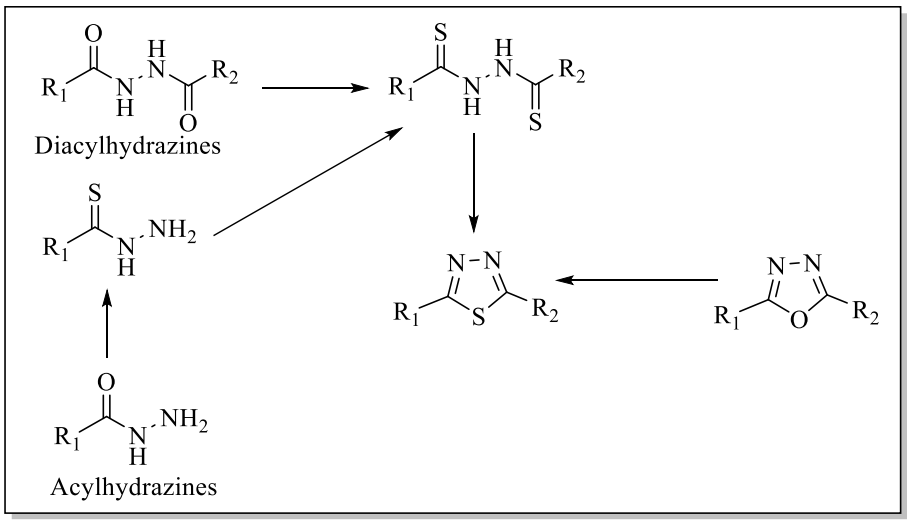

Scheme 1: General Preparation of 1,3,4-Thiadiazoles from Acylhydrazines or 1,3,4-Oxadiazoles.

1.1. From Acylhydrazines:

As shown in **Scheme 2**, phosphorus sulfide reagents such as P_2S_5 and Lawesson's reagent can be employed to sulfurate the respective 1,4-dicarbonyl or acyl precursors, producing 1,3,4-thiadiazoles [2–4]. However, severe conditions or the stoichiometric formation of an intractable byproduct are persistent issues with the commonly reported procedures.

1.1.1. From Acid Hydrazides:

Numerous one-pot syntheses of 1,3,4-thiadiazole have been reported in recent decades, eliminating the laborious multistep synthesis process. While some of these techniques have been refined, others are still employed in challenging circumstances. Propylphosphonic anhydride (T3P) (**Scheme 2a**) is utilised by Augustine et al. in a one-pot synthesis of 1,3,4-thiadiazoles (**3a-3c**) directly from carboxylic acids (**1a-1c**) and acid hydrazides (**2a-2c**). T3P acts as a coupling and cyclodehydration reagent. The reaction typically proceeds with excellent efficiency and broad compatibility with various functional groups. However, a small amount of the byproduct 1,3,4-oxadiazole (3–5%) contaminates the products, which are easily purified by column chromatography or recrystallisation [5].

In a single step, Polshettiwar et al. used microwave irradiation to create 1,3,4-thiadiazoles from acid hydrazides (**Scheme 2b**). With the help of solid-supported NafionNR50 and the thionating agent phosphorus pentasulfide in alumina (P_4S_{10}/Al_2O_3), a variety of aromatic and heterocyclic hydrazides (**4a−4f**) reacted effectively with triethyl orthoformate, triethyl orthoproponate, and triethyl orthobenzoate (**5a−5c**) without the need for a solvent, yielding moderate to good yields of 1,3,4-thiadiazoles (**6a−6j**) [6].

There are two or more steps involved in the reaction between acid hydrazide and the sulfur reagents CS_2 [7,8], isothiocyanate, or dithiocarbamates to produce thiadiazoles. The first step is to synthesise pertinent thiosemicarbazides or dithiacarbazides, which subsequently transform into thiadiazoles (see sections **1.2.1** and **1.2.3**). This type of reaction is rarely synthesised in a single pot. In the presence of water and triethylamine, isothiocyanate **7** has been shown to

immediately react with acid hydrazide to produce 2-substituted-1,3,4-thiadiazole (**Scheme 3a**) [9–12]. They used dithiocarbamates and acid hydrazides in water to create a series of high-yield 5-substituted-2-amino-1,3,4-thiadiazoles under the same conditions (**Scheme 3b**).

Lawesson's reagent, P_2S_5, along with H_2S/HCl, causes the thionation of acyl hydrazines to thioacylhydrazides (**Scheme 4**), which can then be cyclized into thiadiazoles [13,14]. We present this portion in section **1.2.4**. Furthermore, as will be covered in the next section, acyl hydrazines can be acylated to create diacyl hydrazines, which can then be cyclo-dehydrated to create thiadiazoles [4,15].

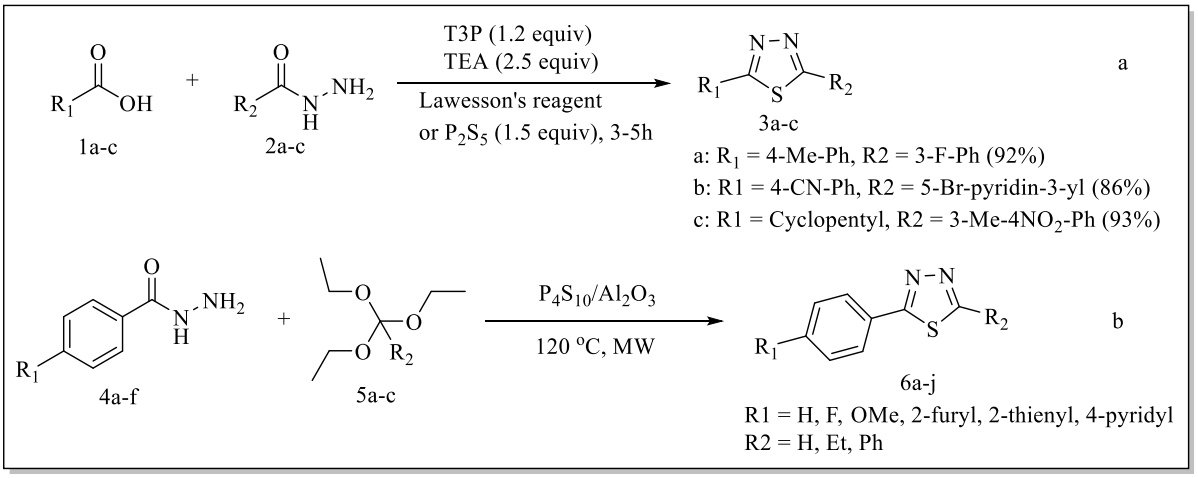

Scheme 2: Synthesis of 1,3,4-Thiadiazoles Directly from Carboxylic Acids and Acid Hydrazides.

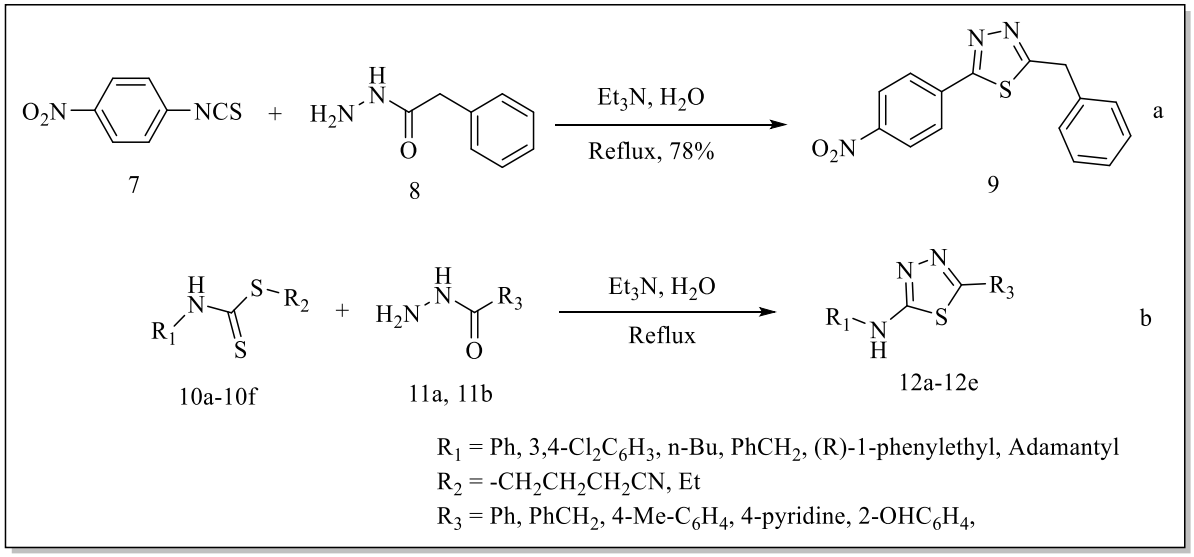

Scheme 3: 1,3,4-thiadiazole synthesis from acid hydrazides and sulfur reagent.

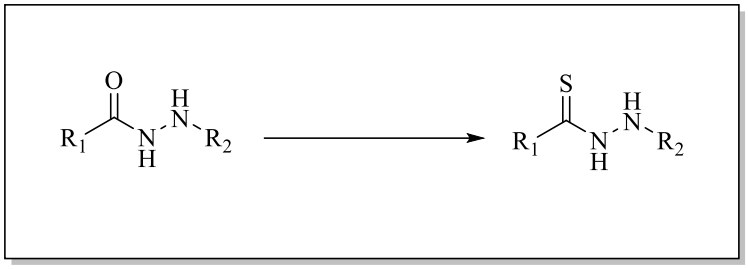

Scheme 4: Synthesis of Thioacylhydrazides from Acylhydrazines.

1.1.2. From Diacylhydrazines:

The cyclisation of N, N′-diacylhydrazines is a popular and practical method for producing 1,3,4-thiadiazoles. Numerous chemists have thoroughly examined this technique using phosphorus sulfides (i.e., P_2S_5 and Lawesson's reagent) in solvents, including DMF, CH_2Cl_2, THF, dioxane, and PhMe [16,17]. Recent studies have also regularly reported on solventless synthesis using microwave radiation. The indolyl-1,3,4-thiadiazoles **14a−14d** (**Scheme 5a**) were produced by thinning diacyl hydrazine **13a−13d** with Lawesson's reagent LR and then cyclized through oxidation in various solvents, such as tetrahydrofuran, toluene, dioxane, and xylene. The best yields were obtained in dry tetrahydrofuran [18]. Typical solvent thiadiazole synthesis methods involve lengthy reaction durations at elevated temperatures, low yields, numerous byproducts, the use of anhydrous hydrocarbon solvent, and a sulfurization reagent, making the process ecologically unfriendly. Conversely, solvent-free processes exposed to microwave radiation are likely to overcome these limitations (**Scheme 5b**) [19].

It can result in less pollution, cheaper expenses, and easier handling and processing. In this field, using microwave radiation as an unconventional energy source has shown great promise. The unsymmetrical N, N′-diacylhydrazine **15** was produced via N-acylation of 4-bromobenzohydrazide with myristoyl chloride. In 13 minutes, this compound cyclized into the corresponding thiadiazole **16** with a yield of 91%. Nevertheless, Lawesson's reagent has also been used in the procedure depicted in Scheme **5a** under solvent-free conditions, utilising

microwave irradiation, which produces a combination of byproducts in addition to the intended thiadiazole **14**. The reactive efficiency can, therefore, likely be increased by suitable reaction conditions, although the reactivities of particular reagents must be taken into consideration.

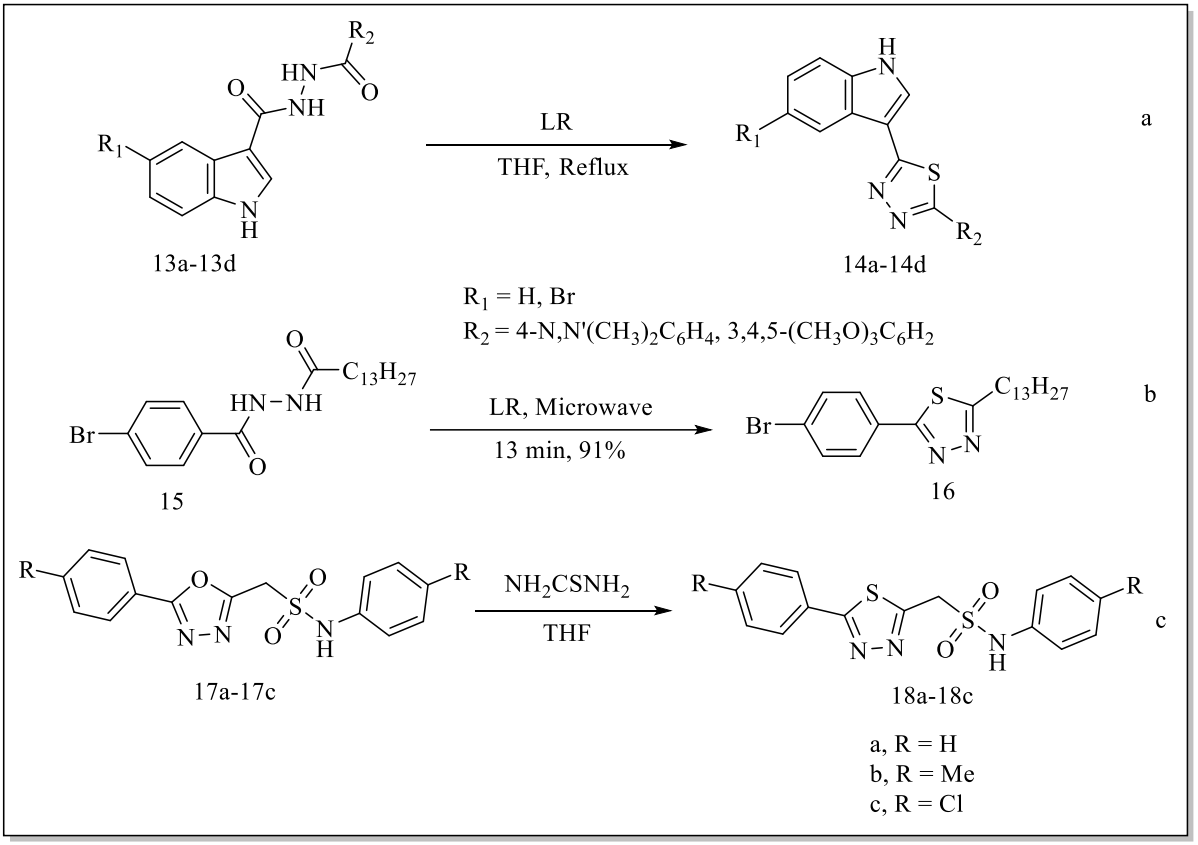

Scheme 5: Synthesis of 1,3,4-thiadiazoles from Diacylhydrazines.

1.2. From Thiohydrazines:

Thiohydrazines and their analogues can also be cyclized to create 1,3,4-thiadiazoles. Unique substituents can be incorporated into the thiadiazole ring from any derivative of thiohydrazines, resulting in 1,3,4-thiadiazoles that exhibit a broad range of reactivity and bioactivity. Here, we classify thiohydrazines into various groups, including bithioureas, thiosemicarbazides, thiocarbazides, dithiocarbazates, and thioacylhydrazines. Below is a summary of the methods used to synthesise 1,3,4-thiadiazole derivatives.

1.2.1. From Thiosemicarbazides:

Thiosemicarbazides, modified thiosemicarbazides, or thiosemicarbazones are the starting point for a number of 1,3,4-thiadiazole synthesis techniques. 2-Amino-1,3,4-thiadiazoles are effectively produced by the cyclisation of thiosemicarbazides or substituted thiosemicarbazides, and they have been extensively researched as essential intermediates in the preparation of 1,3,4-thiadiazole derivatives. The cyclisation of thiosemicarbazides is initiated in this reaction by acylation (**Scheme 6**) or Schiff base formation on the α-amino group. The action of a dehydrating agent such as EDCI, DCC, TMSCl, TsCl, PPh_3, $SOCl_2$, PCl_5, and diphenyl chlorophosphate then produces thiadiazoles. Numerous common acylating agents have been utilised, including acid halides [20], carboxylic acids [21–24], and acid anhydrides (**Scheme 7a** and **7b**) [25–27]. Schiff bases were created using metal oxidants such as ferric chloride, acidic aluminium oxide, and aldehydes (**Schemes 7c** and **7d**) [25,28,29].

Thiosemicarbazide can also become (thio)acylated as a result of nucleophilic attack on iso(thio)cyanates [30]. Furthermore, thiosemicarbazides can be produced by directly reacting thiourea with acetamide [31]. Both mono- and bicyclic 2-amino-1,3,4-thiadiazole derivatives have been prepared via an interaction between carboxylic acids and thiosemicarbazide in ionic liquids, which have been widely used as potential replacements for conventional solvents for a range of chemical processes (**Scheme 7e**) [32]. N-substituted 5-amino-1,3,4-thiadiazole **28** or analogue **27** without the amine group was produced by treating sulfinyl-bis((2,4-dihydroxyphenyl) methanethione) (STB) with the proper thiosemicarbazides or hydrazides in methanol (**Scheme 7f**). Prior to converting into the thiol form, the linear product of the thioacyl derivative is created in the interaction of STB with nucleophiles. The 1,3,4-thiadiazole ring is ultimately obtained by eliminating the H_2S or H_2O molecule. Additionally, STB functions as an endogenous cyclizing reagent due to its electrophilic nature as a substrate. Furthermore, the synthesis of thiadiazoles from thiosemicarbazides also involves nitriles [33,34]. In a PPA

(phenylpropanolamine) media, the nitriles **29** are easily transformed into PPA iminoesters, which react with thiosemicarbazide to form amidazones **30** and then lose an ammonia molecule to form compounds **31** (**Scheme 7g**).

The structure of 1,3,4-thiadiazolium mesoionic derivatives is characterised by the formula (**Figure 2**), featuring distinct positive and negative charge zones that enable a neutral overall balance. This feature has drawn much interest in photochemical research. They can interact with biomolecules due to their structure, which is linked to a polyheteroatomic system, and their generally neutral nature facilitates membrane transport, a process essential in medicinal chemistry. **Scheme 8** illustrates the synthesis of a group of 4-phenyl-5-styryl-1,3,4-thiadiazolium-2-phenylamines whose antiparasitic properties have been thoroughly investigated [35–38]. Thiosemicarbazides react with CS_2 to produce 1,3,4-thiadiazoles, although they first generate dithiocarbazates (**Scheme 8**), which we will describe in Section **1.2.3** [39,40].

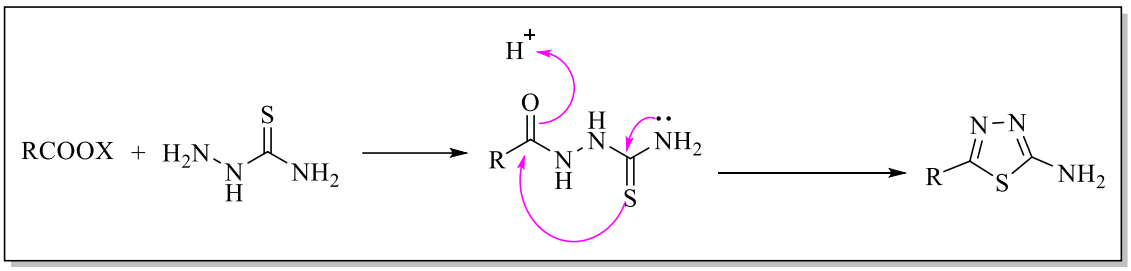

Scheme 6: Mechanism of Thiadiazole formation from Thiosemicarbazide.

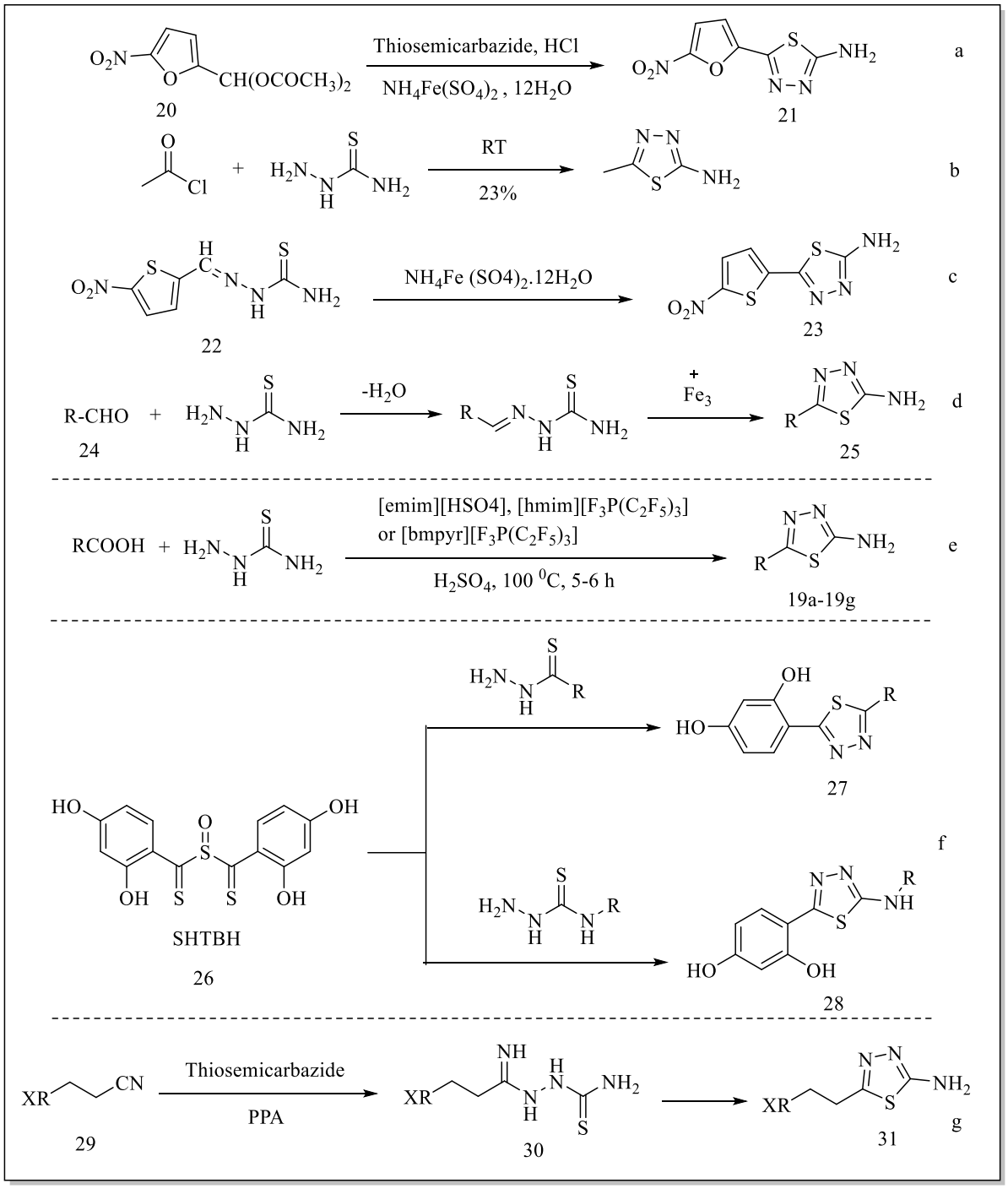

Scheme 7: 1,3,4-thiadiazole synthesis from thiosemicarbazides.

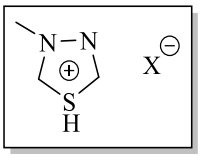

Figure 2: Chemical structure of the mesoionic salt derivative formed by 1,3,4-thiadiazole compounds.

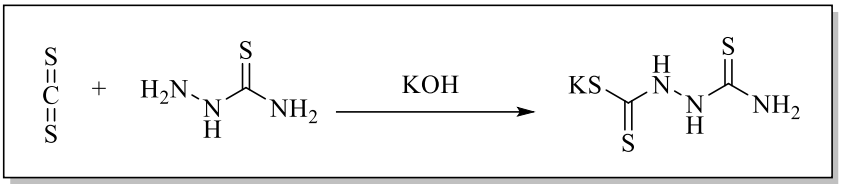

Scheme 8: Synthesis of 4-Phenyl-5-styryl-1,3,4-thiadiazolium-2-phenylamines.

1.2.2. From Thiocarbazides:

The synthesis of thiadiazole using thiocarbazide, also known as carbonothioic dihydrazide, and its derivatives is comparable to that of thiosemicarbazide. The added substituents on 1,3,4-thiadiazole, specifically 2-amino (from thiosemicarbazide) and 2-acyl hydrazine (from thiocarbazide), are the only sources of variation. Hydrazides or 1,3,4-thiadiazol-2-yl hydrazones have been synthesised using thiocarbazides. Thiadiazoles 33a−33g are produced when carbonothioic dihydrazide is treated with the appropriate hydrazonoyl halide 32a−32g (**Scheme 9a**) [41]. Bis(1,3,4-thiadiazole-2-yl) hydrazones were also synthesised by the chemists using the same procedure in the same study (**Scheme 9b**). To obtain the desired hydrazones, Sayed et al. treated aldehydes with 2- (phenylmethylene) carbonothioic dihydrazide, in addition to the hydrazonoyl halide [41–43]. Li et al. described a novel, quick, and environmentally friendly method for preparing (un)substituted benzaldehyde (5-aryl-1,3,4-thiadiazol-2-yl) hydrazones using thiocarbo-hydrazide as the starting reagent [44], readily recoverable silica-supported dichlorophosphate as the dehydrant, and a microwave as the heat source to circumvent the long-term environmental problems associated with conventional procedures. This approach proved to be a high-yield technique worth mentioning. Furthermore,

scheme 9c illustrates how to prepare 1,3,4-thiadiazol-2-yl hydrazides using thiocarbazide and microwave radiation.

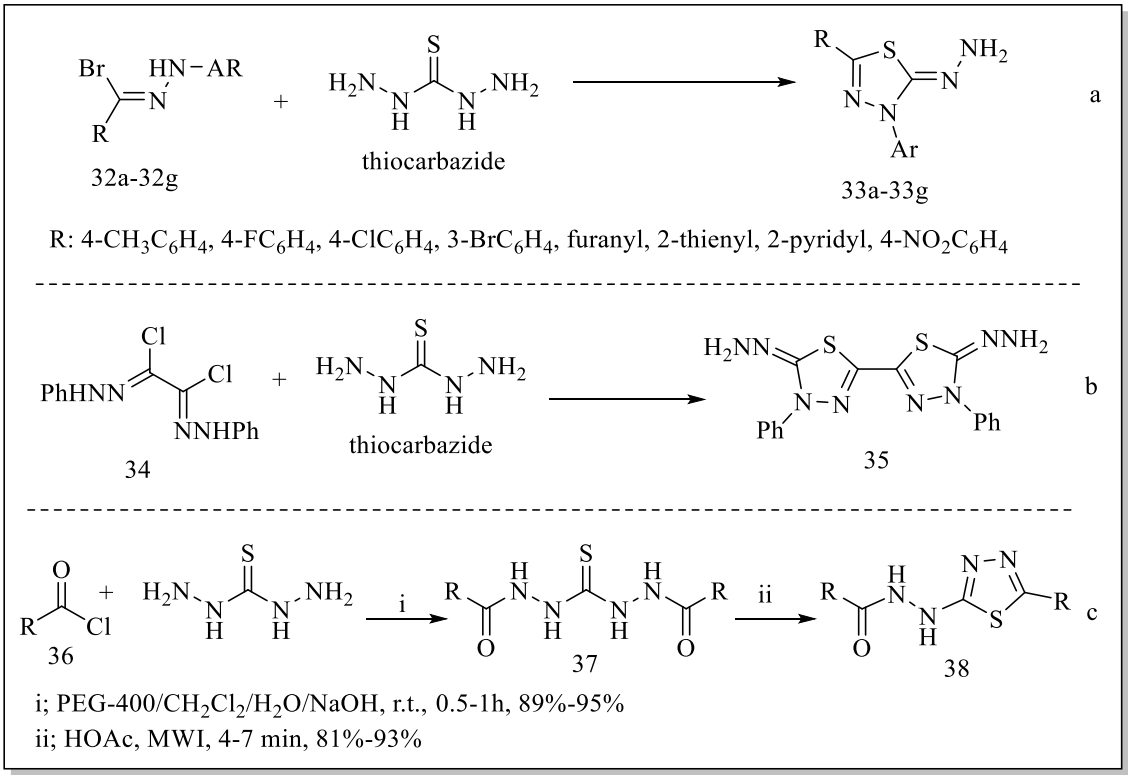

Scheme 9: Synthesis of 1,3,4-Thiadiazoles from Thiocarbazides.

1.2.3. From Dithiocarbazates:

As previously stated, carbon disulfide, the sulfur source reagent, reacts with hydrazine, hydrazides, hydrazone, thiosemicarbazide (listed in **Scheme 8**), or thioacylhydrazine, often under essential circumstances (**Scheme 10**), to create dithiocarbazates. In order to produce 2-thiol/thione 1,3,4-thiadiazoles, dithiocarbazates were usually acylated and then cyclodehydrated (concentrated sulphuric acid was always the dehydrant, sometimes CF_3COOH). A broad procedure for creating dithiocarbazate and 1,3,4-thiadiazole using acylhydrazide was described by Wei et al. and Kadi et al. (**Scheme 11a**) [45,46]. According to Sayed et al., dithiocarbazates with hydrazonoyl halides **32a**, **32g**, and **34** may also produce compounds **33a**, **33g** and **35** [41]. Another method of making 1,3,4-thiadiazole involves first acylating dithiocarbazate with chloroacetyl chloride, followed by dehydration (**Scheme 11b**)

[47]. There have also been several reports of the selective, reagent-based cyclisation of acyldithiocarbazate to produce 1,3,4-thiadiazole derivatives in solid phase. Using CS_2 in the presence of sodium hydride at room temperature to make several acyldithiocarbazate resins 44 and cyclodehydrated to create the target compounds **45**, Gong et al. compiled a number of appropriate techniques for solid-phase synthesis of 1,3,4-thiadiazoles (**Scheme 11c**) [48]. EDCI, DCC, TMSCl, TsCl, PPh_3, $SOCl_2$, PCl_5, and diphenyl chlorophosphate were among the reagents that Gong et al. examined for the cyclisation reactions of the acyldithiocarbazate **44** using Merrifield resin as a polymer support. They discovered that TMSCl and diphenyl chlorophosphate were comparatively good options for the 1,3,4-thiadiazole **45**.

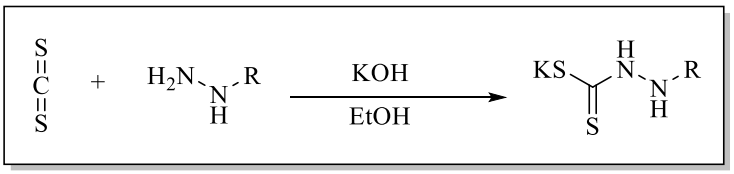

Scheme 10. Synthesis of Dithiocarbazates from Thioacylhydrazine.

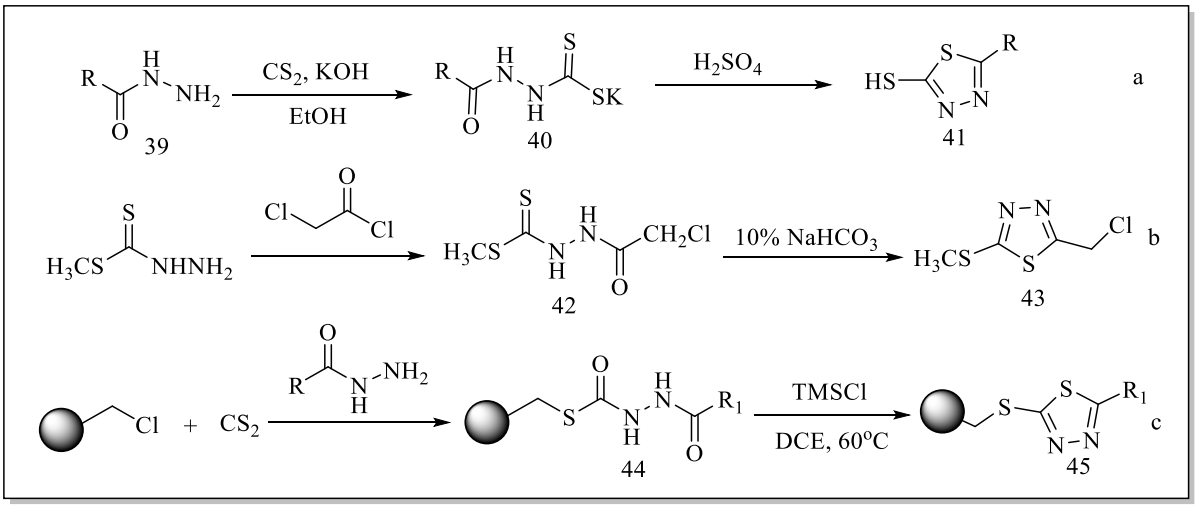

Scheme 11: Synthesis of 1,3,4-Thiadiazoles from Dithiocarbazates.

1.2.4. From Thiohydrazides:

The absence of the α-amino group in thiohydrazide is the sole structural difference between it and thiosemicarbazide. Because of this, thiohydrazide is also often used in the "hodgepodge" synthesis of 1,3,4-thiadiazoles, utilizing techniques that are similar to those used for

thiosemicarbazide. According to reports, 1,3,4-thiadiazoles are created by acylating thiohydrazides (with carboxylic acid, acid halide, or acid anhydride) or by forming Schiff base (with aldehyde) and hydrazone (with nitrile), followed by in situ cyclodehydration. Using $K_2S_2O_8$ and I_2/pyridine as oxidants, Fararr et al. prepared 2,5-dimethylphenyl-1,3,4-thiadiazole 48 by treating thiobenzhydrazide **46** with benzaldehyde to produce the thiohydrazide derivative **47** (**Scheme 12a**) and with benzonitrile to produce N-thiobenzoylbenzamidrazone **49** (**Scheme 12b**) [49]. The deprotonation of thiohydrazide, followed by the intramolecular assault of the thiolate anion on the amidinyl or iminyl carbon atom and the loss of ammonia or hydrogen after proton transfer, may be used to explain the formation of the thiadiazole ring. While it has a negative impact on the synthesis of thiadiazoles in **Scheme 12b**, a neutral or acidic environment is most likely advantageous in **Scheme 12a**. A variety of 1,3,4-thiadiazolyl phenyl oxazolidinone analogues **51** were produced in excellent yield when thiobenzhydrazide **50** reacted with acid chlorides in refluxing THF. The Fmoc-protected 2-aminomethyl-1,3,4-thiadiazole analogues **52** (**Scheme 12c**) were obtained by refluxing THF with Fmoc–glycyl chloride or Fmoc–sarcosine acid chloride (made from Fmoc–sarcosine and thionyl chloride using a catalytic amount of DMF). The Fmoc protecting group can be eliminated by treating with piperidine [50]. It has also been reported that coumarin-3-carbothiohydrazide may be condensed with esters (ethyl orthoformate, trimethyl orthoacetate, and trimethyl orthobenzoate) to produce coumarin-1,3,4-thiadiazole derivatives. 1,3,4-thiadiazoles may also be made using diethyl chlorophosphate [51].

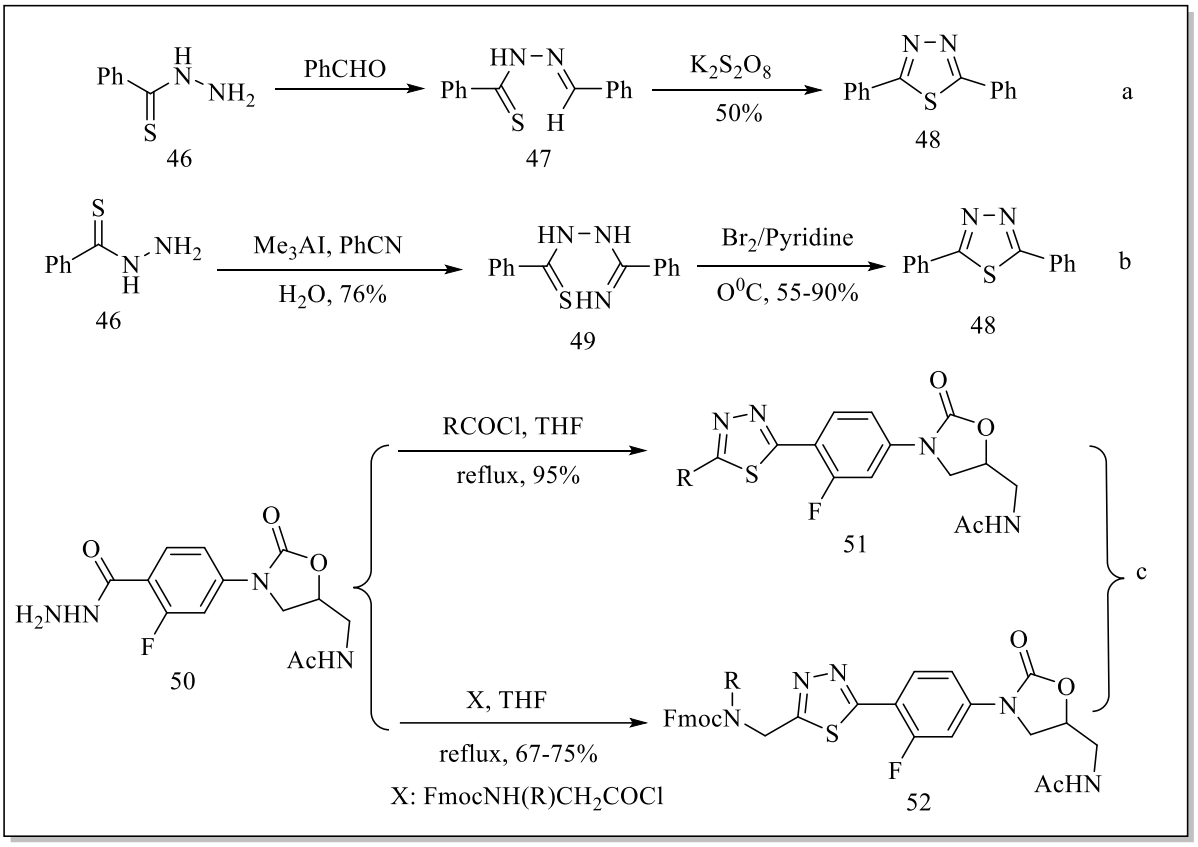

Scheme 12: Synthesis of 1,3,4-Thiadiazoles from Thiohydrazides.

1.2.5. From Bithioureas:

It is possible to create bithiourea with α-amino groups on both ends by reacting isothiocyanates with thiosemicarbazides or hydrazines (**Scheme 13a**) [52,53]. The crucial intermediary for the subsequent preparation of various 2,5-bis-substituent-1,3,4-thiadiazoles, 2,5-amino-1,3,4-thiadiazole, may be obtained through cyclodehydration. The formation can be explained by the detachment of the RNH or HS moiety, as shown in **Scheme 13b**, followed by an intramolecular nucleophilic attack from either the 2-thiol or the NH group. The elimination of aniline or allylamine would yield 5-substituted amino-3H-[1,3,4] thiadiazole-2-thione **55**, while the displacement of H_2S would yield N, N-disubstituted [1,3,4] thiadiazole-2,5-diamine [54]. The 2,5-disubstituted amino-1,3,4-thiadiazoles **58a–58c** were minor products from quinoxaline derivatives, generated by adding tetrahydrofuran (THF) solutions of **56a–56c** to a 2:1 solution of **57a** and **57b** in the same solvent (yields of 12–15% for **57a** and 21–26% for **57b**) (**Scheme**

13c) [55]. Compared to the standard procedure of adding **56a–56c** to ethyl acetate or chlorobenzene without ethylenetetracarbonitrile (TCNE) for 96 hours, which resulted in compounds **56a–56c** again, not following the previous sequence of chemical reactions, it was shown that TCNE, a highly electron-deficient and strongly electrophilic reagent, was crucial in the condensation of **56a–56c** to obtain the corresponding thiadiazoles and thiadiazole-2-thiones [56].

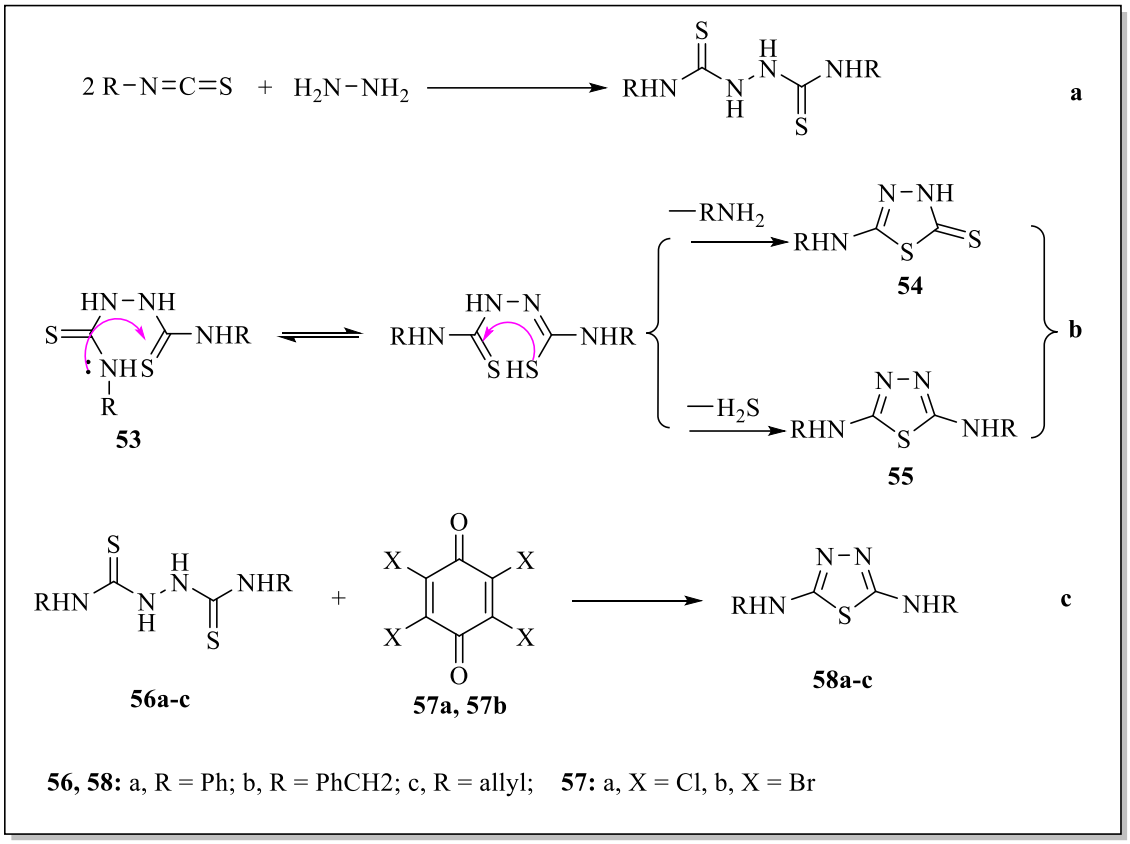

Scheme 13: Synthesis of 1,3,4-Thiadiazoles from Bithioureas

2. Synthesis of 1,3-thiazolidine-4-one scaffold-based molecules:

O.A. Ali and coresearchers synthesised sulfaguanidine incorporating thiazolidine-4-one moieties. Additionally, the design and construction of the prepared compounds are displayed in **Scheme 14**. The nucleophilic substitution reaction of the sulfaguanidine **1** with the cyanoacetylating agent **2** in a non-polar solvent (toluene) produced the starting material, N-(4-(N-carbamimidoylsulfamoyl) phenyl)-2-cyanoacetamide **3** (**Scheme 14**). Furthermore, as

shown in **Scheme 14**, the non-isolable sulfide salt **4** was produced by the reactivity of the starting material **3** with certain electrophiles, such as the isothiocyanate derivative in DMF solvent. Lastly, intramolecular cycloalkylation of the non-isolable salt **4** with halogenated alkylating agents, such as ethyl 2-chloroacetate, methyl 2-bromopropanoate, methyl 2-bromobutanoate, and dimethyl acetylenedicarboxylate, led to the preparation of several novel thiazolidine-4-one derivatives, yielding new thiazolidine-4-one derivatives **5–8**, respectively [57].

In a separate study, several approaches were investigated for the synthesis of derivatives of 2-(3-halo-phenyl)-3-(2-methoxy-phenyl) thiazolidine-4-one. The nucleophilic inclusion of the amine derivative to the aldehyde carbon results in the synthesis of an imine via the removal of water in all applicable ways, depending on the reaction mechanism. An intramolecular cyclisation is the consequence of the thioglycolic acid's ─SH group being added to the C═N carbon, the amine attacking the acid's carbonyl carbon, and the removal of water. **Scheme 15a** states that a one-pot, three-component synthesis method was conducted in dry benzene, tetrahydrofuran, and chloroform medium for 24 hours at the reflux temperature. In dry benzene, compounds **11a–c** yielded the highest yields (66%, 63%, and 72%, respectively) under these conditions. Additionally, **scheme 15a** utilised the produced chiral ionic liquid 1-(S-2′-methylbutyl)-3-methylimidazolium tetrafluoroborate [mbmi][BF4] at 0, 25, 50, and 75 °C for 4, 8, and 12 hours to create **11a–c** derivatives (**Scheme 15a**). Then, under ideal circumstances of 4 hours and 75 °C, the yields of the produced compounds were computed as 89%, 87%, and 81% for compounds **11a–c**, respectively [58].

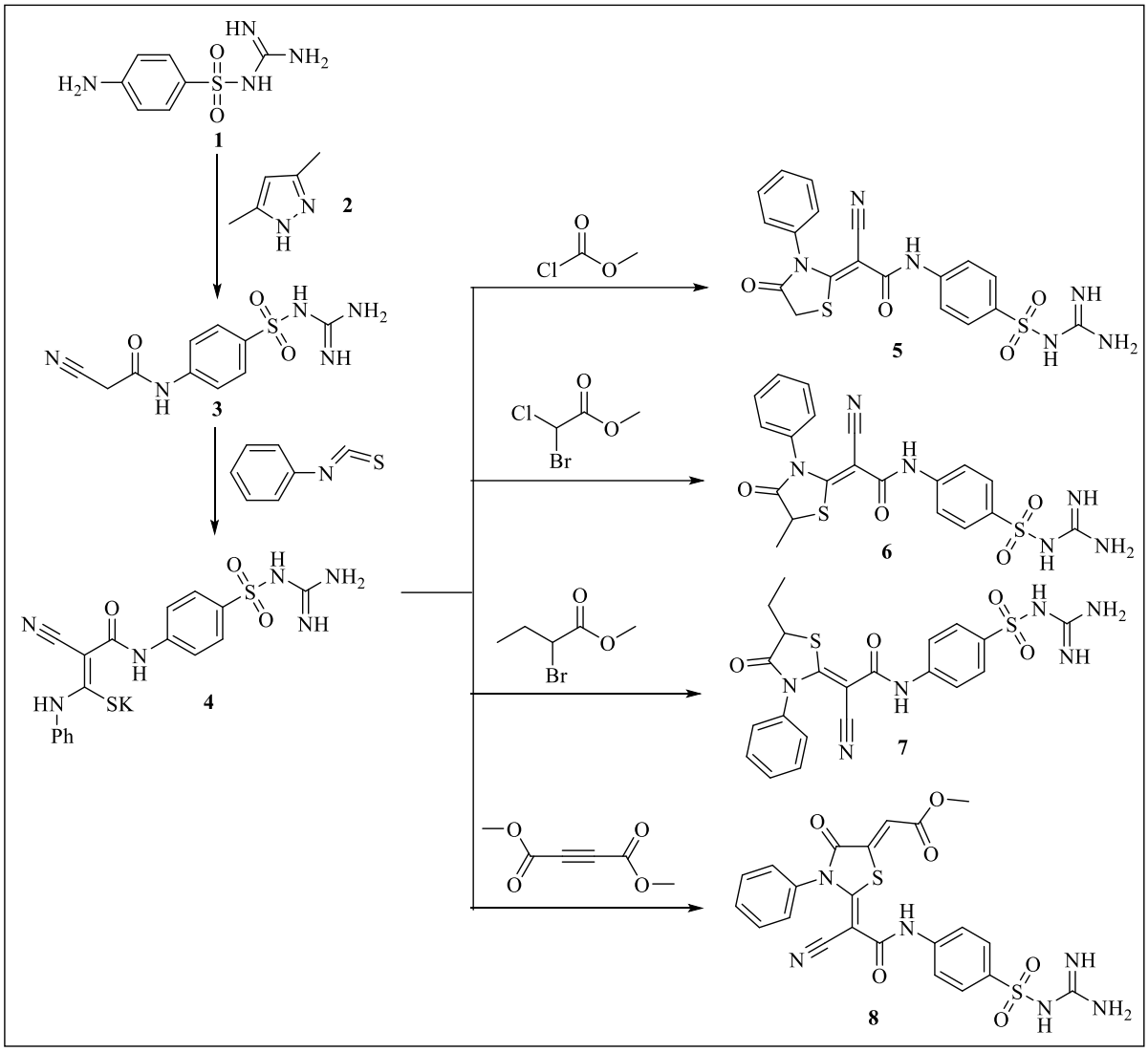

Scheme 14: Synthesis of thiazolidin-4-one derivatives from sulfide salt containing the sulfaguanidine scaffold.

Using DCC as a catalyst for 4 hours at 0 °C and 25 °C, the tests were conducted again in **scheme 15b** with the same solvents present. Examining the experimental data, it was found that the efficiency of dry benzene was excellent, and the yields produced in THF and $CHCl_3$ at 25 °C were lower than those obtained with the chiral ionic liquid. However, several of the documented techniques have several drawbacks, including the need for expensive catalysts, hazardous solvents, specialised equipment, lengthy reaction periods, and time-consuming handling processes, and they often yield only poor to moderate amounts of products. As a result, the need to develop a more effective and valuable method for synthesising this

significant heterocyclic framework is increasing. Moreover, another method included doing microwave-assisted tests for 5 and 10 minutes at 80 °C and 600 W, both without a solvent and with the chiral ionic liquid [mbmi][BF4] present. Compounds **11a–c** yielded 96%, 95%, and 92%, respectively, when the chiral ionic liquid was present and the reaction was run for 10 minutes (**Scheme 15d**) [58].

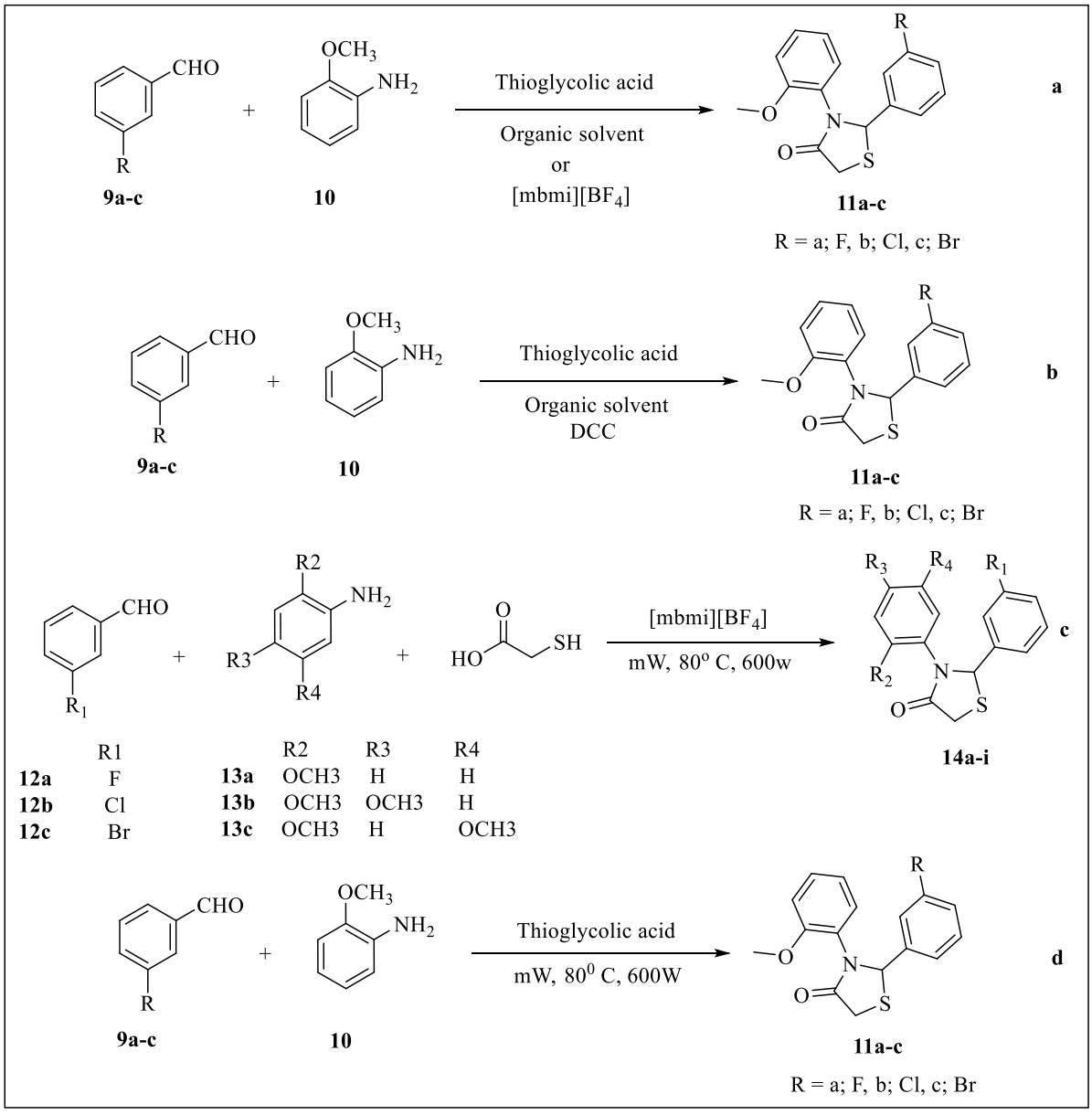

Scheme 15: Synthesis of thiazolidine-4-one from imine and thioglycolic acid under different conditions using organic solvents, ionic liquids, and microwave irradiation.

Ranade et al. described the synthesis of new 4-(2-(4-oxo-2-(phenylimino) thiazolidin-3-yl) ethyl) benzenesulfonamide or compound **18**. 4-(2-(3-phenylthioureido) ethyl) benzenesulfonamide **(17)** was obtained by the reaction between 4-(2-aminoethyl) benzenesulfonamide **(15)** and phenylisothiocyanate (**16**) in the presence of a catalytic amount of triethylamine (**Scheme 16a**). Finally, compound **18** was obtained by refluxing **17** and chloroacetic acid in the presence of sodium acetate (**Scheme 16b**) [59]

In various studies, thioureas **22a-k** were reacted with either diethyl acetylenedicarboxylate (DEAD) or dimethyl acetylenedicarboxylate (DMAD) to produce a range of novel thiazolidine-5-ylidenes **24a-n** compounds in a straightforward and efficient manner. Spectroscopic evidence validated the suggested structures of these novel compounds. DMAD and DEAD (**23a-b**) react smoothly with the generated thioureas **22a-k** (**Scheme 17**) when exposed to microwave radiation, yielding thiazolidine-4-ones **24a-n** [60].

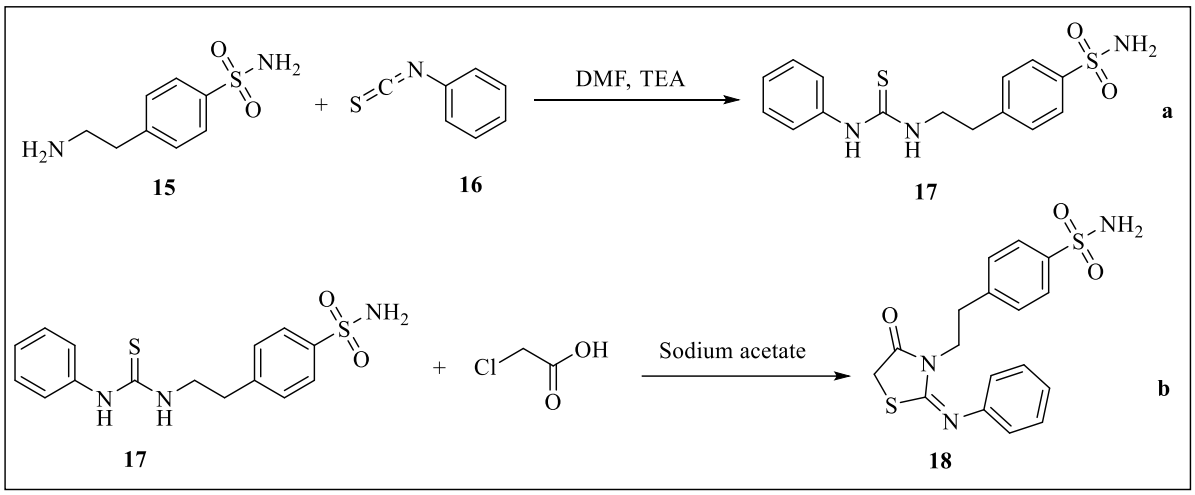

Scheme 16: Synthesis of thiazolidine-4-one derivative from thiourea and chloroacetic acid.

Targeted thiazolidine-4-one and intermediate compounds were synthesised using the process shown in **Scheme 18**. 9H-Fluoren-9-one (**25**) produced 2-(9H-fluoren-9 ylidene) hydrazine carbothioamide upon reaction with thiosemicarbazide in ethanol and a catalytic quantity of acetic acid (**26**). Chloroacetic acid treatment of **26** in the presence of ethanol and sodium acetate produced 2-(2-(9H-fluoren-9-ylidene) hydrazinyl) thiazol-4(5H)-one (**27**) [61].

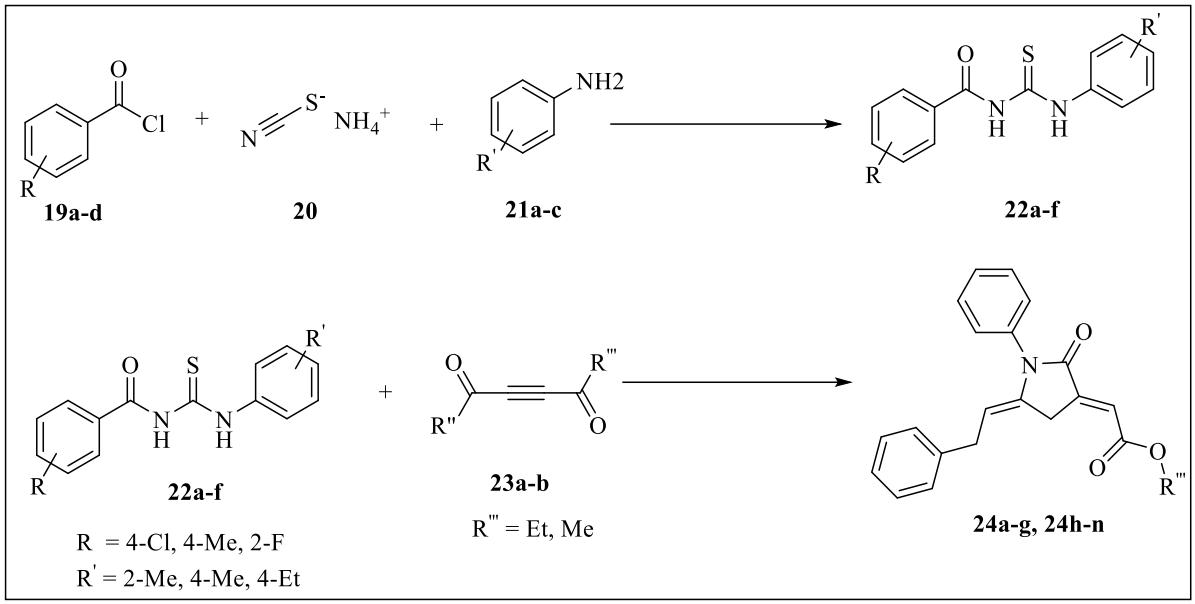

Scheme 17: Synthesis of thiazolidine-4-one using thiourea and diethyl acetylenedicarboxylate (DEAD) or dimethyl acetylenedicarboxylate (DMAD).

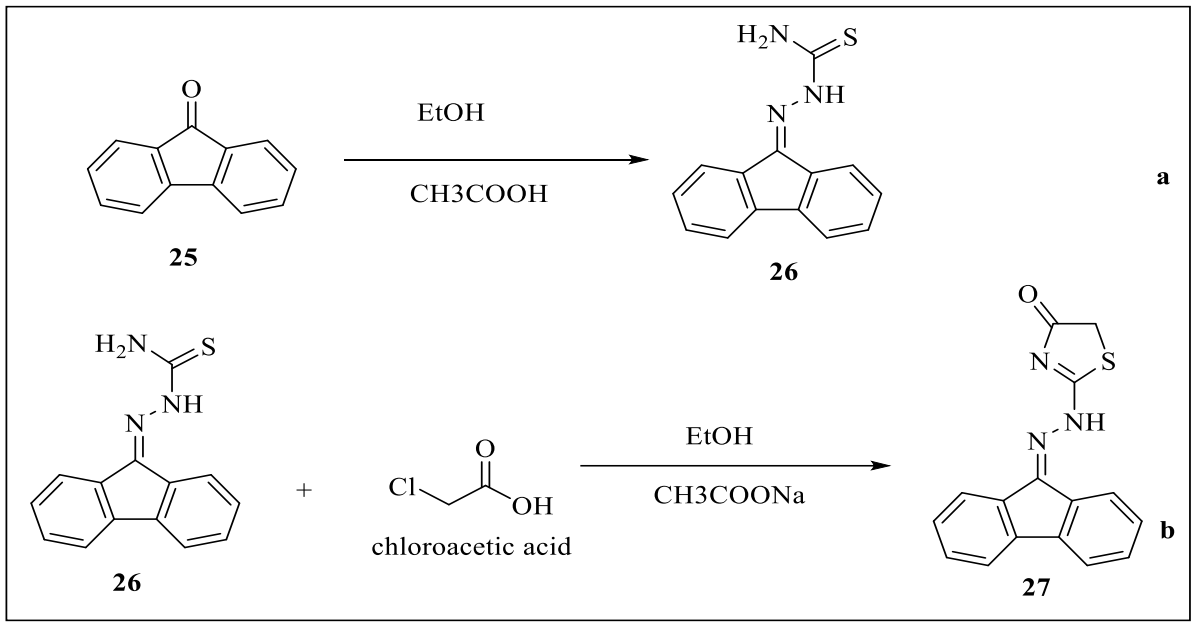

Scheme 18: Synthesis of thiazolidine-4-one from hydrazine carbothioamide and chloroacetic acid.

In order to create new bioactive 2-aryl-3-(1H-pyrazol-3-yl) thiazolidin-4-one derivatives (**28a-o**) with a respectable yield that are safe for Mother Earth, Sharmistha Das et al. developed a new one-pot multi-component reaction (MCR) scheme (**Scheme 19**), which is supported by the PTSA and employing a green protocol in an aqueous medium without the use of hazardous

solvents or metal catalysts. Reaction parameters were carefully investigated to determine the viability and screening conditions of our existing methodology. They used benzaldehyde, 1H-pyrazol-3-amine, and thioglycolic acid in a 1:1:1 molar ratio as the model reaction to initiate the learning of the outlined scheme. They have run the model reaction in a variety of solvents, with varying amounts of catalyst, at different temperatures, and for varying durations to optimise the designed MCR [62]. Noor et al. carry out the multi-step synthesis of a heterocyclic series of thiazolidine-4-one derivatives (**Scheme 20**). To create the first series from thiazolidin-4-one, thiosemicarbazone was first produced and then treated with chloroacetic acid as a cyclisation agent in ethanol under reflux conditions [63].

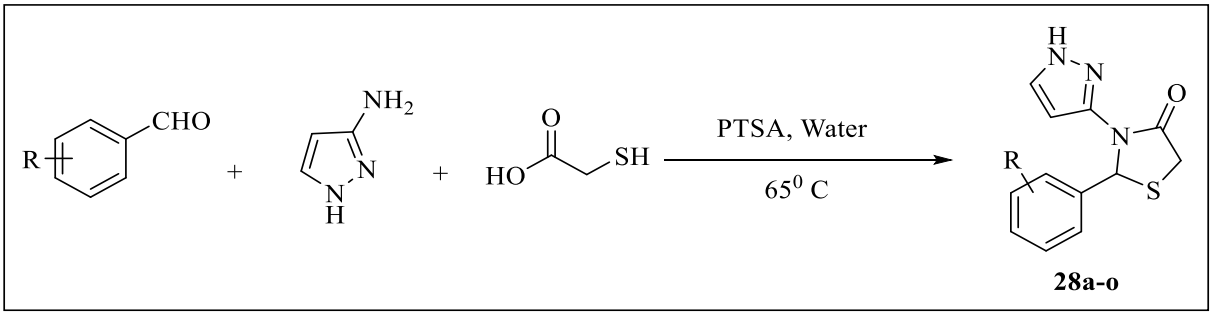

Scheme 19: Reaction of imine and thioglycolic acid in water using paratoluene sulfonic acid (PTSA) to create thiazolidine-4-one.

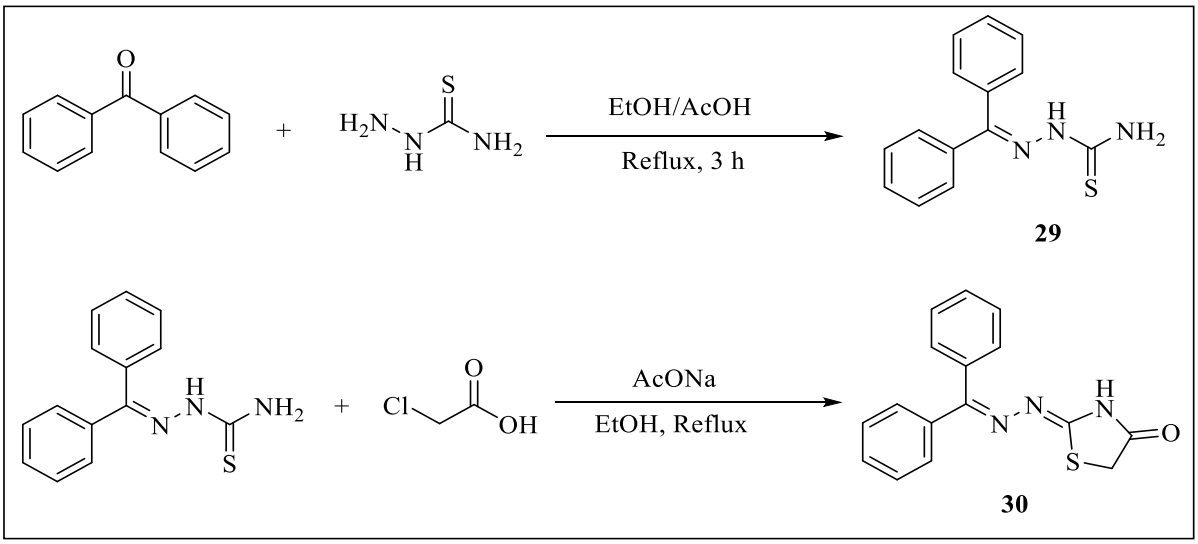

Scheme 20: Synthesis of thiazolidine-4-one from hydrazine carbothioamide and chloroacetic acid.

The reaction between diethyl azodicarboxylate (**32**) and hydrazine carbothioamides **31a-h** is shown in **Scheme 21**. Using a cheap catalyst, the reaction between hydrazine carbothioamide **31a, b** and diethyl azodicarboxylate (**32**) was first carried out in several solvents, including EtOH, CH_3CN, CH_2Cl_2, and AcOEt, to optimise the reaction conditions. However, regrettably, no products were found. Reacting with compound **32** in the presence of triphenylphosphine (Ph_3P) and triethylamine (Et_3N) in absolute ethanol (abs. EtOH) under reflux conditions for six hours, then repeating the reactions of hydrazine carbothioamides (**31a, b**) produced (Z) 2-(substituted imino)-3-(phenylamino) thiazolidin-4-ones (**33a, b**). The remaining reactions involving hydrazine carbothioamides (**31c-h**) and diethyl azodicarboxylate (**32**) under the same circumstances to complete the chain are based on the earlier findings. However, hydrazonothiazolidin-4-ones (**34a-f**), which were unexpected products, were also found (**Scheme 21a**). To enhance the study, another reaction was carried out between substituted hydrazine carbothioamides (**31c-h**) and chloroacetyl chloride (35) in ethyl acetate, catalysed by triethylamine (TEA). In the case of 2-(2,4-dinitrophenyl)-N-substituted hydrazine carbothioamide (**31c-h**), this reaction has produced hydrazonothiazolidinone (**34a-f**). Hydrazine carbothioamide **31b** and **35** interacted to produce (Z)-2-chloro-N-(2-(cyclohexylimino)-4-oxo-thiazolidin-3-yl)-N-phenyacetamide **36** (**Scheme 21b**) [64].

In another research study, using **Scheme 22**, the synthesis of 1,3-thiazolidine-4-one (**39**) was conducted. The initial stage of the synthesis involved the creation of the dithiocarbamate salt (**38**) as described below. Ten millilitres of triethylamine were mixed with 0.1 mole of paratoluidine (**37**). N-Paramethyltoluidine triethylammonium dithiocarbamate (**38**) was then formed by adding 0.11 mole of carbon disulfide. To be employed in the second phase, the resultant solid was cleaned and allowed to dry. At 0°C, the dithiocarbamate salt (**38**) was dissolved in 50 ml of water while being stirred magnetically for an hour. After that, sodium chloroacetate was added. At 0°C, the mixture is mechanically stirred for 15 minutes. To acidify

the medium, concentrated HCl (0.1–0.2 N) was added. At 100°C, the reaction mixture underwent reflux. The title compound **39** yielded a reasonable 65% after the precipitate was filtered off [65]

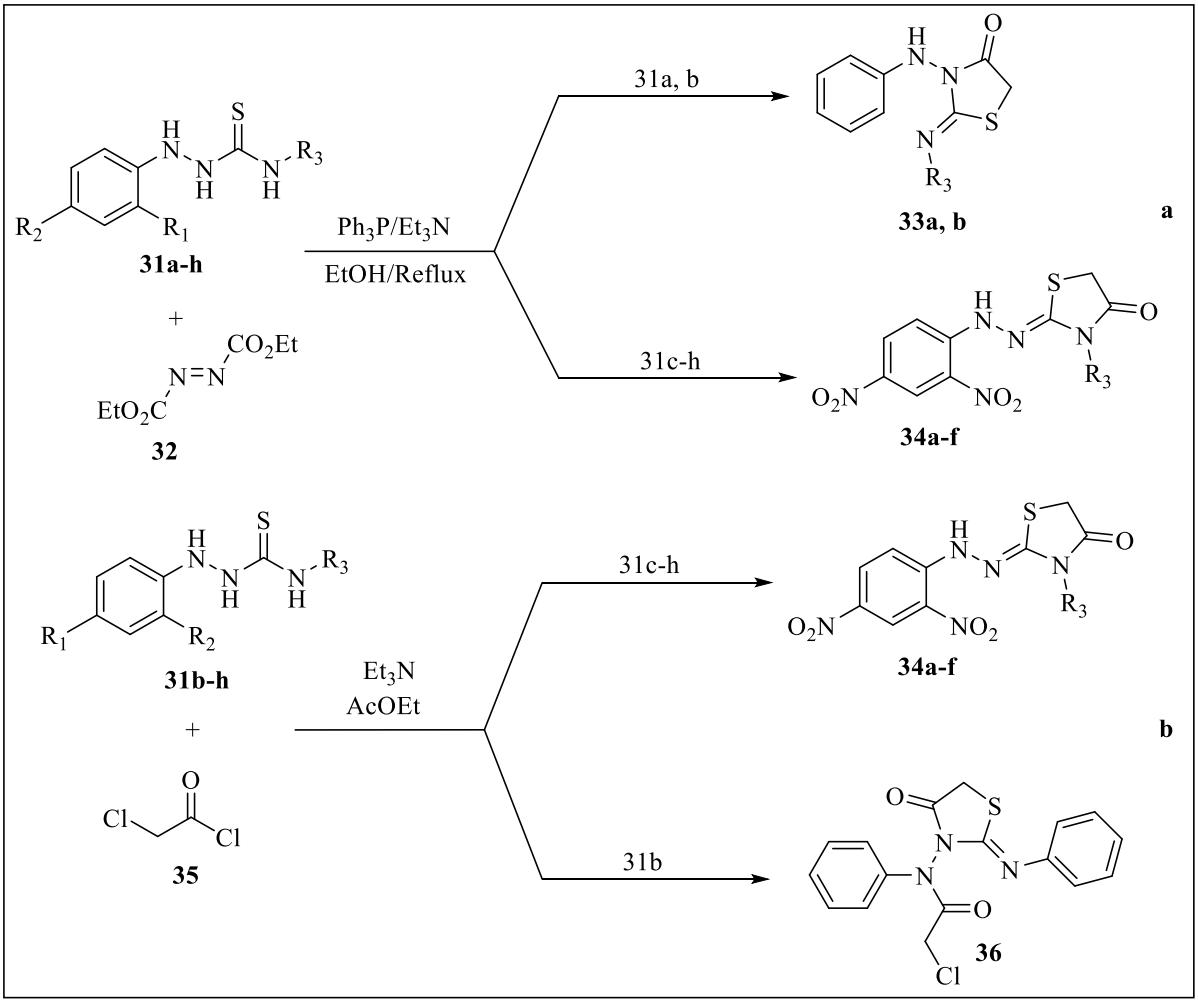

Scheme 21: Synthesis of thiazolidine-4-one by the reaction between hydrazine carbothioamide and diethyl azodicarboxylate/chloroacetyl chloride.

The synthesis of molecular hybrids (**44–57**) based on thiazolidine-4-one and pyrazole was accomplished using the synthetic approach depicted in **Scheme 23**. When 4-substituted arylthioureas (**41a-b**) were condensed with ethyl 2-bromoacetate in glacial acetic acid with sodium acetate as a base, the crucial reactant 2-(p-arylimino) thiazolidin-4-one (**42a-b**) was created. Using piperidine as a base, the resulting product **42a-b** was condensed with 3-(aryl)-

1-phenyl-1H-pyrazole-4-carbaldehyde (**43a-g**) in refluxing ethanol for 10 to 12 hours to obtain thiazolidine-4-one and pyrazole molecular hybrids **44-57** [66].

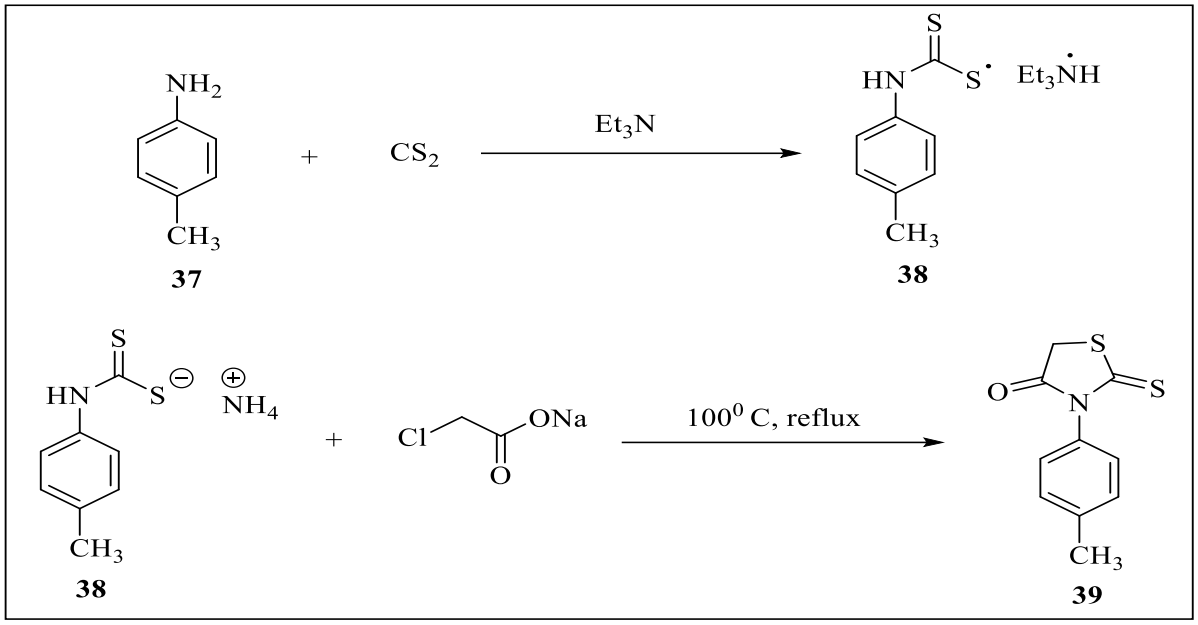

Scheme 22: The reaction of dithiocarbamate salt and sodium chloroacetate to produce thiazolidine-4-one.

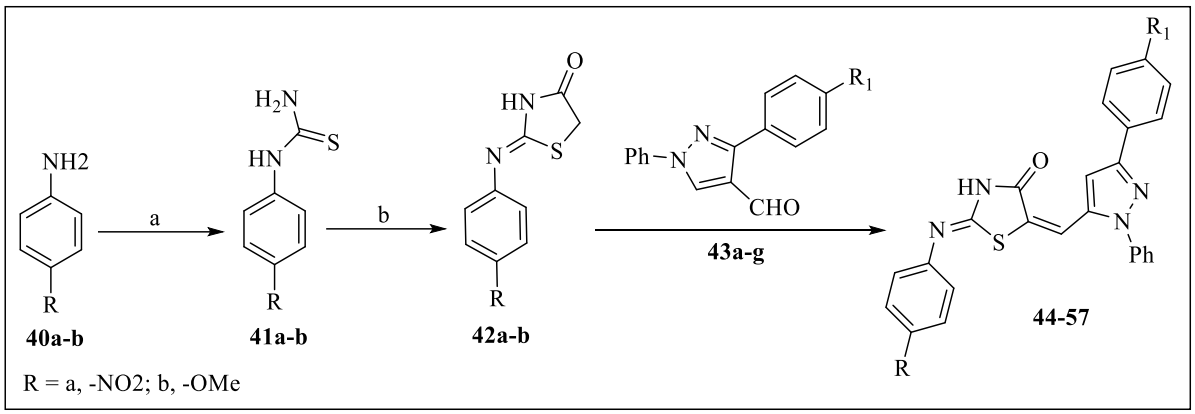

Scheme 23: Synthesis of thiazolidine-4-one from thiourea and ethyl 2-bromoacetate.

The research work of Haque and coresearchers synthesised 4-thiazolidinone **61** in another study, following the protocol available in the literature and depicted in **Scheme 24**. Intermediate compounds 1-cyclopropyl-3-phenyl thiourea (**60**) and 4-thiazolidinone core, i.e., 3-cyclopropyl-2-(phenylimino) thiazolidin-4-one (**61**), were obtained following the reported method [67]. The synthesis of new hybrid spiro[indeno[1,2-b] quinoxaline-[11,2′]-thiazolidine]-4′-ones (**65a-k**) utilizing a multi-component reaction of indeno[1,2-b]

quinoxalinone, α-mercaptocarboxylic acids, and different types of amines with urea-choline chloride as a green deep eutectic solvent and carbon-SO3H as a solid acid catalyst was described in another study (**Scheme 25**). This innovative method yields good to outstanding results in the formation of a thiazolidine ring linked to an indeno[1,2-b] quinoxaline via a spirocarbon. This protocol's benefits include avoiding hazardous and toxic catalysts and solvents, as well as the fact that both the catalyst and DES were quantitatively recovered and reused several times from the reaction mixture [68].

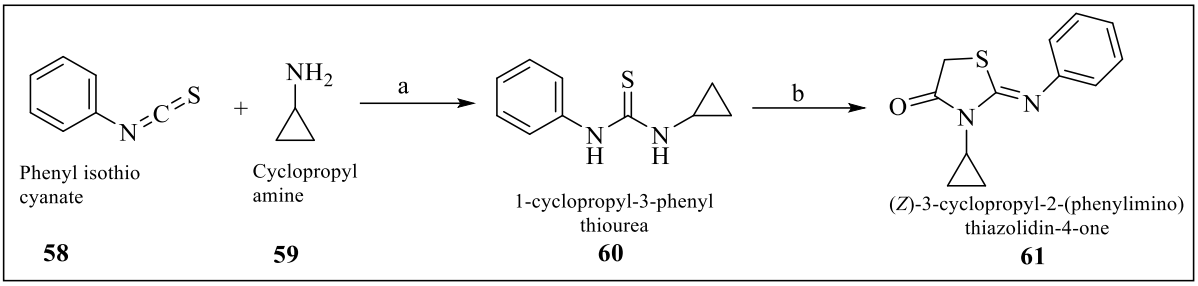

Scheme 24: Synthesis of thiazoline-4-one from thiourea.

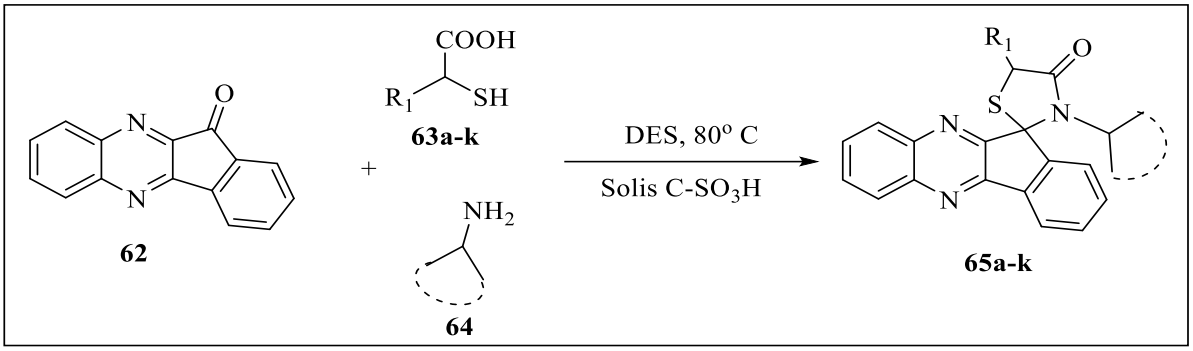

Scheme 12: Synthesis of thiazolidine-4-one using indeno[1,2-b] quinoxalinone, α-mercaptocarboxylic acids, and amines in deep eutectic solvent as a catalyst.

Leila Zare Fekri et al. developed new avenues for the organic synthesis of thiazolidine-4-one using the ionic liquid urazolium acetate as a catalyst. They describe a simple, environmentally friendly, unique, and effective task-specific ionic liquid, urazolium diacetate, for the first time in organic transformations. This liquid is used to create novel thiazolidine-4-ones (**69**) via a three-component reaction involving different aldehydes, thioglycolic acid, and 4-aminoazobenzene (**Scheme 26a**). TSIL urazolium diacetate was initially generated by heating

azole and excess acetic acid to 80 °C for four hours (**Scheme 26b**). To remove any unreacted components, 3 × 10 mL of diethyl ether was used to wash the yellow-orange TSIL [69]. Triphenylphosphine catalyzed the reaction between 3-aroyl-1-arylthioureas and dimethyl but-2-ynedioate in dichloromethane at -5 °C, resulting in (Z)-methyl 2-[(Z)-2-(4-aroylimino)-4-oxo-3-aryl-1,3-thiazolidin-5-ylidene] acetates (**72a-f**) in high quantities. The following procedure (**Scheme 27**) was employed. For four hours, a solution of two was combined with triphenylphosphine at temperatures ranging from –5 °C to 0 °C. After adding N-Aroyl-N'-arylthiourea (**70a–f**) at 0°C, the reaction mixture was agitated for 12–24 hours at room temperature [70].

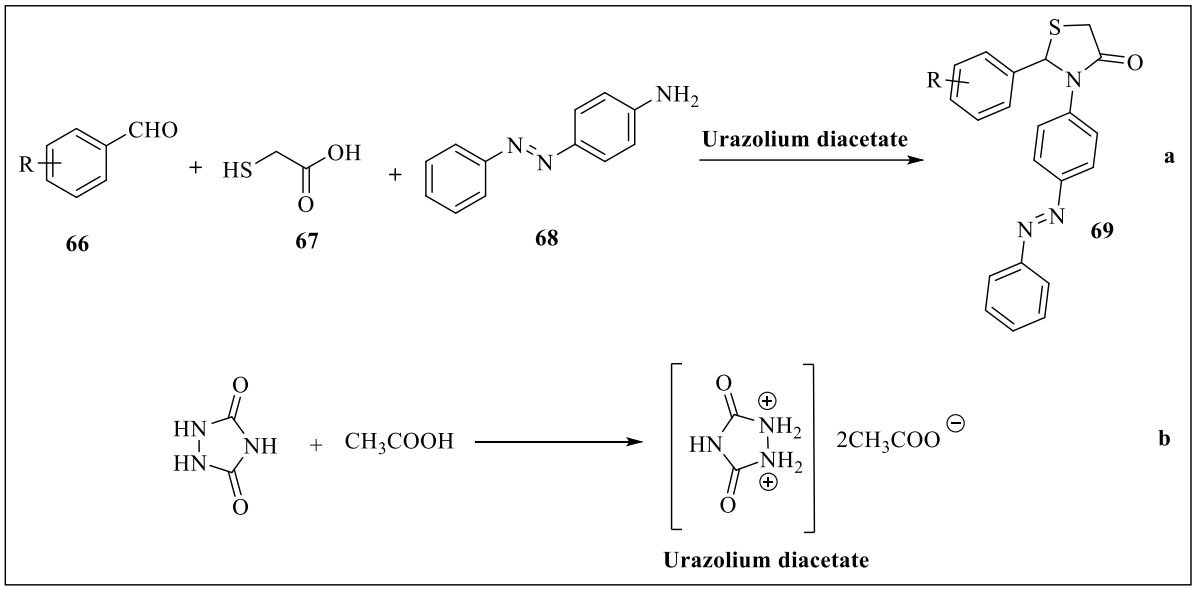

Scheme 26: Synthesis of thiazolidine-4-one by the reaction of aldehyde, amine, and thioglycolic acid using task-specific ionic liquid, urazolium diacetate.

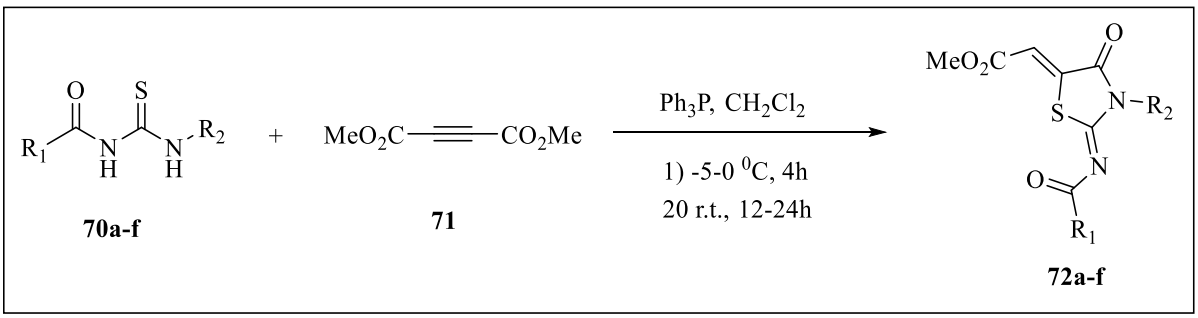

Scheme 27: Synthesis of thiazolidine-4-one from thiourea derivative and acetylene dicarboxylate.

3. Biological Activity of 1,3,4-thiadiazole Derivatives:

Following the discovery of the carbonic anhydrase inhibitor acetazolamide (AAZ), the synthesis and biological activities of numerous 1,3,4-thiadiazoles have been reported. Recent research studies have described the various biological actions of 1,3,4-thiadiazole derivatives, and the most current and pertinent research has shown that these compounds exhibit a wide range of pharmacological activities. To support this research work, the current scenario of developing 1,3,4-thiadiazole molecules as potent antitumor agents has been emphasised [71]. As prospective EGFR inhibitors, five sets of novel 1,3,4-thiadiazole hybrids were designed and prepared. The *in vitro* antiproliferative activity of these hybrid compounds was evaluated using the MTT assay on three human cancer cell lines, viz. breast cancer (MCF-7), liver cancer (HepG-2), and colon cancer (HCT-116). Compound **2** exhibits better cytotoxicity against MCF-7 compared to doxorubicin (IC_{50} = 3.31 μM), while being safe for normal cells, WI-38 (IC_{50} = 43.99 μM). In comparison to the reference compound, gefitinib (IC_{50} = 0.04 μM), compound **1** (IC_{50} = 0.15 μM) and compound **2** (IC_{50} = 0.08 μM) exhibited the most significant EGFR inhibitory action. The subsequent mechanistic investigation of compound **2** revealed significant cell cycle arrest (28.92%) at the G2/M phase and a 14.24-fold increase in total apoptosis. It also activated the mitochondrial apoptotic pathway, as indicated by an apoptosis study. Additionally, it increased the accumulation of reactive oxygen species (ROS) in MCF-7 cells. A molecular docking study was also performed for the most potent EGFR inhibitors, compounds **1** and **2** (**Table 1**), and all of the results were consistent with the biological findings [72]. The biological activities of twelve novel N-[5-(3,5-dichlorophenoxy) methyl]-1,3,4-thiadiazole derivatives were examined in lung cancer cells. The A549 and L929 cell lines were used to evaluate the anticancer properties of the compounds. Compound **4**, even at the lowest tested dose, demonstrated superior action than cisplatin, with strong inhibitory potency (IC_{50}:

<0.98 μg/mL) and selectivity against the A549 cell line. In comparison to cisplatin, compounds **3**, **4**, and **5** (**Table 1**), which had the lowest IC_{50} values, demonstrated a good percentage of apoptosis, ranging from 72.48 to 91.95%. The effects of the aforementioned three drugs on caspase-3 activation and mitochondrial membrane potential were also investigated. Additionally, the matrix metalloproteinase-9 (MMP-9) inhibition capacity of all final compounds was examined; two compounds showed promising activity. These compounds were subjected to molecular docking and molecular dynamics simulation studies to investigate their inhibition of the matrix metalloproteinase-9 (MMP-9) enzyme. The nitrogen atoms of the amide and thiadiazole moieties were found to be important in chelating with Zn metal, while the (thio)ether moieties permit conformational change, which enables the ligand to form more stable contacts [73]. To create multifunctional compounds for the treatment of cancer, two heterocyclic nuclei, 1,2,3-triazole and 1,3,4-thiadiazole, were incorporated to form a set of 1,3,4-thiadiazole analogues. Cell viability test (MTT) was used to evaluate the *in vitro* anticancer activity of the resulting 1,2,3-triazole-1,3,4-thiadiazoles against human cancer cell lines, specifically fibrosarcoma (HT-1080), lung carcinoma (A-549), and breast carcinoma (MCF-7 and MDA-MB-231). The most active heterocycle was compound **6 (Table 1)**, which had cytotoxic activity three times lower than that of the reference drug doxorubicin (6 μM). To clarify the possible modes of action, molecular docking experiments were performed against two antiapoptotic proteins, BCL-2 and BCL-XL. The findings show that compound **6** interacts well with the target proteins via hydrogen bonding, hydrophobic interactions, and electrostatic interactions (binding energy = −7.6 to −9.8 kcal/mol) [74]. Compounds containing an N-(benzimidazol-5-yl)-1,3,4-thiadiazol-2-amine scaffold were developed using a scaffold combination technique, and their ability to block the interleukin-6 (IL-6)/JAK/STAT3 pathway was evaluated in HEK-Blue IL-6 reporter cells. Following optimisation, lead compound **7** (**Table 1**) was identified as a selective STAT3 inhibitor that blocks STAT3 phosphorylation,

translocation, and downstream gene transcription by directly binding to the SH2 domain. Additionally, compound **7** induced cell death and cell cycle arrest, exhibiting antiproliferative effects against STAT3-overexpressed DU145 (IC_{50} value, 2.97 μM) and MDA-MB-231 (IC_{50} value, 3.26 μM) cancer cells. Compound **7** demonstrated *in vivo* anticancer activity after intraperitoneal injection in the DU145 xenograft model, with a tumour growth suppression rate of 65.3% at 50 mg/kg, suggesting potential for further development as an anticancer medicine [75].

MNKs, or mitogen-activated protein kinase-interacting protein kinases, phosphorylate eukaryotic initiation factor 4E (eIF4E) and control the migration and invasion of cancer cells as well as the cell cycle and proliferation. It may be possible to cure tumours by specifically blocking MNK activity. Compound **8** (**Table 1**) of the new MNK inhibitors reported by Xin Jin et al. in this work, which contains an imidazo [2,1-b] [1,3,4] thiadiazole scaffold, effectively suppressed the phosphorylation of eIF4E in a variety of cancer cell lines. Compound **8** showed more effectiveness against MNK2 than MNK1. It also reduced the levels of cyclin-B1, cyclin-D3, and MMP-3 in A549 and MDA-MB-231 cells, inhibited colony formation and cell growth, arrested the cell cycle in the G0/G1 phase, and prevented A549 cells from migrating and secreting TNF-α, MCP-1, and IL-8. It serves as a building block for the development of further inhibitors that specifically target MNKs and are used to treat different illnesses [76]. For the synthesis of 1,3,4-thiadiazole-based molecules, an environmentally friendly and effective technique has been developed. Both conventional and microwave (MW) irradiation techniques were used to create the compounds. All of the novel 1,3,4-thiadiazole compounds were tested against the HepG-2, MCF-7, HCT-116, and PC-3 cancer cell lines. With IC_{50} values ranging from 3.97 to 9.62 μM, the majority of the synthesised compounds demonstrated excellent broad-spectrum cytotoxicity against the tested cancer cell lines. Additionally, five

derivatives showed potent inhibitory effects against VEGFR-2 tyrosine kinase in an enzymatic evaluation. Subsequent research using the DNA/methyl green test demonstrated a substantial DNA-binding affinity of 36.06 μM for compound **9** (**Table 1**). Additionally, a molecular docking investigation was conducted to identify the binding interaction of the compounds with the VEGFR-2 enzyme, revealing a notable inhibitory effect of the derivatives. Lastly, in order to forecast the pharmacokinetics of the synthesised molecules, ADME/Tox experiments were conducted [77].

One possible method of treating cancer is to inhibit angiogenesis. In order to assess the anticancer effectiveness of thieno[2,3-d] pyrimidine-1,3,4-thiadiazole-aryl urea derivatives in the chick chorioallantoic membrane (CAM) experiment, their design, synthesis and biological activity were tested. Compound **10** (**Table 1**) was one of the target compounds with the highest activity against the PC3 prostate cancer cell line (IC_{50} = 3.6 μM). Furthermore, it is presumed that compound **10** may be a viable option for the development of new medications to treat tumours, especially those related to prostate cancer, due to its induction of apoptosis, strong inhibitory activity against the growth of capillary blood vessels, and inhibition of VEGFR-2 phosphorylation [78]. Monika et al. developed and assessed the anti-glioblastoma (GBM) properties of new 1,3,4-thiadiazole derivatives. Both patient-derived GBM cells and all GBM cell lines investigated were significantly cytotoxically affected by the substances under investigation. Compared to temozolomide, the first-line chemotherapeutic treatment for GBM, all molecules were 15–110 times more effective. Interestingly, three of the compounds did not harm human astrocytes at anticancer doses. With IC_{50} values for GBM cells ranging from 45 to 68 μM and for astrocytes over 100 μM, compound **11** seemed to be the most promising molecule. It increased the effectiveness of temozolomide and prevented GBM cells from proliferating, migrating, and invading. Compound **11** treatment reduced the phosphorylation

levels of GSK3β and AKT. Additionally, cells were partially resistant to compound **11-**induced mortality by pretreatment with the AKT activator PDGF-BB, suggesting that the inhibition of the AKT pathway is linked to the compound **11**-promoted reduction in cell viability (**Table 1**) [79]. As new anticancer molecules, several C-3 modified ciprofloxacin derivatives with an N-(5-(benzylthio)-1,3,4-thiadiazol-2-yl)-carboxamide moiety have been developed. In the MTT experiment, the majority of compounds showed notable anticancer action against the tested cancer cell lines (MCF-7, A549, and SKOV-3). Specifically, it was revealed that compounds were just as effective against the MCF-7 cell line as the standard medication doxorubicin (IC_{50} = 3.26–3.90 μM). The ability of two intriguing compounds, **12** and **13**, to induce cell cycle arrest and apoptosis was further investigated. Both compounds were capable of inducing apoptosis in MCF-7 cells, although compound **12** was a more potent inducer of apoptosis, increasing the percentage of apoptotic cells in MCF-7 cells by 18 times at the IC_{50} dose. Compounds **12** and **13** (**Table 1**) may increase cell fractions in the sub-G1 phase, leading to oligonucleosomal DNA fragmentation and cell death, as indicated by the comet test, according to the cell cycle analysis [80].

A new series of 1,3,4-thiadiazole-thiazolone hybrids was developed, characterised, and tested against the basal and microtubule (MT)-stimulated ATPase activity of Eg5. With an IC_{50} value of 13.2 μM against the MT-stimulated Eg5 ATPase activity, compound **14** (**Table 1**) showed the most significant inhibition of the assessed derivatives. The SAR was further validated by an in silico molecular docking study that utilised the crystal structure of Eg5 to elucidate the significance of key molecular protein-ligand interactions in modulating the suppression of Eg5's ATPase activity. The compounds' increased *in vitro* potency was a result of both the crucial molecular interactions and the strength of their electron-withdrawing functions compared to the hybrids. Key pharmacokinetic parameters (ADME) were computationally

determined, and Lipinski's rule of five was applied to assess the drug-like characteristics of the synthetic compounds. As a result, these hybrid compounds are revealed in this study to be new Eg5 inhibitors with intriguing drug-like properties for further research [81]. Derivatives of [1,2,4] triazolo[3,4-b] [1,3,4] thiadiazole have been developed, and their biological activity has been assessed. The majority of these substances exhibited potent anti-c-Met kinase and anti-cell growth properties. The most promising compound, **15**, inhibits c-Met kinase activity and cell proliferation in the MKN45 cell line, with IC_{50} values of 2.02 and 88 nM, respectively. Furthermore, compound **15** shows over 2500-fold selective inhibition (**Table 1**) to 16 tyrosine kinases tested and is highly specific to c-Met kinase [82]. Six 2,5-disubstituted 1,3,4-thiadiazole compounds were created, and their cytotoxic effects on breast cancer cells (MCF-7 and MDA-MB-231) were investigated. The capacity of compounds **16**, **17**, and **18** to decrease the growth of MCF-7 and MDA-MB-231 cells was validated by the MTT test (**Table 1**). The IC_{50} values for the chemicals in question varied from 70 to 170 μM (MDA-MB-231 cells) and from 120 to 160 μM (MCF-7 cells). Furthermore, it was shown that whereas compounds **17** and **18** may stabilise the DNA-topoII cleavage complex and are hence topoII poisons, compound **16** is a human topoisomerase II (topoII) catalytic inhibitor [83]. A number of new indole derivatives were produced by adding 1,3,4-thiadiazole moieties and urea structural fragments. Using four human cancer cell lines (A549, PC-3, K562, and 5637), the antiproliferative activity of these substances was evaluated using the MTT assay. The findings revealed that several compounds possess antiproliferative properties. Compound **19** (**Table 1**), with an IC_{50} value of 9.42 μM, demonstrated encouraging efficacy against K562 cells. The mode of action of compound **19** was further examined through apoptosis studies, which showed its notable capacity to induce cell death [84]. As sorafenib analogues, a new class of 1-(5-(benzylthio)-1,3,4-thiadiazol-2-yl)-3-phenylurea derivatives was produced. Four distinct human cancer cell lines (MCF-7, HepG2, A549, and HeLa) were used to test the *in vitro*

cytotoxicity effects of the developed compounds. The majority of the substances strongly inhibited the growth of the examined cancer cells, as indicated by the biological data. Notably, 2-F, 4-Cl, and 2,6-diF substituted derivatives, i.e. compounds **20, 21, and 22** (**Table 1**) showed encouraging actions, particularly against Hela cancer cells (IC_{50} = 0.37, 0.73, and 0.95 μM), which were noticeably more effective than the reference sorafenib (IC_{50} = 7.91 μM). The prototype compounds (**20, 21, and 22**) strongly induced apoptotic cell death in HeLa cancer cells and arrested the cell cycle in the sub-G1 phase, as determined by flow cytometry analysis. Furthermore, the binding interaction of prototype compounds to the VEGFR-2 active site was validated by an *in silico* docking investigation [85].

Table 1: Literature-reported compounds with 1,3,4-thiadiazole scaffold having antiproliferative activity.

S. No	Compound Structure	Cancer	References
01	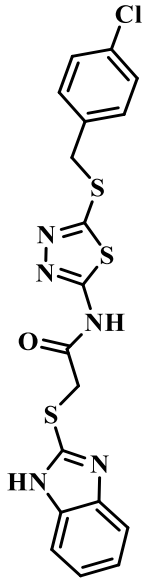 **Cpd 1**	Colon cancer (IC_{50} = 23.48 μM), Hepatocellular cancer (IC_{50} = 17.64 μM), Breast cancer (IC_{50} = 12.27 μM).	[72]

02	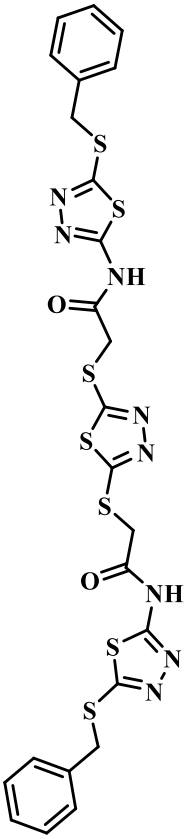 **Cpd 2**	Colon cancer (IC_{50} = 14.54 μM), Hepatocellular cancer (IC_{50} = 5.80 μM), Breast cancer (IC_{50} = 3.31 μM).	
03	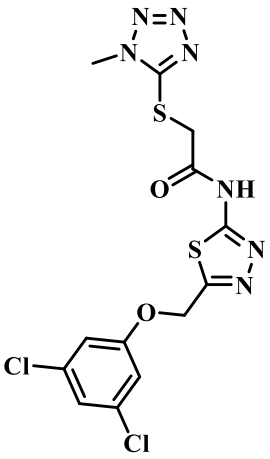 **Cpd 3**	Lung cancer (IC_{50} = 2.93 μg/ml).	[73]

04	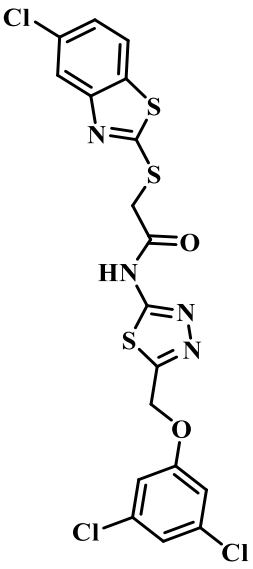 **Cpd 4**	Lung cancer (IC_{50} < 0.98 µg/ml).	
05	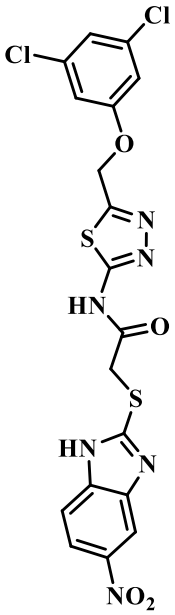 **Cpd 5**	Lung cancer (IC_{50} = 14.67 µg/ml).	

06	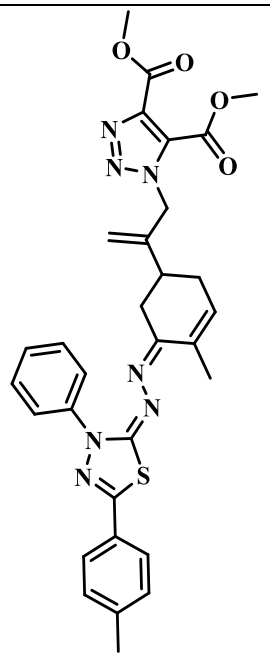 **Cpd 6**	Breast cancer, MCF-7 (IC_{50} = 19.34 μM), MDA-MB-231 (IC_{50} = 21.81 μM).	[74]
07	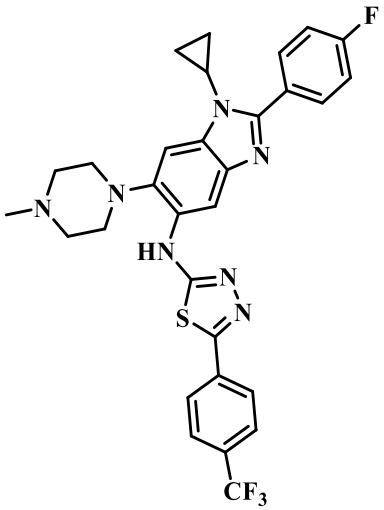 **Cpd 7**	Prostate cancer, DU145 (IC_{50} = 2.97 μM), Breast cancer, MDA-MB-231 (IC_{50} = 3.26 μM).	[75]
08	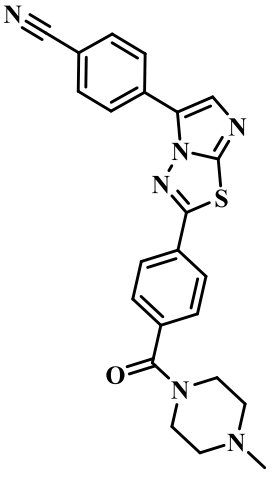 **Cpd 8**	Breast cancer, Lung cancer.	[76]

09	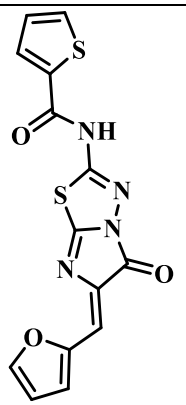 **Cpd 9**	Liver cancer (IC_{50} = 6.8 μM), Breast cancer (IC_{50} = 4.36 μM), Colon cancer (IC_{50} = 5.26 μM), Prostate cancer (IC_{50} = 8.01 μM).	[77]
10	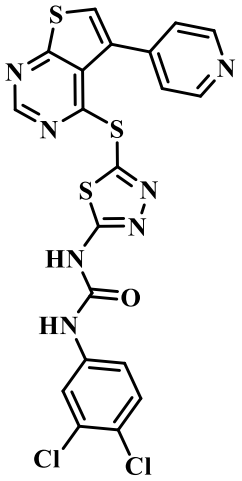 **Cpd 10**	Prostate cancer (IC_{50} = 3.6 μM).	[78]
11	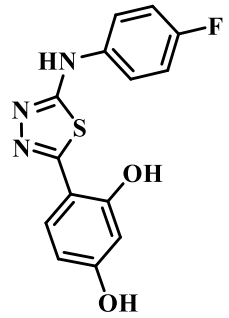 **Cpd 11**	Glioblastoma.	[79]

12	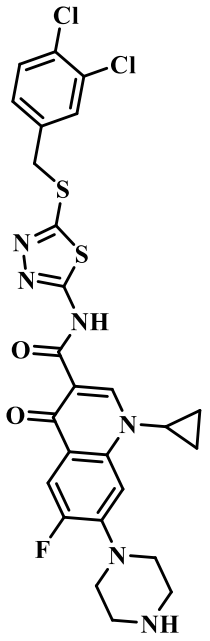 **Cpd 12**	Breast cancer.	[80]
13	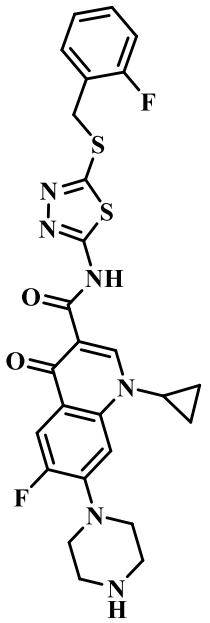 **Cpd 13**	Breast cancer.	

14	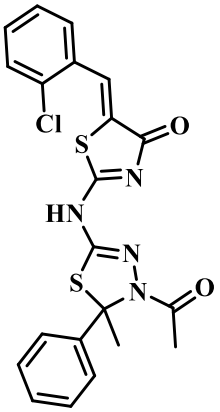 **Cpd 14**	Hepatocellular cancer, Lung cancer, Breast cancer.	[81]
15	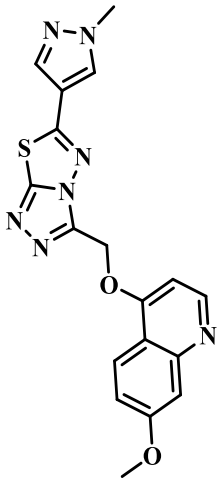 **Cpd 15**	Gastric cancer.	[82]
16	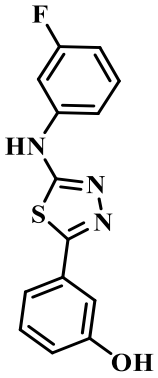 **Cpd 16**	Breast cancer.	[83]
17	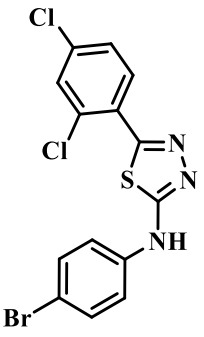 **Cpd 17**	Breast cancer.	

18	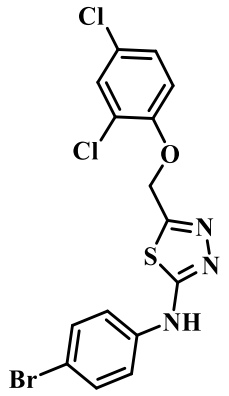 **Cpd 18**	Breast cancer.	
19	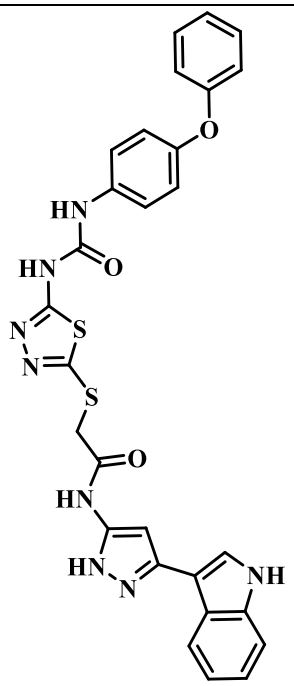 **Cpd 19**	Leukemia (IC_{50} = 9.42 µM).	[84]
20	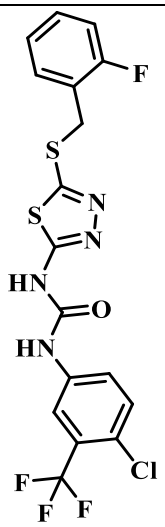 **Cpd 20**	Cervical cancer (IC_{50} = 0.37 µM).	[85]

21	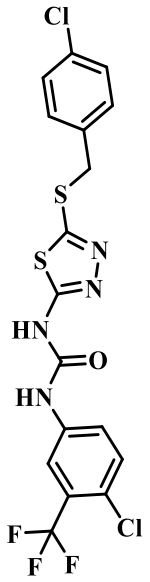 **Cpd 21**	Cervical cancer (IC_{50} = 0.73 μM).	
22	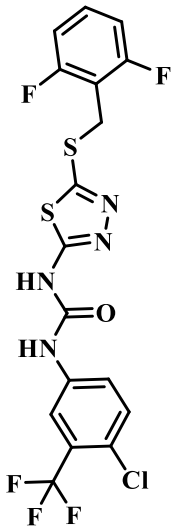 **Cpd 22**	Cervical cancer (IC_{50} = 0.95 μM).	

4. Biological activity of 1,3-thiazolidine-4-one:

In the realm of medicinal chemistry, compounds based on thiazolidinones have garnered significant interest as potential sources of new molecules that resemble existing drugs. The study of 4-thiazolidinone derivatives as antitumour agents has emerged as a possible line of inquiry in recent years [86]. In addition to interacting with various anticancer drugs, these compounds have demonstrated effectiveness against a range of cancer cell lines, including those of melanoma, lung, colon, ovarian, renal, prostate, and breast cancers [87].

Rahaman et al. developed thiazolidine-4-one hybrid molecules having a 4-aminoquinoline moiety and evaluated their anti-inflammatory and anticancer activities. Compound **23** exhibited the most promising anti-inflammatory (IC_{50} = 2.38 μM) and anticancer activity (IC_{50} = 3.26 μM) in the RAW 267.7 cell line and the triple-negative breast cancer (TNBC) cell line, respectively. Further investigation revealed that compound **23** induced G2/M phase cell cycle arrest, ROS generation, and inhibited MDA-MB-231 cell migration, suggesting an anticancer mechanism**.** Additionally, compound **23** possesses anti-inflammatory activity by reducing LPS activity, which is associated with TLR4 and cell activation. SAR study followed by MD simulation showed the binding interaction mechanism of compound **23** with TLR4 **(Table 2)** [88]. New benzenesulfonamide analogues containing 4-thiazolidinone were synthesised in a research work by Belma Zengin Kurt and co-researchers. The compounds were tested for anticancer activity against different cancer cell lines, including HT-29, DLD-1, COLO-205, and CCD-986Sk. Compounds **24** (IC_{50} = 111.06 μM) and **25** (IC_{50} = 62.94 μM) exhibited the highest potency against colorectal cancer cell lines. Compound **24** emerged as a notably promising candidate, exhibiting elevated early apoptotic cell percentages akin to those induced by 5-FU. Molecular docking and molecular dynamics simulations demonstrated that compounds **24** and **25** maintain stable interactions with critical cancer-associated protein targets, notably TGFβ2. These interactions indicate their potential as therapeutic agents. The anticipated ADME parameters further emphasised compounds **24** and **25 (Table 2)** for their advantageous lipophilicity, solubility, permeability, and oral absorption characteristics, reinforcing their potential as candidates for future drug development [89]. A novel series of imidazothiazole derivatives containing a thiazolidinone moiety was designed, synthesised, and assessed for their potential as epidermal growth factor receptor (EGFR) kinase inhibitors, as well as for anticancer activity. Compound **26** inhibited EGFR kinase at a concentration of 18.35 μM, while the standard drug erlotinib exhibited an IC_{50} value of 6.12 μM. Molecular docking,

dynamics simulation, and MM-GBSA binding energy calculations demonstrated a robust interaction between compound **26 (Table 2)** and the EGFR binding site. Compound **26** exhibited the highest cytotoxicity, with IC_{50} values of 10.74 and 18.73 against the A549 and MCF-7 cancer cell lines, respectively. It also promoted apoptosis of the A549 cell line [90]. Through a multi-step synthesis method, Shahjahan et al. developed a variety of oxindoline-containing thiazolidine-4-ones linked triazole hybrids, which were then evaluated for their cytotoxic efficacy against four human cancer cell lines. Liver cancer cells (HepG2) showed a markedly increased vulnerability to the tested compounds. Among them, compounds **27** (IC_{50} = 1.64 μM) and **28** (IC_{50} = 2.07 μM) demonstrated encouraging cytotoxicity against the HepG2 cell line, compared to the reference drug 5-fluorouracil (IC_{50} = 20.8 μM) **(Table 2)**. Subsequently, these compounds altered the shape of HepG2 cells in a dose-dependent manner, dramatically reducing the development of colonies in HepG2 cells. These substances inhibited cell migration and reduced wound size, as indicated by the scratch test. It is noteworthy that they caused cell cycle arrest during the S phase. Additionally, AO/Eb staining revealed a higher number of apoptotic cells at higher dosages, and the DCFDA test demonstrated ROS generation proportional to the dose of the compound. They functioned as antimitotic drugs, inhibiting microtubules, as indicated by the tubulin polymerisation test. This scaffold is a great template and is anticipated to have enormous promise for the development of cancer treatments [91].

Xuwen Chen and co-researchers synthesised thiazolidine-4-one sulfone analogues to develop compounds against osteosarcoma. **Compound 29** exhibited remarkable *in vitro* anticancer activity, as revealed by cell viability (IC_{50} = 0.217 μM) and colony formation assays. Further *in vivo* anticancer studies on the tumour xenograft model using BALB/c mice showed that **compound 29** causes a 44.6% inhibition of osteosarcoma growth. **Compound 7** exhibited a superior pharmacokinetic profile (*in vivo* bioavailability F = 115%, intraperitoneal injection) and a much longer half-life ($T_{1/2}$ = 73.8 min, mouse liver microsome). These findings imply

that **compound 29** may be a viable therapeutic option for osteosarcoma **(Table 2)** [92]. According to the research work of Tawfeek et al, 1,4-disubstituted hydrazine carbothioamide derivatives were reacted with diethyl azodicarboxylate to create new thiazolidine-4-one. The antiproliferative properties of the compounds were evaluated against four human cancer cell lines using the MTT assay. With GI_{50} values ranging from 0.70 µM to 1.20 µM, compounds **30, 31,** and **32** had the most antiproliferative effect in comparison to doxorubicin, which had a GI_{50} value of 1.10 µM. Compounds **31** (IC_{50} = 18 nM) and **32** (IC_{50} = 14 nM) have demonstrated intense inhibitory action against the CDK2 enzyme, outperforming dinaciclib (IC_{50} = 20 nM). Furthermore, when compared to the reference erlotinib (IC_{50} = 70 nM), compounds **31** (IC_{50} = 93 nM) and **32** (IC_{50} = 87 nM) were the most effective EGFR inhibitors, respectively. Furthermore, the apoptotic activity examination indicated that compounds **30, 31,** and **32 (Table 2)** increased the number of active caspases 3, 8, and 9, as well as the cyt-C level, more than doxorubicin. The most effective CDK2 and EGFR inhibitor compounds also had the highest docking score, as determined by a molecular docking study examining the binding sites of these compounds within the active sites of CDK2 and EGFR targets [93].

A unique series of 1,3-thiazolidine-4-ones is synthesised by Nosrat O. Mahmoodi et al. via a cycloaddition reaction between N-aryl-N'-acyl thioureas and acetylenic esters in the absence of solvents and under microwave irradiation. Based on analytical, chemical, and spectral investigations, the structural validity and characterisation of the products were verified. In comparison to a control sample, **compound 33** (IC_{50} = 8.7 µM) exhibited the maximum cytotoxicity against MKN-45 gastric cancer cells in the MTT assay **(Table 2)**. The results suggested that the target-produced thiazolidine-4-ones were found to be toxic in cellular tests, and they may be utilised as potential anticancer agents for MKN-45 gastric adenocarcinoma cells [94]. A number of thiazolidine-4-one urea analogues were synthesised by Baohui Qi et

al., and their anticancer properties were evaluated *in vitro* using various cancer cell lines. Compound **34** was the most effective, with IC_{50} values of 0.65 μM and 0.11 μM against the A549 and HT-29 cancer cell lines, respectively **(Table 2)**. Compound **34** is a multikinase inhibitor that effectively inhibits FLT3 (IC_{50} = 8.6 nM) and VEGFR2 (IC_{50} = 18.7 nM), as indicated by the kinase profile data. Compound **34** demonstrated exceptional cytotoxicity and anti-proliferative activity against HT-29 cancer cells in a time- and dose-dependent manner, which was noticeably more effective than that of Cabozantinib, according to the findings of real-time live-cell imaging. Furthermore, the ability of compound **34** to induce cancer cell death and inhibit cancer cell migration was linked to its *in vitro* anticancer efficacy [95].

A novel series of 2,3-diaryl-1,3-thiazolidin-4-one derivatives has been developed and tested for its ability to inhibit COX enzymes, cytotoxicity, and antioxidant properties. Compound **35**, besides showing antioxidant (IC_{50} = 45.27 μM) and COX-2 (IC_{50} = 0.06 μM) enzyme inhibitory properties, also exhibited the most potent cytotoxic activity (IC_{50} = 2.31 μM) on HepG2 cell lines. Additionally, anticancer mechanistic studies revealed that compound **35** induces significant apoptosis and cell cycle arrest in the G1 phase of HePG2 cancer cells. These biological findings could also suggest a role that COX-2 inhibition plays in the antiproliferative properties of these compounds. The findings of the *in vitro* COX-2 inhibition test were consistent with the molecular docking results for compound **35 (Table 2)** into the COX-2 active site [96]. A combination of aryl thiosemicarbazone and β-aroylacrylic acid was refluxed to produce thiazolidin-4-one derivatives, which were then characterised using ^{1}H NMR and IR spectroscopy. The SwissADME online tool was used to evaluate pharmacokinetic characteristics and physicochemical descriptors in silico. Additionally, synthesised compounds were subjected to docking experiments to investigate their binding to p53 (PDB: 6MXZ) and cyclooxygenase-2 (COX-2) (PDB: 5IKT). The *in vitro* cytotoxic effects of several compounds against the Caco-2 cell line were assessed. **Compound 36** had the highest impact of all the

compounds tested, with an IC_{50} of 70 µg/ml **(Table 2)**. Moreover, reduced expression of the p53 and caspase-3 genes was observed for the compounds, indicating that they have antitumor effects [97].

The potential therapeutic benefits of combining tubulin-targeting anticancer drugs with selective COX-2 inhibitors have been suggested by several studies. The pharmacophoric characteristics of many COX inhibitors and tubulin polymerisation inhibitors were combined in the present investigation to create a new series of thiazolidin-4-one derivatives. The cytotoxic activity of the compounds against the MCF7, HT29, and A2780 cancer cell lines was assessed (IC_{50} = 0.02–17.02 µM). Additionally, the compounds' cytotoxicity was evaluated against normal MRC5 cells (IC_{50} = 0.47–13.46 µM). The most active compounds, **37, 38,** and **39,** significantly reduced the number of HT29 colonies compared to the control. In Ehrlich solid carcinoma-bearing mice, compounds **37, 38,** and **39 (Table 2)** also considerably reduced tumour masses and volumes compared to the control. In the wound-healing test, the three substances likewise showed intense anti-HT29 migration action. Additionally, they have caused cell cycle arrest by inhibiting HT-29 cells throughout the S and G2/M phases. Additionally, when HT29 cells were compared to the control, compounds showed a significant increase in both early and late apoptotic events, with compound **39** having the most critical impact. In contrast to colchicine (3 µM), compound **39** (1 µM) showed little inhibitory effect against tubulin polymerisation. However, compared to celecoxib (IC_{50} = 0.86 µM), all compounds reduced the activity of COX-2 (IC_{50} = 0.42–29.11 µM). Compounds **37**, **38**, and **39** exhibit larger binding free energies to COX-2 than to COX-1, as revealed from molecular docking research. According to the findings above, **compound 39** may be a viable option for developing anticancer medication [98].

Table 2: Literature-reported 1,3-thiazolidine-4-one derivatives having anticancer potency.

S. No.	Compound Structure	Cancer	Reference
01	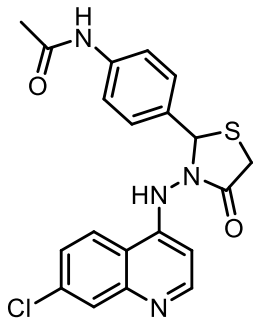 **Cpd 23**	Leukaemia (IC_{50} = 2.38 µM), Breast cancer (IC_{50} = 3.26 µM).	[88]
02	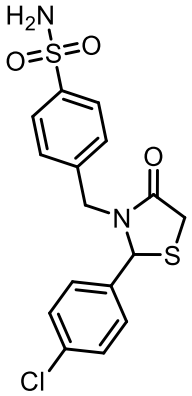 **Cpd 24**	Colon cancer (IC_{50} = 111.06 µM).	[89]
03	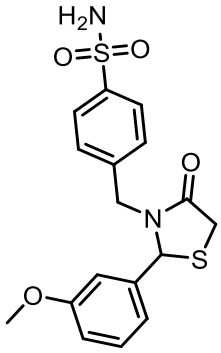 **Cpd 25**	Colon cancer (IC_{50} = 62.94 µM).	
04	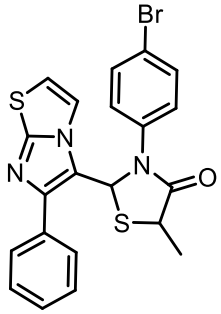 **Cpd 26**	Lung cancer (IC_{50} = 10.74 µM), Breast cancer (IC_{50} = 18.73 µM)	[90]

05	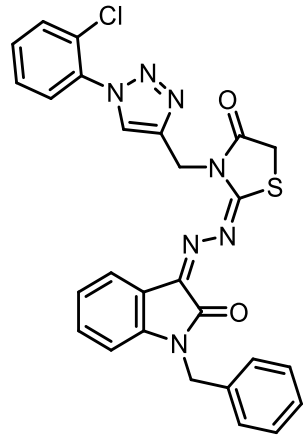 **Cpd 27**	Hepatocellular cancer (IC_{50} = 1.64 μM).	[91]
06	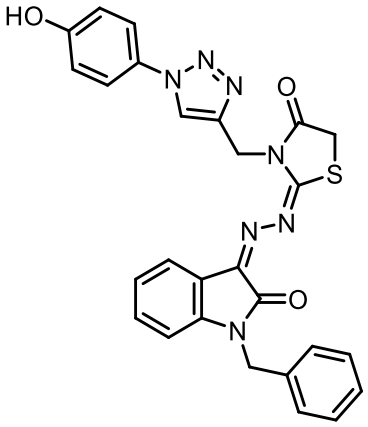 **Cpd 28**	Hepatocellular cancer (IC_{50} = 2.07 μM).	
07	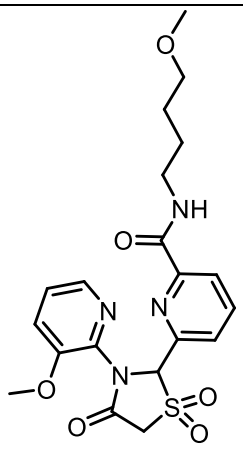 **Cpd 29**	Osteosarcoma (IC_{50} = 0.217 μM).	[92]

08	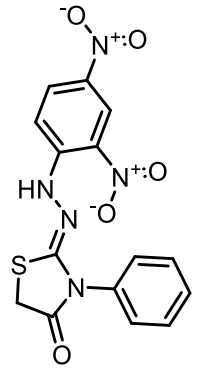 **Cpd 30**	Breast cancer (IC_{50} = 1.05 μM).	[93]
09	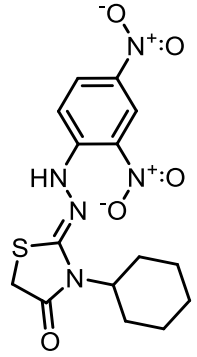 **Cpd 31**	Breast cancer (IC_{50} = 0.80 μM).	
10	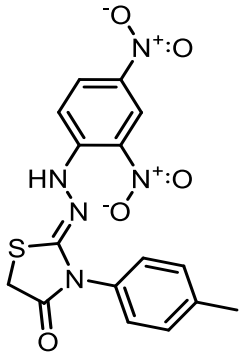 **Cpd 32**	Breast cancer (IC_{50} = 0.70 μM).	
11	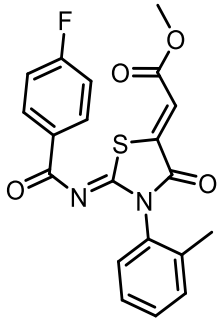 **Cpd 33**	Gastric cancer (IC_{50} = 8.7 μM).	[94]

12	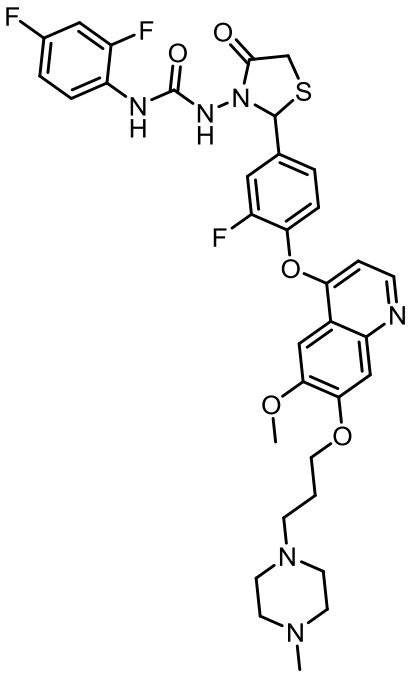 **Cpd 34**	Lung cancer (IC_{50} = 0.65 µM), Colorectal cancer (IC_{50} = 0.11 µM).	[95]
13	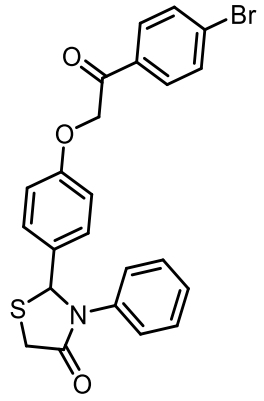 **Cpd 35**	Hepatocellular cancer (IC_{50} = 2.31 µM).	[96]
14	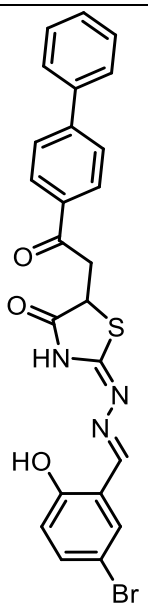 **Cpd 36**	Colon cancer (IC_{50} = 70 µg/ml).	[97]

15	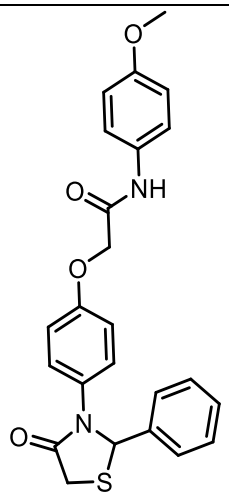 **Cpd 37**	Colon cancer	[98]
16	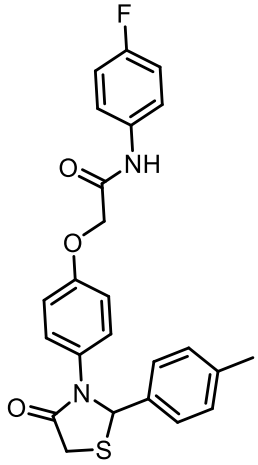 **Cpd 38**	Colon cancer	
17	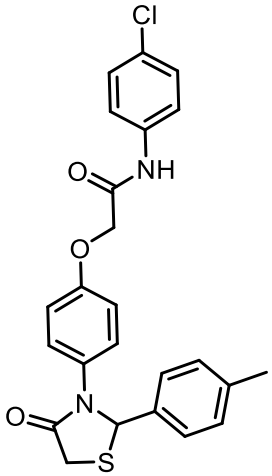 **Cpd 39**	Colon cancer	

References:

[1] Y. Hu, C.-Y. Li, X.-M. Wang, Y.-H. Yang, H.-L. Zhu, 1,3,4-Thiadiazole: Synthesis, Reactions, and Applications in Medicinal, Agricultural, and Materials Chemistry, Chem Rev 114 (2014) 5572–5610. https://doi.org/10.1021/cr400131u.

[2] M. Saitoh, J. Kunitomo, E. Kimura, H. Iwashita, Y. Uno, T. Onishi, N. Uchiyama, T. Kawamoto, T. Tanaka, C.D. Mol, D.R. Dougan, G.P. Textor, G.P. Snell, M. Takizawa, F. Itoh, M. Kori, 2-{3-[4-(Alkylsulfinyl)phenyl]-1-benzofuran-5-yl}-5-methyl-1,3,4-oxadiazole Derivatives as Novel Inhibitors of Glycogen Synthase Kinase-3β with Good Brain Permeability, J Med Chem 52 (2009) 6270–6286. https://doi.org/10.1021/jm900647e.

[3] Z. Kaleta, B.T. Makowski, T. Soós, R. Dembinski, Thionation Using Fluorous Lawesson's Reagent, Org Lett 8 (2006) 1625–1628. https://doi.org/10.1021/ol060208a.

[4] J. Garfunkle, C. Ezzili, T.J. Rayl, D.G. Hochstatter, I. Hwang, D.L. Boger, Optimization of the Central Heterocycle of α-Ketoheterocycle Inhibitors of Fatty Acid Amide Hydrolase, J Med Chem 51 (2008) 4392–4403. https://doi.org/10.1021/jm800136b.

[5] J.K. Augustine, V. Vairaperumal, S. Narasimhan, P. Alagarsamy, A. Radhakrishnan, Propylphosphonic anhydride (T3P®): an efficient reagent for the one-pot synthesis of 1,2,4-oxadiazoles, 1,3,4-oxadiazoles, and 1,3,4-thiadiazoles, Tetrahedron 65 (2009) 9989–9996. https://doi.org/10.1016/j.tet.2009.09.114.

[6] V. Polshettiwar, R.S. Varma, Greener and rapid access to bio-active heterocycles: one-pot solvent-free synthesis of 1,3,4-oxadiazoles and 1,3,4-thiadiazoles, Tetrahedron Lett 49 (2008) 879–883. https://doi.org/10.1016/j.tetlet.2007.11.165.

[7] G. Rai, N. Joshi, J.E. Jung, Y. Liu, L. Schultz, A. Yasgar, S. Perry, G. Diaz, Q. Zhang, V. Kenyon, A. Jadhav, A. Simeonov, E.H. Lo, K. van Leyen, D.J. Maloney, T.R. Holman, Potent and Selective Inhibitors of Human Reticulocyte 12/15-Lipoxygenase as Anti-Stroke Therapies, J Med Chem 57 (2014) 4035–4048. https://doi.org/10.1021/jm401915r.

[8] V. Padmavathi, P. Thriveni, B.J.M. Reddy, A. Padmaja, Synthesis of thiadiazoles, triazoles and oxadiazoles from sulfonyl acetic acids *via* a common route, J Heterocycl Chem 42 (2005) 113–116. https://doi.org/10.1002/jhet.5570420116.

[9] U. Salgın-Gökşen, N. Gökhan-Kelekçi, Ö. Göktaş, Y. Köysal, E. Kılıç, Ş. Işık, G. Aktay, M. Özalp, 1-Acylthiosemicarbazides, 1,2,4-triazole-5(4H)-thiones, 1,3,4-thiadiazoles and hydrazones containing 5-methyl-2-benzoxazolinones: Synthesis, analgesic-anti-inflammatory and antimicrobial activities, Bioorg Med Chem 15 (2007) 5738–5751. https://doi.org/10.1016/j.bmc.2007.06.006.

[10] F. Aryanasab, A.Z. Halimehjani, M.R. Saidi, Dithiocarbamate as an efficient intermediate for the synthesis of 2-amino-1,3,4-thiadiazoles in water, Tetrahedron Lett 51 (2010) 790–792. https://doi.org/10.1016/j.tetlet.2009.11.100.

[11] K. Matsuno, Y. Masuda, Y. Uehara, H. Sato, A. Muroya, O. Takahashi, T. Yokotagawa, T. Furuya, T. Okawara, M. Otsuka, N. Ogo, T. Ashizawa, C. Oshita, S. Tai, H. Ishii, Y. Akiyama, A. Asai, Identification of a New Series of STAT3 Inhibitors by Virtual Screening, ACS Med Chem Lett 1 (2010) 371–375. https://doi.org/10.1021/ml1000273.

[12] J. Mirzaei, H. Pirelahi, M. Amini, A. Shafiee, Convenient syntheses of 5-[(2-methyl-5-nitro-1 *H* -imidazol-1-yl)methyl]-1,3,4-oxadiazole-2(3 *H*)thione and N-substituted 2-amino-5-[(2-methyl-5-nitro-1 *H* -imidazol-1-yl)methyl]-1,3,4-thiadiazoles, J Heterocycl Chem 45 (2008) 921–925. https://doi.org/10.1002/jhet.5570450343.

[13] B.G. Szczepankiewicz, G. Liu, H.-S. Jae, A.S. Tasker, I.W. Gunawardana, T.W. von Geldern, S.L. Gwaltney, J.R. Wu-Wong, L. Gehrke, W.J. Chiou, R.B. Credo, J.D. Alder, M.A. Nukkala, N.A. Zielinski, K. Jarvis, K.W. Mollison, D.J. Frost, J.L. Bauch, Y.H. Hui, A.K. Claiborne, Q. Li, S.H. Rosenberg, New Antimitotic Agents with Activity in Multi-Drug-Resistant Cell Lines and in Vivo Efficacy in Murine Tumor Models, J Med Chem 44 (2001) 4416–4430. https://doi.org/10.1021/jm010231w.

[14] A.R. Angeles, L. Yang, C. Dai, A. Brunskill, A.D. Basso, M.A. Siddiqui, Synthesis, determination of absolute configuration, and biological evaluation of spiro-fused thiadiazoline inhibitors of kinesin spindle protein (KSP), Tetrahedron Lett 51 (2010) 6236–6239. https://doi.org/10.1016/j.tetlet.2010.09.066.

[15] Y. Zuo, S.-G. Yang, L.-L. Jiang, G.-F. Hao, Z.-F. Wang, Q.-Y. Wu, Z. Xi, G.-F. Yang, Quantitative structure–activity relationships of 1,3,4-thiadiazol-2(3H)-ones and 1,3,4-oxadiazol-2(3H)-ones as human protoporphyrinogen oxidase inhibitors, Bioorg Med Chem 20 (2012) 296–304. https://doi.org/10.1016/j.bmc.2011.10.079.

[16] S.A.S. Ghozlan, M.A. Al-Omar, A.E.E. Amr, K.A. Ali, A.A.A. El-Wahab, Synthesis and antimicrobial activity of some heterocyclic 2,6-bis(substituted)-1,3,4-thiadiazolo-, oxadiazolo-, and oxathiazolidino-pyridine derivatives from 2,6-pyridine dicarboxylic acid dihydrazide, J Heterocycl Chem 48 (2011) 1103–1110. https://doi.org/10.1002/jhet.690.

[17] C.-T. Liao, Y.-J. Wang, C.-S. Huang, H.-S. Sheu, G.-H. Lee, C.K. Lai, New metallomesogens derived from unsymmetric 1,3,4-thiodiazoles: synthesis, single crystal structure, mesomorphism, and optical properties, Tetrahedron 63 (2007) 12437–12445. https://doi.org/10.1016/j.tet.2007.09.031.

[18] D. Kumar, N. Maruthi Kumar, K.-H. Chang, K. Shah, Synthesis and anticancer activity of 5-(3-indolyl)-1,3,4-thiadiazoles, Eur J Med Chem 45 (2010) 4664–4668. https://doi.org/10.1016/j.ejmech.2010.07.023.

[19] A.A. Kiryanov, P. Sampson, A.J. Seed, Synthesis of 2-Alkoxy-Substituted Thiophenes, 1,3-Thiazoles, and Related S-Heterocycles via Lawesson's Reagent-Mediated Cyclization under Microwave Irradiation: Applications for Liquid Crystal Synthesis, J Org Chem 66 (2001) 7925–7929. https://doi.org/10.1021/jo016063x.

[20] A.W. Schüttelkopf, L. Gros, D.E. Blair, J.A. Frearson, D.M.F. van Aalten, I.H. Gilbert, Acetazolamide-based fungal chitinase inhibitors, Bioorg Med Chem 18 (2010) 8334–8340. https://doi.org/10.1016/j.bmc.2010.09.062.

[21] H. Rajak, A. Agarawal, P. Parmar, B.S. Thakur, R. Veerasamy, P.C. Sharma, M.D. Kharya, 2,5-Disubstituted-1,3,4-oxadiazoles/thiadiazole as surface recognition moiety: Design and synthesis of novel hydroxamic acid based histone deacetylase inhibitors, Bioorg Med Chem Lett 21 (2011) 5735–5738. https://doi.org/10.1016/j.bmcl.2011.08.022.

[22] G. Tu, S. Li, H. Huang, G. Li, F. Xiong, X. Mai, H. Zhu, B. Kuang, W.F. Xu, Novel aminopeptidase N inhibitors derived from 1,3,4-thiadiazole scaffold, Bioorg Med Chem 16 (2008) 6663–6668. https://doi.org/10.1016/j.bmc.2008.05.081.

[23] M.A. Hilfiker, N. Wang, X. Hou, Z. Du, M.A. Pullen, M. Nord, R. Nagilla, H.E. Fries, C.W. Wu, A.C. Sulpizio, J.-P. Jaworski, D. Morrow, R.M. Edwards, J. Jin, Discovery of novel aminothiadiazole amides as selective EP3 receptor antagonists, Bioorg Med Chem Lett 19 (2009) 4292–4295. https://doi.org/10.1016/j.bmcl.2009.05.074.

[24] S. Ferrari, F. Morandi, D. Motiejunas, E. Nerini, S. Henrich, R. Luciani, A. Venturelli, S. Lazzari, S. Calò, S. Gupta, V. Hannaert, P.A.M. Michels, R.C. Wade, M.P. Costi, Virtual Screening Identification of Nonfolate Compounds, Including a CNS Drug, as Antiparasitic Agents Inhibiting Pteridine Reductase, J Med Chem 54 (2011) 211–221. https://doi.org/10.1021/jm1010572.

[25] A. Foroumadi, Z. Kiani, F. Soltani, Antituberculosis agents VIII, Il Farmaco 58 (2003) 1073–1076. https://doi.org/10.1016/S0014-827X(03)00158-7.

[26] A. Foroumadi, A. Asadipour, M. Mirzaei, J. Karimi, S. Emami, Antituberculosis agents. V. Synthesis, evaluation of in vitro antituberculosis activity and cytotoxicity of some 2-(5-nitro-2-furyl)-1,3,4- thiadiazole derivatives, Il Farmaco 57 (2002) 765–769. https://doi.org/10.1016/S0014-827X(02)01277-6.

[27] S.G. Alegaon, K.R. Alagawadi, P. V. Sonkusare, S.M. Chaudhary, D.H. Dadwe, A.S. Shah, Novel imidazo[2,1-b][1,3,4]thiadiazole carrying rhodanine-3-acetic acid as potential antitubercular agents, Bioorg Med Chem Lett 22 (2012) 1917–1921. https://doi.org/10.1016/j.bmcl.2012.01.052.

[28] V. Jatav, P. Mishra, S. Kashaw, J.P. Stables, CNS depressant and anticonvulsant activities of some novel 3-[5-substituted 1,3,4-thiadiazole-2-yl]-2-styryl quinazoline-4(3H)-ones, Eur J Med Chem 43 (2008) 1945–1954. https://doi.org/10.1016/j.ejmech.2007.12.003.

[29] V. Jatav, S. Kashaw, P. Mishra, Synthesis, antibacterial and antifungal activity of some novel 3-[5-(4-substituted phenyl) 1,3,4-thiadiazole-2-yl]-2-styryl quinazoline-4(3H)-ones, Medicinal Chemistry Research 17 (2008) 169–181. https://doi.org/10.1007/s00044-007-9047-2.

[30] H. Kumar, S.A. Javed, S.A. Khan, M. Amir, 1,3,4-Oxadiazole/thiadiazole and 1,2,4-triazole derivatives of biphenyl-4-yloxy acetic acid: Synthesis and preliminary

evaluation of biological properties, Eur J Med Chem 43 (2008) 2688–2698. https://doi.org/10.1016/j.ejmech.2008.01.039.

[31] U. Salgın-Gökşen, N. Gökhan-Kelekçi, Ö. Göktaş, Y. Köysal, E. Kılıç, Ş. Işık, G. Aktay, M. Özalp, 1-Acylthiosemicarbazides, 1,2,4-triazole-5(4H)-thiones, 1,3,4-thiadiazoles and hydrazones containing 5-methyl-2-benzoxazolinones: Synthesis, analgesic-anti-inflammatory and antimicrobial activities, Bioorg Med Chem 15 (2007) 5738–5751. https://doi.org/10.1016/j.bmc.2007.06.006.

[32] M.A. Epishina, A.S. Kulikov, N. V. Ignat'ev, M. Schulte, N.N. Makhova, Synthesis of 5-alkyl-2-amino-1,3,4-thiadiazoles and α,ω-bis(2-amino-1,3,4-thiadiazol-5-yl)alkanes in ionic liquids, Mendeleev Communications 21 (2011) 331–333. https://doi.org/10.1016/j.mencom.2011.11.013.

[33] M.E. Layton, M.J. Kelly, K.J. Rodzinak, P.E. Sanderson, S.D. Young, R.A. Bednar, A.G. DiLella, T.P. Mcdonald, H. Wang, S.D. Mosser, J.F. Fay, M.E. Cunningham, D.R. Reiss, C. Fandozzi, N. Trainor, A. Liang, E. V. Lis, G.R. Seabrook, M.O. Urban, J. Yergey, K.S. Koblan, Discovery of 3-Substituted Aminocyclopentanes as Potent and Orally Bioavailable NR2B Subtype-Selective NMDA Antagonists, ACS Chem Neurosci 2 (2011) 352–362. https://doi.org/10.1021/cn200013d.

[34] M.A. Kukaniev, M.D. Osimov, Z.G. Sangov, S.S. Safarov, M.B. Karimov, T.R. Radjabov, Polyfunctional nitriles in the synthesis of derivatives of 1,3,4-thiadiazolo-[3,2-a]pyrimidines, Chem Heterocycl Compd (N Y) 44 (2008) 882–885. https://doi.org/10.1007/s10593-008-0125-2.

[35] R.F. Rodrigues, D. Castro-Pinto, A. Echevarria, C.M. dos Reis, C.N. Del Cistia, C.M.R. Sant'Anna, F. Teixeira, H. Castro, M. Canto-Cavalheiro, L.L. Leon, A. Tomás, Investigation of trypanothione reductase inhibitory activity by 1,3,4-thiadiazolium-2-aminide derivatives and molecular docking studies, Bioorg Med Chem 20 (2012) 1760–1766. https://doi.org/10.1016/j.bmc.2012.01.009.

[36] G. Mloston, R. Huisgen, Acid–base reactions of adamantanethione S -methylide and its spiro-1,3,4-thiadiazoline precursor, Tetrahedron 57 (2001) 145–151. https://doi.org/10.1016/S0040-4020(00)00988-1.

[37] A. do R.A. Pires, M.B.M. de Oliveira, A. Echevarria, E.F. Silva, M.E.M. Rocha, E.G.S. Carnieri, G.R. Martinez, G.R. Noleto, S.M.S.C. Cadena, Comparative study of the effects of 1,3,4-thiadiazolium mesoionic derivatives on energy-linked functions of rat liver mitochondria, Chem Biol Interact 186 (2010) 1–8. https://doi.org/10.1016/j.cbi.2010.04.001.

[38] E. DASILVA, M. CANTOCAVALHEIRO, V. BRAZ, L. CYSNEFINKELSTEIN, L. LEON, A. ECHEVARRIA, Synthesis, and biological evaluation of new 1,3,4-thiadiazolium-2-phenylamine derivatives against promastigotes and amastigotes, Eur J Med Chem 37 (2002) 979–984. https://doi.org/10.1016/S0223-5234(02)01401-0.

[39] M. Yusuf, R.A. Khan, B. Ahmed, Syntheses and anti-depressant activity of 5-amino-1, 3, 4-thiadiazole-2-thiol imines and thiobenzyl derivatives, Bioorg Med Chem 16 (2008) 8029–8034. https://doi.org/10.1016/j.bmc.2008.07.056.

[40] M.K. Abdel-Hamid, A.A. Abdel-Hafez, N.A. El-Koussi, N.M. Mahfouz, A. Innocenti, C.T. Supuran, Design, synthesis, and docking studies of new 1,3,4-thiadiazole-2-thione derivatives with carbonic anhydrase inhibitory activity, Bioorg Med Chem 15 (2007) 6975–6984. https://doi.org/10.1016/j.bmc.2007.07.044.

[41] A.R. Sayed, Synthesis of novel thiadiazoles and bis-thiadiazoles from carbonothioic dihydrazide, Tetrahedron Lett 51 (2010) 4490–4493. https://doi.org/10.1016/j.tetlet.2010.06.060.

[42] A.S. Shawali, A.R. Sayed, Tandem regioselective 1,5-electrocyclizations of *bis* -nitrilimines—a new convenient synthesis of 1,2,4-triazolo[3,4-b][1,3,4]thiadiazoles, Journal of Sulfur Chemistry 27 (2006) 233–244. https://doi.org/10.1080/17415990600649193.

[43] A. Sami Shawali, A.R. Sayed, A new convenient synthesis of alditol C-glycosides of 1,2,4-triazolo[3,4-b][1,3,4]thiadiazole, Journal of Sulfur Chemistry 28 (2007) 23–29. https://doi.org/10.1080/17415990601101020.

[44] Z. Li, X. Feng, Y. Zhao, Microwave induced efficient synthesis of (un)substituted benzaldehyde (5-aryl-1,3,4-thiadiazol-2-yl)hydrazones using silica-supported dichlorophosphate as a recoverable dehydrant, J Heterocycl Chem 45 (2008) 1489–1492. https://doi.org/10.1002/jhet.5570450540.

[45] A.A. Kadi, E.S. Al-Abdullah, I.A. Shehata, E.E. Habib, T.M. Ibrahim, A.A. El-Emam, Synthesis, antimicrobial and anti-inflammatory activities of novel 5-(1-adamantyl)-1,3,4-thiadiazole derivatives, Eur J Med Chem 45 (2010) 5006–5011. https://doi.org/10.1016/j.ejmech.2010.08.007.

[46] M.-X. Wei, L. Feng, X.-Q. Li, X.-Z. Zhou, Z.-H. Shao, Synthesis of new chiral 2,5-disubstituted 1,3,4-thiadiazoles possessing γ-butenolide moiety and preliminary evaluation of in vitro anticancer activity, Eur J Med Chem 44 (2009) 3340–3344. https://doi.org/10.1016/j.ejmech.2009.03.023.

[47] T. Wang, W. Miao, S. Wu, G. Bing, X. Zhang, Z. Qin, H. Yu, X. Qin, J. Fang, Synthesis, Crystal Structure, and Herbicidal Activities of 2-Cyanoacrylates Containing 1,3,4-Thiadiazole Moieties, Chin J Chem 29 (2011) 959–967. https://doi.org/10.1002/cjoc.201190196.

[48] Y.-D. Gong, T. Lee, Combinatorial Syntheses of Five-Membered Ring Heterocycles Using Carbon Disulfide and a Solid Support, J Comb Chem 12 (2010) 393–409. https://doi.org/10.1021/cc100049u.

[49] J.M. Farrar, M.K. Patel, P. Kaszynski, V.G. Young, A New Thiatriazine Isomer: Synthesis, Tautomerism, and Molecular Structure of 3,6-Diphenyl-4 *H* -1,2,4,5-thiatriazine as a Precursor to the 1,2,4,5-Thiatriazinyl Radical, J Org Chem 65 (2000) 931–940. https://doi.org/10.1021/jo991126l.

[50] L.M. Thomasco, R.C. Gadwood, E.A. Weaver, J.M. Ochoada, C.W. Ford, G.E. Zurenko, J.C. Hamel, D. Stapert, J.K. Moerman, R.D. Schaadt, B.H. Yagi, The synthesis and antibacterial activity of 1,3,4-Thiadiazole phenyl oxazolidinone analogues, Bioorg Med Chem Lett 13 (2003) 4193–4196. https://doi.org/10.1016/j.bmcl.2003.07.018.

[51] H. TAKECHI, Y. ODA, N. NISHIZONO, K. ODA, M. MACHIDA, Fluorescent Labeling Reagents. Part 3. Screening Search for Organic Fluorophores: Syntheses and Fluorescence Properties of 3-Azolyl-7-diethylaminocoumarin Derivatives., Chem Pharm Bull (Tokyo) 48 (2000) 1702–1710. https://doi.org/10.1248/cpb.48.1702.

[52] M.D. Hall, N.K. Salam, J.L. Hellawell, H.M. Fales, C.B. Kensler, J.A. Ludwig, G. Szakács, D.E. Hibbs, M.M. Gottesman, Synthesis, Activity, and Pharmacophore Development for Isatin-β-thiosemicarbazones with Selective Activity toward Multidrug-Resistant Cells, J Med Chem 52 (2009) 3191–3204. https://doi.org/10.1021/jm800861c.

[53] T.A. Yousef, O.A. El-Gammal, S.E. Ghazy, G.M. Abu El-Reash, Synthesis, spectroscopic characterization, pH-metric and thermal behavior on Co(II) complexes formed with 4-(2-pyridyl)-3-thiosemicarbazide derivatives, J Mol Struct 1004 (2011) 271–283. https://doi.org/10.1016/j.molstruc.2011.08.020.

[54] A.A. Hassan, A.E. Mourad, K.M. El-Shaieb, A.H. Abou-Zied, D. Doepp, Thermolysis of Symmetrical Dithiobiurea and Thioureidoethylthiourea Derivatives., ChemInform 34 (2003). https://doi.org/10.1002/chin.200351044.

[55] A. Hassan, A. Mourad, K. El-Shaieb, A. Abou-Zied, Synthesis of 1,3,4-Thiadiazole, 1,3,4-Thiadiazine, 1,3,6-Thiadiazepane and Quinoxaline Derivatives from Symmetrical Dithiobiureas and Thioureidoethylthiourea Derivatives, Molecules 10 (2005) 822–832. https://doi.org/10.3390/10070822.

[56] A.A. Hassan, A.-F.E. Mourad, K.M. El-Shaieb, A.H. Abou-Zied, Ethenetetracarbonitrile and Heterocyclization of Symmetrical Dithiobiurea as well as Thioureidoethylthiourea Derivatives, Zeitschrift Für Naturforschung B 59 (2004) 910–916. https://doi.org/10.1515/znb-2004-0807.

[57] O.A.A. Ali, A. Ragab, Y.A. Ammar, M.S. Abusaif, Discovery of new thiazolidin-4-one and thiazole nucleus incorporation sulfaguanidine scaffold as new class of antimicrobial agents: Design, synthesis, in silico ADMET, and docking simulation, J Mol Struct 1334 (2025) 141879. https://doi.org/10.1016/j.molstruc.2025.141879.

[58] C. Gundogdu Hizliates, S. Oncuoglu, Eco-Friendly Synthesis of 2,3-Disubstituted Thiazolidine-4-One Derivatives Via A Multicomponent Reaction with Microwave Irradiation in a Chiral Ionic Liquid Medium, ChemistrySelect 10 (2025). https://doi.org/10.1002/slct.202404712.

[59] S.D. Ranade, S.G. Alegaon, N.A. Khatib, S. Gharge, R.S. Kavalapure, B.R.P. Kumar, Design, synthesis, molecular dynamic simulation, DFT analysis, computational pharmacology and decoding the antidiabetic molecular mechanism of sulphonamide-

thiazolidin-4-one hybrids, J Mol Struct 1311 (2024) 138359. https://doi.org/10.1016/j.molstruc.2024.138359.

[60] N.O. Mahmoodi, M. Mohammadi Zeydi, E. Biazar, Z. Kazeminejad, Synthesis of novel thiazolidine-4-one derivatives and their anticancer activity, Phosphorus Sulfur Silicon Relat Elem 192 (2017) 344–350. https://doi.org/10.1080/10426507.2016.1239197.

[61] M.A. Doddagaddavalli, V.K.A. Kalalbandi, T.R.R. Naik, S.D. Joshi, J. Seetharamappa, Fluorenone–thiazolidine-4-one scaffolds as antidiabetic and antioxidant agents: design, synthesis, X-ray crystal structures, and binding and computational studies, New Journal of Chemistry 47 (2023) 13581–13599. https://doi.org/10.1039/D3NJ01922E.

[62] S. Das, S. Paul, B. Mitra, G. Chandra Pariyar, P. Ghosh, *p* -Toluene Sulphonic Acid (PTSA): An Efficient Catalyst for One-Pot Three-Component Synthesis of Novel 3-Pyrazolyl-Thiazolidin-4-One Derivatives, ChemistrySelect 9 (2024). https://doi.org/10.1002/slct.202401822.

[63] N.M. Nasir, T.A. Alsalim, A.A. El-Arabey, M. Abdalla, Anticancer, antioxidant activities and molecular docking study of thiazolidine-4-one and thiadiazol derivatives, J Biomol Struct Dyn 41 (2023) 3976–3992. https://doi.org/10.1080/07391102.2022.2060306.

[64] H.N. Tawfeek, A.A. Hassan, S. Bräse, M. Nieger, Y.A. Mostafa, H.A.M. Gomaa, B.G.M. Youssif, E.M. El-Shreef, Design, synthesis, crystal structures and biological evaluation of some 1,3-thiazolidin-4-ones as dual CDK2/EGFR potent inhibitors with potential apoptotic antiproliferative effects, Arabian Journal of Chemistry 15 (2022) 104280. https://doi.org/10.1016/j.arabjc.2022.104280.

[65] B. Baroudi, K. Argoub, D. Hadji, A.M. Benkouider, K. Toubal, A. Yahiaoui, A. Djafri, Synthesis and DFT calculations of linear and nonlinear optical responses of novel 2-thioxo-3-N,(4-methylphenyl) thiazolidine-4 one, Journal of Sulfur Chemistry 41 (2020) 310–325. https://doi.org/10.1080/17415993.2020.1736073.

[66] P. Kumar, M. Duhan, J. Sindhu, K. Kadyan, S. Saini, N. Panihar, Thiazolidine-4-one clubbed pyrazoles hybrids: Potent α-amylase and α-glucosidase inhibitors with NLO properties, J Heterocycl Chem 57 (2020) 1573–1587. https://doi.org/10.1002/jhet.3882.

[67] A. Haque, M.W.A. Khan, K.M. Alenezi, R. Soury, M.S. Khan, S. Ahamad, Md. Mushtaque, D. Gupta, Synthesis, Characterization, Antiglycation Evaluation, Molecular Docking, and ADMET Studies of 4-Thiazolidinone Derivatives, ACS Omega 9 (2024) 1810–1820. https://doi.org/10.1021/acsomega.3c08463.

[68] R. Singh, S. Ahmad Ganaie, A. Singh, A. Chaudhary, Carbon-SO 3 H catalyzed expedient synthesis of new spiro-[indeno[1,2- *b*]quinoxaline-[11,2′]-thiazolidine]-4′-ones as biologically important scaffold, Synth Commun 49 (2019) 80–93. https://doi.org/10.1080/00397911.2018.1542003.

[69] L.Z. Fekri, H. Hamidian, M.A. Chekosarani, Urazolium diacetate as a new, efficient and reusable Brønsted acid ionic liquid for the synthesis of novel derivatives of

thiazolidine-4-ones, RSC Adv 10 (2020) 556–564. https://doi.org/10.1039/C9RA08649H.

[70] A.A. Aly, A.B. Brown, M. Abdel-Aziz, G.E.A.A. Abuo-Rahma, M.F. Radwan, M. Ramadan, A.M. Gamal-Eldeen, An Efficient Synthesis of Thiazolidine-4-ones with Antitumor and Antioxidant Activities, J Heterocycl Chem 49 (2012) 726–731. https://doi.org/10.1002/jhe.641.

[71] A.K. Jain, S. Sharma, A. Vaidya, V. Ravichandran, R.K. Agrawal, 1,3,4-Thiadiazole and its Derivatives: A Review on Recent Progress in Biological Activities, Chem Biol Drug Des 81 (2013) 557–576. https://doi.org/10.1111/cbdd.12125.

[72] M.I. Serag, S.S. Tawfik, H.M. Eisa, S.M.I. Badr, Design, Synthesis, Biological Evaluation and Molecular Docking Study of New 1,3,4-Thiadiazole-Based Compounds as EGFR Inhibitors, Drug Dev Res 86 (2025). https://doi.org/10.1002/ddr.70035.

[73] L. Yurttaş, A.E. Evren, H. AlChaib, H.E. Temel, G. Akalin Çiftçi, Synthesis, molecular docking, and molecular dynamic simulation studies of new 1,3,4-thiadiazole derivatives as potential apoptosis inducers in A549 lung cancer cell line, J Biomol Struct Dyn 43 (2025) 3814–3829. https://doi.org/10.1080/07391102.2023.2300125.

[74] A. Oubella, A. Bimoussa, M.T. Rehman, M.F. AlAjmi, A. Auhmani, M.L. Taha, H. Morjani, M.Y.Ait. Itto, Molecular hybrids based on 1,2,3-triazole and 1,3,4-thiadiazole cores: Synthesis, characterization, anticancer activity and in silico study, J Mol Struct 1311 (2024) 138339. https://doi.org/10.1016/j.molstruc.2024.138339.

[75] R. Wang, T.-T. Du, W.-Q. Liu, Y.-C. Liu, Y.-D. Yang, J.-P. Hu, M. Ji, B.-B. Yang, L. Li, X.-G. Chen, Discovery, Optimization, and Evaluation of Novel *N* -(Benzimidazol-5-yl)-1,3,4-thiadiazol-2-amine Analogues as Potent STAT3 Inhibitors for Cancer Treatment, J Med Chem 66 (2023) 12373–12395. https://doi.org/10.1021/acs.jmedchem.3c00863.

[76] X. Jin, T. Qiu, J. Xie, X. Wei, X. Wang, R. Yu, C. Proud, T. Jiang, Using Imidazo[2,1-*b*][1,3,4]thiadiazol Skeleton to Design and Synthesize Novel MNK Inhibitors, ACS Med Chem Lett 14 (2023) 83–91. https://doi.org/10.1021/acsmedchemlett.2c00442.

[77] S.R. Atta-Allah, A.M. AboulMagd, P.S. Farag, Design, microwave assisted synthesis, and molecular modeling study of some new 1,3,4-thiadiazole derivatives as potent anticancer agents and potential VEGFR-2 inhibitors, Bioorg Chem 112 (2021) 104923. https://doi.org/10.1016/j.bioorg.2021.104923.

[78] A. Faraji, T. Oghabi Bakhshaiesh, Z. Hasanvand, R. Motahari, E. Nazeri, M.A. Boshagh, L. Firoozpour, H. Mehrabi, A. Khalaj, R. Esmaeili, A. Foroumadi, Design, synthesis and evaluation of novel thienopyrimidine-based agents bearing diaryl urea functionality as potential inhibitors of angiogenesis, Eur J Med Chem 209 (2021) 112942. https://doi.org/10.1016/j.ejmech.2020.112942.

[79] M. Szeliga, M. Karpińska, R. Rola, A. Niewiadomy, Design, synthesis and biological evaluation of novel 1,3,4-thiadiazole derivatives as anti-glioblastoma agents targeting

the AKT pathway, Bioorg Chem 105 (2020) 104362. https://doi.org/10.1016/j.bioorg.2020.104362.

[80] H. Ahadi, M. Shokrzadeh, Z. Hosseini-khah, N. Ghassemi barghi, M. Ghasemian, E. Emadi, M. Zargari, N. Razzaghi-Asl, S. Emami, Synthesis and biological assessment of ciprofloxacin-derived 1,3,4-thiadiazoles as anticancer agents, Bioorg Chem 105 (2020) 104383. https://doi.org/10.1016/j.bioorg.2020.104383.

[81] S.P. Khathi, B. Chandrasekaran, S. Karunanidhi, C.L. Tham, F. Kozielski, N. Sayyad, R. Karpoormath, Design and synthesis of novel thiadiazole-thiazolone hybrids as potential inhibitors of the human mitotic kinesin Eg5, Bioorg Med Chem Lett 28 (2018) 2930–2938. https://doi.org/10.1016/j.bmcl.2018.07.007.

[82] L. Zhang, J. Zhao, B. Zhang, T. Lu, Y. Chen, Discovery of [1,2,4]triazolo[3,4-b][1,3,4]thiadiazole derivatives as novel, potent and selective c-Met kinase inhibitors: Synthesis, SAR study, and biological activity, Eur J Med Chem 150 (2018) 809–816. https://doi.org/10.1016/j.ejmech.2018.03.049.

[83] T. Plech, B. Kaproń, A. Paneth, M. Wujec, R. Czarnomysy, A. Bielawska, K. Bielawski, N. Trotsko, E. Kuśmierz, P. Paneth, Search for human DNA topoisomerase II poisons in the group of 2,5-disubstituted-1,3,4-thiadiazoles, J Enzyme Inhib Med Chem 30 (2015) 1021–1026. https://doi.org/10.3109/14756366.2014.995179.

[84] G. Wu, N. Feng, Y. Zhou, C. Li, X. Yang, Z. Li, C. Li, D. Chen, Z. Wang, Design, Synthesis and Antitumor Activity Evaluation of Indole Derivatives Containing Thiadiazole and Urea Motifs, ChemistrySelect 10 (2025). https://doi.org/10.1002/slct.202500692.

[85] A. Aghcheli, M. Toolabi, A. Ayati, S. Moghimi, L. Firoozpour, T.O. Bakhshaiesh, E. Nazeri, M. Norouzbahari, R. Esmaeili, A. Foroumadi, Design, synthesis, and biological evaluation of 1-(5-(benzylthio)-1,3,4-thiadiazol-2-yl)-3-phenylurea derivatives as anticancer agents, Medicinal Chemistry Research 29 (2020) 2000–2010. https://doi.org/10.1007/s00044-020-02616-2.

[86] S.V. Laxmi, P. Anil, G. Rajitha, A.J. Rao, P.A. Crooks, B. Rajitha, Synthesis of thiazolidine-2,4-dione derivatives: anticancer, antimicrobial and DNA cleavage studies, J Chem Biol 9 (2016) 97–106. https://doi.org/10.1007/s12154-016-0154-8.

[87] V. Asati, D.K. Mahapatra, S.K. Bharti, Thiazolidine-2,4-diones as multi-targeted scaffold in medicinal chemistry: Potential anticancer agents, Eur J Med Chem 87 (2014) 814–833. https://doi.org/10.1016/j.ejmech.2014.10.025.

[88] S.K. Batin Rahaman, S. Halder, K.K. Roy, P.K. Halder, U. Debnath, K. Jana, Discovery of New 4-Aminoquinoline–Thiazolidinone Hybrid Analogs as Antiproliferative Agents Inhibiting <scp>TLR4</scp> – <scp>LPS</scp> -Mediated Migration in Triple-Negative Breast Cancer Cells, Chem Biol Drug Des 105 (2025). https://doi.org/10.1111/cbdd.70089.

[89] B. Zengin Kurt, M. Gökçe, H. Şenol, D. Öztürk Civelek, G. Dandin, I. Gazioglu, Synthesis, cytotoxic evaluation, and in silico studies of novel benzenesulfonamide-

thiazolidinone derivatives against colorectal carcinoma, J Mol Struct 1321 (2025) 140153. https://doi.org/10.1016/j.molstruc.2024.140153.

[90] P. Kamboj, Anjali, K. Imtiyaz, M.A. Rizvi, V. Nath, V. Kumar, A. Husain, Mohd. Amir, Design, synthesis, biological assessment and molecular modeling studies of novel imidazothiazole-thiazolidinone hybrids as potential anticancer and anti-inflammatory agents, Sci Rep 14 (2024) 8457. https://doi.org/10.1038/s41598-024-59063-x.

[91] S. Shahjahan, L.T. Naraharisetti, A. Begum, P.A. Yakkala, P.S. Lakshmi Soukya, C. Godugu, S.A. Begum, A. Kamal, Oxindoline Containing Thiazolidine-4-one Tethered Triazoles Act as Antimitotic Agents by Targeting Microtubule Dynamics, ChemistrySelect 9 (2024). https://doi.org/10.1002/slct.202400539.

[92] X. Chen, Z. Luo, Z. Hu, D. Sun, Y. He, J. Lu, L. Chen, S. Liu, Discovery of potent thiazolidin-4-one sulfone derivatives for inhibition of proliferation of osteosarcoma in vitro and in vivo, Eur J Med Chem 266 (2024) 116082. https://doi.org/10.1016/j.ejmech.2023.116082.

[93] H.N. Tawfeek, A.A. Hassan, S. Bräse, M. Nieger, Y.A. Mostafa, H.A.M. Gomaa, B.G.M. Youssif, E.M. El-Shreef, Design, synthesis, crystal structures and biological evaluation of some 1,3-thiazolidin-4-ones as dual CDK2/EGFR potent inhibitors with potential apoptotic antiproliferative effects, Arabian Journal of Chemistry 15 (2022) 104280. https://doi.org/10.1016/j.arabjc.2022.104280.

[94] N.O. Mahmoodi, M. Mohammadi Zeydi, E. Biazar, Z. Kazeminejad, Synthesis of novel thiazolidine-4-one derivatives and their anticancer activity, Phosphorus Sulfur Silicon Relat Elem 192 (2017) 344–350. https://doi.org/10.1080/10426507.2016.1239197.

[95] B. Qi, X. Xu, Y. Yang, Y. Zhou, T. Chen, G. Gong, X. Yue, X. Xu, L. Hu, H. He, Discovery of thiazolidin-4-one urea analogues as novel multikinase inhibitors that potently inhibit FLT3 and VEGFR2, Bioorg Med Chem 27 (2019) 2127–2139. https://doi.org/10.1016/j.bmc.2019.03.049.

[96] Y.O. Mekhlef, A.M. AboulMagd, A.M. Gouda, Design, Synthesis, Molecular docking, and biological evaluation of novel 2,3-diaryl-1,3-thiazolidine-4-one derivatives as potential anti-inflammatory and cytotoxic agents, Bioorg Chem 133 (2023) 106411. https://doi.org/10.1016/j.bioorg.2023.106411.

[97] S.S. Saad, S.S.A. El-Sakka, M.H.A. Soliman, M.H.A. Gadelmawla, N.M. Mahmoud, Thiazolidin-4-one derivatives as antitumor agents against (Caco-2) cell line: synthesis, characterization, in silico and in vitro studies, Phosphorus Sulfur Silicon Relat Elem 199 (2024) 732–745. https://doi.org/10.1080/10426507.2024.2419634.

[98] A.M. Shawky, F.A. Almalki, A.N. Abdalla, B.G.M. Youssif, M.M. Abdel-Fattah, F. Hersi, H.A.M. El-Sherief, N.A. Ibrahim, A.M. Gouda, Discovery and optimization of 2,3-diaryl-1,3-thiazolidin-4-one-based derivatives as potent and selective cytotoxic agents with anti-inflammatory activity, Eur J Med Chem 259 (2023) 115712. https://doi.org/10.1016/j.ejmech.2023.115712.

CHAPTER-III

Synthesis and antiproliferative potency of 1,3,4-thiadiazole and 1,3-thiazolidine-4-one based new binary heterocyclic molecules: *in vitro* cell-based anticancer studies

1. Introduction:

The majority of chemists' interests over the past few decades have been in heterocyclic compounds, their various derivatives, and their applications in the chemical and pharmaceutical industries. Numerous recent research studies have been published that discuss the synthesis and application of a wide variety of heterocyclic compounds, including pyrazole, tetrahydroquinolines, benzotriazole, 1,2,3,4-tetrazine, thiazole, 2-thiazoline, pyrimidine, and others. 1,3,4-thiadiazole is a prevalent and essential five-membered heterocyclic system containing two nitrogen atoms and a sulfur atom [1]. Thiadiazole exists in various isomers, including 1,2,3-thiadiazole, 1,2,4-thiadiazole, and 1,2,5-thiadiazole, among others. A quick review of high-quality research articles revealed that 1,3,4-thiadiazole has received more research attention than other isomers [2]. Accordingly, recent research by Yang Li and colleagues has developed some quinoline and 1,3,4-thiadiazole molecular hybrids that show potential anti-breast cancer activity on *in vitro* and *in vivo* preclinical settings. Compounds also inhibited EGFR and HER2 proteins, as evident from *in vitro* kinase assays and molecular docking studies [3]. One significant resource for identifying new therapeutic possibilities is the growing diversity of small chemical libraries. Heterocycles, specifically 1,3-thiazolidine-4-ones, are among the most studied groups of chemicals in this context. These are heterocyclic nuclei containing a carbonyl group at position four and nitrogen and sulfur atoms at positions **1** and **3**, respectively. Research on the production of these compounds and their bioactivity has garnered considerable interest [4,5]. Numerous pharmacological actions, including anticancer activity, have been demonstrated by thiazolidine-4-one and its derivatives [6]. Similarly, a recent research study by Senol et al. reported the discovery of new thiazolidine-4-one derivatives exhibiting impressive cytotoxicity against MCF-7 breast cancer cell lines in the MTT assay. Potent compounds also exhibited excellent binding interactions with the HER2 (PDB; 3PP0) protein, a growth factor involved in the development and progression of breast

cancer [6]. Cancer is the second leading cause of death among diseases, compared to heart disease, and the latter is the primary cause of death across the global mortality incidence due to diseases [7]. Uncontrolled cell division and lack of cellular apoptotic activity led to cancer development by significantly increasing the number of malignant cells [8]. As per the WHO reports, in 2021, breast cancer is predicted to be the most common cancerous disease worldwide, with about 2.3 million diagnosed cases and 685 thousand deaths in 2020. Breast cancer accounts for 25% of total cancer cases in women and 15% of cancer-related mortalities. Moreover, breast cancer was shown to be the most frequently diagnosed cancer globally in 2022 [9]. This kind of cancer is more common in women and has very rare cases in males [10]. The primary treatment for breast cancer involves surgery, which is followed by radiation therapy to the breast and lymph nodes to lower the chances of recurrence [11]. The recent cancer therapies depend on the mechanisms that lead to genetic damage, an imbalance in kinase and phosphatase activity, problems with the division spindle, and differences in cell cycle checkpoints. The majority of treatment approaches fail to effectively destroy cancer cells, as they attempt to inhibit the growth of these cells. Complete remission of cancer is often caused by cancer cell apoptosis, which provides better results and reduces the chances of recurrence [12]. However, the alternative systemic therapies that have been developed recently are not entirely effective in treating breast cancer. In addition, osteoporosis, cardiovascular issues, and medication resistance may develop as side effects. Thus, there is a pressing need for ongoing advancements in identifying and synthesising new potent lead compounds for long-term cancer treatment with fewer adverse effects [13–16]. In this context, twenty-one 1,3,4-thiadiazole and 1,3-thiazolidine-4-one-based heterocyclic hybrid molecules have been synthesised and evaluated for cytotoxicity on a panel of *in vitro* cancer cell lines (MCF-7, PC3, 4T1, MDA-MB-231, and MOC2, etc.). The final compound series (**5a-g**, **6a-g**, and **7a-g**) have been synthesised in excellent yields (84-96%) via the Knoevenagel condensation (KC) method using

urea as the catalyst and glacial acetic acid as solvent [17]. The compound series was also tested for its mechanism of anticancer activity through cell cycle analysis, nuclear fragmentation, and ROS generation studies. Hence, additional mechanisms of action are derived thereof.

2. Experimental methods:

2.1. Chemical materials and devices:

Chemicals and solvents of the highest grades for this research work were purchased from reputable vendors, including Merck, Sigma-Aldrich, Spectrochem, SRL, and LOBA Chemicals. Purification techniques were employed as specified in the literature to achieve the maximum purity level. A thin-layer chromatography (TLC) plate and an ultraviolet (UV) light chamber (with both short and long wavelengths) were used to monitor the synthesis process. The melting point of the synthesised compounds was determined using the VEEGO melting point apparatus. NMR (^{1}H, ^{13}C, and ^{19}F) spectroscopy and HRMS (Q-TOF) data were used for the structure elucidation of the compounds. Advanced equipment, such as the Bruker Advance NMR Spectrophotometer (Germany), was used to record the ^{1}H-NMR, ^{13}C-NMR, and ^{19}F-NMR spectra at 400/300 MHz (^{1}H-NMR), 101/75 MHz (^{13}C-NMR), and 376 MHz (^{19}F-NMR), respectively, using DMSO-d_6 as the solvent. Chemical shifts were reported in parts per million (ppm) with respect to the internal standard tetramethylsilane (δ = 0.00 ppm), and coupling constant values were reported in Hertz (Hz). The following are the descriptions of the peak splitting: dd (doublet of doublets), t (triplet), q (quartet), m (multiplet), and s (singlet). High-resolution mass spectra (HRMS, *m/z*) were recorded using an ESI (Q-TOF and Orbitrap, positive ion mode) mass spectrometry instrument (Agilent).

2.2. Synthesis and structural analysis of intermediate compounds:

2.2.1. Synthesis of 5-amino 1,3,4-thiadiazol-2-thiol (compound **1**):

Hydrazine carbothioamide/thiosemicarbazide (20 mmol, 1.82 g) was added to a 150 mL flat-bottom flask containing Ethanol (30 mL) and KOH (24 mmol, 0.96 g). Carbon disulfide (25

mmol, 1.44 mL) was added dropwise, and the entire mixture was refluxed (80 °C) with stirring (600-700 rpm) for 10 h in an oil bath fitted to a magnetic stirrer with a heating plate. After the reaction (TLC), the mixture was poured into ice-cold water and acidified with 20% HCl to a pH of 4-5. The precipitated product was filtered and washed with water. Then, the filtrated product was dried and purified by recrystallizing from EtOH/MeOH **(Scheme 1)**:

5-amino 1,3,4-thiadiazol-2-thiol (compound **1**)**:** Pale yellow crystal, 2.55g, Yield 96%; MP = 231-233 ^{0}C; ^{1}H NMR (300 MHz, DMSO-*d*$_6$) δ_H: 13.14 (s, 1H), 7.04 (s, 2H) ppm; ^{13}C NMR (75 MHz, DMSO-*d*$_6$) δ_C: 181.0, 161.5, 40.3, 40.0, 39.8, 39.2, 38.9, 38.6 ppm; HRMS (ESI/TOF-Q) *m/z*: $[M + H]^+$ Calcd. for $C_2H_4N_3S_2^+$ 133.9841; Found 133.9837.

2.2.2. Synthesis of 5-(substituted benzylthio)-1,3,4-thiadiazol-2-amine (compound **2a-c):** Compound **1** (0.01 mol) was dissolved in dry DMF (25 mL) containing anhydrous K_2CO_3 (2 equiv) in a 100 mL flat-bottom flask. Then, substituted benzyl chlorides (1.2 equiv) were added and stirred (600-700 rpm) on a magnetic stirrer at room temperature for 10-12h. After the reaction (TLC), the content was poured into crushed ice in a beaker. The precipitated solid was filtered, dried, and recrystallised from EtOH/Methanol to obtain pure products **(Scheme 1)**:

5-(benzylthio)-1,3,4-thiadiazol-2-amine (compound **2a**): White solid, 1.89g, Yield 85%; MP = 138-140 ^{0}C; ^{1}H NMR (400 MHz, DMSO-*d*$_6$) δ_H: 7.36 – 7.33 (m, 3H), 7.31 (s, 1H), 7.30 (s, 2H), 7.28 – 7.23 (m, 1H), 4.29 (s, 1H) ppm; ^{13}C NMR (101 MHz, DMSO-*d*$_6$) δ_C: 169.9, 149.5, 137.1, 129.0, 128.5, 127.4, 40.1, 39.9, 39.9, 39.7, 39.7, 39.5, 39.4, 39.3, 39.2, 39.1, 39.0, 38.89, 38.4 ppm; HRMS (ESI/TOF-Q) *m/z*: $[M + H]^+$ Calcd. for $C_9H_{10}N_3S_2^+$ 224.0311; Found 224.0309.

5-((4-chlorobenzyl) thio)-1,3,4-thiadiazol-2-amine (compound **2b)**: White solid, 2.24g, Yield 87%; MP =145-148 ^{0}C; ^{1}H NMR (400 MHz, DMSO-*d*$_6$) δ_H: 7.38 – 7.36 (m, 4H), 7.34 – 7.31 (m, 2H), 4.28 (s, 2H) ppm; ^{13}C NMR (101 MHz, DMSO-*d*$_6$) δ_C: 170.0, 149.0, 136.4,

132.0, 130.8, 128.4, 40.1, 39.9, 39.7, 39.5, 39.3, 39.1, 38.8, 37.6 ppm; HRMS (ESI/TOF-Q) *m/z*: $[M + H]^+$ Calcd. for $C_9H_9ClN_3S_2^+$ 257.9921; Found 257.9918.

5-((2,4-dichloro benzyl) thio)-1,3,4-thiadiazol-2-amine (compound **2c**): White solid, 2.51g, Yield 86%; MP = 156-158 ^{0}C; ^{1}H NMR (400 MHz, DMSO-d_6) δ_H: 8.32 (s, 2H), 7.64 (dd, *J* = 6.4, 2.0 Hz, 1H), 7.46 – 7.33 (m, 1H), 4.34 (s, 2H) ppm; ^{13}C NMR (101 MHz, DMSO-d_6) δ_C: 166.8, 151.6, 134.2, 134.1, 132.9, 132.6, 132.4, 129.0, 128.9, 127.4, 127.4, 79.2, 40.1, 39.9, 39.7, 39.5, 39.3, 39.1, 38.9, 35.5 ppm; HRMS (ESI/TOF-Q) *m/z*: $[M + H]^+$ Calcd. for $C_9H_8Cl_2N_3S_2^+$ 291.9531; Found 291.9526.

2.2.3. Synthesis of 5-(substituted benzylthio)-1,3,4-thiadiazol-2-yl)-2-chloroacetamide (compound **3a-c):**

To the stirring solution of **2a-c** (0.01 mol) and TEA (1.2 equiv) in dry tetrahydrofuran (THF, 20 mL) in a 50 mL flat-bottom flask, chloroacetyl chloride (1.2 equiv) was added dropwise, maintaining the temperature at 0-10°C. The reaction mixture was stirred at room temperature for about 7-8 hours. After the reaction (TLC) was completed, excess THF was evaporated under reduced pressure using a rotary evaporator. The resultant residue obtained was washed with water, filtered, and dried. Crude products, **3a-c**, thus obtained, were purified by recrystallisation using methanol/DMF **(Scheme 1)**:

N-(5-(benzylthio)-1,3,4-thiadiazol-2-yl)-2-chloroacetamide (compound **3a**): White solid, 2.78g, Yield 93%; MP = 182-184 ^{0}C; ^{1}H NMR (300 MHz, DMSO-d_6) δ_H: 12.98 (s, 1H), 7.42 – 7.38 (m, 2H), 7.36 – 7.27 (m, 3H), 4.50 (s, 2H), 4.43 (s, 2H) ppm; ^{13}C NMR (75 MHz, DMSO-d_6) δ_C: 165.4, 158.6, 136.6, 128.9, 128.5, 127.6, 42.2, 40.3, 40.0, 39.8, 39.5, 39.2, 38.9, 38.6, 37.5 ppm; HRMS (ESI/TOF-Q) *m/z*: $[M + H]^+$ Calcd. for $C_{11}H_{11}ClN_3OS_2^+$ 300.0027; Found 300.0023.

2-chloro-N-(5-((4-chlorobenzyl) thio)-1,3,4-thiadiazol-2-yl) acetamide (compound **3b**): White solid, 3.04g, Yield 91%; MP = 205-207 ^{0}C; ^{1}H NMR (400 MHz, DMSO-d_6) δ_H: 13.02(s,

1H), 7.42 (dd, *J* = 8.80, 2.24 Hz, 2H), 7.37 (dd, *J* = 6.56, 2.12 Hz, 2H), 4.48 (s, 2H), 4.44 (s, 2H) ppm; ^{13}C NMR (101 MHz, DMSO-*d*$_6$) δ_C: 171.6, 165.5, 158.8, 158.6, 158.3, 157.7, 136.0, 135.9, 132.2, 132.1, 130.8, 128.5, 128.5, 42.2, 40.1, 39.9, 39.7, 39.5, 39.3, 39.1, 39.1, 38.9, 36.6 ppm; HRMS (ESI/TOF-Q) *m/z*: $[M + H]^+$ Calcd. for $C_{11}H_{10}Cl_2N_3OS_2^+$ 333.9637; Found 333.9632.

2-chloro-N-(5-((2,4-dichloro benzyl) thio)-1,3,4-thiadiazol-2-yl) acetamide (compound **3c**): White solid, 3.19g, Yield 87%; MP = 214-217 ^{0}C; ^{1}H NMR (400 MHz, DMSO-*d*$_6$) δ_H: 13.08 (s, 1H), 7.64 (d, *J* = 2.16 Hz, 1H), 7.53 – 7.50 (m, 1H), 7.39 (dd, *J* = 8.28, 2.12 Hz, 1H), 4.54 (s, 2H), 4.46 (s, 2H) ppm; ^{13}C NMR (101 MHz, DMSO-*d*$_6$) δ_C: 171.7, 165.5, 159.1, 159.0, 157.5, 156.9, 134.3, 133.5, 133.4, 133.3, 133.2, 132.6, 129.0, 127.5, 127.5, 42.2, 40.1, 39.9, 39.7, 39.5, 39.3, 39.1, 38.9, 35.1 ppm; HRMS (ESI/TOF-Q) *m/z*: $[M + H]^+$ Calcd. for $C_{11}H_9Cl_3N_3OS_2^+$ 367.9247; Found 367.9241.

2.2.4. Synthesis of 5-(substituted benzylthio)-1,3,4-thiadiazol-2-yl) imino) thiazolidine-4-one (compound **4a-c):**

Compounds **3a-c** (0.01 mol) and ammonium thiocyanate (NH_4SCN, 3 equiv) were suspended in Ethanol in a 100 mL flat-bottom flask. The mixture was refluxed in an oil bath with stirring (600-700 rpm) overnight using a magnetic stirrer hot plate. After confirmation of the reaction completion (TLC), the mixture was poured into ice-cold water in a beaker. The precipitated solid was filtered and washed with water, then dried and recrystallised from EtOH/MeOH plus DMF to obtain pure product **4a-c** (**Scheme 1**):

2-((5-(benzylthio)-1,3,4-thiadiazol-2-yl) imino) thiazolidine-4-one (compound **4a**): Beige solid, 2.86g, Yield 89%; MP = 216-218 ^{0}C; ^{1}H NMR (300 MHz, DMSO-*d*$_6$) δ_H: 12.31 (s, 1H), 7.43 (d, *J* = 9.76 Hz, 2H), 7.36 – 7.28 (m, 3H), 4.51 (s, 2H), 4.10 (s, 2H) ppm; ^{13}C NMR (101 MHz, DMSO-*d*$_6$) δ_C: 174.0, 170.37, 165.9, 160.5, 136.5, 129.1, 128.6, 127.6, 40.1, 39.9, 39.73,

39.5, 39.3, 39.2, 39.1, 38.8, 37.3, 35.7 ppm; HRMS (ESI/TOF-Q) *m/z*: $[M + H]^+$ Calcd. for $C_{12}H_{11}N_4OS_3^+$ 323.0089; Found 323.0084.

2-((5-((4-chlorobenzyl) thio)-1,3,4-thiadiazol-2-yl) imino) thiazolidine-4-one (compound **4b**): Beige solid, 3.31g, Yield 93%; MP = 210-213 ^{0}C; ^{1}H NMR (400 MHz, DMSO-*d*$_6$) δ_H: 12.32 (s, 1H), 7.46 – 7.43 (m, 2H), 7.41 – 7.38 (m, 2H), 4.50 (s, 2H), 4.10 (s, 2H)ppm; ^{13}C NMR (101 MHz, DMSO-*d*$_6$) δ_C: 174.0, 170.4, 165.9, 160.2, 135.9, 132.2, 130.9, 128.5, 40.1, 39.9, 39.7, 39.5, 39.3, 39.2, 39.1, 38.8, 36.3, 35.7 ppm; HRMS (ESI/TOF-Q) *m/z*: $[M + H]^+$ Calcd. for $C_{12}H_{10}ClN_4OS_3^+$ 356.9700; Found 356.9706.

2-((5-((2,4-dichlorobenzyl) thio)-1,3,4-thiadiazol-2-yl) imino) thiazolidine-4-one (compound **4c**): Beige solid, 3.67g, Yield 94%; MP = 215-217 ^{0}C; ^{1}H NMR (400 MHz, DMSO-*d*$_6$) δ_H: 12.34 (s, 1H), 7.66 (d, *J* = 2.20 Hz, 1H), 7.57 (d, *J* = 8.36 Hz, 1H), 7.41 (dd, *J* = 8.28, 2.16 Hz, 1H), 4.57 (s, 2H), 4.10 (s, 2H) ppm; ^{13}C NMR (101 MHz, DMSO-d$_6$) δ_C: 174.0, 170.8, 166.1, 159.3, 134.3, 133.3, 133.3, 132.7, 129.1, 127.6, 40.1, 39.9, 39.7, 39.5, 39.3, 39.1, 38.8, 35.8, 34.7 ppm; HRMS (ESI/TOF-Q) *m/z*: $[M + H]^+$ Calcd. for $C_{12}H_9Cl_2N_4OS_3^+$ 390.9310; Found 390.9306.

2.3. Synthesis procedure and structural analysis of final compounds series (5a-g, 6a-g, and 7a-g):

Compound **4a-c** (1 mmol) and urea/thiourea (1.5 equiv) were taken in a 50 mL flat-bottom flask, followed by the addition of glacial acetic acid (10 mL). The suspension was stirred for a few minutes, and then different benzaldehydes (1.2 equiv) were added portion-wise. The mixture was refluxed by heating it on a hot plate with a magnetic stirrer at 120 °C for 16-20 hours. After confirmation of the reaction completion by TLC checking, the mixture was poured into crushed ice in a beaker. The precipitated crude solid products were filtered and washed several times with distilled water to remove acetic acid. The crude solid products were then

dried and recrystallised from a methanol and DMF mixture (2:1) to obtain pure final compounds **(Scheme 1)**:

5-(benzylidene)-2-((5-(benzylthio)-1,3,4-thiadiazol-2-yl) imino) thiazolidine-4-one (compound **5a**): Yellow solid, 0.336g, Yield 82%; MP = 208-212 ^{0}C; ^{1}H NMR (400 MHz, DMSO-d_6) δ_H: 12.94 (s, 1H), 7.78 (s, 1H), 7.67 – 7.65 (m, 2H), 7.58 (t, *J* = 7.44 Hz, 2H), 7.52 – 7.48 (m, 1H), 7.46 – 7.43 (m, 2H), 7.37 – 7.33 (m, 2H), 7.31 – 7.27 (m, 1H), 4.54 (s, 2H) ppm; ^{13}C NMR (101 MHz, DMSO-d_6) δ_C: 169.9, 166.9, 161.5, 158.4, 136.4, 133.1, 132.9, 130.5, 130.2, 129.4, 129.1, 128.6, 127.7, 123.8, 40.1, 39.9, 39.7, 39.5, 39.3, 39.1, 38.8, 37.2 ppm; HRMS (ESI/TOF-Q) *m/z*: $[M + H]^+$ Calcd. for $C_{19}H_{15}N_4OS_3^+$ 411.0402; Found 411.0389.

2-((5-(benzylthio)-1,3,4-thiadiazol-2-yl) imino)-5-(3-fluoro benzylidene) thiazolidine-4-one (compound **5b**): Yellow solid, 0.359g, Yield 84%; MP = 231-234 ^{0}C; ^{1}H NMR (400 MHz, DMSO-d_6) δ_H: 12.98 (s, 1H), 7.75 (s, 1H), 7.63 – 7.58 (m, 1H), 7.48 – 7.42 (m, 4H), 7.36 – 7.32 (m, 3H), 7.31 – 7.26 (m, 1H), 4.53 (s, 2H) ppm; ^{13}C NMR (101 MHz, DMSO-d_6) δ_C: 169.8, 166.7, 163.5, 161.6, 161.0, 158.0, 136.4, 135.4, 131.5, 131.4, 129.1, 128.6, 127.7, 125.6, 117.3, 117.1, 117.0, 116.8, 40.1, 39.9, 39.7, 39.5, 39.3, 39.1, 38.8, 37.2 ppm; ^{19}F NMR (376 MHz, DMSO-d_6) δ_F: -111.61 ppm; HRMS (ESI/TOF-Q) *m/z*: $[M + H]^+$ Calcd. for $C_{19}H_{14}FN_4OS_3^+$ 429.0308; Found 429.0300.

2-((5-(benzylthio)-1,3,4-thiadiazol-2-yl) imino)-5-(4-fluoro benzylidene) thiazolidine-4-one (compound **5c**): Yellow solid, 0.389g, Yield 91%; MP = 179-181 ^{0}C; ^{1}H NMR (300 MHz, DMSO-d_6) δ_H: 12.93 (s, 1H), 7.76 (s, 1H), 7.72 – 7.67 (m, 2H), 7.46 – 7.42 (m, 2H), 7.40 (s, 1H), 7.37 – 7.32 (m, 3H), 7.31 – 7.25 (m, 1H), 4.53 (s, 2H) ppm; ^{13}C NMR (75 MHz, DMSO-d_6) δ_C: 169.8, 166.9, 164.6, 162.3, 161.4, 161.2, 158.2, 136.4, 132.7, 132.6, 131.8, 129.7, 129.1, 128.6, 127.7, 123.5, 116.7, 116.4, 40.3, 40.0, 39.8, 39.5, 39.2, 38.9, 38.6, 37.1 ppm; ^{19}F NMR (376 MHz, DMSO-d_6) δ_F: -108.50 ppm; HRMS (ESI/TOF-Q) *m/z*: $[M + H]^+$ Calcd. for $C_{19}H_{14}FN_4OS_3^+$ 429.0308; Found 429.0304.

2-((5-(benzylthio)-1,3,4-thiadiazol-2-yl) imino)-5-(4-chlorobenzylidene) thiazolidine-4-one (compound **5d**): Yellow solid, 0.396g, Yield 89%; MP = 193-195 ^{0}C; ^{1}H NMR (400 MHz, DMSO-d_6) δ_H: 12.93 (s, 1H), 7.72 (s, 1H), 7.64 – 7.59 (m, 4H), 7.45 – 7.43 (m, 2H), 7.36 – 7.32 (m, 2H), 7.30 – 7.26 (m, 1H), 4.53 (s, 2H) ppm; ^{13}C NMR (101 MHz, DMSO-d_6) δ_C: 169.7, 166.7, 161.4, 157.9, 136.3, 135.0, 131.9, 131.7, 131.4, 129.3, 129.0, 128.5, 127.6, 124.5, 40.1, 39.9, 39.7, 39.5, 39.3, 39.1, 38.9, 37.2 ppm; HRMS (ESI/TOF-Q) *m/z*: $[M + H]^+$ Calcd. for $C_{19}H_{14}ClN_4OS_3^+$ 445.0013; Found 445.0003.

2-((5-(benzylthio)-1,3,4-thiadiazol-2-yl) imino)-5-(4-methoxy benzylidene) thiazolidine-4-one (compound **5e**): Yellow solid, 0.405g, Yield 92%; MP = 228-230 ^{0}C; ^{1}H NMR (400 MHz, DMSO-d_6) δ_H: 12.83 (s, 1H), 7.75 (s, 1H), 7.63 (d, J = 8.2 Hz, 2H), 7.46 – 7.41 (m, 2H), 7.35 (t, J = 7.60 Hz, 2H), 7.31 – 7.28 (m, 1H), 7.16 (d, J = 8.28 Hz, 2H), 4.55 (s, 2H), 3.84 (s, 3H) ppm; ^{13}C NMR (101 MHz, DMSO-d_6) δ_C: 170.0, 167.0, 161.2, 161.1, 158.6, 136.4, 133.0, 132.3, 129.1, 128.6, 128.6, 127.7, 125.5, 120.5, 115.0, 55.5, 40.1, 39.9, 39.7, 39.5, 39.3, 39.1, 38.8, 37.2 ppm; HRMS (ESI/TOF-Q) *m/z*: $[M + H]^+$ Calcd. for $C_{20}H_{17}N_4O_2S_3^+$ 441.0508; Found 441.0502.

2-((5-(benzylthio)-1,3,4-thiadiazol-2-yl) imino)-5-(4-hydroxy benzylidene) thiazolidine-4-one (compound **5f**): Yellow solid, 0.388g, Yield 91%; MP = 233-235 ^{0}C; ^{1}H NMR (400 MHz, DMSO-d_6) δ_H: 12.87 – 12.61 (m, 1H), 10.37 (s, 1H), 7.68 (s, 1H), 7.52 – 7.50 (m, 2H), 7.45 – 7.41 (m, 2H), 7.36 – 7.32 (m, 2H), 7.30 – 7.26 (m, 1H), 6.97 – 6.95 (m, 2H), 4.53 (s, 2H) ppm; ^{13}C NMR (101 MHz, DMSO-d_6) δ_C: 170.0, 167.1, 162.2, 161.0, 160.1, 158.6, 136.4, 133.5, 132.6, 129.0, 128.5, 128.5, 127.6, 127.6, 123.9, 119.1, 116.4, 40.1, 39.9, 39.7, 39.5, 39.3, 39.1, 38.8, 37.2. HRMS (ESI/TOF-Q) *m/z*: $[M + H]^+$ Calcd. for $C_{19}H_{15}N_4O_2S_3^+$ 427.0352; Found 427.0344.

2-((5-(benzylthio)-1,3,4-thiadiazol-2-yl) imino)-5-(4-hydroxy-3-methoxy benzylidene) thiazolidine-4-one (compound **5g**): Yellow solid, 0.429g, Yield 94%; MP = 189-191 ^{0}C; ^{1}H

NMR (300 MHz, DMSO-d_6) δ_H: 12.80 (s, 1H), 10.03 (s, 1H), 7.71 (s, 1H), 7.46 – 7.41 (m, 2H), 7.38 – 7.30 (m, 3H), 7.28 – 7.26 (m, 1H), 7.13 (dd, *J* = 8.31, 1.98 Hz, 1H), 7.00 (d, *J* = 8.31 Hz, 1H), 4.53 (s, 2H), 3.83 (s, 3H) ppm; ^{13}C NMR (75 MHz, DMSO-d_6) δ_C: 172.0, 170.0, 167.1, 161.1, 158.7, 149.7, 148.0, 136.5, 136.4, 133.9, 129.1, 128.6, 128.6, 127.7, 127.7, 124.5, 123.5, 119.5, 116.4, 115.6, 55.7, 40.3, 40.0, 39.8, 39.6, 39.5, 39.2, 38.9, 38.6, 37.3 ppm; HRMS (ESI/TOF-Q) *m/z*: $[M + H]^+$ Calcd. for $C_{20}H_{17}N_4O_3S_3^+$ 457.0457; Found 457.0449.

5-(benzylidene)-2-((5-((4-chlorobenzyl) thio)-1,3,4-thiadiazol-2-yl) imino) thiazolidine-4-one (compound **6a**): Yellow solid, 0.413g, Yield 93%; MP = 207-209 ^{0}C; ^{1}H NMR (300 MHz, DMSO-d_6) δ_H: 12.95 (s, 1H), 7.78 (s, 1H), 7.67 – 7.64 (m, 2H), 7.57 (t, *J* = 6.96 Hz, 2H), 7.52 – 7.46 (m, 3H), 7.42 – 7.36 (m, 2H), 4.53 (s, 2H) ppm; ^{13}C NMR (75 MHz, DMSO-d_6) δ_C: 170.0, 166.9, 161.1, 158.5, 135.8, 133.0, 132.9, 132.2, 130.9, 130.5, 130.2, 129.4, 128.5, 128.5, 123.8, 40.0, 39.8, 39.5, 39.2, 38.9, 38.6, 36.3 ppm; HRMS (ESI/TOF-Q) *m/z*: $[M + H]^+$ Calcd. for $C_{19}H_{14}ClN_4OS_3^+$ 445.0013; Found 445.0033.

2-((5-((4-chlorobenzyl) thio)-1,3,4-thiadiazol-2-yl) imino)-5-(3-fluoro benzylidene) thiazolidine-4-one (compound **6b**): Yellow solid, 0.422g, Yield 91%; MP = 222-224 ^{0}C; ^{1}H NMR (300 MHz, DMSO-d_6) δ_H: 13.00 (s, 1H), 7.76 (s, 1H), 7.65 – 7.58 (m, 1H), 7.50 – 7.45 (m, 4H), 7.41 – 7.30 (m, 3H), 4.53 (s, 2H) ppm; ^{13}C NMR (75 MHz, DMSO-d_6) δ_C: 169.9, 166.7, 163.9, 161.2, 160.6, 158.1, 135.7, 132.3, 131.5, 131.4, 130.9, 128.5, 125.6, 125.5, 117.1, 40.3, 40.0, 39.8, 39.5, 39.2, 38.9, 38.6, 36.3 ppm; ^{19}F NMR (376 MHz, DMSO-d_6) δ_F: -111.60 ppm; HRMS (ESI/TOF-Q) *m/z*: $[M + H]^+$ Calcd. for $C_{19}H_{13}ClFN_4OS_3^+$ 462.9919; Found 462.9939.

2-((5-((4-chlorobenzyl) thio)-1,3,4-thiadiazol-2-yl) imino)-5-(4-fluoro benzylidene) thiazolidine-4-one (compound **6c**): Yellow solid, 0.435g, Yield 94%; MP = 196-198 ^{0}C; ^{1}H NMR (300 MHz, DMSO-d_6) δ_H: 12.95 (s, 1H), 7.78 (s, 1H), 7.72 (dd, *J* = 8.43, 5.34 Hz, 2H), 7.48 – 7.38 (m, 7H), 4.53 (s, 2H) ppm; ^{13}C NMR (75 MHz, DMSO-d_6) δ_C: 170.0, 166.9, 161.16,

158.3, 135.8, 132.7, 132.6, 132.2, 131.8, 130.9, 129.7, 128.5, 123.5, 116.7, 116.4, 40.3, 40.0, 39.8, 39.5, 39.2, 38.9, 38.6, 36.2 ppm; ^{19}F NMR (376 MHz, DMSO-d_6) δ_F: -108.49 ppm; HRMS (ESI/TOF-Q) *m/z*: $[M + H]^+$ Calcd. for $C_{19}H_{13}ClFN_4OS_3^+$ 462.9919; Found 462.9916.

2-((5-((4-chlorobenzyl) thio)-1,3,4-thiadiazol-2-yl) imino)-5-(4-chloro benzylidene) thiazolidine-4-one (compound **6d**): Yellow solid, 0.421g, Yield 88%; MP = 230-233 ^{0}C; ^{1}H NMR (400 MHz, DMSO-d_6) δ_H: 12.99 (s, 1H), 7.77 (s, 1H), 7.68 – 7.62 (m, 4H), 7.47 (d, *J* = 8.12 Hz, 2H), 7.40 (d, *J* = 8.12 Hz, 2H), 4.53 (s, 2H) ppm; ^{13}C NMR (101 MHz, DMSO-d_6) δ_C: 170.0, 166.9, 161.3, 158.2, 135.8, 135.1, 132.3, 132.0, 131.8, 131.6, 131.0, 129.5, 128.6, 124.6, 40.1, 39.9, 39.7, 39.5, 39.3, 39.1, 38.8, 36.3 ppm; HRMS (ESI/TOF-Q) *m/z*: $[M + H]^+$ Calcd. for $C_{19}H_{13}Cl_2N_4OS_3^+$ 478.9623; Found 478.9629.

2-((5-((4-chlorobenzyl) thio)-1,3,4-thiadiazol-2-yl) imino)-5-(4-methoxy benzylidene) thiazolidine-4-one (compound **6e**): Yellow solid, 0.455g, Yield 96%; MP = 204-207 ^{0}C; ^{1}H NMR (300 MHz, DMSO-d_6) δ_H: 12.86 (s, 1H), 7.74 (s, 1H), 7.63 (dd, *J* = 6.72, 2.04 Hz, 2H), 7.49 – 7.45 (m, 2H), 7.43 – 7.39 (m, 2H), 7.17 – 7.13 (m, 2H), 4.54 (s, 2H), 3.83 (s, 3H) ppm; ^{13}C NMR (75 MHz, DMSO-d_6) δ_C: 170.1, 167.1, 161.1, 160.9, 158.7, 135.8, 133.1, 132.4, 132.2, 130.9, 128.5, 125.5, 120.5, 115.0, 55.5, 40.3, 40.0, 39.8, 39.5, 39.2, 38.9, 38.6, 36.3 ppm; HRMS (ESI/TOF-Q) *m/z*: $[M + H]^+$ Calcd. for $C_{20}H_{16}ClN_4O_2S_3^+$ 475.0118; Found 475.0115.

2-((5-((4-chlorobenzyl) thio)-1,3,4-thiadiazol-2-yl) imino)-5-(4-hydroxy benzylidene) thiazolidine-4-one (compound **6f**): Yellow solid, 0.402g, Yield 87%; MP = 239-241 ^{0}C; ^{1}H NMR (400 MHz, DMSO-d_6) δ_H: 12.81 (s, 1H), 10.39 (s, 1H), 7.69 (s, 1H), 7.52 (d, *J* = 8.36 Hz, 2H), 7.48 – 7.46 (m, 2H), 7.42 – 7.40 (m, 2H), 6.97 (d, *J* = 8.32 Hz, 2H), 4.54 (s, 2H) ppm; ^{13}C NMR (101 MHz, DMSO-d_6) δ_C: 170.1, 167.2, 160.7, 160.1, 158.8, 135.8, 133.6, 132.7, 132.2, 130.9, 128.5, 128.5, 123.9, 119.1, 116.5, 40.1, 39.9, 39.7, 39.5, 39.3, 39.1, 39.1, 38.8,

36.3 ppm; HRMS (ESI/TOF-Q) *m/z*: $[M + H]^+$ Calcd. for $C_{19}H_{14}ClN_4O_2S_3^+$ 460.9962; Found 460.9962.

2-((5-((4-chlorobenzyl) thio)-1,3,4-thiadiazol-2-yl) imino)-5-(4-hydroxy-3-methoxy benzylidene) thiazolidine-4-one (compound **6g**): Yellow solid, 0.436g, Yield 89%; MP = 207-210 ^{0}C; ^{1}H NMR (400 MHz, DMSO-d_6) δ_H: 12.81 (s, 1H), 10.02 (s, 1H), 7.71 (s, 1H), 7.48 – 7.46 (m, 2H), 7.41 – 7.38 (m, 2H), 7.27 (d, *J* = 2.12 Hz, 1H), 7.12 (dd, *J* = 8.36, 2.04 Hz, 1H), 7.00 (d, *J* = 8.28 Hz, 1H), 4.53 (s, 2H), 3.83 (s, 3H) ppm; ^{13}C NMR (101 MHz, DMSO-d_6) δ_C: 170.1, 167.1, 160.7, 158.8, 149.7, 148.0, 135.8, 133.9, 132.2, 130.9, 130.8, 128.5, 128.5, 128.5, 124.4, 123.5, 119.5, 116.4, 115.6, 55.7, 40.1, 39.9, 39.7, 39.5, 39.3, 39.1, 38.8, 36.3 ppm; HRMS (ESI/TOF-Q) *m/z*: $[M + H]^+$ Calcd. for $C_{20}H_{16}ClN_4O_3S_3^+$ 491.0068; Found 491.0063.

5-(benzylidene)-2-((5-((2,4-dichloro benzyl) thio)-1,3,4-thiadiazol-2-yl) imino) thiazolidine-4-one (compound **7a**): Yellow solid, 0.436g, Yield 89%; MP = 187-190 ^{0}C; ^{1}H NMR (300 MHz, DMSO-d_6) δ_H: 12.97 (s, 1H), 7.79 (s, 1H), 7.68 – 7.65 (m, 3H), 7.61 – 7.48 (m, 4H), 7.43 (dd, *J* = 8.28, 2.19 Hz, 1H), 4.61 (s, 2H) ppm; ^{13}C NMR (75 MHz, DMSO-d_6) δ_C: 170.6, 166.6, 160.3, 158.9, 134.3, 133.4, 133.2, 133.0, 132.7, 130.5, 130.2, 129.4, 129.1, 127.6, 123.8, 40.3, 40.0, 39.8, 39.5, 39.2, 38.9, 38.6, 34.7 ppm; HRMS (ESI/TOF-Q) *m/z*: $[M + H]^+$ Calcd. for $C_{19}H_{13}Cl_2N_4OS_3^+$ 478.9623; Found 478.9612.

2-((5-((2,4-dichloro benzyl) thio)-1,3,4-thiadiazol-2-yl) imino)-5-(3-fluoro benzylidene) thiazolidine-4-one (compound **7b**): Yellow solid, 0.462g, Yield 93%; MP = 174-177 ^{0}C; ^{1}H NMR (400 MHz, DMSO-d_6) δ_H: 13.04 (s, 1H), 7.79 (s, 1H), 7.67 (d, *J* = 2.22 Hz, 1H), 7.65 – 7.58 (m, 2H), 7.53 – 7.48 (m, 2H), 7.43 (dd, *J* = 8.4, 2.4 Hz, 1H), 7.39 – 7.33 (m, 1H), 4.61 (s, 2H) ppm; ^{13}C NMR (101 MHz, DMSO-d_6) δ_C: 170.3, 168.8, 166.8, 163.5, 161.1, 160., 158.4, 135.5, 134.4, 133.4, 133.3, 132.8, 131., 131.5, 129.1, 129.1, 127.7, 125.7, 125.5, 117.5, 117.2, 117.1, 116.9, 40.2, 40.1, 39.9, 39.7, 39.5, 39.3, 39.1, 38.9, 38.9, 34.7 ppm; ^{19}F NMR (376 MHz,

DMSO-d_6) δ_F: -111.59 ppm; HRMS (ESI/TOF-Q) *m/z*: $[M + H]^+$ Calcd. for $C_{19}H_{12}Cl_2FN_4OS_3^+$ 496.9529; Found 496.9525.

2-((5-((2,4-dichloro benzyl) thio)-1,3,4-thiadiazol-2-yl) imino)-5-(4-fluoro benzylidene) thiazolidine-4-one (compound **7c**): Yellow solid, 0.452g, Yield 91%; MP = 186-190 ^{0}C; ^{1}H NMR (300 MHz, DMSO-d_6) δ_H: 12.97 (s, 1H), 7.79 (s, 1H), 7.72 (t, *J* = 8.64, 5.46 Hz, 2H), 7.67 (d, *J* = 2.1 Hz, 1H), 7.59 (d, *J* = 8.4 Hz, 1H), 7.45 – 7.39 (m, 3H), 4.60 (s, 2H) ppm; ^{13}C NMR (75 MHz, DMSO-d_6) δ_C: 170.3, 166.9, 160.3, 158.5, 134.3, 133.4, 133.2, 132.7, 131.9, 129.7, 129.1, 127.6, 123.5, 116.7, 116.4, 40.3, 40.0, 39.8, 39.5, 39.2, 38.9, 38.6, 34.6 ppm; ^{19}F NMR (376 MHz, DMSO-d_6) δ_F: -108.46 ppm; HRMS (ESI/TOF-Q) *m/z*: $[M + H]^+$ Calcd. for $C_{19}H_{12}Cl_2FN_4OS_3^+$ 496.9529; Found 496.9527.

5-(4-chloro benzylidene)-2-((5-((2,4-dichloro benzyl) thio)-1,3,4-thiadiazol-2-yl) imino) thiazolidine-4-one (compound **7d**): Yellow solid, 0.488g, Yield 95%; MP = 245-248 ^{0}C; ^{1}H NMR (300 MHz, DMSO-d_6) δ_H: 13.00 (s, 1H), 7.78 (s, 1H), 7.70 – 7.56 (m, 6H), 7.45 – 7.40 (m, 1H), 4.61 (s, 2H) ppm; ^{13}C NMR (75 MHz, DMSO-d_6) δ_C: 170.3, 168.8, 166.8, 158.3, 135.1, 134.3, 133.4, 133.2, 132.7, 131.8, 131.6, 129.5, 129.1, 127.6, 124.5, 40.3, 40.0, 39.8, 39.5, 39.2, 38.9, 38.6, 34.7 ppm; HRMS (ESI/TOF-Q) *m/z*: $[M + H]^+$ Calcd. for $C_{19}H_{12}Cl_3N_4OS_3^+$ 514.9204; Found 514.9201.

2-((5-((2,4-dichloro benzyl) thio)-1,3,4-thiadiazol-2-yl) imino)-5-(4-methoxy benzylidene) thiazolidine-4-one (compound **7e**): Yellow solid, 0.478g, Yield 94%; MP = 208-212 ^{0}C; ^{1}H NMR (300 MHz, DMSO-d_6) δ_H: 12.88 (s, 1H), 7.75 (s, 1H), 7.68 (d, *J* = 2.19 Hz, 1H), 7.61 (t, *J* = 8.73 Hz, 3H), 7.43 (dd, *J* = 8.28, 2.19 Hz, 1H), 7.15 (d, *J* = 8.55 Hz, 2H), 4.61 (s, 2H), 3.83 (s, 3H) ppm; ^{13}C NMR (75 MHz, DMSO-d_6) δ_C: 170.5, 167.1, 161.1, 160.1, 134.3, 133.4, 133.3, 132.7, 132.3, 129.1, 127.6, 125.5, 120.5, 115.0, 55.5, 40.3, 40.0, 39.8, 39.5, 39.2, 38.9, 38.6, 34.7 ppm; HRMS (ESI/TOF-Q) *m/z*: $[M + H]^+$ Calcd. for $C_{20}H_{15}Cl_2N_4O_2S_3^+$ 508.9729; Found 508.9720.

2-((5-((2,4-dichlorobenzyl) thio)-1,3,4-thiadiazol-2-yl) imino)-5-(4-hydroxybenzylidene) thiazolidine-4-one (compound **7f**): Yellow solid, 0.450g, Yield 91%; MP = 219-223 ^{0}C; ^{1}H NMR (400 MHz, DMSO-d_6) δ_H: 12.82 (s, 1H), 10.40 (s, 1H), 7.69 (s, 1H), 7.66 (d, *J* = 2.20 Hz, 1H), 7.59 (d, *J* = 8.36 Hz, 1H), 7.52 (d, *J* = 8.36 Hz, 2H), 7.42 (dd, *J* = 8.24, 2.20 Hz, 1H), 6.96 (d, *J* = 8.52 Hz, 2H), 4.59 (s, 2H) ppm; ^{13}C NMR (101 MHz, DMSO-d_6) δ_C: 170.5, 167.2, 160.1, 159.9, 158.9, 134.3, 133.7, 133.4, 133.3, 132.7, 129.1, 127.6, 124.0, 119.1, 116.5, 40.1, 39.9, 39.7, 39.5, 39.3, 39.1, 38.8, 34.7 ppm; HRMS (ESI/TOF-Q) *m/z*: $[M + H]^+$ Calcd. for $C_{19}H_{13}Cl_2N_4O_2S_3^+$ 494.9572; Found 494.9589.

2-((5-((2,4-dichloro benzyl) thio)-1,3,4-thiadiazol-2-yl) imino)-5-(4-hydroxy-3-methoxy benzylidene) thiazolidine-4-one (compound **7g**): Yellow solid, 0.467g, Yield 89%; MP = 192-195 ^{0}C; ^{1}H NMR (400 MHz, DMSO-d_6) δ_H: 12.84 (s, 1H), 10.04 (s, 1H), 7.72 (s, 1H), 7.68 (d, *J* = 2.20 Hz, 1H), 7.59 (d, *J* = 8.32 Hz, 1H), 7.43 (dd, *J* = 8.36, 2.24 Hz, 1H), 7.28 (d, *J* = 2.08 Hz, 1H), 7.13 (dd, *J* = 8.32, 2.08 Hz, 1H), 7.00 (d, *J* = 8.28 Hz, 1H), 4.60 (s, 2H), 3.83 (s, 3H) ppm; ^{13}C NMR (101 MHz, DMSO-d_6) δ_C: 170.5, 167.1, 160.0, 159.0, 149.7, 148.0, 134.3, 134.0, 133.4, 133.3, 132.7, 129.1, 127.6, 124.4, 123.5, 119.4, 116.4, 115.6, 55.8, 40.1, 39.9, 39.7, 39.5, 39.3, 39.1, 38.9, 34.8 ppm; HRMS (ESI/TOF-Q) *m/z*: $[M + H]^+$ Calcd. for $C_{20}H_{15}Cl_2N_4O_3S_3^+$ 524.9678; Found 524.9697.

2.4. Anticancer activity study:

2.4.1. Materials and methods:

The *in vitro* cytotoxicity of all the synthesised compounds was evaluated on different cancer cell lines and normal human cell lines using the MTT assay procedure. The MTT assay was performed on a mouse triple-negative breast cancer cell line (4T1), human luminal A breast cancer cell line (MCF-7), human triple-negative breast cancer (TNBC) cell line (MDA-MB-231), human prostate cancer cell line (PC3) and mouse oral squamous cell carcinoma cell line (MOC2)**,** and normal human embryonic kidney cell line (HEK-293). All the cell lines were

procured from the National Centre for Cell Science (NCCS, Pune, India). 4T1, MCF-7, MDA-MB-231, PC3, MOC2, and HEK-293 cell lines were primarily cultured in DMEM (Dulbecco's modified eagle medium, high glucose media: AL007S) enriched with 10% fetal bovine serum (FBS) and 1% antibiotic (Pen strep: A001). The cultures were incubated at 37 °C under a 5% CO_2 atmosphere during the experiment. MTT [3-(4,5-dimethylthiazol-2-yl)-2,5-diphenyltetrazolium bromide], a yellow dye, was used to determine cell viability. All the required reagents were directly purchased from Himedia Laboratories Pvt. Ltd., Mumbai, India.

2.4.2. Chemicals:

The DMSO stock solutions of all compounds at a 100 mM concentration were prepared and stored at 4 °C. Staining solutions for the nuclear staining assay, including DAPI, Acridine Orange (AO), DCFH-DA for ROS generation and cell cycle analysis, propidium iodide, and RNase, were purchased directly from Sigma-Aldrich. The apoptosis assay used the TACs Annexin-V/FITC-PI assay kit purchased from BioLegend.

2.4.3. MTT assay:

The cell viability assay was performed using MTT to determine the *in vitro* cytotoxicity of all the synthesised compounds against different cancer cell lines and normal cell lines, as well as their selectivity over normal human cell lines. 4T1, MCF-7, MDA-MB-231, PC3, and MOC2 cell lines were seeded in a 96-well plate with about 100µL/well at a density of $1x10^4$ cells and incubated overnight. After incubation, the old media were aspirated, and the cells were treated with a wide range of concentrations of test compounds, followed by an additional 48-hour incubation. After the treatment period, the media containing the compounds was aspirated, and 50 µL of a 5 mg/mL MTT solution in PBS was added. The mixture was then incubated for 3 h to form formazan crystals. After incubation, the MTT solution was aspirated, and 150 µL of DMSO was added to dissolve crystals. The absorbance was measured at the wavelengths 570

nm and 650 nm. The percentage cell viability was calculated, and the results were illustrated as a dose-response curve for the IC_{50} analysis using GraphPad Prism version 8.0.1. [18].

2.4.4. Apoptosis assay:

The Apoptosis Assay was performed using MCF-7 cells utilising the TACs/Annexin V kit from Biolegend, US. MCF-7 cells were seeded at a density of 5×10^4 cells per well in a flat-bottomed 12-well plate and allowed to attach overnight. After that, the medium was aspirated, and the cells were treated with compound **6e** in triplicate for 48 hours to determine its *in vitro* IC_{50} values. Trypsinization was performed after the cells were washed with ice-cold PBS twice. After trypsinisation, the cells were collected and centrifuged; the resulting cell pellet was washed with ice-cold PBS. It was then resuspended in 100 µL of freshly prepared Annexin V reagent, which consisted of 100 µL of double-distilled water, 10 µL of 10X binding buffer, 10 µL of propidium iodide (PI), and 1 µL of fluorescein isothiocyanate (FITC). Following a 30-minute dark incubation period, 400 µL of 1X binding buffer was added to dilute the samples to a final volume of 500 µL. Following incubation, the samples were examined using BD Biosciences' flow cytometry (BDAriaTM III).

2.4.5. Cell cycle analysis:

Flow cytometry was used to evaluate the cell cycle of cells treated with **compound 6e** using a BDAriaTM III. A 12-well plate was seeded with 5 x 10^4 MCF-7 cells per well and then incubated. The other day, the medium was aspirated, and the IC_{50} concentration of **compound 6e** was added. The treatment period was 48 h. Following the treatment, the cells were washed with PBS, trypsinized, and collected as a cell pellet. Following two ice-cold PBS washes of the pellet, 70% ice-cold ethanol was added dropwise and gently vortexed to yield the single-cell suspension. The fixed cells were kept overnight at -20 °C. After centrifuging the samples, the cell pellet was recovered and then resuspended in 500 µL of the staining solution, which was made with 20% w/v RNase, 2% w/v PI, and approximately 0.1% v/v Triton X-100 solution in

PBS. Following a 30-minute dark incubation period at room temperature, the dissolved samples were examined using flow cytometry in BD Biosciences BDAriaTM III. The X- and Y-axes of the dot plot were used to display the data as PI width vs. PI area, respectively. The histogram plotted with PI area vs. count on the X- and Y-axes, respectively, was used to examine the percentage population of DNA. Flow Jo_V10.7.1_CL software was used to analyse the data and determine the proportion of cells in each cell cycle phase.

2.4.6. Nuclear staining with DAPI and acridine orange (AO):

A nuclear staining assay was performed with the lead **compound 6e** in MCF-7 cells to determine the extent of DNA disintegration of the cancer cells. Flat-bottomed 12-well plates with coverslips were seeded with MCF-7 cells and left overnight for attachment. This was followed by media aspiration and treatment with a control of 1% DMSO solution, **compound 6e,** at the *in vitro* IC_{50} concentrations in the MCF-7 cells. After treatment, the 12-well plate was incubated for 48 hours. The cells were fixed using a 4% paraformaldehyde solution and stained with DAPI and AO. The extent of nuclear staining was visualised under a Laser Scanning Confocal Microscope (LSCM) DMI8 (Leica Microsystems, Germany) on 20x Magnification. The quantification of the apoptosis percentage was performed using ImageJ software. Significance was analysed using one-way ANOVA analysis, and the graph was plotted in GraphPad Prism™ version 8.0.1[18–20].

2.4.7. Intracellular ROS generation by DCFH-DA staining assay:

Using the 2, 7-dichlorofluorescein diacetate (DCFH-DA) assay, the generation of reactive oxygen species in MCF-7 cells following **compound 6e** treatment was examined. MCF-7 cells were seeded onto 12-well plates with coverslips, cultured for 24 hours, and then treated with the IC_{50} of **compound 6e** for 48 h. Following incubation, the old medium was removed by aspiration, and the cells were treated with 10 µM DCFH-DA (S0033-Beyotime) for 10 minutes at 37 °C in the dark, as per the standard protocol. Then, using a Laser Scanning Confocal

Microscope (LSCM) DMI8 (Leica Microsystems, Germany), set to 20x magnification and with excitation wavelengths of 485 nm and 535 nm, the intensity of the fluorescence was measured. The DCF-DA fluorescence in **compound 6e-**treated MCF-7 cells was compared to that of untreated (negative control) cells, where a fluorescence value of 1 was assumed. Concurrently, the rise in fluorescence intensity was computed compared to the control group. The relative fluorescence intensity (%) was calculated using Image J software. A one-way ANOVA analysis was used to determine significance, and GraphPad PrismTM version 8.0.1 was used to visualise the data [21–23]

3. Results and discussion:

3.1. Chemistry:

This research work reported new 1,3,4-thiadiazole and 1,3-thiazolidine-4-one-based binary heterocyclic compounds (**Table 2**), starting with thiosemicarbazide. Compound **1** was synthesised by reacting thiosemicarbazide/hydrazine carbothioamide with carbon disulfide (CS_2) in the presence of KOH in ethanol, leading to the production of a carbazate salt. This salt, upon acidification with dilute HCl (20%), undergoes cyclisation and produces compound **1**. The thiol group in compound **1** undergoes a substitution reaction with different benzyl chlorides in the presence of a weak base (K_2CO_3) in anhydrous dimethylformamide (DMF) at room temperature, producing various benzyl-substituted compounds **2(a-c)**.

Compound **3(a-c)** was obtained from the reaction of chloroacetyl chloride with **2(a-c)** in the presence of TEA in anhydrous THF at room temperature (RT). In the next step, chloroacetamide derivatives **3(a-c)** were reacted with ammonium thiocyanate (NH_4SCN) in ethanol under reflux conditions (80 °C) to yield compounds **4(a-c)**. Whereas compound **4 (a-c)** was reacted with seven different aromatic aldehydes using urea (NH_2CONH_2) as the catalyst and glacial acetic acid as a solvent under reflux (120 ^{0}C) yielded titled benzylidene derivatives **5(a-g)**, **6(a-g)**, and **7(a-g)** via Knoevenagel condensation (**Scheme 1**).

All the synthesised compounds were extensively characterised via spectral data analysis of ^{1}H NMR, ^{13}C NMR, ^{19}F NMR, and HRMS (Q-TOF). Furthermore, X-ray crystallographic analysis data (single-crystal XRD) confirmed the structure and geometry of compounds **6g** and **7f**. Compound **1's** ^{1}H-NMR spectra showed that the 5-amino-1,3,4-thiadiazole-2-thiol resonated at two singlet signals 13.137 (-SH) and 7.043 (-NH_2) ppm. Furthermore, two sharply distinct ^{13}C NMR signals at 181.02 ppm and 161.55 ppm are associated with the number '**2**' and '**5**' carbon atoms of the 1,3,4-thiadiazole ring. The disappearance of the sulfhydryl proton in compound **2 (a-c)** confirmed the substitution with the benzyl group. Additionally, the S-CH_2 benzylic proton and carbon resonated at 4.28-4.34 ppm (^{1}H NMR) and 36.053-38.935 ppm (^{13}C NMR), respectively, as well as new aromatic protons of the benzyl moiety appear in the ^{1}H NMR spectrum. In compounds **3 (a-c)**, the amide proton resonated at 12.8-13 ppm (^{1}H NMR) along with additional methylene protons (4.48-4.53 ppm) other than the S-CH_2 group. The amide carbonyl carbon in **3 (a-c)** resonated at 169-170 ppm. In compound **4 (a-c),** the amide proton in the thiazolidine-4-one ring shifted to 12.3 ppm (^{1}H NMR), and two methylene protons in the same ring resonated at 4.09-4.10 ppm. In the ^{1}H NMR of the final compound series (**5a-g, 6a-g, and 7a-g**), the disappearance of those methylene protons confirms the substitution with the benzylidene group, and the new vinylic proton resonated at 7.72-7.78 ppm. ^{19}F NMR showed that fluorine-atom in few compounds (**5b-c, 6b-c and 7b-c**) resonated at -108 to -111 ppm. HRMS (Q-TOF) data generated via ESI scanning in positive mode also supported the molar mass of the final compound series, as the experimental $(M+H)^{+}$ m/z value of the compound agreed with the calculated value (**Spectral Data**). The exact structure and geometry of the compound's series were verified by analogy with the single-crystal XRD-generated diagram of compound **6g** (CCDC-**2366716**) and compound **7f** (CCDC-**2366780**). Crystallographic data confirmed that compounds are Z, Z geometry isomers in their stereochemical features with respect to imine and vinylic double bonds present in the 1,3-thiazolidine-4-one ring.

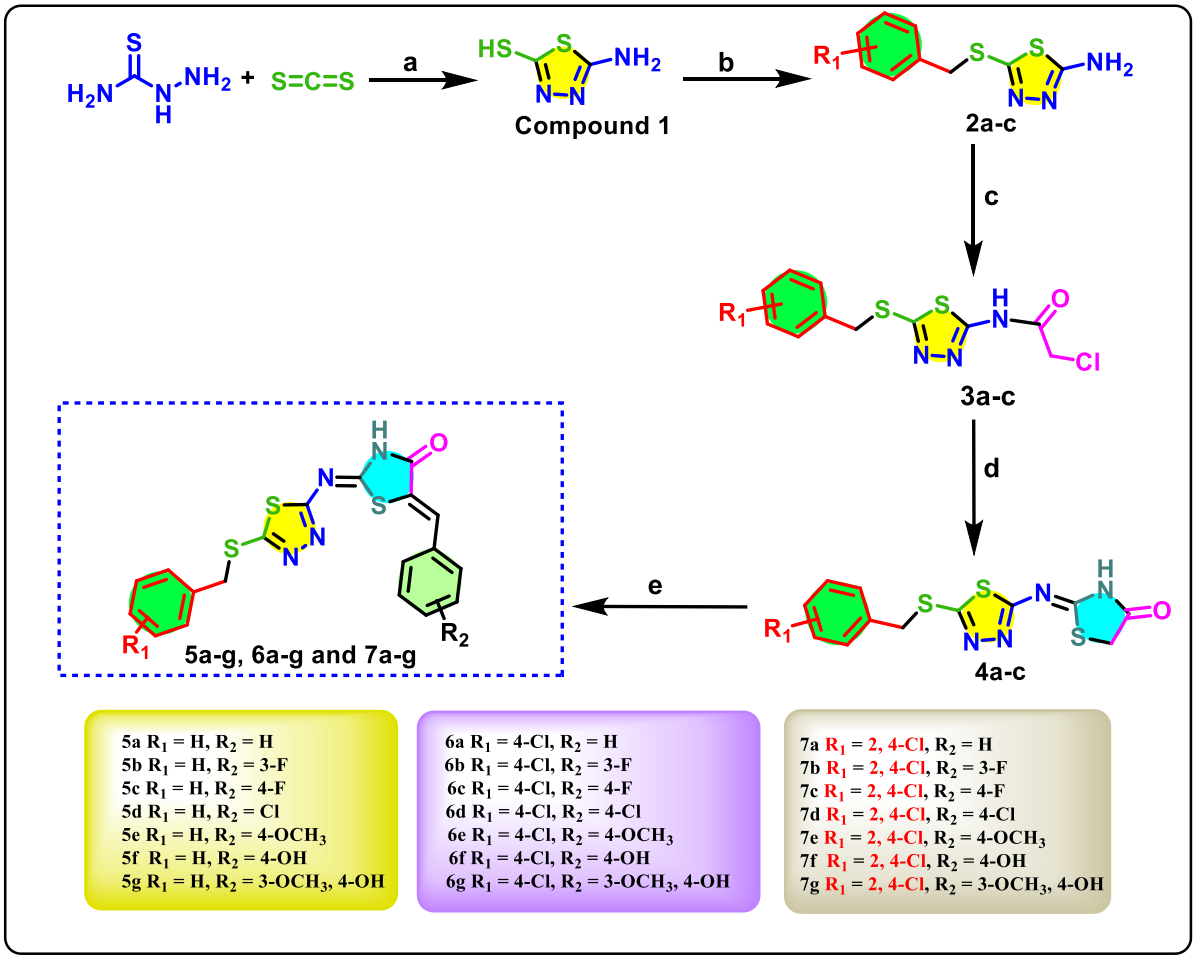

Scheme 1: Synthesis of hybrid compounds **5a-g**, **6a-g,** and **7a-g**. **Reagents and conditions:** a) i. Carbon disulfide (CS_2), Ethanol, 70-80 ^{0}C, reflux; ii. Dilute (20%) HCl; b) Substituted benzyl chlorides, K_2CO_3, dry DMF, rt; c) Chloroacetylchloride, TEA, dry THF, rt; d) Ammonium thiocyanate (NH_4SCN), Ethanol, 80 ^{0}C, Reflux; e) Benzaldehydes, Urea (1.5 equiv), Glacial acetic acid, 120 ^{0}C, Reflux.

3.2. Single-crystal (SC)-XRD Study (Compound 6g and 7f):

An X-ray crystallographic analysis was performed on two single crystals obtained, compounds **6g** and **7f** (**Figures 1** and **2**), using a single-crystal X-ray diffractometer (XRD, Bruker SMART, Germany). The XRD data helps to verify the actual structure and geometry of the developed compound series. The structures and geometries of all the other compounds were confirmed by analogy and verified through spectral data analysis, including NMR (^{1}H, ^{13}C, and ^{19}F) and HRMS (Q-TOF) studies. Crystallisation was achieved for compounds **6g** and **7f** using 1,4-dioxane and DMSO solvents via a gradual evaporation method at room temperature. We were

interested in the stereochemistry of the products, for which we provided the molecular geometry data in the crystals. These data can also be easily accessed from the Cambridge Crystallographic Data Centre (CCDC) through the link www.ccdc.cam.ac.uk/data_request/cif, with the unique identification numbers **2366716 (**Compound **6g)** and **2366780 (**Compound **7f)** for the deposited crystals. Crystal structures confirmed that the compounds exhibit Z, Z geometric isomerism regarding their stereochemical features in relation to the imine and vinylic double bonds present in the 1,3-thiazolidine-4-one ring (**S.F49 & Table S1**).

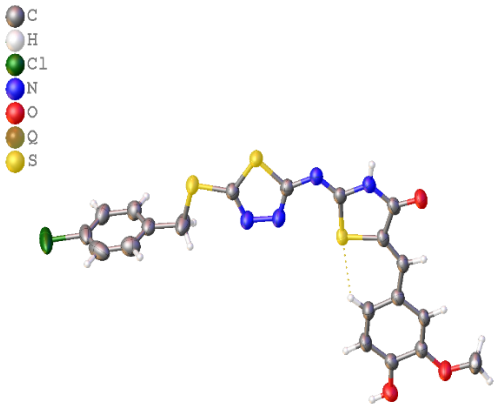

Figure 1: ORTEP diagram of compound **6g**.

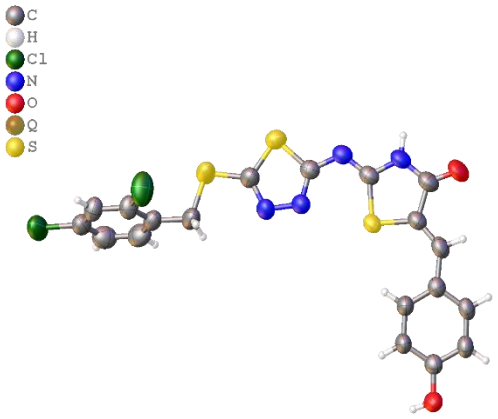

Figure 2: ORTEP diagram of compound **7f**.

3.3. Anticancer activity:

3.3.1. Cytotoxicity:

The cytotoxic effects of 1,3,4-thiadiazole-2-yl-imino-thiazolidine-4-one derivatives (**5a-g**, **6a-g**, and **7a-g**) were investigated on *in vitro* breast cancer cells (MCF-7, 4T1, and MDA-MB-231), prostate cancer cells (PC3), and oral cancer cells (MOC2) cell line using the MTT assay protocol [18–20]. The compounds were evaluated for their IC_{50} determination at concentrations ranging from 200 µM to 0.195 µM. The tested compounds were found to be more potent against MCF-7 cancer cell lines, with IC_{50} values ranging from 3.85 µM to 43.5 µM. The dose-cytotoxicity response curves of the molecules against MCF-7 (A), PC3 (B), 4T1 (C), MDA-

MB-231 (D) and MOC2 (E) are presented as sigmoidal curves (**Figure 3)**. Based on the results obtained from the *in vitro* cytotoxicity evaluation using the MTT assay, we identified the lead compound **6e** as the most active anticancer molecule, with an IC_{50} value of 3.85 μM against the MCF-7 cell line. The cytotoxic potency of the compounds was compared with that of **BG45,** a selective inhibitor of class I histone deacetylase (HDAC) that preferentially targets the HDAC3 isoform. It has been mentioned in the literature as a possible antitumour agent [24]. The maximum number of compounds displayed higher cytotoxicity than **BG45** in the MTT assay, where compound **6e (**IC_{50}: 3.85 μM) is the most active and identified as a lead molecule. Additionally, the results indicate a higher inhibitory potential against human breast cancer cell lines compared to other cancer cell lines.

Further, we have tested the synthesised compounds for their *in vitro* cytotoxicity against normal human embryonic kidney cell lines (HEK-293). **Table 2** presents the selectivity index (SI) of compounds on cancer cells compared to normal cells. Interestingly, it was found that all the compounds showed well-defined preferential selectivity towards cancer cell lines and had less cytotoxicity towards normal cell lines. The lead compound **6e** from the series exhibited more than 35-fold selectivity towards MCF-7 cell lines **(**IC_{50}: **3.85 μM)** than normal HEK-293 cell lines (IC_{50}: **138.10 μM**). The dose-response curves, along with the IC_{50} values of different compounds on various cancer cell lines and normal cell lines, are presented in the article (**Figure 3** and **Table 1**). Additionally, other mechanistic *in vitro* studies (outlined below) have been performed on the MCF-7 cell line using compound **6e** to deduce possible mechanisms of anticancer potency.

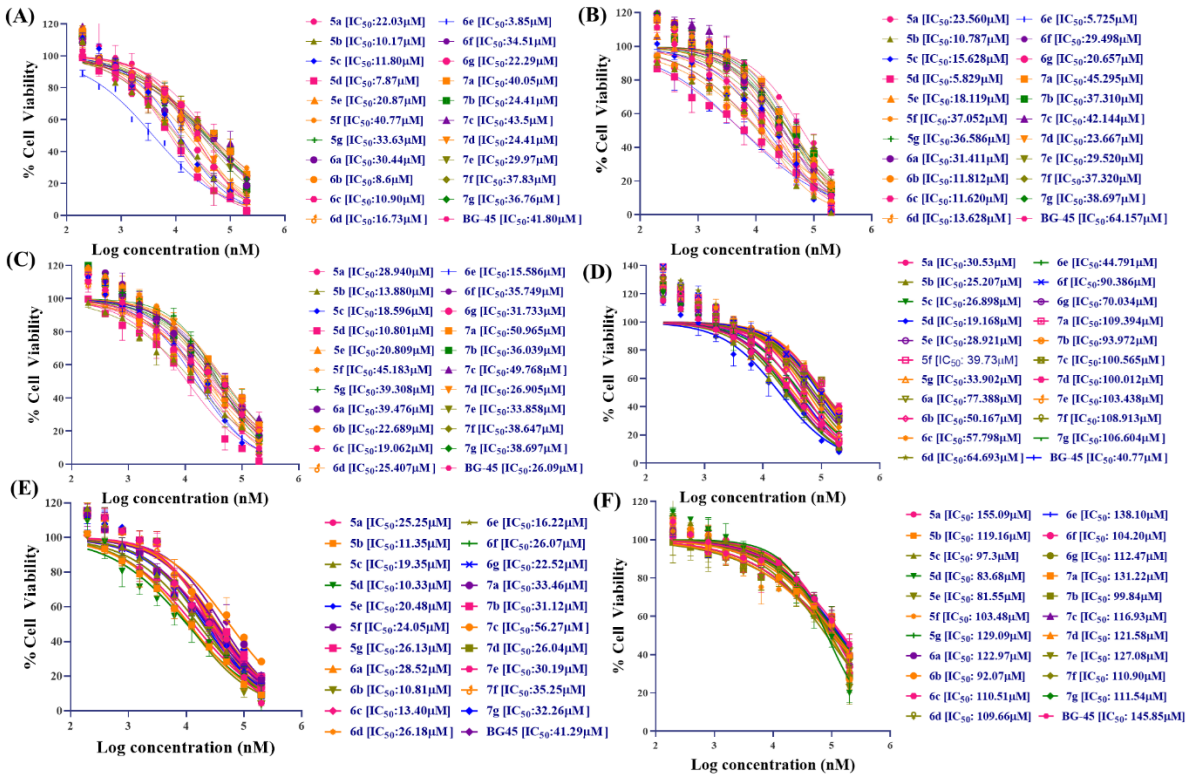

Figure 3: Dose-cytotoxicity response curve of the compound series (**5a-g, 6a-g and 7a-g**).

3.3.2. Structure-cytotoxic activity relationship (SAR):

When we investigated the structure-activity relation (SAR) of the compound series, we observed that the compound with the 4-OCH_3 arylidene moiety on the thiazolidine-4-one ring and a 4-Cl-benzyl thio moiety on the '2' positions of the 1,3,4-thiadiazole ring (**6e**) showed remarkably potent cytotoxic activity than compounds with either benzyl thio or 2,4-Cl-benzyl thio moiety on the exact position of 1,3,4-thiadiazole ring (**5e & 7e**). Whereas compounds with either 3-F (**5b** & **6b**) or 4-F (**5c** & **6c**) on arylidene moiety in the case of the first two series (**5a-g** & **6a-g**) showed better tolerability for cytotoxic effect than other functional groups or atoms, although exception for compound **6e** with 4-OCH_3 group on the same moiety having most potent activity. However, compounds (**7a-g**) with 2,4-Cl benzyl thio groups on '2' positions of the 1,3,4-thiadiazole showed less tolerability and very low cytotoxic potential (**Figure 4**).

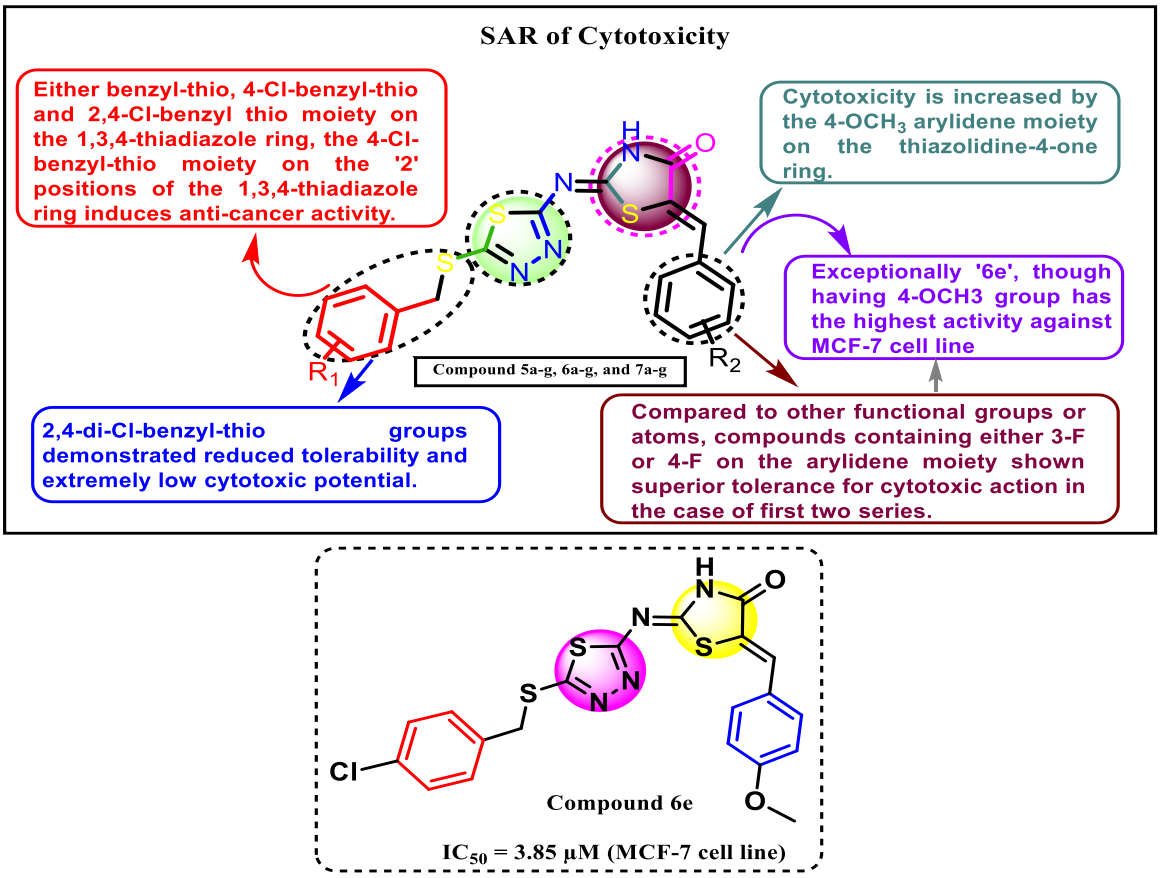

Figure 4: SAR of compound series (**5a-g, 6a-g and 7a-g**) for cytotoxic activity on various cancer cell lines.

3.3.3. Apoptosis and cell cycle analysis:

The cytotoxicity of the lead molecule compound **6e** has also been explored and validated using apoptosis and cell cycle analysis experiments with MCF-7 cells. The results indicated significant apoptotic activity and cell cycle arrest in the G0/G1 phase of the cell cycle when treated with compound **6e** (**Figure 6**). Cells were given treatment with an IC_{50} concentration as per the provided protocol [20]. Compound **6e** showed significant early and late apoptotic activity compared to the control group. **Figure 5** illustrates the percentage of apoptotic cells (early and late apoptosis). The lead compound **6e** induced 25.3% apoptotic death of MCF-7 cells in the Annexin-V apoptosis assay (**Figure 5**).

Cell cycle analysis of MCF-7 cells treated with compound **6e** revealed that it primarily blocked the G0/G1 phase, leading to an accumulation of the cell population in the G2/M phase.

Compound **6e** decreased the cell population in the G2/M phase from 11.6% in control cells to 5.6% in compound **6e**-treated MCF-7 cells. Additionally, there was a simultaneous increase in the cell population in the G0/G1 phase, resulting in cell cycle arrest at this stage of the cell cycle.

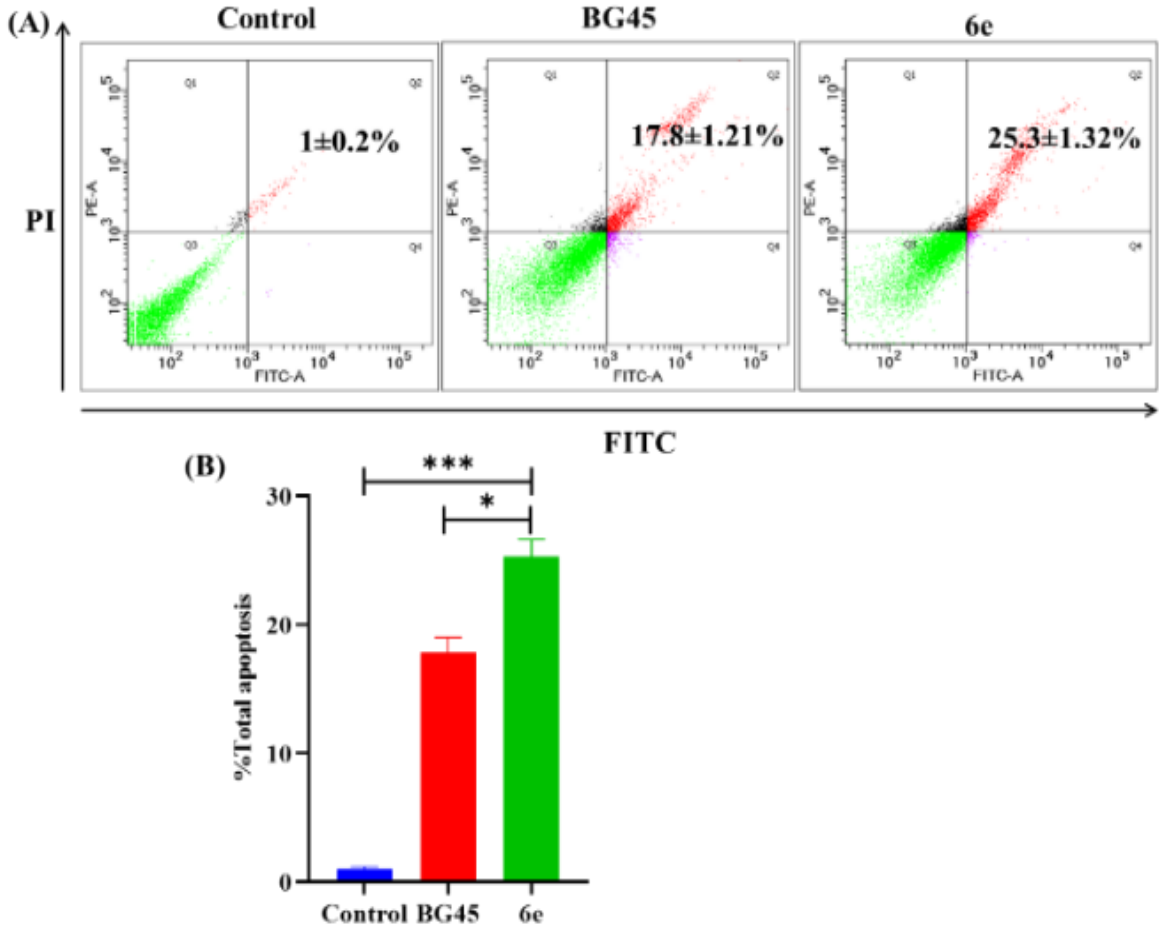

Figure 5: (A) Apoptosis analysis using Annexin V/PI assay double staining by flow cytometry. MCF-7 cells from the same cultures were treated with vehicle **Control**, **BG45**, and compound **6e** at their respective in vitro IC_{50} concentrations for 48 h (Q1 – Necrotic cells, Q2 - late apoptosis, Q3 – Live cells, Q4 – early apoptotic cells (X and Y-axis represent the intensities of annexin V and propidium iodide respectively); **(B)** Graphical representation of the total apoptotic percentage analysis in MCF-7 cells.

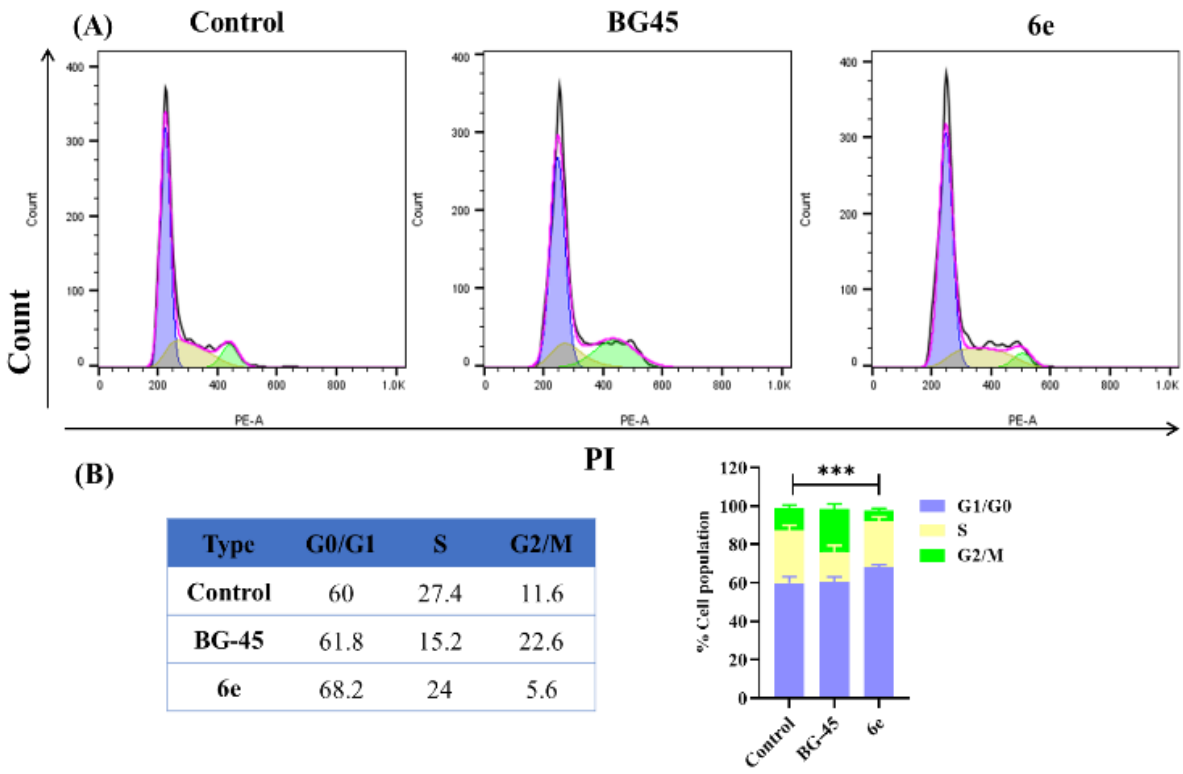

Type	G0/G1	S	G2/M
Control	60	27.4	11.6
BG-45	61.8	15.2	22.6
6e	68.2	24	5.6

Figure 6: (A) Cell cycle analysis using a Flow cytometer (BD Aria III) after treatment with vehicle **control**, reference compound **BG45**, and compound **6e** for 48 h. **(B)** Tabular and graphical representation of the percentage cell population at various cell cycle stages in MCF-7 cells, i.e., G1, S, and G2/M phases.

Table 1: The IC_{50} (cytotoxic effects) values of the final compound series (**5a-g, 6a-g and 7a-g**) and reference **BG45** on different cancer cell lines and normal HEK-293 cell lines.

Compounds	MCF-7 IC_{50} (µM)	PC3 IC_{50} (µM)	4T1 IC_{50} (µM)	MDA-MB-231 IC_{50} (µM)	MOC2 IC_{50} (µM)	HEK-293 IC_{50} (µM)
5a	22.03±0.13	23.56±0.22	28.94±0.22	25.29±0.27	30.53±0.19	155.09±0.23
5b	10.17±0.17	10.78±0.25	13.88±0.15	11.35±0.12	25.20±0.22	119.16±0.22
5c	11.80±0.18	15.62±0.21	18.59±0.16	19.52±0.25	26.89±0.23	97.3±0.20
5d	7.87±0.09	5.8±0.23	10.80±0.20	10.33±0.28	19.16±0.22	83.68±0.19
5e	20.87±0.09	18.11±0.17	20.80±0.19	20.63±0.22	28.92±0.23	81.55±0.30
5f	40.77±0.27	37.05±0.23	45.18±0.27	24.08±0.23	39.73±0.43	103.48±0.32
5g	33.63±0.25	36.58±0.21	39.30±0.23	26.44±0.25	33.90±0.31	129.09±0.23
6a	30.44±0.24	31.41±0.27	39.47±0.27	28.22±0.26	77.38±0.42	122.97±0.15
6b	8.6±0.09	11.81±0.15	22.68±0.28	10.39±0.13	50.16±0.34	92.07±0.18
6c	10.90±0.21	11.62±0.14	19.06±0.19	13.64±0.12	57.79±0.40	110.51±0.17

6d	16.73±0.25	13.62±0.21	25.40±0.15	26.10±0.25	64.69±0.52	109.66±0.19
6e	3.85±0.12	5.72±0.17	15.58±0.22	16.26±0.12	44.79±0.35	138.10±0.17
6f	34.51±0.23	29.49±0.26	35.74±0.28	26.02±0.25	90.38±0.52	104.20±0.21
6g	22.29±0.13	20.65±0.22	31.73±0.27	22.29±0.24	70.03±0.42	112.47±0.28
7a	40.05±0.29	45.29±0.21	50.96±0.26	33.81±0.31	109.39±0.56	131.22±0.18
7b	24.41±0.27	37.31±0.26	36.03±0.25	31.17±0.29	93.97±0.38	99.84±0.32
7c	43.5±0.35	42.14±0.28	49.76±0.31	56.30±0.31	100.56±0.42	116.93±0.16
7d	24.41±0.14	23.66±0.17	26.90±0.21	26.13±0.25	100.01±0.49	121.58±0.15
7e	29.97±0.22	29.52±0.28	33.85±0.25	30.49±0.28	103.43±0.43	127.08±0.32
7f	37.83±0.26	37.32±0.30	38.64±0.31	35.46±0.29	108.9±0.48	110.90±0.16
7g	36.76±0.24	38.69±0.33	38.69±0.30	32.59±0.29	106.60±0.41	111.54±0.30
BG45	50.80±0.30	64.15±0.25	26.03±0.34	41.80±0.25	40.77±0.31	145.85±0.19

Table 2: Final compounds series (**5a-g**, **6a-g,** and **7a-g**) with selectivity indices (SI) on different cancer cells.

Compounds	**Structure**	**SI**				
		MCF-7	**PC3**	**4T1**	**MDA-MB-231**	**MOC2**
5a	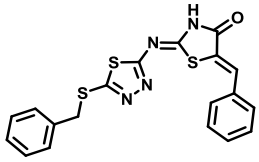	7.03	6.58	5.35	6.13	5.07
5b	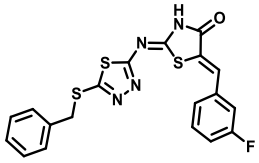	11.71	11.05	8.58	10.49	4.72
5c	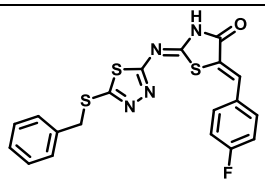	8.24	6.22	5.23	4.98	3.61
5d	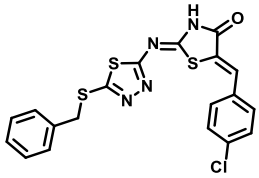	10.63	14.42	7.74	8.10	4.36

Compounds	Structure	SI				
		MCF-7	**PC3**	**4T1**	**MDA-MB-231**	**MOC2**
5e	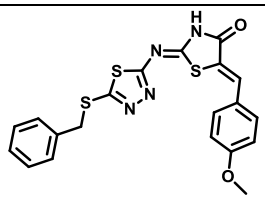	3.90	4.50	3.92	3.95	2.81
5f	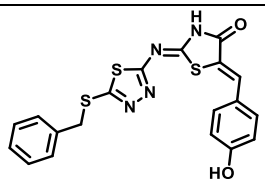	2.53	2.79	2.29	4.29	2.60
5g	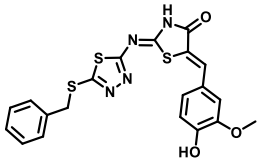	3.83	3.52	3.28	4.88	3.80
6a	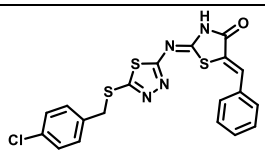	4.03	3.91	3.11	4.35	1.58
6b	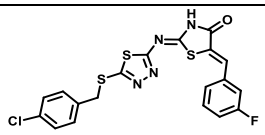	10.70	7.79	4.05	8.86	1.83
6c	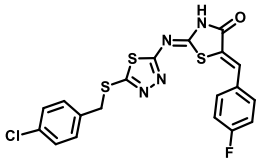	10.13	9.51	5.79	8.10	1.91
6d	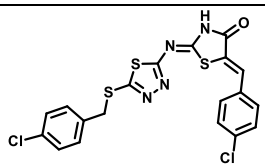	6.55	8.05	4.31	4.20	1.69
6e	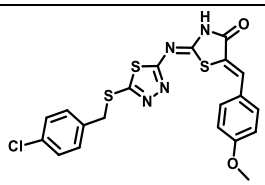	35.87	24.14	8.86	8.49	3.08
6f	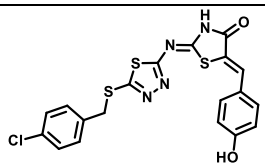	3.01	3.53	2.91	4.00	1.15

Compounds	Structure	SI				
		MCF-7	PC3	4T1	MDA-MB-231	MOC2
6g	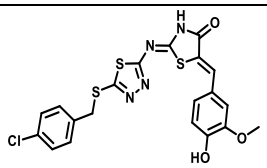	5.04	5.44	3.54	5.04	1.60
7a	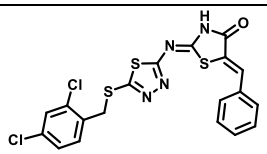	3.27	2.89	2.57	3.88	1.19
7b	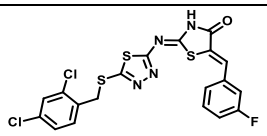	4.09	2.67	2.77	3.20	1.06
7c	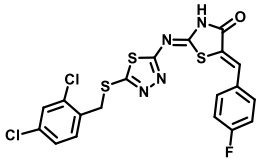	2.68	2.77	2.34	2.07	1.16
7d	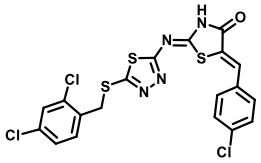	4.98	5.13	4.51	4.65	1.21
7e	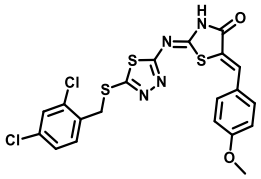	4.24	4.30	3.75	4.16	1.22
7f	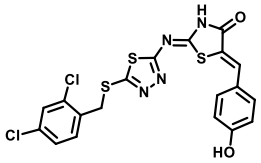	2.93	2.97	2.87	3.12	1.01
7g	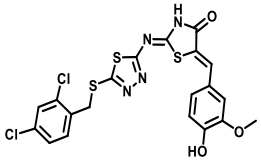	3.03	2.88	2.88	3.42	1.04

3.3.4. Nuclear staining assay (DAPI and AO):

DAPI is used to stain and detect apoptotic bodies. The cells that had undergone apoptosis will be stained brightly with DAPI, and they exhibit chromatin condensation and nuclear fragmentation, which are the characteristic features of apoptosis. Untreated or control cells will

have less fluorescence. Acridine orange (AO) is typically used to stain acidic vesicles in live cells, producing orange-to-red signals that help distinguish apoptotic cells from normal cells, which exhibit green fluorescence. A nuclear staining assay was performed using the lead molecule (compound **6e**) to assess the cytotoxicity of MCF-7 cell lines after treatment, employing DAPI and AO as the staining dyes and examining the results under a fluorescence microscope [19]. MCF-7 cells were treated with an IC_{50} concentration of the compound **6e** for 48h, followed by staining with DAPI/AO. There is a change in fluorescence pattern in AO staining from green to orange-red (**Figure 7**). Increased AO fluorescence in compound **6e**-treated cancer cells confirmed significant nuclear fragmentation (NF-cleavage of chromosomal DNA into fragments), accompanied by chromosomal condensation and cell shrinkage (CS-shrunken morphology of cells), which were attributed to the induction of apoptosis compared to the untreated control cells. This indicated the compound's cytotoxicity and suggested the apoptotic cell death mechanism.

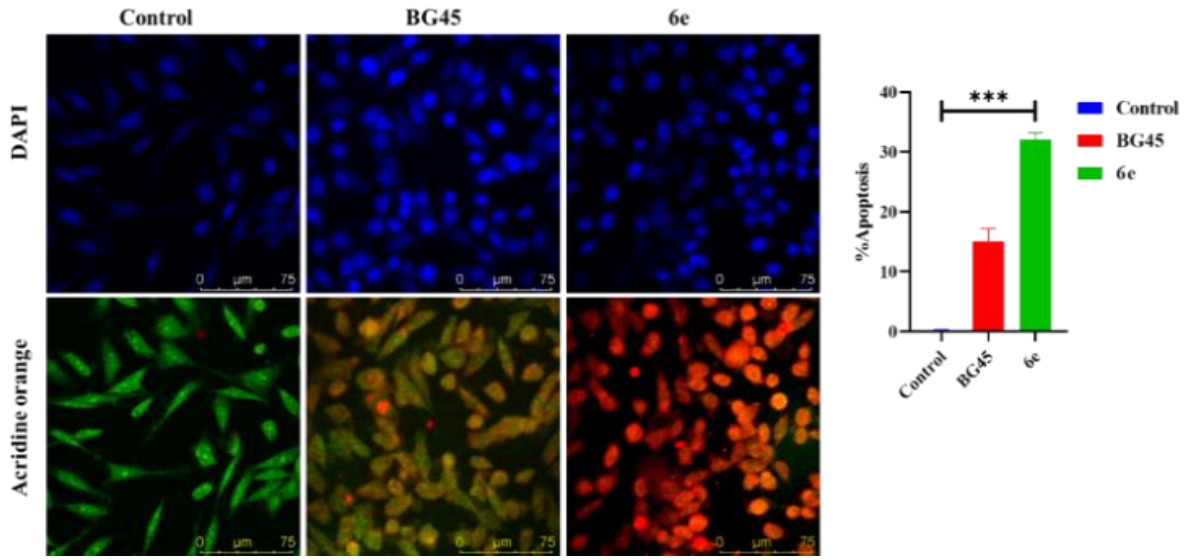

Figure 7: Analysis of the nuclear morphology by nuclear staining experiment after treatment with **BG45** and compound **6e**, along with control (A) MCF-7 cells using the staining solutions of DAPI and AO after the treatment period, and **(B)** Graph representing the % apoptosis quantified by ImageJ software. The values represent the mean ± SD (n = 3); ***p < 0.001. A laser scanning confocal microscope (DMI8, Leica Microsystems, Germany) was used at 20× magnification to visualise the stained nuclei.

3.3.5. Reactive oxygen species (ROS) formation in cancer cells:

The literature reports found that intracellular ROS generation plays a significant role in tumour suppression via cell death, inducing apoptosis through damage to nucleic acids and other cellular components. DCFH-DA enters the cells, where cellular esterases remove the acetyl groups, generating non-fluorescent DCFH. Upon oxidation by reactive oxygen species (ROS), DCFH is converted into DCF, which emits green fluorescence. Cancerous cells proliferate well under a moderate level of ROS, whereas a high level of ROS creates a stressful microenvironment, depolarising the mitochondria and killing the cells. We assessed whether the compound **6e** could promote the formation of reactive oxygen species (ROS) in the MCF-7 cell lines [25]. According to **Figure 8,** there is a marked enhancement of relative fluorescence intensity in MCF-7 cells after treatment with **compound 6e** at the IC_{50} dose compared to control, untreated cells (1% DMSO-treated cells). The results revealed the apoptosis mechanism of cancer cell death and the cytotoxicity of the compounds.

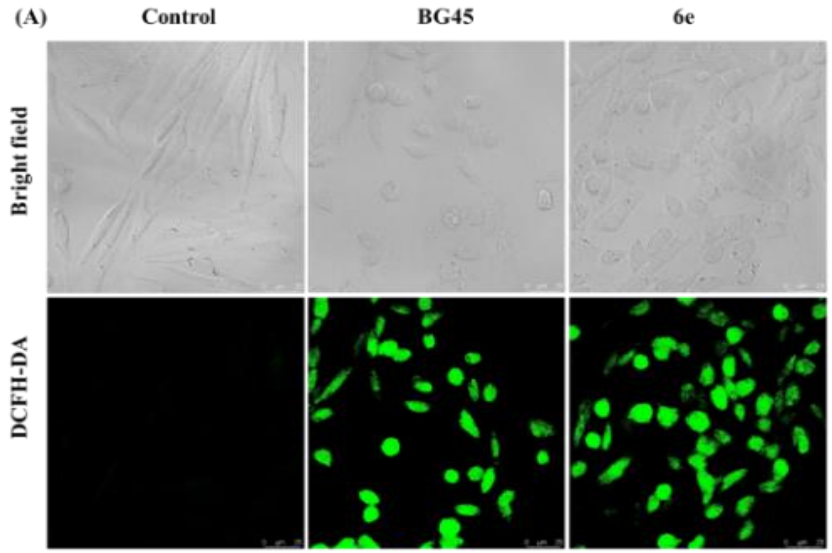

(B)

Type	Fluorescence intensity
Control	0.906
BG-45	18.287
6e	37.511

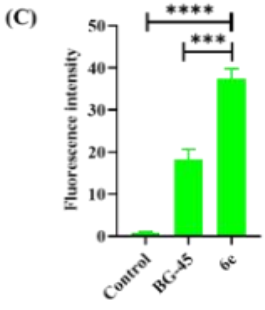

Figure 8: Detection of intracellular ROS generation by DCFH-DA. **(A)** 4T1 cells were stained using DCFH-DA dye after the treatment period, **(B)** a table representing the fluorescence intensity values quantified by Image J software, and **(C)** a plot of fluorescence intensity quantification obtained using Image J. A laser scanning confocal microscope (DMI8, Leica Microsystems, Germany) at 20× magnification was used to visualise ROS generation. Scale bars: 25 μm. The obtained values represent the mean ± SD (n = 3); ****$p < 0.0001$.

Spectral Data:

1. Copy of ^{1}H, ^{13}C and ^{19}F NMR data:

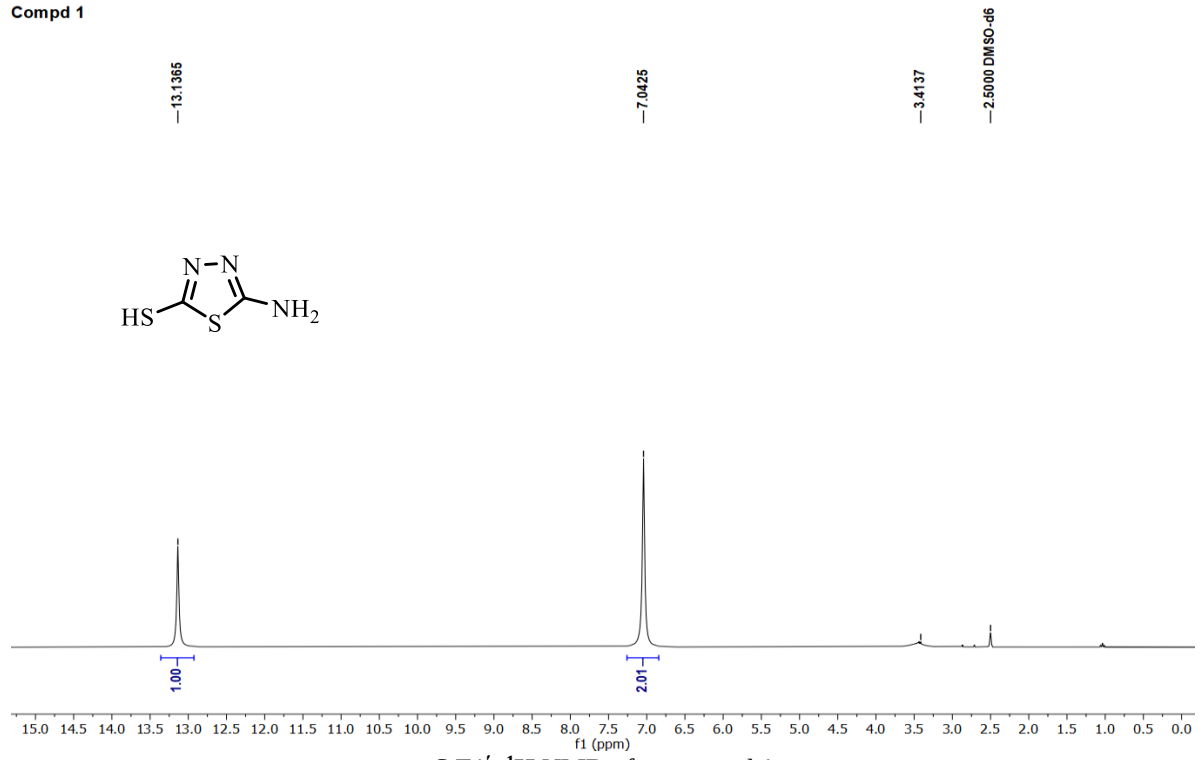

S.F1′: ^{1}H NMR of compound **1**

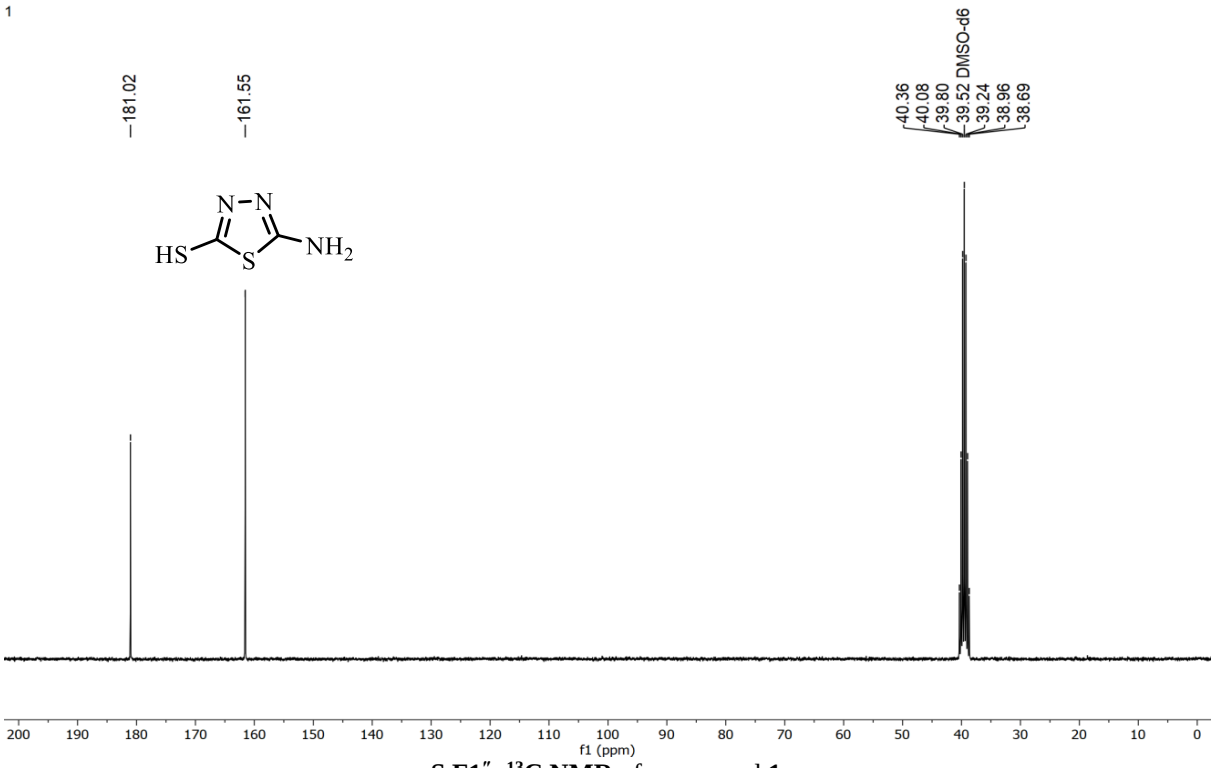

S.F1″: ^{13}C NMR of compound **1**

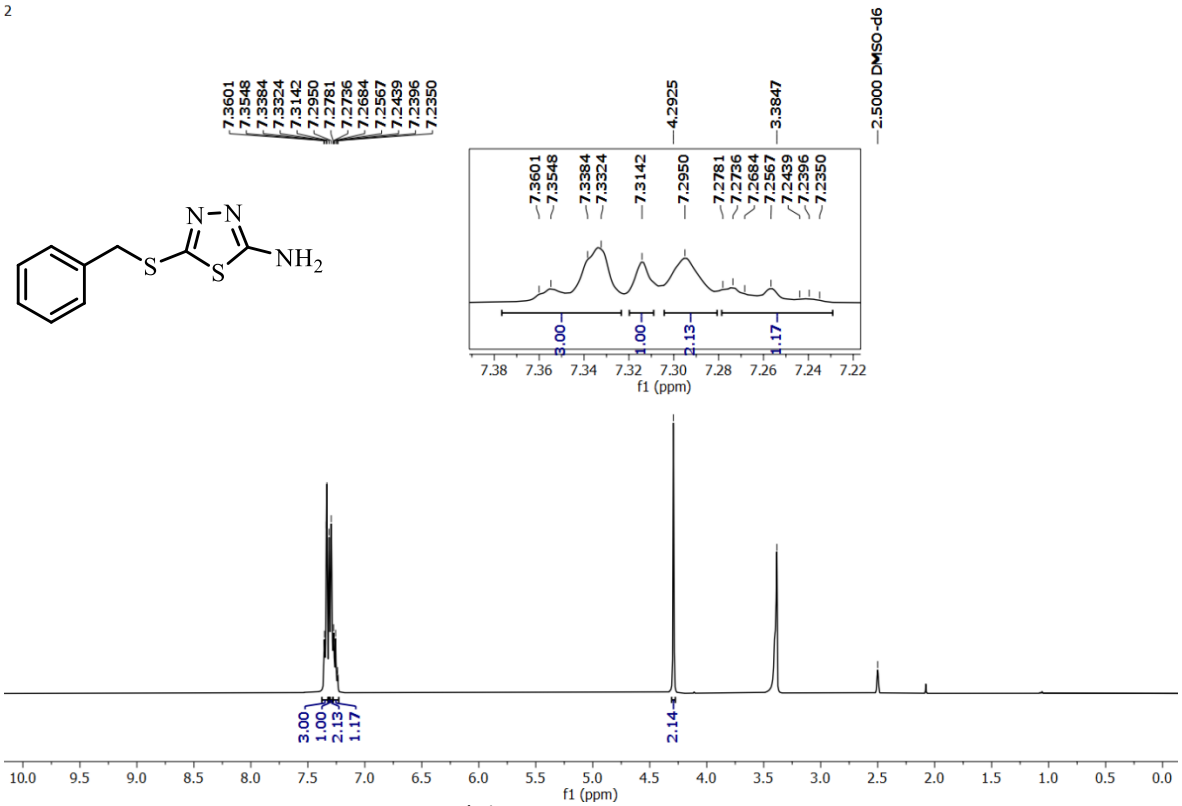

S.F2′: ^{1}H NMR of compound **2a**

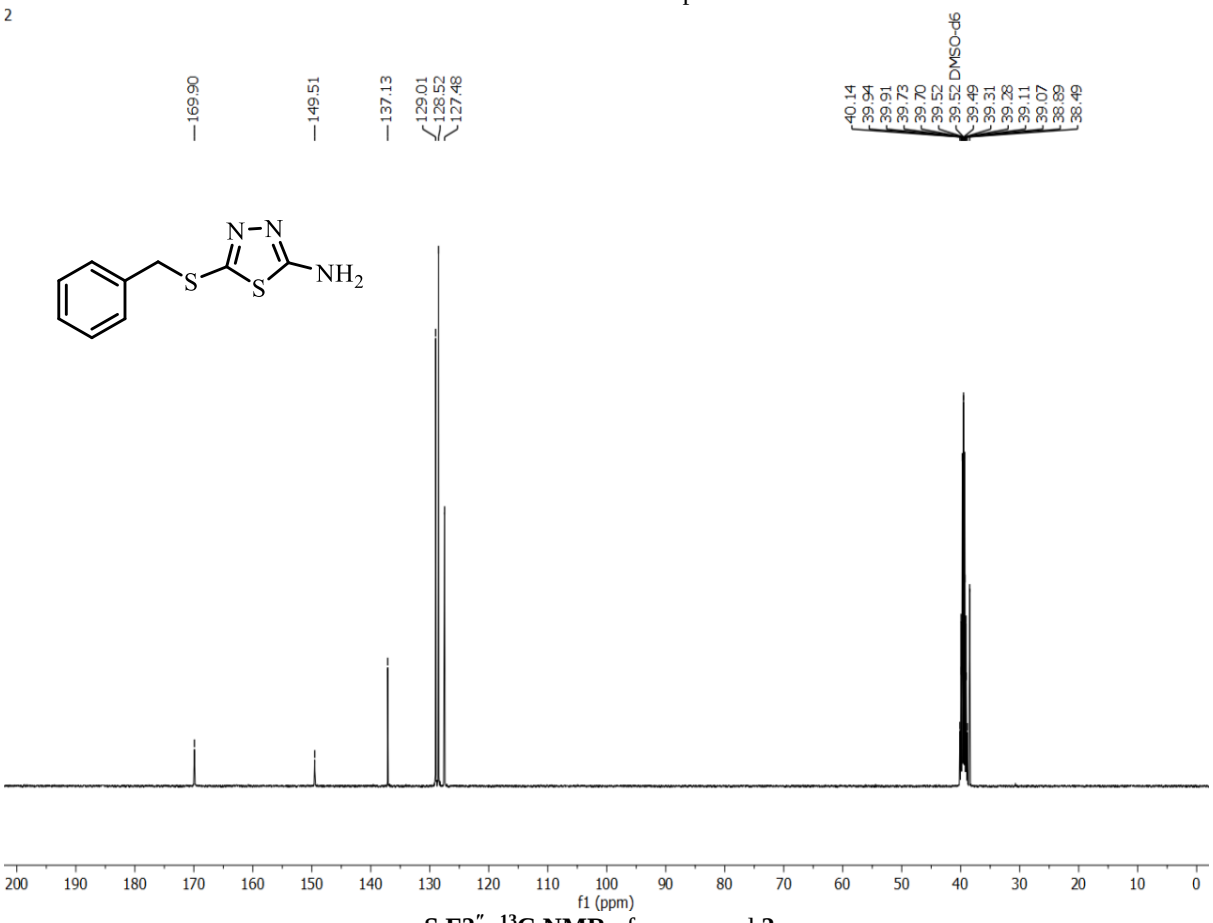

S.F2″: ^{13}C NMR of compound **2a**

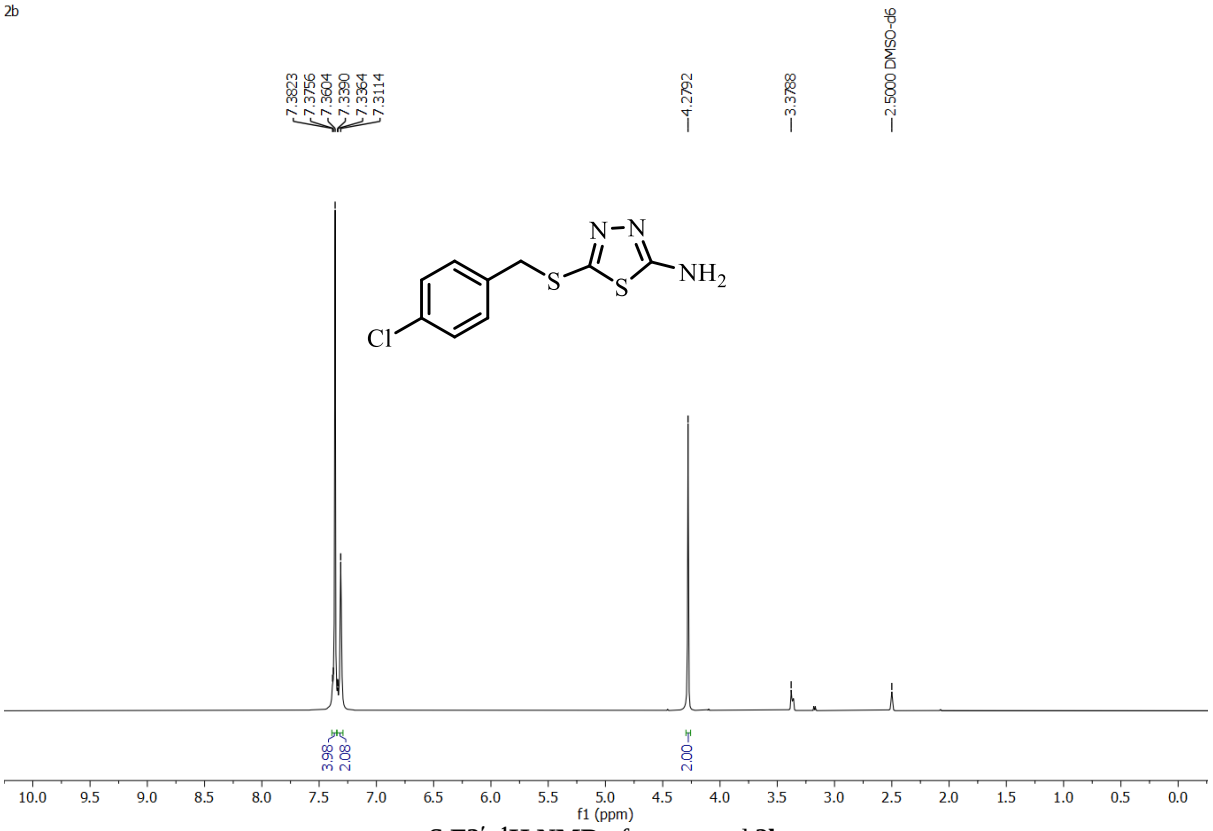

S.F3′: ^{1}H NMR of compound **2b**

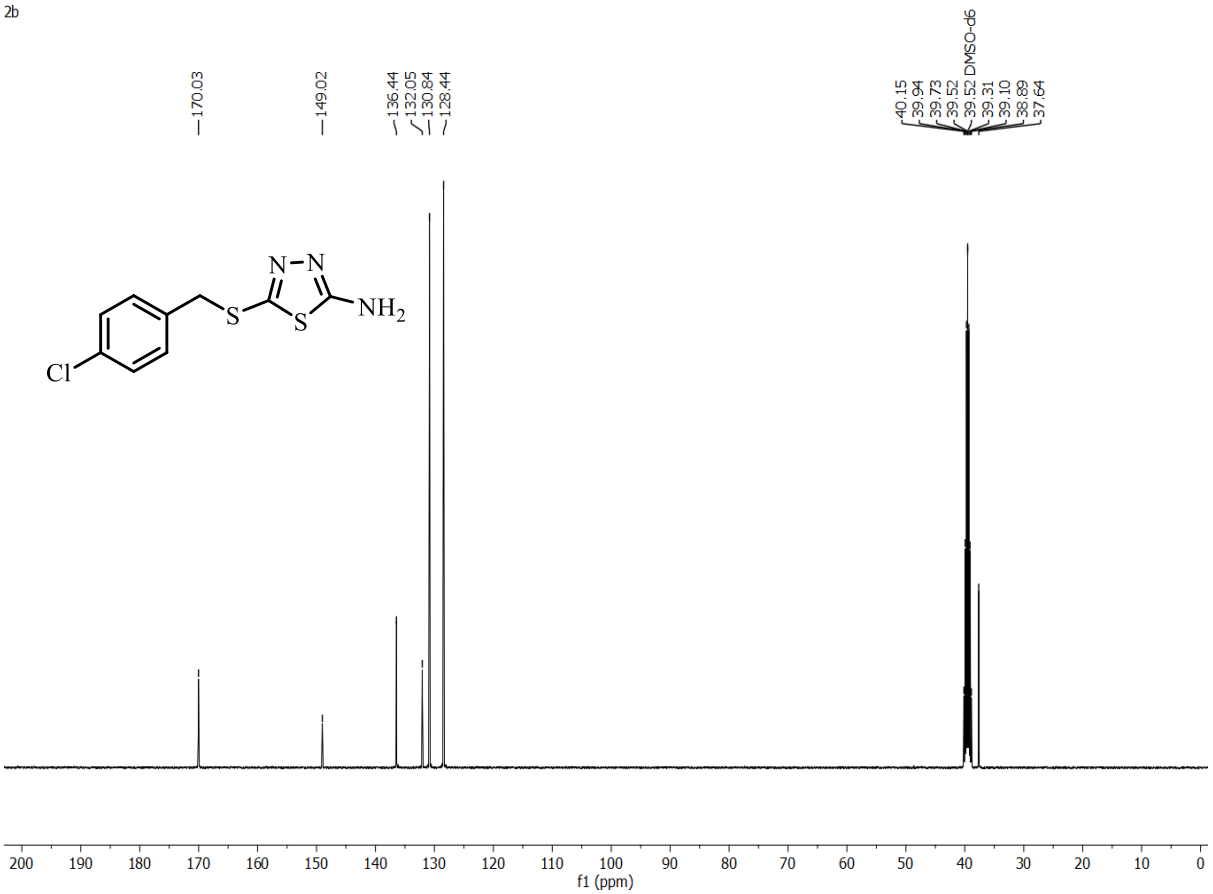

S.F3″: ^{13}C NMR of compound **2b**

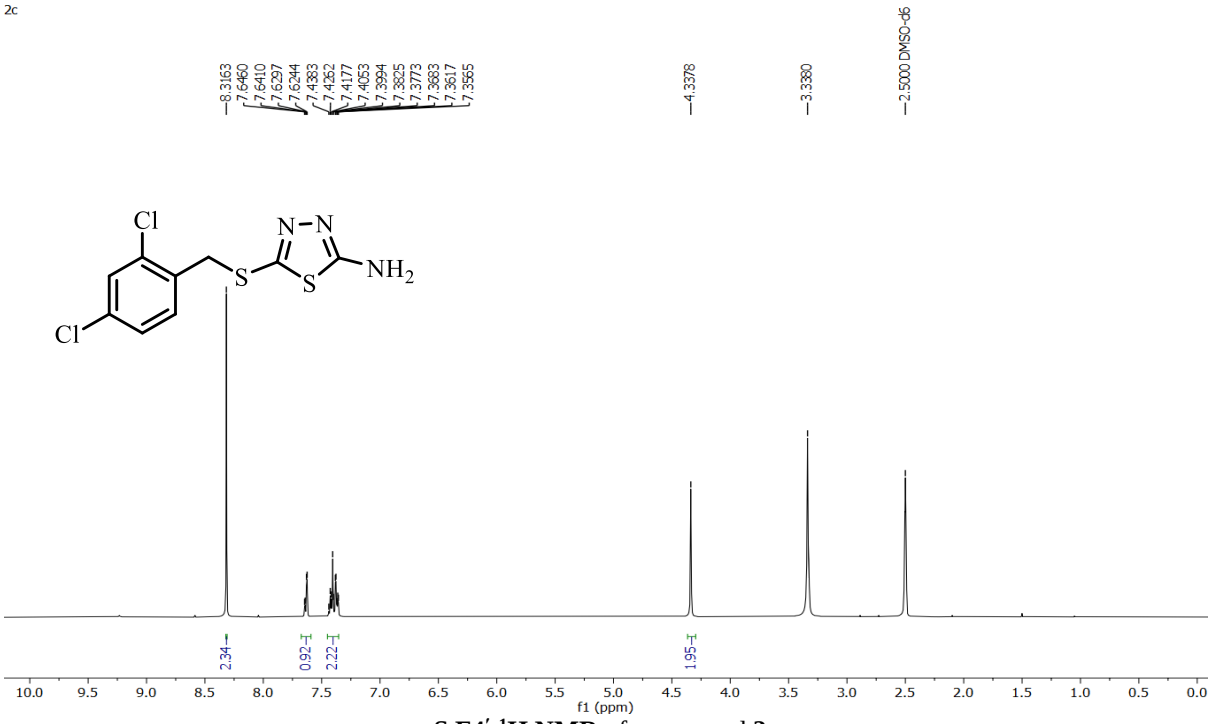

S.F4′:^{1}H NMR of compound **2c**

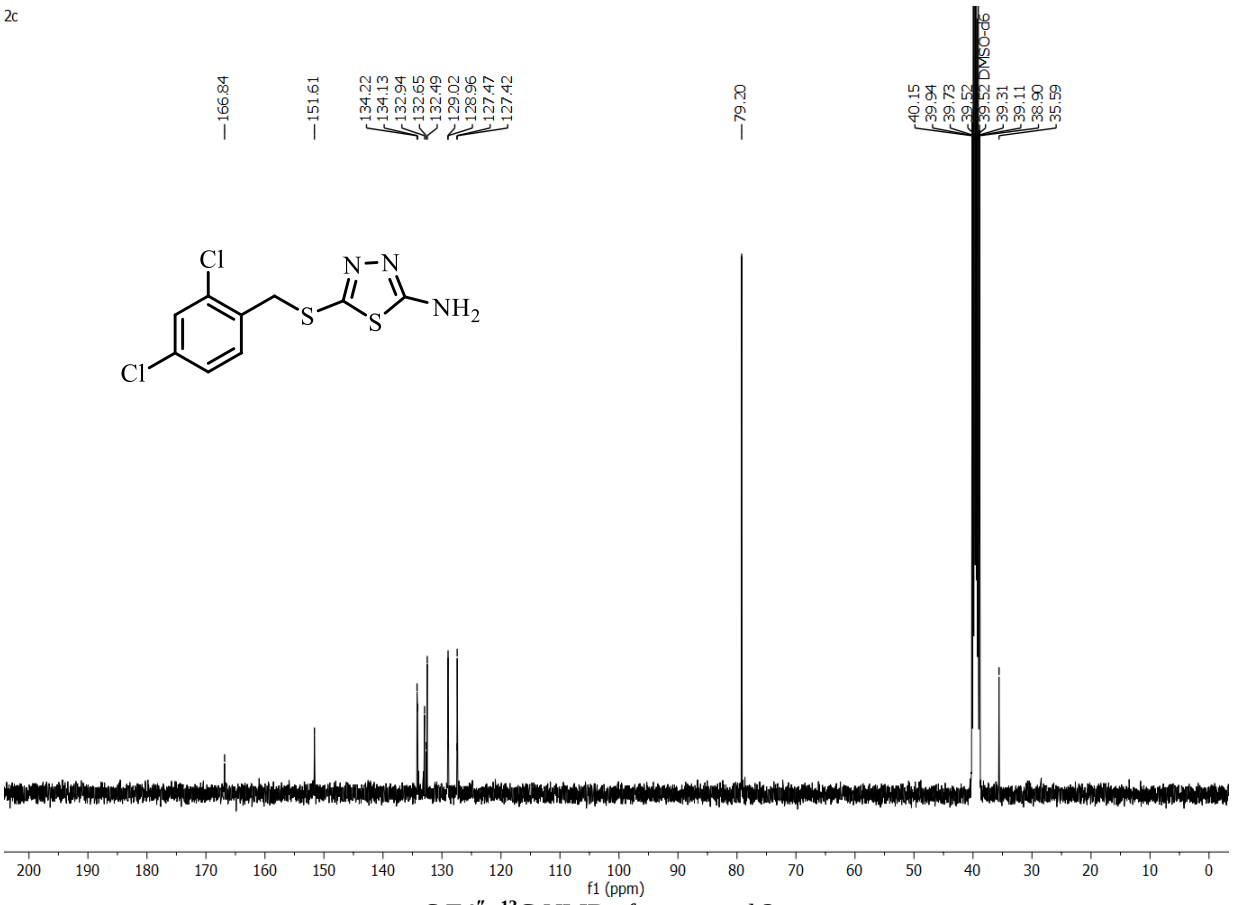

S.F4″: ^{13}C NMR of compound **2c**

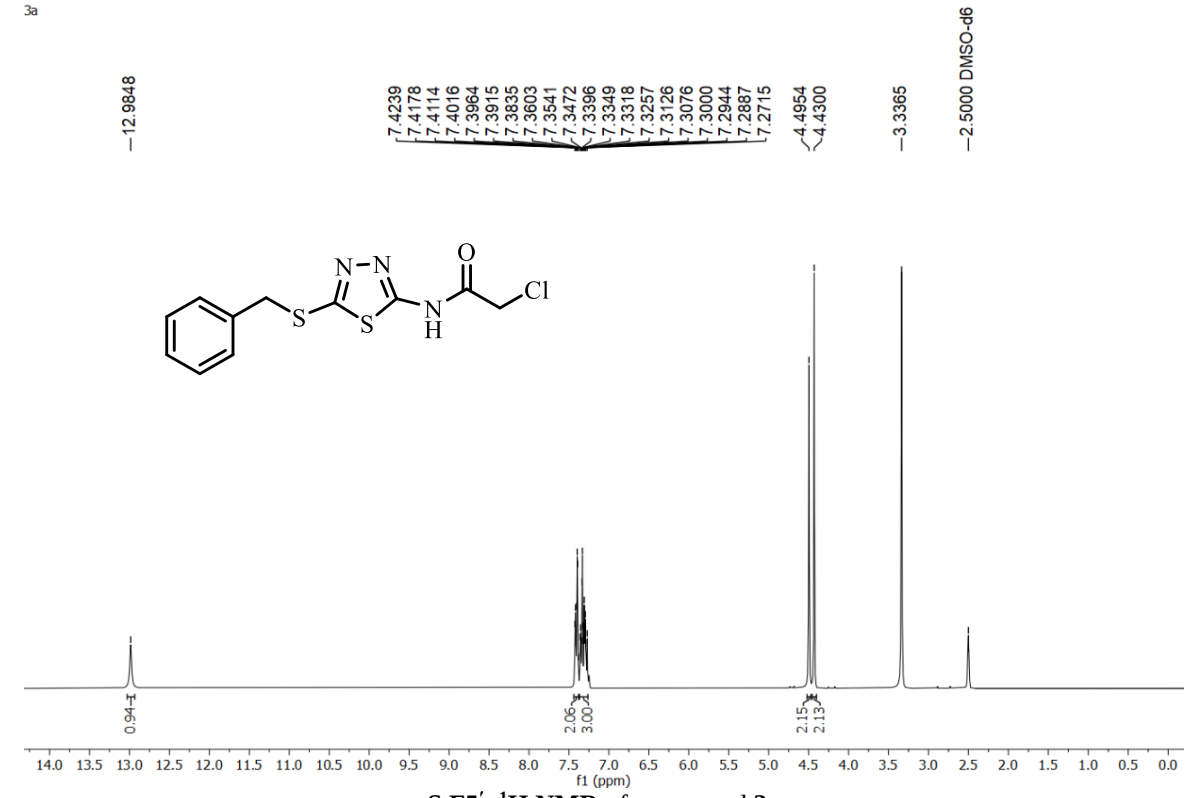

S.F5′: ^{1}H NMR of compound **3a**

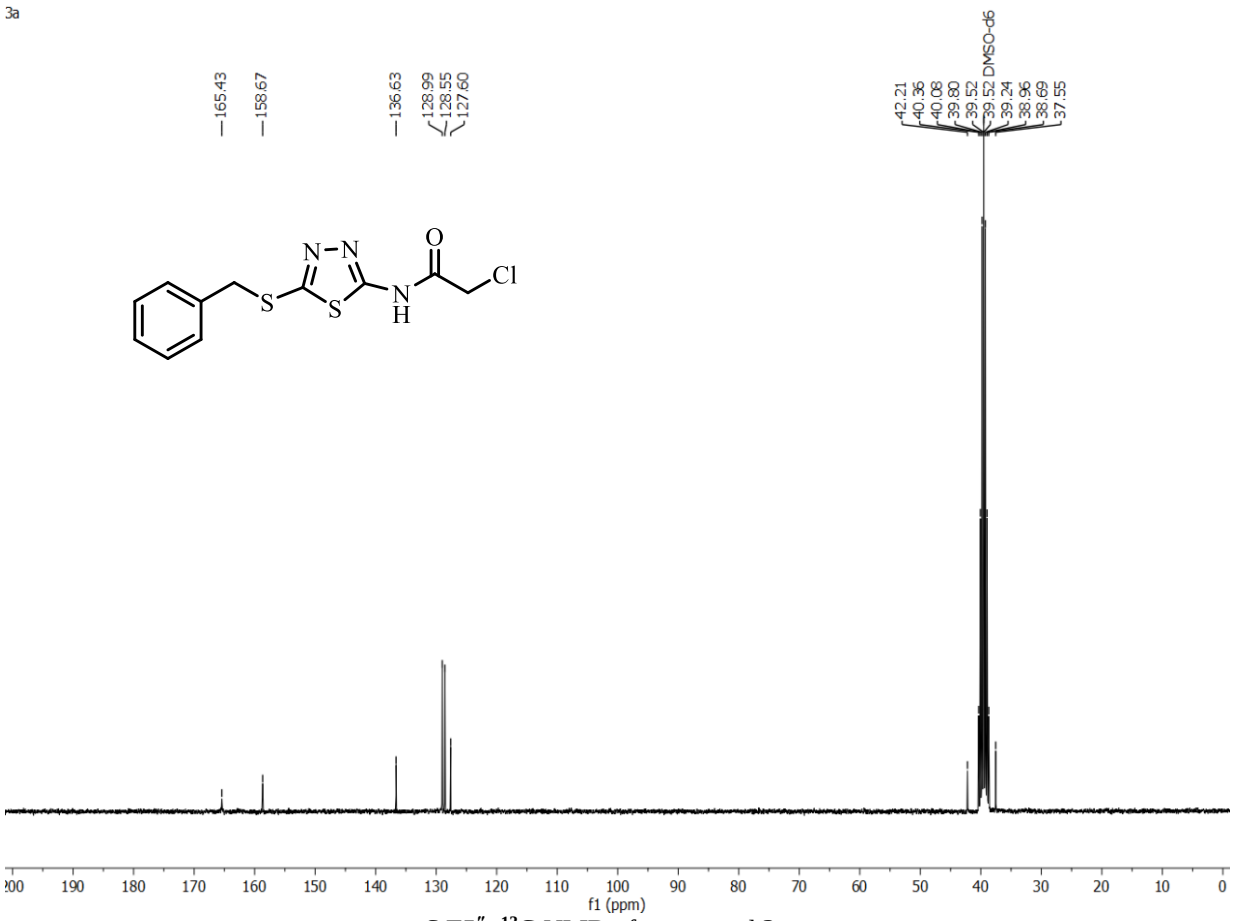

S.F5″: ^{13}C NMR of compound **3a**

S.F6′: ^{1}H NMR of compound **3b**

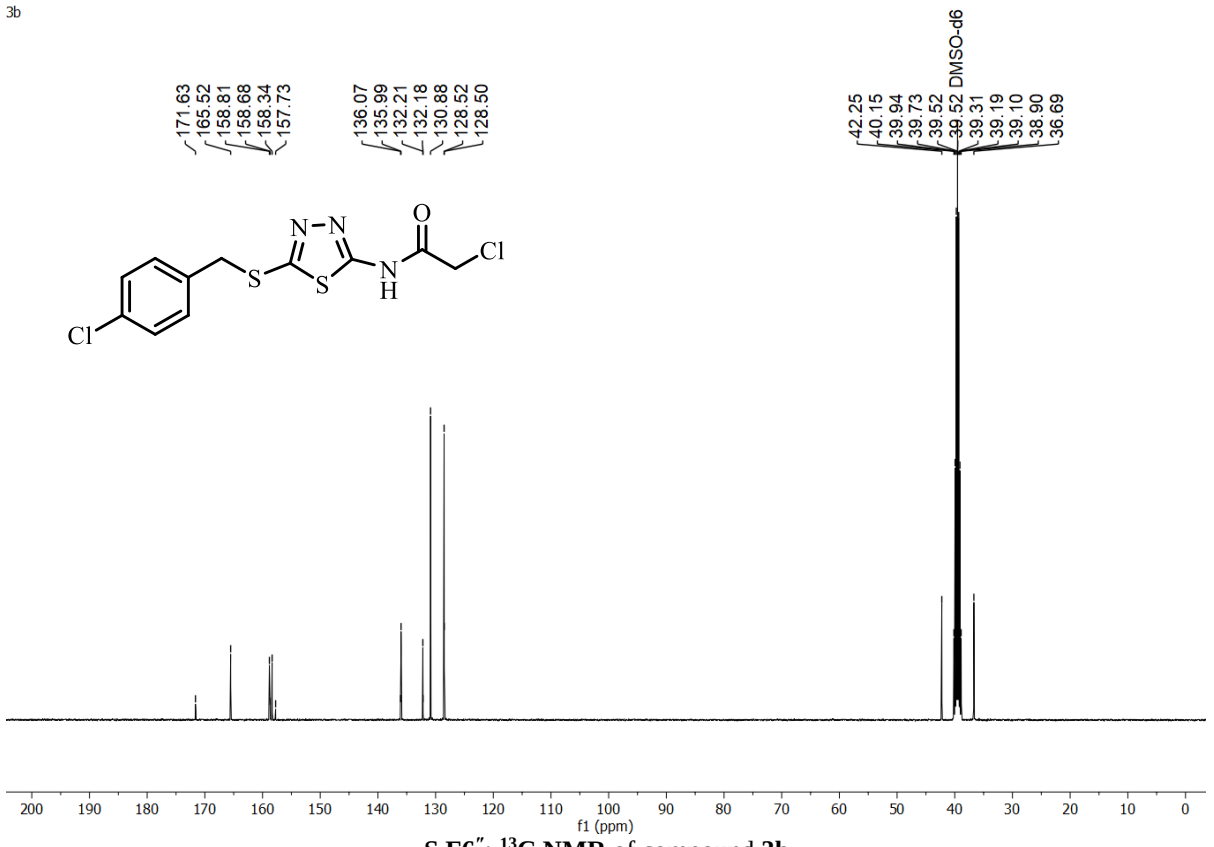

S.F6″: ^{13}C NMR of compound **3b**

S.F7′: ^{1}H NMR of compound **3c**

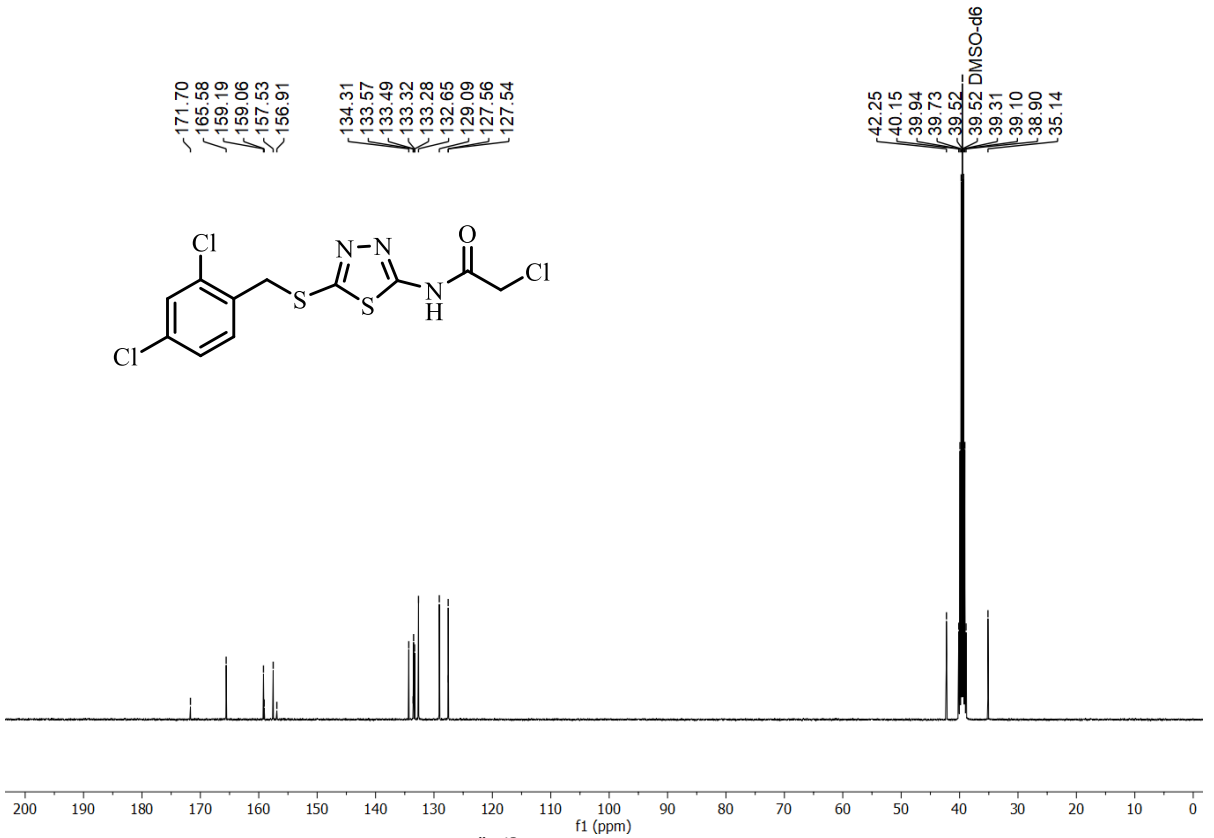

S.F7″: ^{13}C NMR of compound **3c**

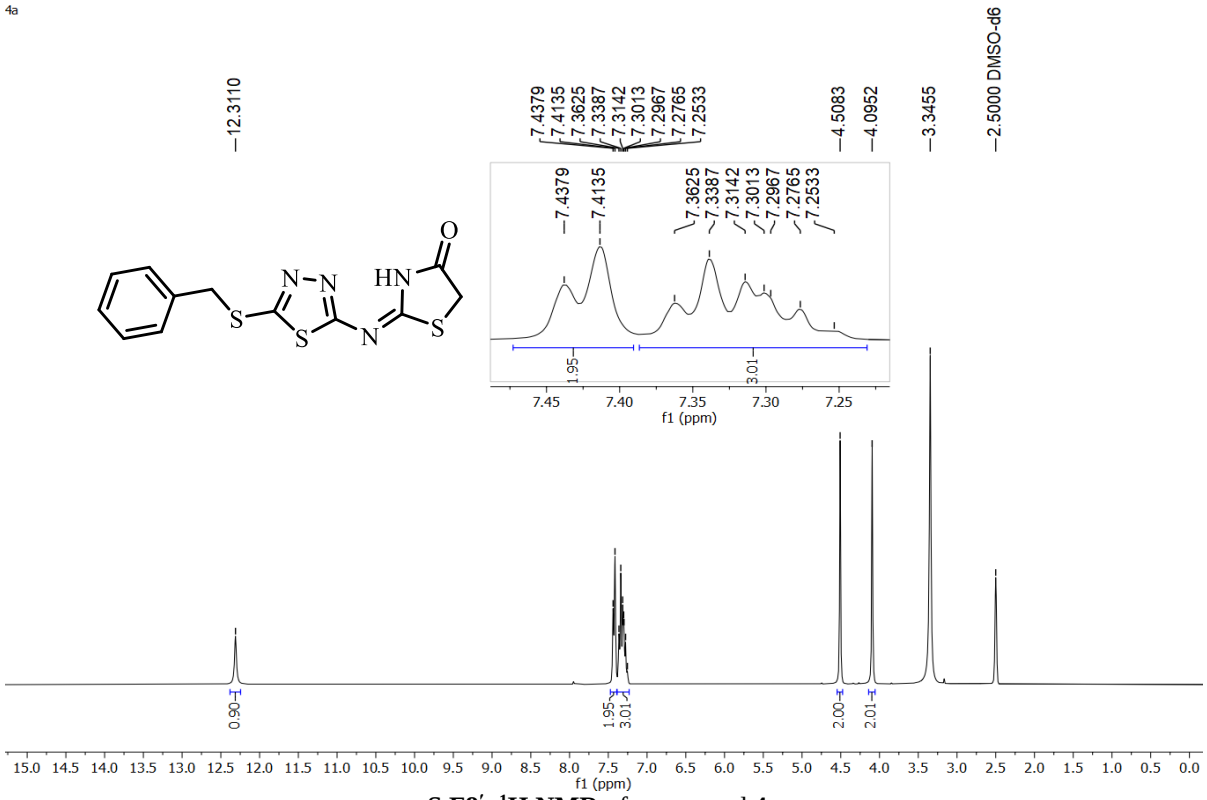

S.F8′: ^{1}H NMR of compound **4a**

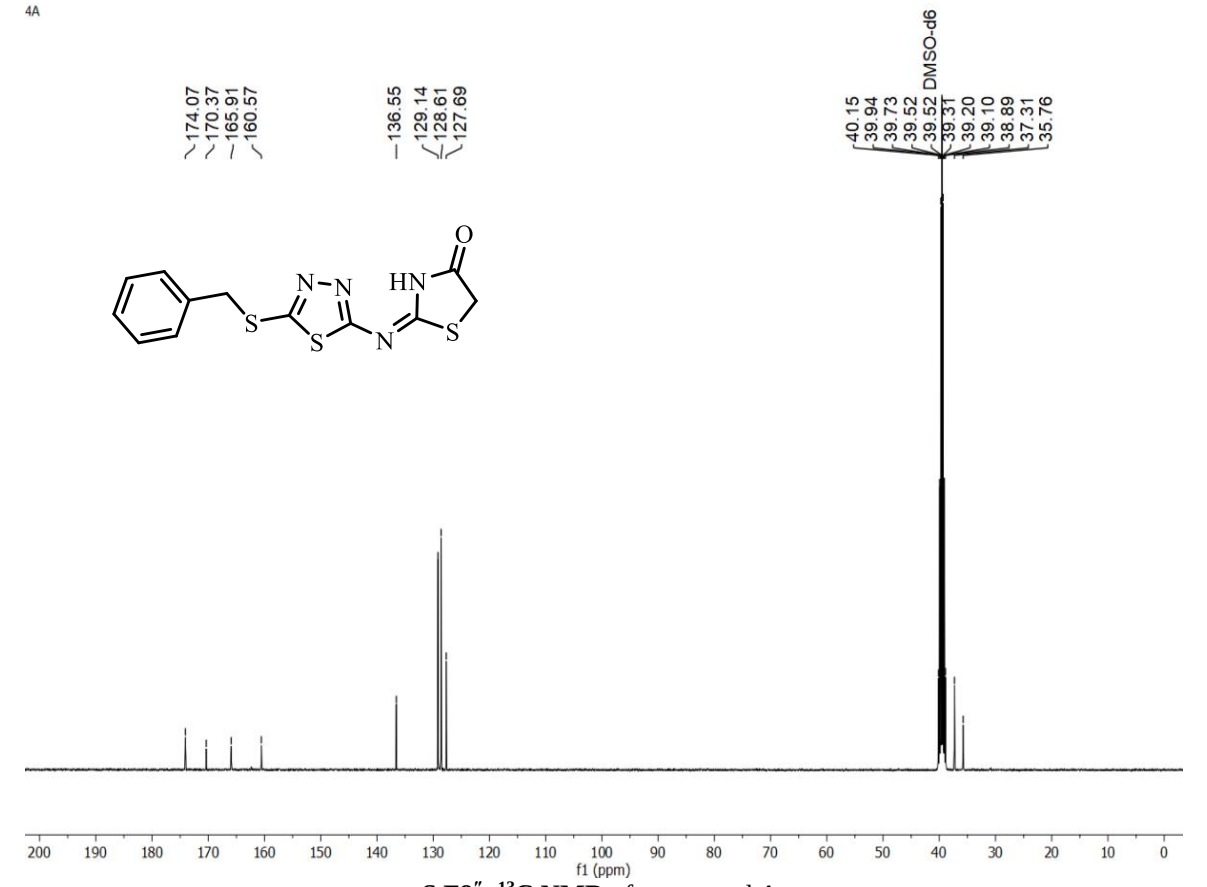

S.F8″: ^{13}C NMR of compound **4a**

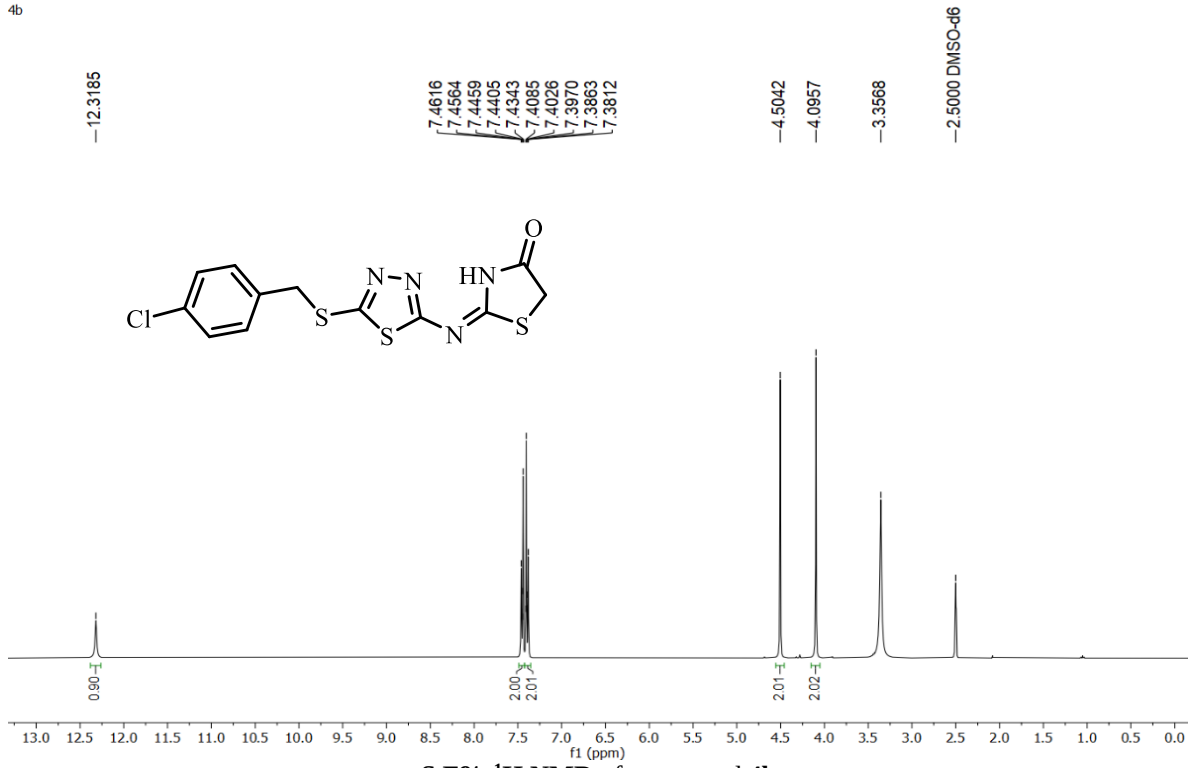

S.F9′: ^{1}H NMR of compound **4b**

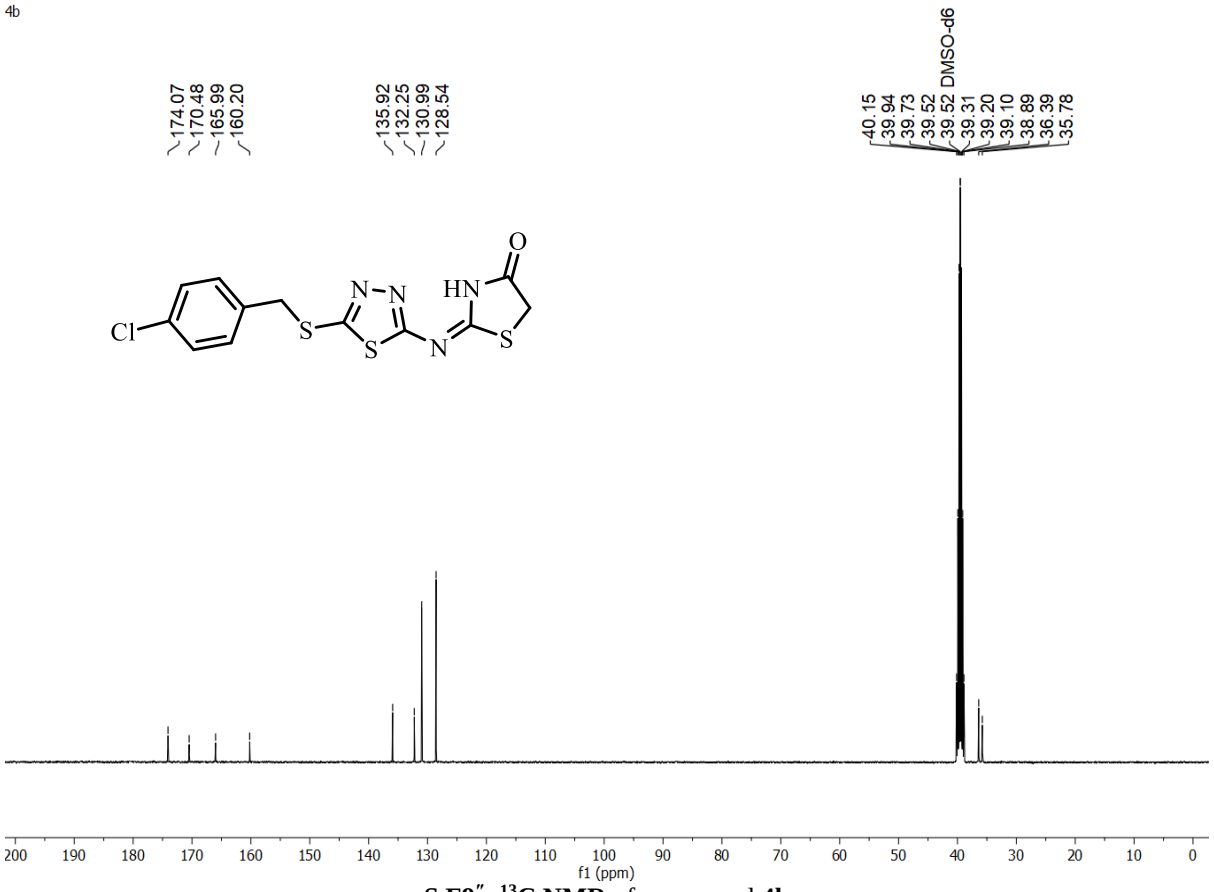

S.F9″: ^{13}C NMR of compound **4b**

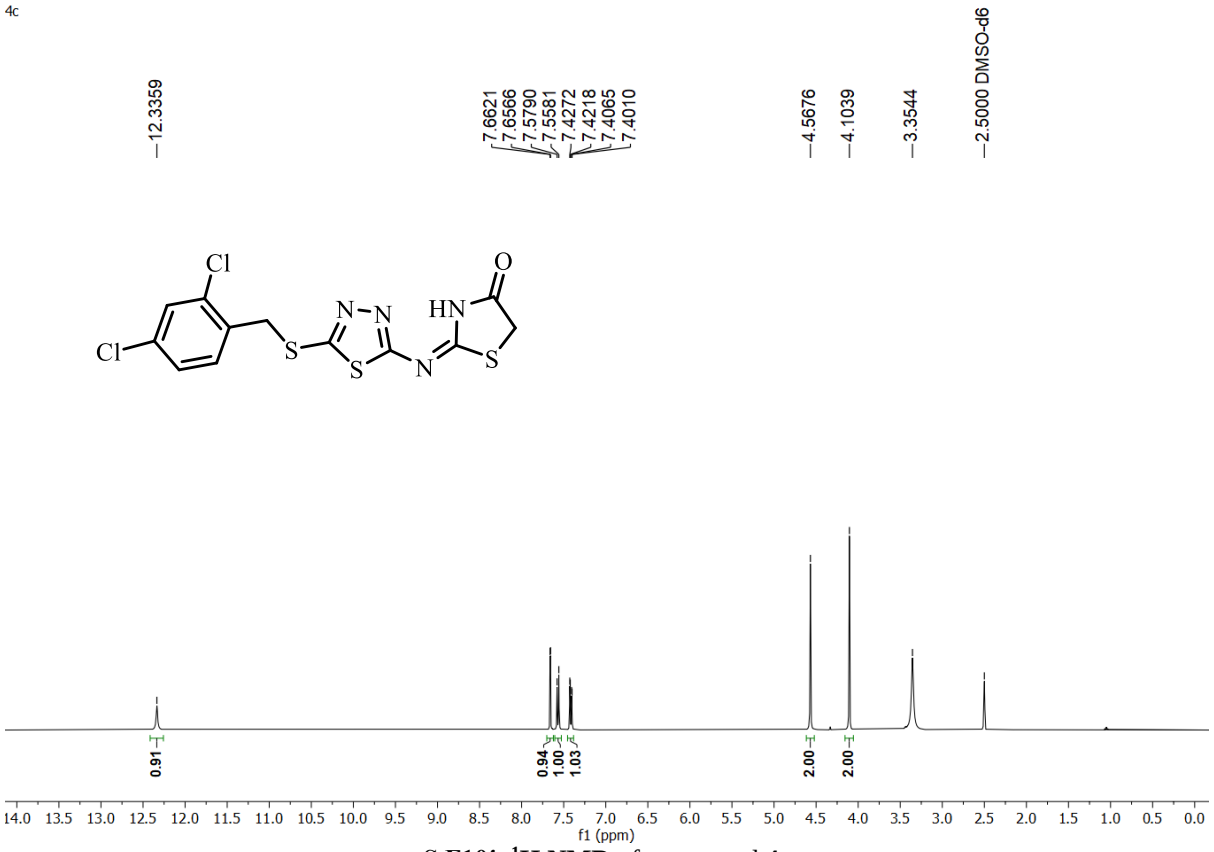

S.F10′: ^{1}H NMR of compound **4c**

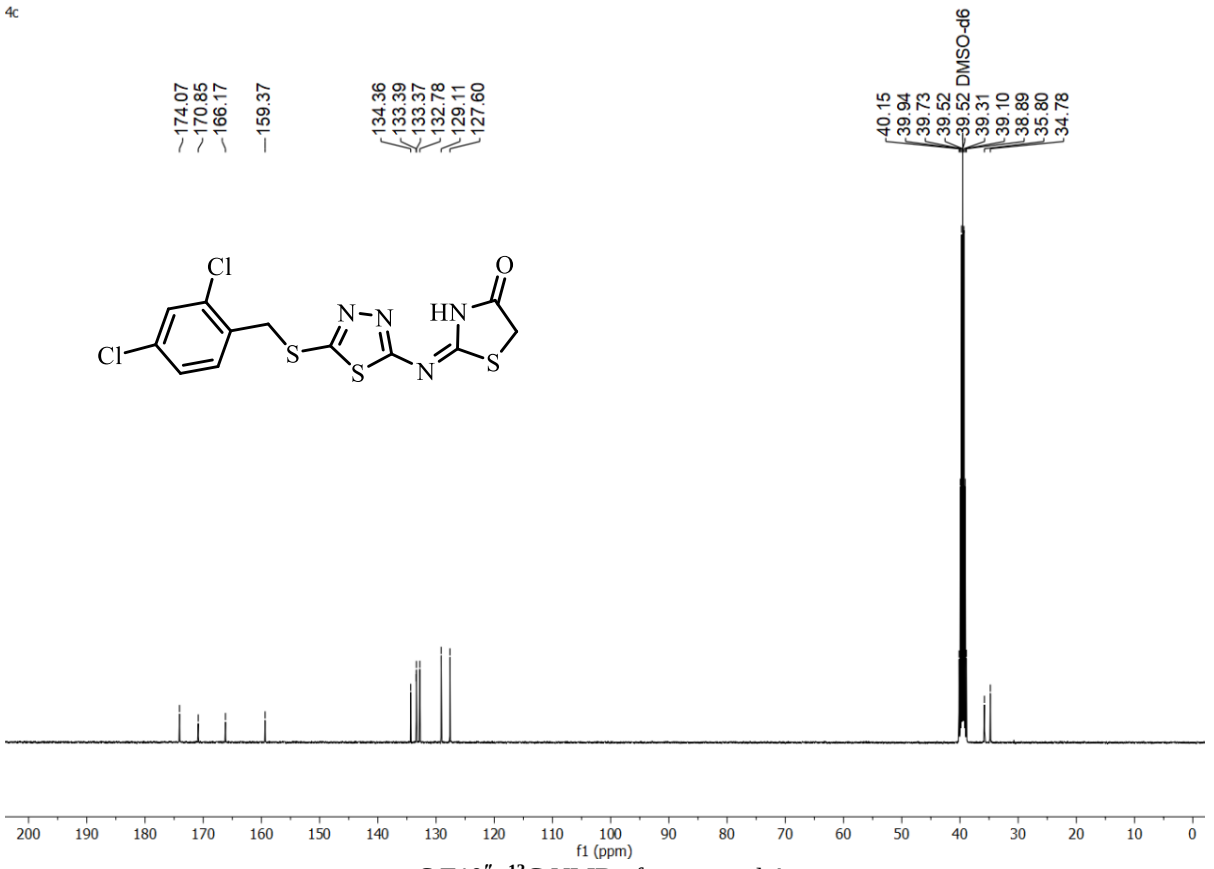

S.F10″: ^{13}C NMR of compound **4c**

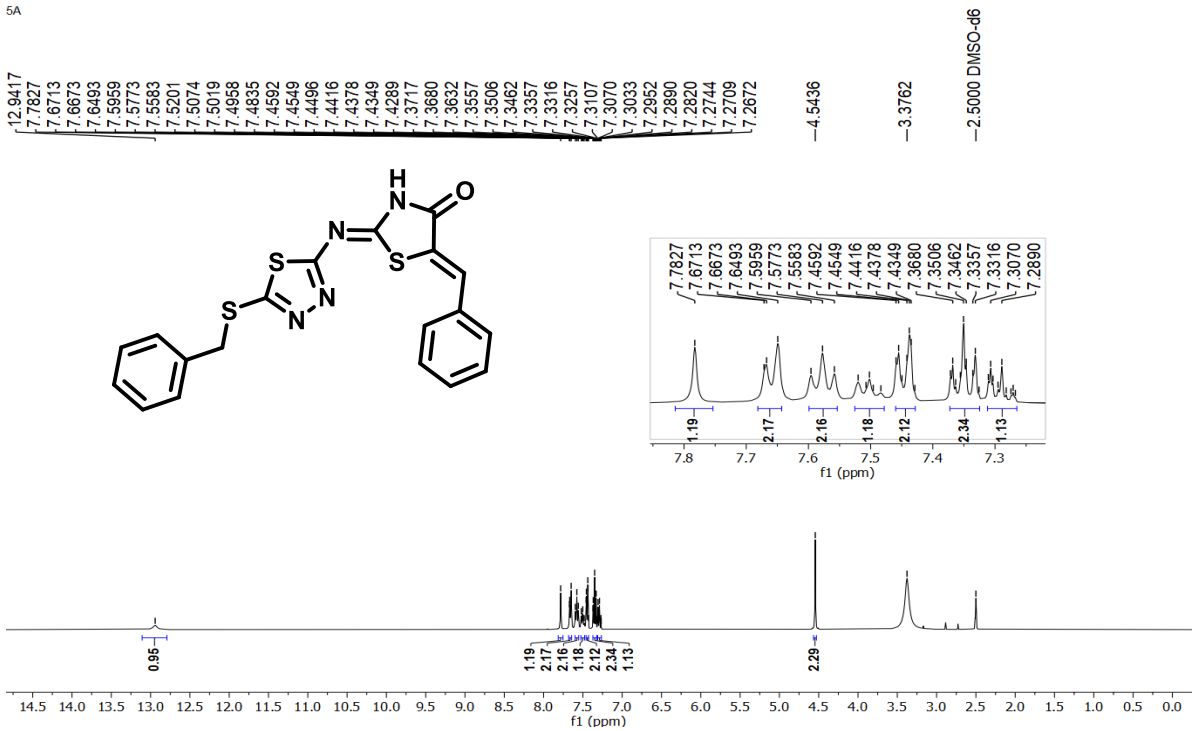

S.F11′: ^{1}H NMR of compound **5a**

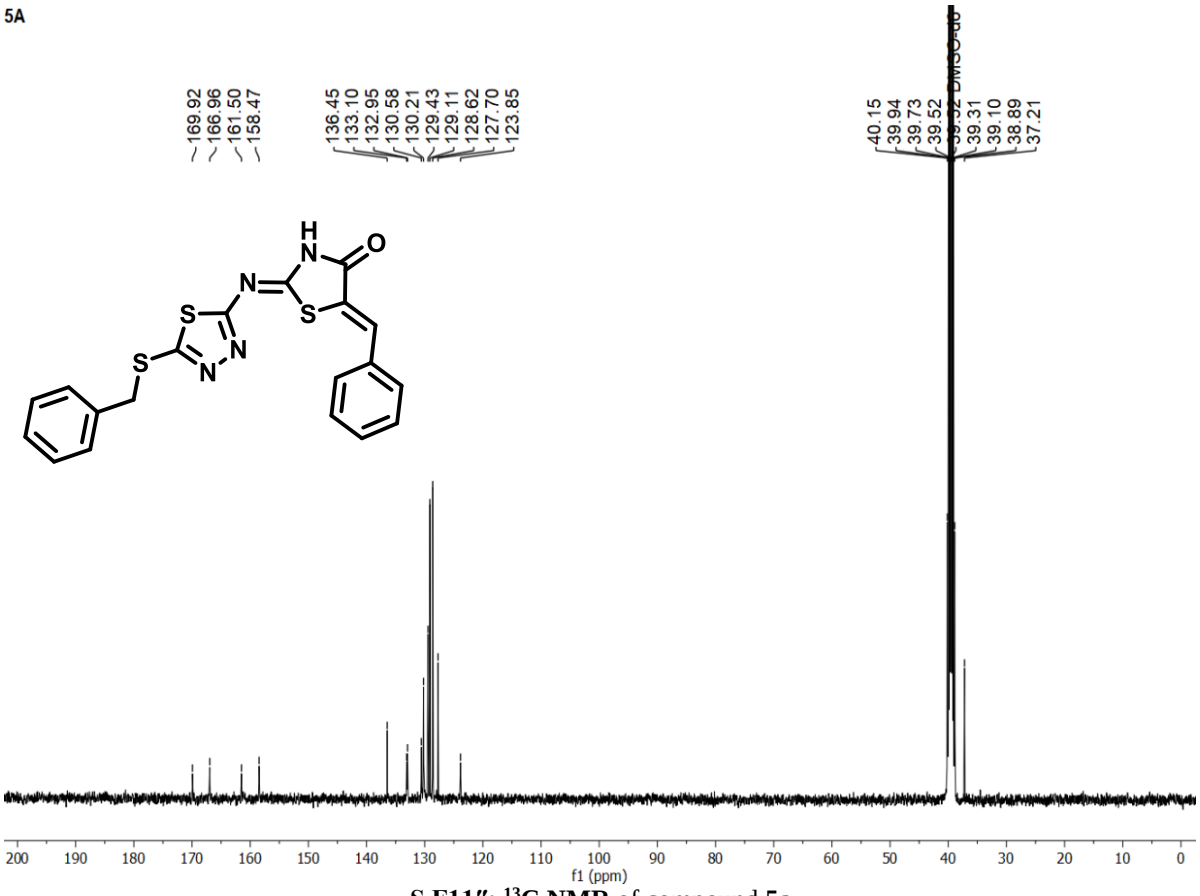

S.F11″: ^{13}C NMR of compound **5a**

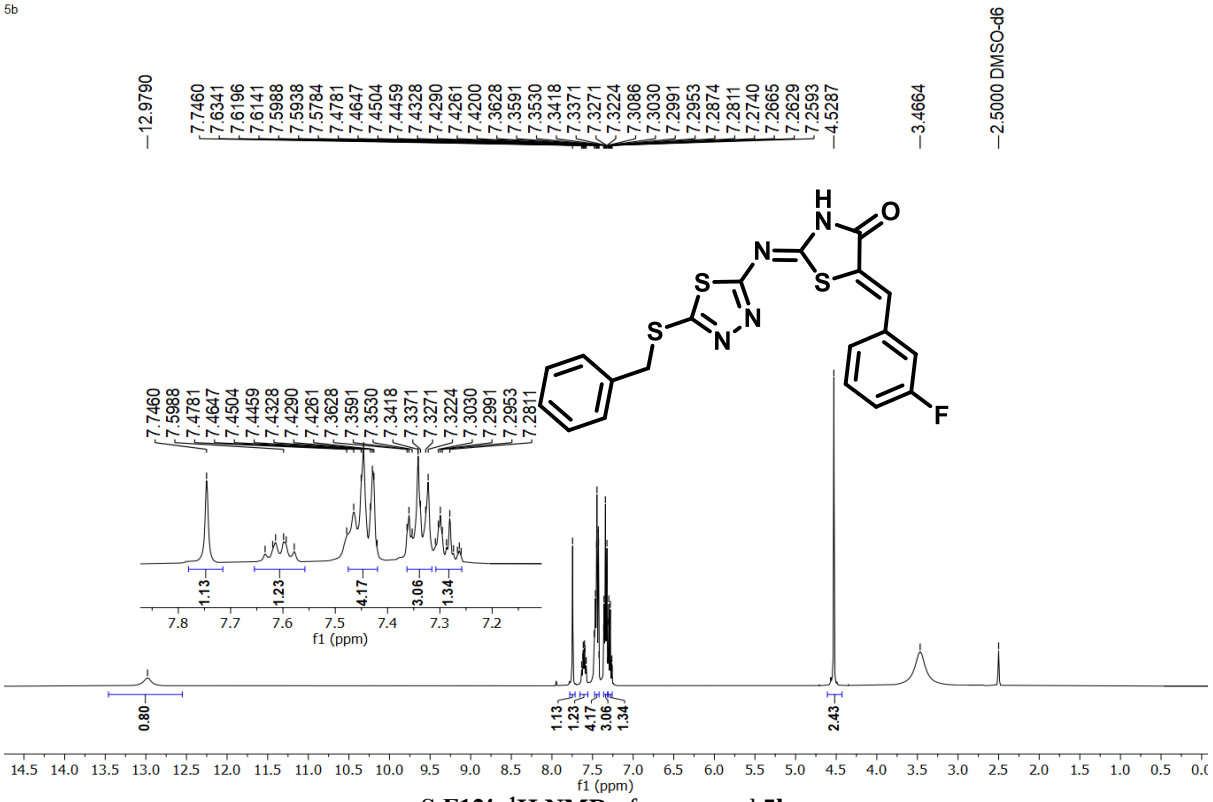

S.F12′: ^{1}H NMR of compound **5b**

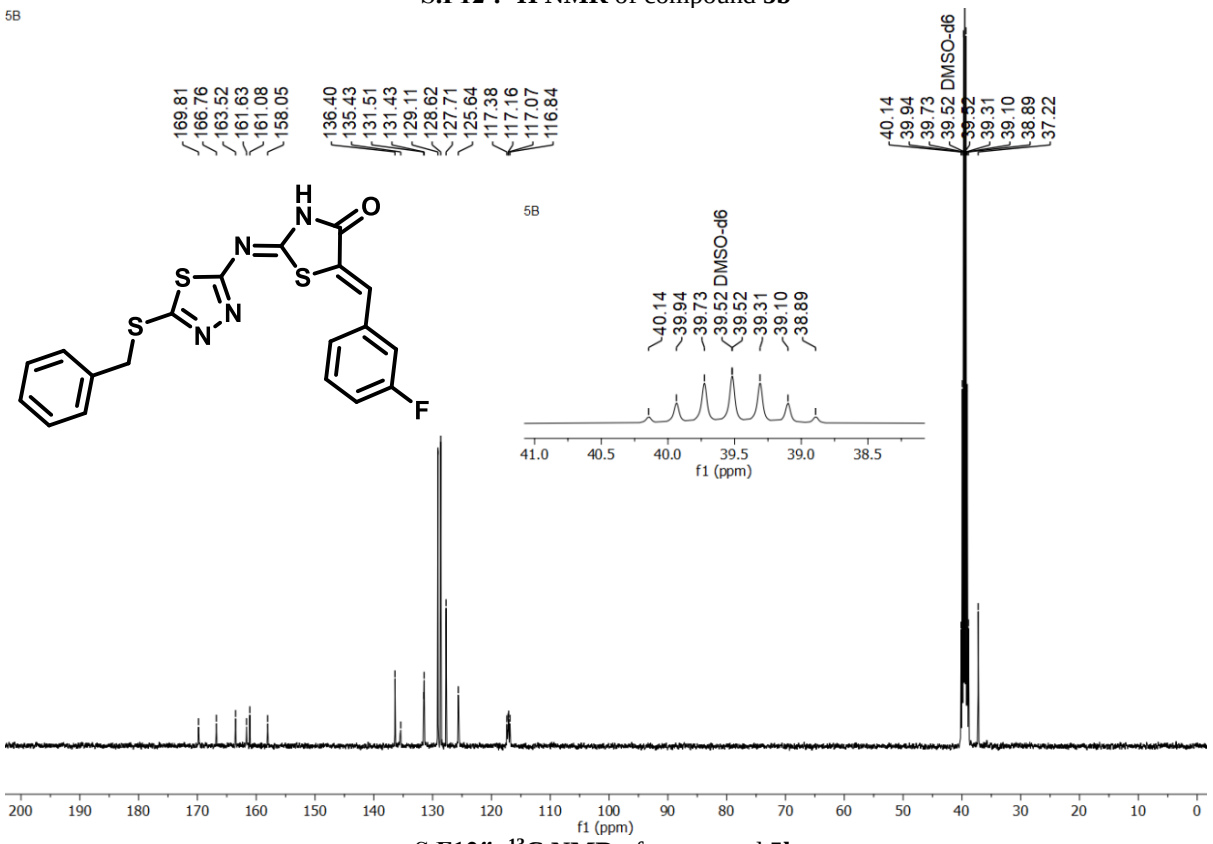

S.F12″: ^{13}C NMR of compound **5b**

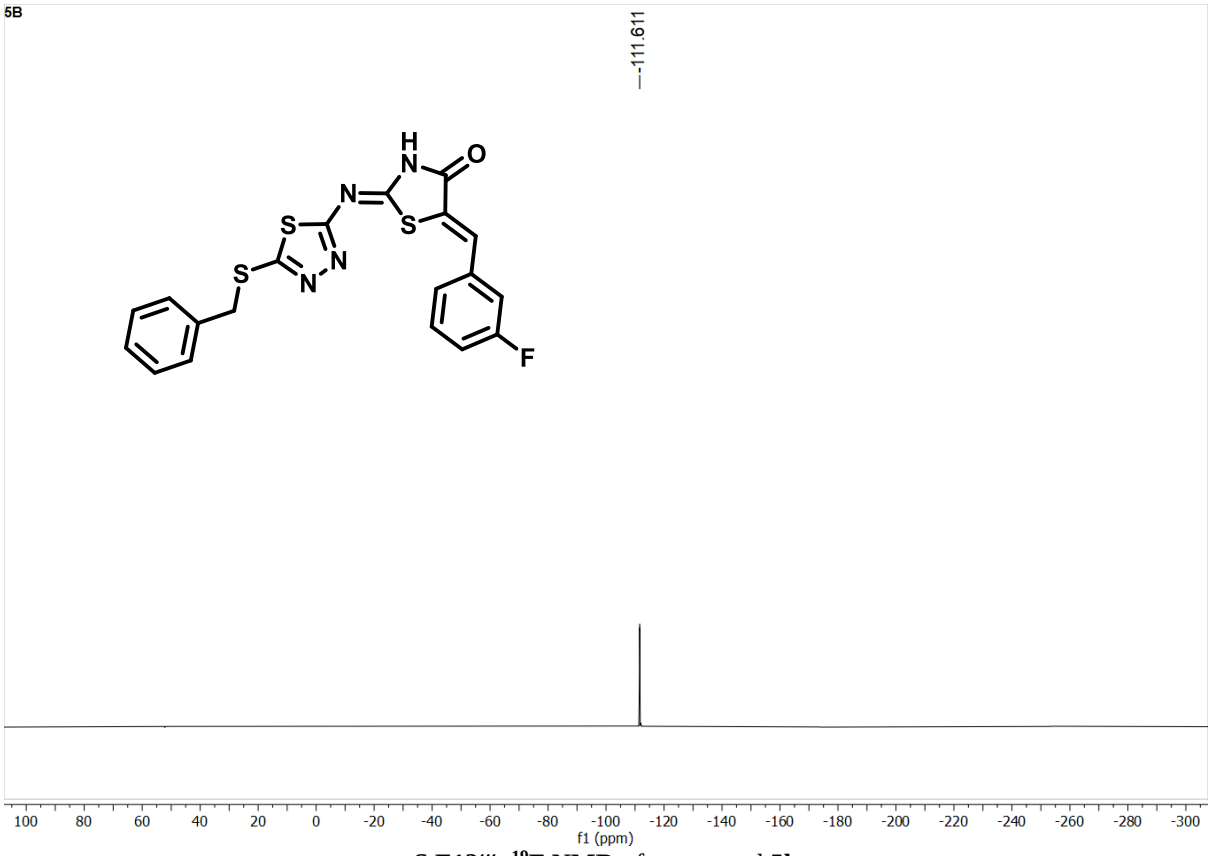

S.F12‴: ^{19}F NMR of compound **5b**

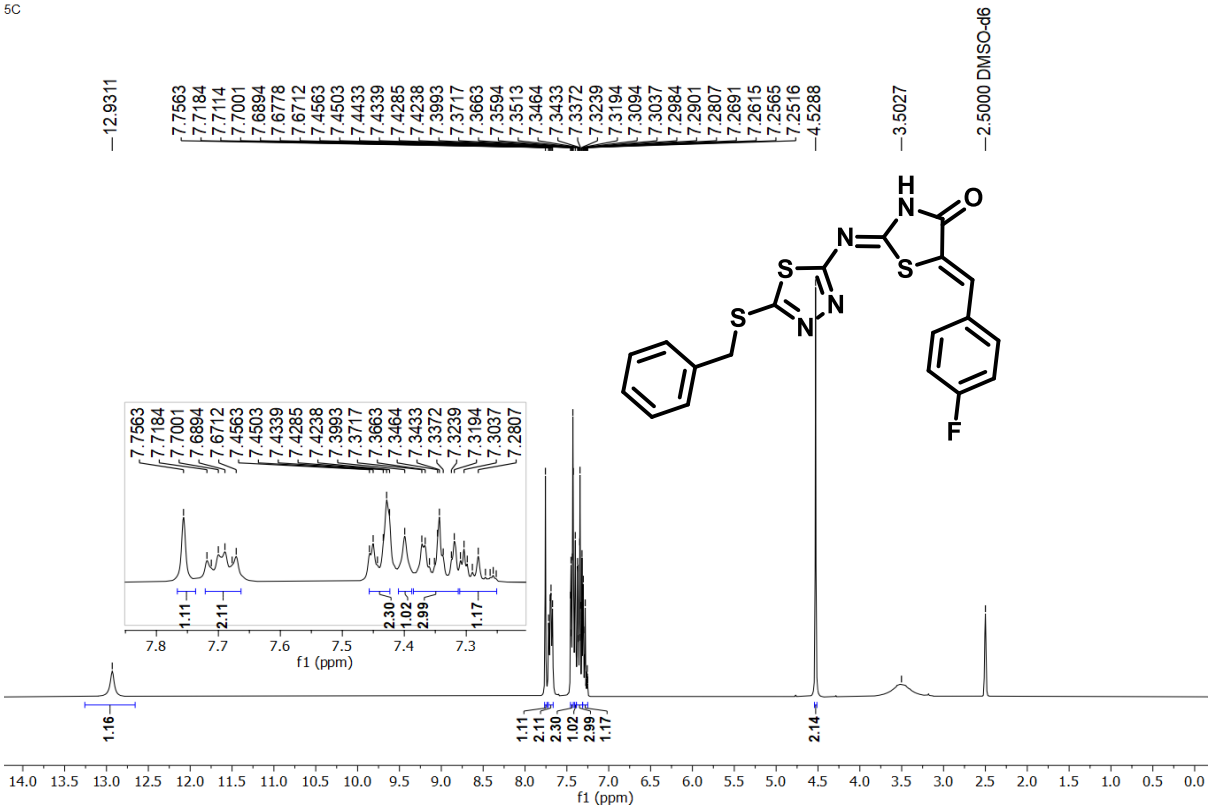

S.F13′: ^{1}H NMR of compound **5c**

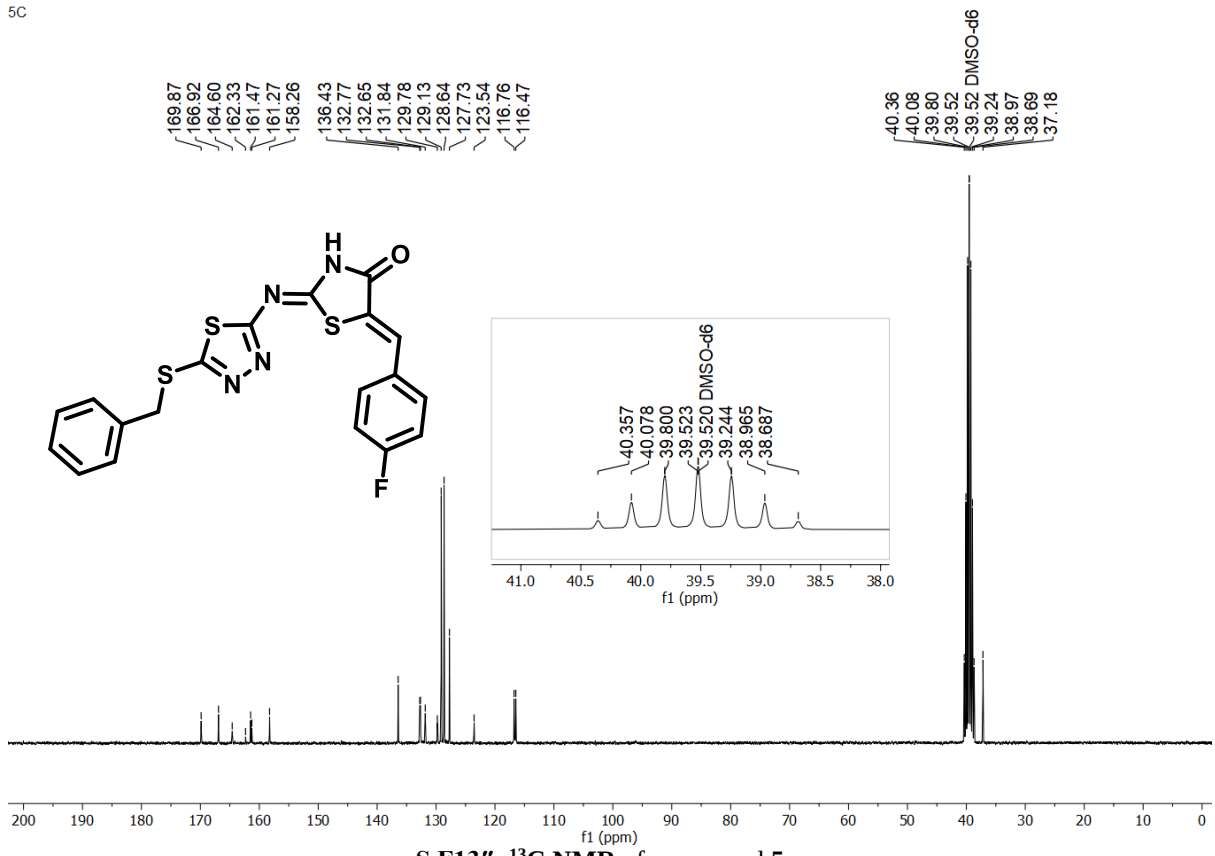

S.F13″: ^{13}C NMR of compound **5c**

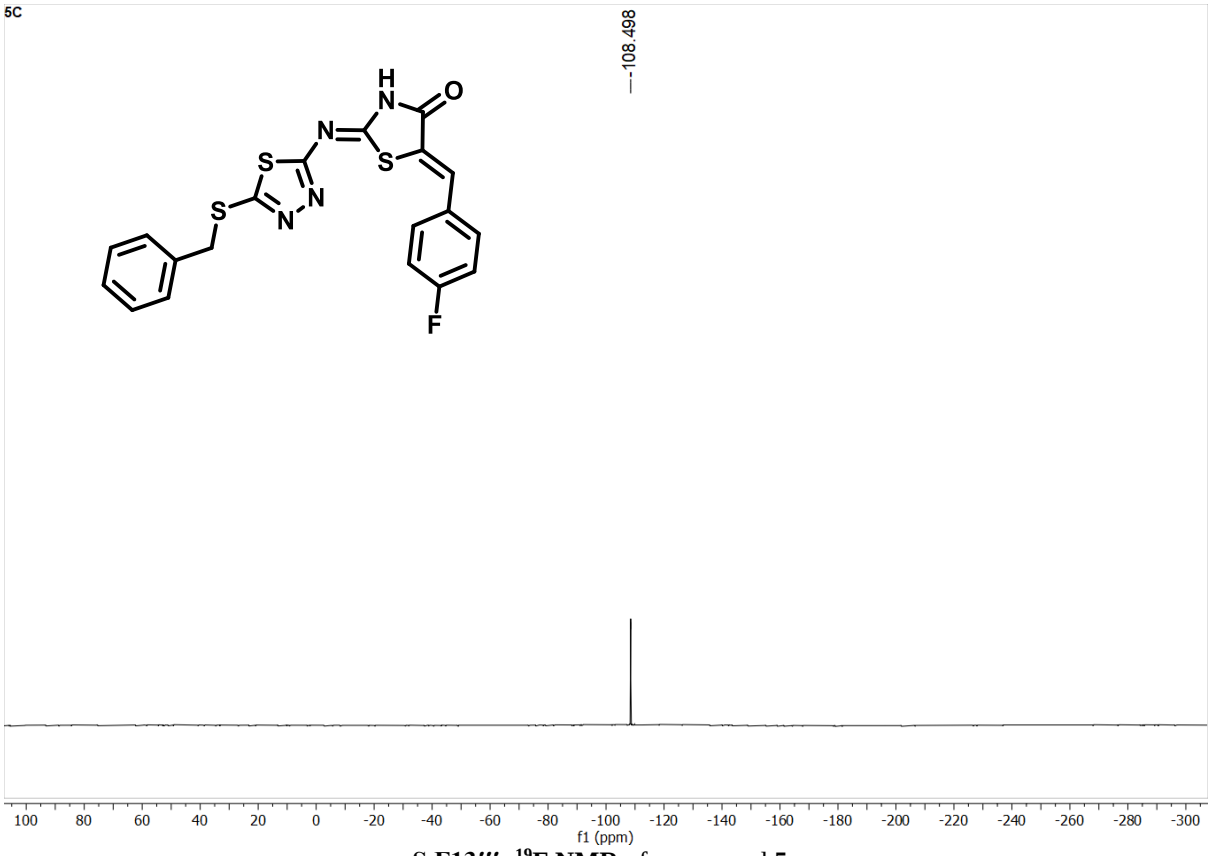

S.F13‴: ^{19}F NMR of compound **5c**

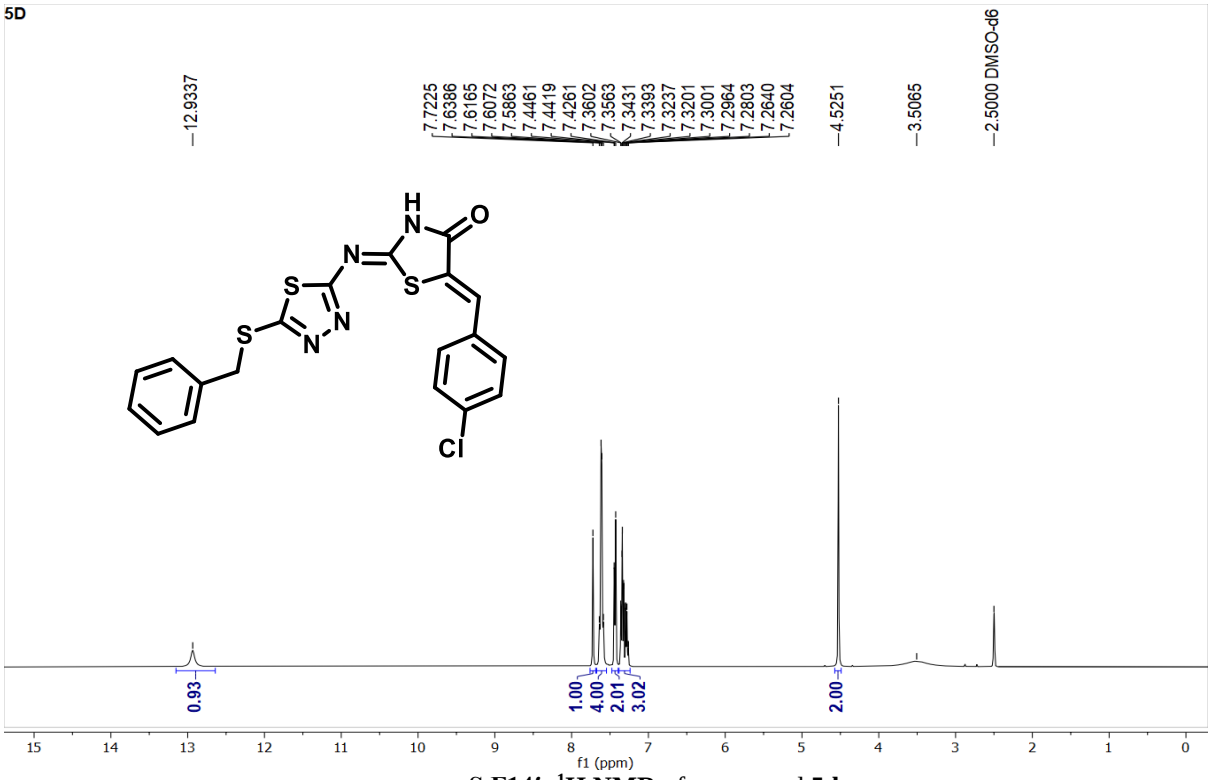

S.F14′: ^{1}H NMR of compound **5d**

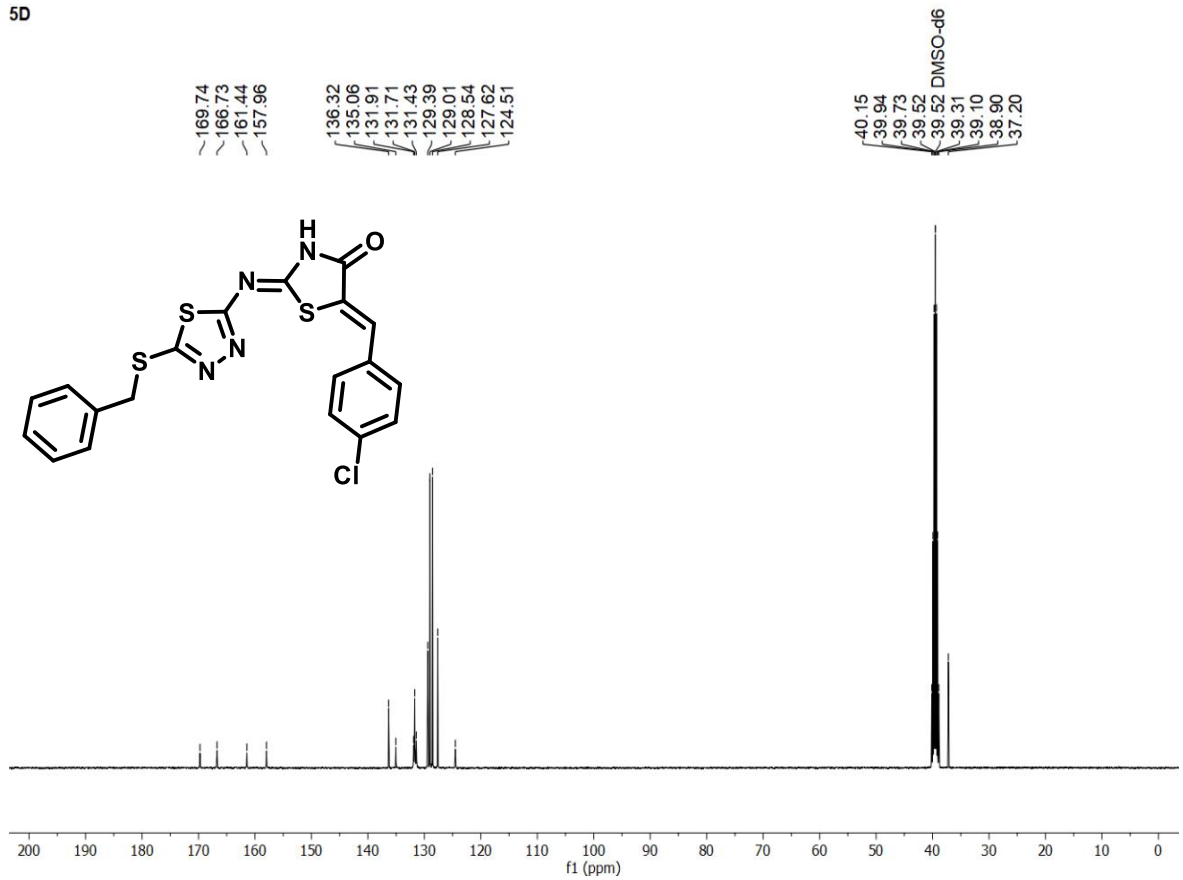

S.F14″: ^{13}C NMR of compound **5d**

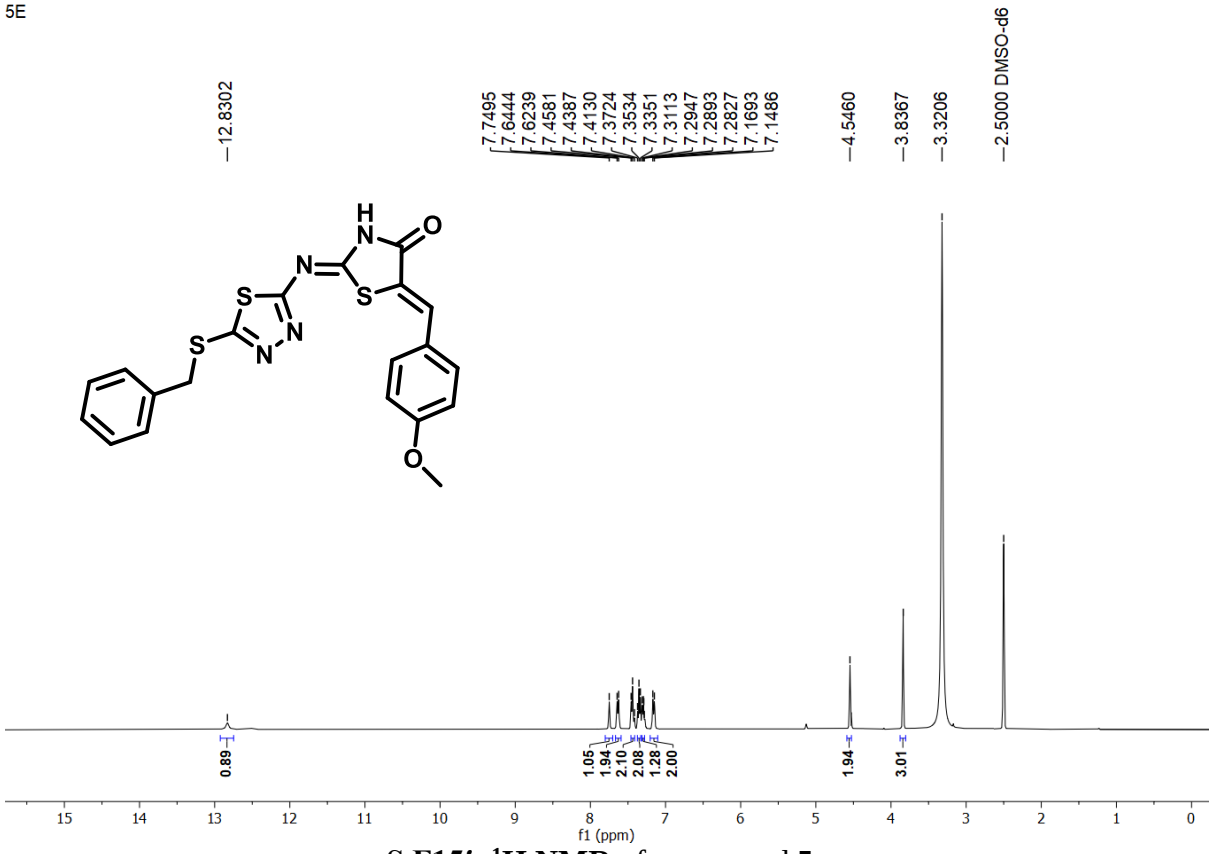

S.F15′: ^{1}H NMR of compound **5e**

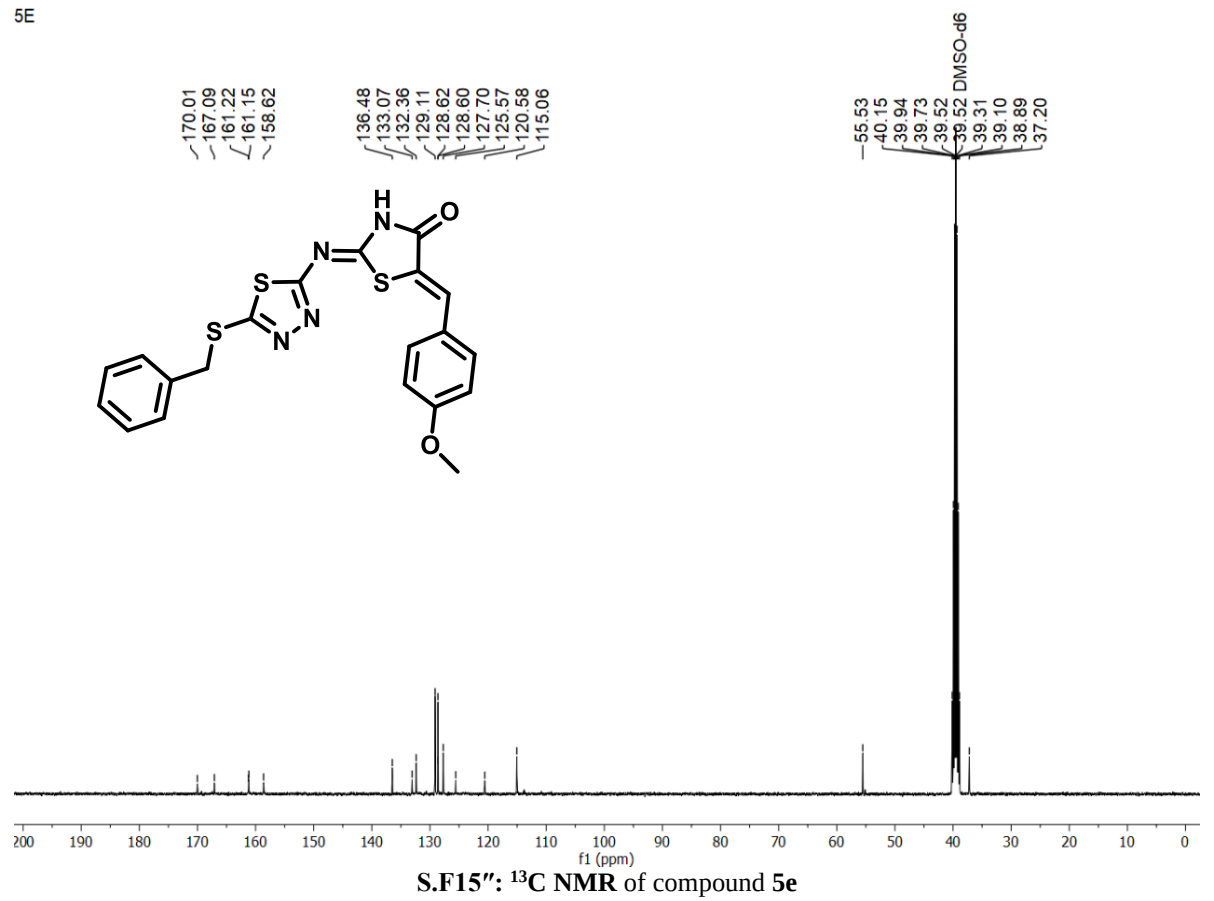

S.F15″: ^{13}C NMR of compound **5e**

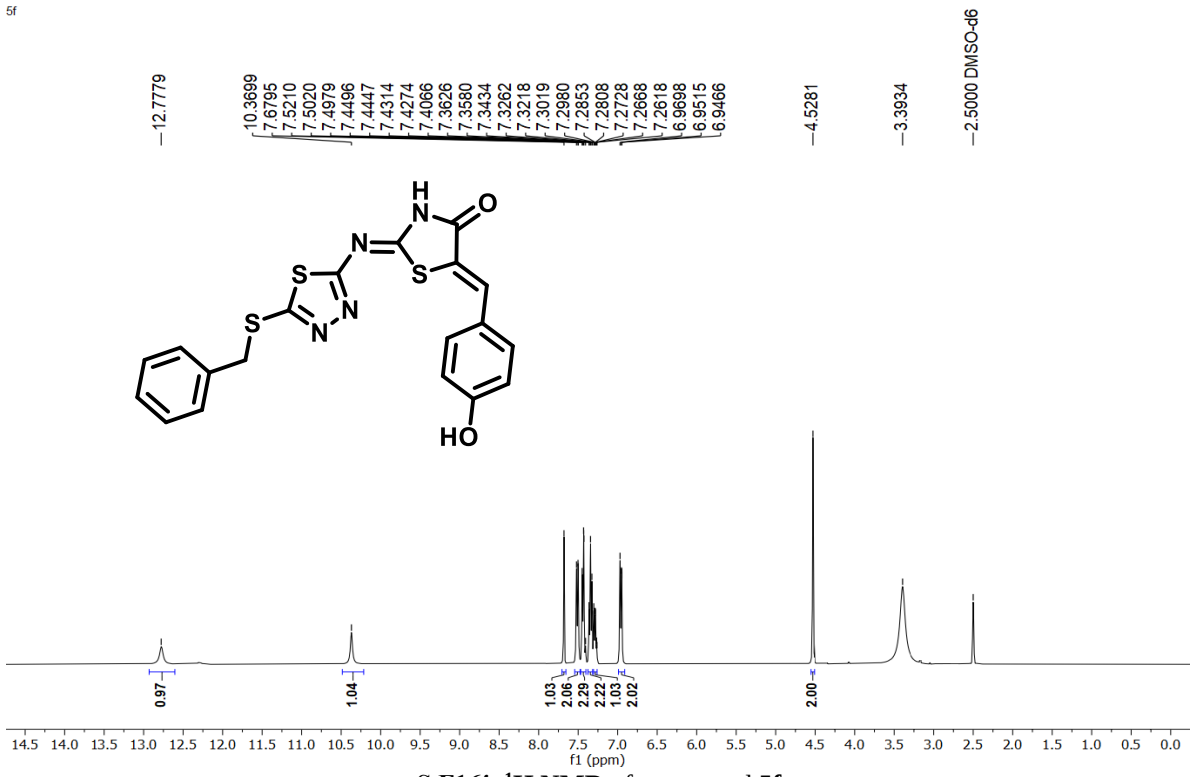

S.F16′: ^{1}H NMR of compound **5f**

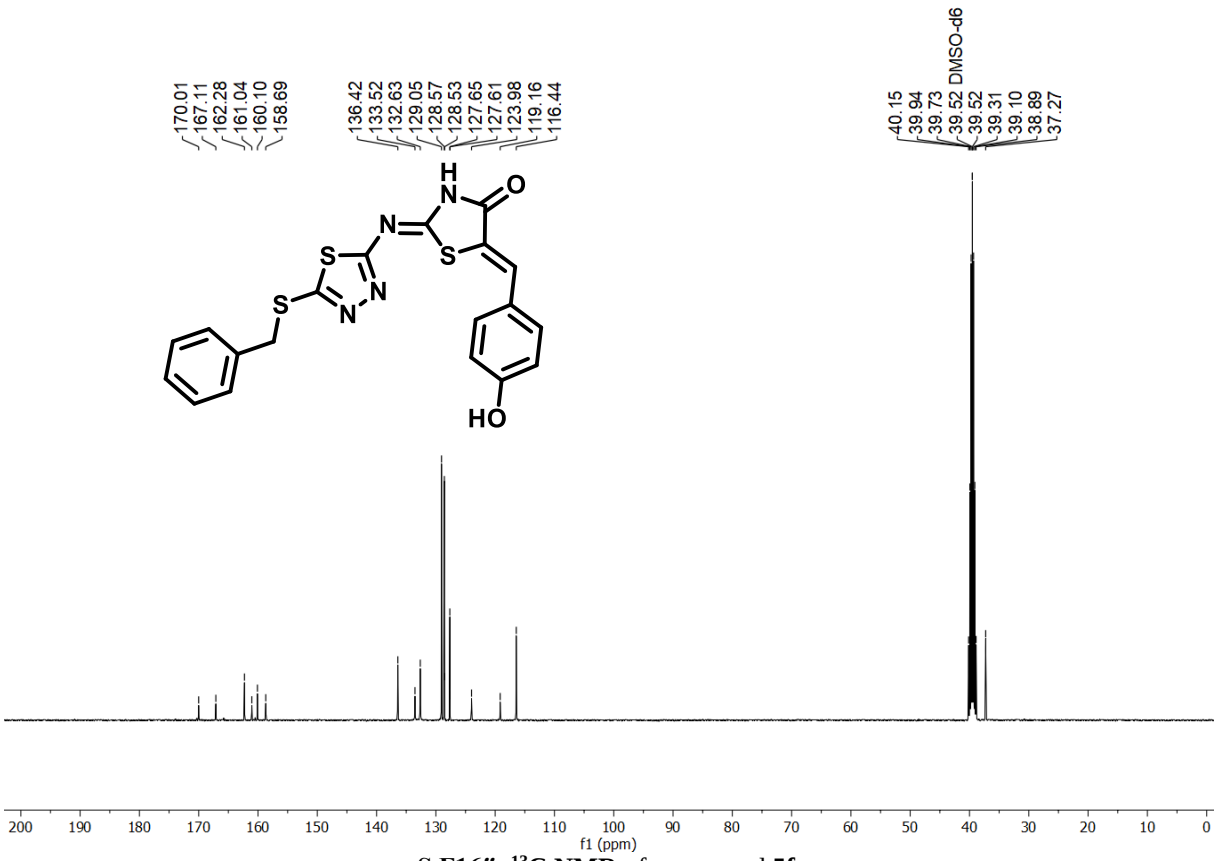

S.F16″: ^{13}C NMR of compound **5f**

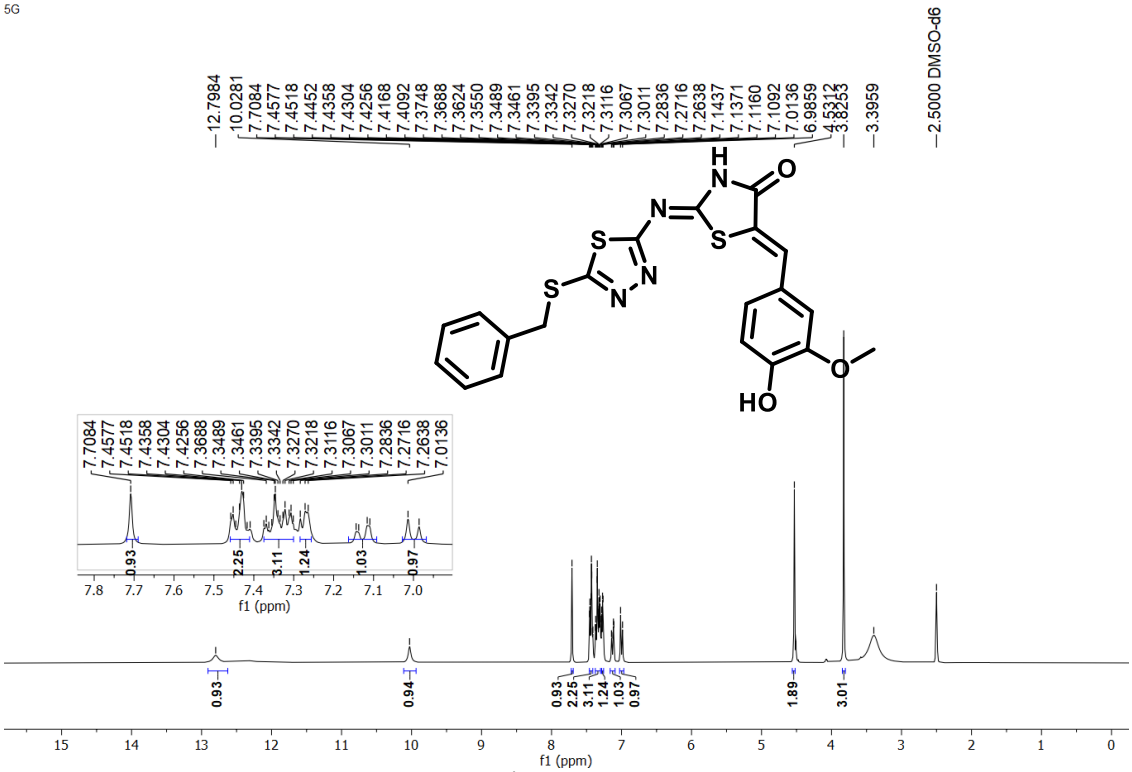

S.F17′: ^{1}H NMR of compound **5g**

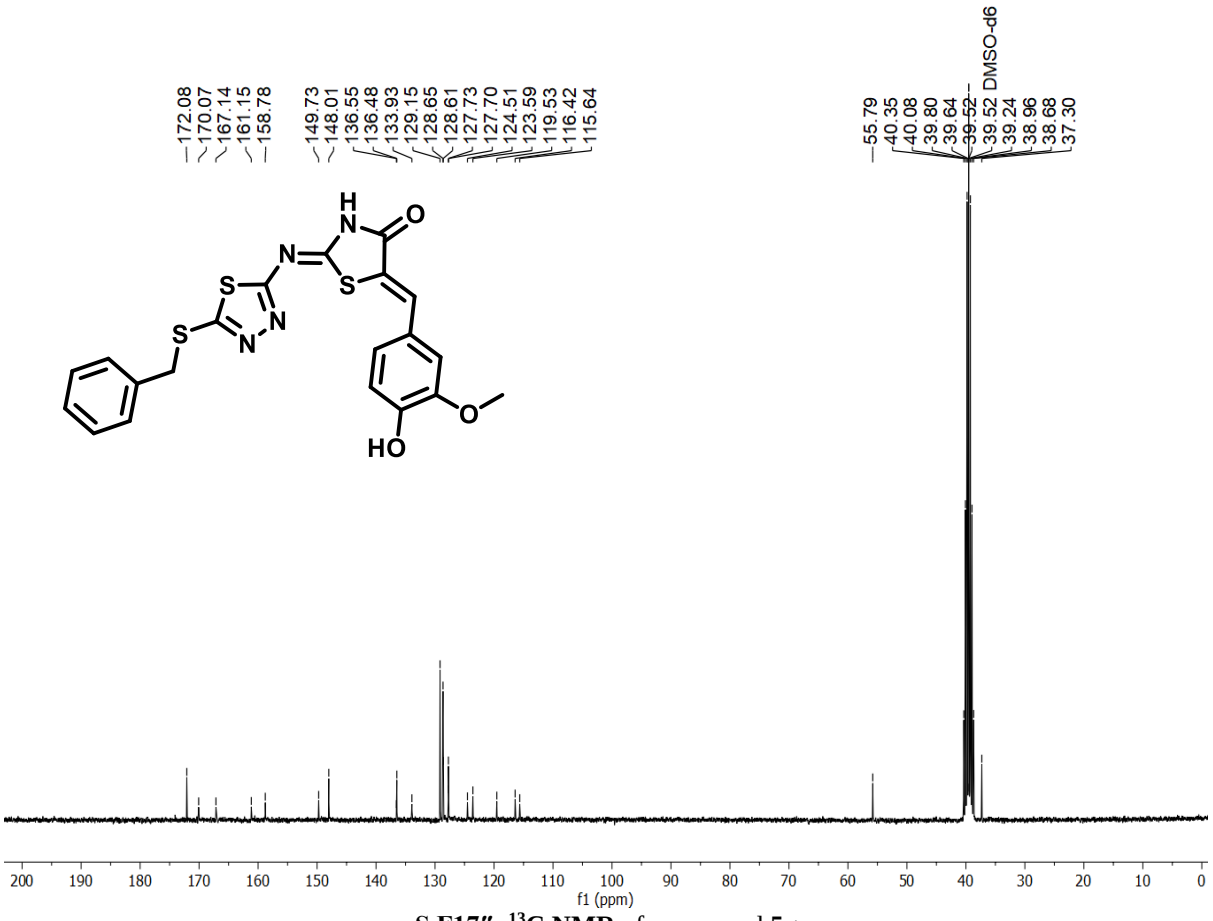

S.F17″: ^{13}C NMR of compound **5g**

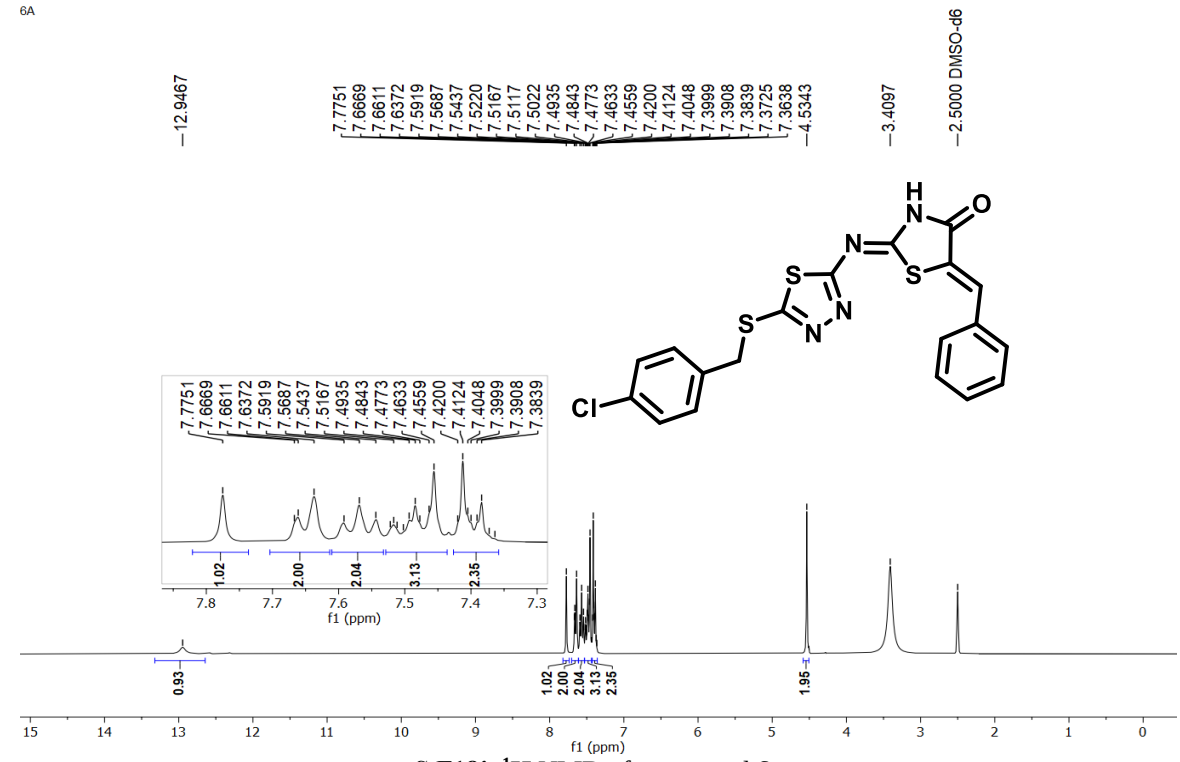

S.F18′: ^{1}H NMR of compound **6a**

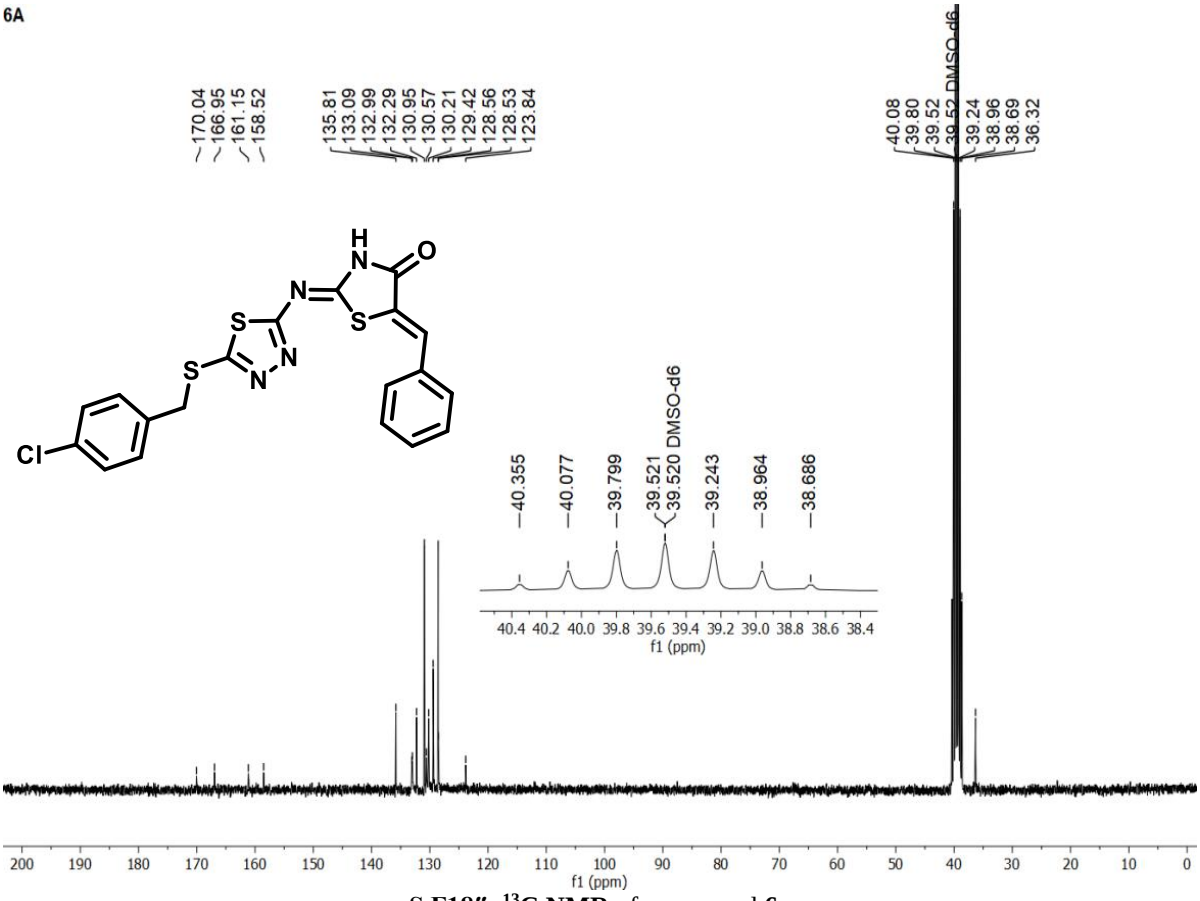

S.F18″: ^{13}C NMR of compound **6a**

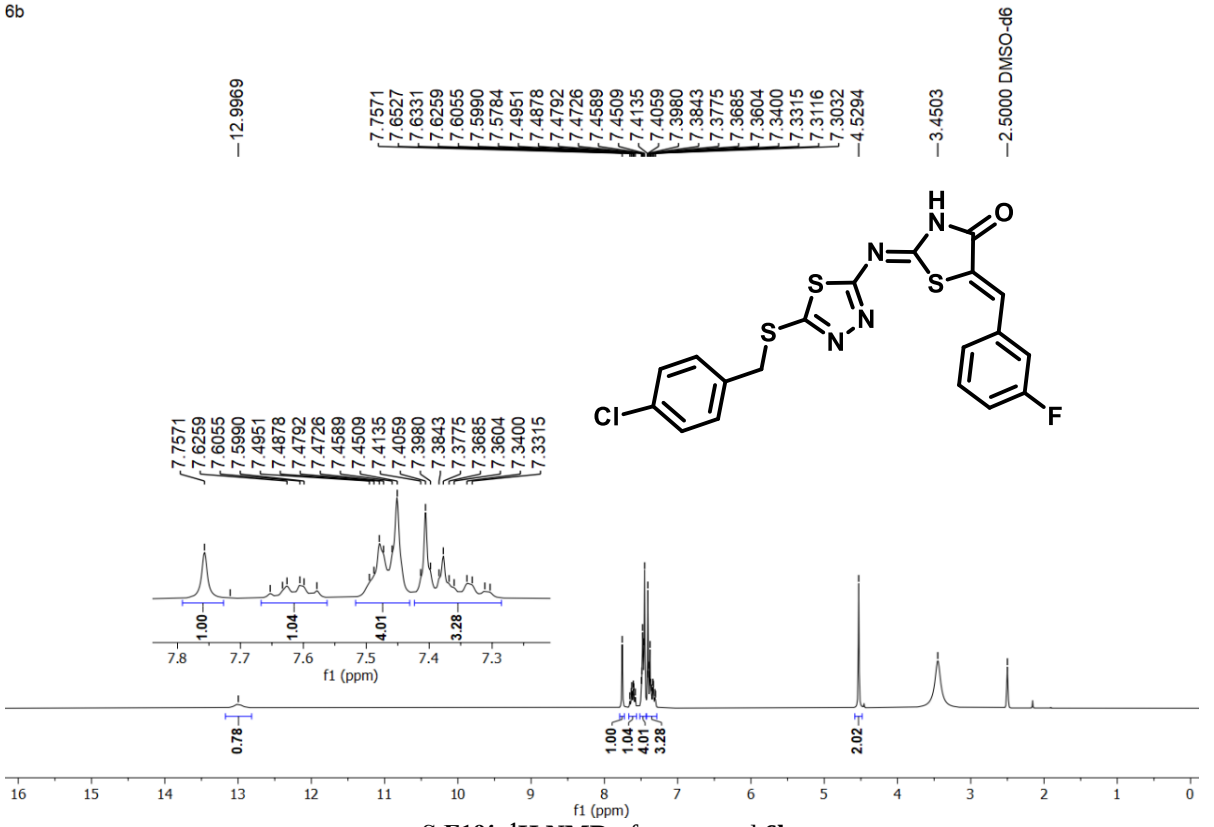

S.F19′: ^{1}H NMR of compound **6b**

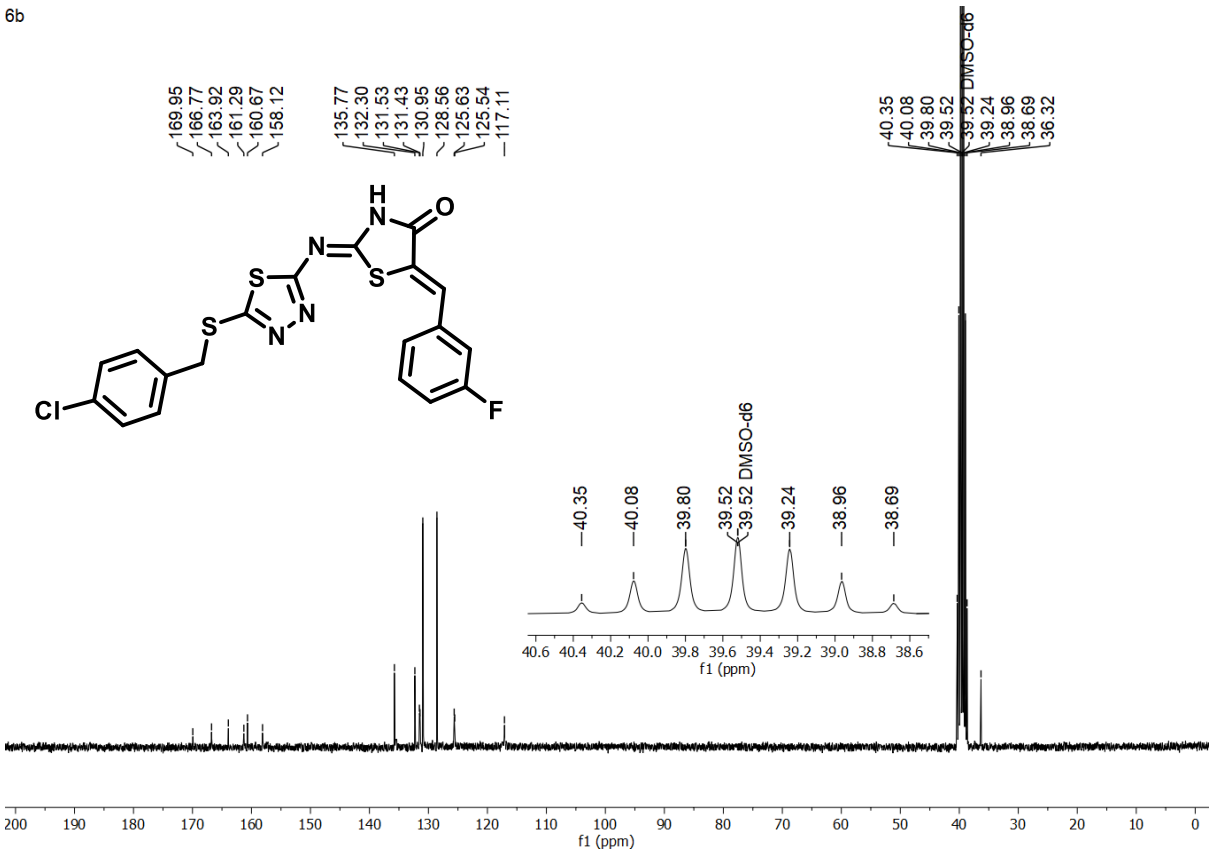

S.F19″: ^{13}C NMR of compound **6b**

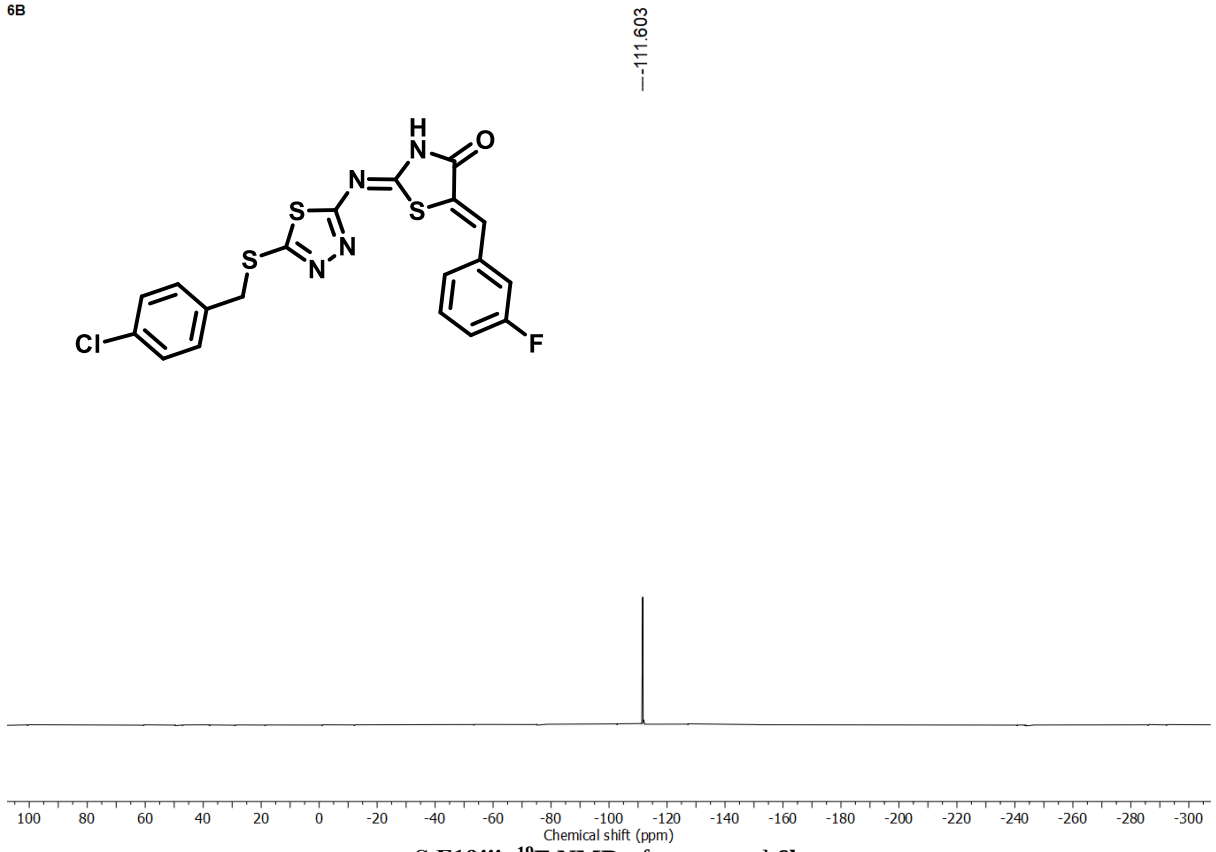

S.F19‴: ^{19}F NMR of compound **6b**

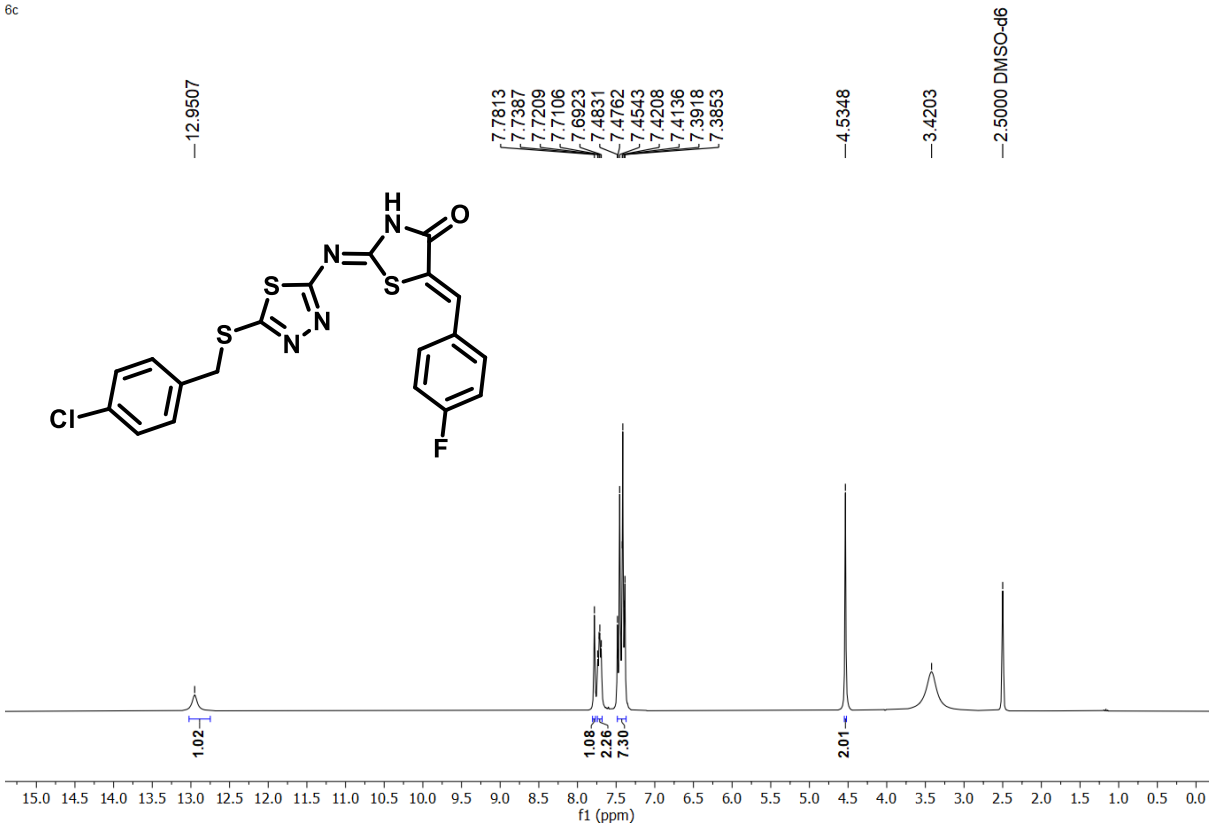

S.F20′: ^{1}H NMR of compound **6c**

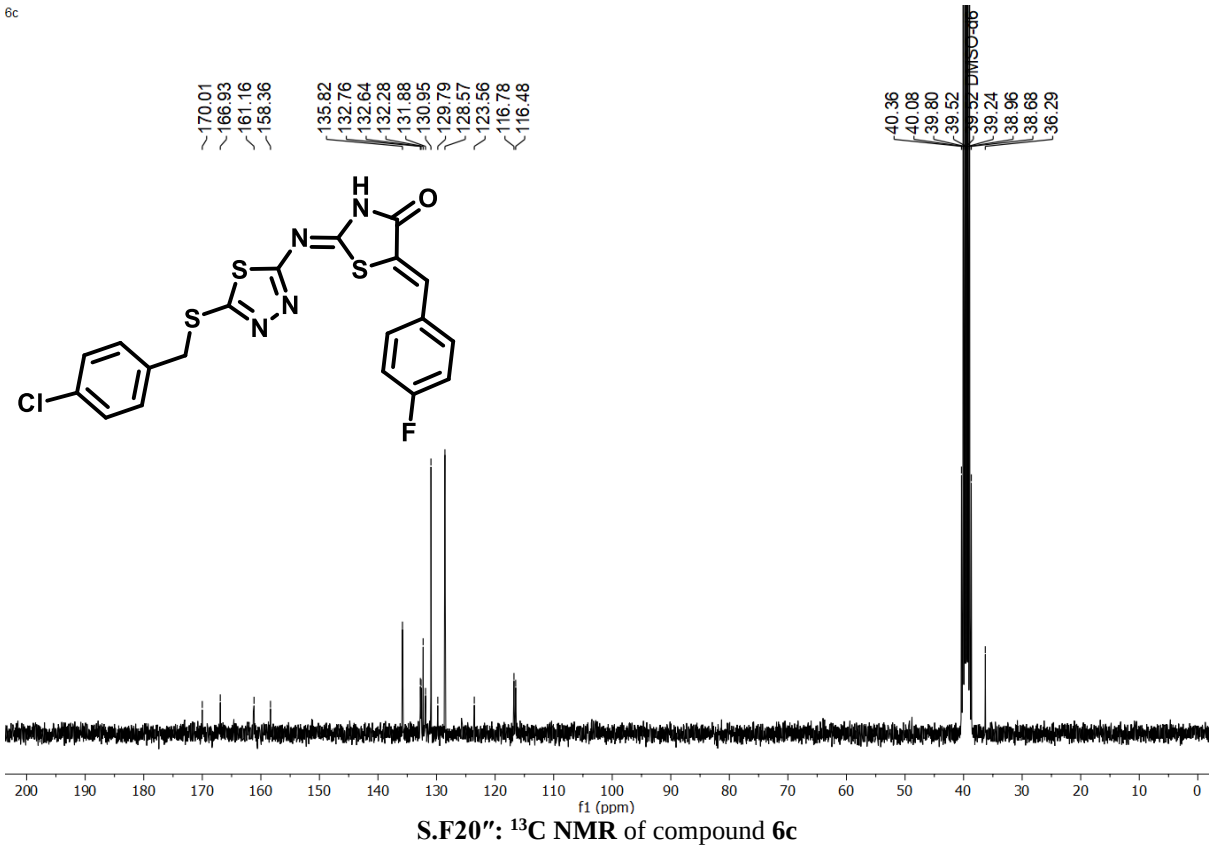

S.F20″: ^{13}C NMR of compound **6c**

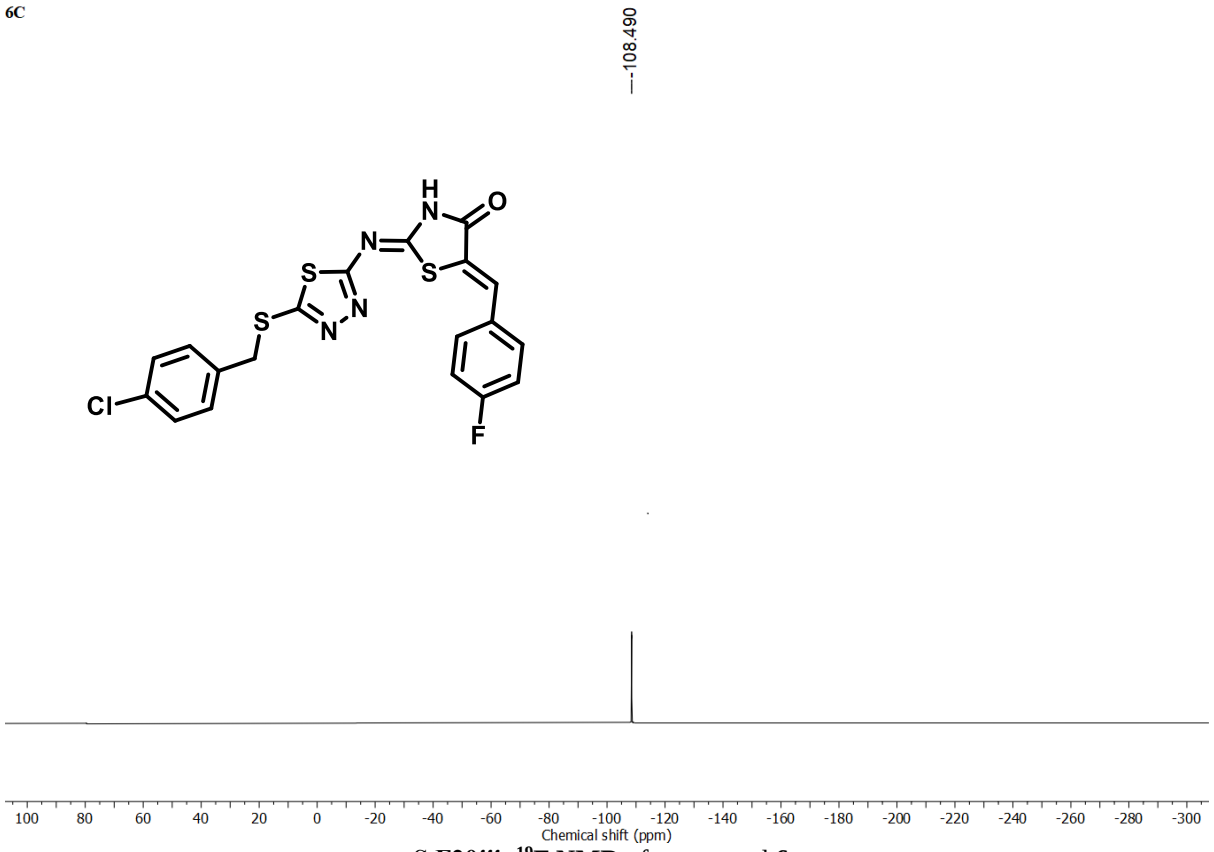

S.F20‴: ^{19}F NMR of compound **6c**

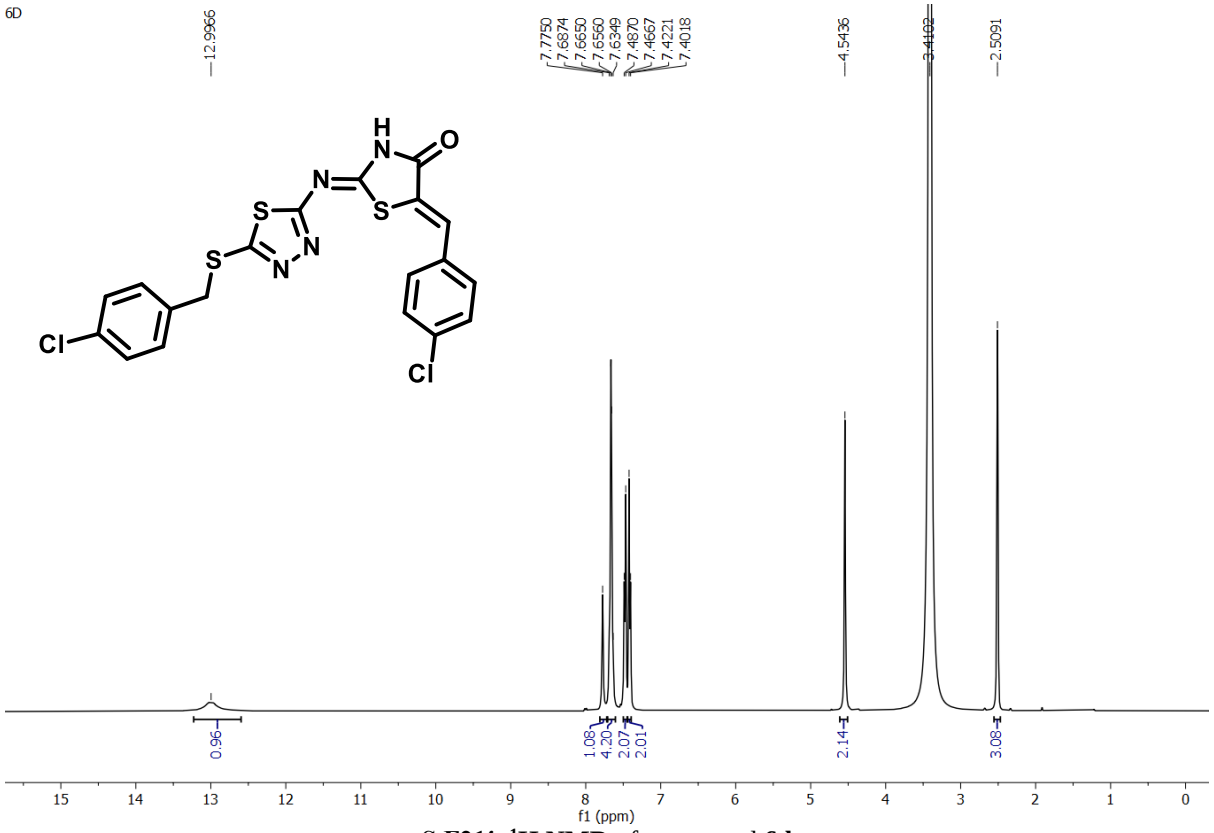

S.F21′: ^{1}H NMR of compound **6d**

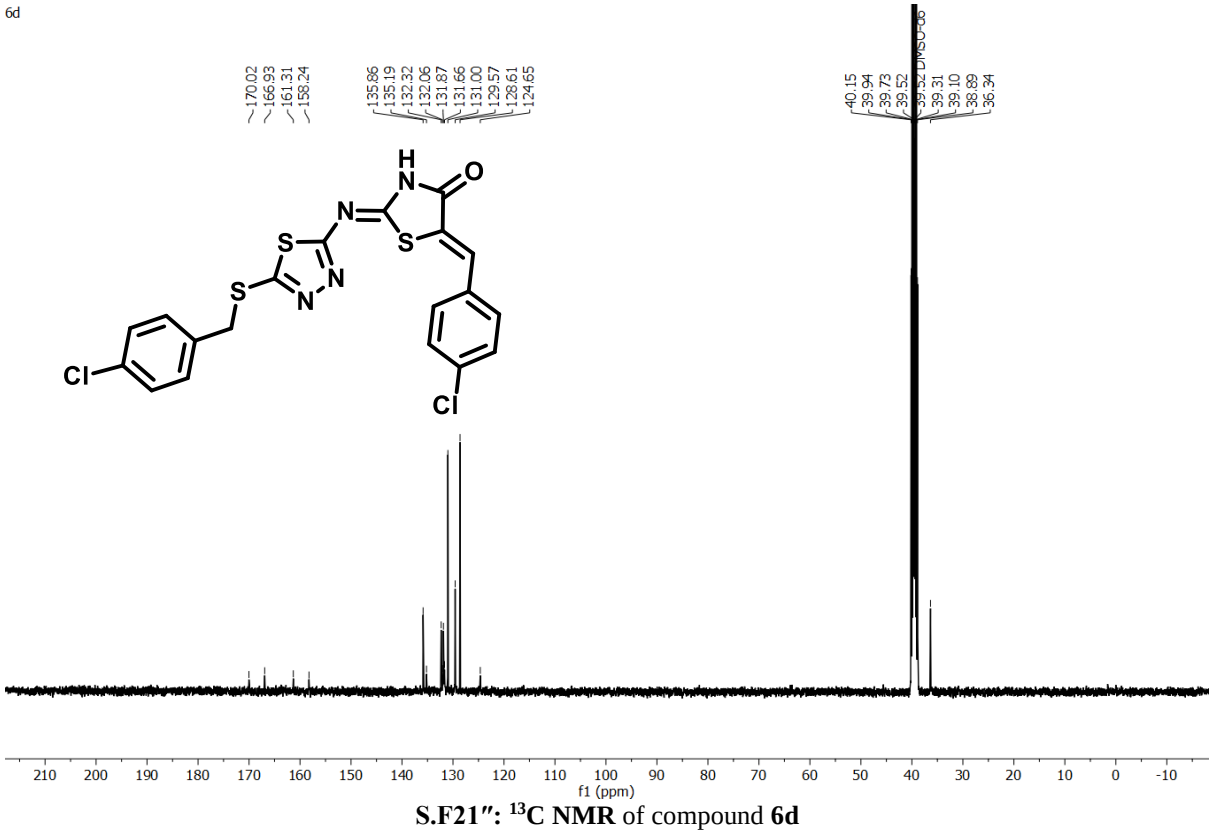

S.F21″: ^{13}C NMR of compound **6d**

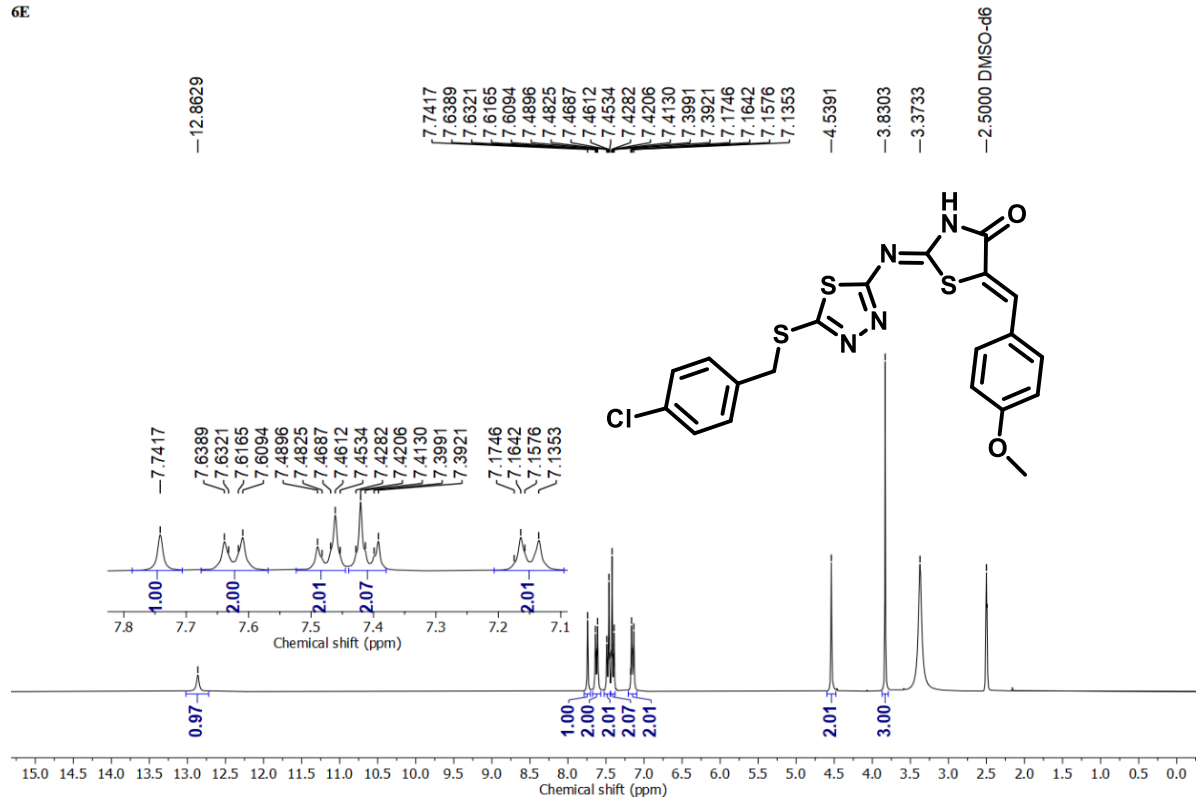

S.F22′: ^{1}H NMR of compound **6e**

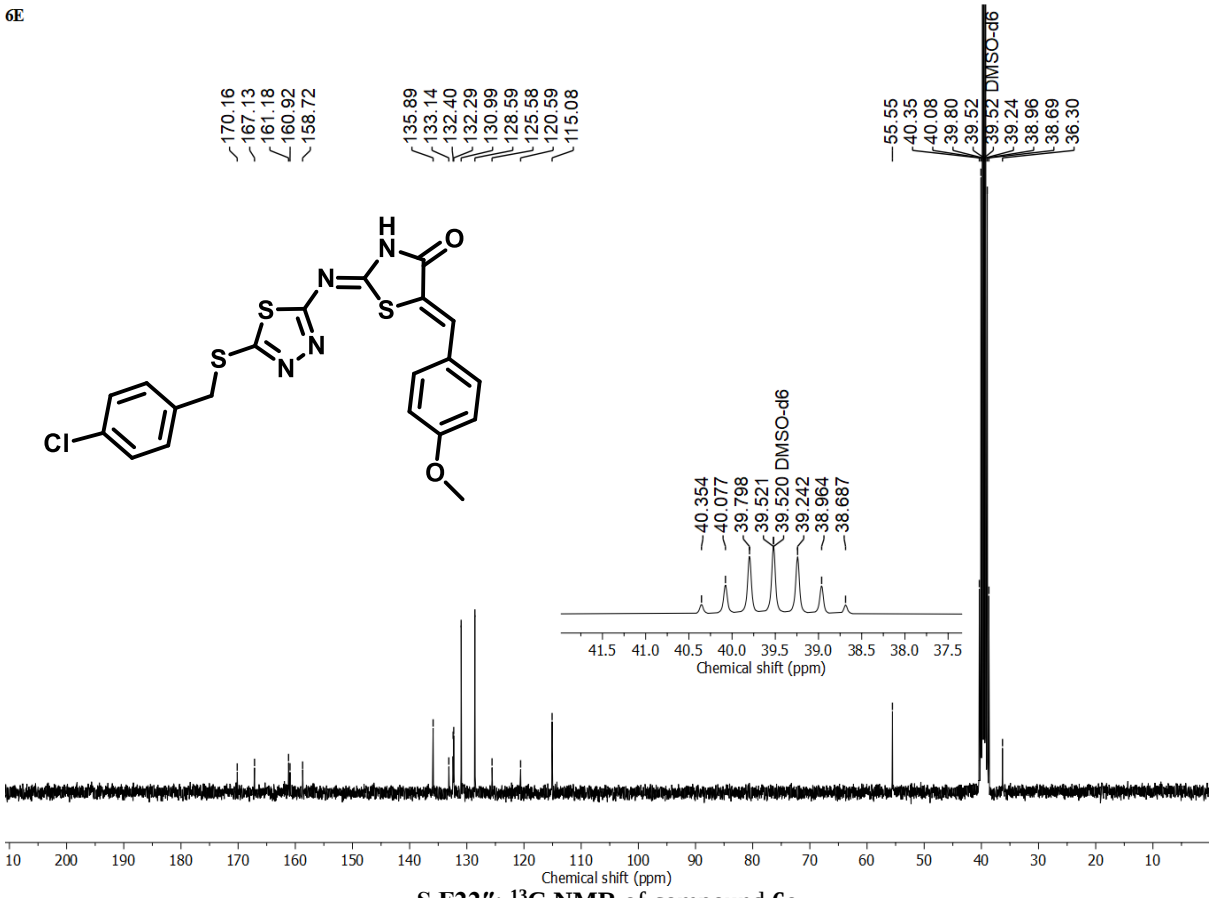

S.F22″: ^{13}C NMR of compound **6e**

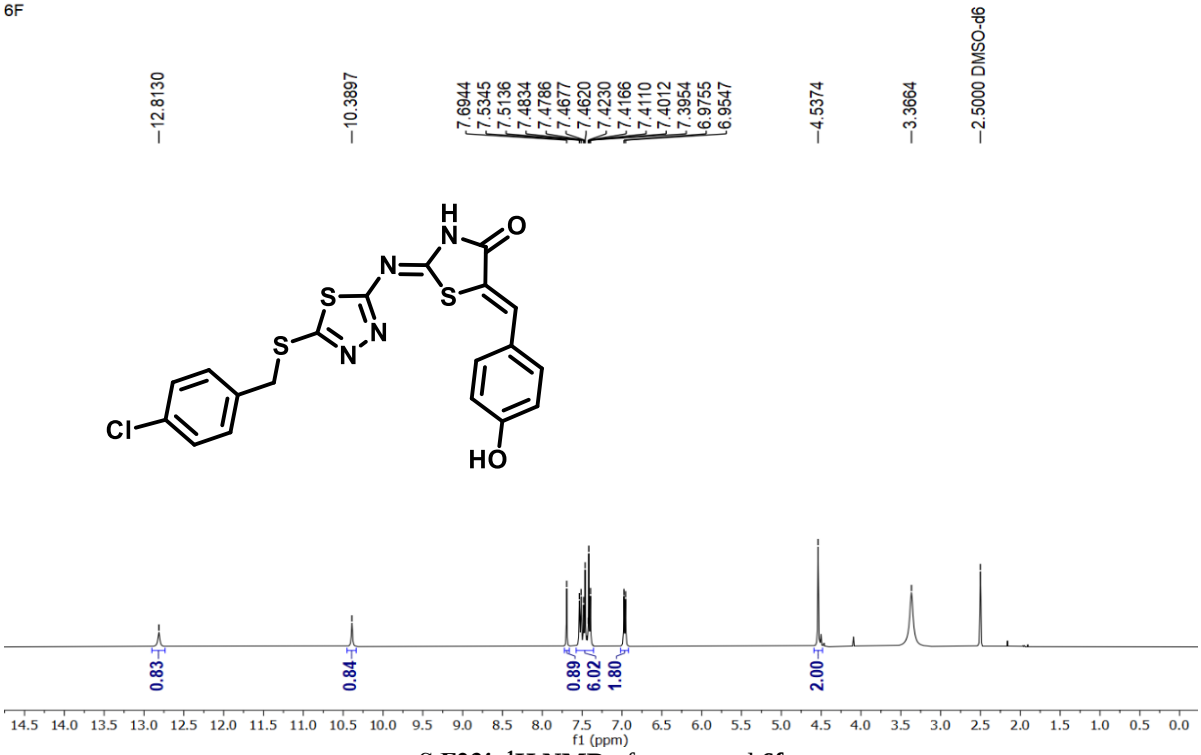

S.F23′: ^{1}H NMR of compound **6f**

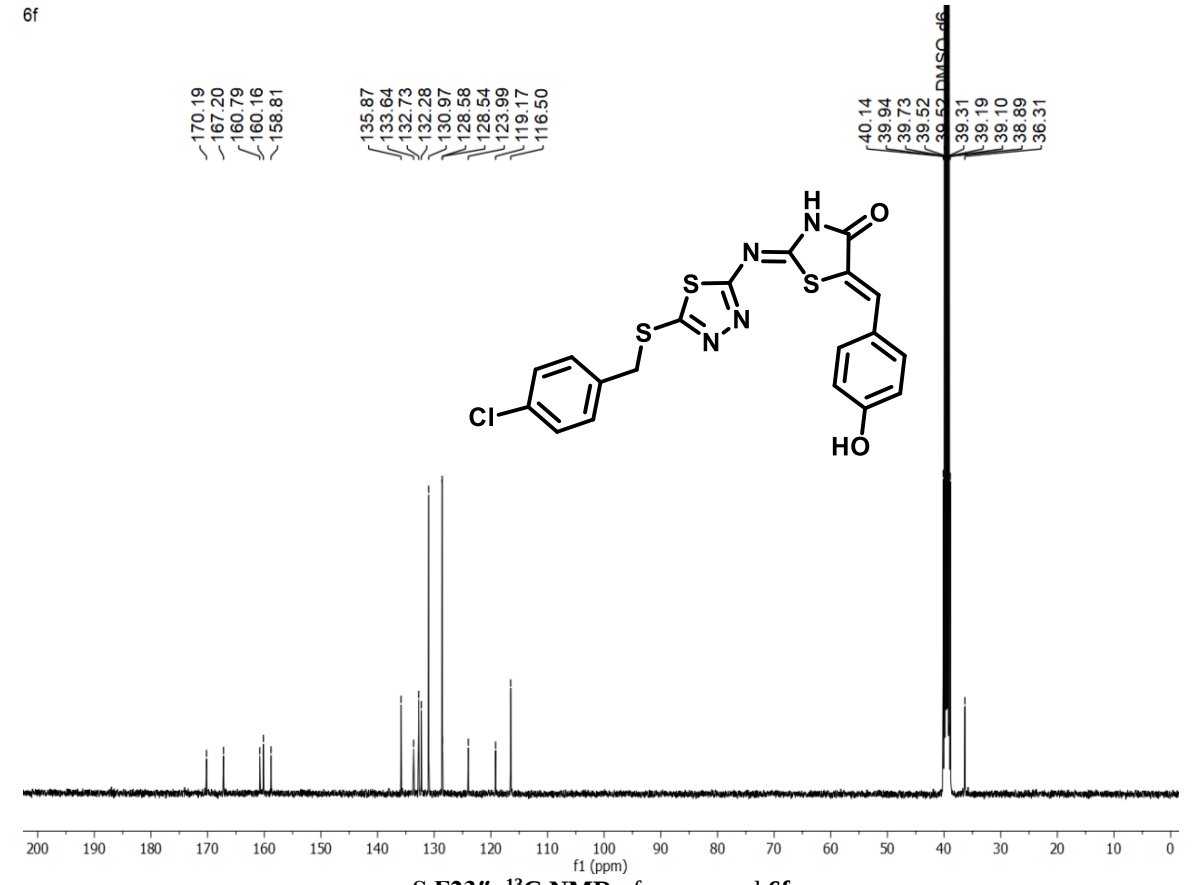

S.F23″: ^{13}C NMR of compound **6f**

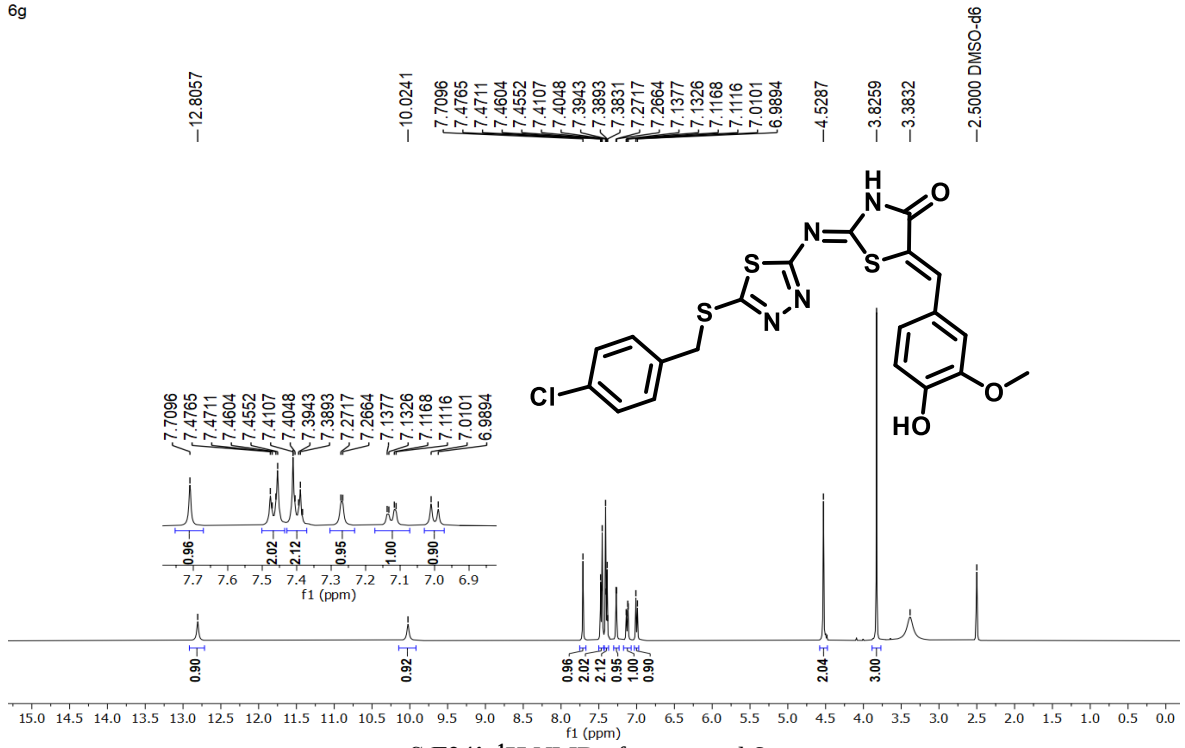

S.F24′: ^{1}H NMR of compound **6g**

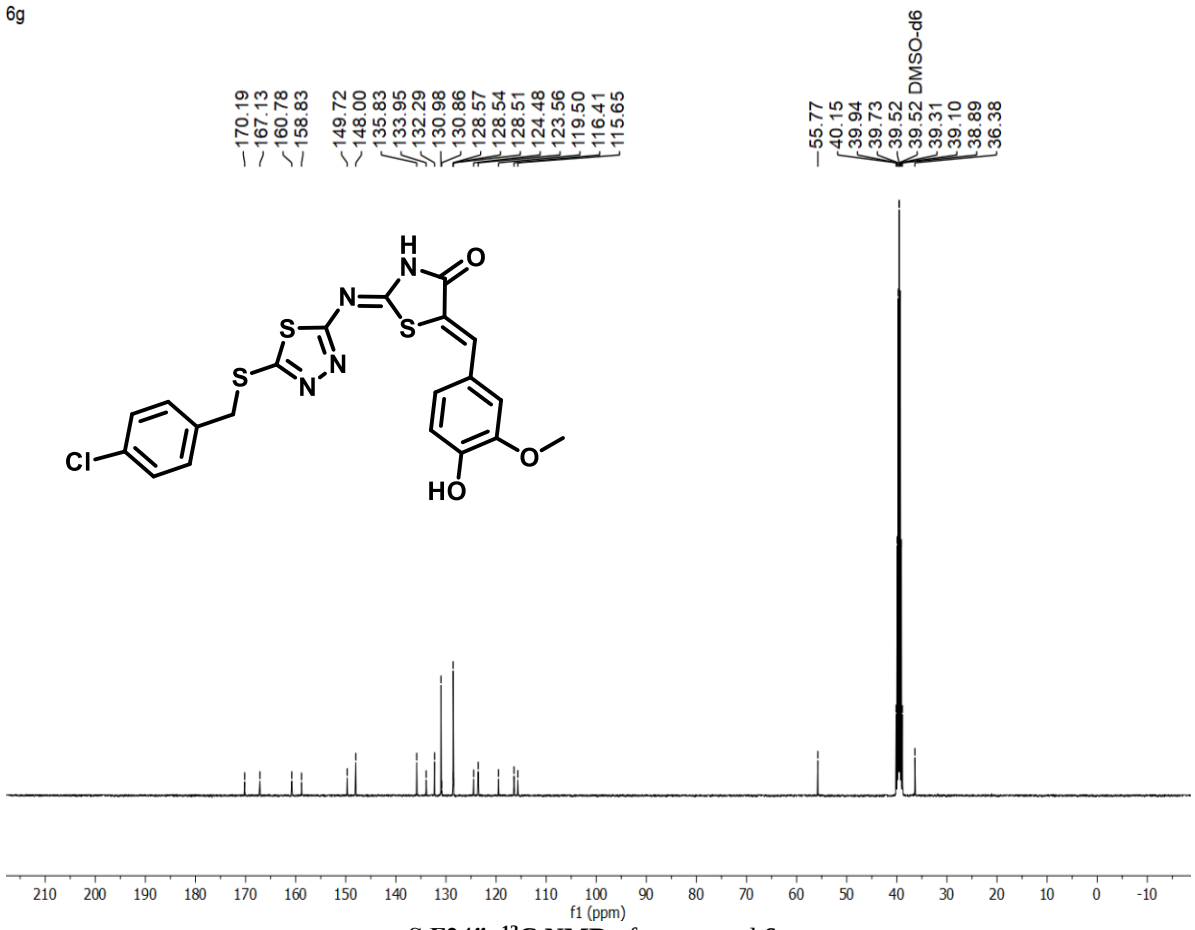

S.F24″: ^{13}C NMR of compound **6g**

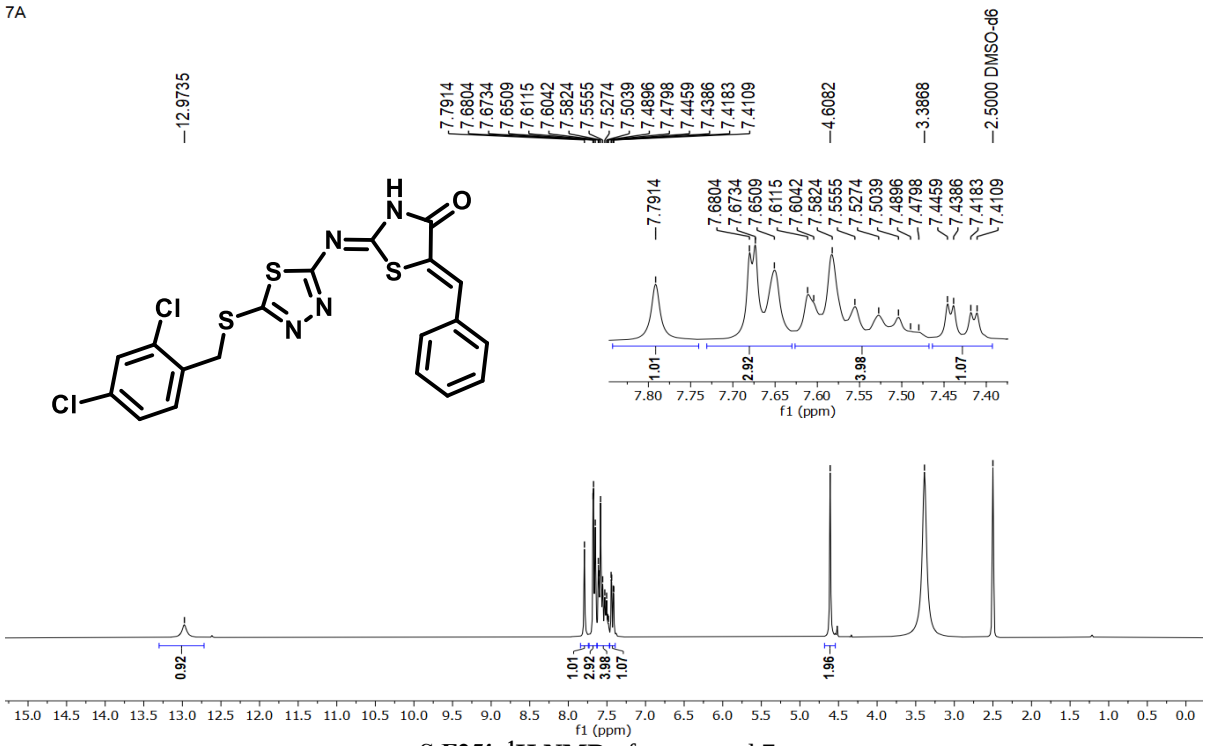

S.F25′: ^{1}H NMR of compound **7a**

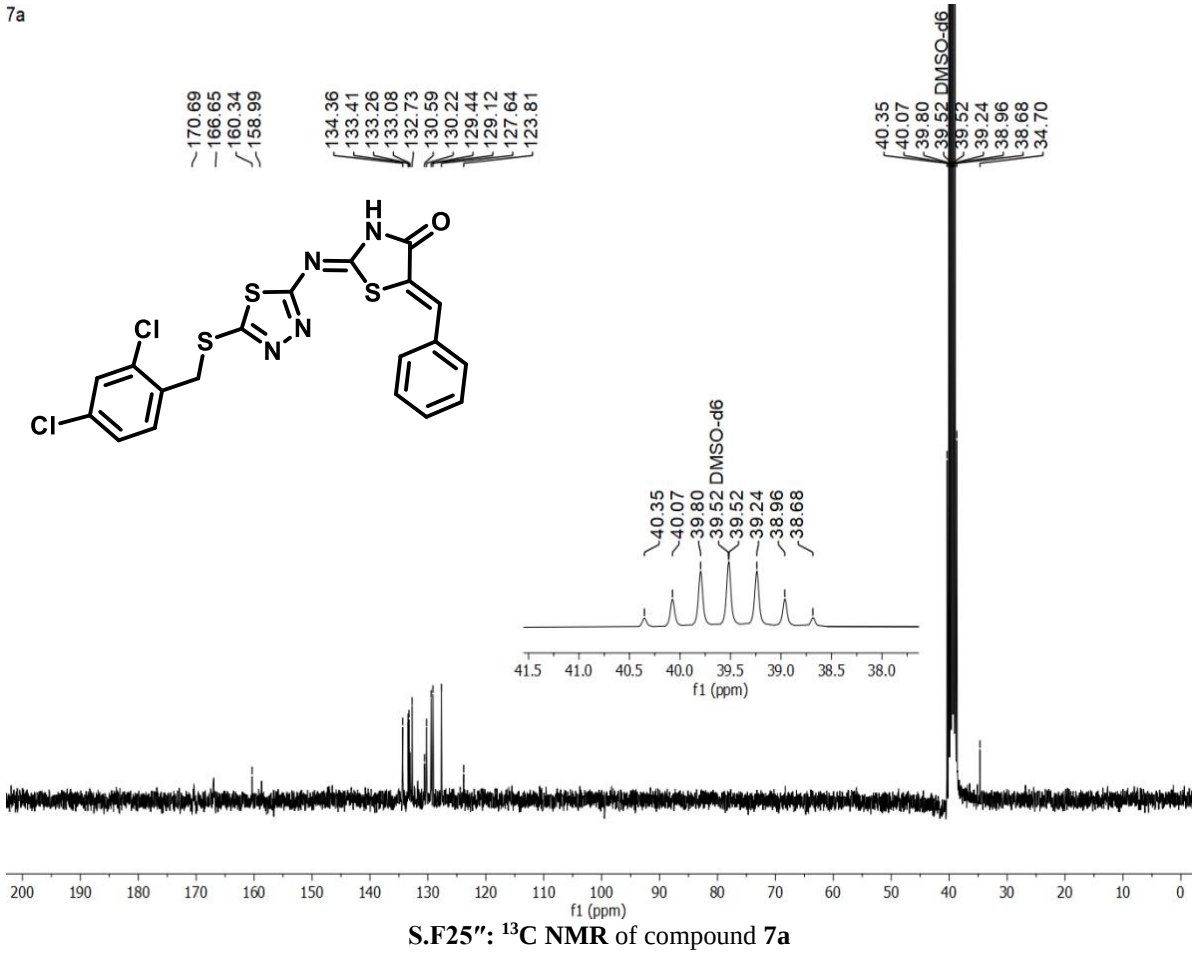

S.F25″: ^{13}C NMR of compound **7a**

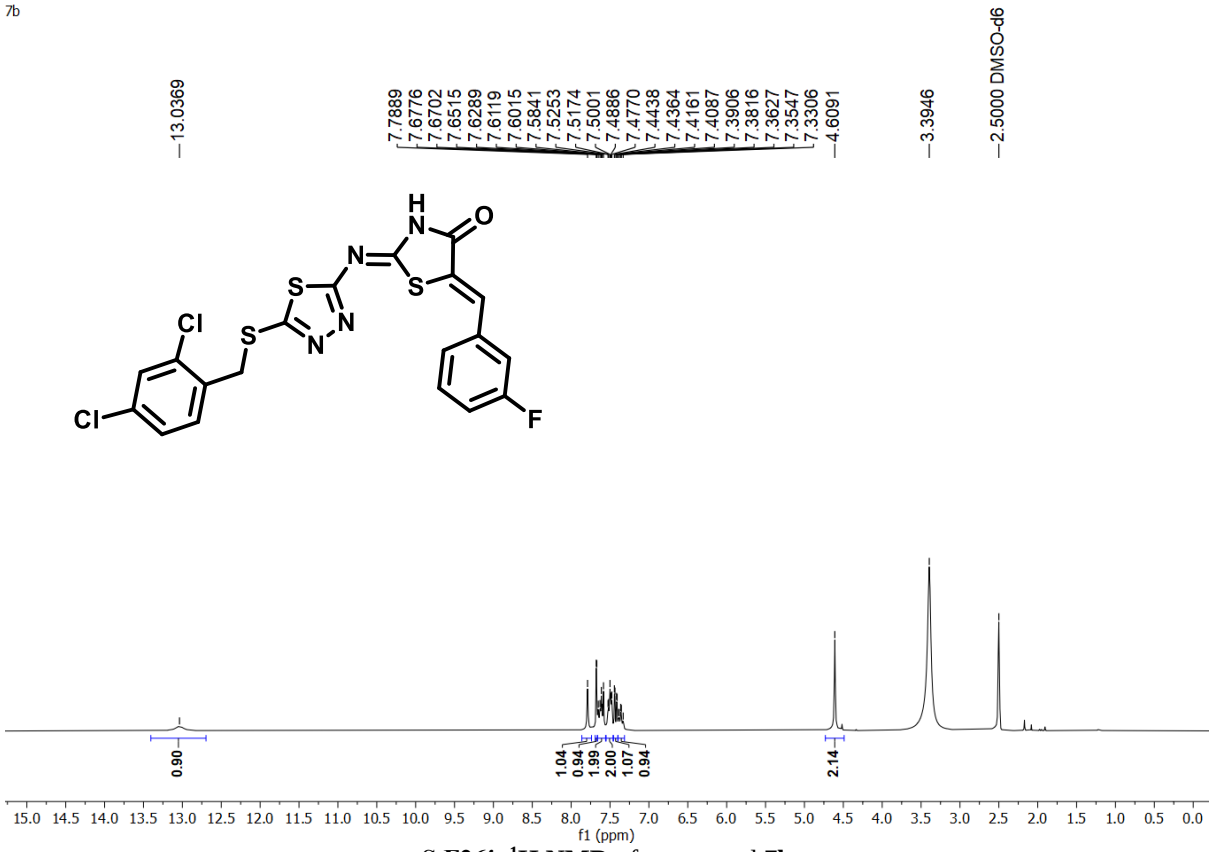

S.F26′: ^{1}H NMR of compound **7b**

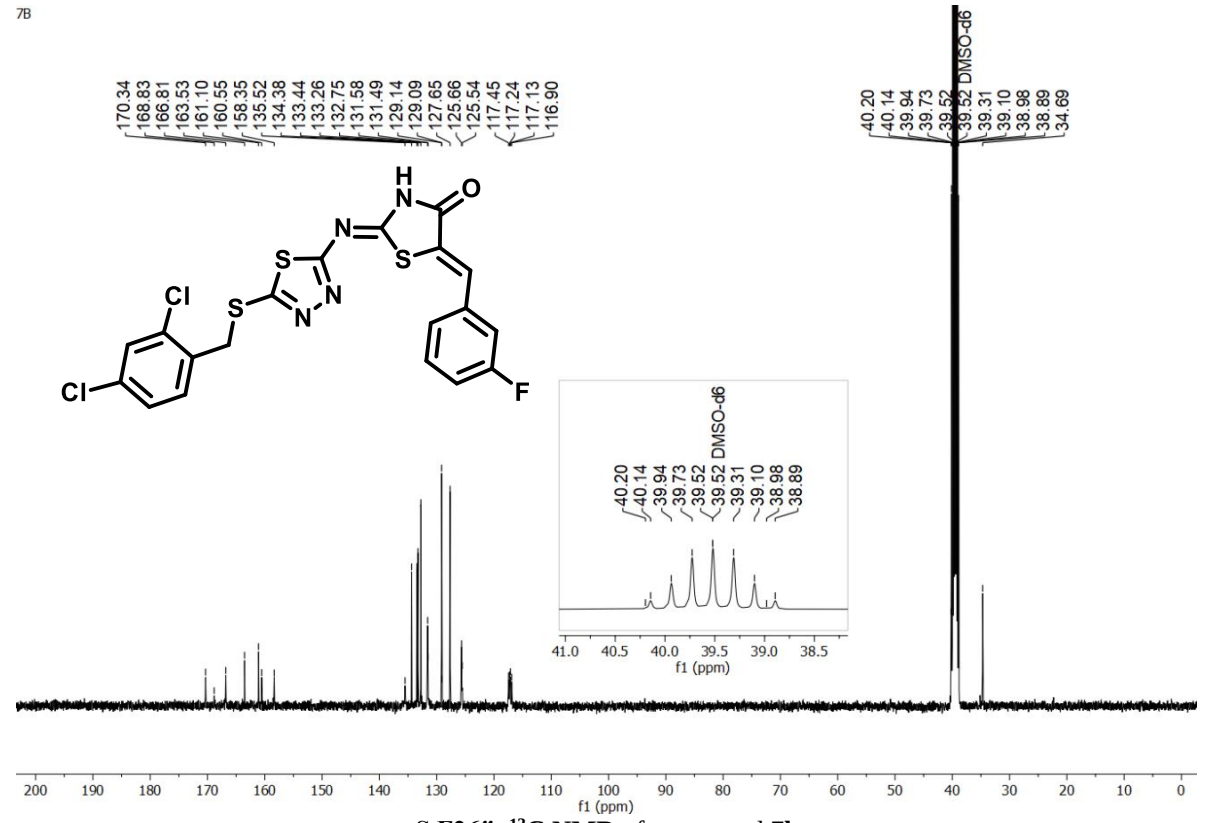

S.F26″: ^{13}C NMR of compound **7b**

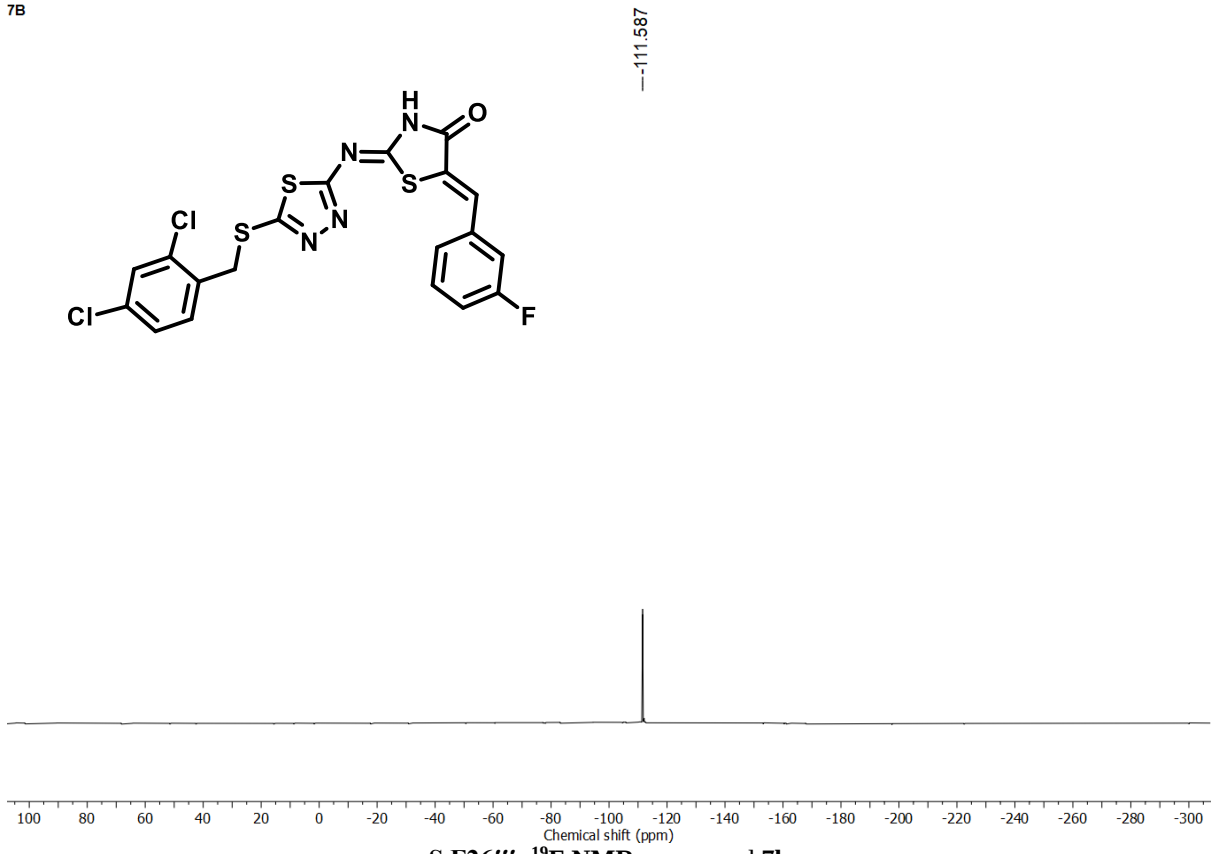

S.F26‴: ^{19}F NMR compound **7b**

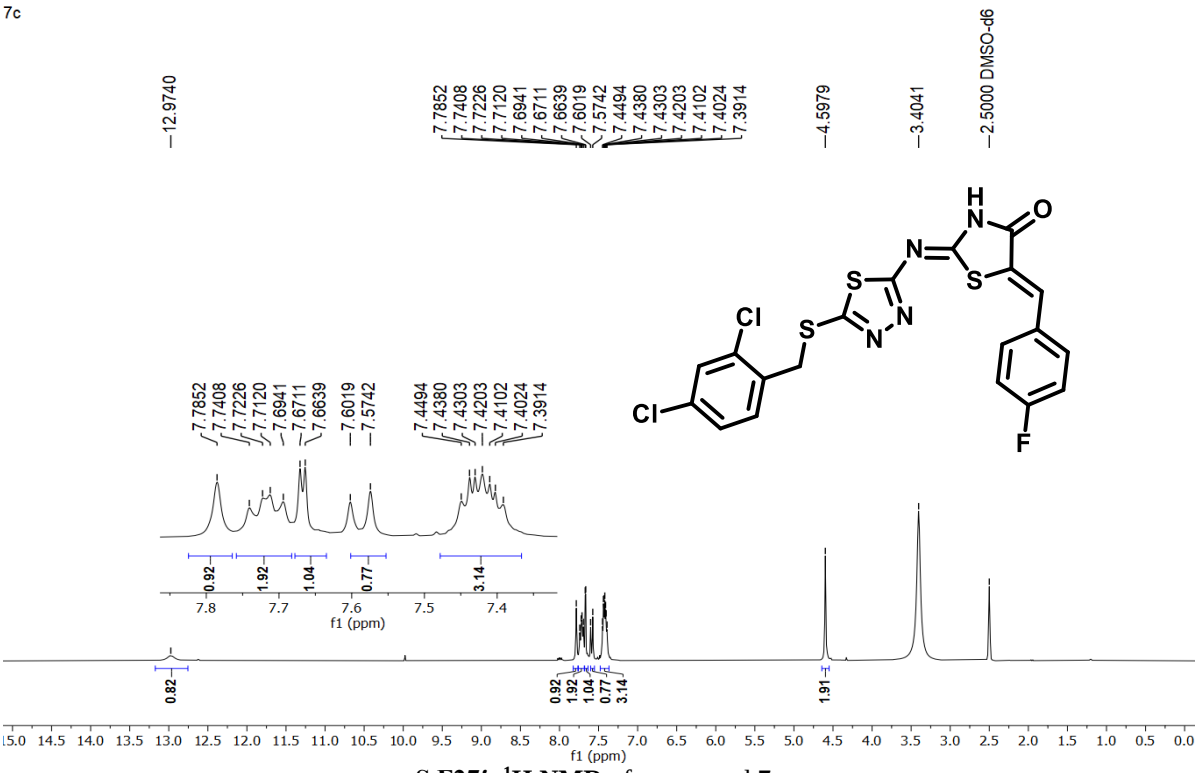

S.F27′: ^{1}H NMR of compound **7c**

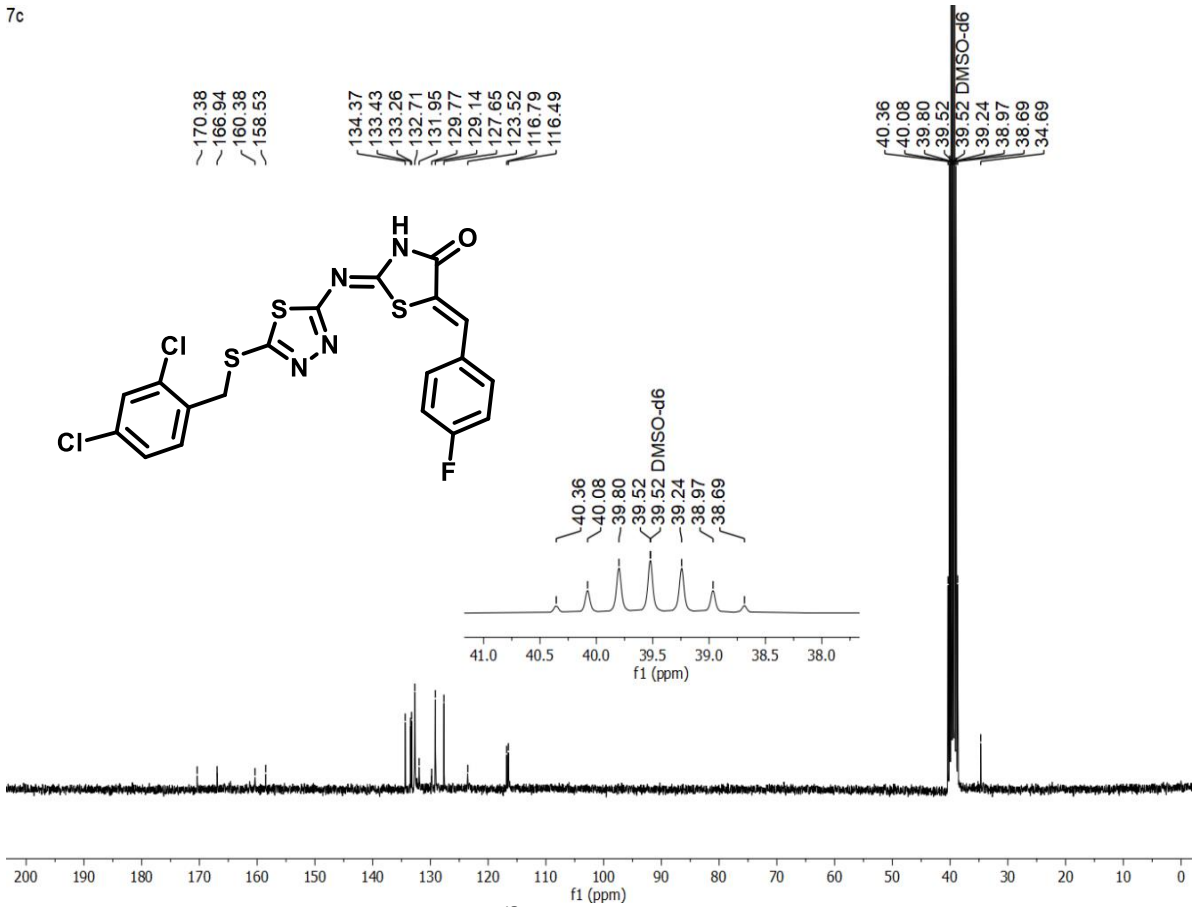

S.F27″: ^{13}C NMR of compound **7c**

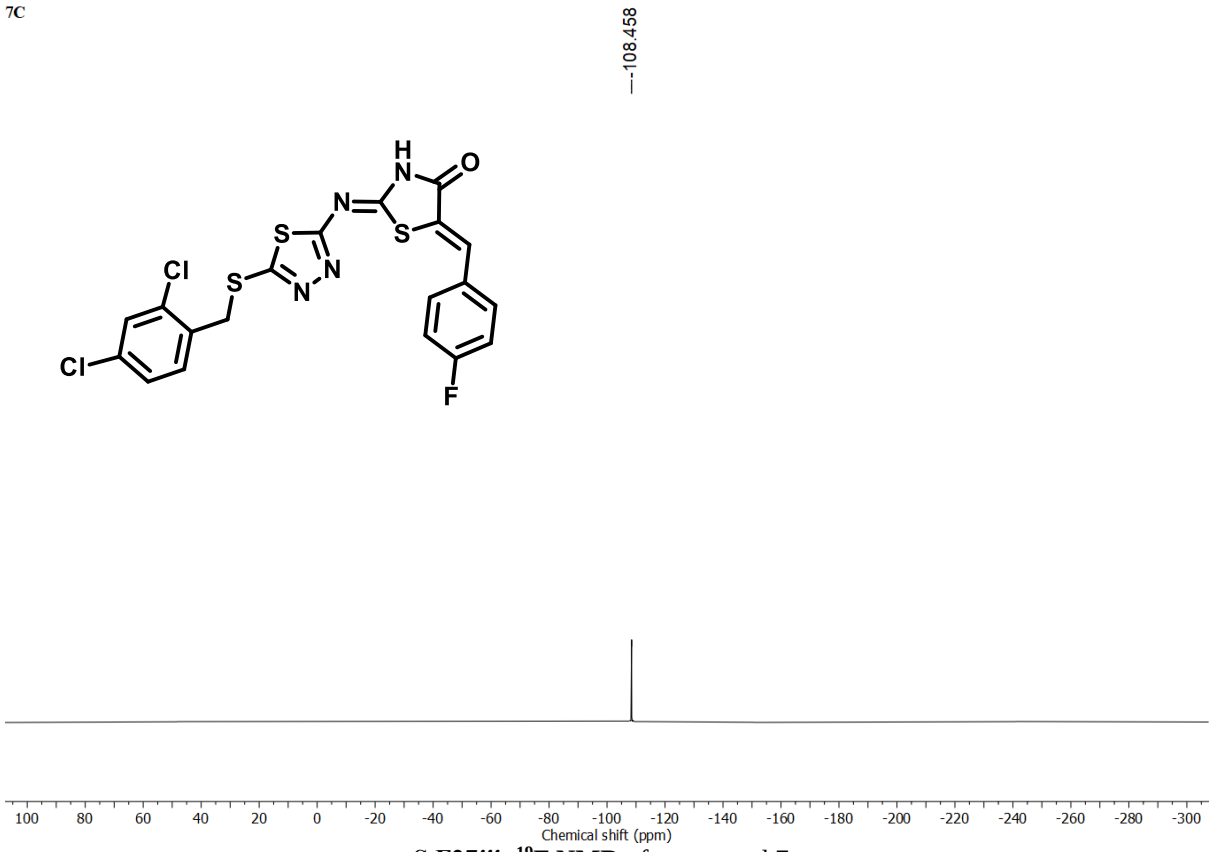

S.F27‴: ^{19}F NMR of compound **7c**

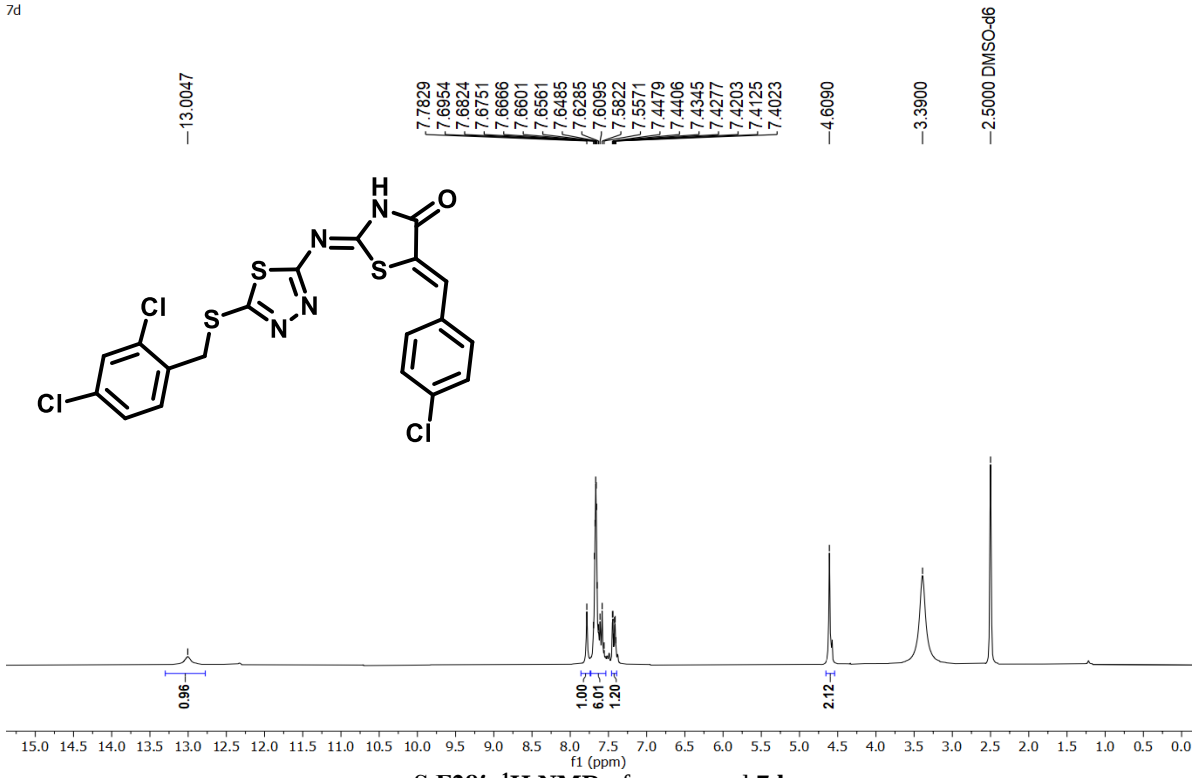

S.F28′: ^{1}H NMR of compound **7d**

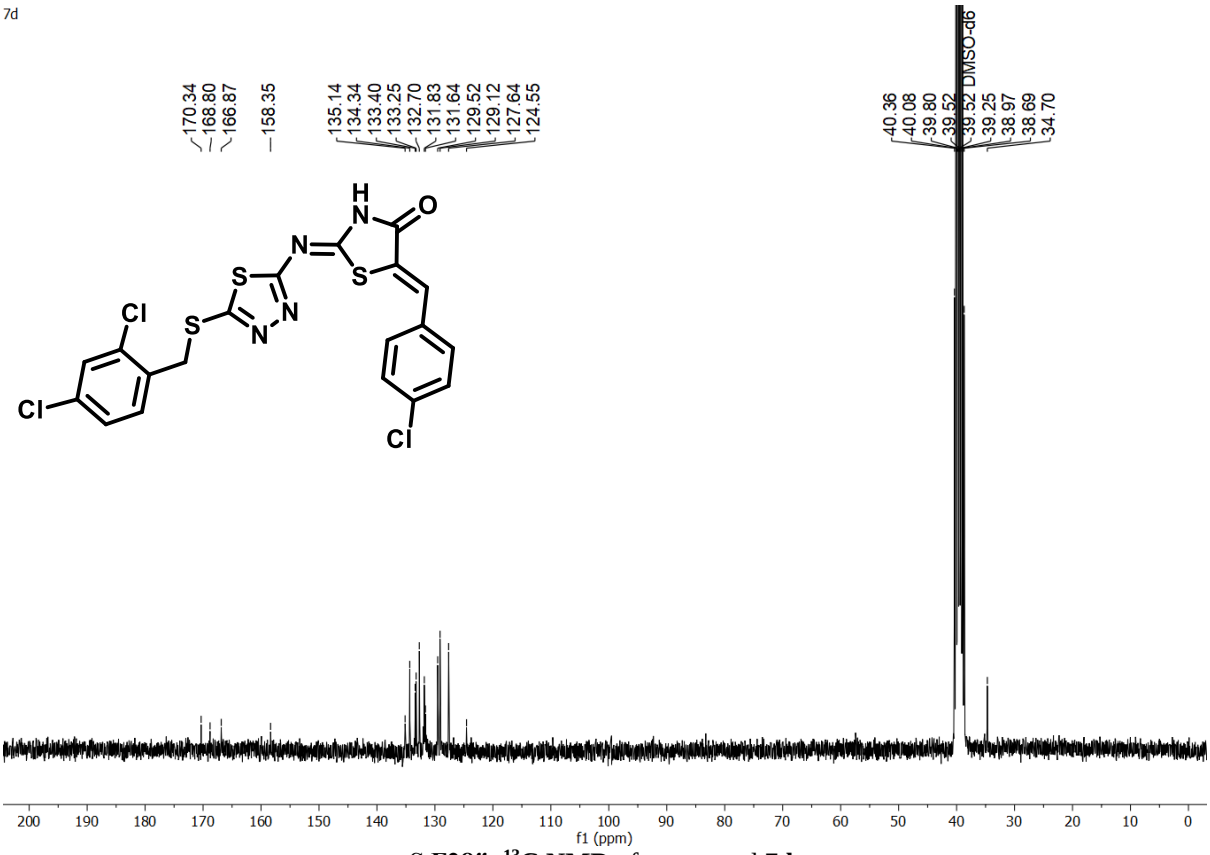

S.F28″: ^{13}C NMR of compound **7d**

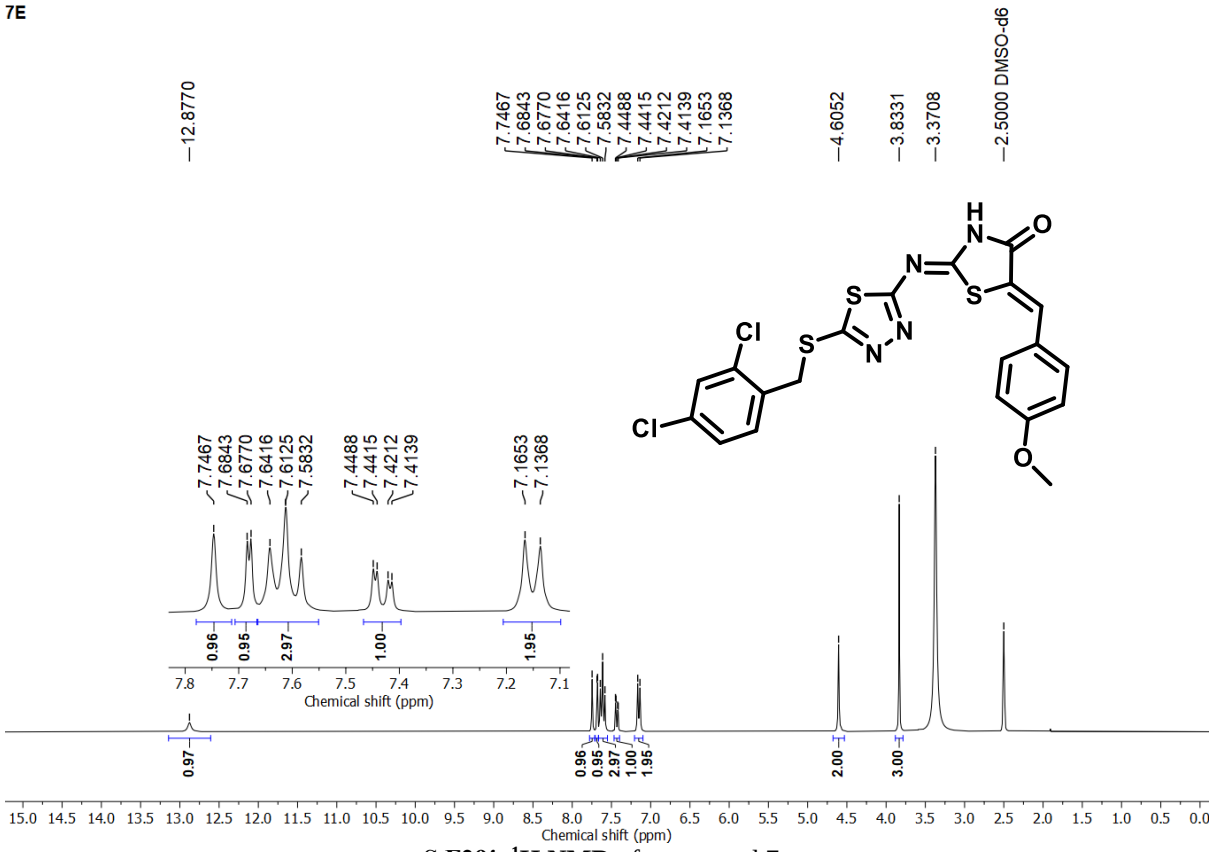

S.F29′: ^{1}H NMR of compound **7e**

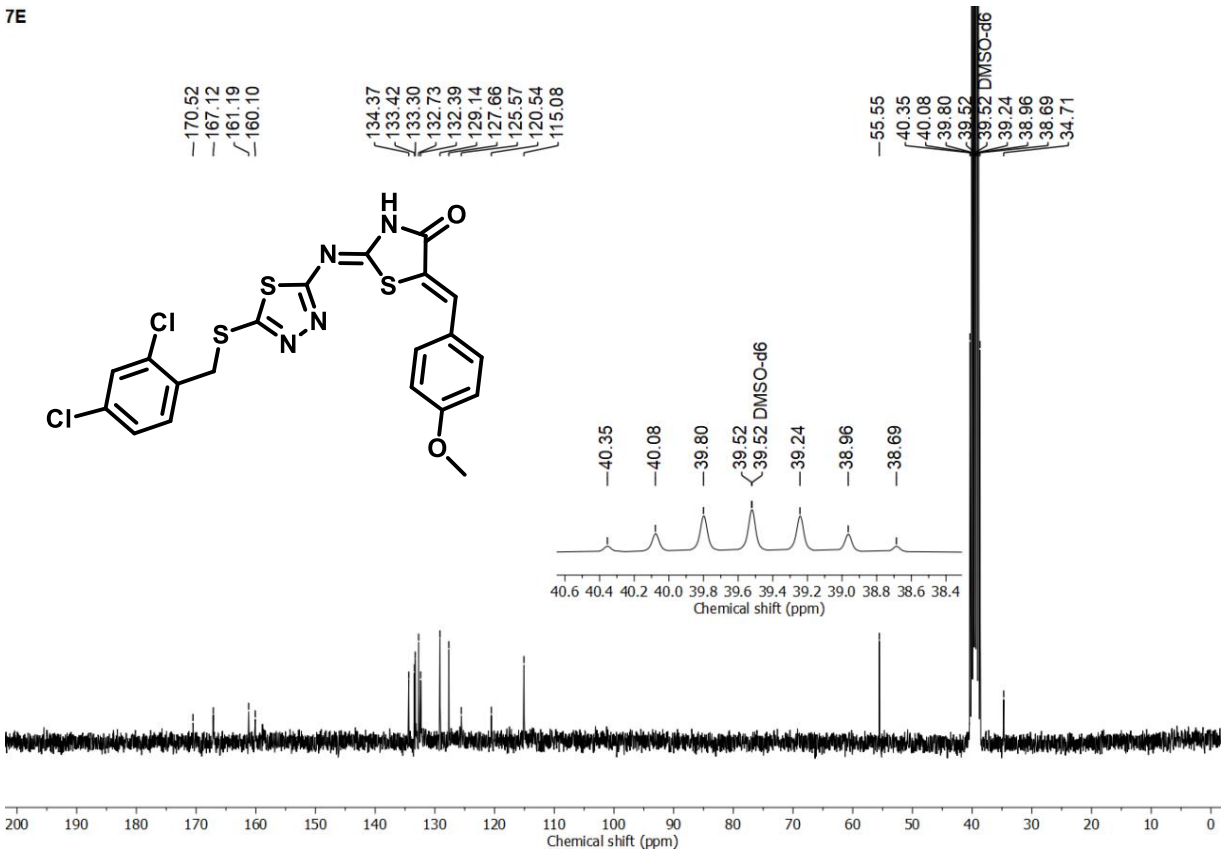

S.F29″: ^{13}C NMR of compound **7e**

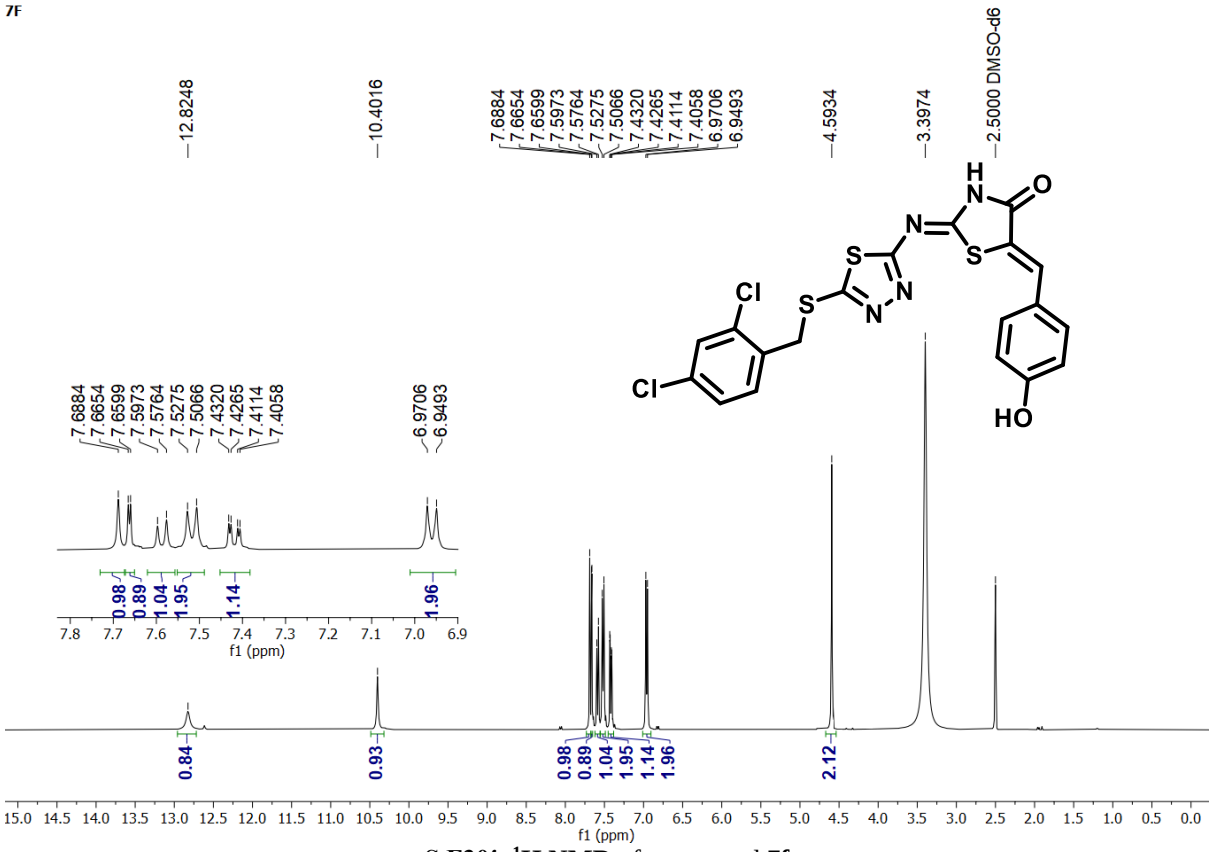

S.F30′: ^{1}H NMR of compound **7f**

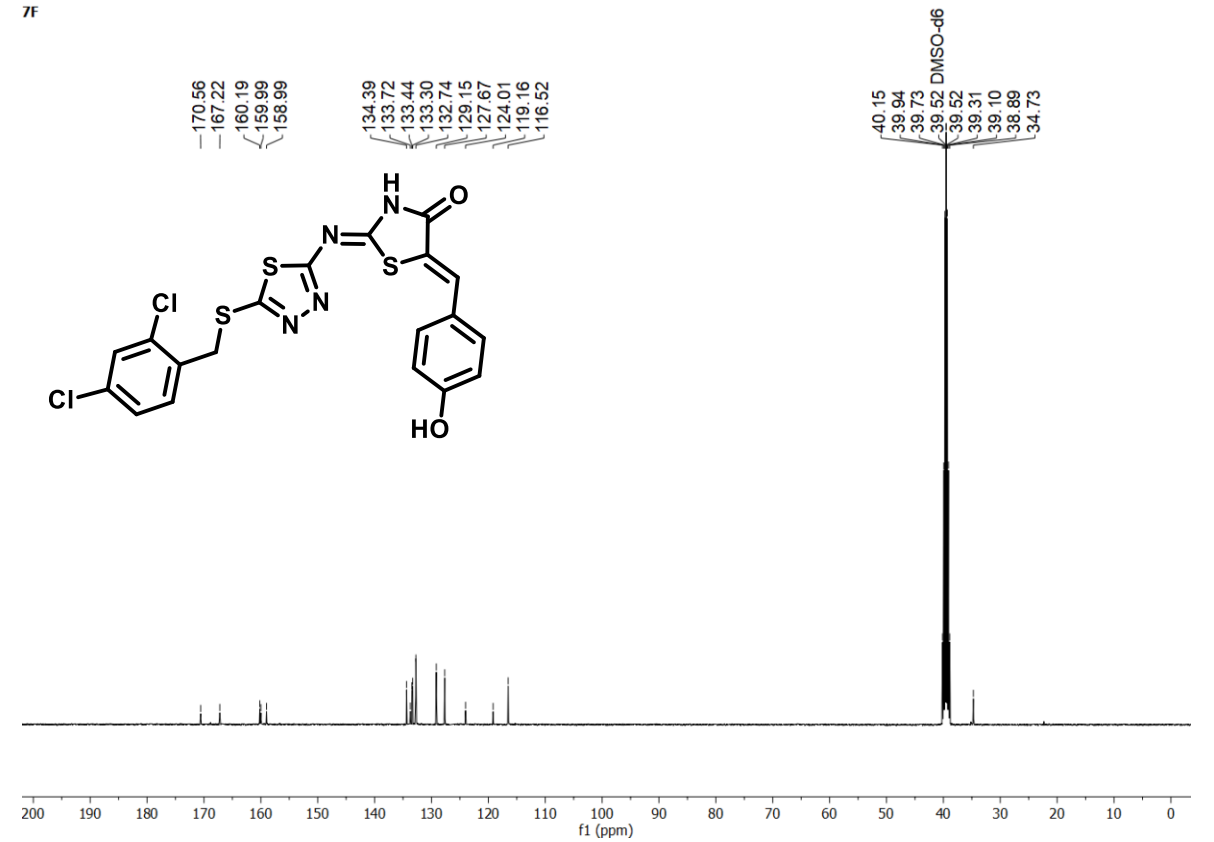

S.F30″: ^{13}C NMR of compound **7f**

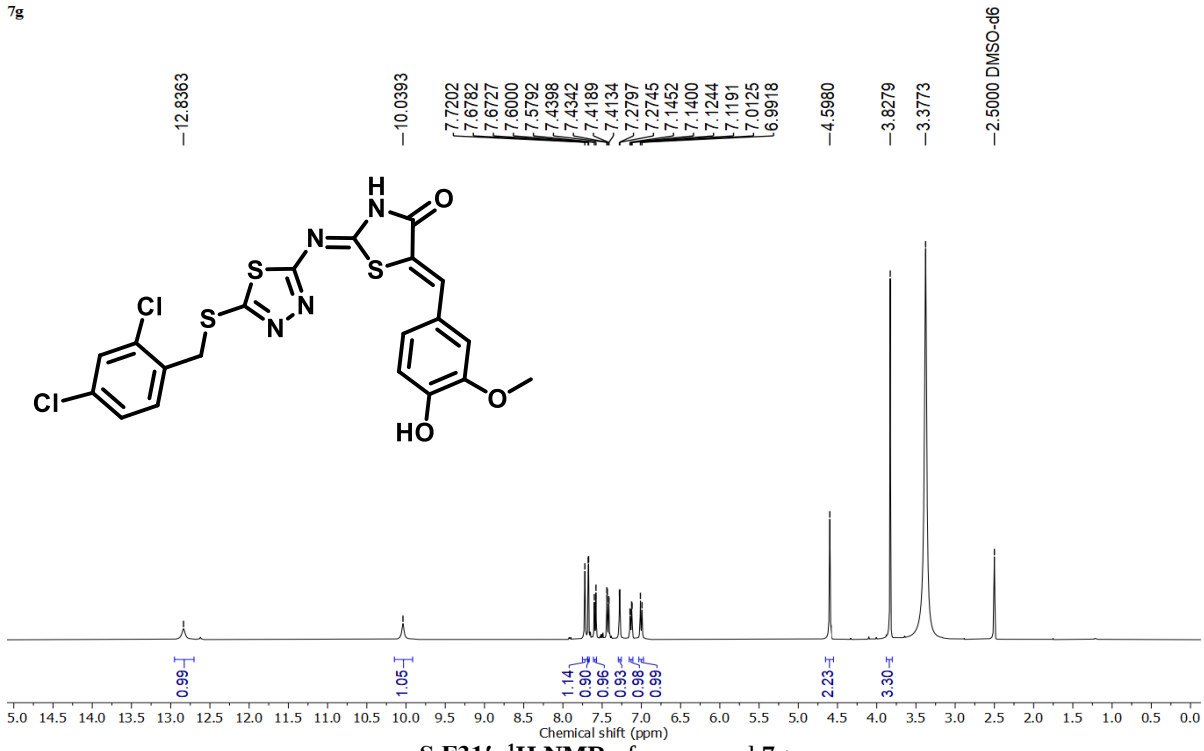

S.F31′: ^{1}H NMR of compound **7g**

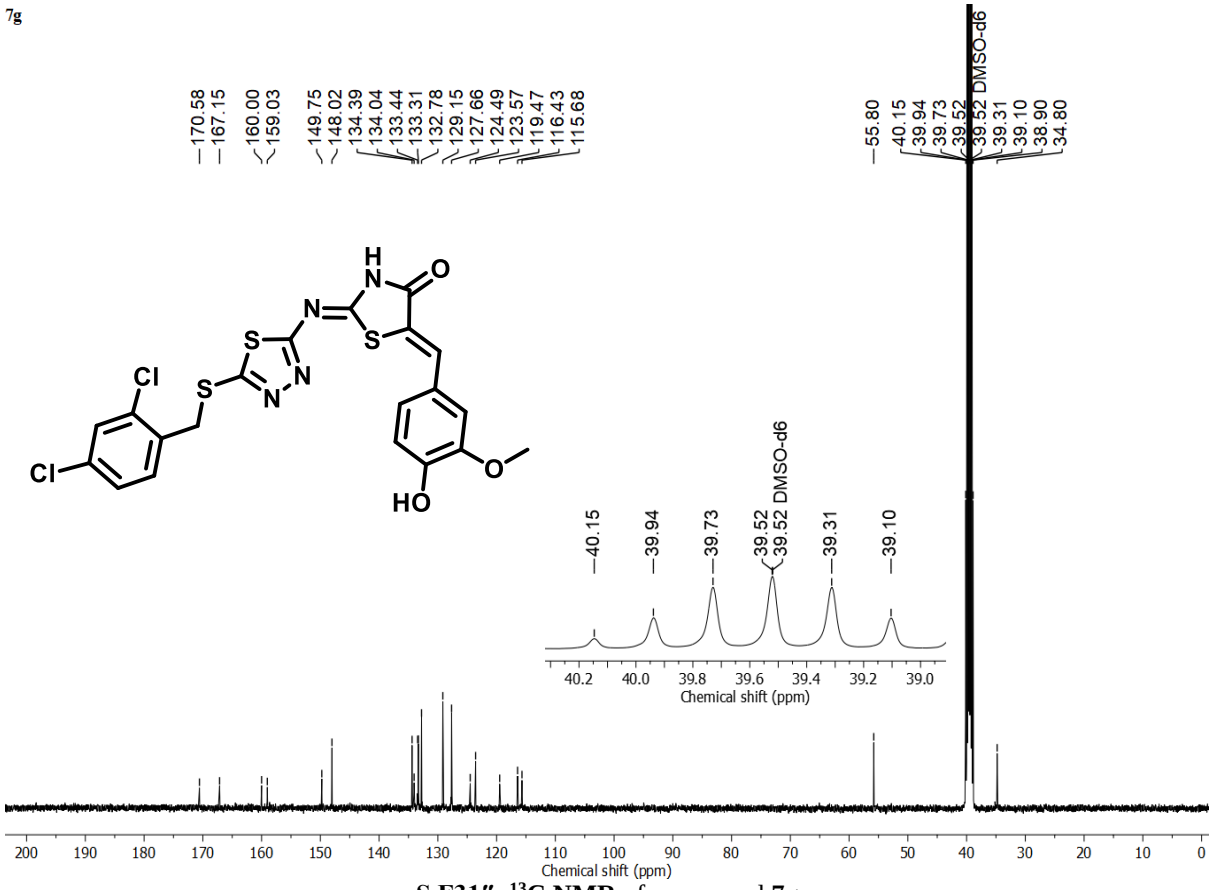

S.F31″: ^{13}C NMR of compound **7g**

2. Copy of HRMS Data (Final Compounds):

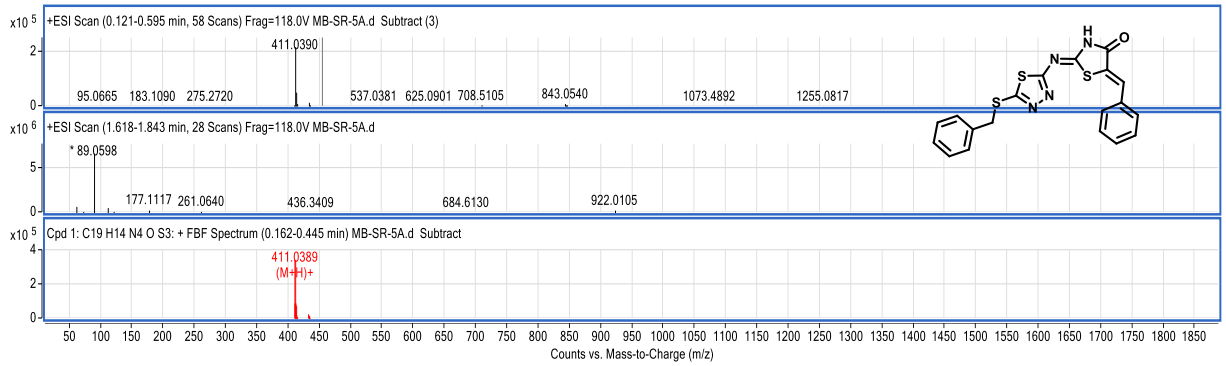

S.F32: HRMS Compound **5a**

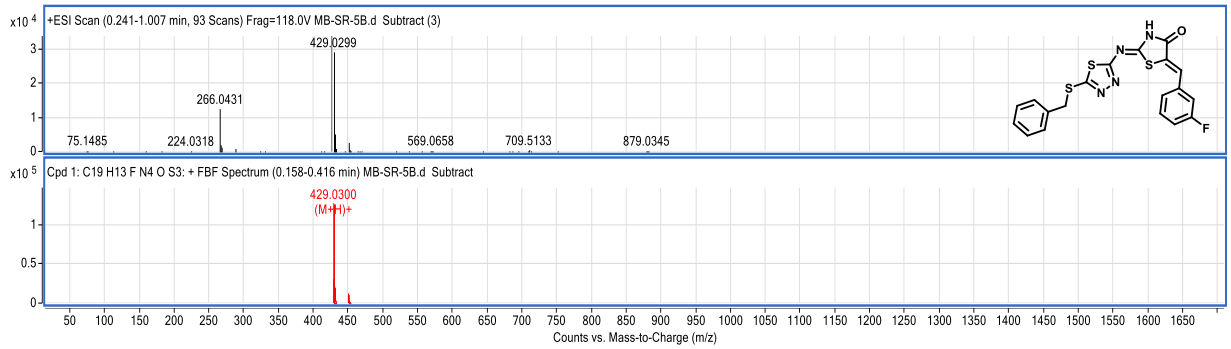

S.F33: HRMS Compound **5b**

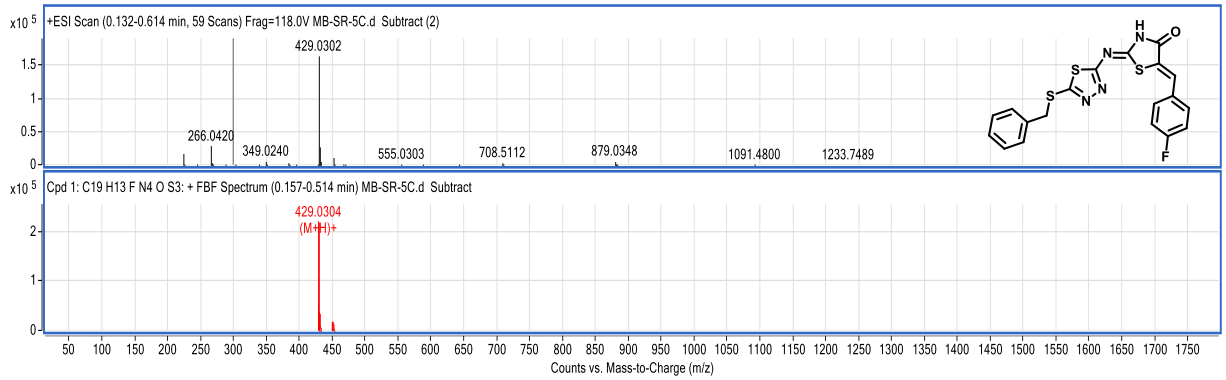

S.F34: HRMS Compound **5c**

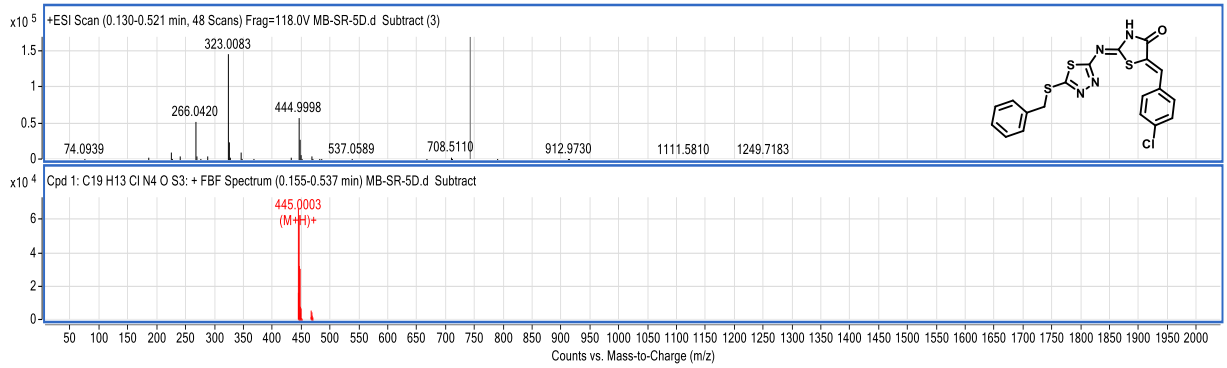

S.F35: HRMS Compound **5d**

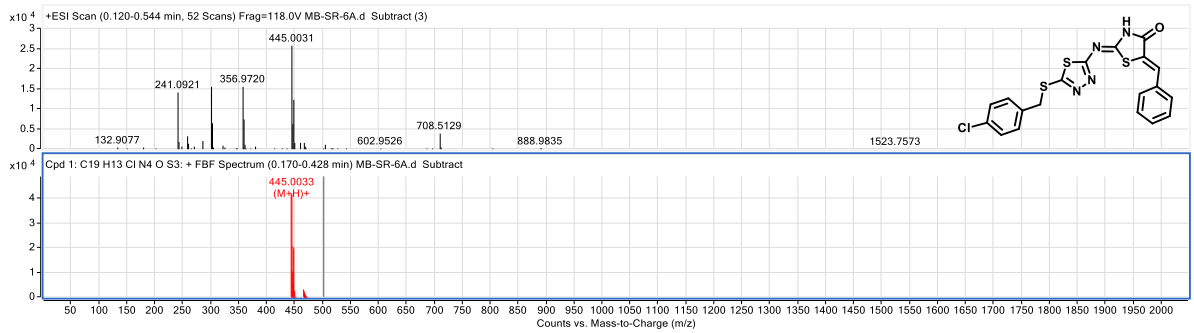

S.F36: HRMS Compound **6a**

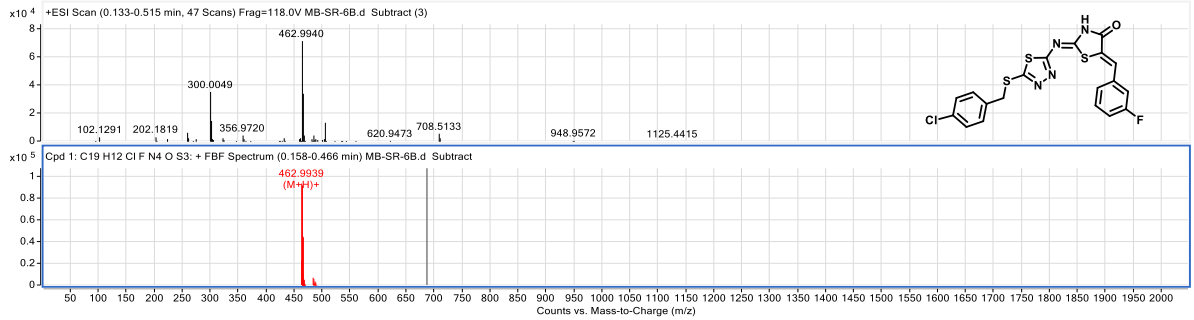

S.F37: HRMS Compound **6b**

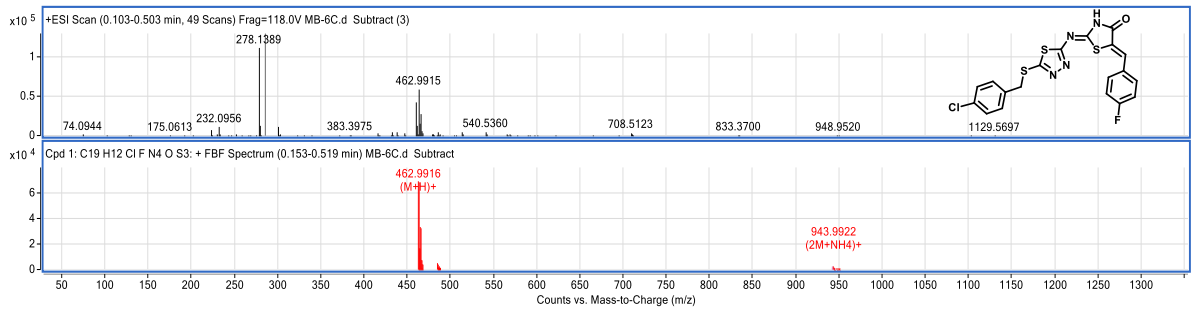

S.F38: HRMS Compound **6c**

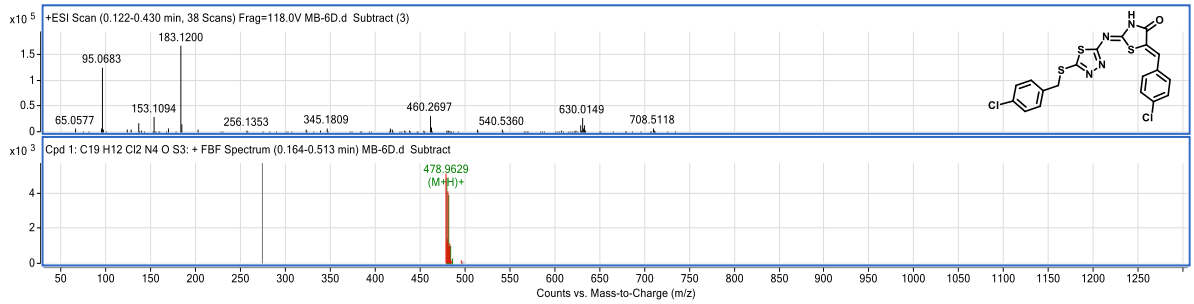

S.F39: HRMS Compound **6d**

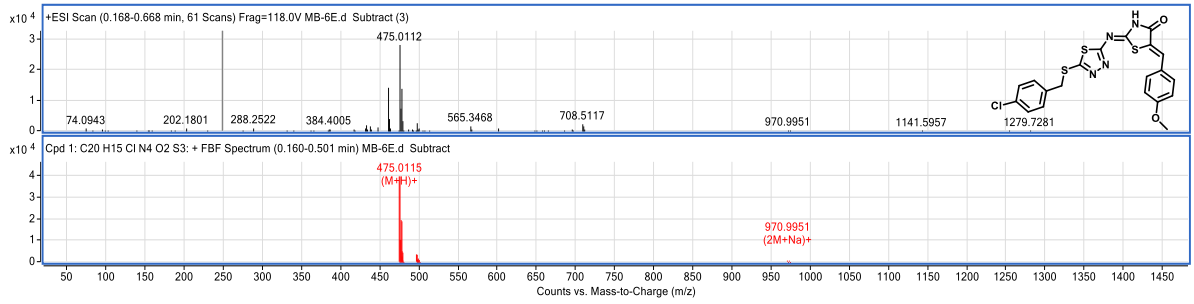

S.F40: HRMS Compound **6e**

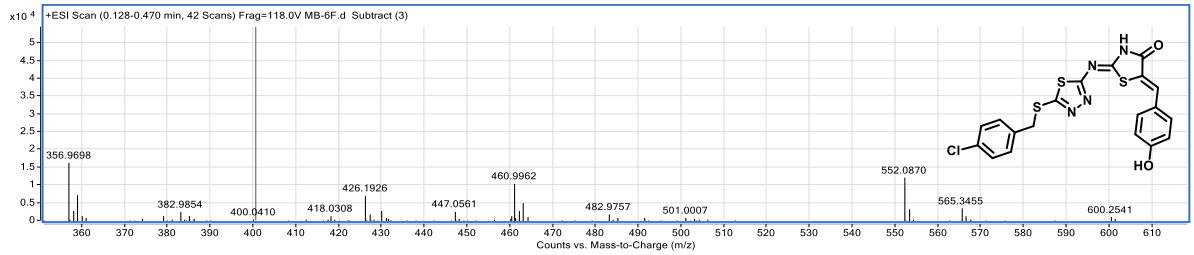

S.F41: HRMS Compound **6f**

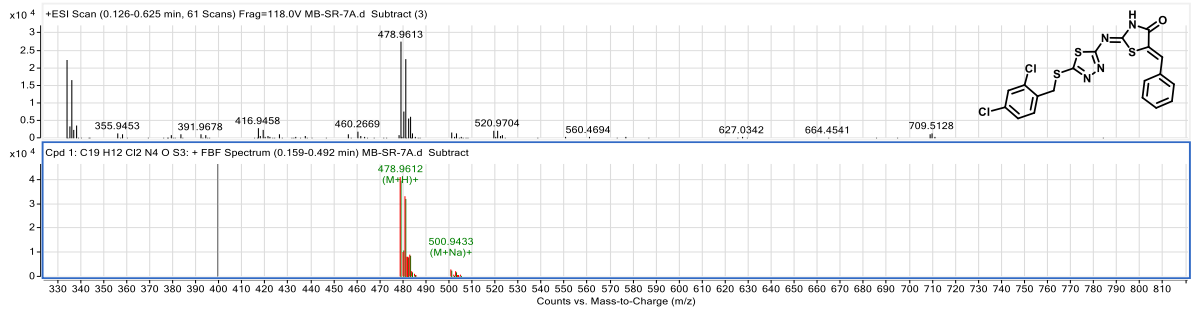

S.F42: HRMS Compound **7a**

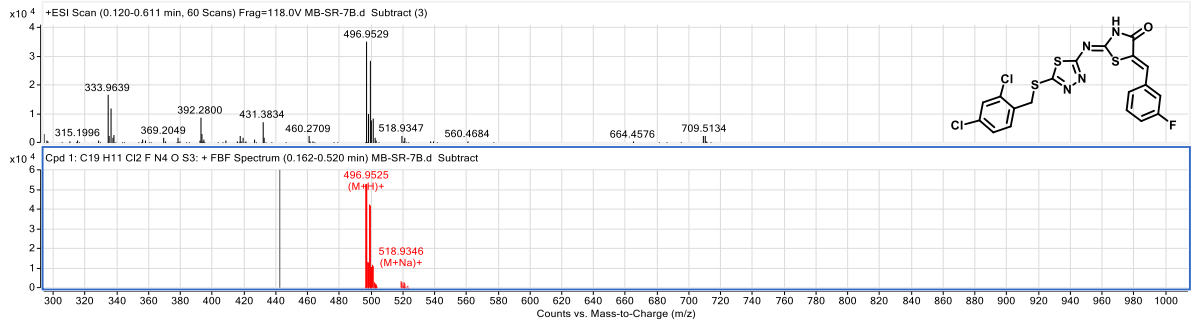

S.F43: HRMS Compound **7b**

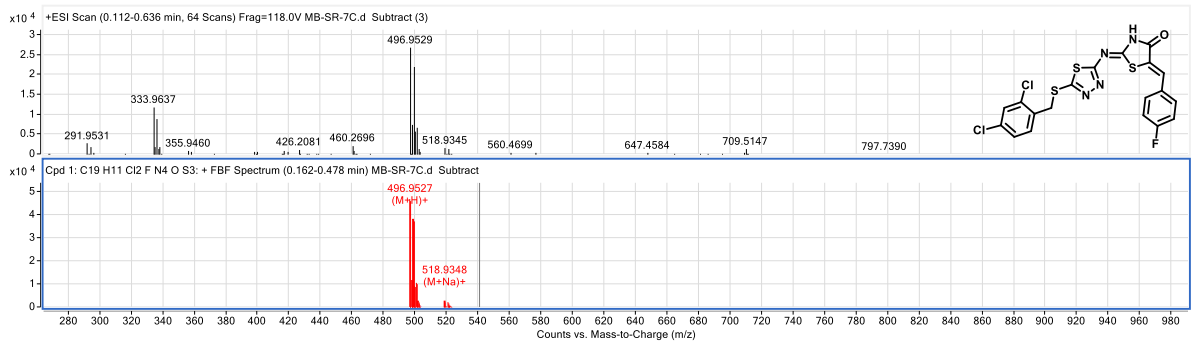

S.F44: HRMS Compound **7c**

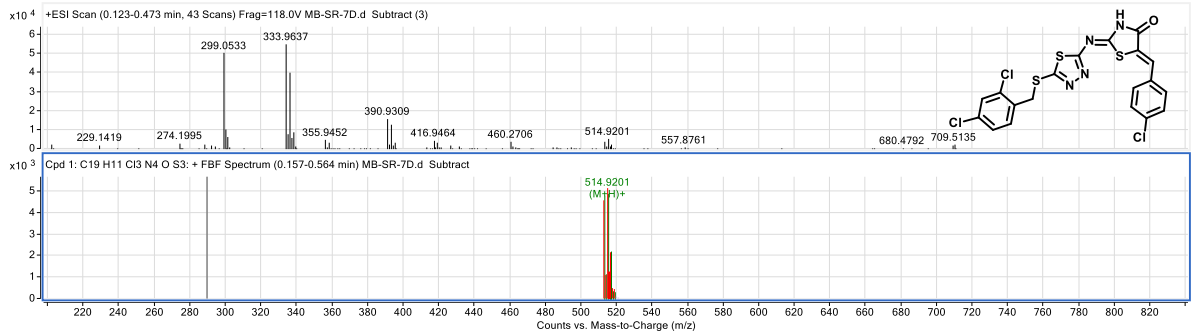

S.F45: HRMS Compound **7d**

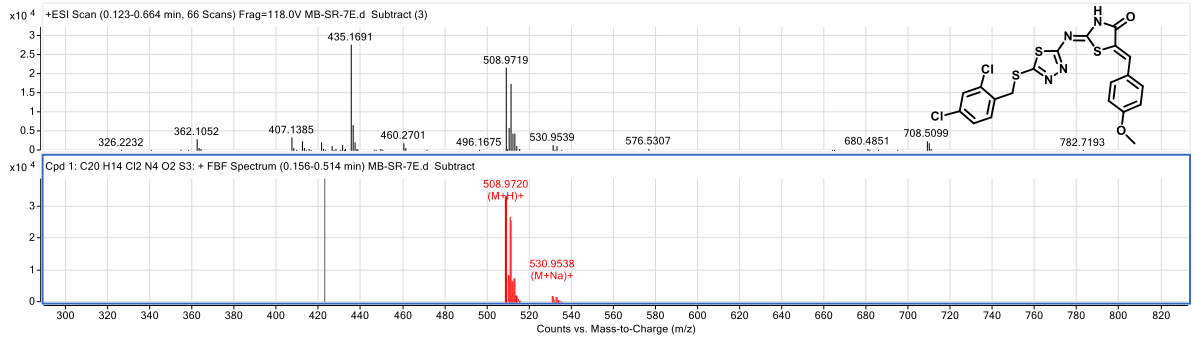

S.F46: HRMS Compound **7e**

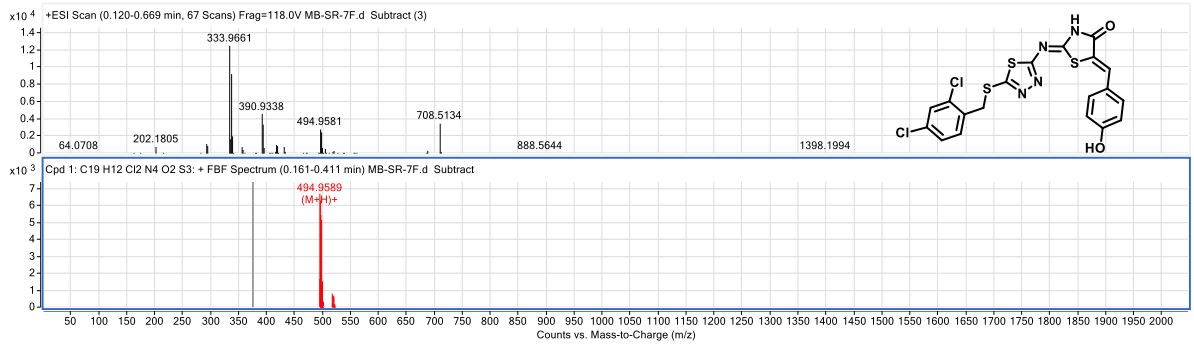

S.F47: HRMS Compound **7f**

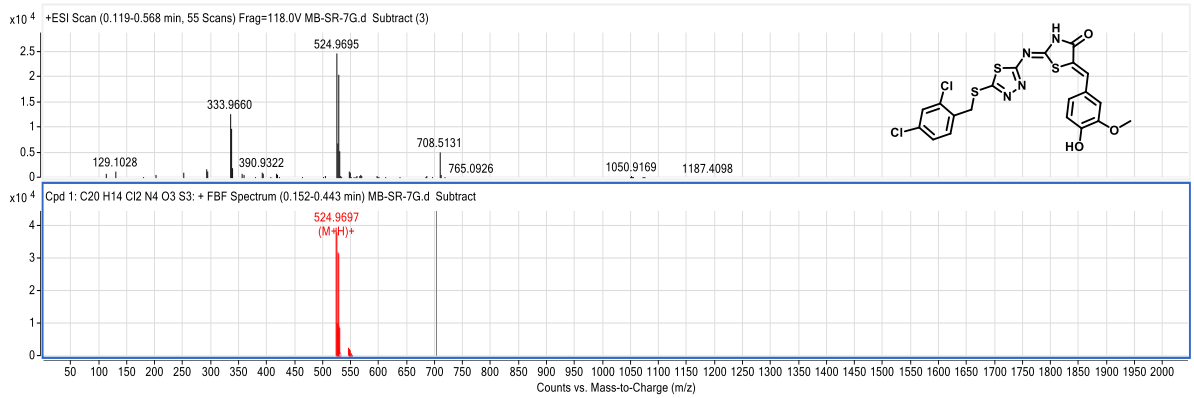

S.F48: HRMS Compound **7g**

3. Copy of supplementary crystal data:

X-ray crystallography of compounds 6g and 7f:

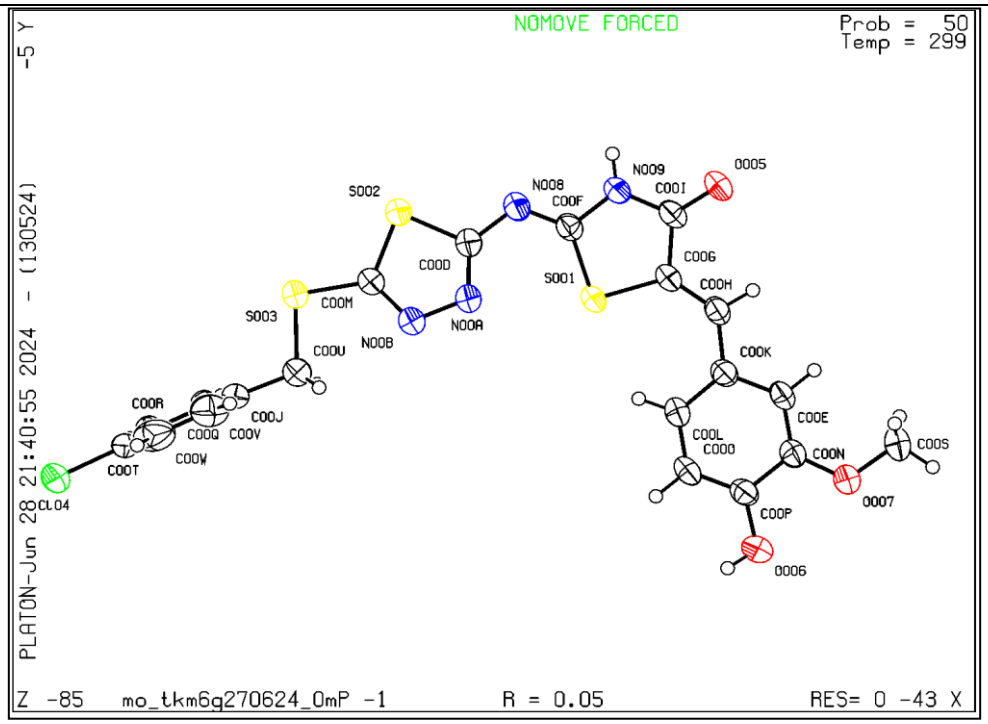

(6g)

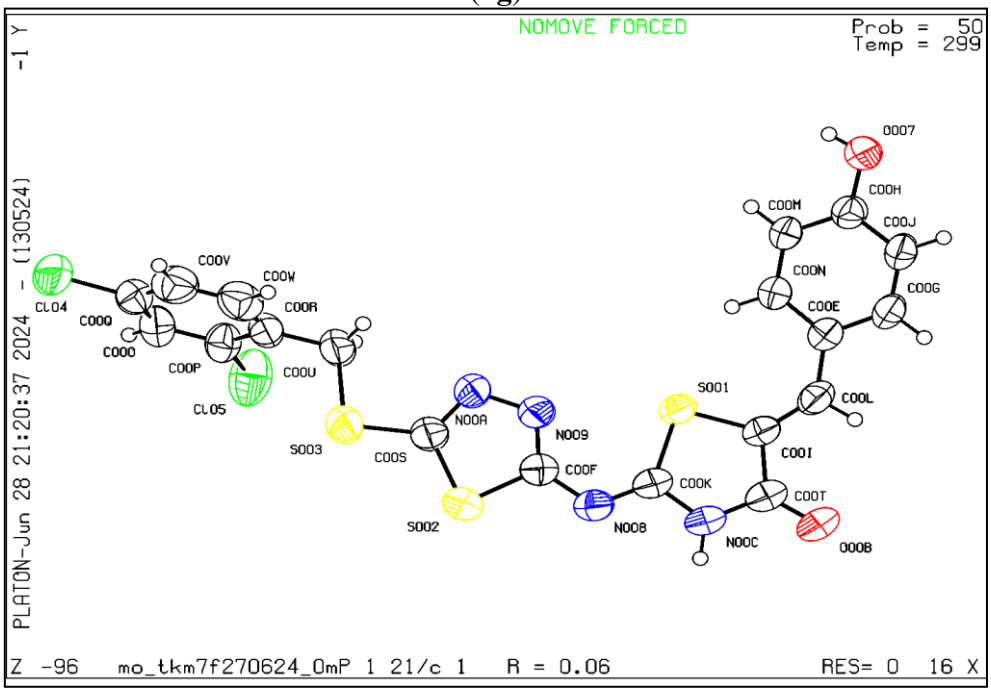

(7f)

S.F49: Molecular geometries of (a) **6g** and (b) **7f** in crystals.

Table S1: Crystallographic table of (a) **6g** and (b) **7f:**

Complexes	**6g**	**7f**
CCDC	2366716	2366780
formula	C_{20} $H_{19}NO_4S$	$C_{19}H_{12}Cl_2N_4O_2S_3$
fw	490.99	495.41
crystal system	triclinic	monoclinic
space group	P -1	P 21/c
a (Å)	10.270(2)	10.146(2)
b (Å)	10.497(2)	17.022(5)
c(Å)	13.887(3)	15.237(4)
α (°)	73.266(7)	90
β (°)	81.446(7)	101.398(7)
γ (°)	85.763(6)	90
V (Å^3)	1416.8(5)	2579.5(11)
Z	4	4
T (K)	299	299
Dx, g cm-3	1.275	1.477
μ (mm^{-1})	0.389	0.607
R1[a][I>2*σ*(I)]/GOF [b]	0.0514/ 1.020	0.0580/ 1.026
*w*R2[c] (I>2*σ* (I))	0.1689	0.1938
observation criterion: [a]R1 = $\Sigma\|\|F_o\|-\|F_c\|\|/\Sigma\|F_o\|$. [b]GOF = $\{\Sigma[w(F_o^2-F_c^2)^2]/(n-p)\}^{1/2}$, [c]*w*R2 = $[\Sigma[w(F_o^2-F_c^2)^2]/\Sigma[w(F_o^2)^2]]^{1/2}$ where $w = 1/[\sigma^2(F_o^2) + (aP)^2+bP]$, $P = (F_o^2+2F_c^2)/3$.		

NB: **S.F**–Spectral Figure

References:

[1] Y. Hu, C.-Y. Li, X.-M. Wang, Y.-H. Yang, H.-L. Zhu, 1,3,4-Thiadiazole: Synthesis, Reactions, and Applications in Medicinal, Agricultural, and Materials Chemistry, Chem Rev 114 (2014) 5572–5610. https://doi.org/10.1021/cr400131u.

[2] A.T. Balaban, D.C. Oniciu, A.R. Katritzky, Aromaticity as a Cornerstone of Heterocyclic Chemistry, Chem Rev 104 (2004) 2777–2812. https://doi.org/10.1021/cr0306790.

[3] X. Li, D. Wang, S. Li, W. Xue, X. Qian, K. Liu, Y. Li, Q. Lin, G. Dong, F. Meng, L. Jian, Discovery of N-(1,3,4-thiadiazol-2-yl)benzamide derivatives containing a 6,7-methoxyquinoline structure as novel EGFR/HER-2 dual-target inhibitors against cancer growth and angiogenesis, Bioorg Chem 119 (2022) 105469. https://doi.org/10.1016/j.bioorg.2021.105469.

[4] A.C. Tripathi, S.J. Gupta, G.N. Fatima, P.K. Sonar, A. Verma, S.K. Saraf, 4-Thiazolidinones: The advances continue…, Eur J Med Chem 72 (2014) 52–77. https://doi.org/10.1016/j.ejmech.2013.11.017.

[5] A.K. Jain, A. Vaidya, V. Ravichandran, S.K. Kashaw, R.K. Agrawal, Recent developments and biological activities of thiazolidinone derivatives: A review, Bioorg Med Chem 20 (2012) 3378–3395. https://doi.org/10.1016/j.bmc.2012.03.069.

[6] H. Şenol, A.G. Ağgül, S. Atasoy, Synthesis, Characterization, Molecular Docking and *in vitro* Biological Studies of Thiazolidin-4-one Derivatives as Anti-Breast-Cancer Agents, ChemistrySelect 8 (2023). https://doi.org/10.1002/slct.202300481.

[7] T. Gregorić, M. Sedić, P. Grbčić, A. Tomljenović Paravić, S. Kraljević Pavelić, M. Cetina, R. Vianello, S. Raić-Malić, Novel pyrimidine-2,4-dione–1,2,3-triazole and furo[2,3-d]pyrimidine-2-one–1,2,3-triazole hybrids as potential anti-cancer agents: Synthesis, computational and X-ray analysis and biological evaluation, Eur J Med Chem 125 (2017) 1247–1267. https://doi.org/10.1016/j.ejmech.2016.11.028.

[8] A. Sarkar, A. Paul, T. Banerjee, A. Maji, S. Saha, A. Bishayee, T.K. Maity, Therapeutic advancements in targeting BCL-2 family proteins by epigenetic regulators, natural, and synthetic agents in cancer, Eur J Pharmacol 944 (2023) 175588. https://doi.org/10.1016/j.ejphar.2023.175588.

[9] A.N. Giaquinto, H. Sung, K.D. Miller, J.L. Kramer, L.A. Newman, A. Minihan, A. Jemal, R.L. Siegel, Breast Cancer Statistics, 2022, CA Cancer J Clin 72 (2022) 524–541. https://doi.org/10.3322/caac.21754.

[10] A. Sarkar, S. Saha, A. Paul, A. Maji, P. Roy, T.K. Maity, Understanding stem cells and its pivotal role in regenerative medicine, Life Sci 273 (2021) 119270. https://doi.org/10.1016/j.lfs.2021.119270.

[11] M.G. Salem, D.M.A. El-Maaty, Y.I.M. El-Deen, B.H. Elesawy, A. El Askary, A. Saleh, E.M. Saied, M. El Behery, Novel 1,3-Thiazole Analogues with Potent Activity against

Breast Cancer: A Design, Synthesis, In Vitro, and In Silico Study, Molecules 27 (2022) 4898. https://doi.org/10.3390/molecules27154898.

[12] A. Maji, A. Paul, A. Sarkar, S. Nahar, R. Bhowmik, A. Samanta, P. Nahata, B. Ghosh, S. Karmakar, T. Kumar Maity, Significance of TRAIL/Apo-2 ligand and its death receptors in apoptosis and necroptosis signalling: Implications for cancer-targeted therapeutics, Biochem Pharmacol 221 (2024) 116041. https://doi.org/10.1016/j.bcp.2024.116041.

[13] S. Arora, P. Narayan, C.L. Osgood, S. Wedam, T.M. Prowell, J.J. Gao, M. Shah, D. Krol, S. Wahby, M. Royce, S. Ghosh, R. Philip, G. Ison, T. Berman, C. Brus, E.W. Bloomquist, M.H. Fiero, S. Tang, R. Pazdur, A. Ibrahim, L. Amiri-Kordestani, J.A. Beaver, U.S. FDA Drug Approvals for Breast Cancer: A Decade in Review, Clinical Cancer Research 28 (2022) 1072–1086. https://doi.org/10.1158/1078-0432.CCR-21-2600.

[14] J. An, C. Peng, X. Xie, F. Peng, New Advances in Targeted Therapy of HER2-Negative Breast Cancer, Front Oncol 12 (2022). https://doi.org/10.3389/fonc.2022.828438.

[15] W. Cui, A. Aouidate, S. Wang, Q. Yu, Y. Li, S. Yuan, Discovering Anti-Cancer Drugs via Computational Methods, Front Pharmacol 11 (2020). https://doi.org/10.3389/fphar.2020.00733.

[16] C.R. Quijia, M. Chorilli, Piperine for treating breast cancer: A review of molecular mechanisms, combination with anticancer drugs, and nanosystems, Phytotherapy Research 36 (2022) 147–163. https://doi.org/10.1002/ptr.7291.

[17] A. Paul, A. Maji, A. Sarkar, S. Saha, P. Janah, T.K. Maity, Recent Approaches in the Synthesis of 5-Arylidene-2,4-thiazolidinedione Derivatives Using Knoevenagel Condensation, Mini Rev Org Chem 20 (2023) 5–34. https://doi.org/10.2174/1570193X19666220331155705.

[18] S. Pulya, A. Himaja, M. Paul, N. Adhikari, S. Banerjee, G. Routholla, S. Biswas, T. Jha, B. Ghosh, Selective HDAC3 Inhibitors with Potent In Vivo Antitumor Efficacy against Triple-Negative Breast Cancer, J Med Chem 66 (2023) 12033–12058. https://doi.org/10.1021/acs.jmedchem.3c00614.

[19] G. Routholla, S. Pulya, T. Patel, Sk. Abdul Amin, N. Adhikari, S. Biswas, T. Jha, B. Ghosh, Synthesis, biological evaluation, and molecular docking analysis of novel linker-less benzamide based potent and selective HDAC3 inhibitors, Bioorg Chem 114 (2021) 105050. https://doi.org/10.1016/j.bioorg.2021.105050.

[20] S. Pulya, T. Patel, M. Paul, N. Adhikari, S. Banerjee, G. Routholla, S. Biswas, T. Jha, B. Ghosh, Selective inhibition of histone deacetylase 3 by novel hydrazide based small molecules as therapeutic intervention for the treatment of cancer, Eur J Med Chem 238 (2022) 114470. https://doi.org/10.1016/j.ejmech.2022.114470.

[21] M. Paul, B. Ghosh, S. Biswas, Human Serum Albumin-Oxaliplatin (Pt(IV)) prodrug nanoparticles with dual reduction sensitivity as effective nanomedicine for triple-

negative breast cancer, Int J Biol Macromol 256 (2024) 128281. https://doi.org/10.1016/j.ijbiomac.2023.128281.

[22] S. Das, M. Paul, B. Ghosh, S. Biswas, Synergistic Anticancer Response via Docetaxel- and Oleanolic Acid-Loaded Albumin/Poly(lactide) Nanoparticles in Triple-Negative Breast Cancer, ACS Appl Nano Mater 6 (2023) 19710–19726. https://doi.org/10.1021/acsanm.3c03499.

[23] A.M. Itoo, M. Paul, B. Ghosh, S. Biswas, Oxaliplatin delivery via chitosan/vitamin E conjugate micelles for improved efficacy and MDR-reversal in breast cancer, Carbohydr Polym 282 (2022) 119108. https://doi.org/10.1016/j.carbpol.2022.119108.

[24] J. Minami, R. Suzuki, R. Mazitschek, G. Gorgun, B. Ghosh, D. Cirstea, Y. Hu, N. Mimura, H. Ohguchi, F. Cottini, J. Jakubikova, N.C. Munshi, S.J. Haggarty, P.G. Richardson, T. Hideshima, K.C. Anderson, Histone deacetylase 3 as a novel therapeutic target in multiple myeloma, Leukemia 28 (2014) 680–689. https://doi.org/10.1038/leu.2013.231.

[25] R. Aluri, A. Natarajan, T. Patel, D. Begum, J. Kumari, D. Sriram, B. Ghosh, K. Rangan, Synthesis, characterisation, single crystal structure and evaluation of a redox innocent carbazate functionalized phenanthroline for antimycobacterial and anticancer activity, J Mol Struct 1323 (2025) 140729. https://doi.org/10.1016/j.molstruc.2024.140729.

CHAPTER-IV

Synthesis, antiproliferative, apoptotic & anti-angiogenic potency of 1,3,4-thiadiazole and 1,3-thiazolidine-4-one scaffold-based hybrid compounds: *in vitro* cell-based anticancer studies

1. Introduction:

Cancer is one of the primary causes of mortality worldwide, making it a serious global health concern. It is expected to have caused the deaths of around 10 million people in the year 2020 alone and roughly one fatality out of six cases worldwide [1]. According to projections, the number of new cases of cancer worldwide is expected to rise steadily from 14.1 million in 2012 to 21.6 million by 2030 [2]. The most familiar type of tumour in women and a major contributor to cancer-related mortality is breast cancer. Thousands of women from all walks of life receive a breast cancer diagnosis every day worldwide. It is the leading cause of cancer-associated mortality and by far the most prevalent malignancy in women worldwide [3]. This highlights how crucial it is to continue studying and implementing focused therapies to lessen the impact of this fatal disorder [4]. Surgery is the primary treatment for breast cancer, and to reduce the risk of recurrence, radiation therapy is administered to the breast and lymph nodes after surgery [5]. Current cancer treatments rely on processes that cause genetic damage, imbalances in kinase and phosphatase activity, spindle issues, and variations in cell cycle checkpoints. Since most treatment methods aim to prevent cancer cells from growing, they are unable to eradicate cancer cells completely. Apoptosis of cancer cells frequently results in complete remission of the disease, improving outcomes and lowering the likelihood of recurrence [6]. However, breast cancer cannot be entirely cured by the alternative systemic medicines that have lately been devised. Furthermore, side effects could include cardiovascular problems, osteoporosis, and drug resistance. Therefore, continuous progress in finding and creating novel lead molecules for long-term cancer therapy with higher potency and minimal side effects is urgently needed [7–10]. In this context, in continuation of our previous research [11], several 1,3,4-thiadiazole and 1,3-thiazolidine-4-one containing hybrid compounds were synthesised and evaluated for *in vitro* anticancer activity. Molecular hybridisation is an attractive approach to drug design that facilitates the development of pharmacologically active compounds for

various disorders, thereby promoting the discovery of novel therapeutics with higher efficacy and fewer adverse effects [12].

A typical five-membered and important heterocyclic structure is 1,3,4-thiadiazole, which contains two nitrogen atoms and one sulfur atom. There are several isomers of thiadiazole; among them, 1,3,4-thiadiazole has gained more research investigation than its other isomers, according to a cursory review of excellent research articles [11]. Numerous interesting compounds have been reported in the literature, indicating that 1,3,4-thiadiazoles have been thoroughly investigated for their potential as anticancer drugs [13–15]. Through a number of mechanisms, such as specific inhibition of RNA and DNA synthesis [16], inhibition of histone deacetylase and antagonism of adenosine A3 receptors [17], inhibition of phosphodiesterase-7 [18], inhibition of carbonic anhydrase [19], the 1,3,4-thiadiazole nucleus produces its antitumor effects. Accordingly, recent studies have proposed new anticancer 1,3,4-thiadiazole derivatives (**Compounds I** and **II**), showing antiproliferative potency against breast cancer cells. They might be developed as potent anti-breast cancer drugs with anti-EGFR activity [20,21]. Similarly, Novel 1,3,4-thiadiazole derivative (**Compound III**) produced by Hossein Zadeh et al. This compound showed strong cytotoxic effects and activated caspases-3 and -9 to cause apoptosis in breast cancer cells [18]. Other research groups developed several 1,3,4-thiadiazole compounds, e.g. **Compound IV** [22]**, Compound V** [23], **Compound VI** [24], and **Compound VII** [25], which showed *in vitro* and *in vivo* anticancer activity by promoting apoptosis, inhibiting angiogenesis, and upregulating ROS levels and other molecular pathways (**Figure 1**).

In recent years, there has been a significant expansion in the study of 1,3-thiazolidin-4-ones, which are heterocycles containing sulfur and nitrogen at the 1st and 3rd positions, respectively, and a carbonyl function at the 4th position [26]. Numerous precise diagnostic and therapeutic agents have utilised the flexible and agile thiazolidinone scaffold [27]. The thiazolidinone

molecule, which features a thiazolidine ring with a carbonyl group, is known to exhibit a range of biological effects and is a key moiety in drug discovery. This moiety contributes uniquely to a variety of pharmacological compounds that aid in the creation and development of several anticancer medications [28]. Moreover, a recent study of a developing 1,3-thiazolidine-4-one scaffold-based anticancer molecule revealed that the most potent compound, **VIII**, promotes apoptosis in cancer cells by upregulating caspase-3, -8, and -9. It also inhibits CDK2, an essential regulator of the cell cycle [29]. Baohui Qi et al. had synthesized thiazolidine-4-one derivatives and biologically evaluated the compounds for possible anticancer activity. The study demonstrated that **Compound IX** exhibits potent antiproliferative effects by inducing apoptosis and inhibiting the metastasis of cancer cells [30]. Furthermore, in view of the anticancer potential of the thiazolidine-4-one scaffold, various research groups developed different anticancer derivatives like **Compound X** [31], **Compound XI** [32], **Compound XII** [33], and **Compound XIII** [34] (**Figure 1**), which displayed promising anticancer activity in *in vitro* and *in vivo* studies and may warrant further development as a possible anticancer drug candidate.

In light of the various research studies discussed above, this study aims to investigate new compounds that could be potential anticancer agents. The main objective of this work is to produce new, potent anticancer compounds by synthesising hybrid molecules using these extensively studied heterocycles.

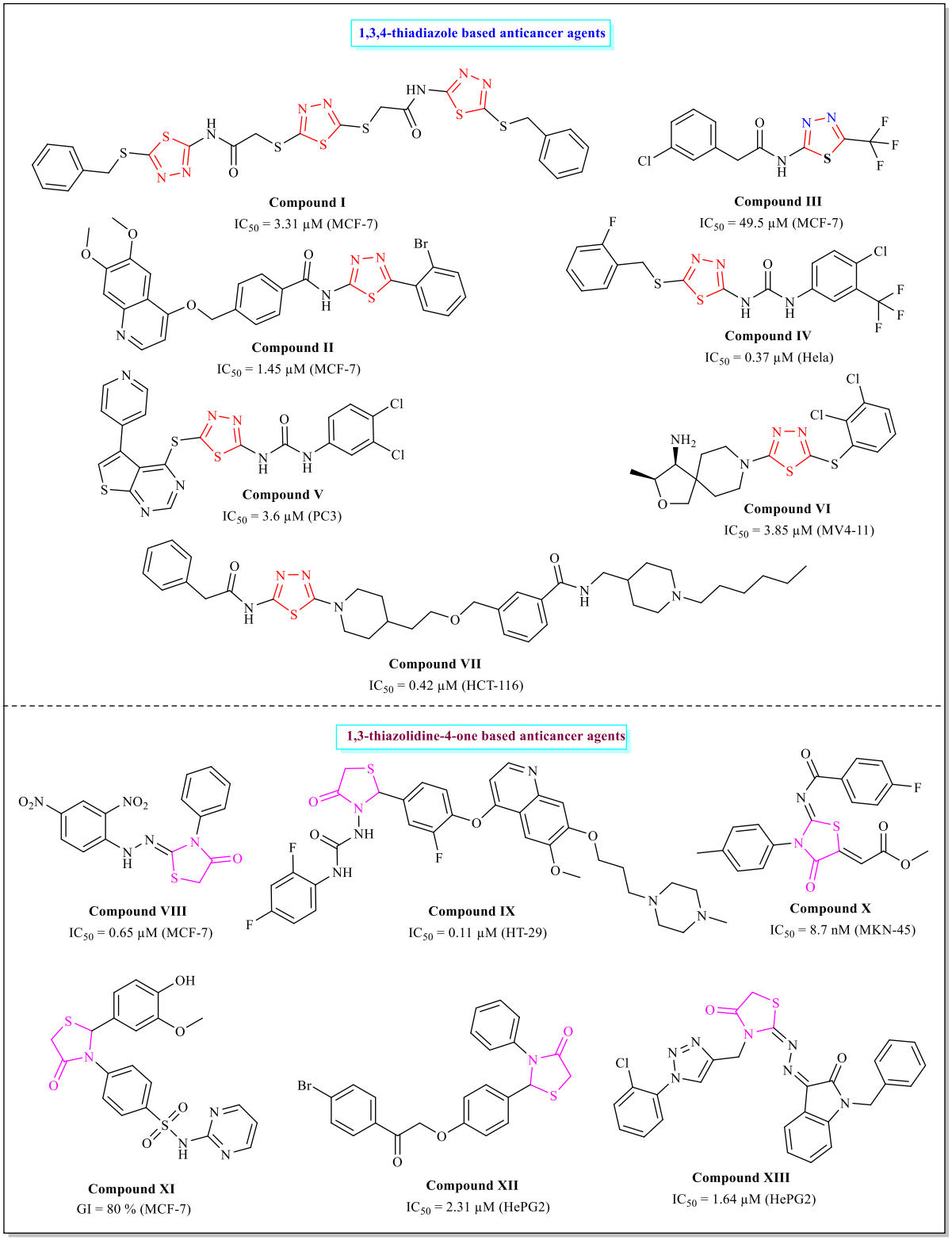

Figure 1: Structure of literature-reported anticancer compounds containing 1,3,4-thiadiazole and 1,3-thiazolidine-4-one scaffold.

2. Materials and Methods:

2.1. Chemicals and devices:

For this study, high-quality solvents and chemicals were purchased from reputable suppliers, including Merck, Spectrochem, LOBA Chemicals, SRL, and other vendors. Purification methods, as outlined in the literature, were applied to achieve the highest grade of pure substances. The synthesis process was observed using a TLC plate and a UV light chamber with both short (254 nm) and long wavelengths (354 nm).

The VEEGO melting point device was used to determine the melting points of the compounds. The compounds were characterised using HRMS and NMR (^{1}H and ^{13}C) spectroscopy. The NMR spectra of the compounds were scanned at 400/300 MHz for ^{1}H-NMR and 101/75 MHz for ^{13}C-NMR, respectively, using a Bruker Advance NMR Spectrometer. In relation to the internal standard tetramethylsilane (δ = 0.00 ppm), chemical shifts of NMR signals were recorded in parts per million (ppm) units using Topspin software, and coupling constant values were reported in Hertz (Hz) units. Splitting patterns, e.g. d (doublet), t (triplet), q (quartet), m (multiplet), and s (singlet), are the terms used to describe the peak splitting of ^{1}H-NMR signals. An ESI (Orbitrap, +Ve & -Ve ion mode) mass spectrometry device (6530 LC/Q-TOF, Agilent) was used to generate HRMS spectra (m/z).

2.2. Synthesis and analysis of intermediates:

2.2.1. Synthesis of compound 1:

In a 150 mL flat-bottom flask containing 30 mL of EtOH and 24 mmol of KOH, 20 mmol of hydrazine carbothioamide/thiosemicarbazide (20 gm) was added. The entire mixture was refluxed (80-90 ^{0}C) with stirring (600-700 rpm) for 10 hours in an oil bath mounted on a magnetic stirrer with a heating plate, following the addition of 25 mmol of carbon disulfide (1.44 ml) dropwise. Following the TLC process, the mixture was placed in ice-cold water and acidified to a pH of 4-5 using 20% HCl to obtain precipitate. The precipitated product was

filtered through Whatman filter paper using a Buchner funnel under a vacuum. The filtrated product was then dried and recrystallised from EtOH/MeOH.

Compound 1 (**5-amino 1,3,4-thiadiazol-2-thiol**)**:** Pale yellow crystal, Yield 96%; Mp = 231-233 ^{0}C; ^{1}H NMR (300 MHz, DMSO-d_6) δ_H: 13.14 (s, 1H), 7.04 (s, 2H) ppm; ^{13}C NMR (75 MHz, DMSO-d_6) δ_C: 181.0, 161.5, 40.3, 40.0, 39.8, 39.2, 38.9, 38.6 ppm; HRMS (Q-TOF) *m/z*: $[M + H]^+$ Cal. for $C_2H_4N_3S_2^+$ 133.9841; Found 133.9853.

2.2.2. Synthesis of 5-(substituted benzylthio)-1,3,4-thiadiazol-2-amine (compound 2d-2f):

Compound **1** (0.01 mol) was dissolved in dry DMF (25 mL) containing anhydrous K_2CO_3 (1.5 equiv) in a 100 mL flat-bottom flask. Substituted benzyl chlorides (1.2 equivalents) were then added dropwise, and the mixture was agitated at 700 rpm for 10-12 hours at room temperature using a magnetic stirrer. Following the completion of the reaction (as indicated by TLC), the material was transferred into a beaker filled with crushed ice, and the compounds were precipitated as white solids. Pure products **2d-2f** were obtained by filtering, drying, and recrystallising the precipitated solid from EtOH/Methanol.

5-((3-chlorobenzyl) thio)-1,3,4-thiadiazol-2-amine (Compound 2d): White solid, Yield = 86%**,** Mp= 130-132^{0}C; ^{1}H NMR (300 MHz, DMSO-d_6) δ_H: 7.42 (d, *J* = 2.1 Hz, 1H), 7.32 (dp, *J* = 4.3, 1.6 Hz, 5H), 4.30 (s, 2H) ppm; ^{13}C NMR (75 MHz, DMSO-d_6) δ_C: 170.04, 148.94, 139.99, 132.96, 130.32, 128.79, 127.70, 127.38, 40.36, 40.08, 39.80, 39.52, 39.24, 38.97, 38.69, 37.62 ppm; HRMS (Q-TOF) *m/z*: $[M + H]^+$ Cal. for $C_9H_9ClN_3S_2^+$ 257.9921; Found 257.9941.

5-((4-fluorobenzyl) thio)-1,3,4-thiadiazol-2-amine (Compound 2e): White solid, Yield = 92%, Mp= 145-147^{0}C; ^{1}H NMR (400 MHz, DMSO-d_6) δ_H: 7.45 – 7.28 (m, 4H), 7.12 (t, *J* = 8.7 Hz, 2H), 4.28 (s, 2H) ppm; ^{13}C NMR (101 MHz, DMSO-d_6) δ_C: 170.08, 162.73, 160.31, 149.36, 133.50, 133.47, 131.07, 130.99, 115.40, 115.19, 40.15, 39.94, 39.73, 39.52, 39.31,

39.10, 38.90, 37.71 ppm; HRMS (Q-TOF) *m/z*: $[M + H]^+$ Cal. for $C_9H_9FN_3S_2^+$ 242.0216; Found 242.0238.

5-((4-methylbenzyl) thio)-1,3,4-thiadiazol-2-amine (Compound 2f): White solid, Yield = 88%, Mp= 150-152^{0}C; ^{1}H NMR (400 MHz, DMSO-d_6) δ_H: 7.28 (s, 2H), 7.22 (d, *J* = 7.9 Hz, 2H), 7.12 (d, *J* = 7.8 Hz, 2H), 4.24 (s, 2H), 2.27 (s, 3H) ppm; ^{13}C NMR (101 MHz, DMSO-d_6) δ_C: 169.83, 149.60, 136.67, 133.97, 129.06, 128.90, 40.15, 39.94, 39.73, 39.52, 39.31, 39.10, 38.89, 38.30, 20.73 ppm; HRMS (Q-TOF) *m/z*: $[M + H]^+$ Cal. for $C_{10}H_{12}N_3S_2^+$ 238.0467; Found 238.0485.

2.2.3. Synthesis of 5-(substituted benzylthio)-1,3,4-thiadiazol-2-yl)-2-chloroacetamide (compound **3d-3f):**

To the stirring solution of **2d-2f** (0.01 mol) and TEA (1.2 equiv) in dry tetrahydrofuran (THF, 20 mL) in a 50 mL flat-bottom flask, chloroacetyl chloride (1.2 equiv) was added dropwise, maintaining the temperature at 0-10 °C. At room temperature, the reaction mixture was agitated for roughly six to eight hours. Following the completion of the reaction (as indicated by TLC), the excess THF was removed using a rotary evaporator at reduced pressure. The leftover residue was treated, washed with water, filtered, and dried. The resulting crude products, **3d-3f**, were purified by recrystallization with a mixture of methanol and DMF (2:1).

2-chloro-N-(5-((3-chlorobenzyl) thio)-1,3,4-thiadiazol-2-yl) acetamide (Compound 3d): White solid, Yield = 83%, Mp= 180-182^{0}C; ^{1}H NMR (300 MHz, DMSO-d_6) δ_H: 13.01 (s, 1H), 7.49 (q, *J* = 1.4 Hz, 1H), 7.35 (dddd, *J* = 6.4, 4.4, 3.5, 1.6 Hz, 3H), 4.50 (s, 2H), 4.44 (s, 2H) ppm; ^{13}C NMR (75 MHz, DMSO-d_6) δ_C: 165.52, 162.65, 158.87, 158.28, 139.51, 133.03, 130.40, 128.85, 127.73, 127.55, 42.27, 36.67 ppm; HRMS (Q-TOF) *m/z*: $[M + H]^+$ Cal. for $C_{11}H_{10}Cl_2N_3OS_2^+$ 333.9637; Found 333.9647.

2-chloro-N-(5-((4-fluorobenzyl) thio)-1,3,4-thiadiazol-2-yl) acetamide (Compound 3e): White solid, Yield = 87%, Mp= 185-190^{0}C; ^{1}H NMR (300 MHz, DMSO-d_6) δ_H: 13.00 (s, 1H),

7.51 – 7.38 (m, 2H), 7.22 – 7.08 (m, 2H), 4.48 (s, 2H), 4.44 (s, 2H) ppm; ^{13}C NMR (75 MHz, DMSO-d_6) δ_C: 165.55, 163.19, 159.96, 158.81, 158.68, 158.51, 157.90, 133.11, 133.07, 133.03, 131.17, 131.06, 115.55, 115.26, 61.18, 42.29, 36.74 ppm; HRMS (Q-TOF) *m/z*: $[M + H]^+$ Cal. for $C_{11}H_{10}ClFN_3OS_2^+$ 317.9932; Found 317.9946.

2-chloro-N-(5-((4-methylbenzyl) thio)-1,3,4-thiadiazol-2-yl) acetamide (Compound 3f): White solid, Yield = 93%, Mp= 198-202^{0}C; ^{1}H NMR (300 MHz, DMSO-d_6) δ_H: 12.99 (s, 1H), 7.32 – 7.23 (m, 2H), 7.12 (d, *J* = 7.8 Hz, 2H), 4.44 (s, 4H), 2.26 (s, 3H) ppm; ^{13}C NMR (75 MHz, DMSO-d_6) δ_C: 165.47, 158.84, 158.64, 136.90, 133.48, 129.15, 128.94, 42.27, 37.39, 20.74 ppm; HRMS (Q-TOF) *m/z*: $[M + H]^+$ Cal. for $C_{12}H_{13}ClN_3OS_2^+$ 314.0183; Found 314.0208.

2.2.4. Synthesis of 5-(substituted benzylthio)-1,3,4-thiadiazol-2-yl) imino) thiazolidine-4-one (compound **4d-4f):**

In a 100 mL flask with a flat bottom, compounds **3d-3f** (0.01 mol) and NH_4SCN (3 equiv) were dispersed in ethanol. Using a magnetic stirrer hot plate, the mixture was refluxed in an oil bath while being stirred (700 rpm) throughout the whole night. Following completion of the reaction (confirmed by TLC), the mixture was transferred to a beaker filled with ice-cold water. The product was deposited as a white solid. To get pure intermediate **4d-4f**, the precipitated material was filtered, cleaned with water, dried, and recrystallized from EtOH/MeOH plus DMF (2:1).

(E)-2-((5-((3-chlorobenzyl) thio)-1,3,4-thiadiazol-2-yl) imino) thiazolidin-4-one (Compound 4d): White solid, Yield = 84%, Mp= 196-198^{0}C; ^{1}H NMR (300 MHz, DMSO-d_6) δ_H: 12.32 (s, 1H), 7.51 (q, *J* = 1.4 Hz, 1H), 7.39 (dt, *J* = 3.1, 1.7 Hz, 1H), 7.37 – 7.31 (m, 2H), 4.51 (s, 2H), 4.10 (s, 2H) ppm; ^{13}C NMR (75 MHz, DMSO-d_6) δ_C: 174.04, 170.52, 166.01, 160.10, 139.43, 133.02, 130.40, 128.91, 127.81, 127.58, 36.40, 35.75 ppm; HRMS (Q-TOF) *m/z*: $[M + H]^+$ Cal. for $C_{12}H_{10}ClN_4OS_3^+$ 356.9700; Found 356.9723.

(E)-2-((5-((4-fluorobenzyl) thio)-1,3,4-thiadiazol-2-yl) imino) thiazolidin-4-one (Compound 4e): White solid, Yield = 91%, Mp= 207-210^{0}C; ^{1}H NMR (400 MHz, DMSO-d$_6$) δ_H: 12.31 (s, 1H), 7.50 – 7.43 (m, 2H), 7.20 – 7.12 (m, 2H), 4.50 (s, 2H), 4.09 (s, 2H) ppm; ^{13}C NMR (101 MHz, DMSO-d$_6$) δ_C: 174.04, 170.41, 165.93, 162.77, 160.34, 160.32, 132.94, 132.91, 131.21, 131.13, 115.48, 115.27, 36.42, 35.75 ppm; HRMS (Q-TOF) *m/z*: $[M + H]^+$ Cal. for $C_{12}H_{10}FN_4OS_3^+$ 340.995; Found 341.0021.

(E)-2-((5-((4-methylbenzyl) thio)-1,3,4-thiadiazol-2-yl) imino) thiazolidin-4-one (Compound 4f): White solid, Yield = 85%, Mp= 216-218^{0}C; ^{1}H NMR (300 MHz, DMSO-d$_6$) δ_H: 12.31 (s, 1H), 7.36 – 7.25 (m, 2H), 7.14 (d, *J* = 7.8 Hz, 2H), 4.46 (s, 2H), 4.09 (s, 2H), 2.27 (s, 3H) ppm; ^{13}C NMR (75 MHz, DMSO-d$_6$) δ_C: 174.15, 170.36, 160.76, 137.04, 133.42, 129.22, 129.11, 37.20, 35.81, 20.80 ppm; HRMS (Q-TOF) *m/z*: $[M + H]^+$ Cal. for $C_{13}H_{13}N_4OS_3^+$ 337.0246; Found 337.0279.

2.3. Synthesis procedure and structural analysis of the final compounds (8a-8h, 9a-9h, and 10a-10h):

In a 50 mL flask with a flat bottom, compound **4d-4f** (1 mmol) and urea/thiourea (1.5 equiv) were added, followed by 15 mL of glacial acetic acid. After a few minutes of stirring, several substituted benzaldehydes (1.2 equiv) were added to the mixture in portions. The mixture was refluxed by heating it for 20-24 hours at 110-120 °C on a hot plate with a magnetic stirrer (600–800 rpm). Following TLC verification of the reaction's completion, the liquid was transferred into a beaker filled with crushed ice, and the final products were deposited as solids. The crude solid compounds were filtered and then cleaned with double-distilled water to remove any remaining acid. To obtain pure final compounds, the crude solid products were subsequently dried and recrystallised or precipitated from a 2:1 combination of ethanol and DMF.

(Z)-5-((Z)-benzylidene)-2-((5-((3-chlorobenzyl) thio)-1,3,4-thiadiazol-2-yl) imino) thiazolidin-4-one (Compound 8a): Yellow solid, Yield = 87%, Mp= 190-193^{0}C; ^{1}H NMR

(300 MHz, DMSO-d_6) δ_H: 12.96 (s, 1H), 7.77 (s, 1H), 7.65 (d, *J* = 7.1 Hz, 2H), 7.60 – 7.46 (m, 4H), 7.44 – 7.39 (m, 1H), 7.36 (dd, *J* = 5.2, 2.5 Hz, 2H), 4.54 (s, 2H) ppm; ^{13}C NMR (75 MHz, DMSO-d_6) δ_C: 170.13, 167.00, 161.10, 158.60, 139.36, 133.09, 130.62, 130.48, 130.24, 129.46, 128.92, 127.83, 127.66, 123.84, 36.34 ppm; HRMS (Q-TOF) *m/z*: $[M + Cl]^-$ Cal. For $C_{19}H_{13}Cl_2N_4OS_3^-$ 478.9634; Found 478.9610.

(Z)-2-((5-((3-chlorobenzyl) thio)-1,3,4-thiadiazol-2-yl) imino)-5-((Z)-3-fluorobenzylidene) thiazolidin-4-one (Compound 8b): Yellow solid, Yield = 88%, Mp= 189-191^{0}C; ^{1}H NMR (300 MHz, DMSO-d_6) δ_H: 13.01 (s, 1H), 7.76 (s, 1H), 7.62 (td, *J* = 8.2, 6.1 Hz, 1H), 7.53 (d, *J* = 2.0 Hz, 1H), 7.47 (dd, *J* = 8.7, 4.3 Hz, 2H), 7.44 – 7.39 (m, 1H), 7.38 – 7.23 (m, 3H), 4.54 (s, 2H) ppm; ^{13}C NMR (75 MHz, DMSO-d_6) δ_C: 170.03, 166.81, 163.95, 161.26, 160.70, 158.21, 139.33, 133.09, 131.57, 131.46, 130.47, 128.93, 127.83, 127.66, 125.67, 117.17, 116.86, 36.33 ppm; HRMS (Q-TOF) *m/z*: $[M + H]^+$ Calcd. For $C_{19}H_{13}ClFN_4OS_3^+$ 462.9919; Found 462.9865.

(Z)-2-((5-((3-chlorobenzyl) thio)-1,3,4-thiadiazol-2-yl) imino)-5-((Z)-4-fluorobenzylidene) thiazolidin-4-one (Compound 8c): Yellow solid, Yield = 87%, Mp= 185-188^{0}C; ^{1}H NMR (400 MHz, DMSO-d_6) δ_H: 12.93 (s, 1H), 7.78 (s, 1H), 7.71 (dd, *J* = 8.5, 5.2 Hz, 2H), 7.53 (d, *J* = 2.3 Hz, 1H), 7.48 – 7.20 (m, 5H), 4.55 (s, 2H) ppm; ^{13}C NMR (101 MHz, DMSO-d_6) δ_C: 171.97, 170.03, 166.88, 164.16, 161.67, 161.02, 158.36, 139.31, 133.04, 132.70, 132.61, 131.85, 130.40, 129.75, 128.83, 127.74, 127.58, 123.49, 116.69, 116.47, 36.32 ppm; HRMS (Q-TOF) *m/z*: $[M + H]^+$ Cal. For $C_{19}H_{13}ClFN_4OS_3^+$ 462.9919; Found 462.9917.

(Z)-2-((5-((3-chlorobenzyl) thio)-1,3,4-thiadiazol-2-yl) imino)-5-((Z)-4-chlorobenzylidene) thiazolidin-4-one (Compound 8d): Yellow solid, Yield = 94%, Mp= 192^{0}C; ^{1}H NMR (400 MHz, DMSO-d_6) δ_H: 12.97 (s, 1H), 7.77 (s, 1H), 7.72 – 7.56 (m, 4H), 7.53 (d, *J* = 2.0 Hz, 1H), 7.44 – 7.32 (m, 3H), 4.55 (s, 2H) ppm; ^{13}C NMR (101 MHz, DMSO-d_6) δ_C: 170.00, 166.83, 161.13, 158.18, 139.29, 135.12, 133.04, 131.97, 131.80, 131.57,

130.41, 129.49, 128.84, 127.75, 127.59, 124.55, 36.31 ppm; HRMS (Q-TOF) *m/z*: $[M + H]^+$ Cal. For $C_{19}H_{13}Cl_2N_4OS_3^+$ 478.9623; Found 478.9618.

(Z)-2-((5-((3-chlorobenzyl) thio)-1,3,4-thiadiazol-2-yl) imino)-5-((Z)-4-methoxy benzylidene) thiazolidin-4-one (Compound 8e): Yellow solid, Yield = 92%, Mp= 200-202^{0}C; ^{1}H NMR (300 MHz, DMSO-d_6) δ_H: 12.86 (s, 1H), 7.74 (s, 1H), 7.62 (d, *J* = 8.4 Hz, 2H), 7.53 (s, 1H), 7.43 – 7.32 (m, 3H), 7.15 (d, *J* = 8.4 Hz, 2H), 4.55 (s, 2H), 3.83 (s, 3H) ppm; ^{13}C NMR (75 MHz, DMSO-d_6) δ_C: 170.21, 161.18, 139.39, 133.07, 132.38, 130.46, 128.89, 127.81, 127.63, 120.56, 115.07, 55.54, 36.35 ppm; HRMS (Q-TOF) *m/z*: $[M + H]^+$ Cal. For $C_{20}H_{16}ClN_4O_2S_3^+$ 475.0118; Found 475.0114.

(Z)-2-((5-((3-chlorobenzyl) thio)-1,3,4-thiadiazol-2-yl) imino)-5-((Z)-4-hydroxy benzylidene) thiazolidin-4-one (Compound 8f): Yellow solid, Yield = 93%, Mp= 210-212^{0}C; ^{1}H NMR (300 MHz, DMSO-d_6) δ_H: 12.81 (s, 1H), 10.39 (s, 1H), 7.69 (s, 1H), 7.58 – 7.47 (m, 3H), 7.41 – 7.32 (m, 3H), 6.96 (d, *J* = 8.3 Hz, 2H), 4.53 (m, 2H) ppm; ^{13}C NMR (75 MHz, DMSO-d_6) δ_C: 174.07, 172.07, 170.25, 167.20, 160.71, 160.17, 158.86, 139.38, 133.65, 133.08, 132.74, 130.47, 130.42, 128.91, 127.82, 127.63, 124.00, 119.14, 116.51, 36.35 ppm; HRMS (Q-TOF) *m/z*: $[M + NH_4]^+$ Cal. For $C_{19}H_{17}ClN_5O_2S_3^+$ 478.0227; Found 478.0098.

(Z)-2-((5-((3-chlorobenzyl) thio)-1,3,4-thiadiazol-2-yl) imino)-5-((Z)-4-hydroxy-3-methoxybenzylidene) thiazolidin-4-one (Compound 8g): Yellow solid, Yield = 88%, Mp= 174^{0}C; ^{1}H NMR (300 MHz, DMSO-d_6) δ_H: 12.81 (s, 1H), 10.03 (s, 1H), 7.71 (s, 1H), 7.52 (d, *J* = 6.0 Hz, 1H), 7.42 – 7.34 (m, 3H), 7.31 – 7.21 (m, 1H), 7.13 (dd, *J* = 8.3, 2.0 Hz, 1H), 7.00 (d, *J* = 8.3 Hz, 1H), 4.52 (m, 2H), 3.82 (s, 3H) ppm; ^{13}C NMR (75 MHz, DMSO-d_6) δ_c: 172.08, 170.25, 167.14, 160.72, 158.90, 149.74, 148.02, 139.45, 139.38, 133.97, 133.08, 133.05, 130.46, 130.43, 128.94, 127.84, 127.64, 124.50, 123.61, 119.49, 116.42, 115.62, 55.79, 36.41, 35.78, 21.09 ppm; HRMS (Q-TOF) *m/z*: $[M + H]^+$ Cal. For $C_{20}H_{16}ClN_4O_3S_3^+$ 491.0068; Found 491.0066.

(Z)-2-((5-((3-chlorobenzyl) thio)-1,3,4-thiadiazol-2-yl) imino)-5-((Z)-4-(dimethylamino) benzylidene) thiazolidin-4-one (Compound 8h): Reddish brown solid, Yield = 84%, Mp= 220-224^{0}C; ^{1}H NMR (300 MHz, DMSO-d_6) δ_H: 12.66 (s, 1H), 7.63 (s, 1H), 7.57 – 7.14 (m, 6H), 6.84 (d, *J* = 8.5 Hz, 1H), 4.52 (m, 2H), 3.01 (s, 6H) ppm; ^{13}C NMR (75 MHz, DMSO-d_6) δ_C: 170.32, 167.20, 160.27, 159.06, 151.61, 139.43, 133.07, 132.49, 130.44, 128.88, 127.80, 127.60, 119.85, 112.14, 36.38, 30.72 ppm; HRMS (Q-TOF) *m/z*: $[M + H]^+$ Cal. For $C_{21}H_{19}ClN_5OS_3^+$ 488.0435; Found 488.0428.

(Z)-5-((Z)-benzylidene)-2-((5-((4-fluorobenzyl) thio)-1,3,4-thiadiazol-2-yl) imino) thiazolidin-4-one (Compound 9a): Yellow solid, Yield = 89%, Mp= 210-212^{0}C; ^{1}H NMR (400 MHz, DMSO-d_6) δ_H: 12.94 (s, 1H), 7.79 (s, 1H), 7.66 (d, *J* = 7.1 Hz, 2H), 7.58 (t, *J* = 7.5 Hz, 2H), 7.50 (ddd, *J* = 8.6, 6.1, 3.3 Hz, 3H), 7.24 – 7.11 (m, 2H), 4.54 (s, 2H) ppm; ^{13}C NMR (101 MHz, DMSO-d_6) δ_C: 169.96, 166.92, 162.77, 161.25, 160.34, 158.48, 133.08, 132.94, 132.83, 132.80, 131.18, 131.10, 130.54, 130.17, 129.39, 123.82, 115.49, 115.28, 40.20, 39.99, 36.33 ppm; HRMS (Q-TOF) *m/z*: $[M + Cl]^-$ Cal. For $C_{19}H_{13}ClFN_4OS_3^+$ 462.9930; Found 462.9824.

(Z)-2-((5-((4-fluorobenzyl) thio)-1,3,4-thiadiazol-2-yl) imino)-5-((Z)-3-fluorobenzylidene) thiazolidin-4-one (Compound 9b): Yellow solid, Yield = 86%**,** Mp= 215^{0}C; ^{1}H NMR (400 MHz, DMSO-d_6) δ_H: 12.99 (s, 1H), 7.77 (s, 1H), 7.62 (q, *J* = 7.6 Hz, 1H), 7.48 (dt, *J* = 8.5, 4.4 Hz, 4H), 7.34 (td, *J* = 8.5, 2.5 Hz, 1H), 7.21 – 7.11 (m, 2H), 4.54 (s, 2H) ppm; ^{13}C NMR (101 MHz, DMSO-d_6) δ_C: 169.86, 166.73, 163.49, 162.77, 161.39, 161.05, 160.34, 158.07, 135.49, 135.41, 132.79, 132.75, 131.48, 131.41, 131.18, 131.09, 125.60, 125.52, 117.35, 117.14, 117.04, 116.82, 115.48, 115.27, 40.20, 36.32 ppm; HRMS (Q-TOF) *m/z*: $[M + H]^+$ Cal. For $C_{19}H_{13}F_2N_4OS_3^+$ 447.0214; Found 447.0213.

(Z)-2-((5-((4-fluorobenzyl) thio)-1,3,4-thiadiazol-2-yl) imino)-5-((Z)-4-fluorobenzylidene) thiazolidin-4-one (Compound 9c): Yellow solid, Yield = 91%, Mp= 190-192^{0}C; ^{1}H NMR

(400 MHz, DMSO-d_6) δ_H: 12.97 (s, 1H), 7.80 (s, 1H), 7.73 (dd, *J* = 8.6, 5.4 Hz, 2H), 7.53 – 7.39 (m, 4H), 7.18 (t, *J* = 8.8 Hz, 2H), 4.54 (s, 2H) ppm; ^{13}C NMR (101 MHz, DMSO-d_6) δ_C: 169.98, 166.96, 164.20, 162.80, 161.71, 161.34, 160.38, 158.37, 132.89, 132.86, 132.77, 132.68, 131.91, 131.23, 131.15, 129.81, 123.58, 116.77, 116.55, 115.55, 115.33, 40.20, 36.30 ppm; HRMS (Q-TOF) *m/z*: $[M + H]^+$ Cal. For $C_{19}H_{13}F_2N_4OS_3^+$ 447.0214; Found 447.0212.

(Z)-5-((Z)-4-chlorobenzylidene)-2-((5-((4-fluorobenzyl) thio)-1,3,4-thiadiazol-2-yl) imino) thiazolidin-4-one (Compound 9d): Yellow solid, Yield = 92%, Mp= 187^{0}C; ^{1}H NMR (300 MHz, DMSO-d_6) δ_H: 12.98 (s, 1H), 7.76 (s, 1H), 7.71 – 7.56 (m, 4H), 7.54 – 7.43 (m, 2H), 7.22 – 7.12 (m, 2H), 4.54 (s, 2H) ppm; ^{13}C NMR (75 MHz, DMSO-d_6) δ_C: 169.93, 166.89, 163.21, 161.40, 159.98, 158.16, 135.16, 132.86, 132.82, 132.01, 131.85, 131.59, 131.24, 131.13, 129.53, 124.61, 115.58, 115.30, 36.31 ppm; HRMS (Q-TOF) *m/z*: $[M + H]^+$ Cal. For $C_{19}H_{13}ClFN_4OS_3^+$ 462.9919; Found 462.9908.

(Z)-2-((5-((4-fluorobenzyl) thio)-1,3,4-thiadiazol-2-yl) imino)-5-((Z)-4-methoxy benzylidene) thiazolidin-4-one (Compound 9e): Yellow solid, Yield = 94% Mp= 220-224^{0}C; ^{1}H NMR (300 MHz, DMSO-d_6) δ_H: 12.84 (s, 1H), 7.71 (s, 1H), 7.60 (d, *J* = 8.5 Hz, 2H), 7.53 – 7.41 (m, 2H), 7.27 – 7.01 (m, 4H), 4.53 (s, 2H), 3.82 (s, 3H) ppm; ^{13}C NMR (75 MHz, DMSO-d_6) δ_C: 170.07, 167.10, 163.22, 161.15, 161.01, 159.98, 158.65, 133.08, 132.90, 132.86, 132.36, 131.25, 131.14, 125.57, 120.58, 115.58, 115.30, 115.03, 55.52, 36.34 ppm; HRMS (Q-TOF) *m/z*: $[M + Na]^+$ Cal. For $C_{20}H_{15}FN_4NaO_2S_3^+$ 481.0233; Found 481.0184.

(Z)-2-((5-((4-fluorobenzyl) thio)-1,3,4-thiadiazol-2-yl) imino)-5-((Z)-4-hydroxybenzylidene) thiazolidin-4-one (Compound 9f): Yellow solid, Yield = 95%, Mp= 257-260^{0}C; ^{1}H NMR (400 MHz, DMSO-d_6) δ_H: 12.81 (s, 1H), 10.39 (s, 1H), 7.69 (s, 1H), 7.64 – 7.34 (m, 4H), 7.18 (t, *J* = 8.7 Hz, 2H), 6.96 (d, *J* = 8.4 Hz, 2H), 4.54 (s, 2H) ppm; ^{13}C NMR (101 MHz, DMSO-d_6) δ_C: 170.14, 167.20, 162.81, 160.93, 160.38, 160.16, 158.79, 133.63,

132.91, 132.88, 132.73, 131.23, 131.15, 124.00, 119.18, 116.50, 115.54, 115.33, 40.20, 36.34 ppm; HRMS (Q-TOF) *m/z*: $[M + H]^+$ Cal. For $C_{19}H_{14}FN_4O_2S_3^+$ 445.0257; Found 445.0249.

(Z)-2-((5-((4-fluorobenzyl) thio)-1,3,4-thiadiazol-2-yl) imino)-5-((Z)-4-hydroxy-3-methoxybenzylidene) thiazolidin-4-one (Compound 9g): Yellow solid, Yield = 89%, Mp= 164-169^{0}C; ^{1}H NMR (300 MHz, DMSO-d_6) δ_H: 12.82 (s, 1H), 10.04 (s, 1H), 7.71 (s, 1H), 7.55 – 7.42 (m, 2H), 7.27 (d, *J* = 2.1 Hz, 1H), 7.22 – 7.06 (m, 3H), 7.00 (d, *J* = 8.3 Hz, 1H), 4.53 (s, 2H), 3.83 (s, 3H) ppm; ^{13}C NMR (75 MHz, DMSO-d_6) δ_C: 170.16, 167.16, 163.23, 160.00, 158.84, 149.74, 148.02, 133.98, 132.92, 132.87, 131.28, 131.17, 124.51, 123.58, 119.53, 116.43, 115.60, 115.32, 55.79, 36.41 ppm; HRMS (Q-TOF) *m/z*: $[M + H]^+$ Cal. For $C_{20}H_{16}FN_4O_3S_3^+$ 475.0363; Found 475.0451.30.

(Z)-5-((Z)-4-(dimethylamino) benzylidene)-2-((5-((4-fluorobenzyl) thio)-1,3,4-thiadiazol-2-yl)imino) thiazolidin-4-one (Compound 9h): Reddish brown solid, Yield = 86%, Mp= 224-228^{0}C; ^{1}H NMR (400 MHz, DMSO-d_6) δ_H: 12.68 (s, 1H), 7.65 (s, 1H), 7.50 (dd, *J* = 8.6, 4.5 Hz, 4H), 7.18 (t, *J* = 8.7 Hz, 2H), 6.86 (d, *J* = 8.6 Hz, 2H), 4.53 (s, 2H), 3.02 (s, 6H) ppm; ^{13}C NMR (101 MHz, DMSO-d_6) δ_C: 170.26, 167.21, 162.79, 160.52, 160.37, 159.02, 151.62, 134.30, 132.97, 132.94, 132.50, 131.23, 131.15, 119.86, 115.83, 115.53, 115.32, 112.16, 36.35, 21.08 ppm; HRMS (Q-TOF) *m/z*: $[M + K]^+$ Cal. For $C_{21}H_{18}FKN_5OS_3^+$ 510.0289, Found 510.0285.

(Z)-5-((Z)-benzylidene)-2-((5-((4-methylbenzyl) thio)-1,3,4-thiadiazol-2-yl) imino) thiazolidin-4-one (Compound 10a): Yellow solid, Yield = 86%, Mp= 210-214^{0}C; ^{1}H NMR (400 MHz, DMSO-d_6) δ_H: 12.95 (s, 1H), 7.77 (s, 1H), 7.65 (d, *J* = 7.6 Hz, 2H), 7.57 (t, *J* = 7.5 Hz, 2H), 7.50 (t, *J* = 7.3 Hz, 1H), 7.32 (d, *J* = 7.7 Hz, 2H), 7.14 (d, *J* = 7.7 Hz, 2H), 4.49 (s, 2H), 2.27 (s, 3H) ppm; ^{13}C NMR (101 MHz, DMSO-d_6) δ_C: 169.89, 167.00, 161.65, 158.44, 137.03, 133.29, 133.12, 132.97, 130.60, 130.25, 129.46, 129.21, 129.07, 123.89, 37.08, 20.77 ppm; HRMS (Q-TOF) *m/z*: $[M + H]^+$ Cal. For $C_{20}H_{17}N_4OS_3^+$ 425.0559; Found 425.0549.

(Z)-5-((Z)-3-fluorobenzylidene)-2-((5-((4-methylbenzyl) thio)-1,3,4-thiadiazol-2-yl) imino) thiazolidin-4-one (Compound 10b): Yellow solid, Yield = 88%, Mp= 217-220^{0}C; ^{1}H NMR (400 MHz, DMSO-d_6) δ_H: 12.99 (s, 1H), 7.75 (s, 1H), 7.61 (q, *J* = 7.5 Hz, 1H), 7.53 – 7.40 (m, 2H), 7.39 – 7.25 (m, 3H), 7.14 (d, *J* = 7.7 Hz, 2H), 4.48 (s, 2H), 2.26 (s, 3H) ppm; ^{13}C NMR (101 MHz, DMSO-d_6) δ_C: 169.77, 166.79, 163.53, 161.78, 161.10, 158.02, 137.04, 135.53, 135.45, 133.23, 131.54, 131.45, 129.21, 129.06, 125.68, 125.66, 125.58, 117.40, 117.19, 117.10, 116.87, 37.09, 20.75 ppm; HRMS (Q-TOF) *m/z*: $[M + H]^+$ Cal. For $C_{20}H_{16}FN_4OS_3^+$ 443.0465; Found 443.0455.

(Z)-5-((Z)-4-fluorobenzylidene)-2-((5-((4-methylbenzyl) thio)-1,3,4-thiadiazol-2-yl) imino) thiazolidin-4-one (Compound 10c): Yellow solid, Yield = 90%, Mp= 170-174^{0}C; ^{1}H NMR (400 MHz, DMSO-d_6) δ_H: 12.93 (s, 1H), 7.77 (s, 1H), 7.71 (dd, *J* = 8.5, 5.4 Hz, 2H), 7.41 (t, *J* = 8.6 Hz, 2H), 7.32 (d, *J* = 7.7 Hz, 2H), 7.14 (d, *J* = 7.7 Hz, 2H), 4.48 (s, 2H), 2.27 (s, 3H) ppm; ^{13}C NMR (101 MHz, DMSO-d_6) δ_C: 169.82, 166.92, 164.18, 161.69, 161.60, 158.23, 137.00, 133.25, 132.74, 132.65, 131.83, 129.77, 129.18, 129.03, 123.57, 116.72, 116.50, 37.05, 20.74 ppm; HRMS (Q-TOF) *m/z*: $[M + H]^+$ Cal. For $C_{20}H_{16}FN_4OS_3^+$ 443.0465; Found 443.0464.

(Z)-5-((Z)-4-chlorobenzylidene)-2-((5-((4-methylbenzyl) thio)-1,3,4-thiadiazol-2-yl) imino) thiazolidin-4-one (Compound 10d): Yellow solid, Yield = 88%, Mp= 170-172^{0}C; ^{1}H NMR (400 MHz, DMSO-d_6) δ_H: 12.98 (s, 1H), 7.77 (s, 1H), 7.66 (t, *J* = 6.2 Hz, 4H), 7.32 (d, *J* = 7.7 Hz, 2H), 7.15 (d, *J* = 7.7 Hz, 2H), 4.49 (s, 2H), 2.27 (s, 3H) ppm. ^{13}C NMR (101 MHz, DMSO-d_6) δ_C: 169.80, 166.91, 161.74, 158.11, 137.01, 133.28, 131.86, 131.58, 129.55, 129.19, 129.04, 124.65, 37.05, 20.74 ppm; HRMS (Q-TOF) *m/z*: $[M + H]^+$ Cal. For $C_{20}H_{16}ClN_4OS_3^+$ 459.0169; Found 459.0163.

(Z)-5-((Z)-4-methoxybenzylidene)-2-((5-((4-methylbenzyl) thio)-1,3,4-thiadiazol-2-yl) imino) thiazolidin-4-one (Compound 10e): Yellow solid, Yield = 92%, Mp= 200-204^{0}C; ^{1}H

NMR (400 MHz, DMSO-d_6) δ_H: 12.85 (s, 1H), 7.73 (s, 1H), 7.62 (d, *J* = 8.4 Hz, 2H), 7.32 (d, *J* = 7.7 Hz, 2H), 7.15 (d, *J* = 7.9 Hz, 4H), 4.49 (s, 2H), 3.83 (s, 3H), 2.27 (s, 3H) ppm; ^{13}C NMR (101 MHz, DMSO-d_6) δ_C: 169.98, 167.13, 161.39, 161.18, 158.60, 137.03, 133.33, 133.10, 132.39, 129.21, 129.06, 125.60, 120.62, 115.08, 55.55, 37.09, 20.76 ppm; HRMS (Q-TOF) *m/z*: $[M + H]^+$ Cal. For $C_{21}H_{19}N_4O_2S_3^+$ 455.0665; Found 455.0659.

(Z)-5-((Z)-4-hydroxybenzylidene)-2-((5-((4-methylbenzyl) thio)-1,3,4-thiadiazol-2-yl)imino) thiazolidin-4-one (Compound 10f): Yellow solid, Yield = 91%, Mp= 230-232^{0}C; ^{1}H NMR (300 MHz, DMSO-d_6) δ_H: 12.81 (s, 1H), 10.41 (s, 1H), 7.69 (s, 1H), 7.52 (d, *J* = 8.4 Hz, 2H), 7.32 (d, *J* = 7.8 Hz, 2H), 7.15 (d, *J* = 7.7 Hz, 2H), 6.96 (d, *J* = 8.4 Hz, 2H), 4.49 (s, 2H), 2.27 (s, 3H) ppm; ^{13}C NMR (75 MHz, DMSO-d_6) δ_C: 170.03, 167.23, 160.17, 158.73, 137.04, 133.62, 133.34, 132.75, 129.22, 129.07, 124.04, 119.22, 116.53, 37.11, 20.78 ppm; HRMS (Q-TOF) *m/z*: $[M + H]^+$ Cal. For $C_{20}H_{17}N_4O_2S_3^+$ 441.0508; Found 441.0498.

(Z)-5-((Z)-4-hydroxy-3-methoxybenzylidene)-2-((5-((4-methylbenzyl) thio)-1,3,4-thiadiazol-2-yl) imino) thiazolidin-4-one (Compound 10g): Yellow solid, Yield = 93%, Mp= 165-167^{0}C; ^{1}H NMR (300 MHz, DMSO-d_6) δ_H: 12.79 (s, 1H), 10.04 (s, 1H), 7.69 (s, 1H), 7.38 – 7.19 (m, 3H), 7.13 (dd, *J* = 8.1, 4.8 Hz, 3H), 6.99 (d, *J* = 8.3 Hz, 1H), 4.47 (s, 2H), 3.82 (s, 3H), 2.26 (s, 3H) ppm; ^{13}C NMR (75 MHz, DMSO-d_6) δ_C: 170.03, 167.17, 161.30, 158.74, 149.74, 148.04, 137.07, 133.94, 133.29, 129.24, 129.21, 129.10, 124.55, 123.64, 119.58, 116.43, 115.61, 55.80, 37.20, 20.80 ppm; HRMS (Q-TOF) *m/z*: $[M + H]^+$ Cal. For $C_{21}H_{19}N_4O_3S_3^+$ 471.0614; Found 471.0609.

(Z)-5-((Z)-4-(dimethylamino) benzylidene)-2-((5-((4-methylbenzyl) thio)-1,3,4-thiadiazol-2-yl) imino) thiazolidin-4-one (Compound 10h): Reddish brown solid, Yield = 89%, Mp= 225^{0}C; ^{1}H NMR (400 MHz, DMSO-d_6) δ_H: 12.67 (s, 1H), 7.63 (s, 1H), 7.48 (d, *J* = 8.6 Hz, 2H), 7.32 (d, *J* = 7.7 Hz, 2H), 7.15 (d, *J* = 7.7 Hz, 2H), 6.85 (d, *J* = 8.6 Hz, 2H), 4.48 (s, 2H), 3.01 (s, 6H), 2.27 (s, 3H) ppm; ^{13}C NMR (101 MHz, DMSO-d_6) δ_C: 170.15, 167.24,

160.85, 158.94, 151.62, 137.01, 134.28, 133.39, 132.52, 129.20, 129.07, 119.88, 115.87, 112.17, 37.11, 20.78 ppm; HRMS (Q-TOF) *m/z*: $[M + H]^+$ Cal. For $C_{22}H_{22}N_5OS_3^+$ 468.0981; Found 468.0973.

2.4. *In vitro* anticancer activity study:

2.4.1. Materials and experimental methods:

The human embryonic kidney cell lines (HEK-293), murine mammary carcinoma (4T1), human breast cancer (MCF-7), prostatic small cell carcinoma (PC3), and human alveolar basal epithelial cell (A549) were obtained from the National Centre for Cell Science (NCCS, Pune, India). Dulbecco's Modified Eagle Medium (DMEM) (Cat No.# 0000671522, HIMEDIA, HiMedia Laboratories Pvt Ltd) was used to culture MCF-7, PC3, A549, and HEK-293 cell lines, whereas 4T1 cell line was cultured in Roswell Park Memorial Institute (RPMI) medium (Gibco, Life Technologies) enriched with 10% fetal bovine serum (Cat No.# 10270106, Gibco, Life Technologies) and 1% of antibiotic solution (10,000 U Penicillin and 10 mg Streptomycin per mL), (Cat No.# 15140-122, Gibco, Life Technologies). Cells were maintained at 37 °C in a humidified atmosphere containing 5% CO_2. All synthesised compounds were dissolved in DMSO at a concentration of 100 mM to prepare stock solutions and stored at 4 °C for subsequent experiments. MTT [3-(4,5-dimethylthiazol-2-yl)-2, 5-diphenyltetrazolium bromide], DAPI (4′,6-diamidino-2-phenylindole), AO (Acridine Orange), propidium iodide, and RNase were purchased from Sigma-Aldrich. TACs Annexin-V/FITC – PI assay kit was purchased from Bio-legend and used according to the manufacturer's protocol.

2.4.2. MTT assay:

The MTT assay was conducted to evaluate the anticancer activity of all synthesised compounds in four cancer cell lines, following standard protocols [35]. For this purpose, cells with a density of 1×10^4 /well were seeded into a 96-well plate with 100 µL of cell suspension and incubated for 24 h. After incubation, cells were treated in duplicate with a range of compound

concentrations (200 µM to 0.195 µM) for 48 hours, along with a 1% DMSO-treated control. Following treatment, the MTT solution was added and incubated for 3 h. Afterwards, the resulting formazan crystals were dissolved in 150 µL of DMSO. Absorbance was measured using a multi-plate spectrophotometer at 570 nm and 650 nm to determine cell viability.

Additionally, following the same protocol, an MTT assay was performed on HEK-293 cells to compare cytotoxic activity and assess selectivity towards the cancerous cells [35]. The percentage of cell viability was calculated, and IC_{50} values were determined using GraphPad Prism™ version 8.0.1.

2.4.3. Apoptosis assay:

The apoptosis assay was conducted in MCF-7 cells using the TACs/Annexin V kit (BioLegend US). MCF-7 cells were seeded at a density of 5×10^4 cells per well in 12-well plates and incubated overnight to facilitate attachment. Cells were then treated in triplicate with the IC_{50} concentration of the compound **9e** (2.87 µM) and the reference compound **BG45** IC_{50} (50.80 µM) along with a 1% DMSO-treated control for 48 h. After treatment, the cells were washed once with PBS, trypsinized, and then centrifuged to form a cell pellet. The pellet was then resuspended in a 100 µL reagent mixture containing 10 µL of 10X Annexin V buffer, 1 µL of FITC, and 10 µL of PI, followed by incubation at ambient temperature for 30 minutes. After incubation, 400 µL of 1X AnnexinV-binding buffer was added to each sample, and samples were analysed using a BDAria™ III flow cytometer (BD Biosciences). FITC versus PI quadrant gating was applied to generate a dot plot, categorizing cells into Q1 (Necrotic cells), Q2 (late apoptosis), Q3 (Live cells), and Q4 (early apoptotic cells). The total apoptotic population was determined by considering both early and late apoptotic events [36].

2.4.4. Cell cycle analysis:

Flow cytometry was employed for cell cycle analysis. MCF-7 cells were seeded at a density of 5×10^4 cells per well in 12-well plates and incubated overnight. Following incubation, the cells

were treated in triplicate with an IC_{50} concentration of compound **9e (**2.87 µM) and the reference compound **BG45** (50.80 µM) along with a 1% DMSO-treated control for 48 h. After treatment, cells were trypsinized and centrifuged, and the resulting cell pellet was washed twice with PBS. Then, the cells were fixed by adding 70% ethanol dropwise to the cell pellet while gently vortexing. The ethanol-fixed cells were stored overnight at -20 ºC. The following day, the samples were subjected to centrifugation at 3500 rpm for 5 min at 4 ºC. The cell pellet of the samples was then re-suspended in 500 µL of staining solution containing 2% (w/v) propidium iodide (PI) and 20% (w/v) RNase in a 0.1% (v/v) Triton X-100 solution in PBS. The samples were incubated at room temperature in the dark for 30 min and analysed using flow cytometry (BDAria^{TM} III). A dot plot was generated to represent PI width versus PI area, and a histogram was plotted with the PI area on the X-axis and cell counts on the Y-axis. The percentage of cells in each phase of the cell cycle was determined using Flow Jo_V10.7.1_CL software [37,38].

2.4.5. Nuclear staining assay:

To evaluate nuclear disintegration in cancerous cells following treatment with the compound **9e**, a nuclear staining was performed. MCF-7 cells were plated into 12-well flat-bottom plates containing embedded sterile coverslips and allowed to adhere overnight. The next day, old media was removed. The cells were treated in triplicate with an IC_{50} concentration of compound **9e** (2.87 µM) and the reference compound **BG45** (50.80 µM), as well as a control (1% DMSO solution), and further incubated for 48 hours. After treatment, the cells were fixed with 4% paraformaldehyde and stained with DAPI (4',6-diamidino-2-phenylindole) and Acridine Orange (AO). Lastly, the stained cells were placed on glass slides with fluoromount-G and examined at 20x Magnification with a Laser Scanning Confocal Microscope (LSCM) DMI8 (Leica Microsystems, Germany) [39].

2.4.6. Reactive oxygen species (ROS) detection:

The production of ROS in MCF-7 cells following treatment with compound **9e** was assessed using the 2,7-Dichlorodihydrofluorescein Diacetate (DCFH-DA) assay. MCF-7 cells were plated into 12-well flat-bottom plates containing embedded sterile coverslips and allowed to adhere overnight. The next day, the old media was removed, and the cells were treated in triplicate with an IC_{50} concentration of compound **9e** (2.87 μM) and the reference compound BG45 (50.80 μM), as well as a control (1% DMSO solution), for 48 h. After treatment, the old media were removed, and a 10 μM concentration of DCFH-DA (S0033-Beyotime) was added. The mixture was then incubated for 10 min at ambient temperature in the dark. Fluorescence intensity was then examined using a Laser Scanning Confocal Microscope (LSCM) DMI8 (Leica Microsystems, Germany) at 20x magnification, with excitation and emission wavelengths of 485 nm and 535 nm, respectively. Image J software was utilized to quantify the relative fluorescence intensity (%). The data was displayed using GraphPad Prism™ version 8.0.1 [11,40].

2.4.7. *In vitro* tube formation assay (angiogenesis assay):

Firstly, the IC_{50} of the compound **9e** in the ACHN cell line was determined by following the MTT assay protocol. Then, an *in vitro* angiogenesis experiment was performed by treating the ACHN cell line with IC_{50} concentrations of the compound **9e** (4.58 μM). A 12-well plate was carefully added with 200 μL/well of Cultrex at 4°C using a pipette after pre-chilling at −20°C. The cells were trypsinised and suspended in 100 μL of complete media in the absence or presence of compound **9e**, with IC_{50} values determined in duplicate. Following the polymerisation of the basement membrane matrix for 1 h at 37°C, cells were gently placed on top. Following 48 h of incubation, the cell arrangement on cultrex was analysed using a microscope. Tubulogenic efficiency was assessed by quantifying the number of meshes, tubes, branches, and nodes using the angiogenesis tool and Imager J software [41–43].

2.4.8. *In vitro* Western blot analysis of apoptotic biomarkers expression:

MCF-7 cells were seeded in a 6-well plate and treated with IC_{50} and 5x IC_{50} concentration of compound **9e** and **BG45**. Following treatment, the cells were homogenised and vortexed 3-4 times with 1x RIPA lysis buffer to extract protein. Protein quantification was done using the BCA protein assay kit (#5000116). A total of 25 µL (30 µg) of cell proteins, mixed with 5 µL of 5x loading buffer, was denatured for 5 min at 95 °C. The denatured proteins were separated using sodium dodecyl sulfate-polyacrylamide gel electrophoresis (SDS-PAGE). Subsequently, the proteins were transferred from the gel to polyvinylidene fluoride (PVDF) membranes (Bio-Rad Laboratories, Inc.). The membranes were blocked by using 5% bovine serum albumin (#9048-46-8, Himedia Laboratories Pvt. Ltd) in tris-buffered saline containing 1% Tween 20 (TBST) and incubated overnight at 4°C with primary antibodies including Caspase-3 (cat#9662), Caspase-7 (#12827), BCL-2 (#3498), and internal control Mouse mAb beta-Actin (#3700) (Cell Signalling Technology, Inc.). The next day, the PVDF membranes were washed twice with TBST before incubation with the corresponding secondary antibodies: anti-rabbit HRP-linked antibody (cat#7074) and anti-mouse IgG HRP-linked antibody (cat#7076) for 1 h at room temperature. Following secondary antibody incubation, the membranes were washed twice with TBST for 10 min each. Protein detection was performed using a chemiluminescence kit (cat#170 S76 5060, Bio-Rad Laboratories, Inc.), and visualisation was carried out using the Fusion Plus 6 Imaging System (Vilber Lourmat, France). The blots were quantified using Image J software, and the graph was plotted using GraphPad Prism™ version 8.0.1 [39].

3. Results and discussion:

3.1. Chemistry:

The synthetic procedure for the development of 1,3,4-thiadiazole and 1,3-thiazolidine-4-one scaffold-based binary heterocyclic compound is depicted in **Scheme 1**. The reaction of thiosemicarbazide with carbon disulfide (CS_2) in ethanol in the presence of KOH produced dithiocarbazate salt, which gets cyclized when acidified with dilute HCl (20%) to deliver

compound **1**. The thiol function of compound **1**, involved in a substitution reaction with various benzyl chloride derivatives in the presence of K_2CO_3 in dry DMF, yields a variety of benzyl-substituted intermediate compounds **2d-2f**. Compound **3d-3f** was produced with excellent yield via the reaction between chloroacetyl chloride and compound **2d-2f** in dry THF at ambient temperature using a TEA catalyst. Ammonium thiocyanate (NH_4SCN) and chloroacetamide derivatives **3d-3f** were reacted under reflux (90 ^{0}C) in ethanol to get the final intermediate compound **4d-4f**. Compound **4d-4f** reacted with eight substituted aromatic aldehydes in the presence of urea (NH_2CONH_2) catalyst and glacial acetic acid (GAA) solvent at reflux (110-120 ^{0}C) to aid the substitution of various benzylidene groups in 5-position of thiazolidinone ring and yield titled compound **8(a-h)**, **9(a-h)**, and **10(a-h)** via Knoevenagel condensation (KC) (**Scheme 1**).

The structure of the compounds was confirmed by ^{1}H NMR, ^{13}C NMR, and HRMS (Q-TOF) data analysis (**Spectral Data**). ^{1}H-NMR spectra of Compound **1** revealed that the thiol and amino groups give two clear singlet signals at 13.137 (-SH) and 7.043 (-NH_2) ppm. Moreover, the carbon atoms in the "2" and "5" positions of the 1,3,4-thiadiazole nucleus correspond to two sharp, different ^{13}C NMR signals at 181.02 ppm and 161.55 ppm. The substitution of the benzyl group was validated by the elimination of the sulfhydryl proton in compound **2 (d-f)**. Also, additional aromatic protons of the benzyl group appeared in the ^{1}H NMR spectrum, and the S-CH_2 protons and carbons give signals at 4.24-4.29 ppm (^{1}H NMR) and 37.61-38.89 ppm (^{13}C NMR). Amide proton resonance at 12.98-13.01 ppm and methylene protons (4.43-4.49 ppm) of the chloroacetamide group, besides the S-CH2 group, are found in compounds **3 (d-f)**. In compound **4 (d-f**), the 1,3-thiazolidine-4-one ring 5-CH_2 proton gives a signal at 4.09 ppm, while the amide proton in the same ring resonated at 12.31 ppm. The new vinylic protons in the ^{1}H NMR of the final product series (**8a-8h, 9a-9h,** and **10a-10h**) resonated at 7.6-7.8 ppm, and the elimination of methylene protons from the 5-position in the 1,3-thiazolidinone ring validates the replacement with the benzylidene group.

HRMS (Q-TOF) data confirmed the actual molecular masses of the titled compounds, where the experimental m/z values of the compounds matched the calculated values (**Spectral Data**). The exact structure and geometry of the compound's series were verified by analogy with the single-crystal XRD-generated structure of compound **9e (Figure 2)**. Crystallographic data (see **Spectral Data**, **S.F59 & Table S1**) confirmed that compounds are Z, Z geometry isomers in their stereochemical features with respect to imine and vinylic double bonds present in the 1,3-thiazolidine-4-one ring.

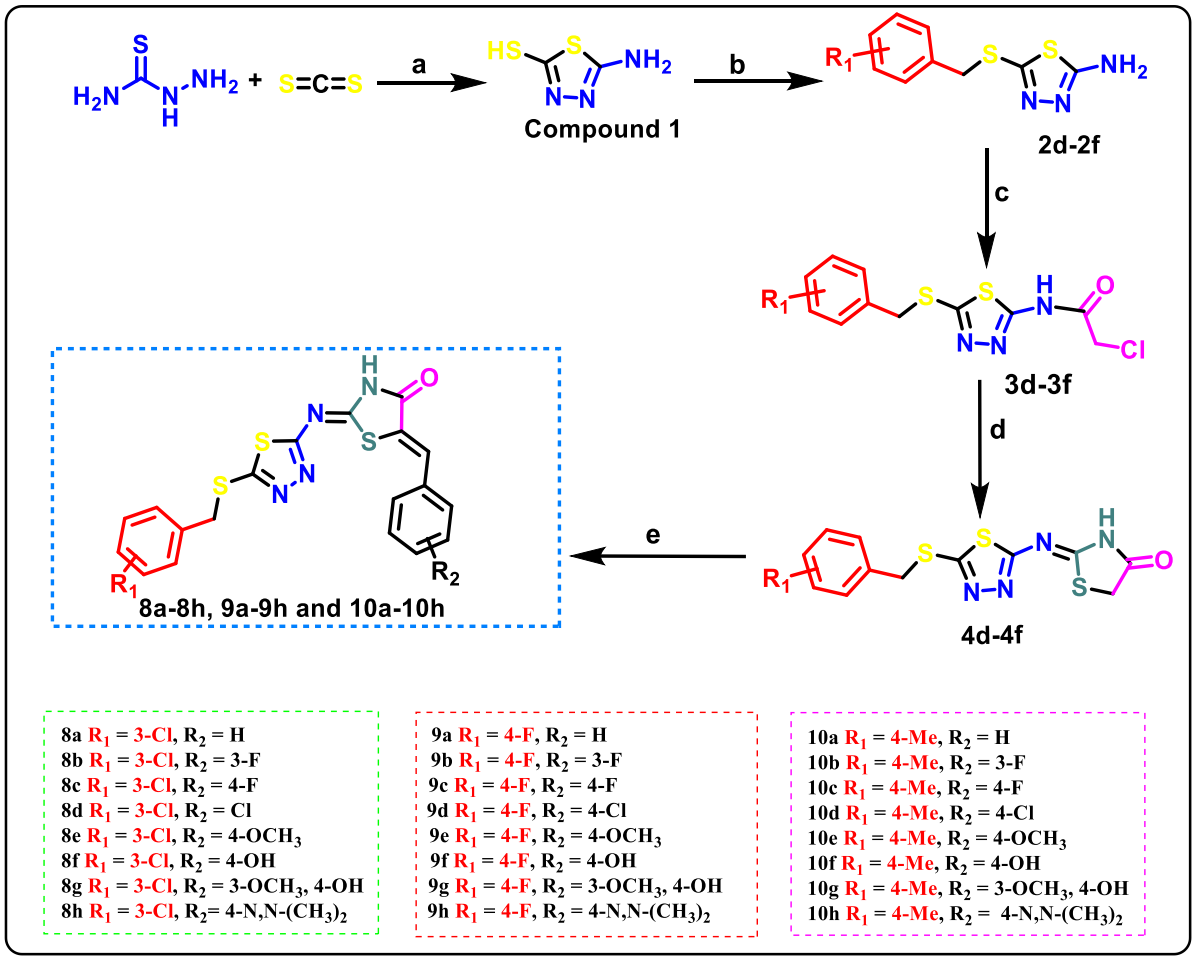

Scheme 1: Synthesis of binary heterocyclic compounds **8(a-h), 9(a-h),** and **10(a-h)**. **Reagents and conditions:** a) i. Carbon disulfide (CS_2), EtOH, 80-90 ^{0}C, reflux, 8-10h; ii. Dilute (20%) HCl, ice-cold water; b) Benzyl chloride derivatives, K_2CO_3, dry DMF, rt, 6-8h; c) Chloroacetylchloride, TEA, dry THF, rt, 6-8h d) NH_4SCN, Ethanol, 90 ^{0}C, Reflux, 10-12h; e) Benzaldehydes, Urea (1.5 equiv), GAA, 110-120 ^{0}C, Reflux, 20-24h.

3.2. Single crystal (SC)-XRD analysis:

To verify the actual structure, geometry, and/or stereochemistry of the compound series, we conducted an X-ray crystallographic analysis on a single crystal obtained from compound **9e** using an XRD instrument (Bruker SMART, Germany). The structures and geometry of other compounds were confirmed by analogy and determined through an analytical study using ^{1}H NMR, ^{13}C NMR, and high-resolution mass spectrometry (HRMS, Q-TOF). Crystallisation of compound **9e** was achieved using 1,4-dioxane as the solvent, employing the evaporation method, which occurred gradually at room temperature. **Figure 2** depicts the asymmetric structure and geometry of the compound **9e** in a single crystal. **S.F59** and **Table S1** provide additional important information on the crystal (**Spectral Data**). These data can also be easily accessed from the Cambridge Crystallographic Data Centre (CCDC) using the link www.ccdc.cam.ac.uk/data_request/cif, with the unique identification number **2422956** for the deposited crystal data.

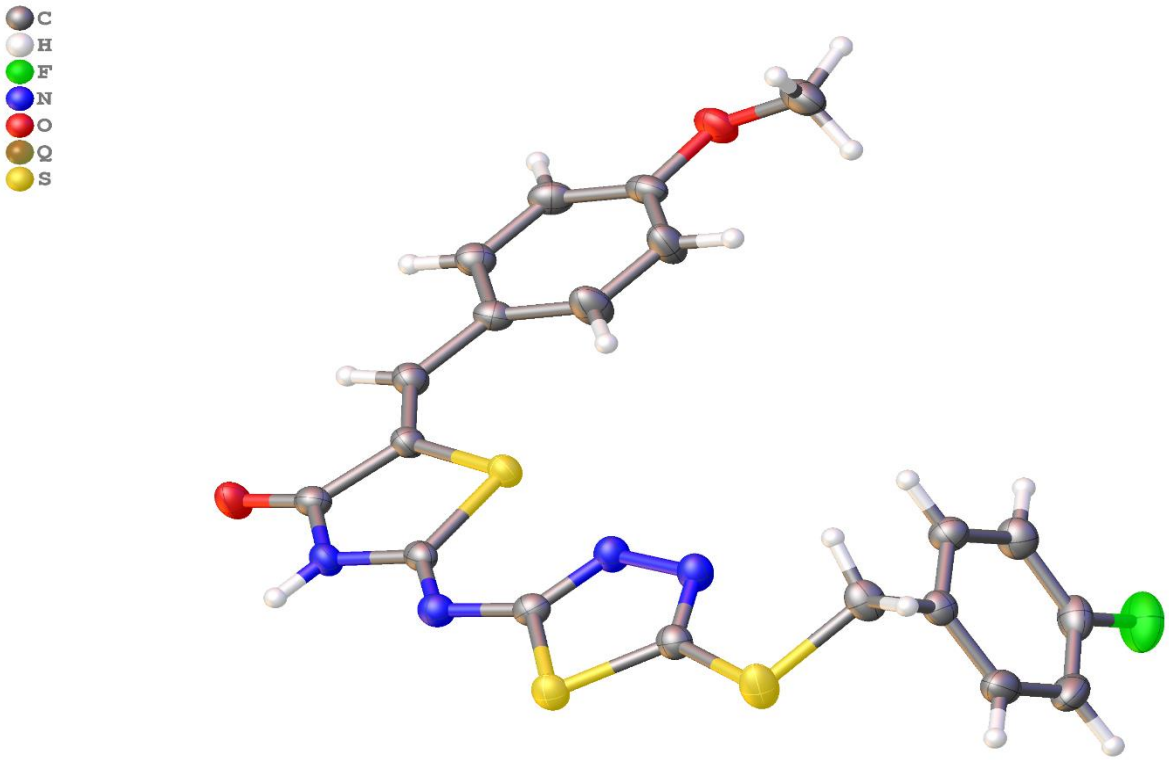

Figure 2: Structure of compound **9e** in crystal (ORTEP Diagram).

3.3. Anticancer activity:

3.3.1. Anti-proliferative activity:

The anticancer activity of all the synthesised final compounds (**8a-h, 9a-h, and 10a-h**) was investigated on murine mammary carcinoma cell line (4T1), human breast cancer cell line (MCF-7), prostatic small cell carcinoma cell line (PC3), and human alveolar basal epithelial cell carcinoma cell lines (A549). All compounds were subjected to a cytotoxicity assay for IC_{50} determination by treating cancer cells with a wide range of concentrations (200 μM to 0.195 μM), following the standard protocol [35]. Results showed that all the compounds exhibited antiproliferative effects on the various cancer cell lines tested (**Figure 3** and **Table 1**). Among the tested cancer cell lines, the maximum anticancer activity against MCF-7 cells was observed for compounds **9e** (IC_{50} = 2.87 μM), **9d** (IC_{50} = 5.19 μM), and **9a** (IC_{50} = 5.50 μM), indicating that these compounds exhibit potent anticancer activity. For the other remaining compounds, the IC_{50} values lie in the range of 7 μM - 27 μM. The dose-cytotoxicity response curves of the molecules against 4T1 (A), MCF-7 (B), PC3 (C), and A549 (D) are presented as sigmoidal curves (**Figure 3)**. Based on the results obtained from the *in vitro* cytotoxicity evaluation using the MTT assay, we identified the lead compound **9e** as the most active anticancer molecule, with an IC_{50} value of 2.87 μM against the MCF-7 cell line. The cytotoxic potency of the compounds was compared with that of **BG45,** a selective inhibitor of class I histone deacetylase (HDAC) that preferentially targets the HDAC3 isoform. It has been mentioned in the literature as a possible antitumour agent. The maximum number of compounds displayed higher cytotoxicity than **BG45** in the MTT assay, where compound **9e (**IC_{50}: 2.87 μM) is the most active and identified as a lead molecule. Additionally, the results indicate a higher inhibitory potential against human breast cancer cell lines compared to other cancer cell lines.

Additionally, we have evaluated the compound's cytotoxicity in normal human embryonic kidney cell lines (HEK-293) using the MTT assay to determine the IC_{50} for this cell line [35].

It is intriguing to note that all the compounds exhibited preferential selectivity towards cancer cell lines, displaying less activity in normal cell lines. The lead compound **9e** showed 40-fold selectivity towards MCF-7 cells. Thus, we considered MCF-7 cells for further experiments to evaluate the mechanism of antiproliferative potency of compounds. The dose-cytotoxicity response curves and IC_{50} of the compound series are presented in this article (**Figure 3** & **Table 1**). The selectivity index (SI) of the compound series on different cancer cell lines is provided in **Table 2**.

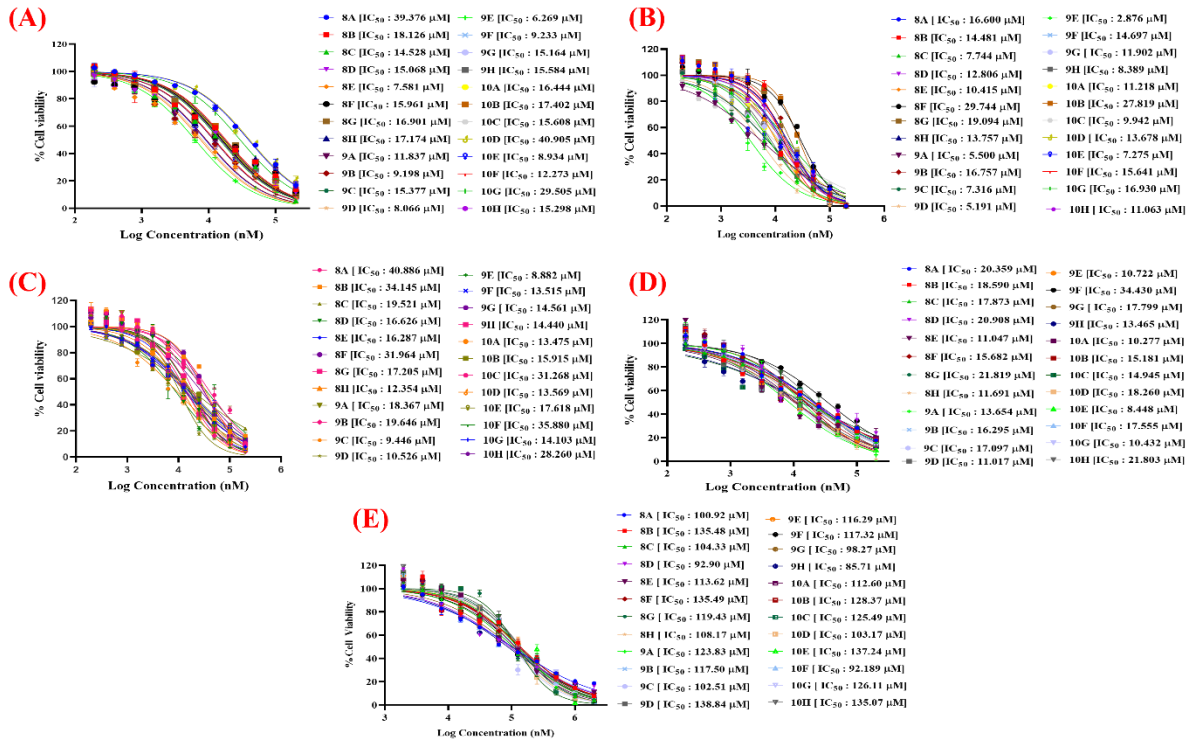

Figure 3: Dose-response curve (DRC) of compounds series (**8a-8h, 9a-9h, and 10a-10h**) on 4T1 (**A**), MCF-7 (**B**), PC-3 (**C**), A549 (**D**) cancer cell lines and normal HEK-293 (**E**) cell lines. Cells were treated with the compound at concentrations ranging from 0.195 µM to 200 µM for 48 hours. Data are presented as mean ± SD, n = 2.

Table 1: The table represents IC_{50} (µM) values of the synthesized final compounds (**8A-8H, 9A-9H, and 10A-10H**) in cancer cell lines (4T1, MCF-7, PC3, A549) and normal cell lines (HEK-293). Data represent mean ± SD (n = 2).

Compounds	**4T1 IC_{50} (µM)**	**MCF-7 IC_{50} (µM)**	**PC3 IC_{50} (µM)**	**A549 IC_{50} (µM)**	**HEK-293 IC_{50} (µM)**
8a	39.37 ± 0.14	16.60 ± 0.15	40.88 ± 2.56	20.35 ± 0.31	100.9 ± 2.06
8b	18.12 ± 0.23	14.48 ± 0.89	34.14 ± 1.59	18.59 ± 0.85	135.48 ± 1.36
8c	14.52 ± 0.51	7.74 ± 0.06	19.52 ± 0.86	17.87 ± 1.02	104.33 ± 0.96
8d	15.06 ± 0.35	12.80 ± 1.02	16.62 ± 0.51	20.90 ± 1.51.	92.90 ± 1.23
8e	7.58 ± 0.12	10.41 ± 0.98	16.28 ± 0.08	11.04 ± 0.35	113.62 ± 0.36
8f	15.96 ± 0.96	29.74 ± 0.13	31.96 ± 1.68	15.68 ± 0.74	135.49 ± 1.69
8g	16.90 ± 0.54	19.09 ± 0.24	17.20 ± 0.85	21.81 ± 1.08	119.43 ± 1.23
8h	17.17 ± 0.25	13.75 ± 0.36	12.35 ± 0.23	11.69 ± 0.29	108.17 ± 0.87
9a	11.83 ± 0.58	5.50 ± 0.07	18.36 ± 0.14	13.65 ± 0.96	123.83 ± 0.96
9b	9.19 ± 0.68	16.75 ± 0.95	19.64 ± 1.98	16.29 ± 0.75	117.50 ± 1.05
9c	15.37 ± 0.65	7.31 ± 0.08	9.44 ± 0.75	17.09 ± 0.63	102.51 ± 2.36
9d	8.06 ± 0.21	5.19 ± 0.53	10.52 ± 0.36	11.01 ± 1.08	138.84 ± 1.69
9e	6.26 ± 0.28	2.87 ± 0.84	8.88 ± 0.12	10.72 ± 0.87	116.29 ± 1.36
9f	9.23 ± 0.68	14.69 ± 0.74	13.51 ± 0.63	34.43 ± 0.52	117.32 ± 1.36
9g	15.16 ± 0.29	11.90 ± 1.23	14.56 ± 1.02	17.79 ± 0.74	98.27 ± 1.05
9h	15.58 ± 0.14	8.38 ± 0.05	14.44 ± 0.09	13.46 ± 0.19	85.71 ± 0.58
10a	16.44 ± 0.89	11.21 ± 2.01	13.47 ± 0.25	10.27 ± 0.85	112.60 ± 2.01
10b	17.40 ± 0.87	27.81 ± 0.13	15.91 ± 0.47	15.18 ± 0.69	128.37 ± 1.02
10c	15.60 ± 0.69	9.94 ± 0.02	31.26 ± 0.35	14.94 ± 0.48	125.49 ± 0.99
10d	40.90 ± 1.25	13.67 ± 0.23	13.56 ± 0.96	18.26 ± 0.63	103.17 ± 1.23
10e	8.93 ± 0.23	7.27 ± 0.38	17.61 ± 0.05	8.44 ± 0.92	137.24 ± 2.63
10f	12.27 ± 0.57	15.64 ± 1.25	35.88 ± 2.04	17.55 ± 1.05	92.189 ± 0.91
10g	29.50 ± 1.25	16.93 ± 1.08	14.10 ± 0.23	10.43 ± 0.47	126.11 ± 1.23
10h	15.29 ± 0.69	11.06 ± 0.97	28.26 ± 1.65	21.80 ± 0.08	135.07 ± 0.95
BG45*	26.03 ± 0.34	50.80 ± 0.30	64.15 ± 0.25	ND	145.85±0.19

*Values reported in previous work [11].

Table 2: Final compounds series (**8a-8h, 9a-9h, and 10a-10h**) and their selectivity index (SI) on various cancer cells.

Compounds	Structure	SI			
		4T1	**MCF-7**	**PC3**	**A549**
8a	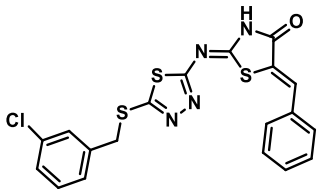	2.56	6.07	2.46	4.95
8b	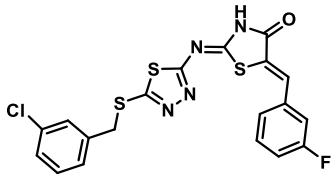	7.47	9.35	3.96	7.28
8c	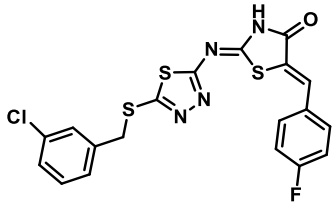	7.18	13.47	5.34	5.83
8d	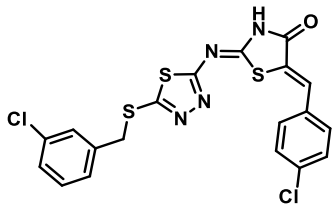	6.16	7.25	5.58	4.44
8e	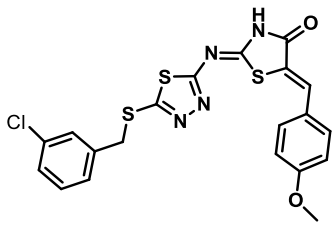	14.98	10.90	6.97	10.28
8f	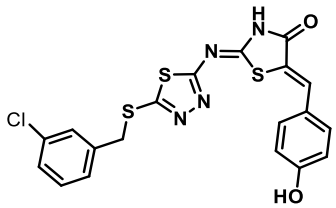	8.48	4.55	4.23	8.63

8g	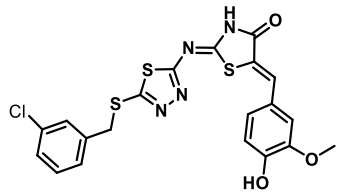	7.06	6.25	6.94	5.47
8h	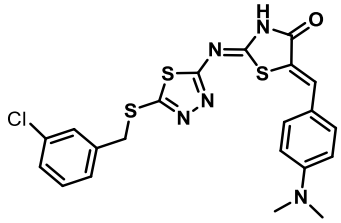	6.29	7.86	8.75	9.25
9a	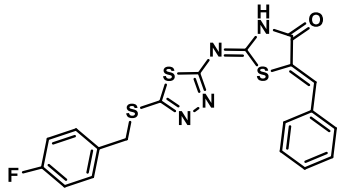	10.46	22.51	6.74	9.06
9b	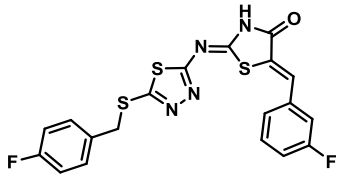	12.77	7.01	5.98	7.21
9c	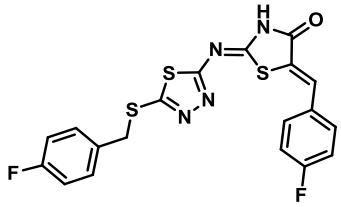	6.66	14.02	10.85	5.99
9d	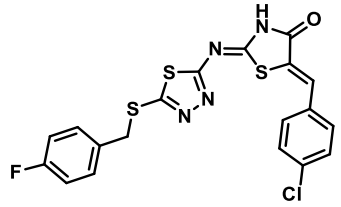	17.21	26.74	13.19	11.01
9e	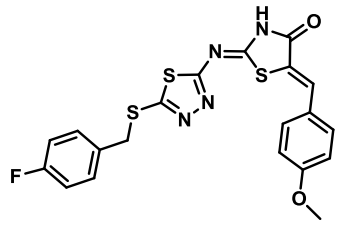	18.55	40.43	13.09	10.84

9f	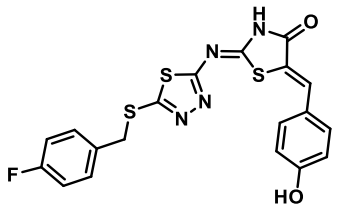	12.70	7.98	8.68	3.40
9g	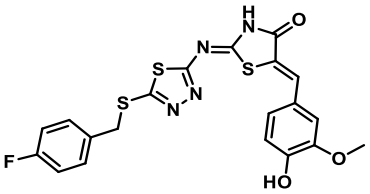	6.48	8.25	6.74	5.52
9h	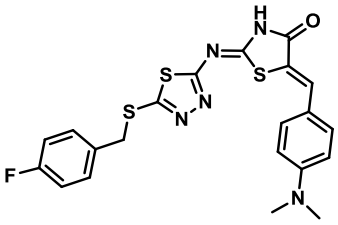	5.49	10.21	5.93	6.36
10a	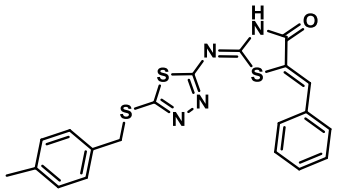	6.84	10.03	8.35	10.95
10b	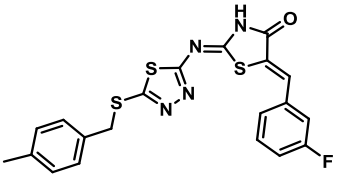	7.37	4.61	8.06	8.45
10c	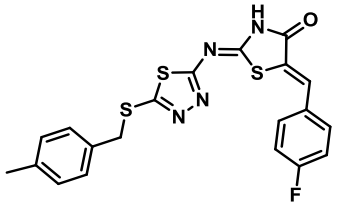	8.04	12.62	4.01	8.39
10d	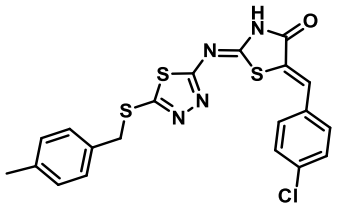	2.52	7.54	7.60	5.65

10e	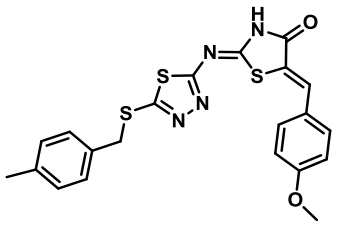	15.36	18.86	7.78	16.24
10f	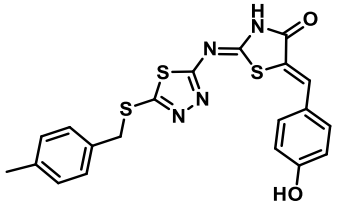	7.51	5.89	2.56	5.25
10g	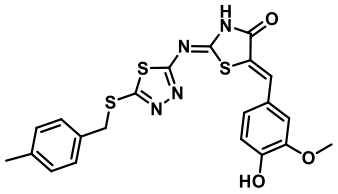	29.505	7.44	8.94	12.0
10h	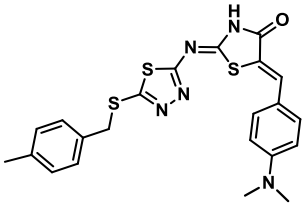	8.82	12.20	4.77	6.19

3.3.2. Structure-activity relationship (SAR):

- From literature reports, it is thought that the binary heterocycle 1,3,4-thiadiazole-2-yl-imino-thiazolidine-4-one scaffold is the central scaffold for anticancer action.
- According to **Table 1** & **Figure 3** the 4-F-benzyl moiety on thio group in the 2-position of 1,3,4-thiadiazole heterocycle revealed superior tolerance for antiproliferative activity (Compounds **9a-9h**).
- The 4-OCH_3 group on the arylidene moiety of the thiazolidine-4-one heterocycle confers better cytotoxic action than other functional groups or atoms (except for compounds **8c**, **9a**, and **9d**). In contrast, compound **9e** (IC_{50} = 2.87 μM), which contains a 4-F-benzyl thio and a 4-OCH_3-arylidene moiety, exhibited superior cytotoxic action against MCF-7 cells.

- Either the 3-Cl or 4-CH_3 group on the benzyl moiety on the thio group in 1,3,4-thiadiazole decreases the anticancer activity for maximum derivatives of the series (Compounds **8a-8h** & **10a-10h**).

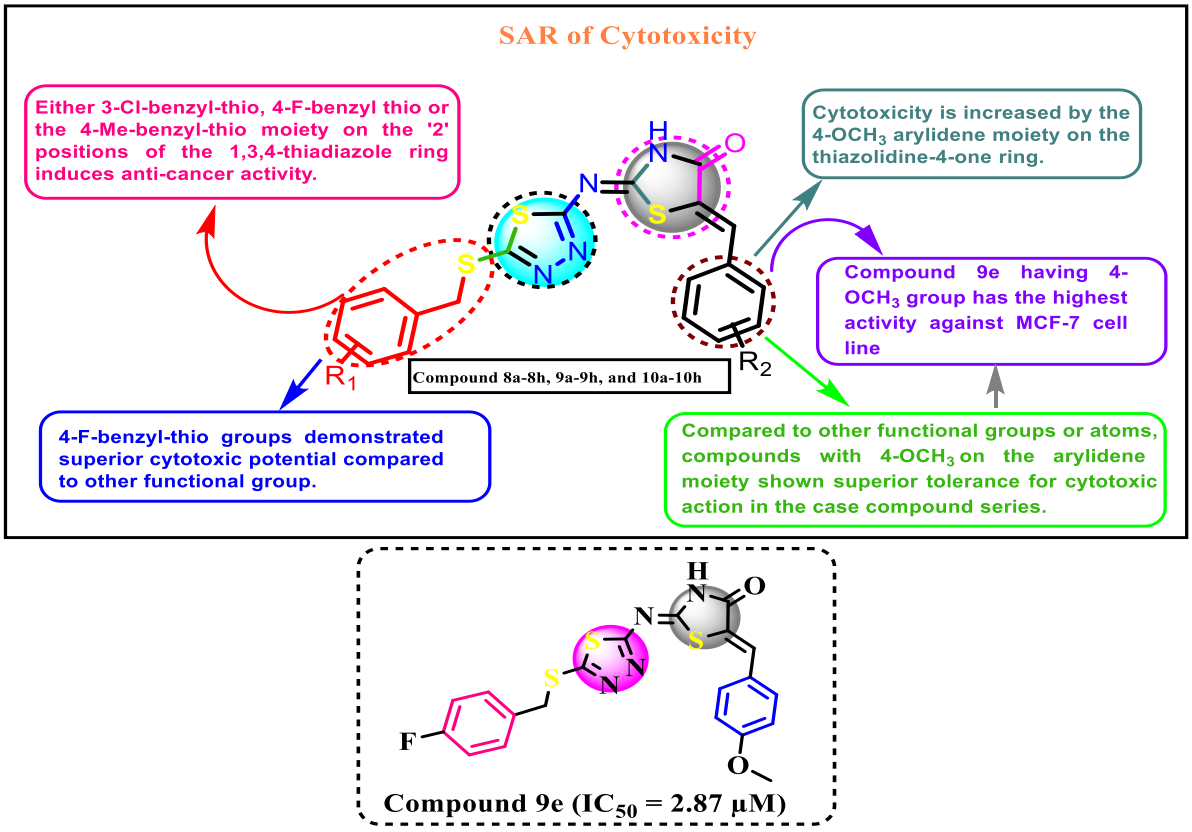

Figure 4: SAR of cytotoxic activity of compounds (**8a-8h, 9a-9h, and 10a-10h**) in various cancer cell lines.

3.3.3. Apoptosis assay:

Several research reports have demonstrated that cytotoxic activity ultimately leads to cell death through apoptotic mechanisms. To evaluate the apoptotic activity of compound **9e**, a FACS analysis was conducted using the Annexin-V/FITC–PI assay in MCF-7 cell lines. The apoptotic influence of compound **9e** was assessed by analyzing its impact on cell cycle status at the IC_{50} concentration (2.87 µM) after 48 hours of treatment (**Figure 5**) [36]. IC_{50} concentrations were chosen based on MTT results, as the tested concentration showed significant activity in the MCF-7 cell line. The results showed marked apoptotic activity in MCF-7 cells after treatment with compound **9e** compared to the reference compound **BG45**. Compound **BG45** at IC_{50}

(50.80 µM) displayed the total % of apoptosis as 23.1 ± 2.61 (Q2 and Q4). In contrast, an enhanced apoptotic population percentage of 28.2 ± 2.15 (Q2 and Q4) was observed for compound **9e** at the IC_{50} concentration, compared to the control, which exhibited an apoptotic percentage of 1.8 ± 1.12 (Q2 and Q4). These results suggest that the programmed cell death mechanism induced by compound **9e** leads to significant apoptosis of cancer cells (MCF-7).

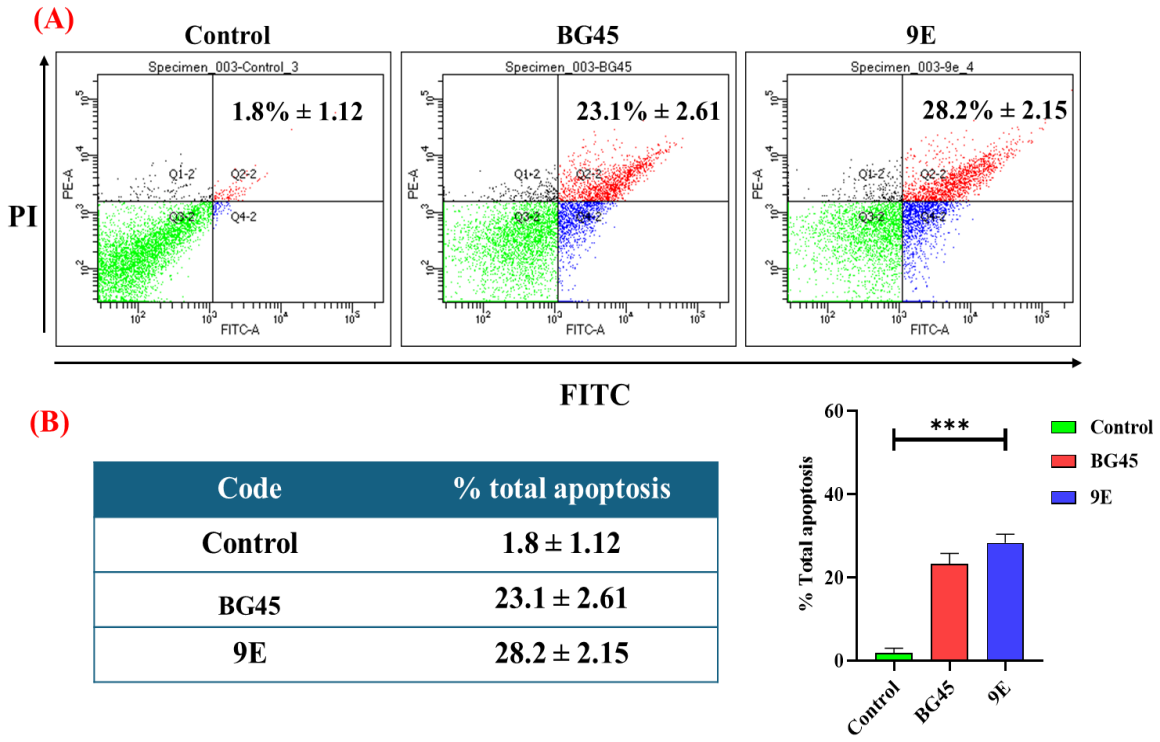

Figure 5: (A) Annexin-V/FITC–PI staining assay using flow cytometry was performed to examine Apoptosis. MCF-7 cells were treated with compound **9e** (2.87 µM) and the reference compound **BG45** (50.80 µM) at their corresponding IC_{50} concentrations for 48 h, along with a vehicle-treated control. The X-axis represents annexin-V intensity, while the Y-axis represents propidium iodide intensity. **(B)** The percentage of apoptotic MCF-7 cells following treatment is illustrated in the accompanying table and graph. Data are expressed as mean ± standard deviation (n =3), ***p < 0.001.

3.3.4. Cell cycle analysis:

In continuation of the outcome from the apoptosis assay, the progress in the cell cycle was determined in MCF-7 cells after the treatment with compound **9e**. The cancer cell population at various stages of the cell cycle was analysed in a flow cytometry assay (**Figure 6**). A cell

cycle experiment was conducted using MCF-7 cell lines after being treated with compound **9e** and **BG45** at the IC_{50} dose for 48 hours [37,38]. The results revealed an enhanced cell population in the G1 stage of the cell cycle for compound **9e** at IC_{50} (76.3%) compared to control (58.9%) and **BG45** (55.4%). This experiment also demonstrated G1/S phase cell cycle arrest, characterised by a rise in the cell population with a 4n DNA count. It was also noticed that compound **9e** at IC_{50} concentration decreased the G2/M population (9.43%) without notable alteration in the S phase (20.1%) compared to the control. These outcomes further emphasize the promising antiproliferative potency of the lead compound **9e**, which might be progressed through G1/S phase cell cycle arrest. Additionally, it validates the results of the apoptotic assay for programmed cell death.

(A)

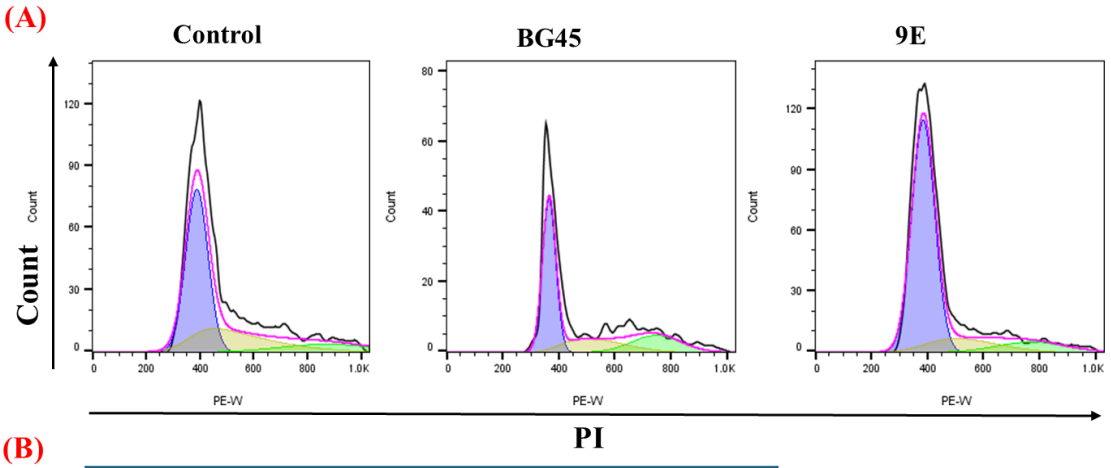

(B)

Code	% cell population G1 phase	% cell population S phase	% cell population G2/M phase
Control	58.9 ± 1.6	27.1 ± 3.5	10.4 ± 1.2
BG45	55.4 ± 2.5	21.4 ± 1.9	22.2 ± 2.3
9E	76.3 ± 3.2	20.1 ± 2.5	9.43 ± 1.8

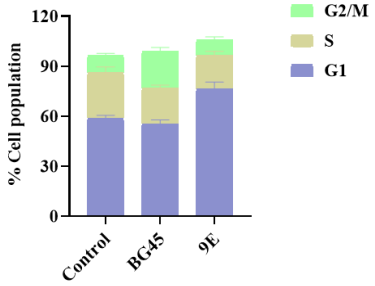

Figure 6: (A) The cell cycle analysis was conducted using flow cytometry (BD Aria III) in MCF-7 cells that were treated with compound **9e** (2.87 µM) and the reference compound **BG45** (50.80 µM) at their corresponding IC_{50} concentrations for 48 h, along with a vehicle-treated control. **(B)** The percentage of the cell population at different cell cycle phases (G1, S, and

G2/M) is presented in the accompanying table and graph. Data are expressed as mean ± standard deviation (n =3).

3.3.5. Nuclear staining assay:

A nuclear staining assay was performed using DAPI and AO as staining dyes to observe the phenomenon of apoptosis in cancer cells, and the samples were examined under a fluorescence microscope [39]. DAPI is used to stain and detect apoptotic bodies. The cells that had undergone apoptosis will be stained brightly with DAPI, and they exhibit chromatin condensation and nuclear fragmentation, which are the characteristic features of apoptosis. Whereas, untreated or control cells will have less fluorescence. Acridine orange (AO) is typically used to stain acidic vesicles in live cells, producing orange-to-red signals that help distinguish apoptotic cells from normal cells, which exhibit green fluorescence. It was observed that treating MCF-7 cells with compound **9e** (IC_{50}: 2.87 µM) for 48 hours, followed by DAPI/AO staining, resulted in a significant difference in the morphology of the treated cancer cells compared to the control, untreated cancer cells (**Figure 7**). Staining of compound **9e**-treated cancer cells with AO showed an alteration in the fluorescence character from green (normal cellular DNA) to orange (nicked cellular DNA). Hence, the enhanced fluorescence intensity of AO in compound **9e**-treated cancer cells suggested that chromosomal condensation happened significantly compared to control, untreated cancer cells. These results suggested the nuclear disintegration of treated cancer cells and revealed an apoptotic mechanism for cell death, indicating the cytotoxicity of the molecule. More apoptotic death was noticed in the compound **9e**-treated cells than in the control.

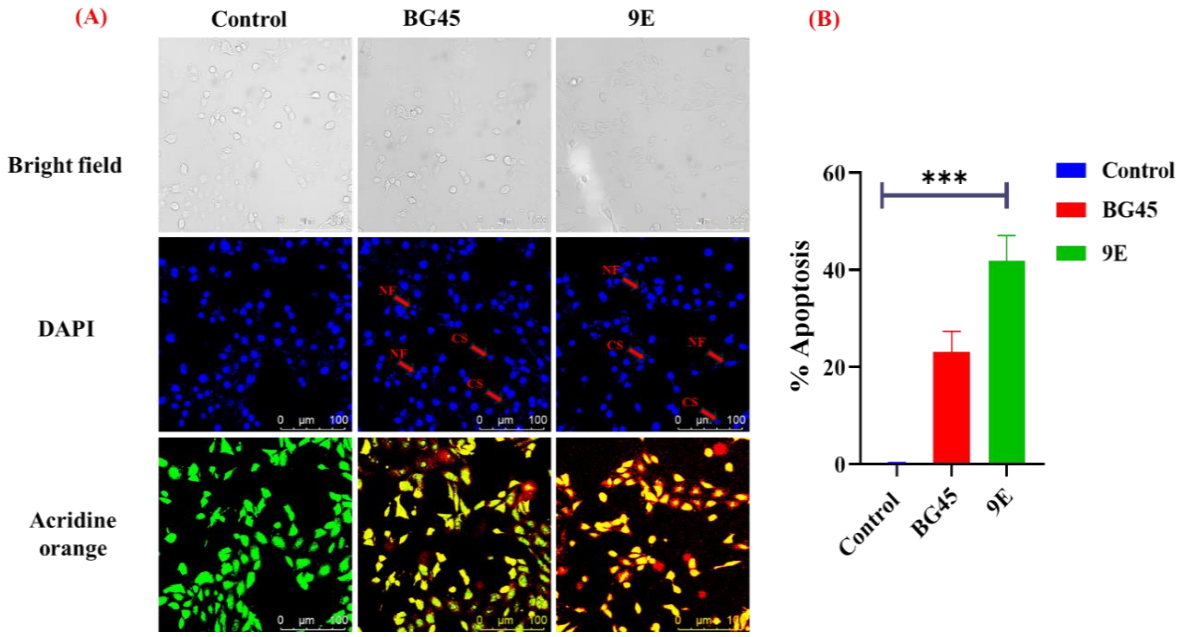

Figure 7: (A) Nuclear staining experiment using DAPI and AO staining solutions to analyse the nuclear morphology in MCF-7 cells following treatment with **BG45** and compound **9e** and a control for 48 h. The stained nuclei were visualised using a laser scanning confocal microscope (DMI8, Leica Microsystems, Germany) with a 20× magnification. **(B)** A graph showing the percentage of apoptosis determined by ImageJ software. NF represents nuclear fragmentation, whereas CS represents cell shrinkage. Data are expressed as mean ± standard deviation (n =3), ***$p < 0.001$.

3.3.6. Reactive oxygen species (ROS) formation in cancer cells:

Research studies reported that intracellular ROS production is a vital factor in cell death, as it promotes apoptosis [44,45]. DCFH-DA enters the cells, where cellular esterases remove the acetyl groups, generating non-fluorescent DCFH. Upon oxidation by ROS, DCFH is converted into DCF, which emits green fluorescence. Cancerous cells proliferate well under a moderate level of ROS, whereas a high level of ROS creates a stressful microenvironment, depolarising the mitochondria and killing the cells. We assessed whether the compound **9e** treatment could promote the formation of ROS in cancer cell lines (MCF-7). According to **Figure 8,** there is a marked enhancement of relative fluorescence intensity in MCF-7 cells after treatment with compound **9e** at the IC_{50} dose compared to control, untreated cells (1% DMSO-treated cells),

as determined by DCFH-DA staining [11,40]. The result of this study supports the apoptosis mechanism of cancer cell death and cytotoxicity.

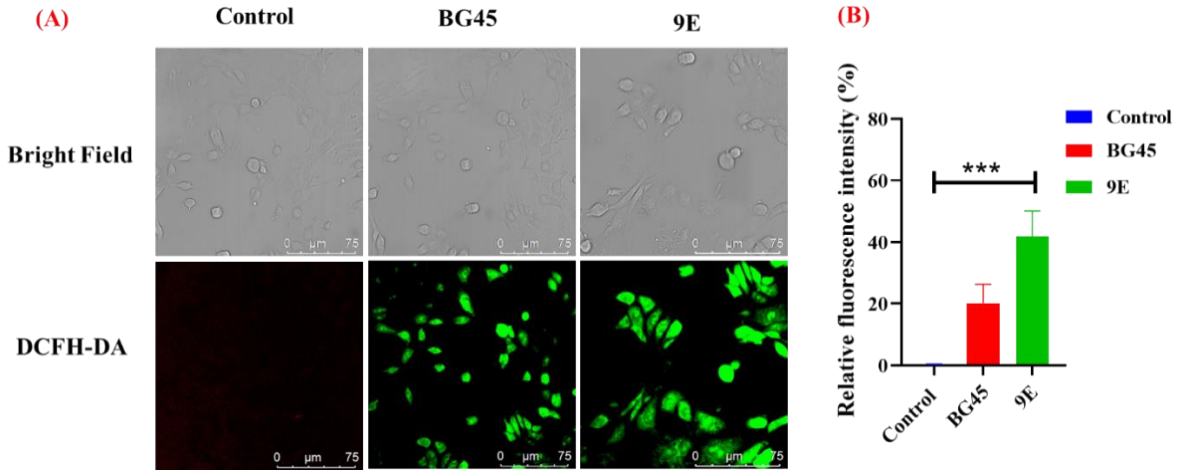

Figure 8: (A) Intracellular ROS levels were detected using DCFH-DA staining in MCF-7 cells following treatment with **BG45**, compound **9e**, and control for 48 h, **(B)** A quantified graph represents fluorescence intensity analyzed using Image J software. ROS generation was visualized using a laser scanning confocal microscope at 20× magnification with scale bars of 75 µm. Data are expressed as mean ± standard deviation (n =3), ***$p < 0.001$.

3.3.7. *In vitro* tube formation assay or angiogenesis assay:

The angiogenesis assay was conducted to assess the antiangiogenic potential of the compound **9e** against the ACHN cell line. After treatment with IC_{50} concentrations (4.58 µM, ACHN) of compound **9e** on ACHN cells (**Figure 11**) for 48 hours, high-quality raw images were acquired along with control, followed by further image processing using ImageJ software [41–43]. In the treatment groups, there was a significant decrease in various parameters like mesh length, branch length, and tube length, which was also clearly visible in the obtained images compared to the control. After the treatment, there was a disruption in the junctions and meshes, resulting in less capillary-like tube formation. This inhibition resulted in a decrease in the formation of the network, as indicated by the significant differences in all other parameters. Statistical analysis was then applied to compare these parameters across the control and compound **9e**. The results analysed highlighted all the above-mentioned features, allowing for a comparison

of the anti-angiogenic potential of compound **9e** to that of the control and aiding in understanding their effects on angiogenesis (**Figures 9 & 10**).

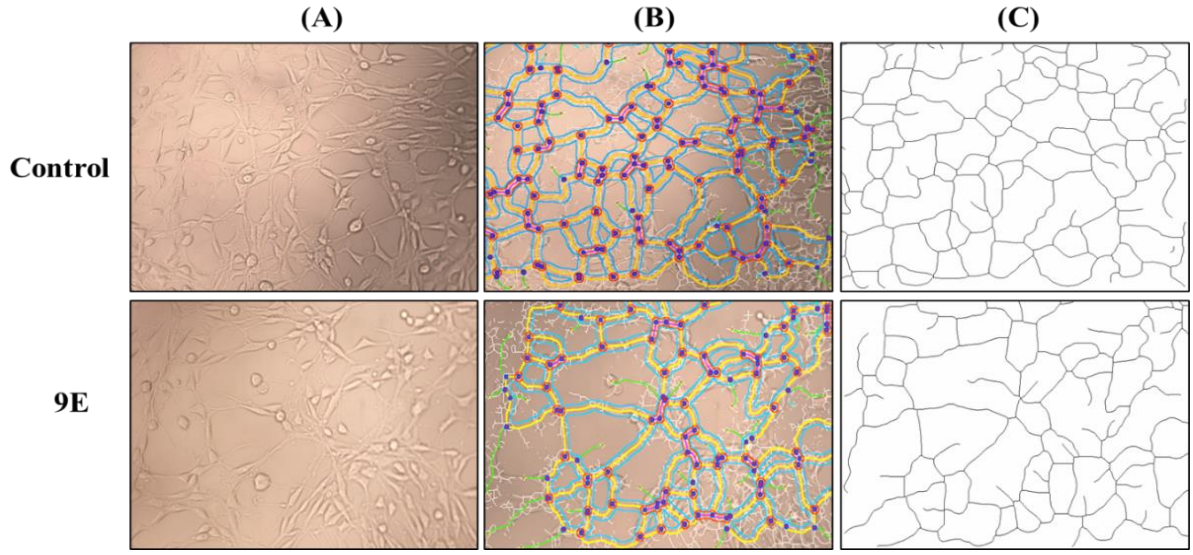

Figure 9: (A) Representative images showing the tubular network formation of ACHN cells treated with control (1% DMSO) and compound **9e** (IC_{50}: 4.58 µM) after 48 h. (B) The corresponding analyzed image using the angiogenesis analysis tool highlights key parameters: Nodes (represented as blue spheres), Branches (depicted in light blue), and Mesh (highlighted in yellow). (C) A binary skeleton representation of the analyzed image illustrates the structural framework of the tubular network**.** Scale bar 100µm.

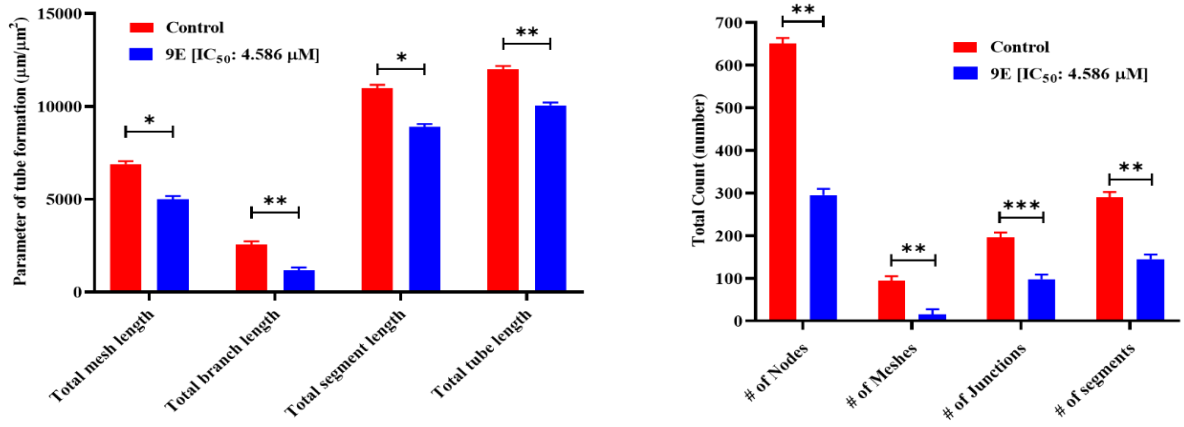

Figure 10: Comparative evaluation of parameters derived from analysis of images in ACHN cells that were treated and untreated after being grown in cultrex for 48 h**.**

Cell viability assay of compound 9e on ACHN cells:

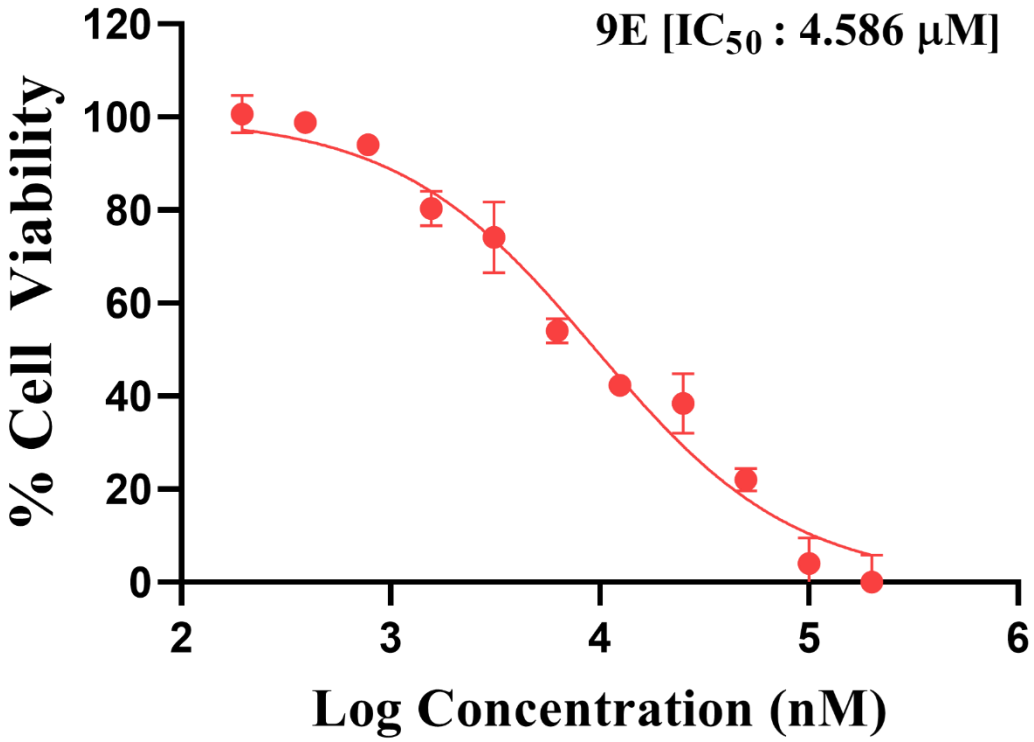

Figure 11: The graph represents the DRC and IC_{50} results of compound **9e** obtained from the MTT assay against ACHN cells. Cells were treated with the compound **9e** at 0.195 µM to 200 µM for 48 h. Data represent mean ± SD, n = 2.

3.3.8. Detection of various apoptotic protein biomarker expression levels by western blot analysis:

We investigated the protein expression levels of caspase-3, caspase-7, and BCL-2 in MCF-7 cells following treatment with compound **9e** and compound **BG45** [39]. In *in vitro* cancer cells, the compound **9e** was found to be highly cytotoxic, particularly against MCF-7 cells. The results depicted in **Figure 12** show an elevation of caspase-3 and caspase-7 levels, along with lower levels of BCL-2 expression, in a concentration-dependent manner in the cell lysate of **compound 9e**-treated MCF-7 cells, indicating an *in vitro* apoptotic cancer cell death mechanism. The preliminary *in vitro* experiments demonstrated that the lead **compound 9e** exhibits cytotoxic activity through apoptosis and cell cycle arrest, mediated by ROS generation

and oxidative stress, ultimately leading to apoptosis via various cellular intrinsic pathways. Overall, these results demonstrated the *in vitro* apoptotic and cytotoxic potential of **compound 9e** on cancer cells.

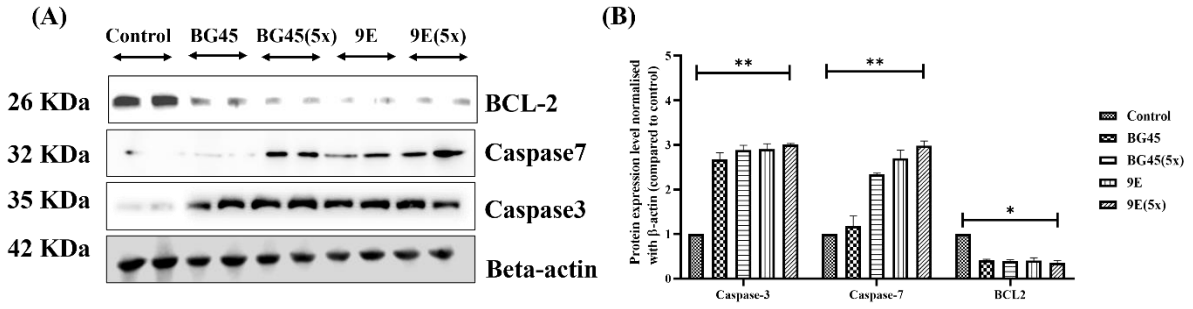

Figure 12: Immunoblotting was performed to evaluate apoptotic biomarkers in MCF-7 cell lysates following treatment with control, compound **9e** at IC_{50} (2.87 µM) and 5x IC_{50} (14.30 µM), as well as **BG45** at IC_{50} (50.80 µM) and 5x IC_{50} (259µM) concentrations. **(A)** Western blot images illustrate the expression levels of caspase-7, caspase-3, and BCL-2 in treated MCF-7 cell lysates. **(B**) Graphical representation of the protein expression level normalized to β-Actin, which served as an internal control. Protein expression was quantified using ImageJ software and normalized against control values. Data are expressed as mean ± standard deviation (n =2).

Spectral Data (Chapter IV):

1. Copy of ^{1}H and ^{13}C NMR data:

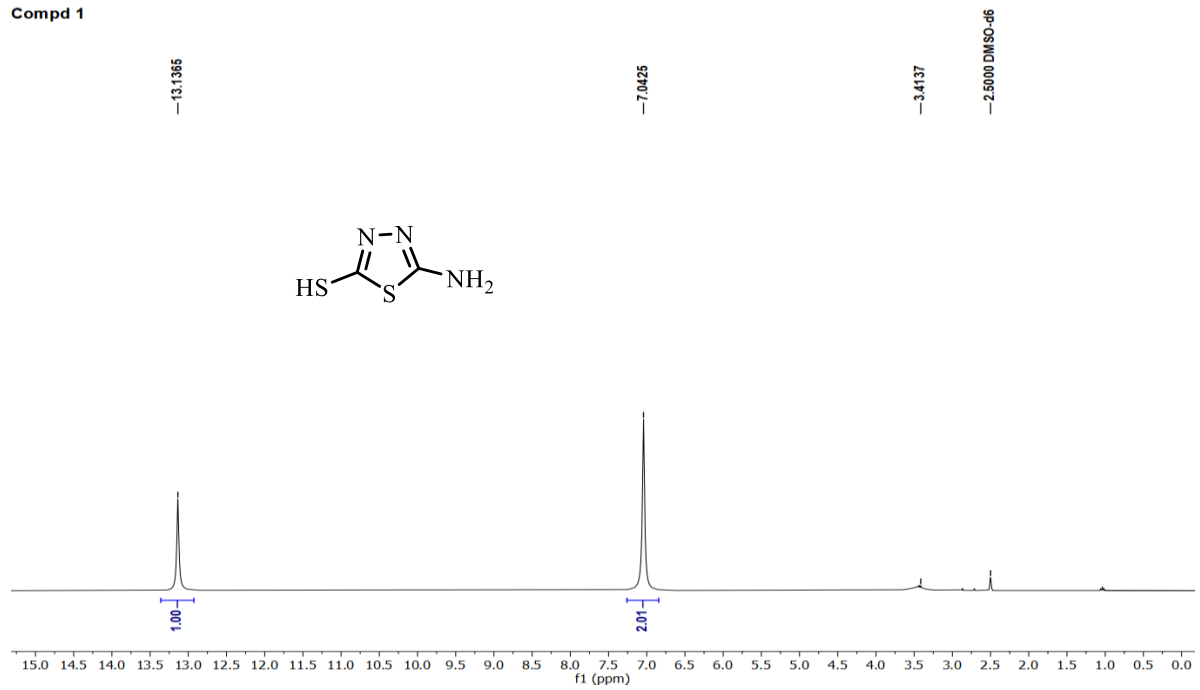

S.F1: ^{1}H NMR of compound **1**

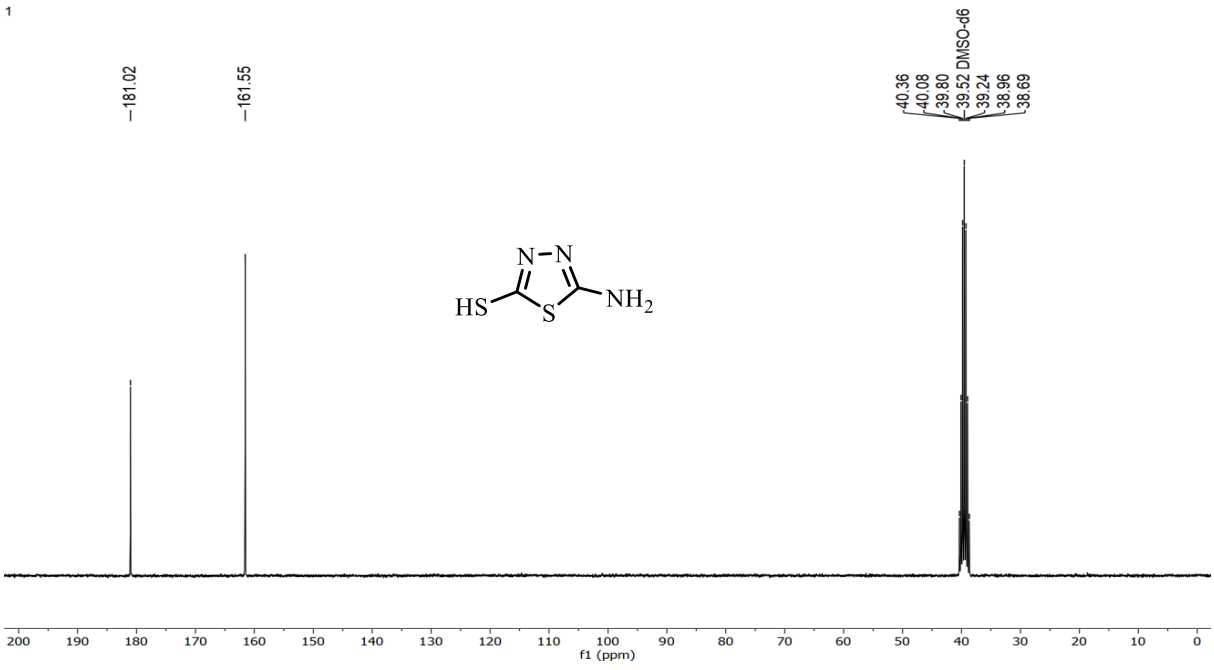

S.F1′: ^{13}C NMR of compound **1**

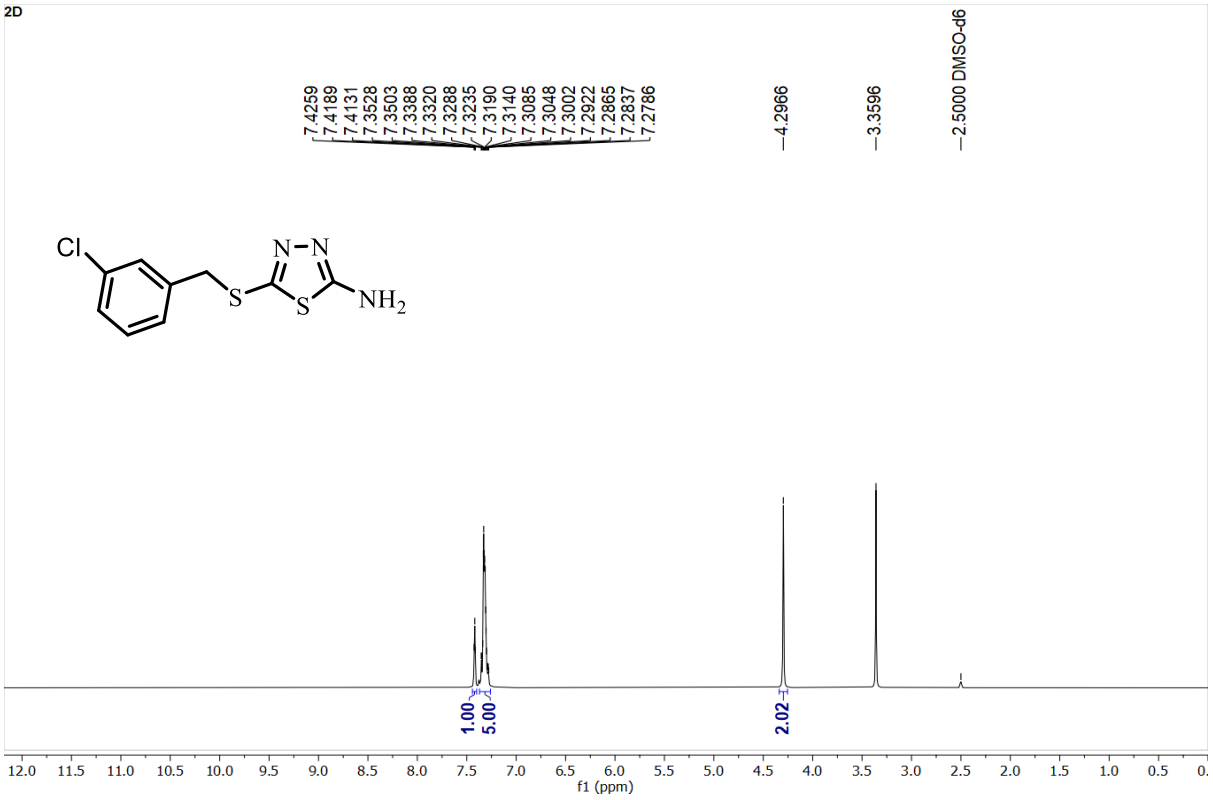

S.F2: ^{1}H NMR of compound **2d**

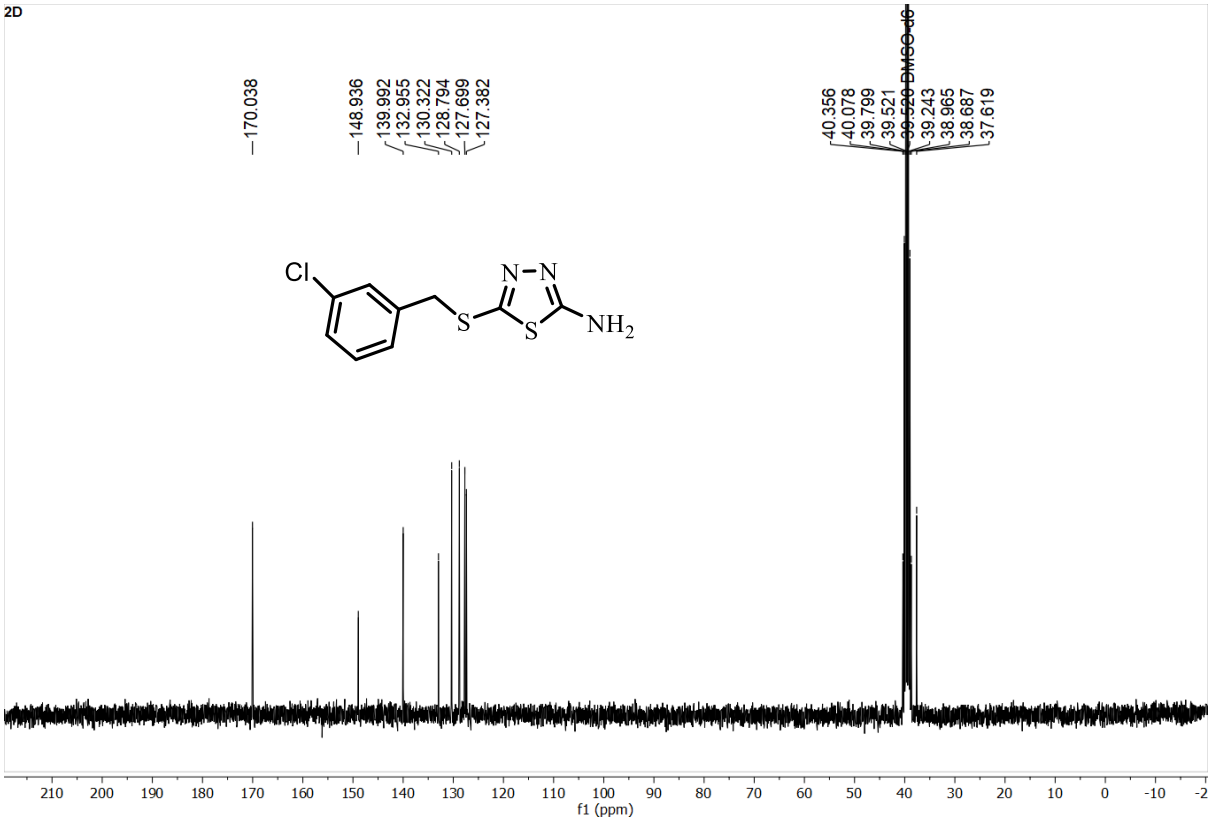

S.F2′: ^{13}C NMR of compound **2d**

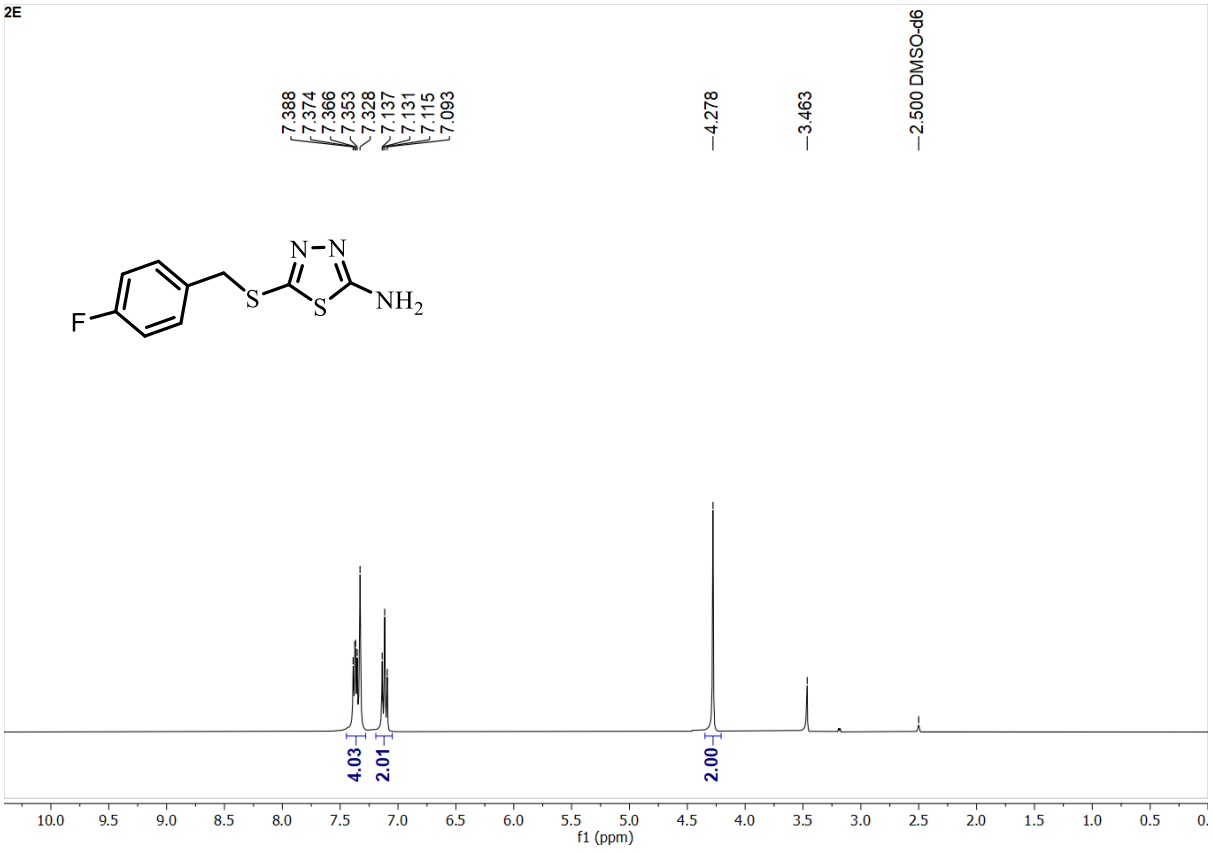

S.F3: ^{1}H NMR of compound **2e**

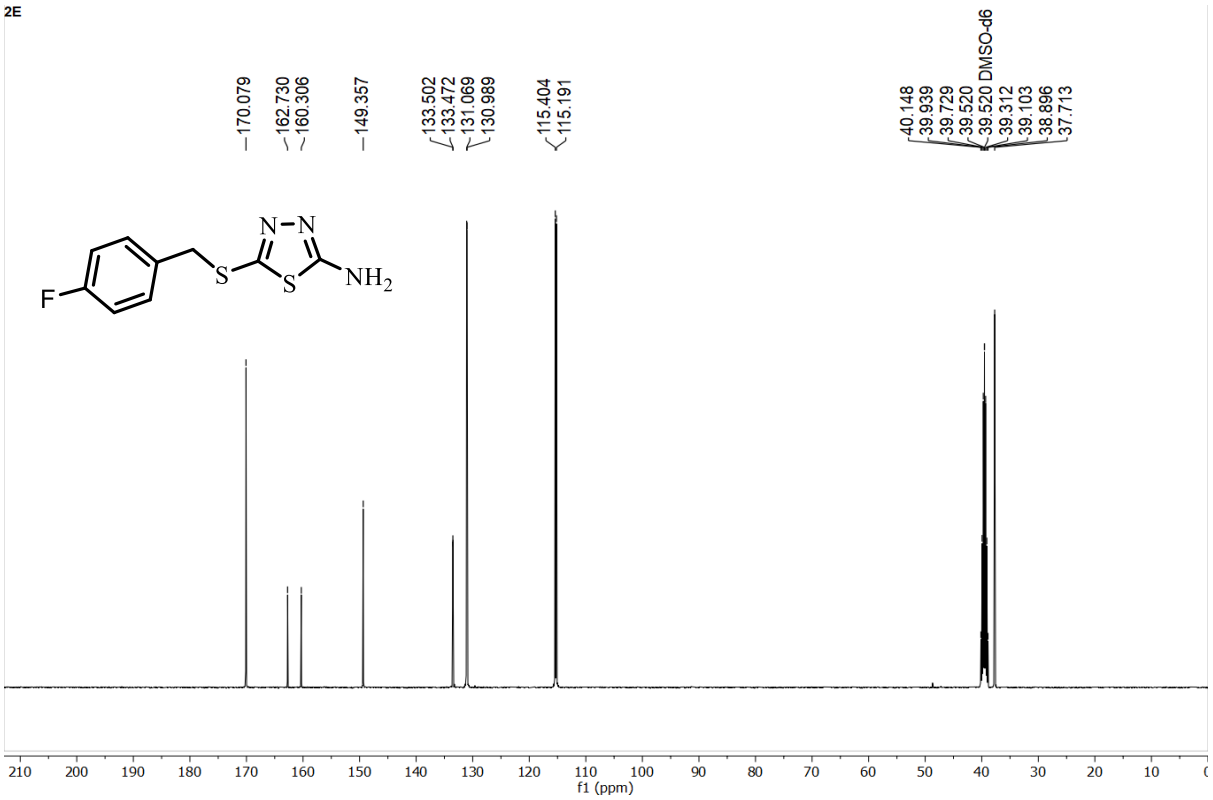

S.F3′: ^{13}C NMR of compound **2e**

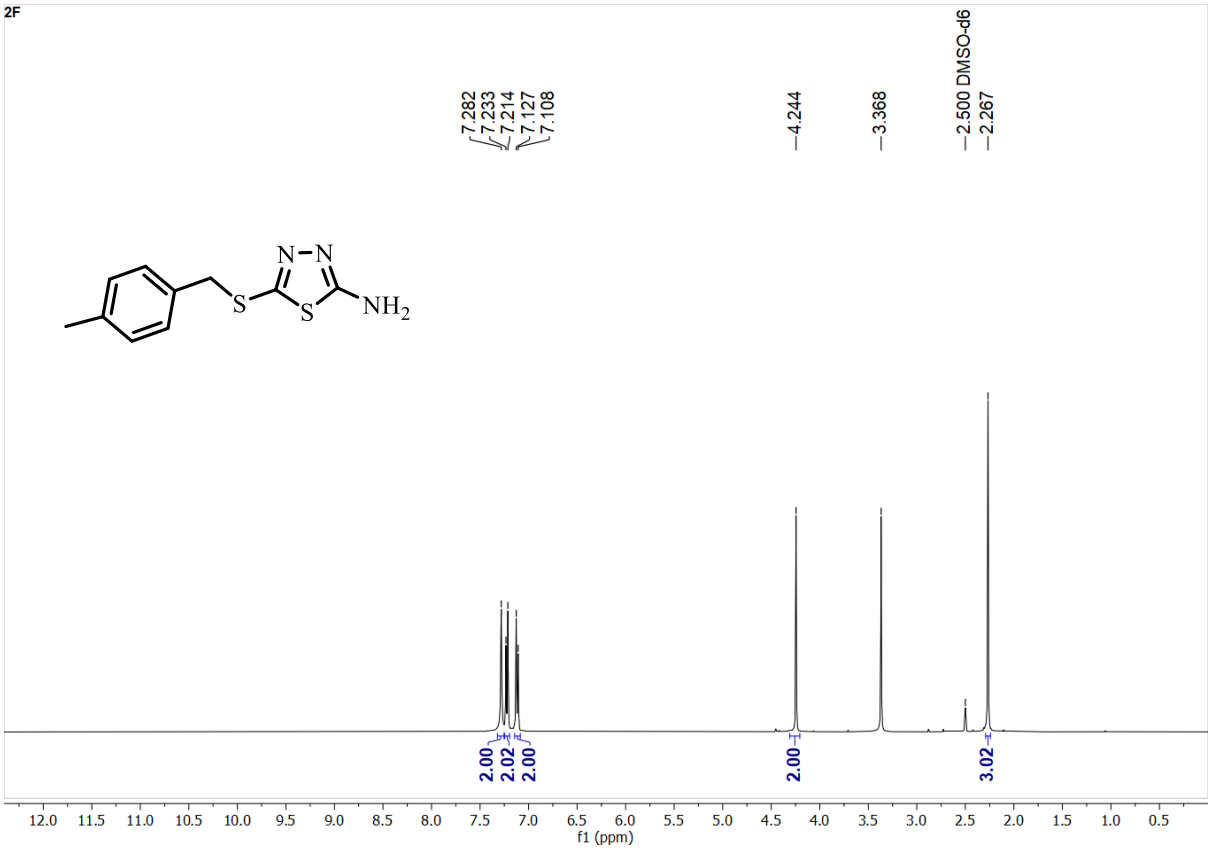

S.F4: ^{1}H NMR of compound **2f**

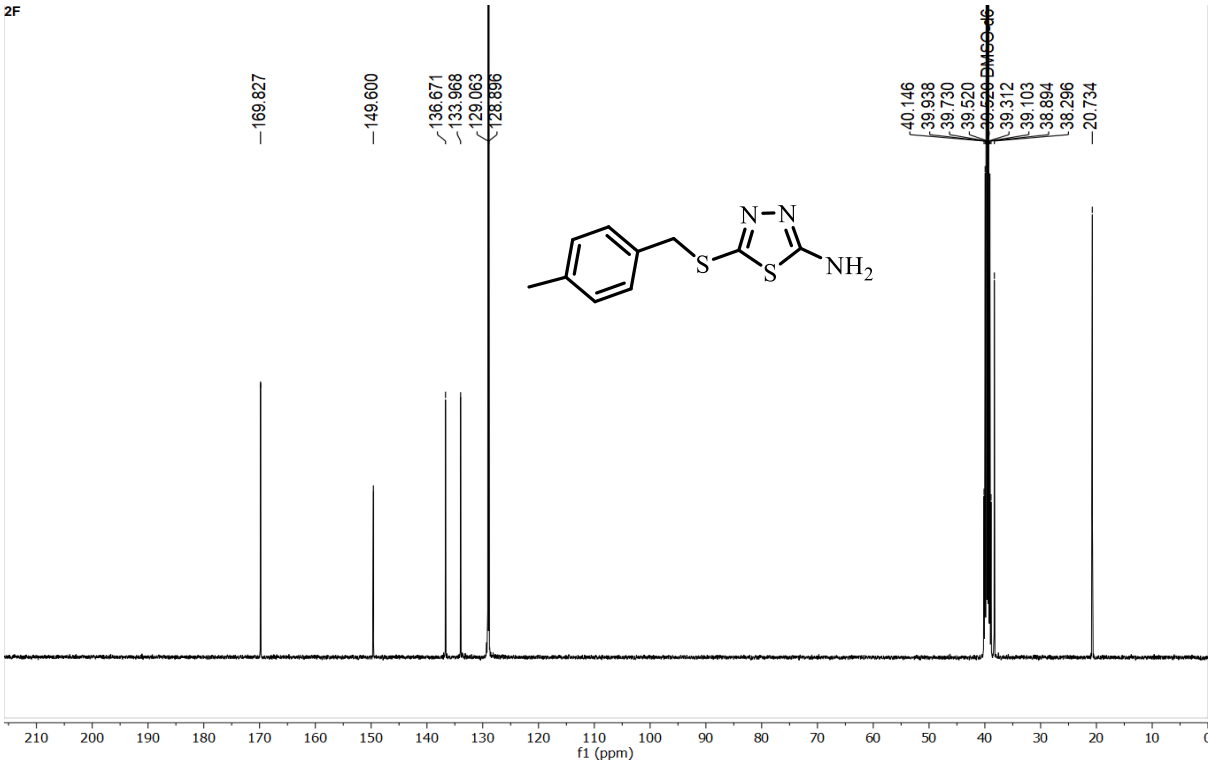

S.F4′: ^{13}C NMR of compound **2f**

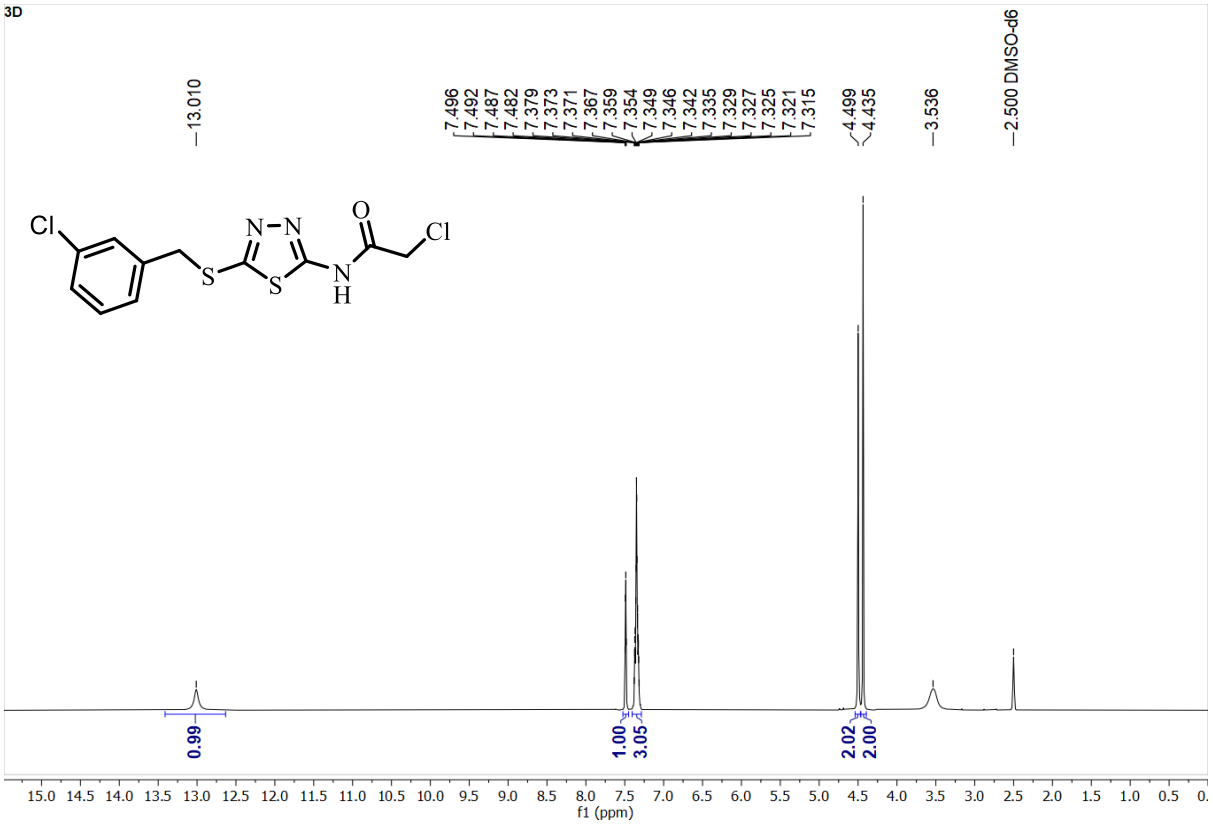

S.F5: ^{1}H NMR of compound **3d**

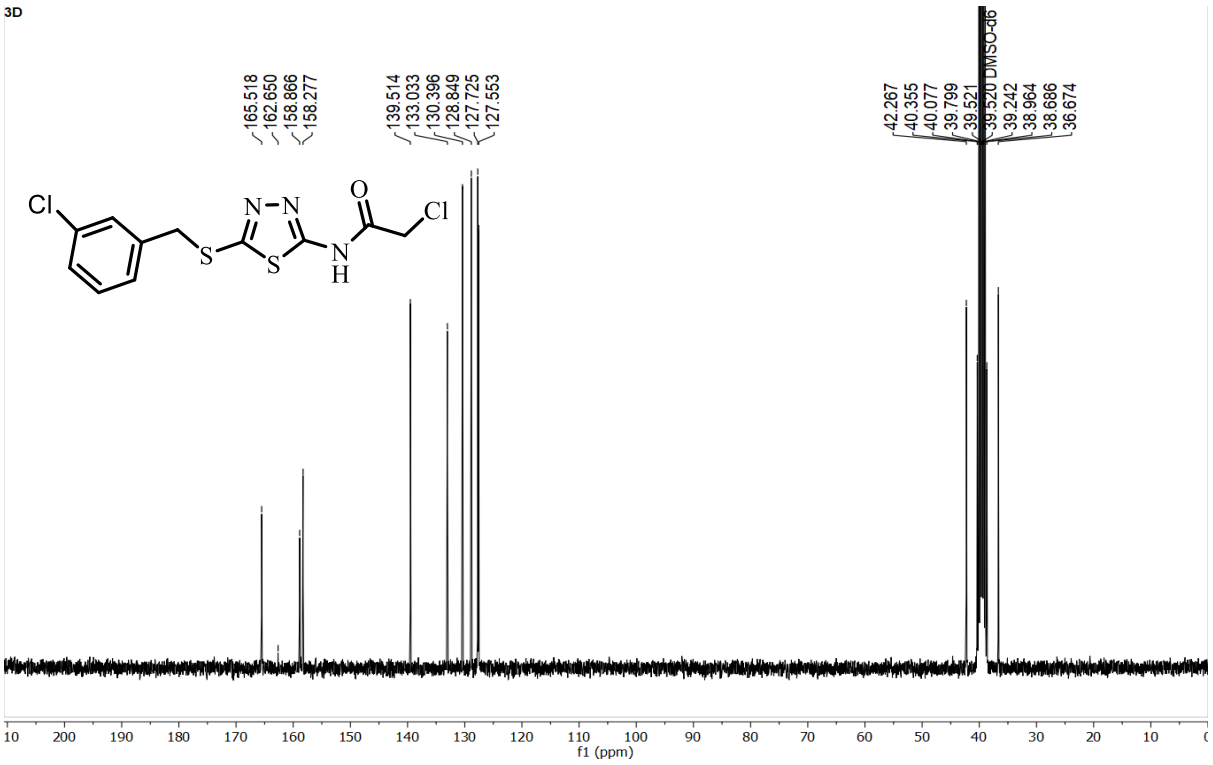

S.F5′: ^{13}C NMR of compound **3d**

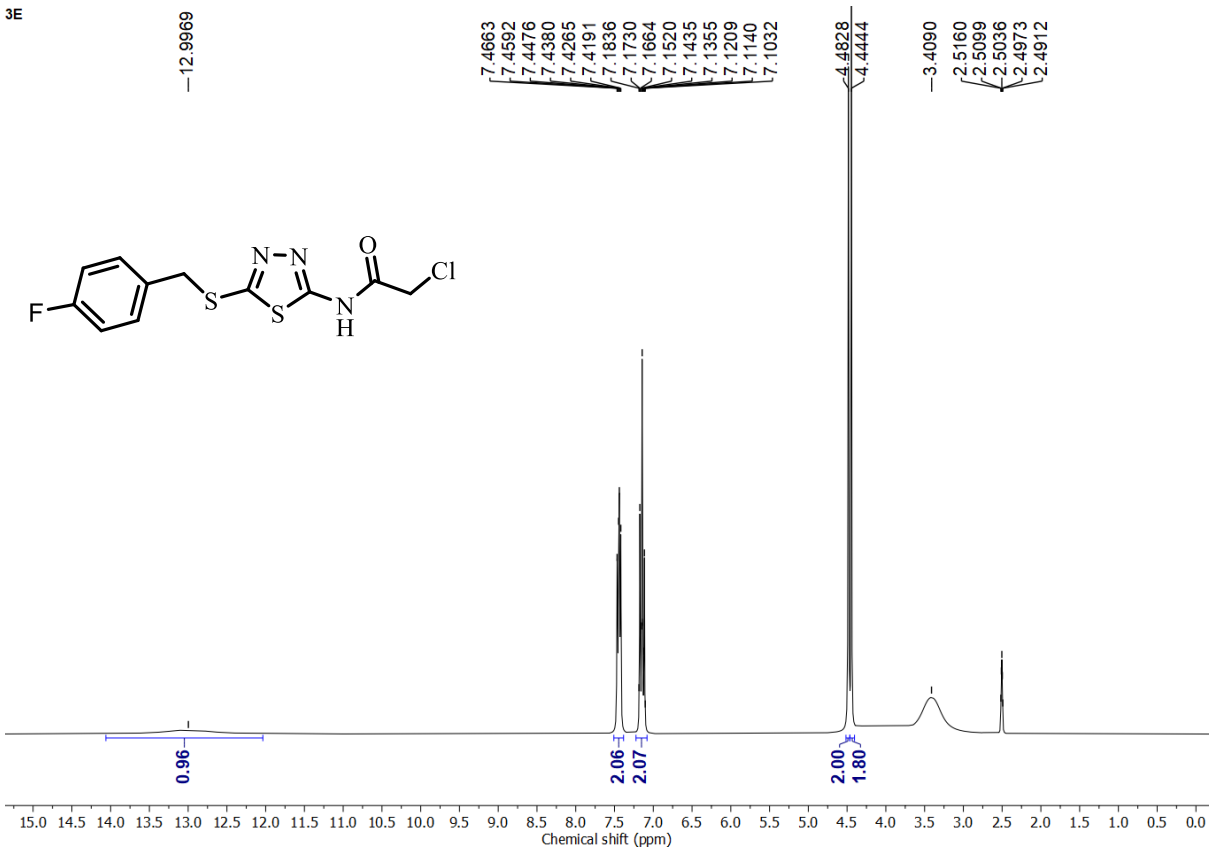

S.F6: ^{1}H NMR of compound **3e**

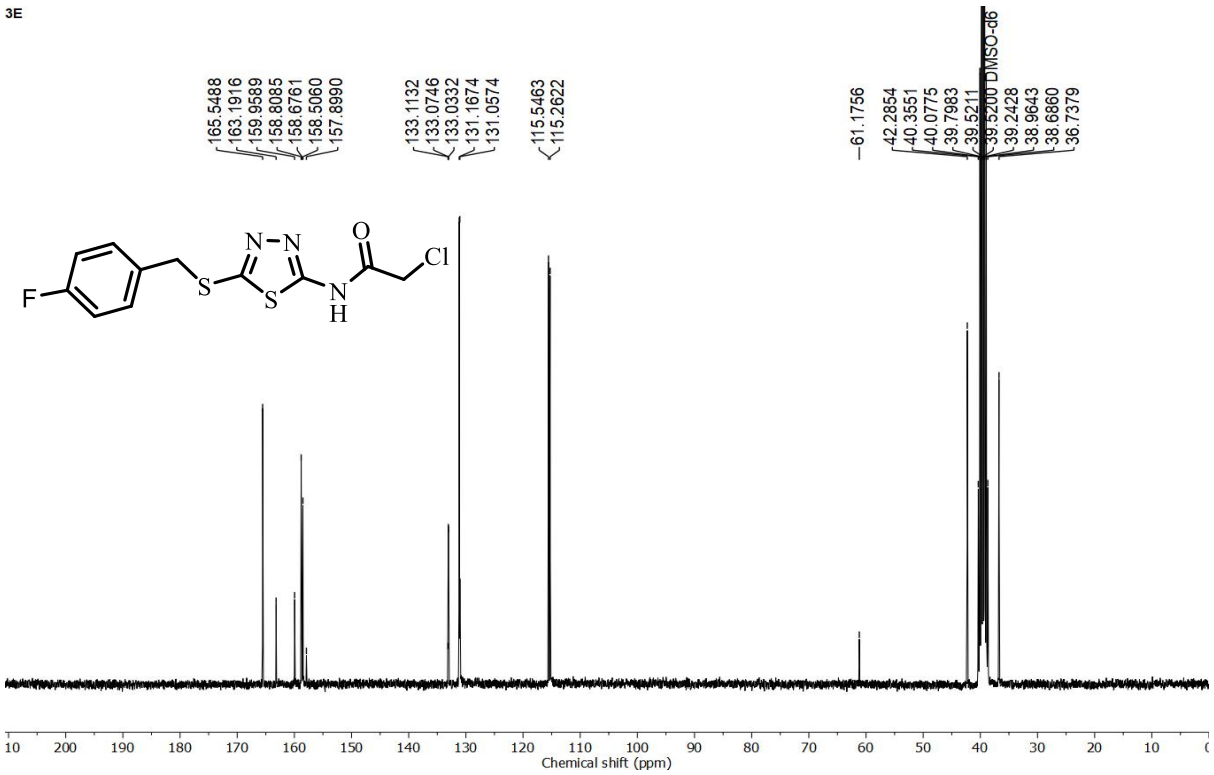

S.F6′: ^{13}C NMR of compound **3e**

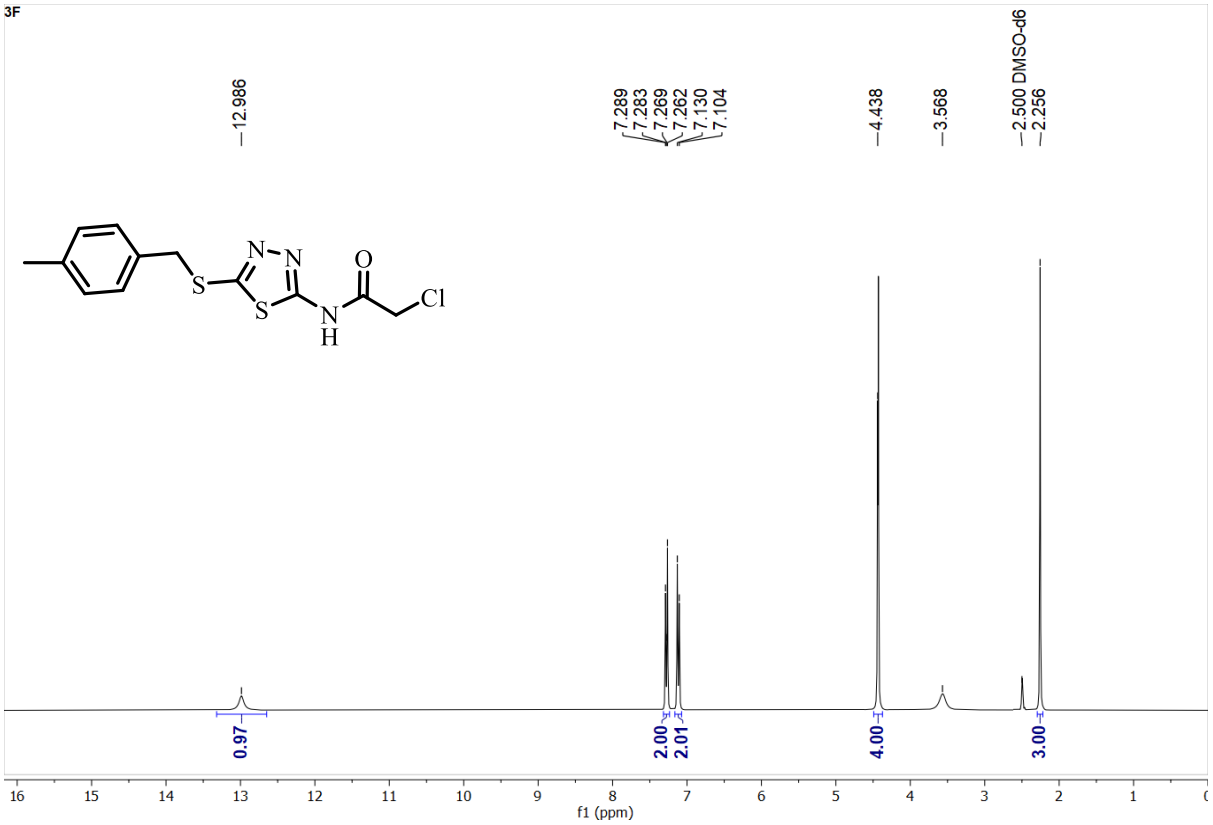

S.F7: ^{1}H NMR of compound **3f**

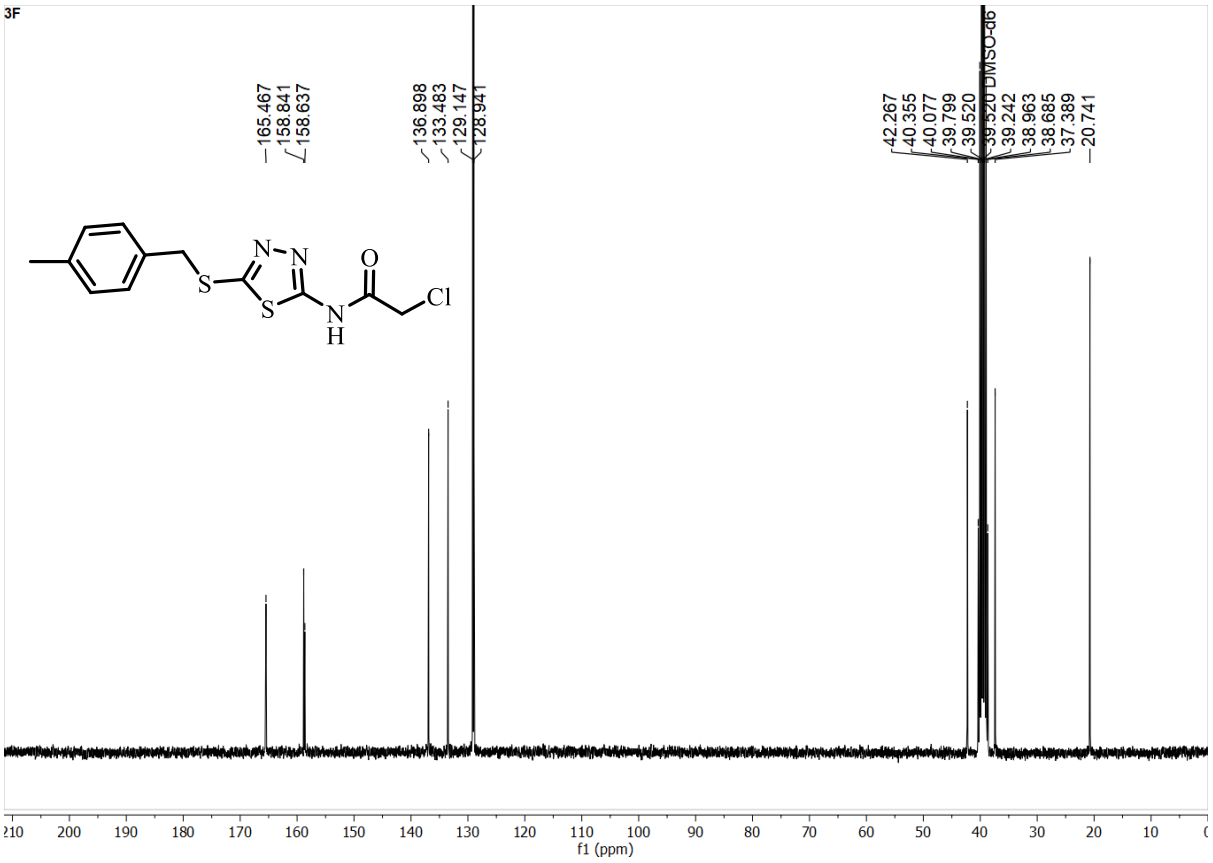

S.F7′: ^{13}C NMR of compound **3f**

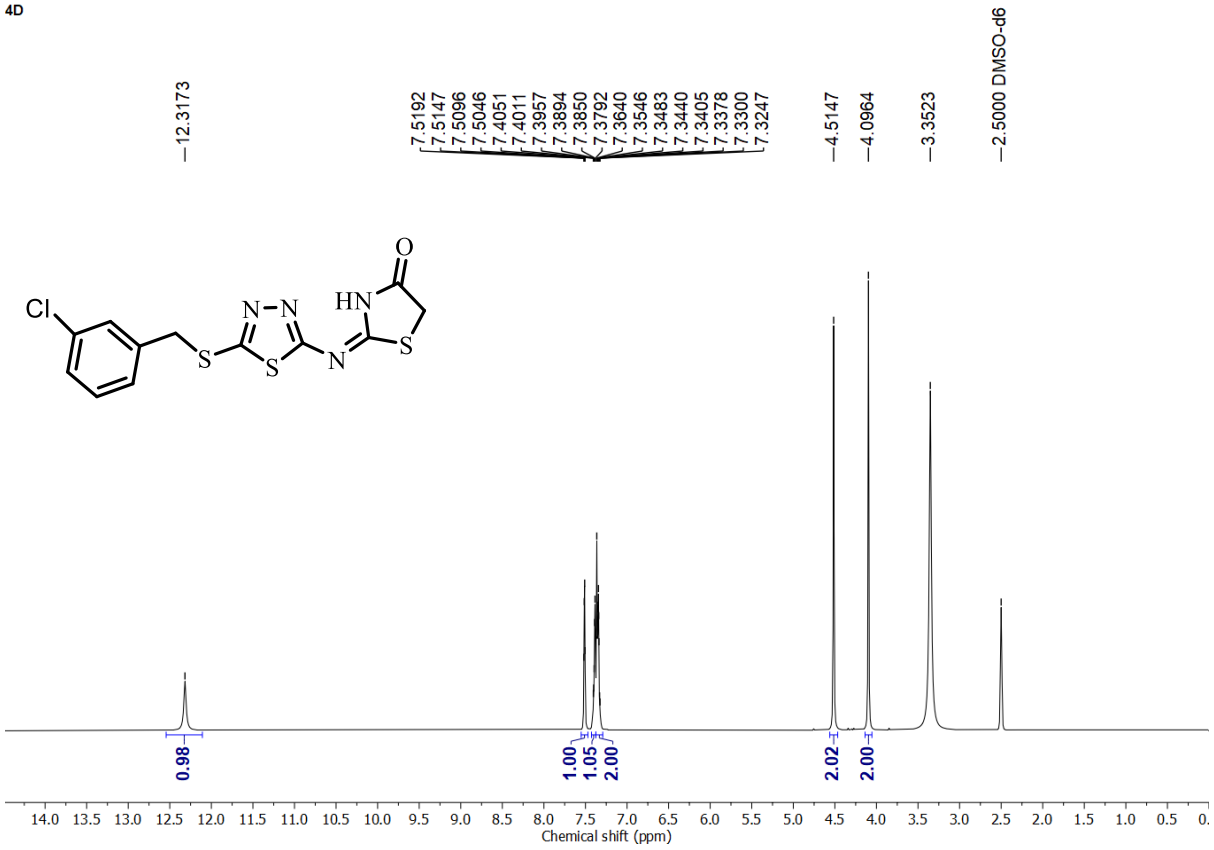

S.F8: ^{1}H NMR of compound **4d**

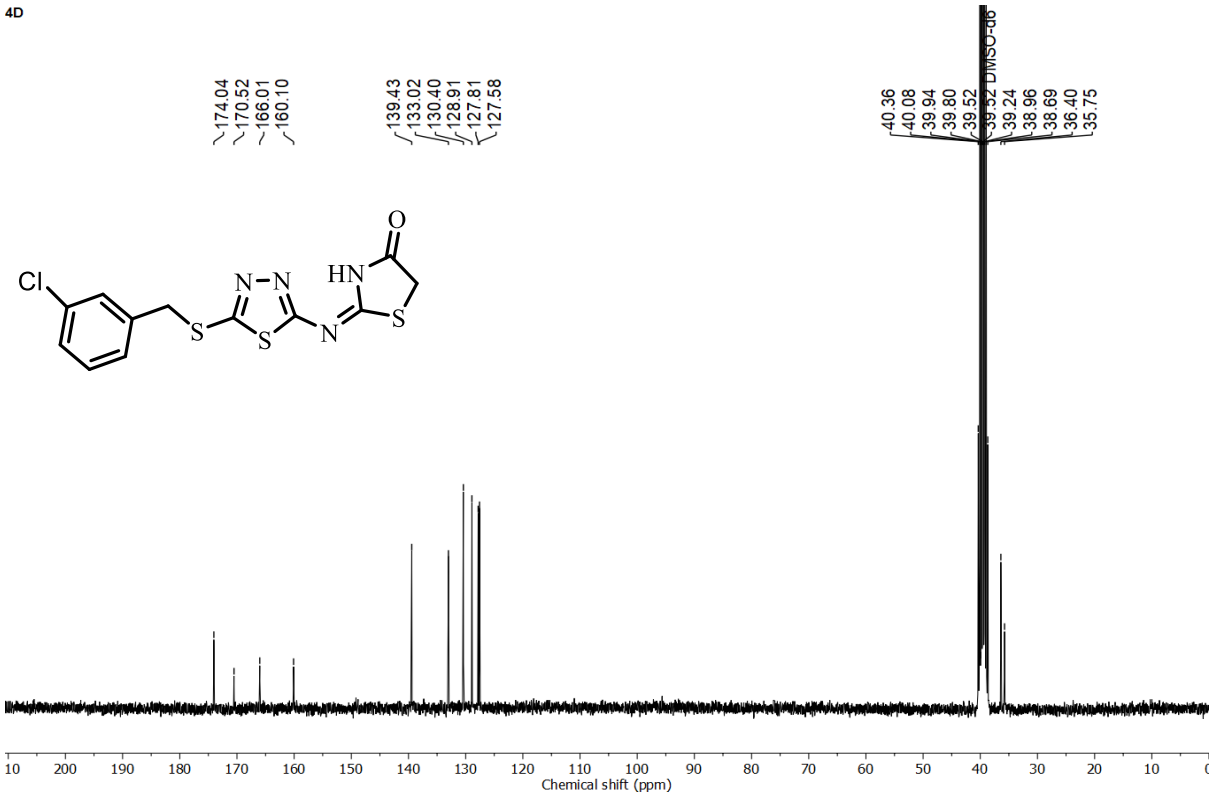

S.F8′: ^{13}C NMR of compound **4d**

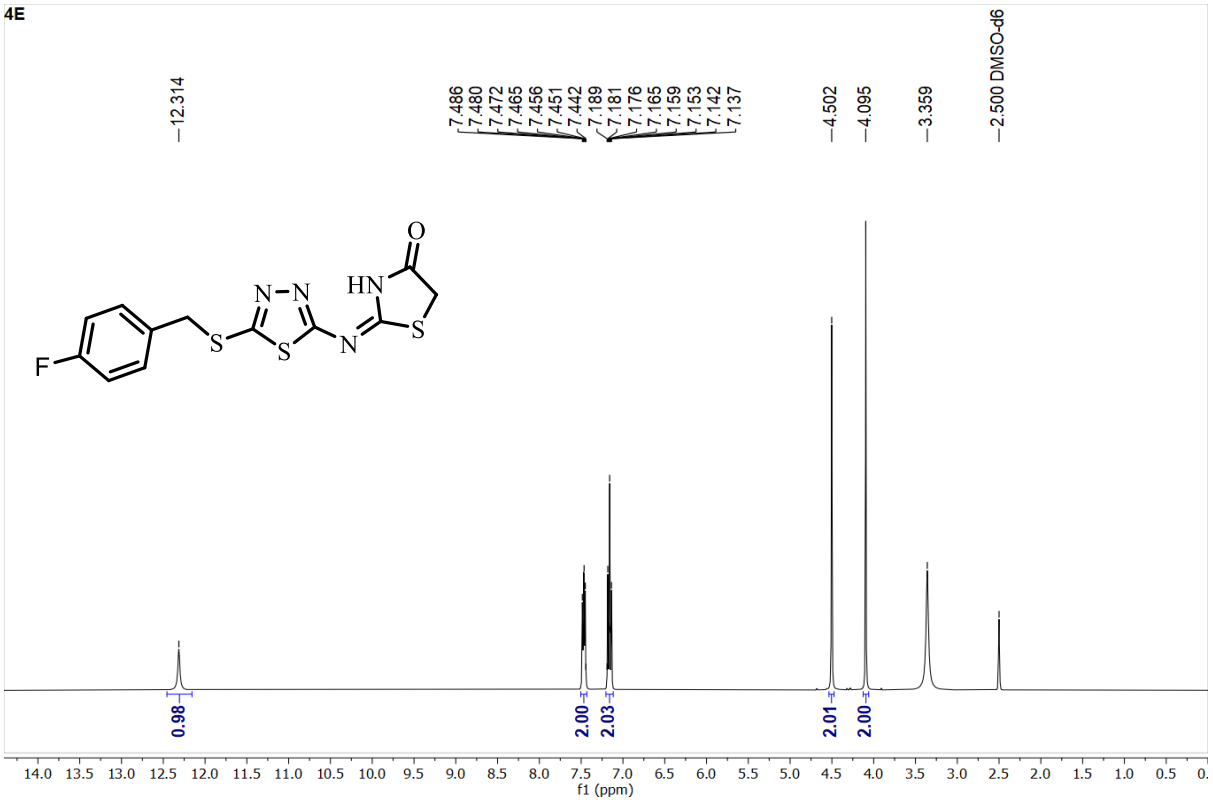

S.F9: ^{1}H NMR of compound **4e**

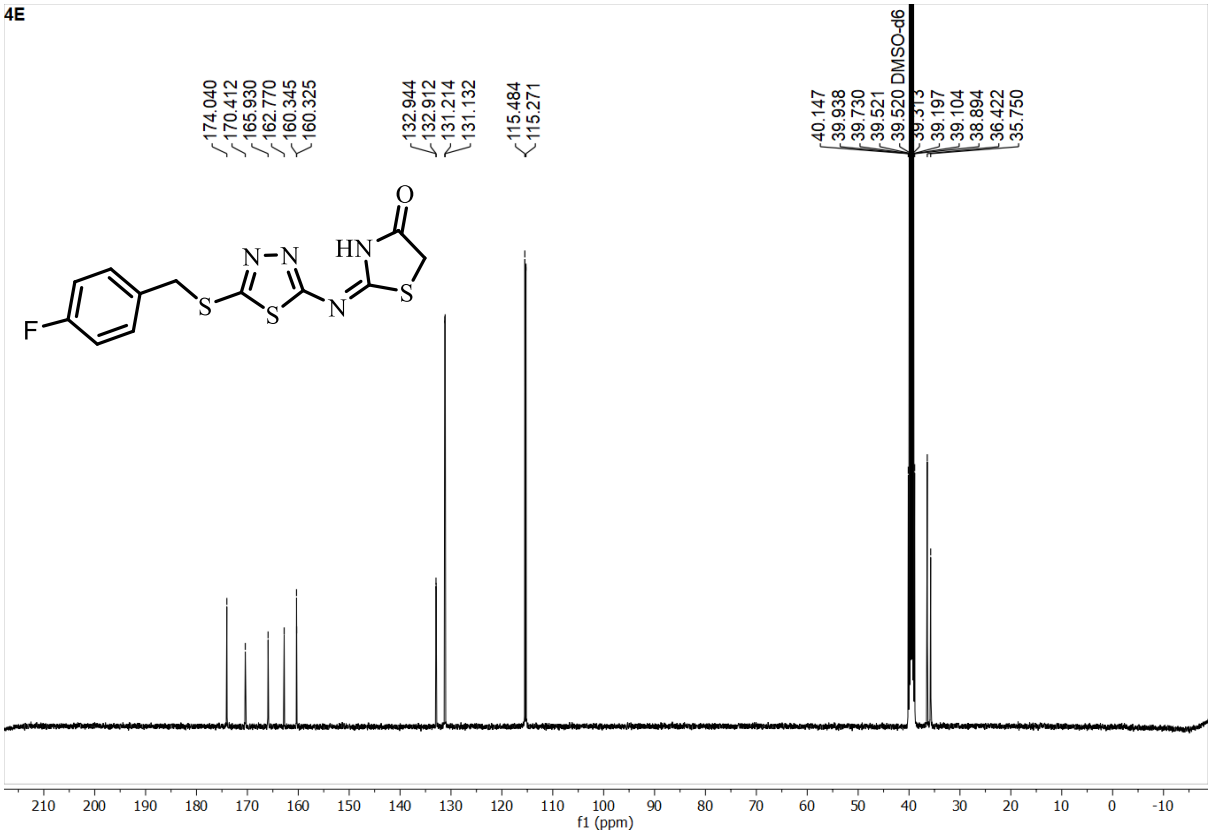

S.F9′: ^{13}C NMR of compound **4e**

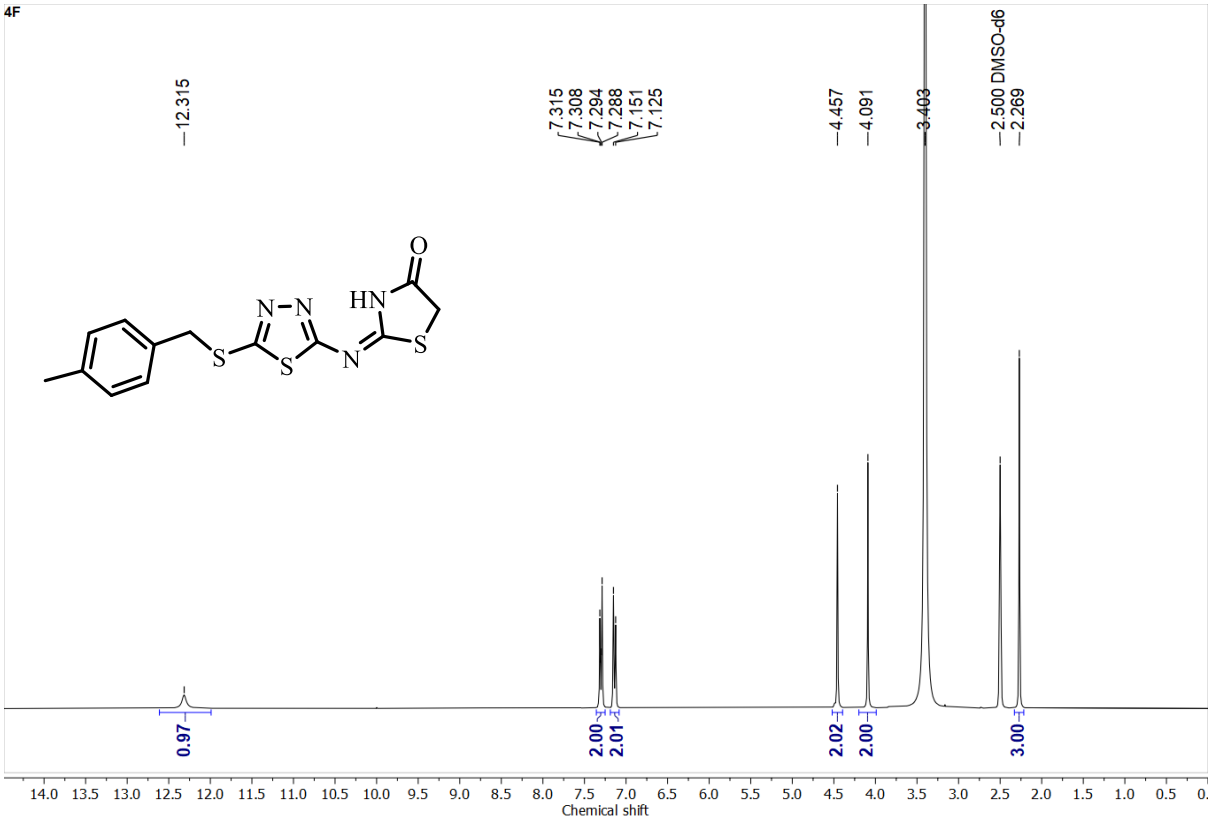

S.F10: ^{1}H NMR of compound **4f**

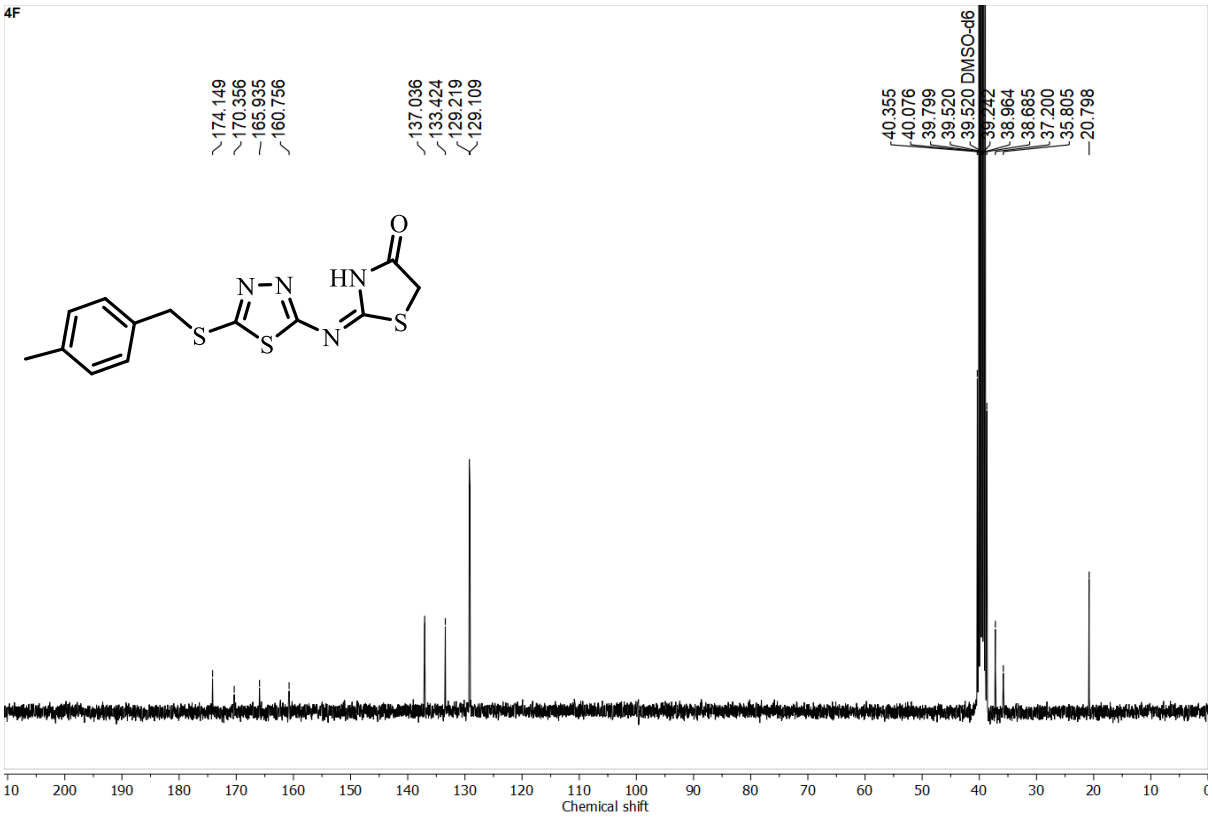

S.F10′: ^{13}C NMR of compound **4f**

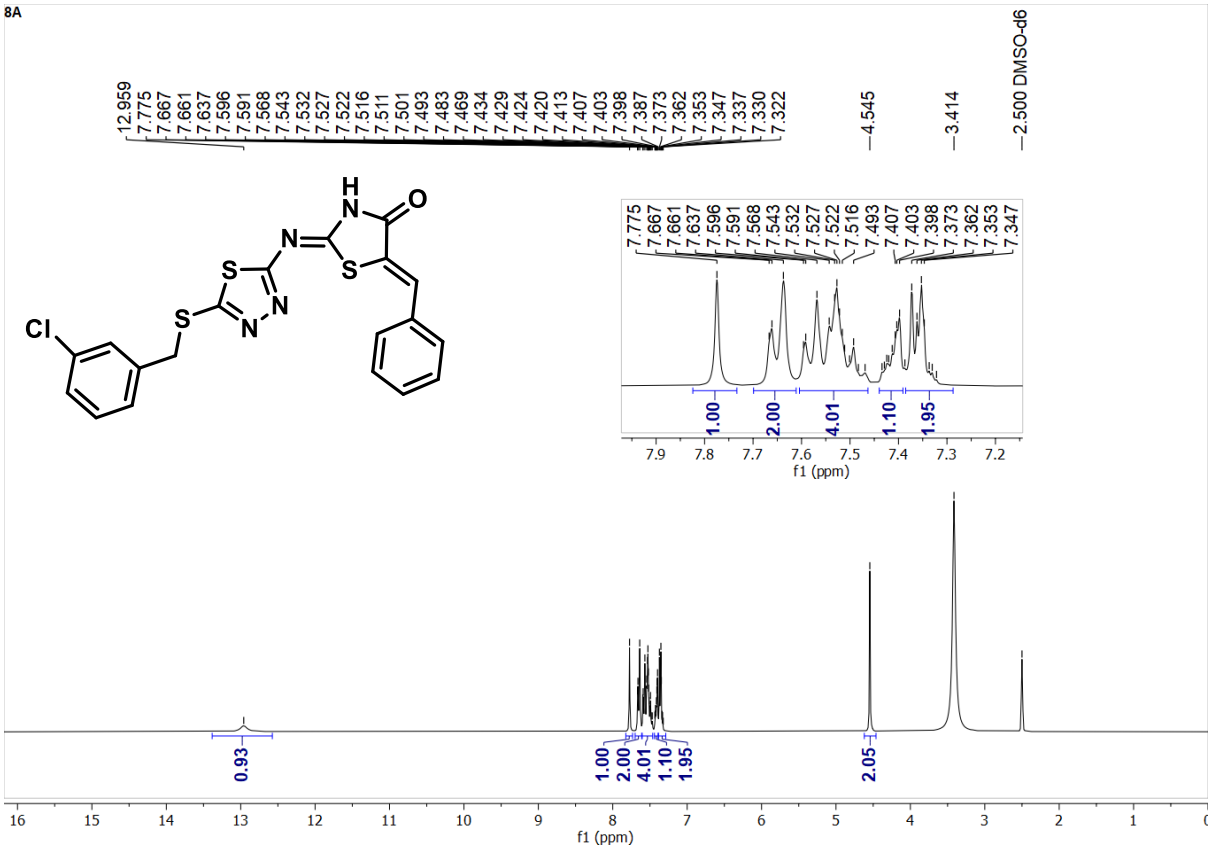

S.F11: ^{1}H NMR of compound **8a**

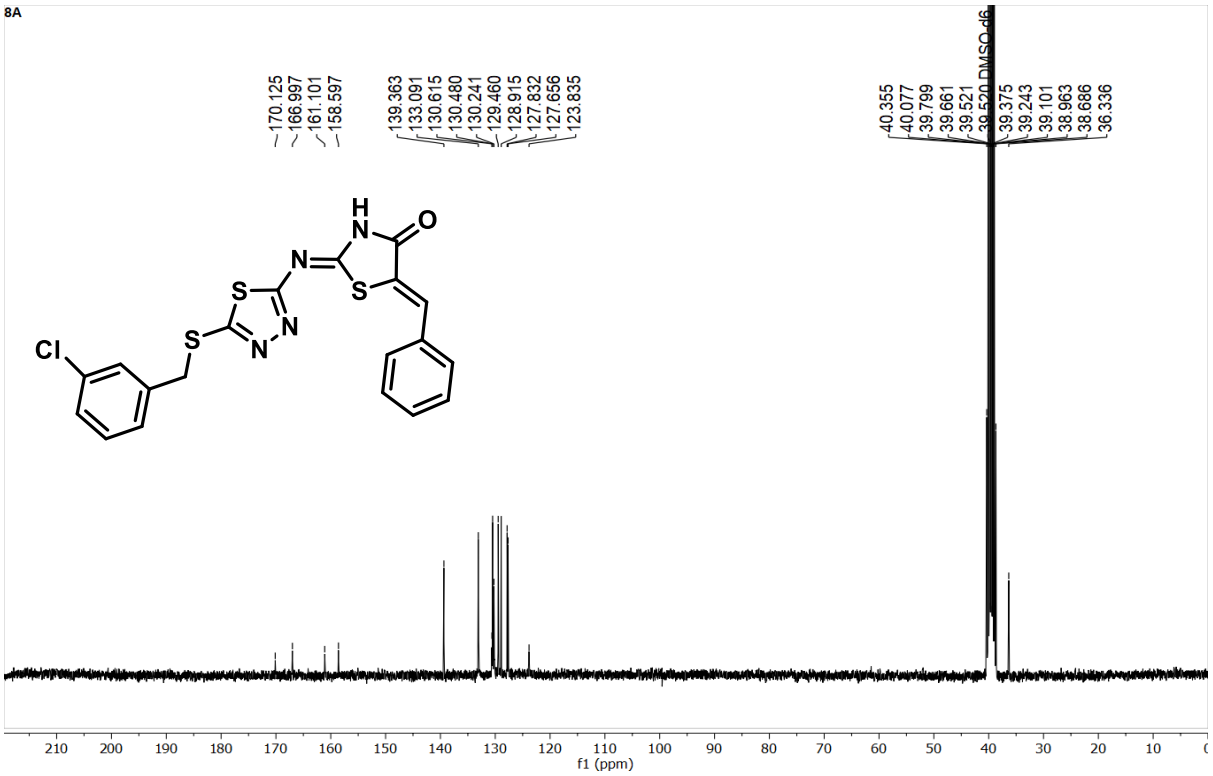

S.F11′: ^{13}C NMR of compound **8a**

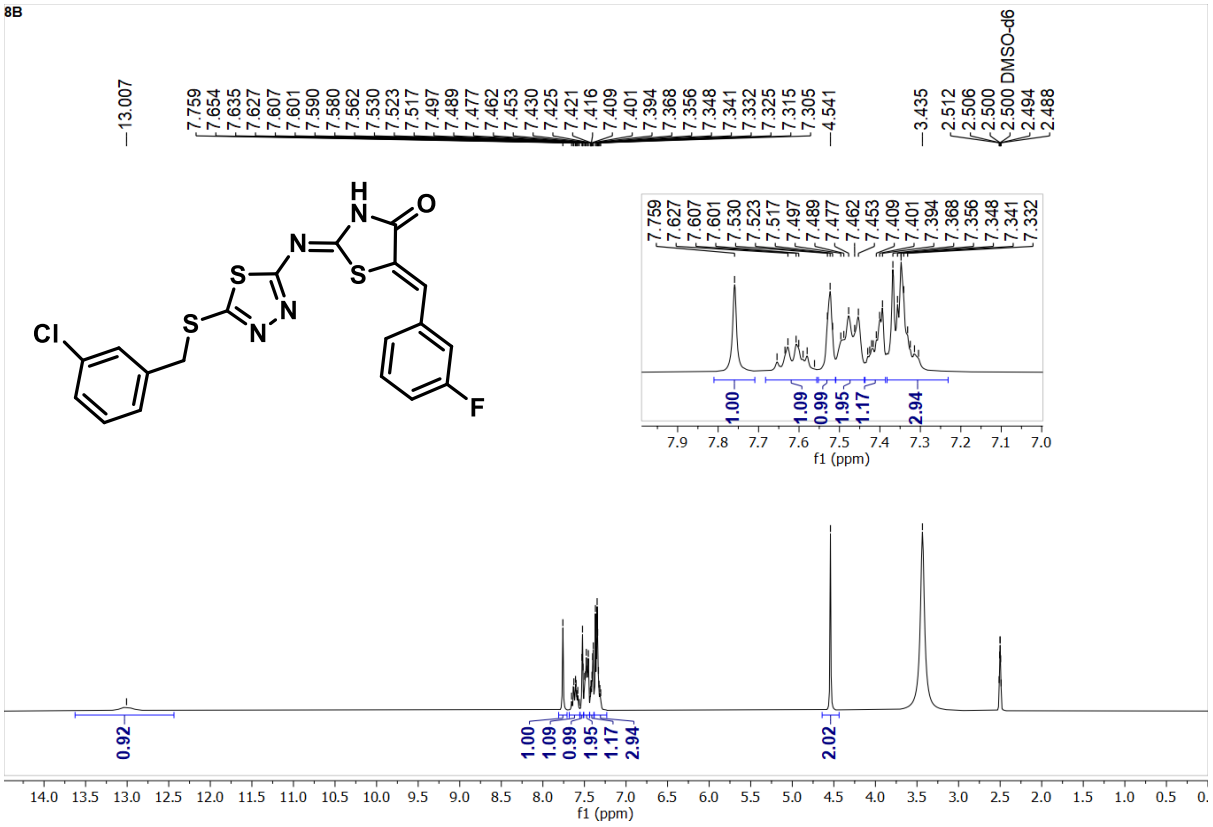

S.F12: ^{1}H NMR of compound **8b**

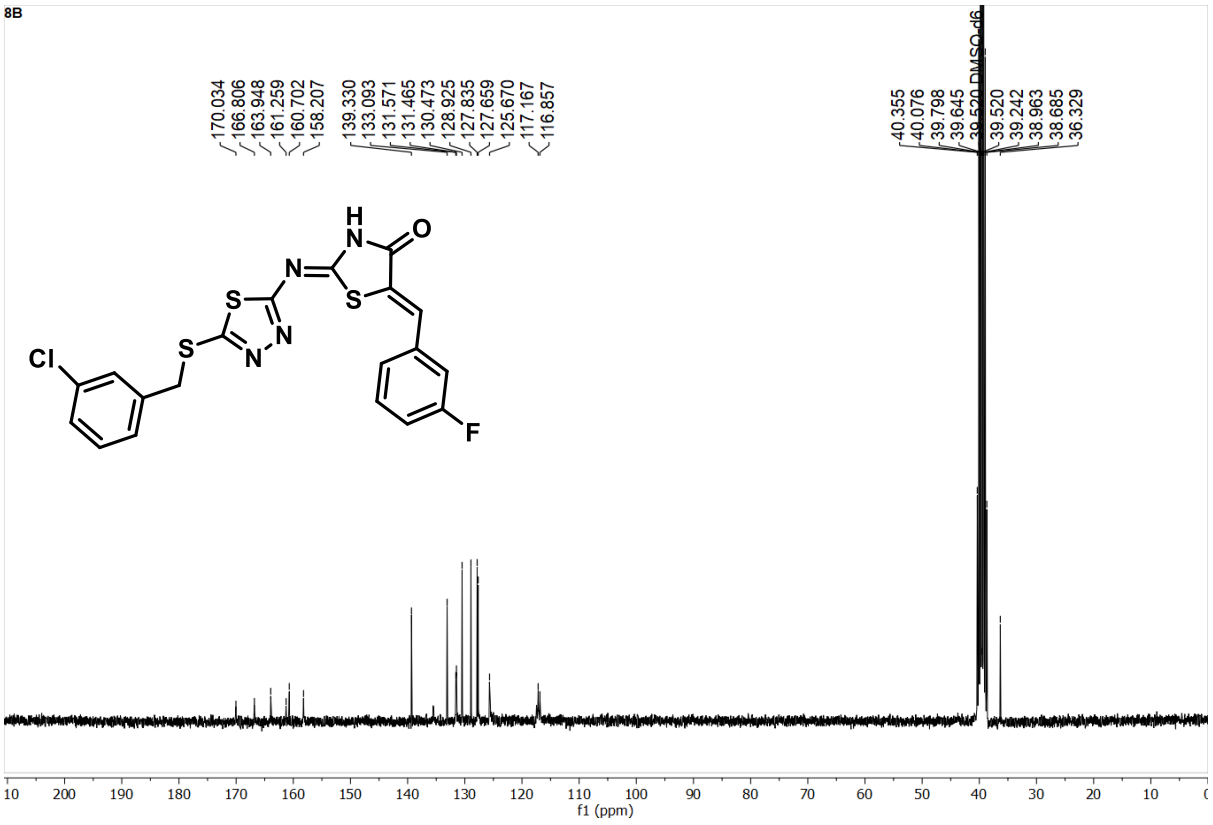

S.F12′: ^{13}C NMR of compound **8b**

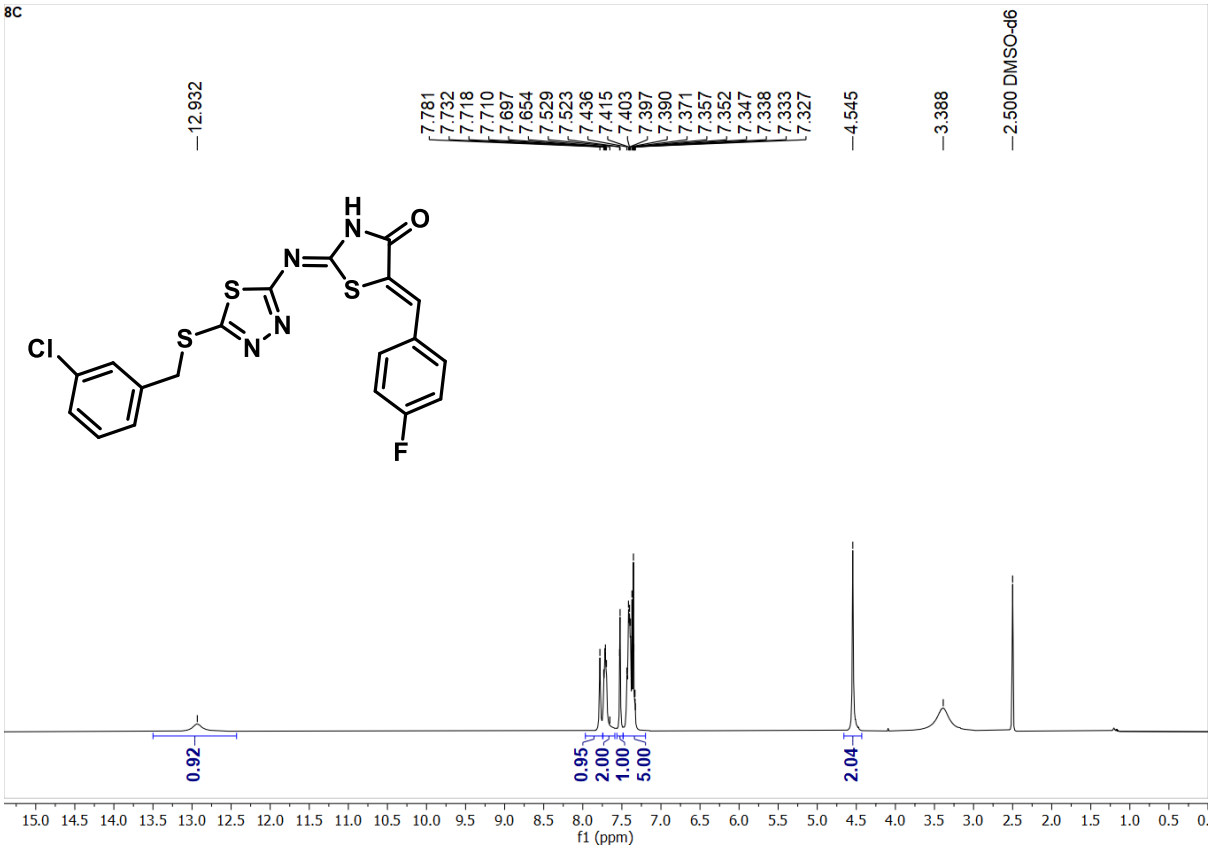

S.F13: ^{1}H NMR of compound **8c**

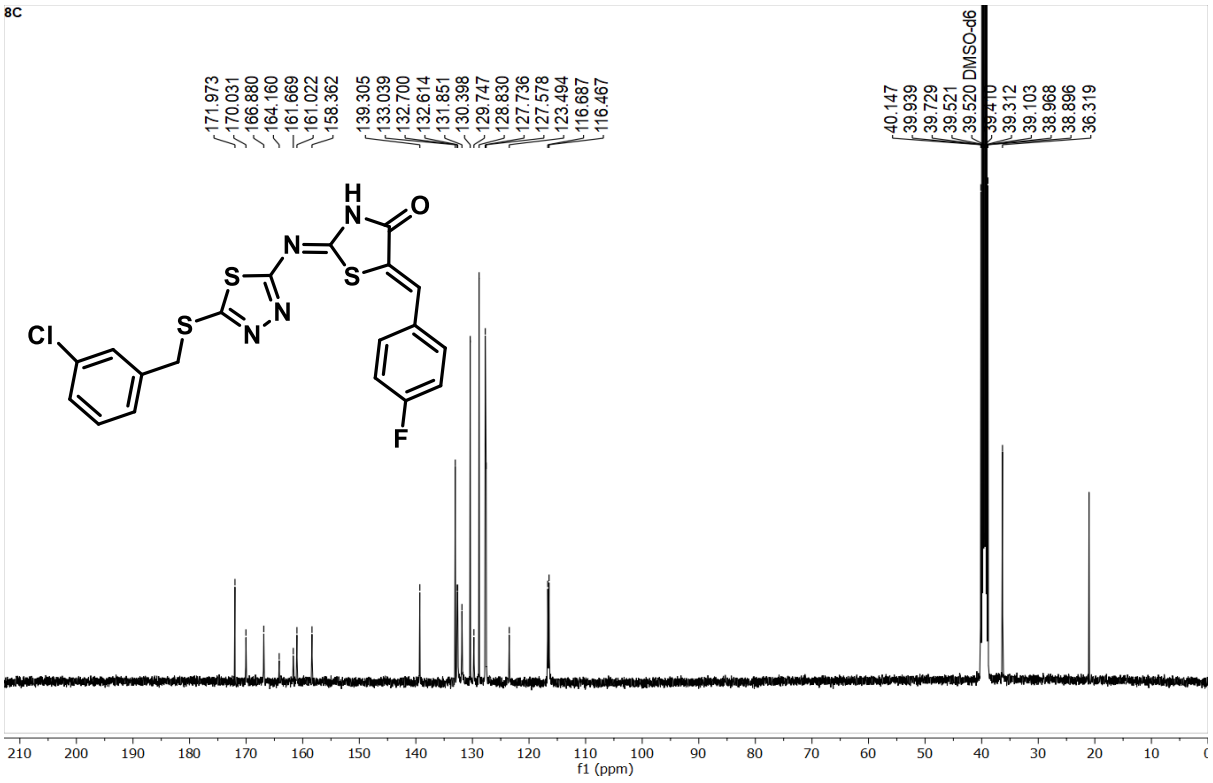

S.F13′: ^{13}C NMR of compound **8c**

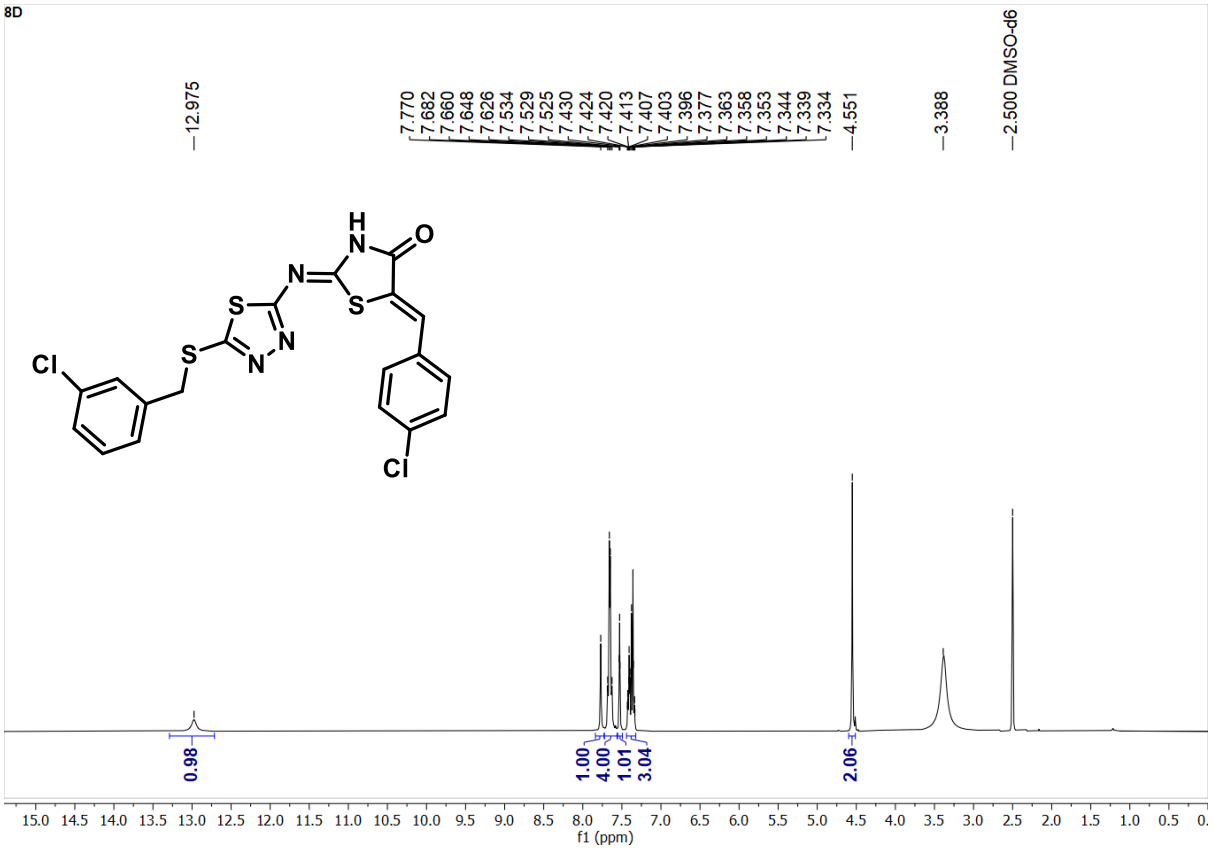

S.F14: ^{1}H NMR of compound **8d**

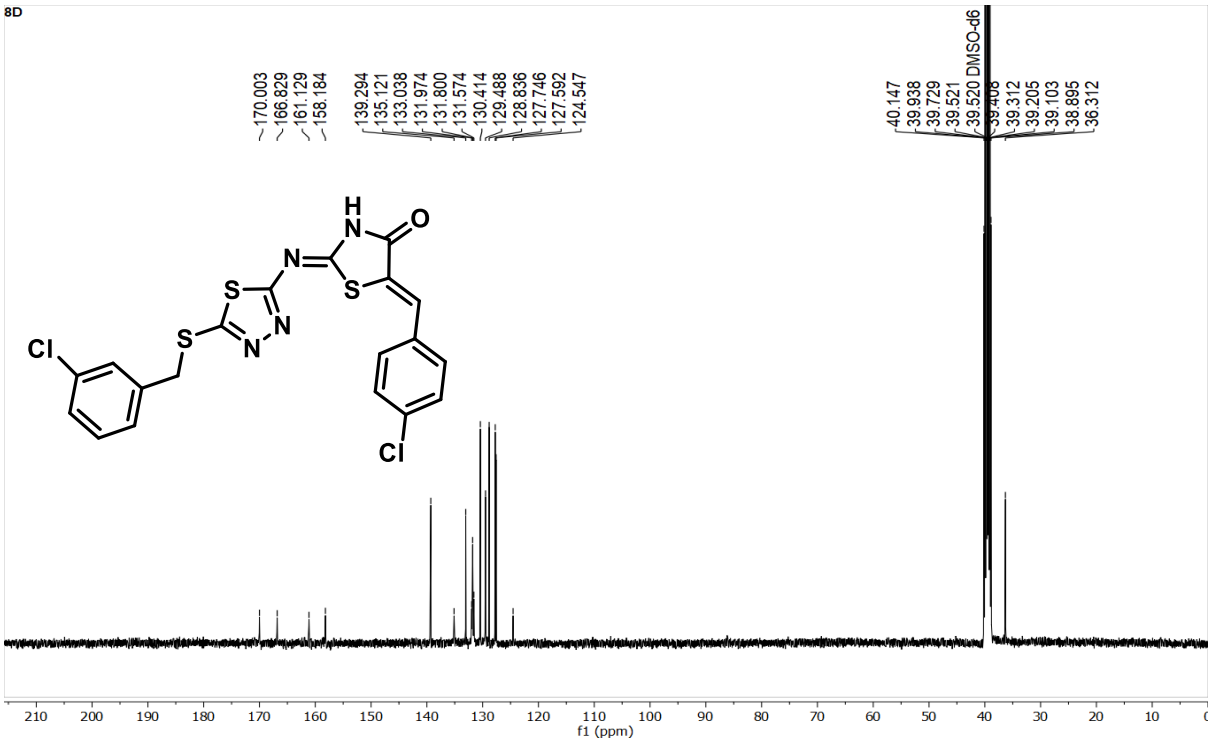

S.F14′: ^{13}C NMR of compound **8d**

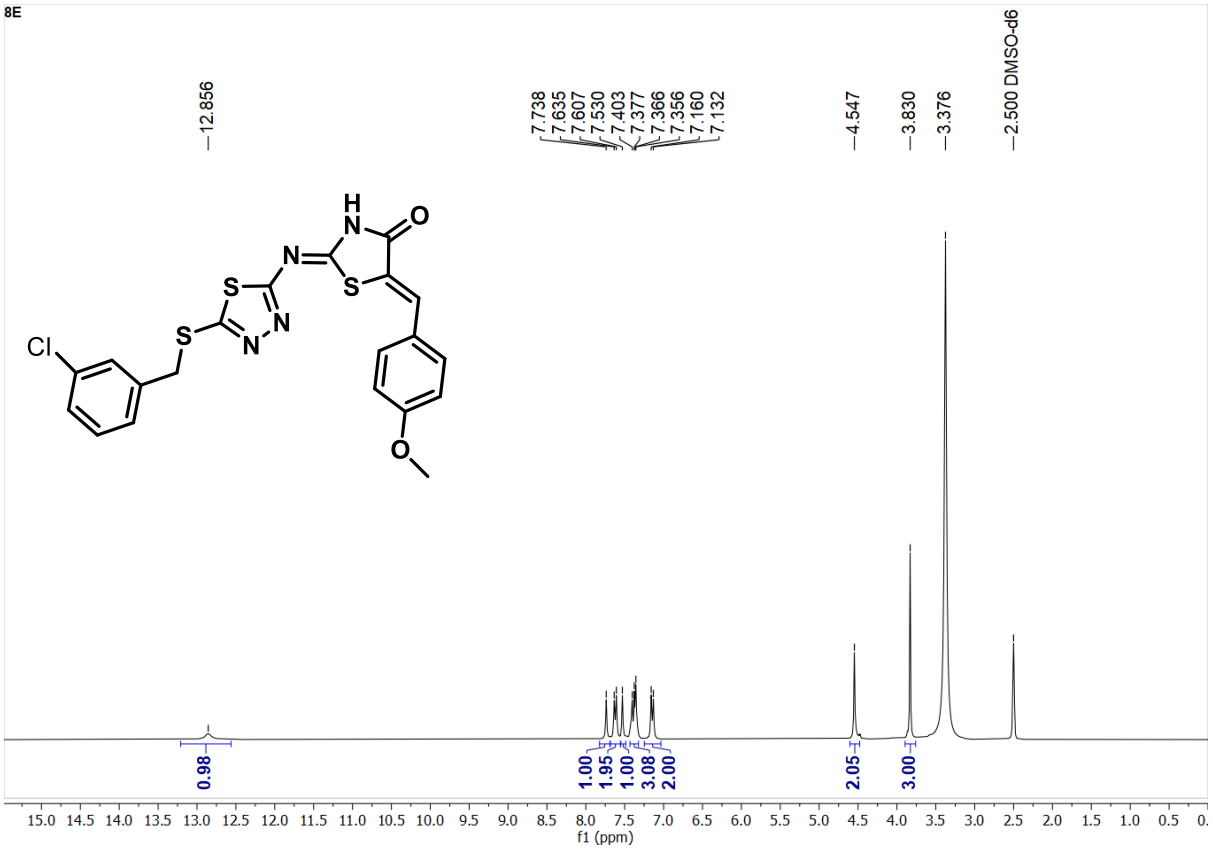

S.F15: ^{1}H NMR of compound **8e**

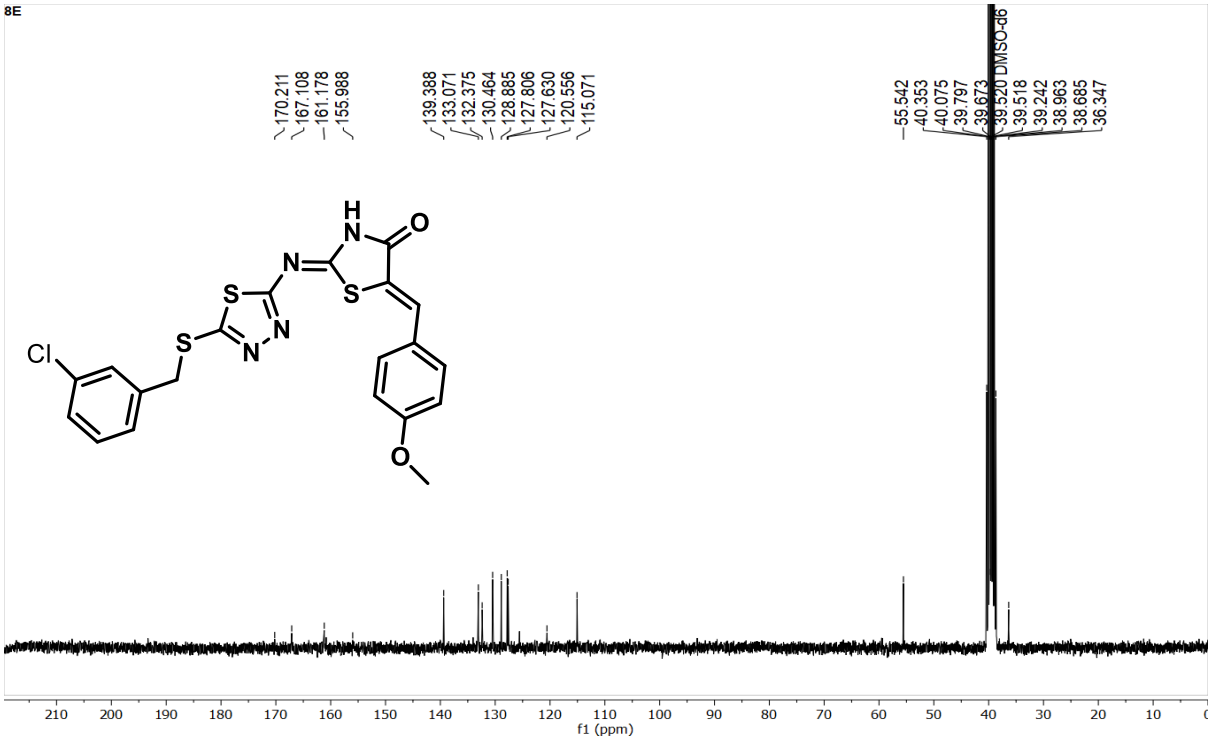

S.F15′: ^{13}C NMR of compound **8e**

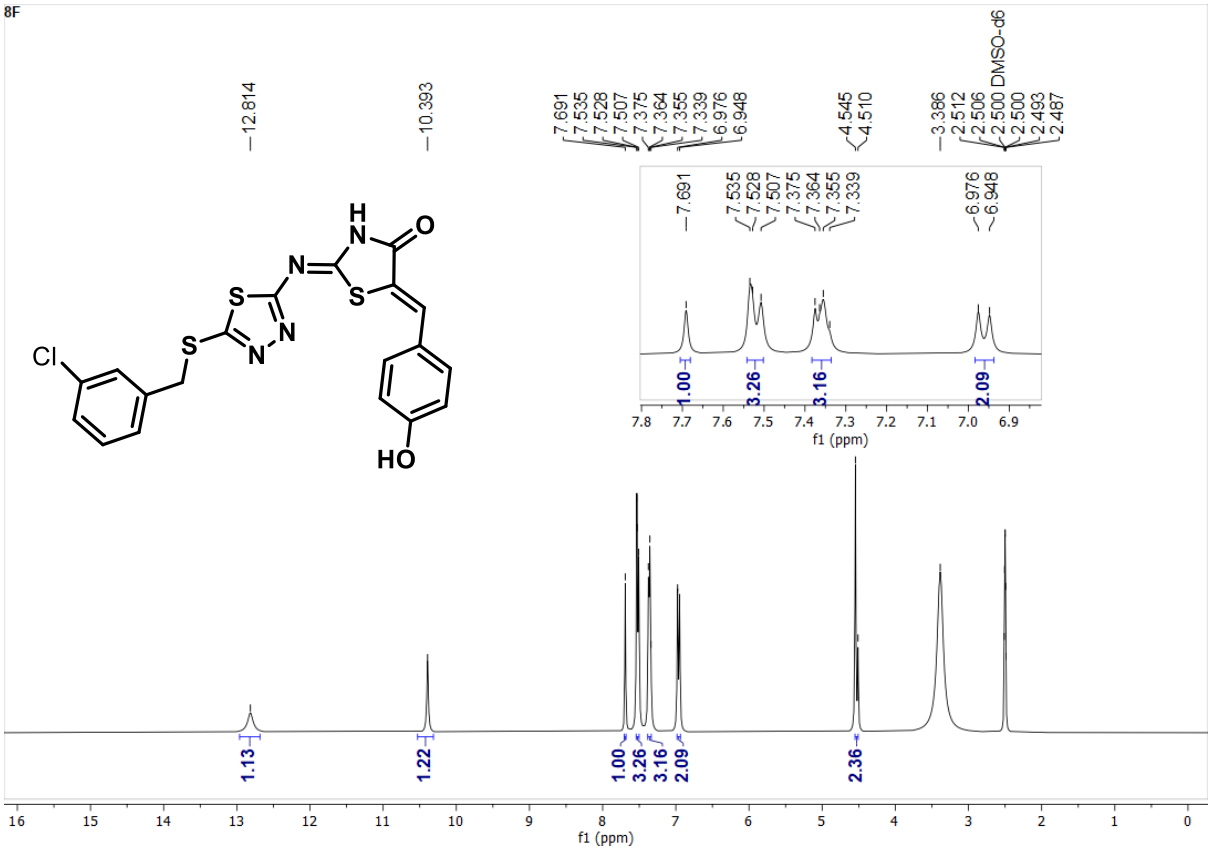

S.F16: ^{1}H NMR of compound **8f**

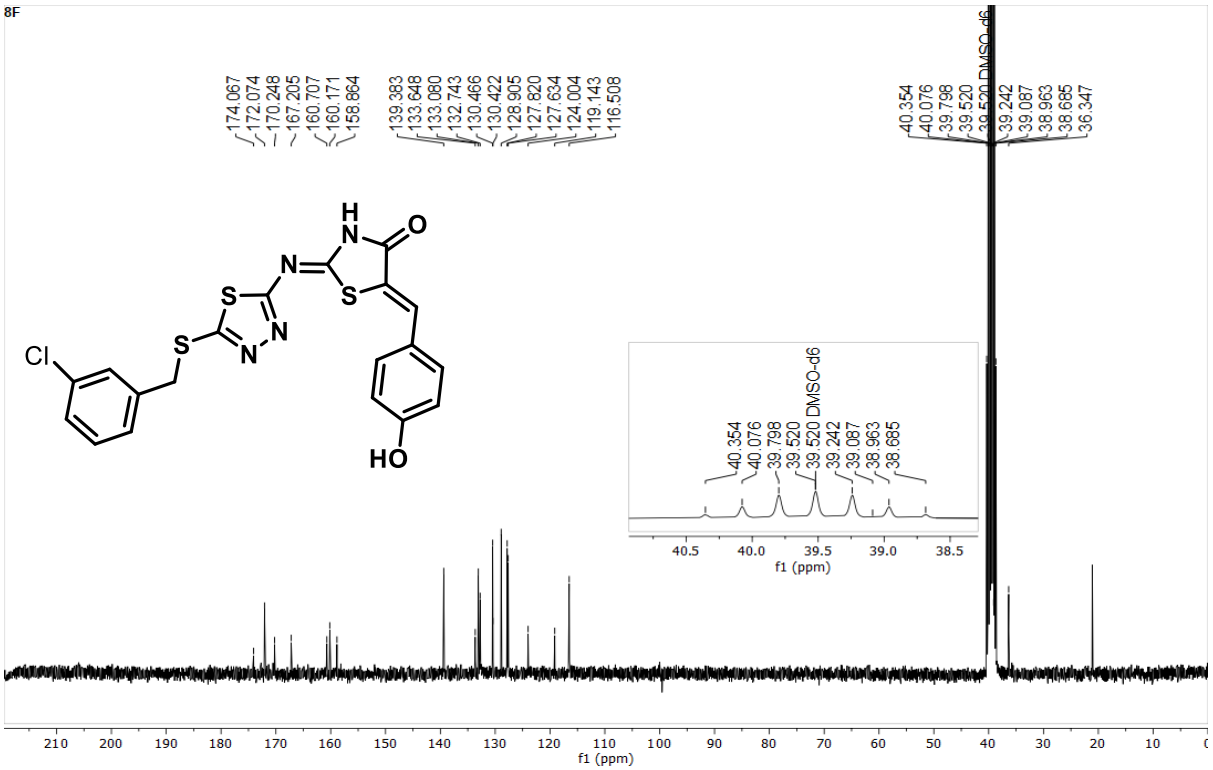

S.F16′: ^{13}C NMR of compound **8f**

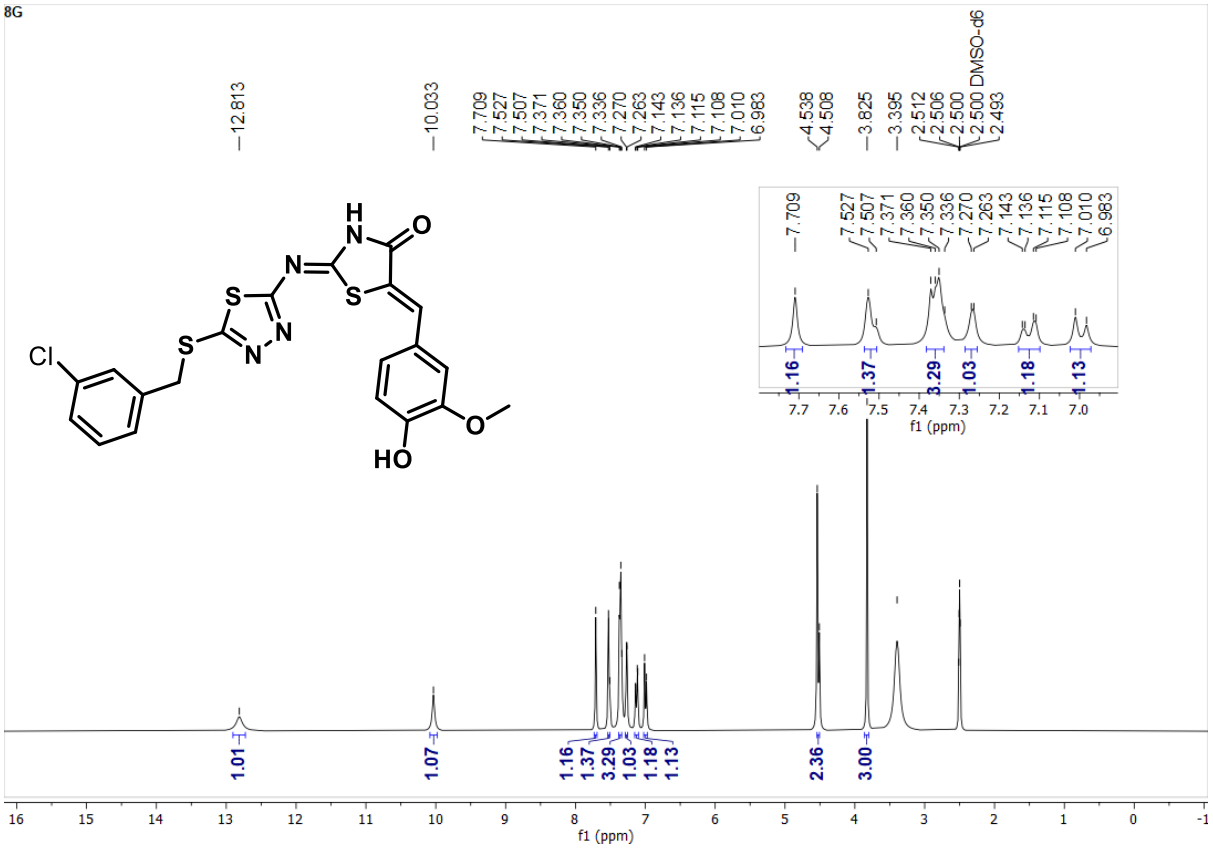

S.F17: ^{1}H NMR of compound **8g**

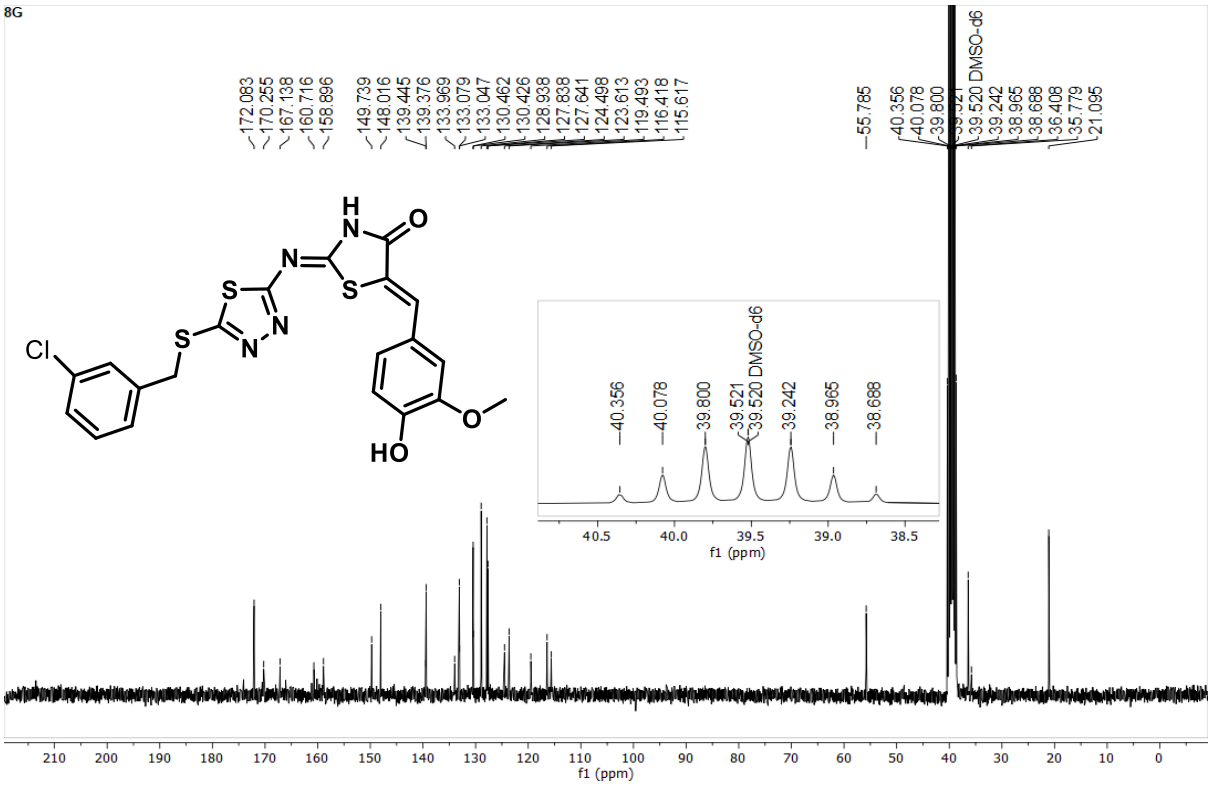

S.F17′: ^{13}C NMR of compound **8g**

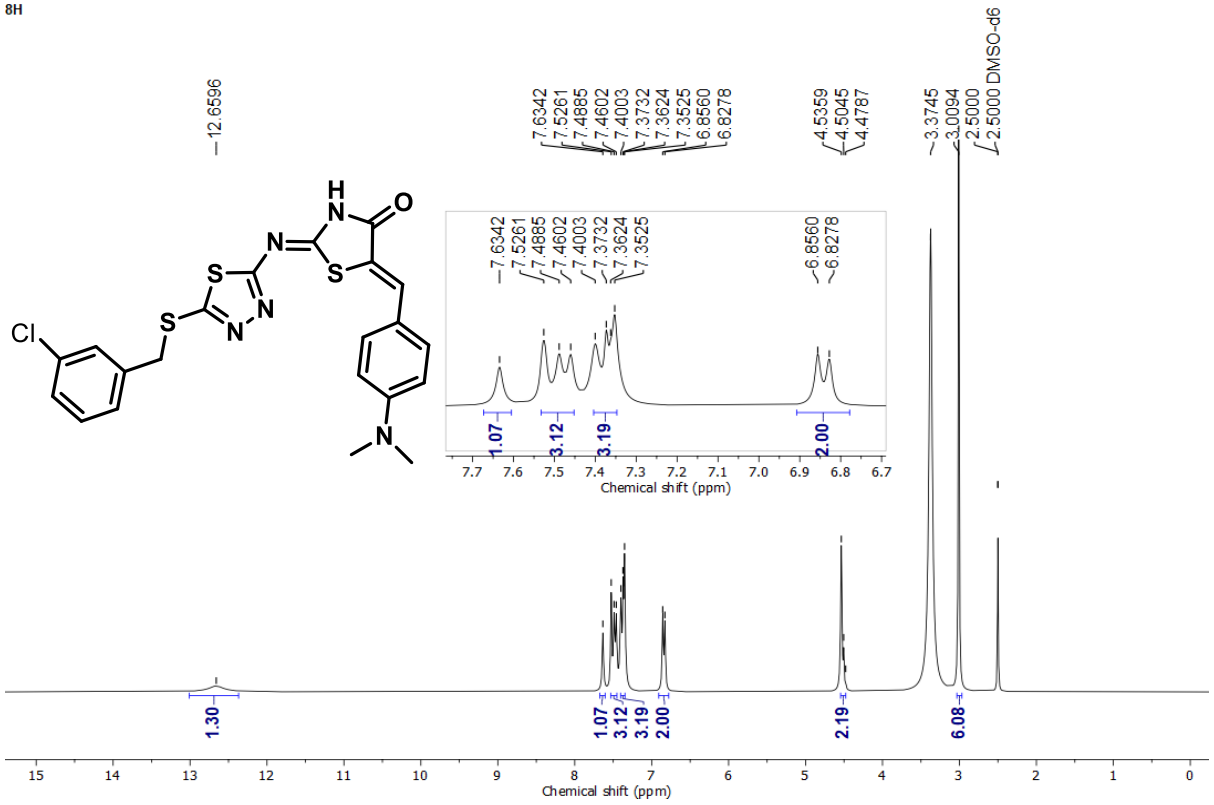

S.F18: ^{1}H NMR of compound **8h**

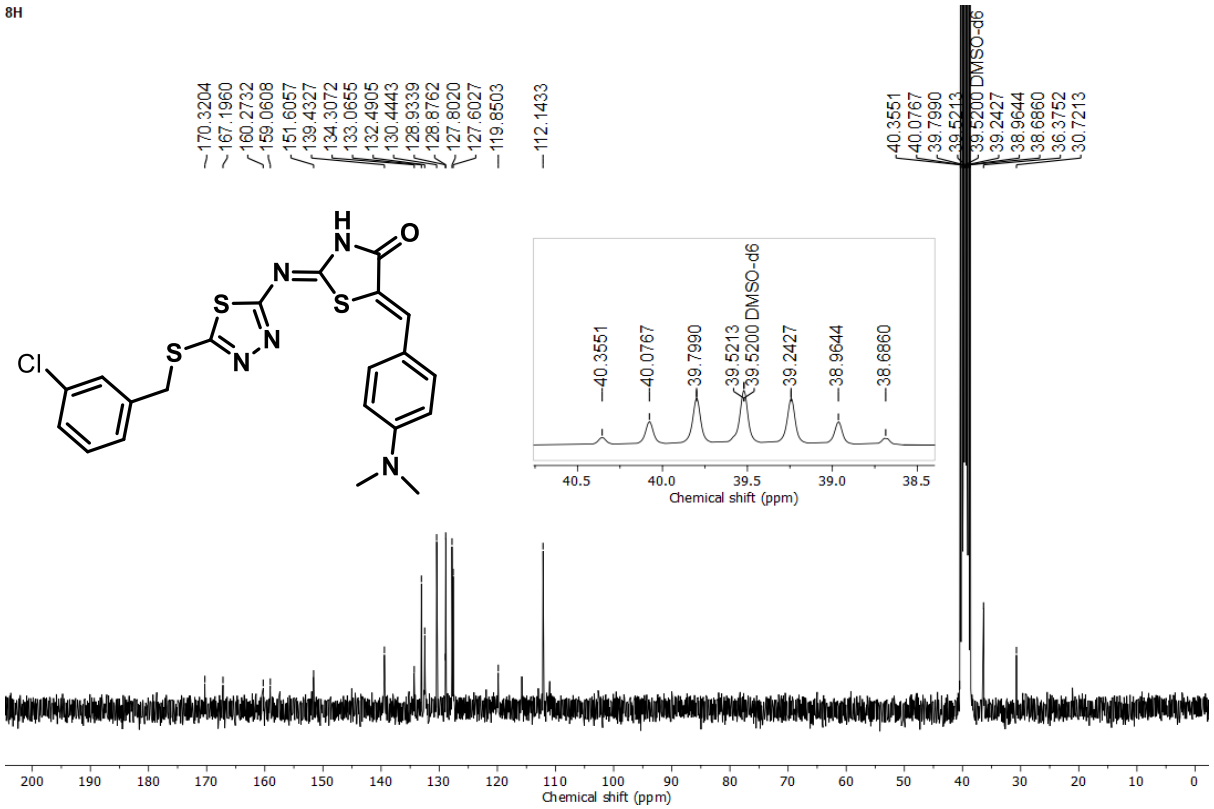

S.F18′: ^{13}C NMR of compound **8h**

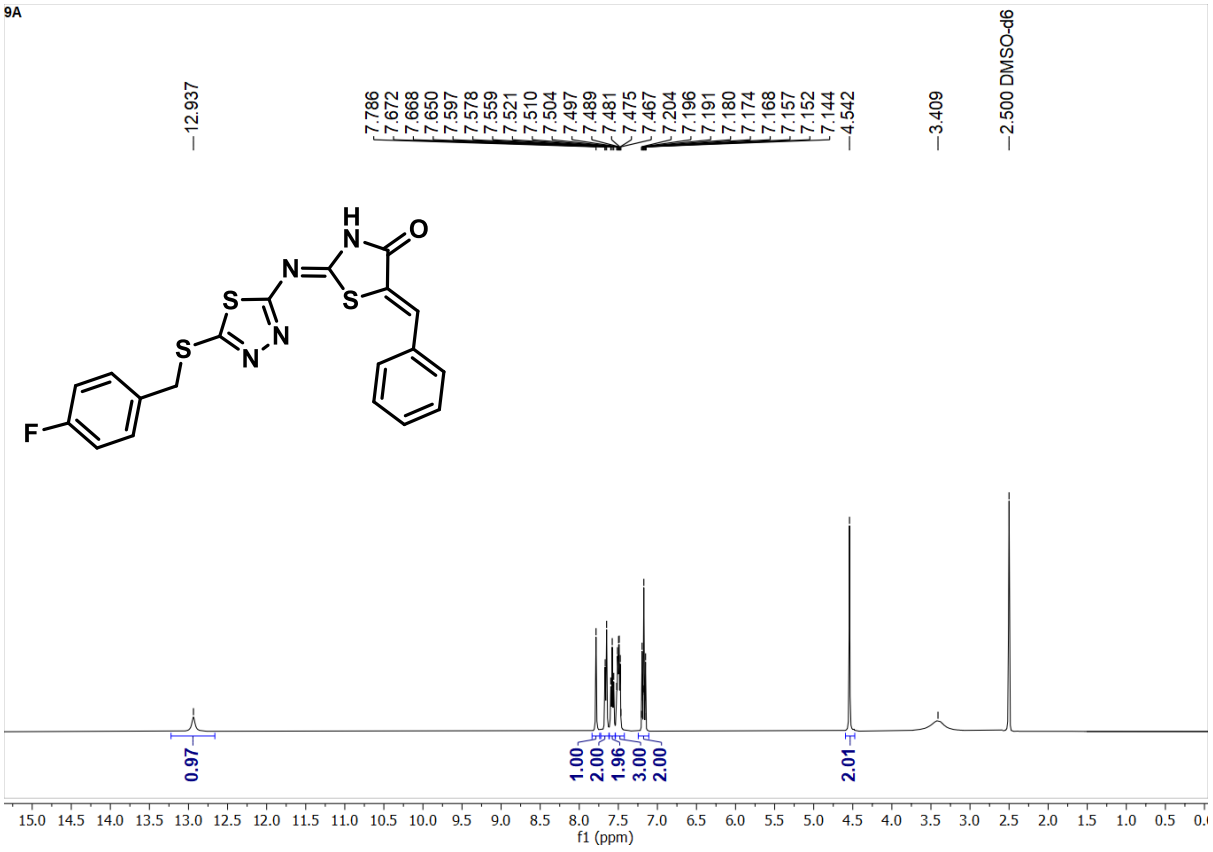

S.F19: ^{1}H NMR of compound **9a**

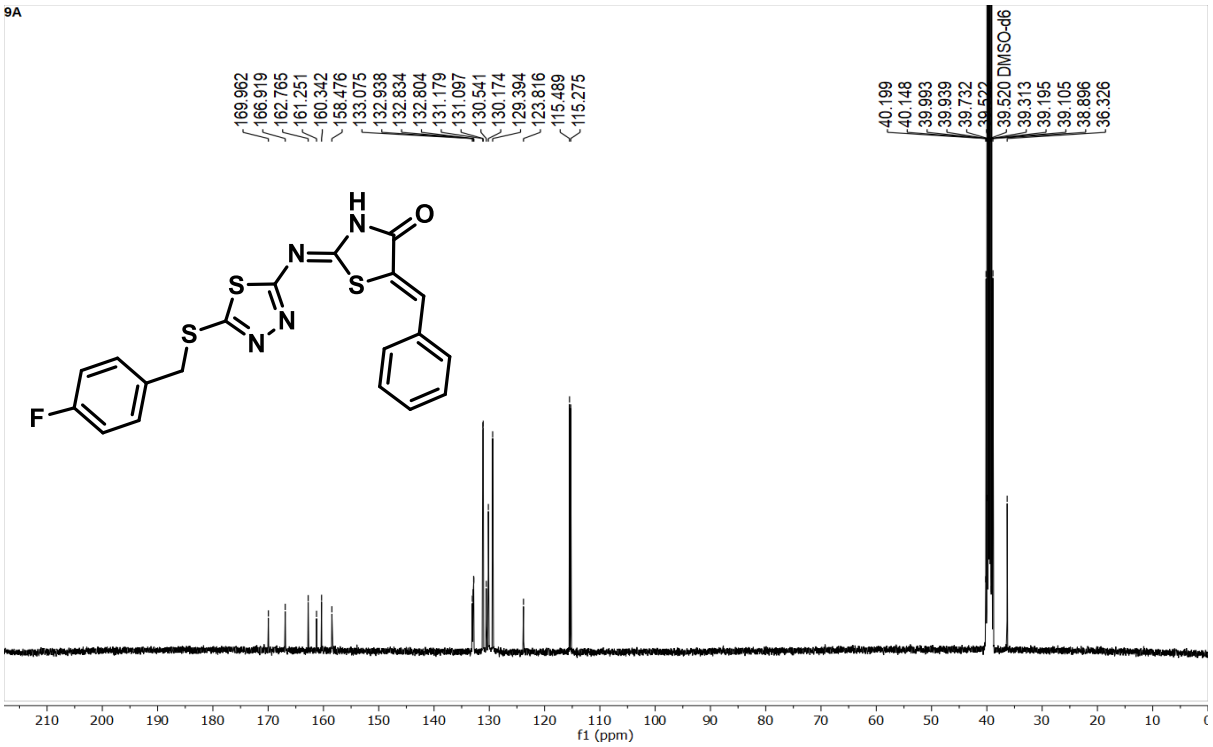

S.F19′: ^{13}C NMR of compound **9a**

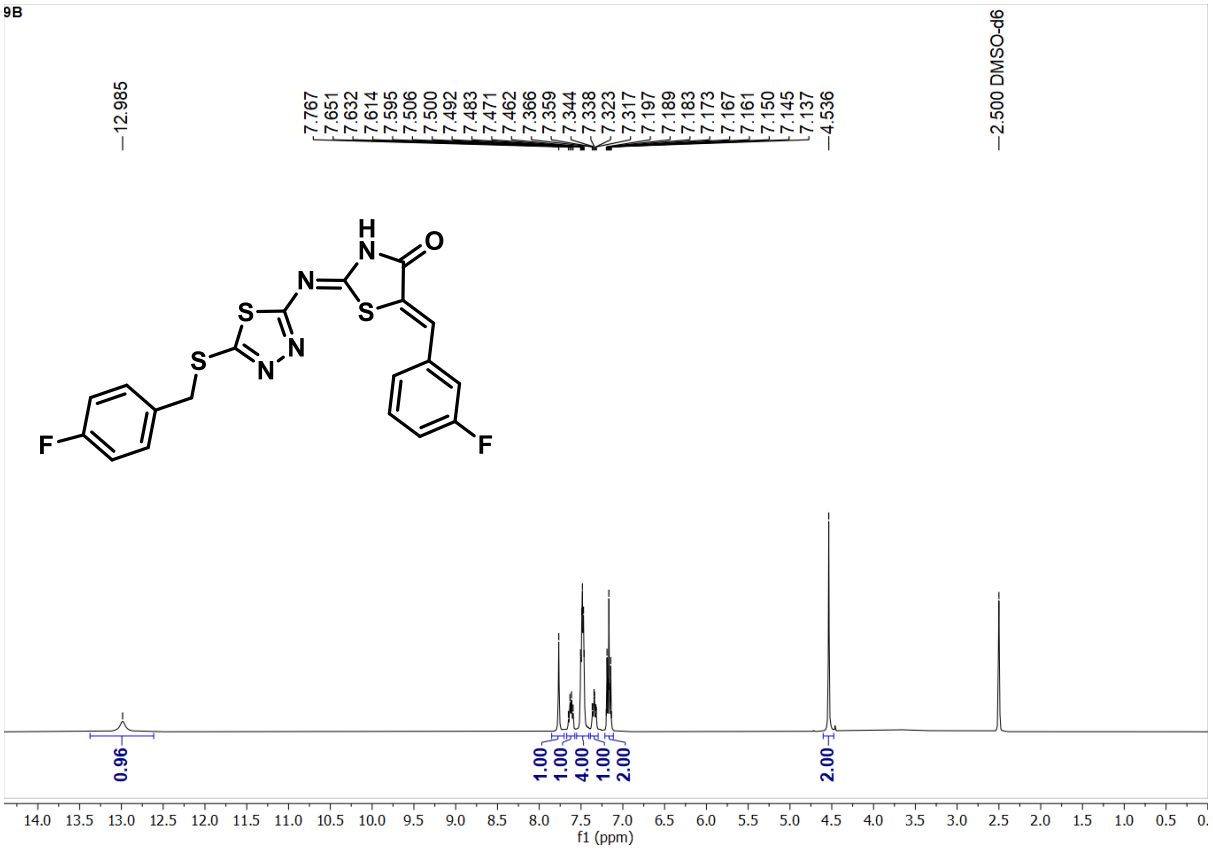

S.F20: ^{1}H NMR of compound **9b**

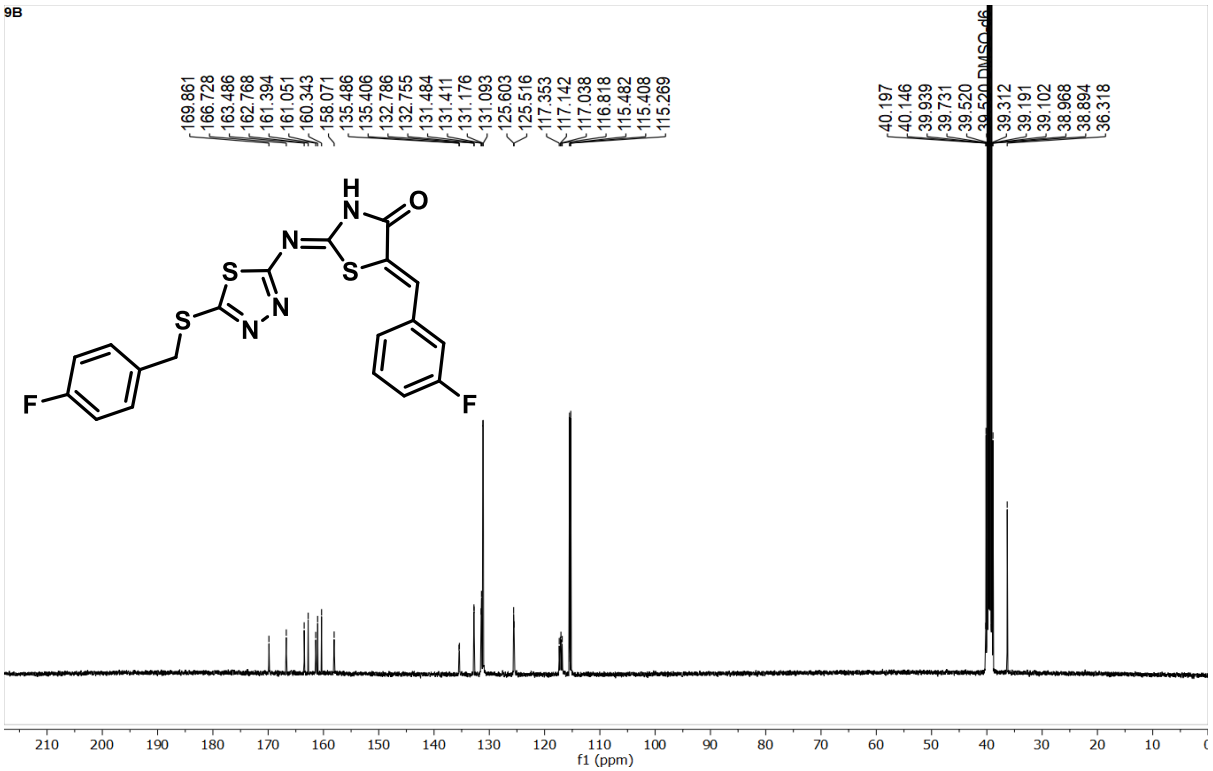

S.F20′: ^{13}C NMR of compound **9b**

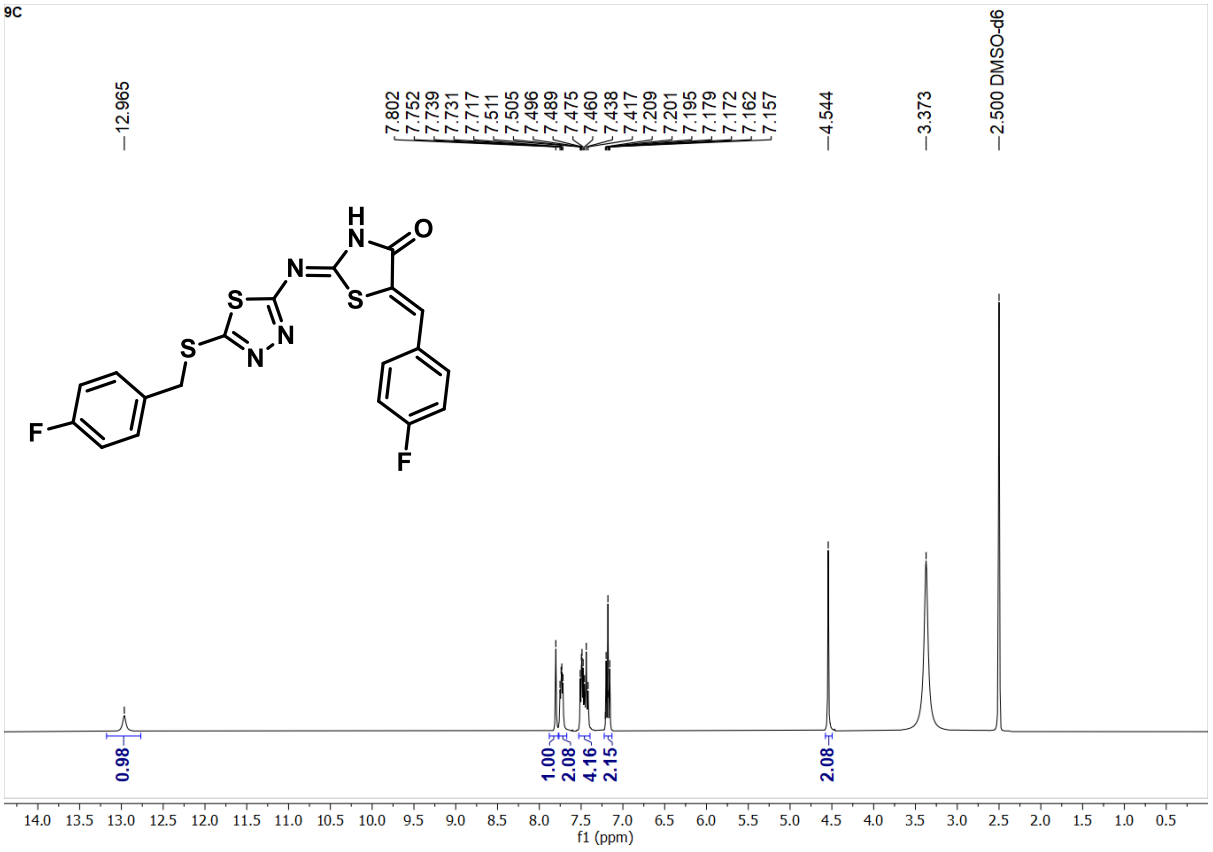

S.F21: ^{1}H NMR of compound **9c**

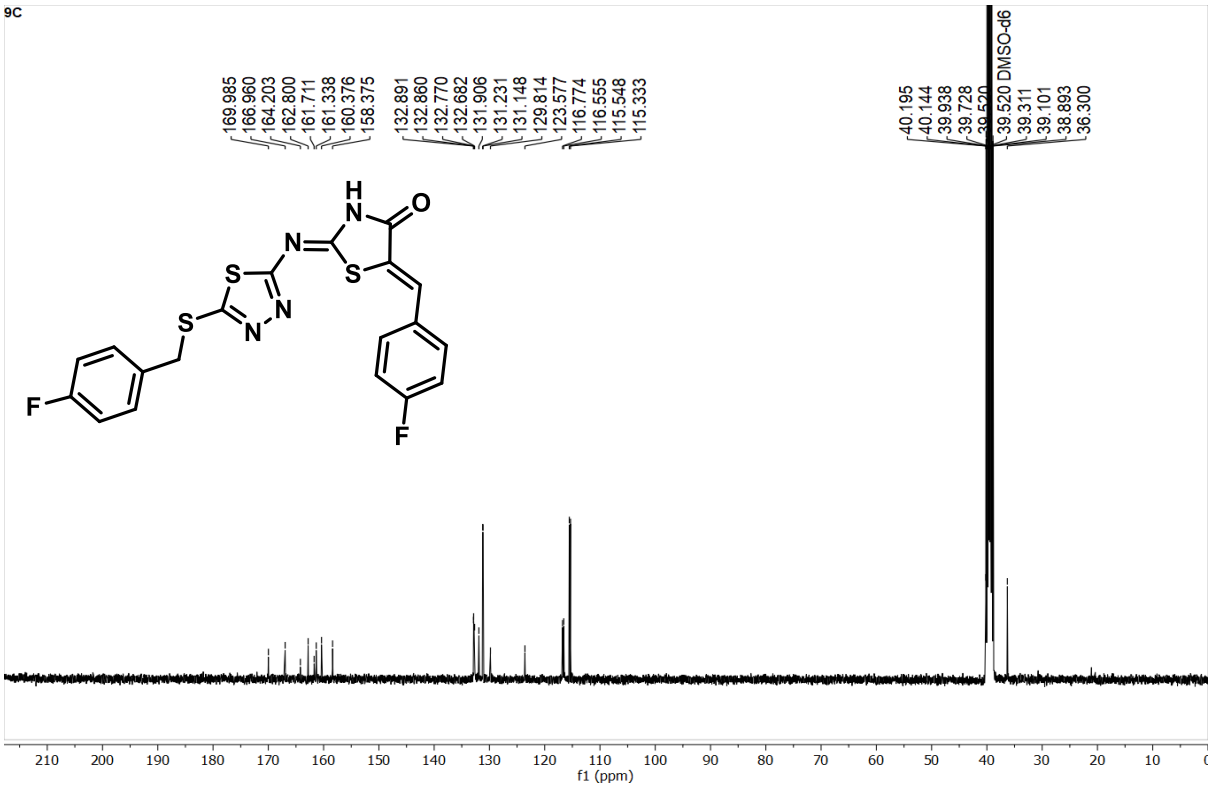

S.F21′: ^{13}C NMR of compound **9c**

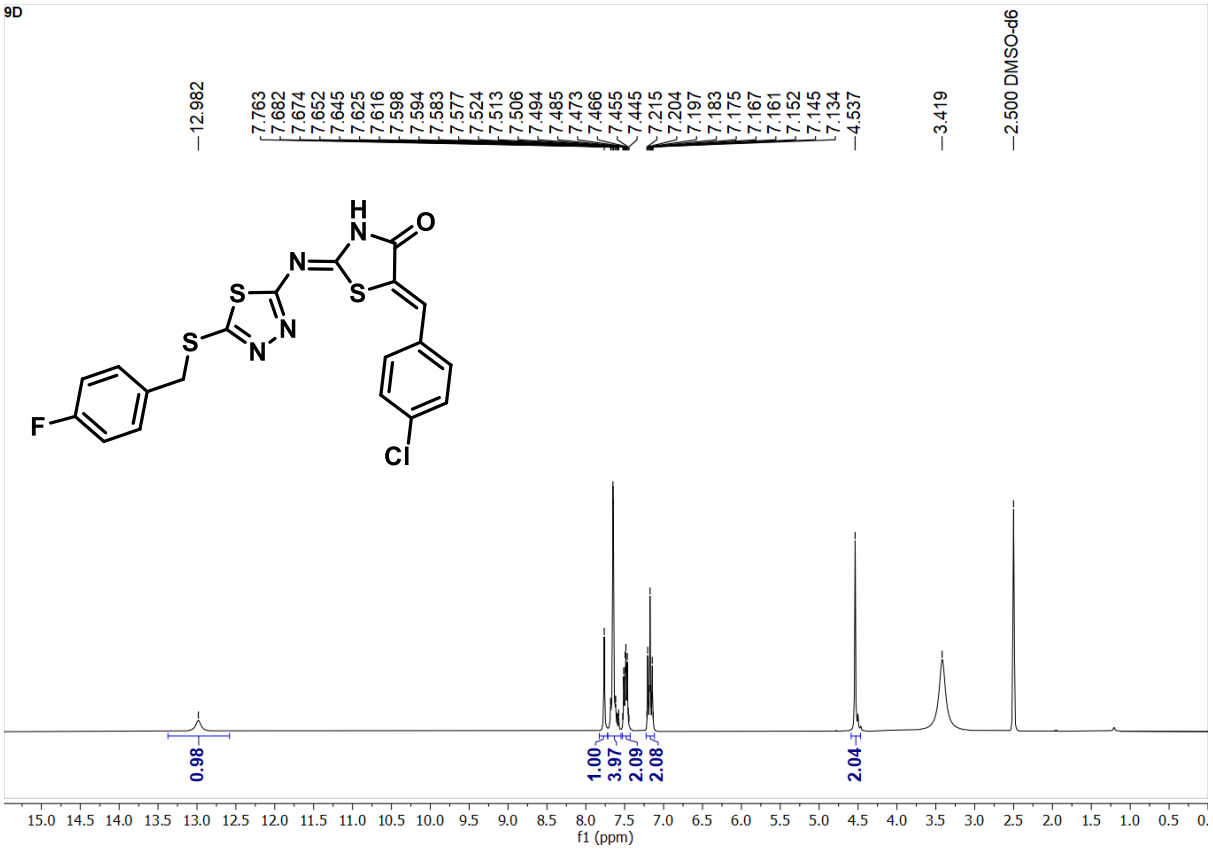

S.F22: ^{1}H NMR of compound **9d**

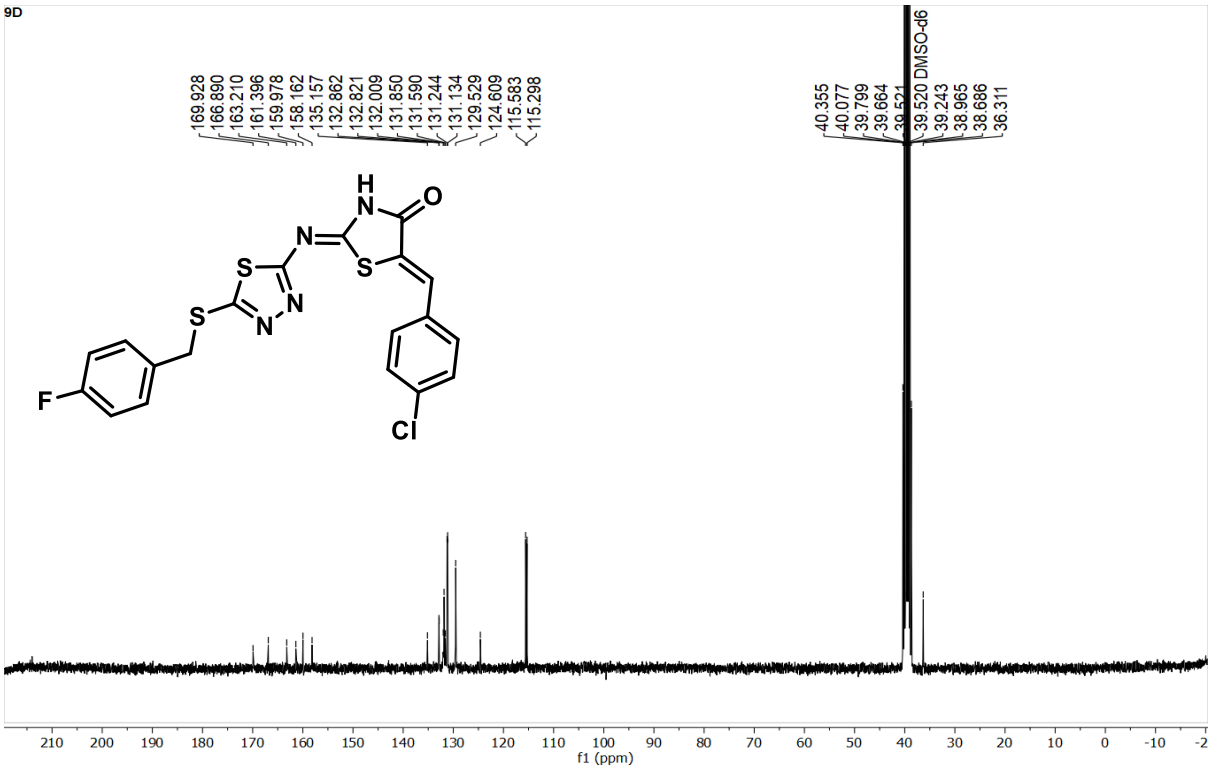

S.F22′: ^{13}C NMR of compound **9d**

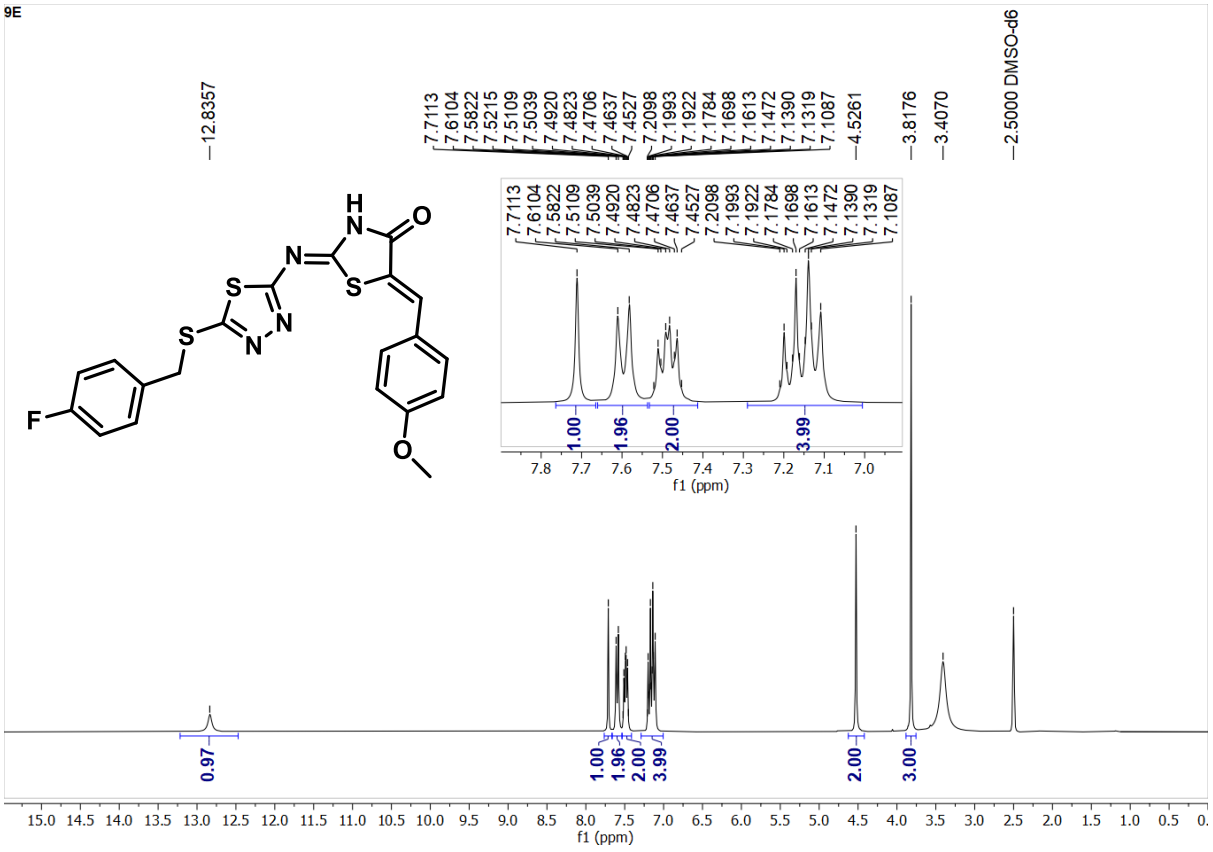

S.F23: ^{1}H NMR of compound **9e**

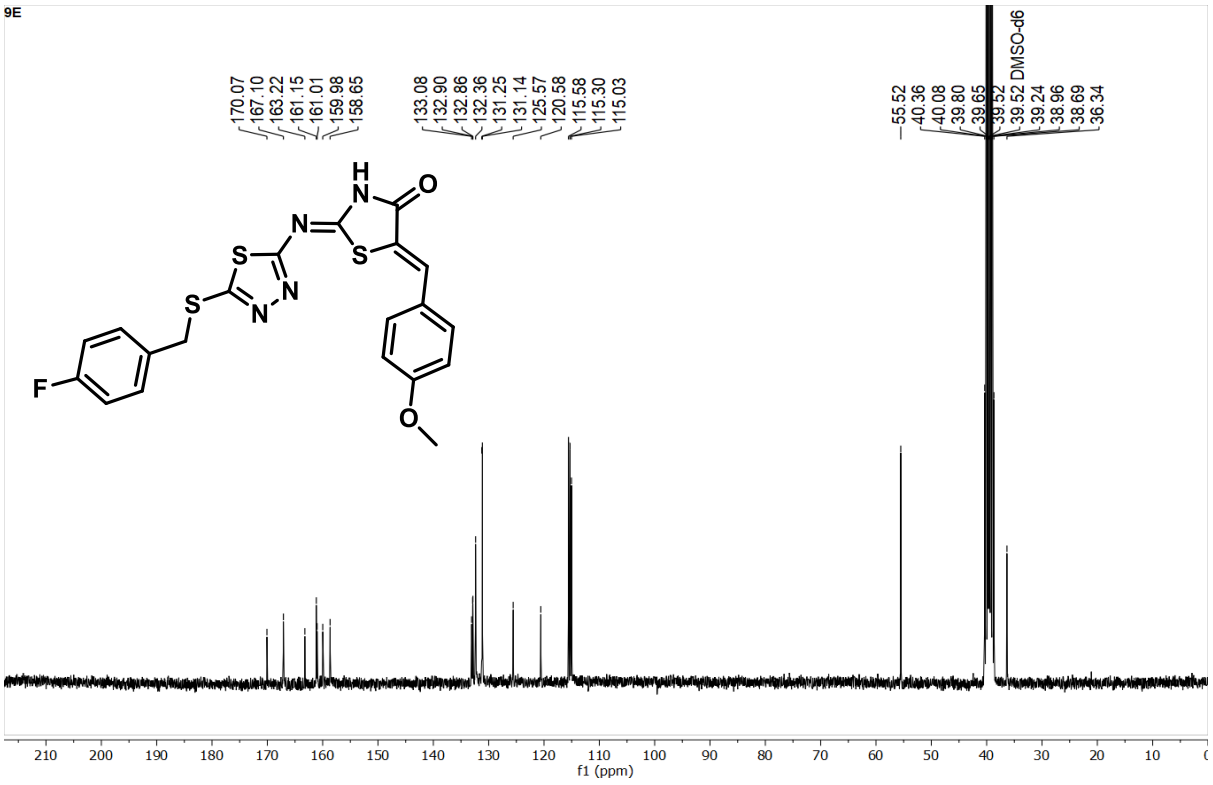

S.F23′: ^{13}C NMR of compound **9e**

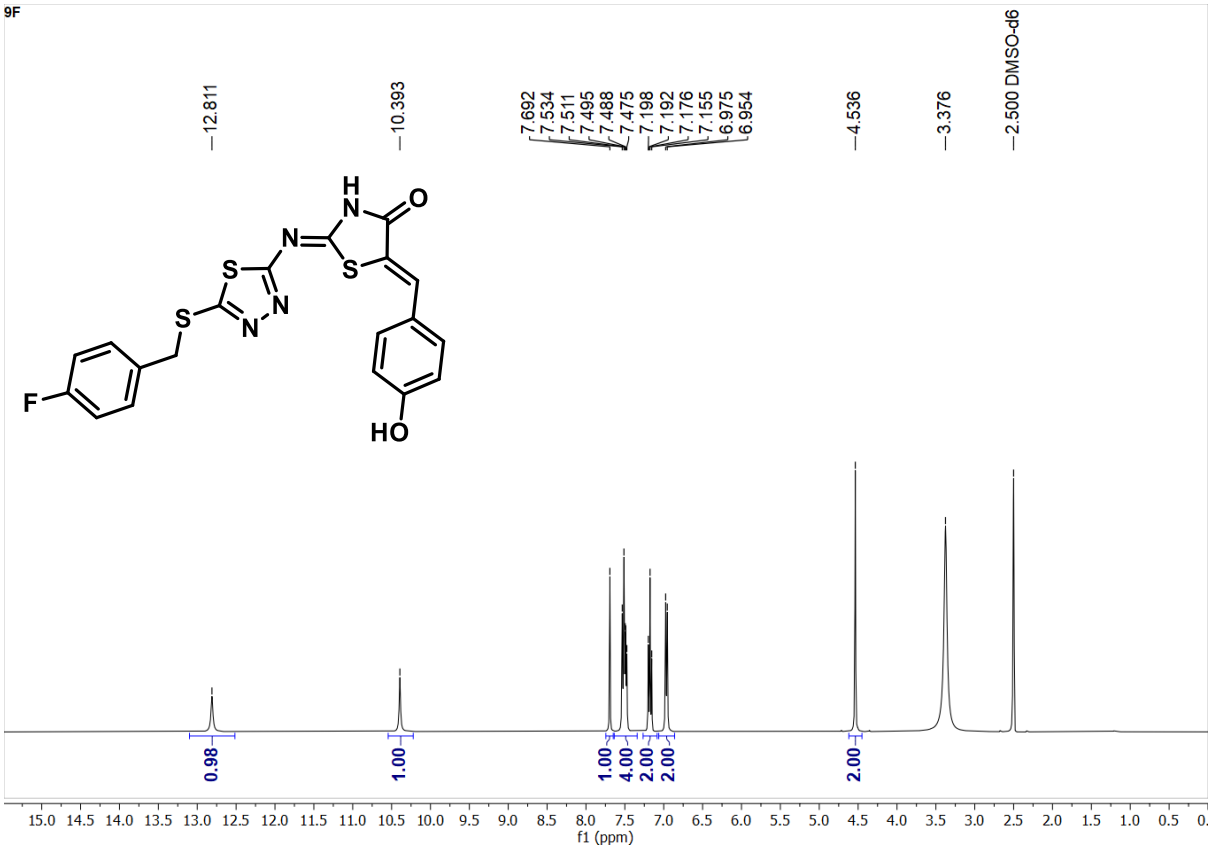

S.F24: ^{1}H NMR of compound **9f**

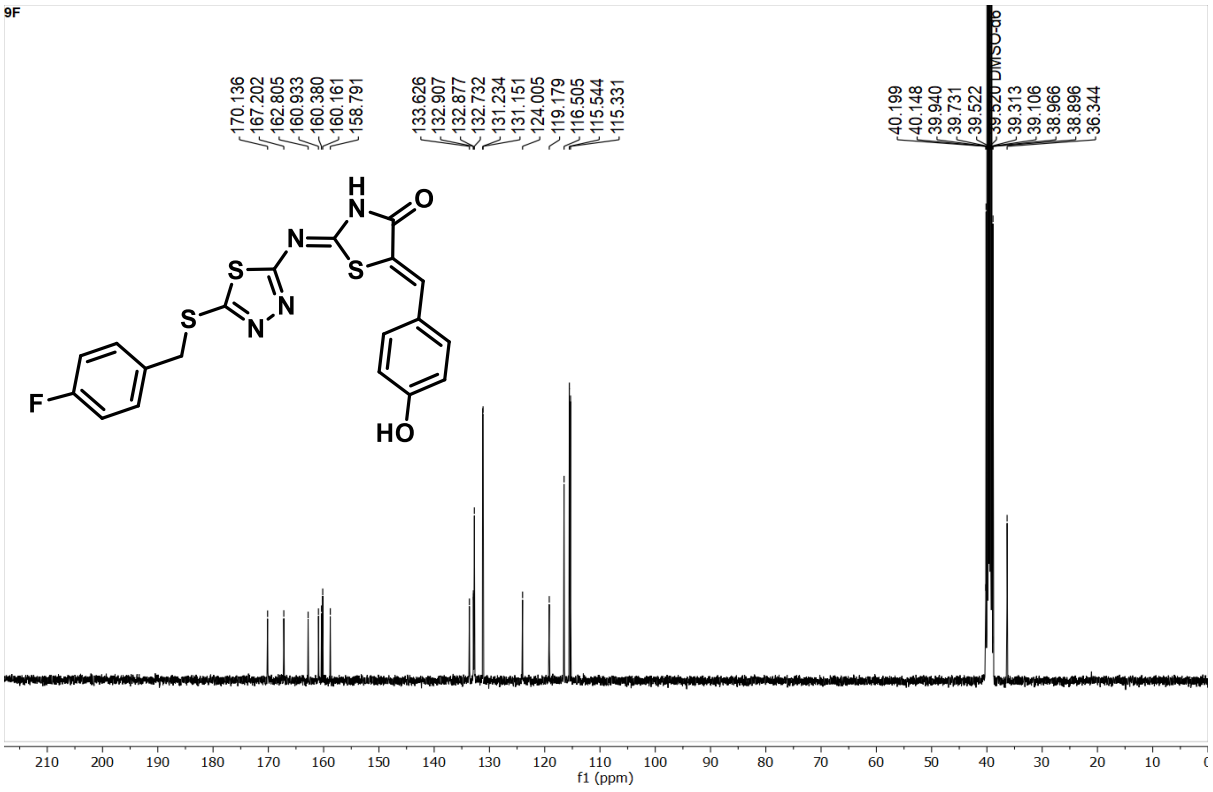

S.F24′: ^{13}C NMR of compound **9f**

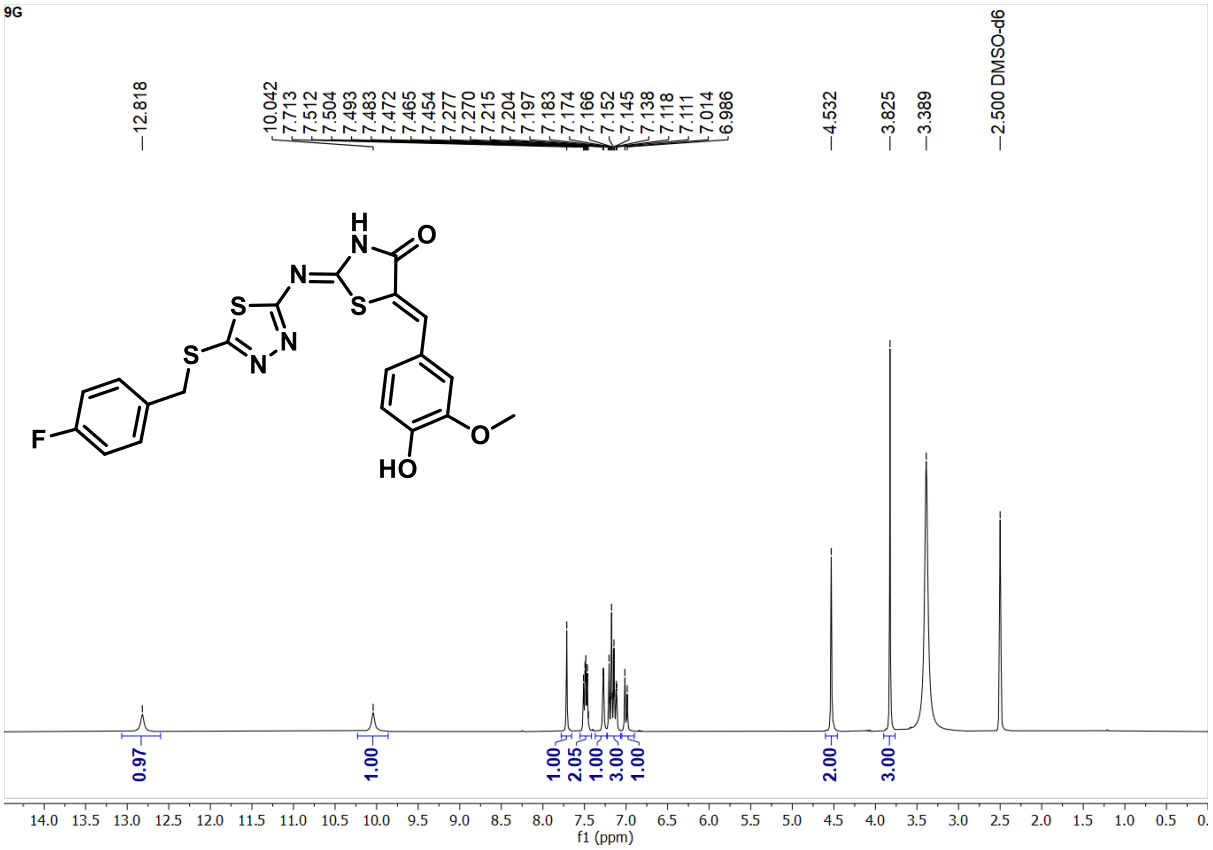

S.F25: ^{1}H NMR of compound **9g**

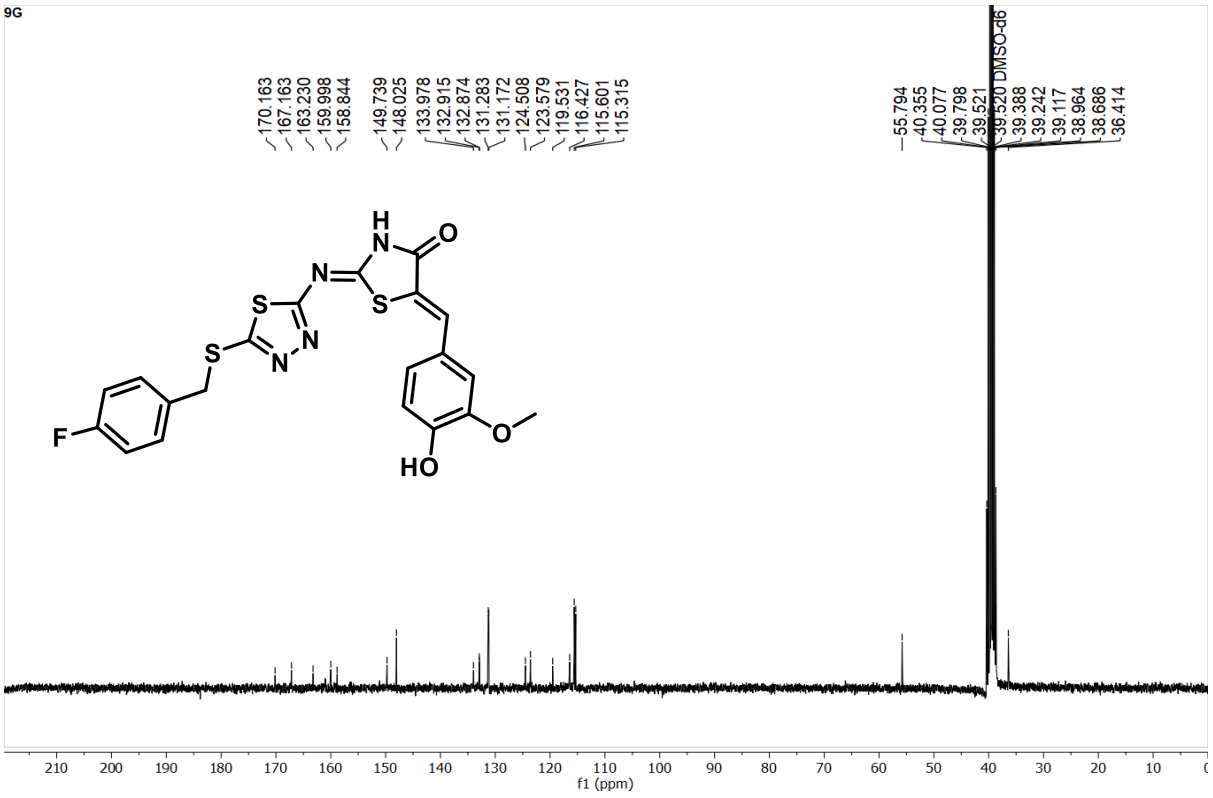

S.F25′: ^{13}C NMR of compound **9g**

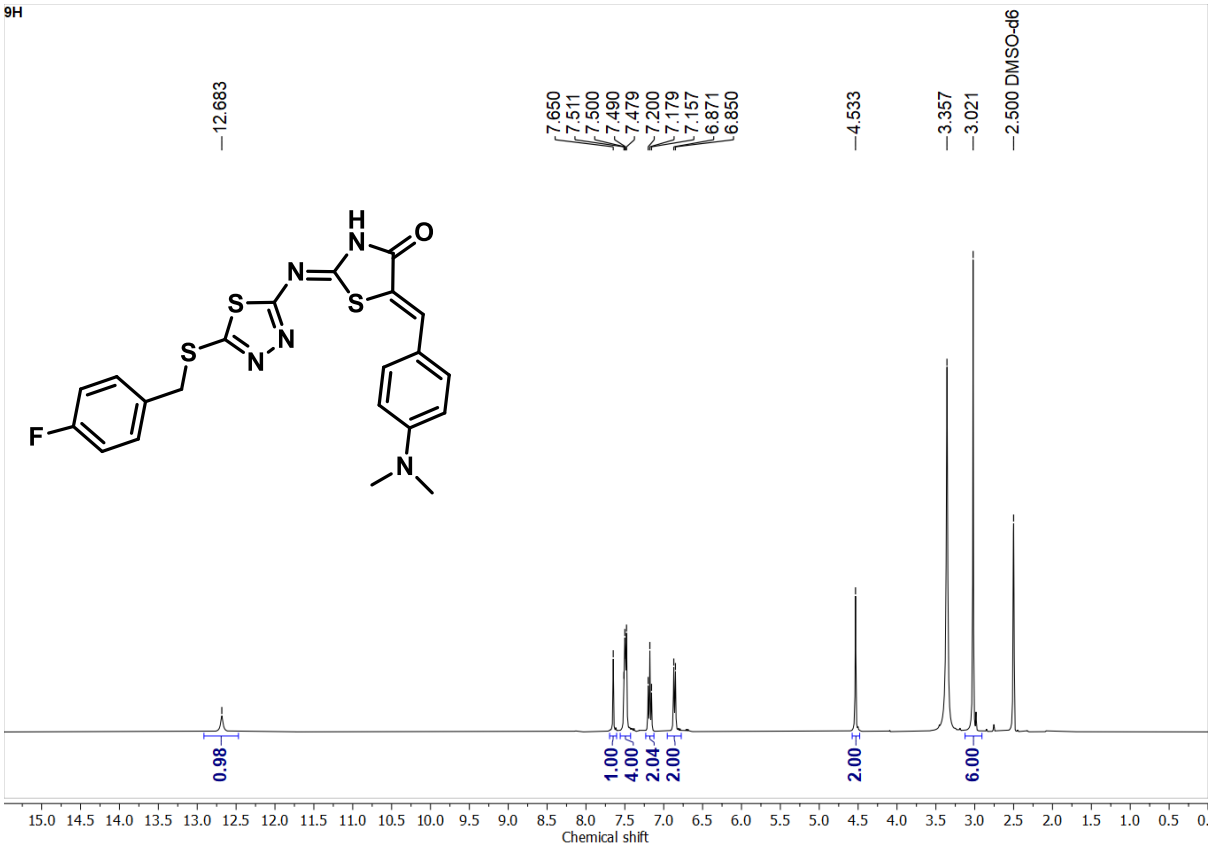

S.F26: ^{1}H NMR of compound **9h**

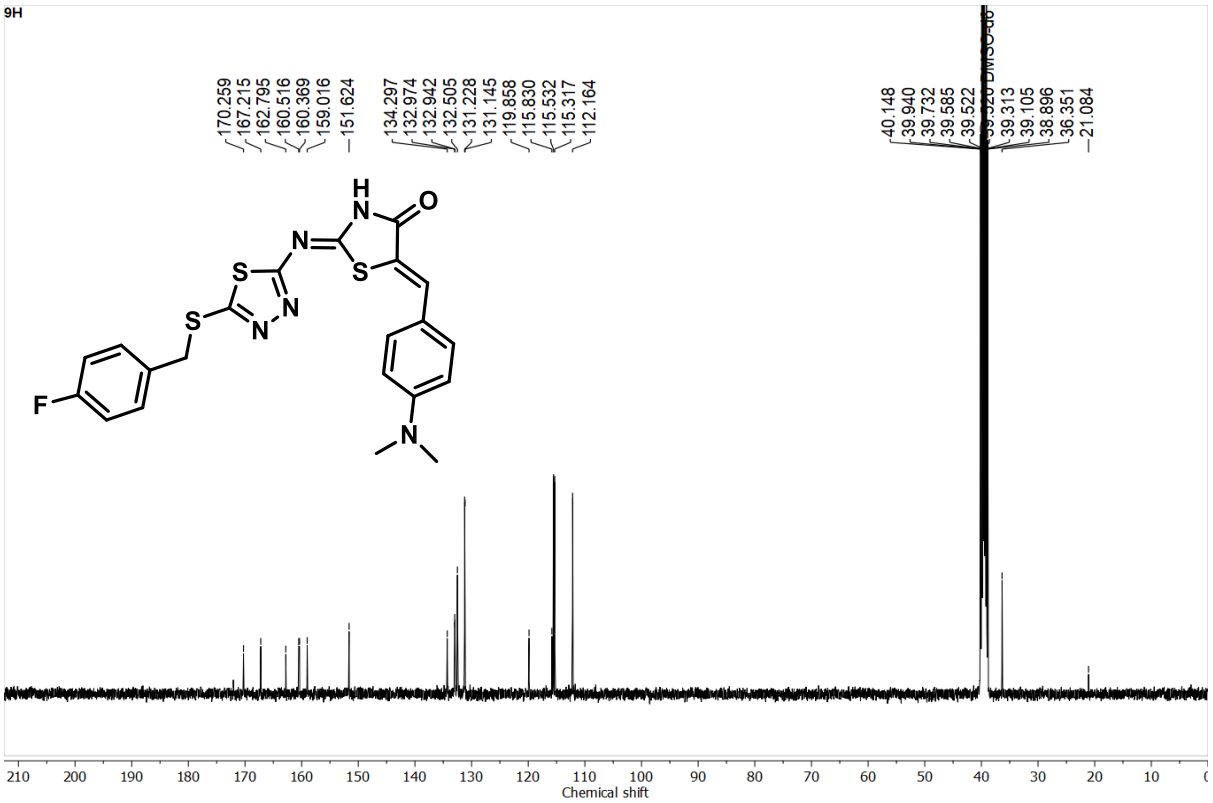

S.F26′: ^{13}C NMR of compound **9h**

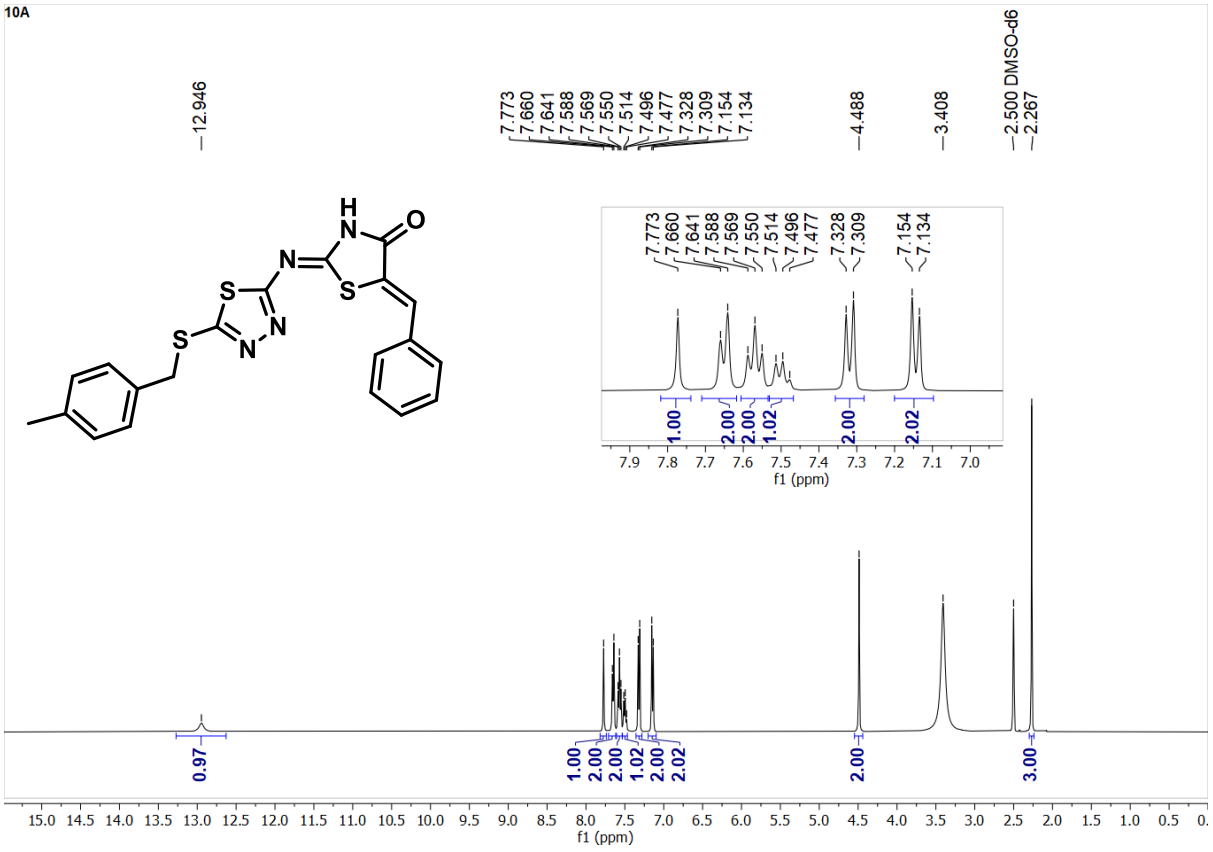

S.F27: ^{1}H NMR of compound **10a**

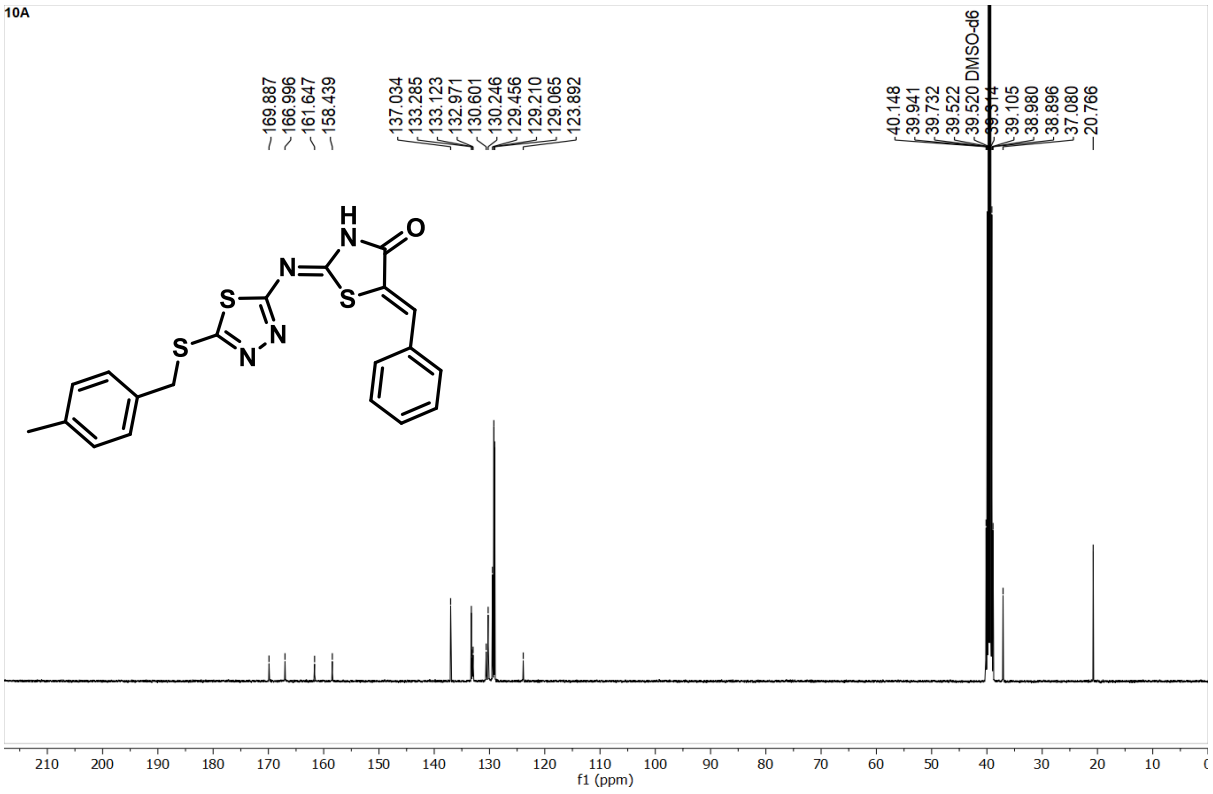

S.F27′: ^{13}C NMR of compound **10a**

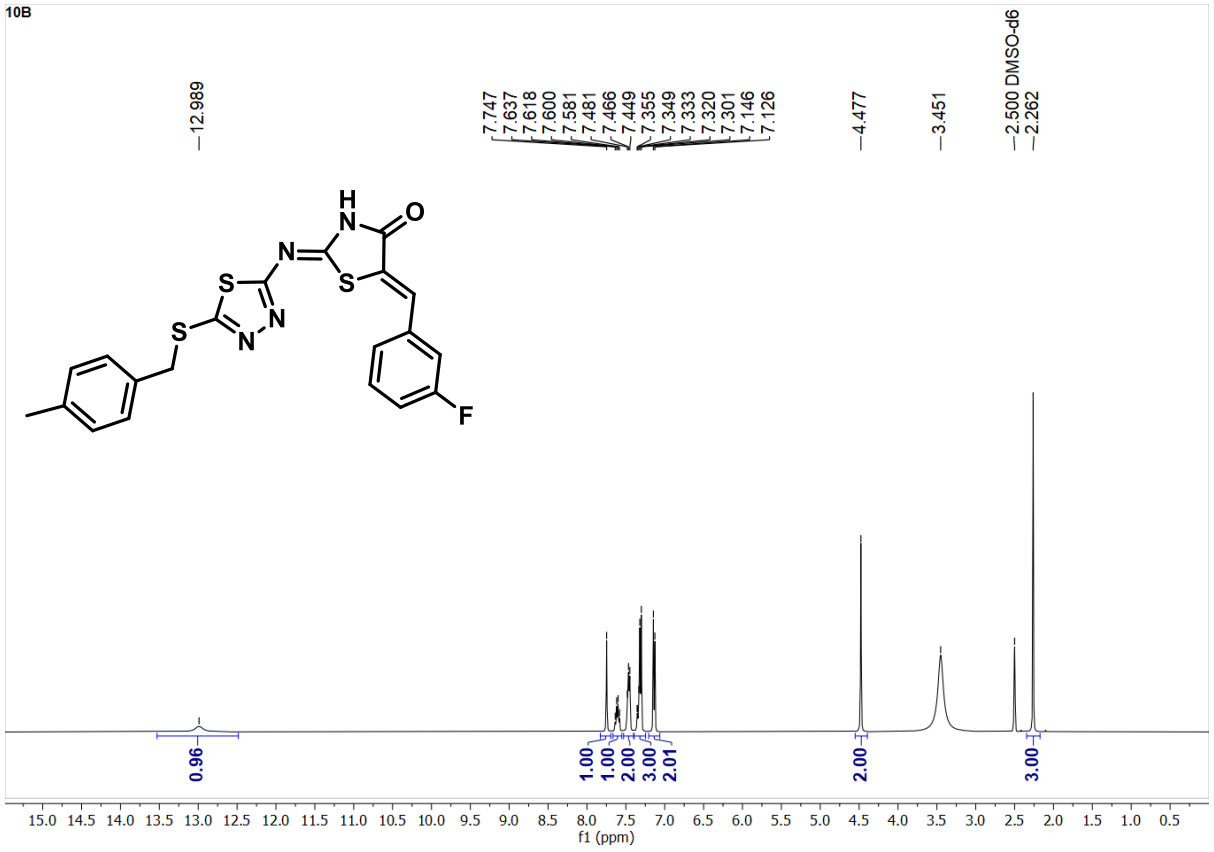

S.F28: ^{1}H NMR of compound **10b**

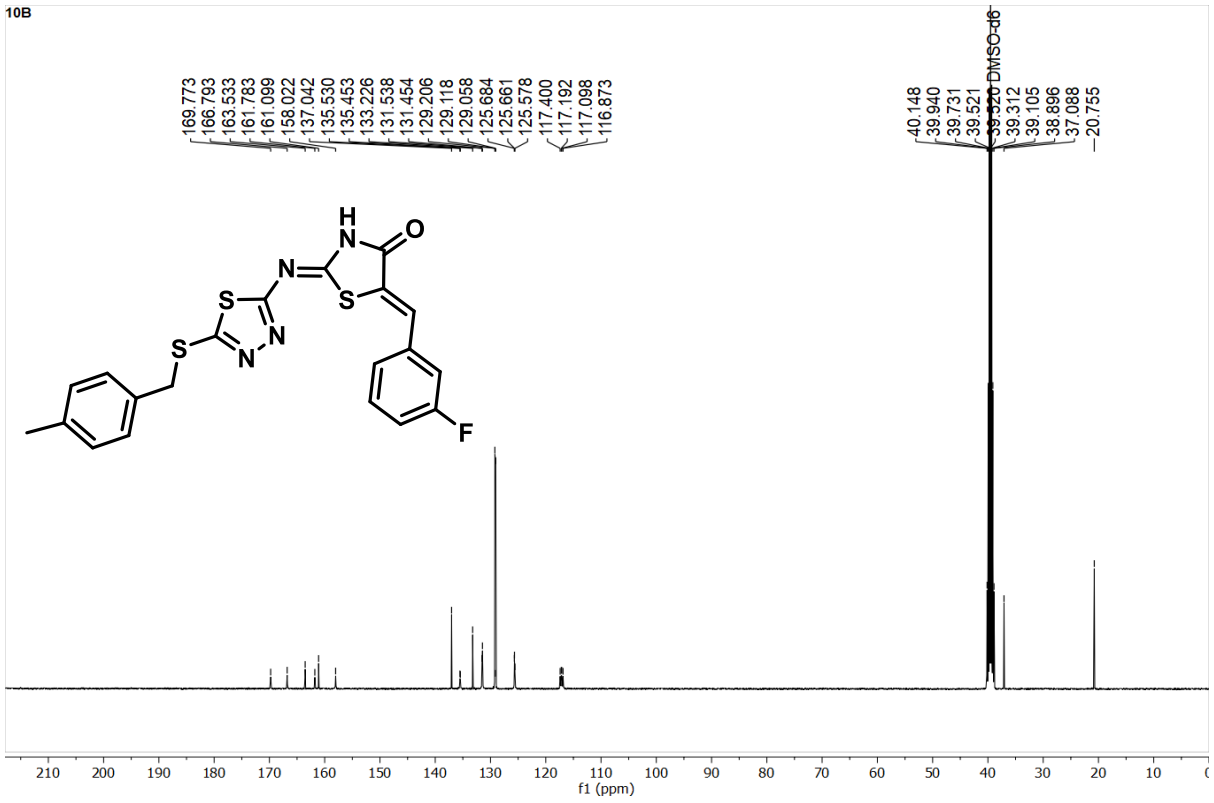

S.F28′: ^{13}C NMR of compound **10b**

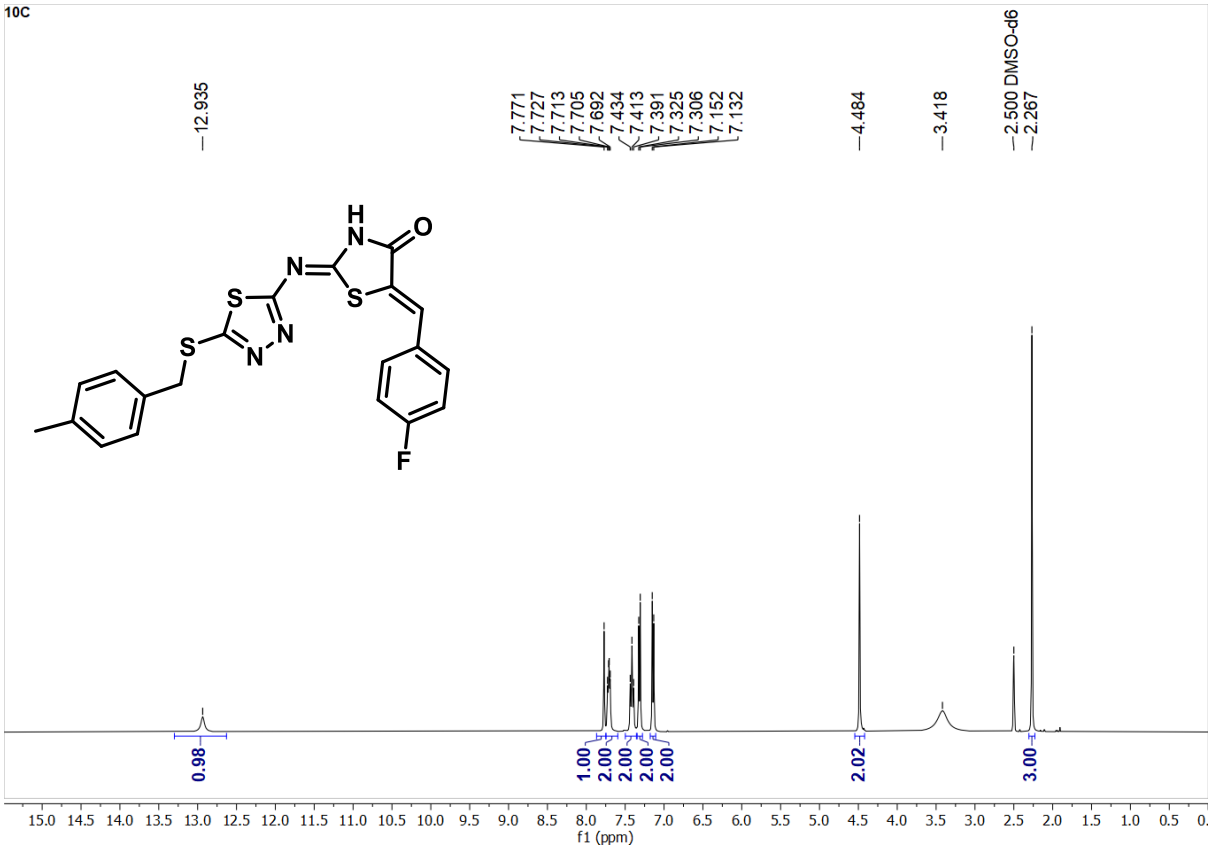

S.F29: ^{1}H NMR of compound **10c**

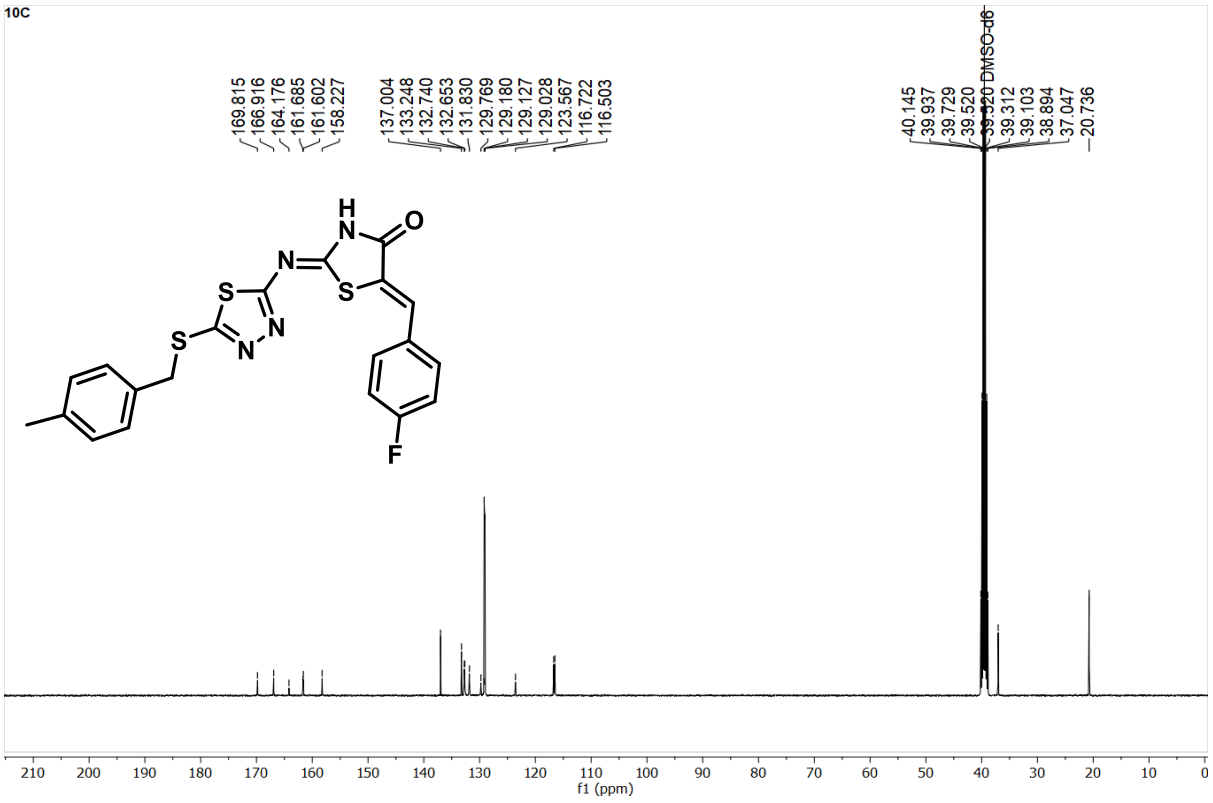

S.F29′: ^{13}C NMR of compound **10c**

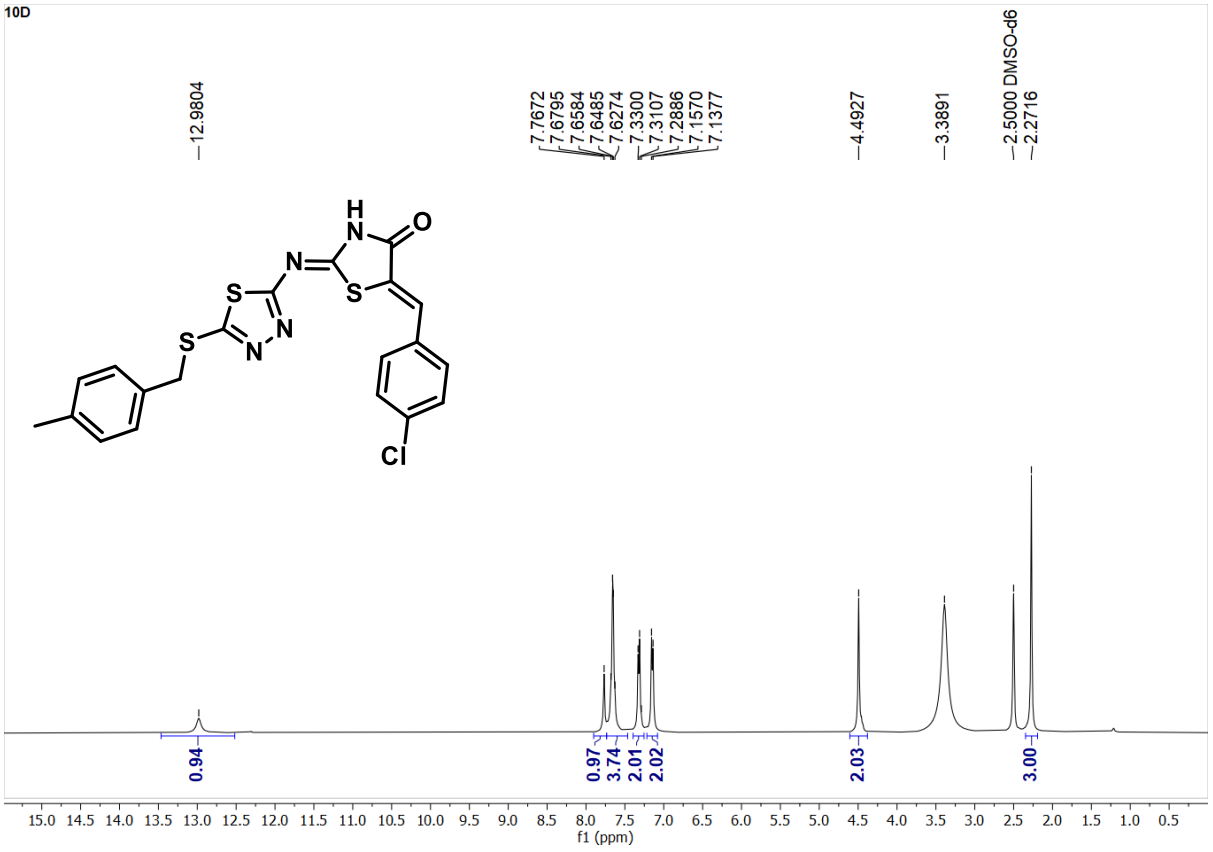

S.F30: ^{1}H NMR of compound **10d**

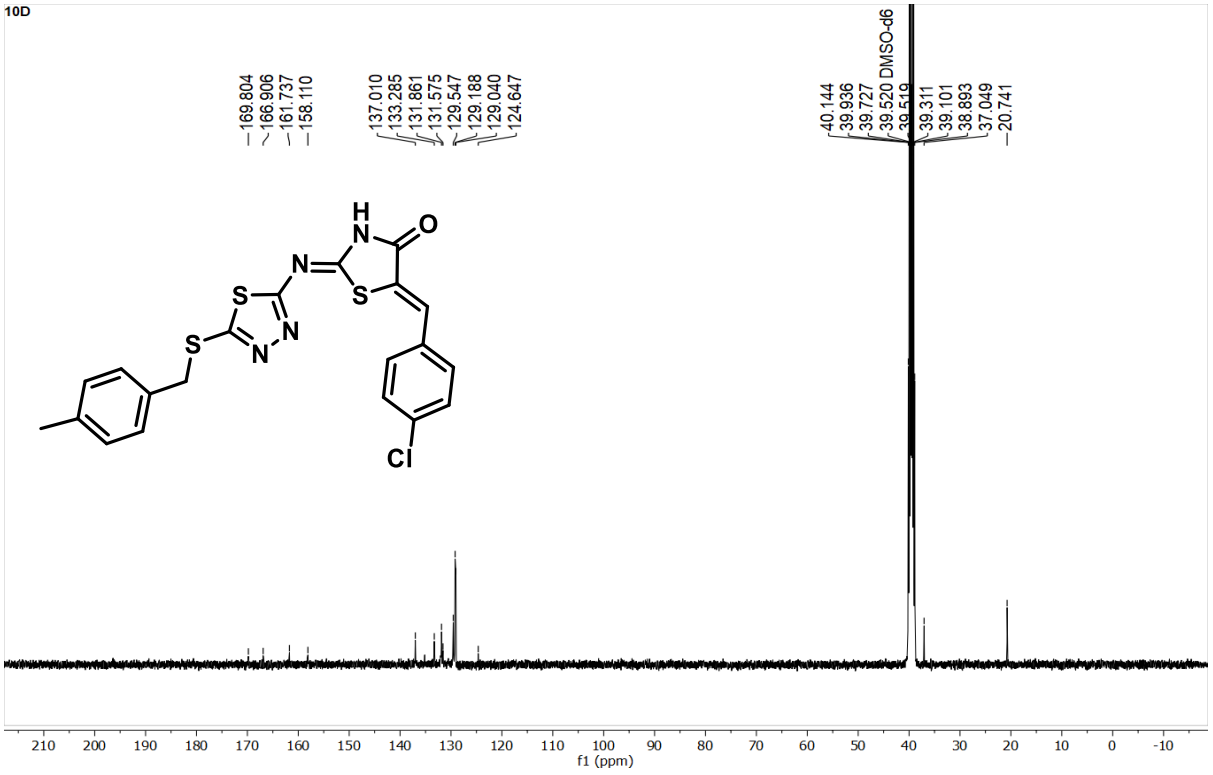

S.F30′: ^{13}C NMR of compound **10d**

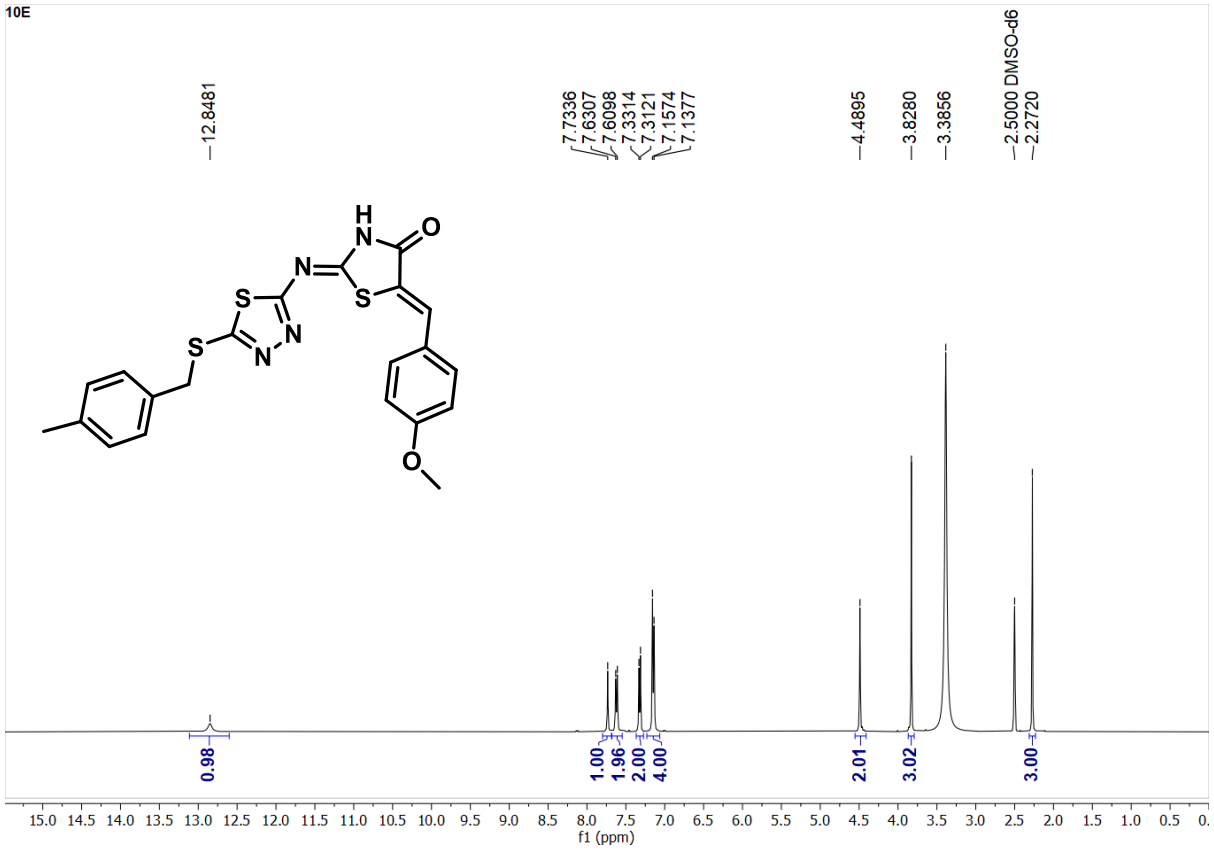

S.F31: ^{1}H NMR of compound **10e**

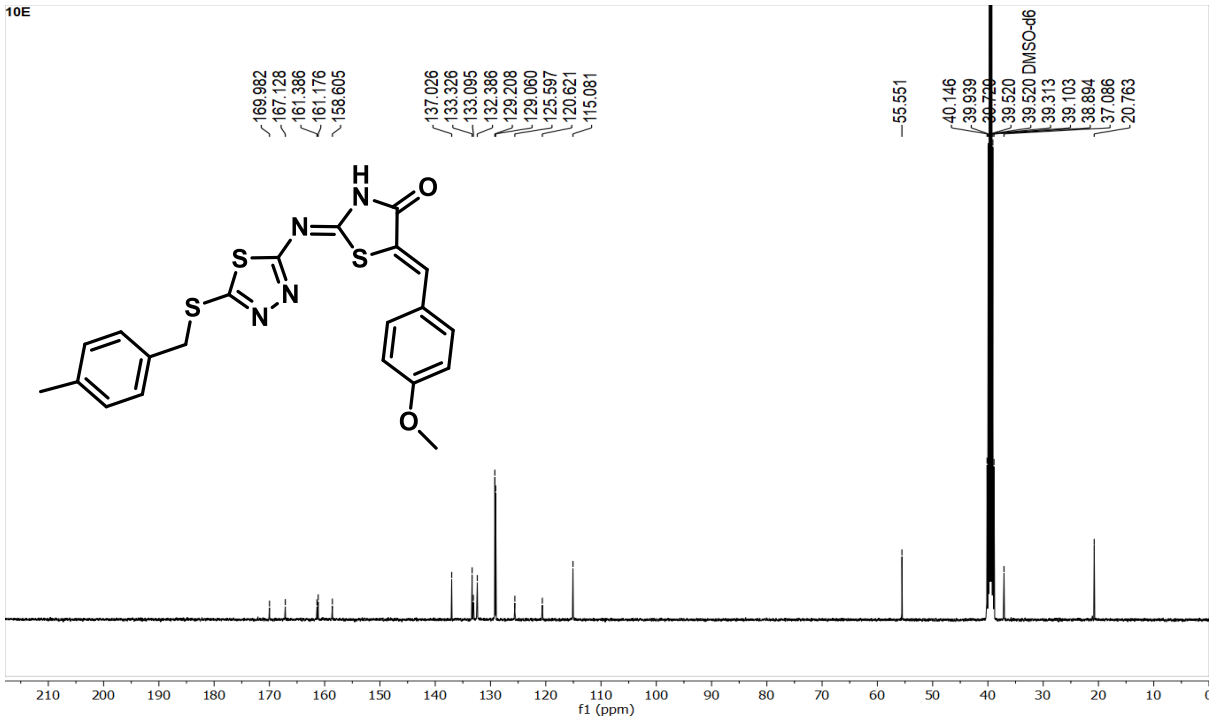

S.F31′: ^{13}C NMR of compound **10e**

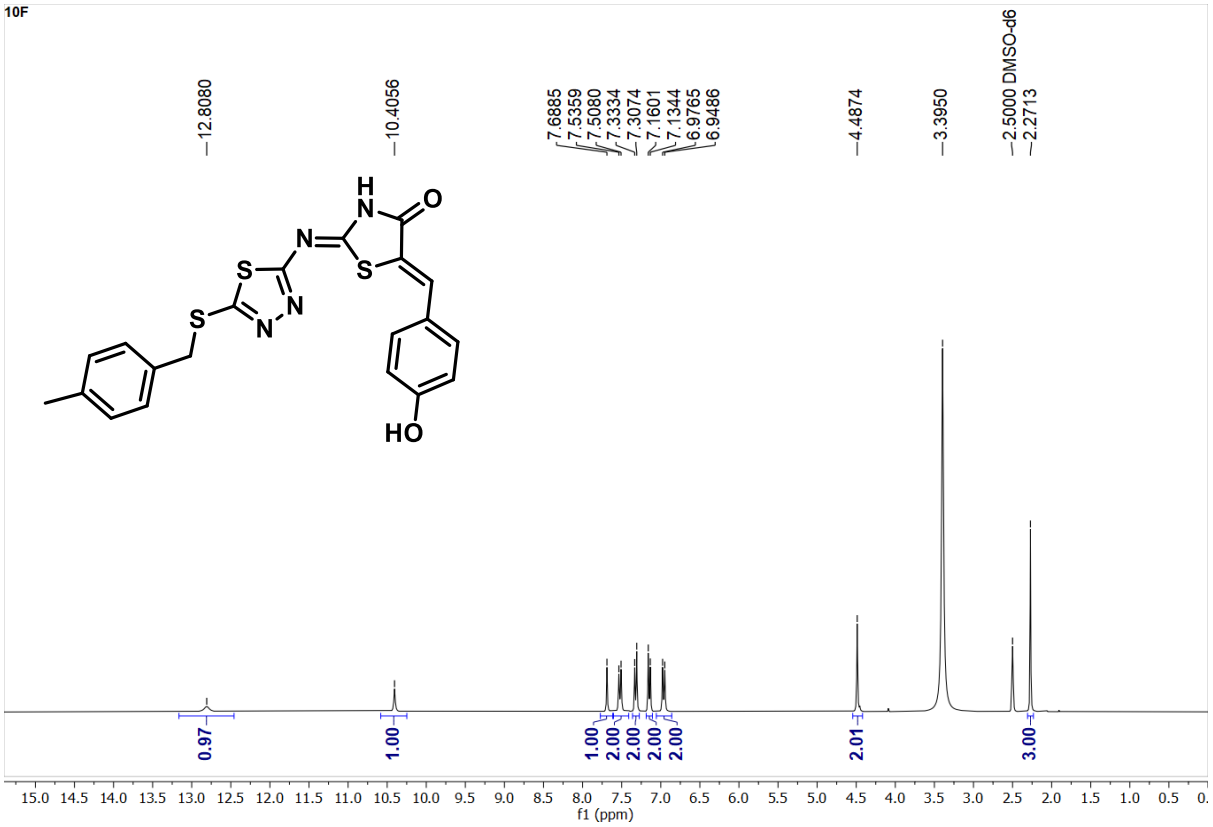

S.F32: ^{1}H NMR of compound **10f**

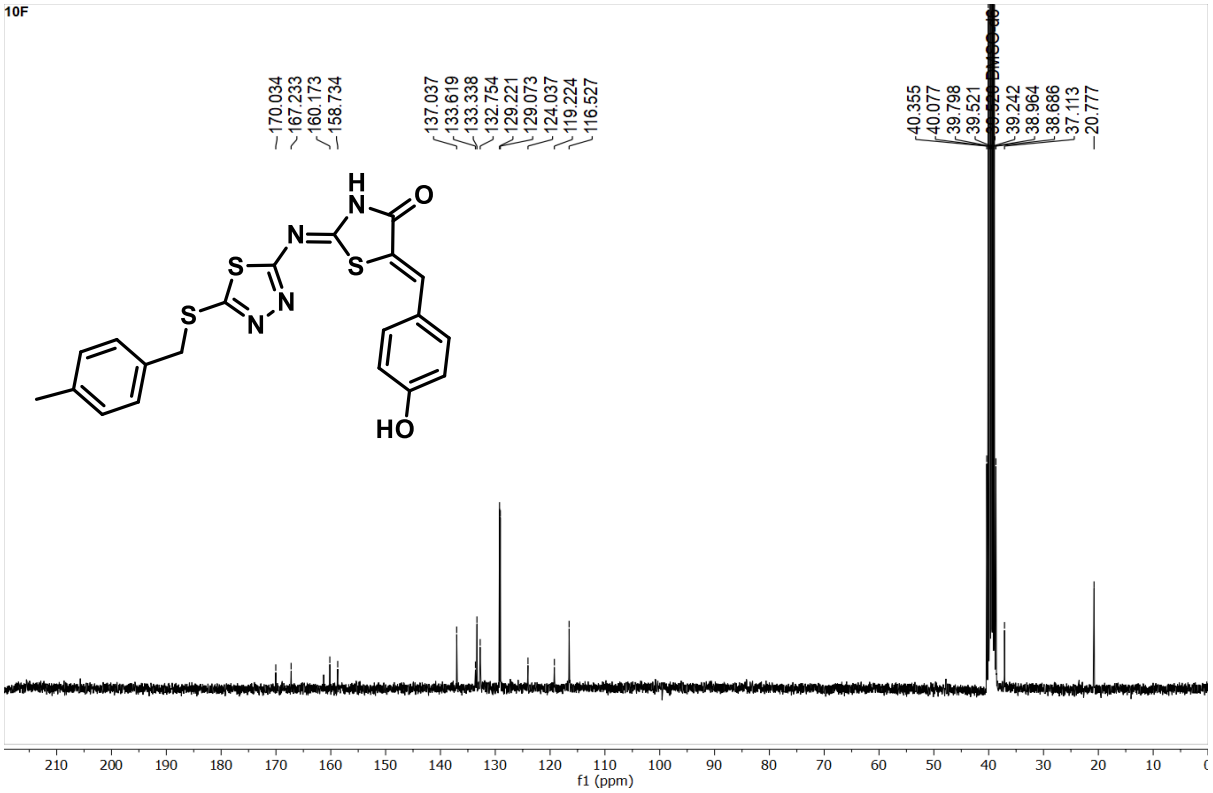

S.F32′: ^{13}C NMR of compound **10f**

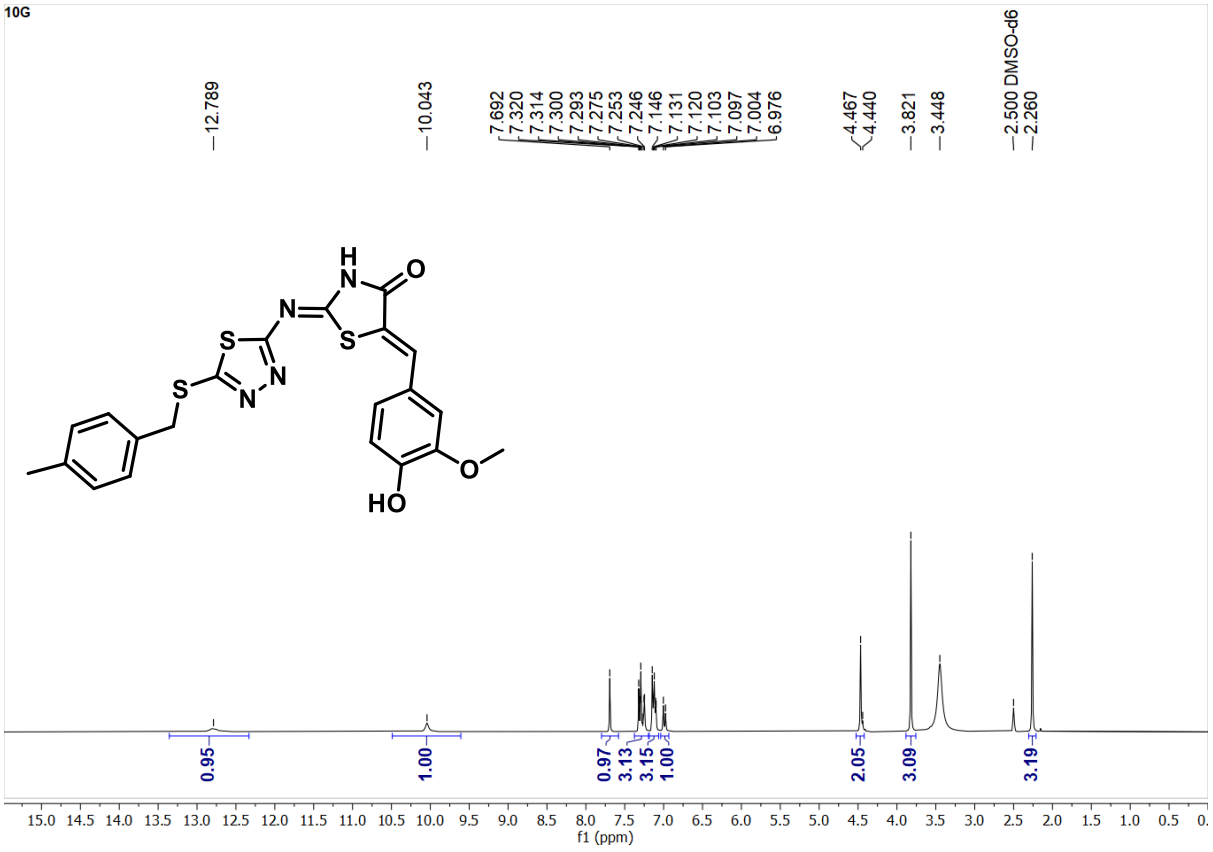

S.F33: ^{1}H NMR of compound **10g**

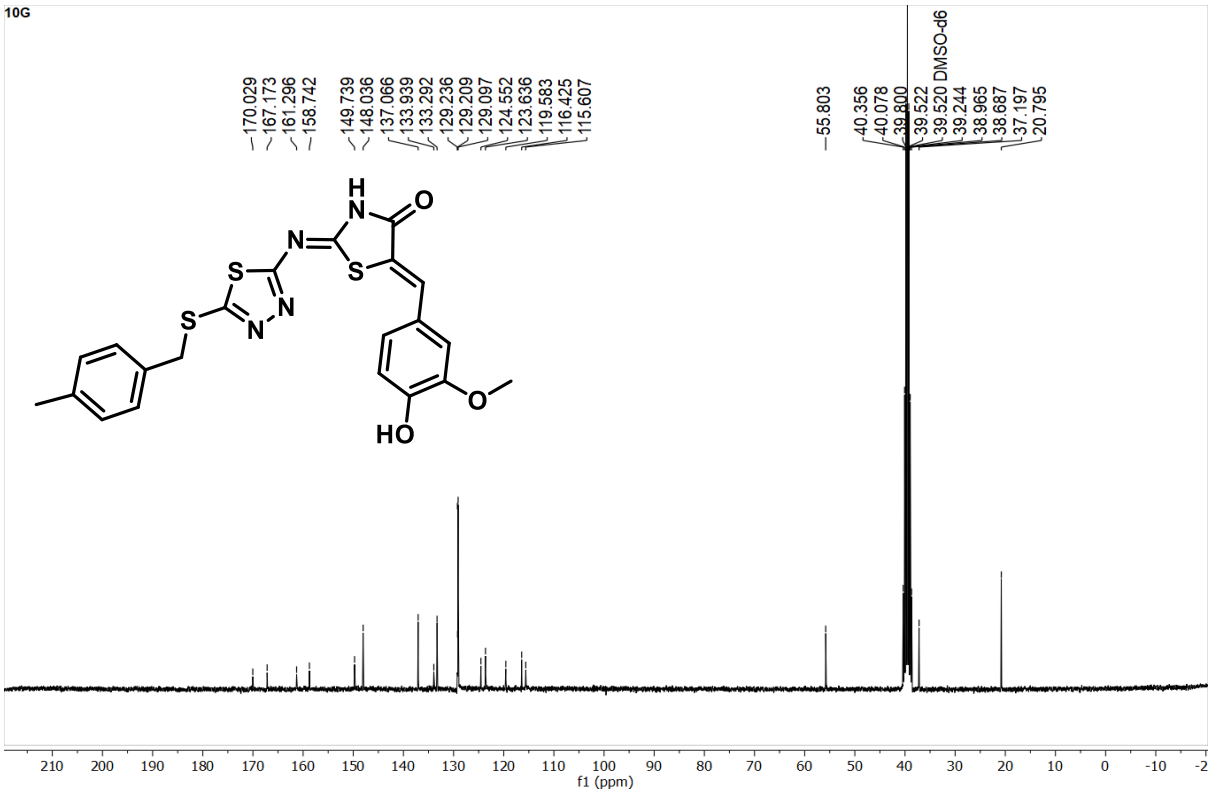

S.F33′: ^{13}C NMR of compound **10g**

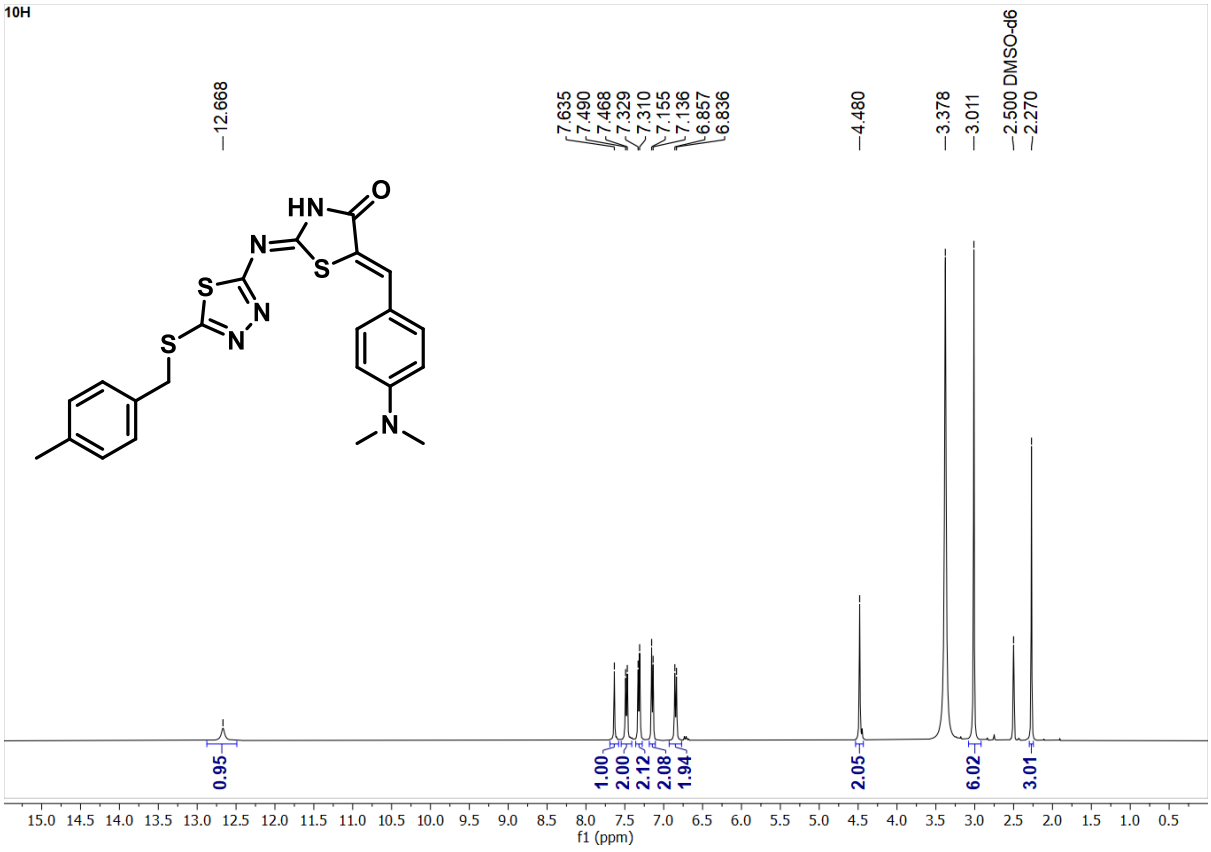

S.F34: ^{1}H NMR of compound **10h**

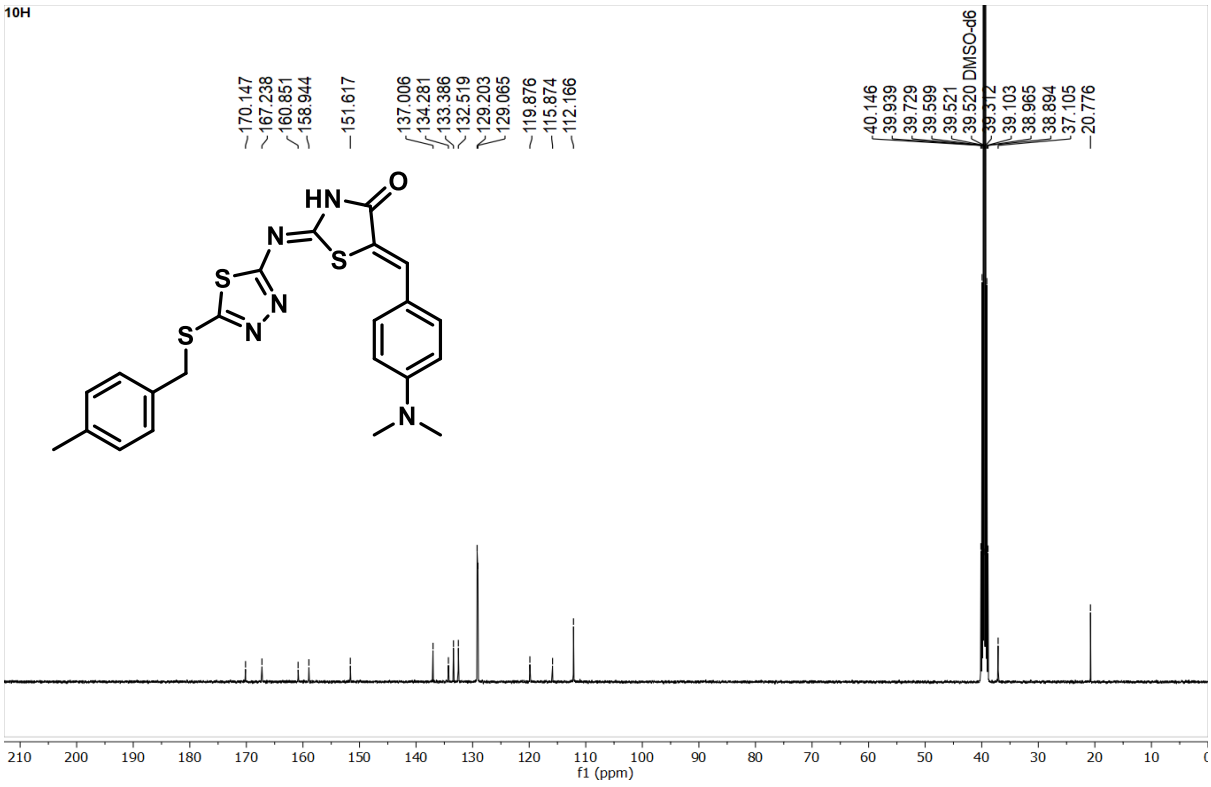

S.F34′: ^{13}C NMR of compound **10h**

2. Copy of HRMS (Q-TOF) Data:

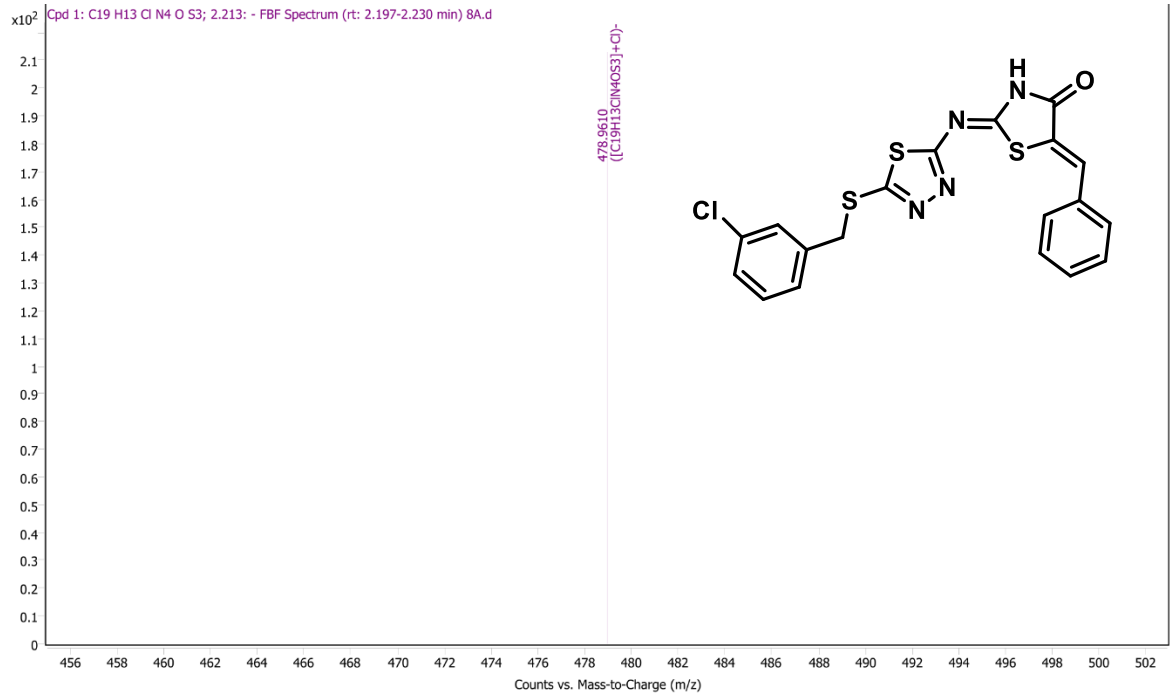

S.F35: HRMS data Compound **8a**

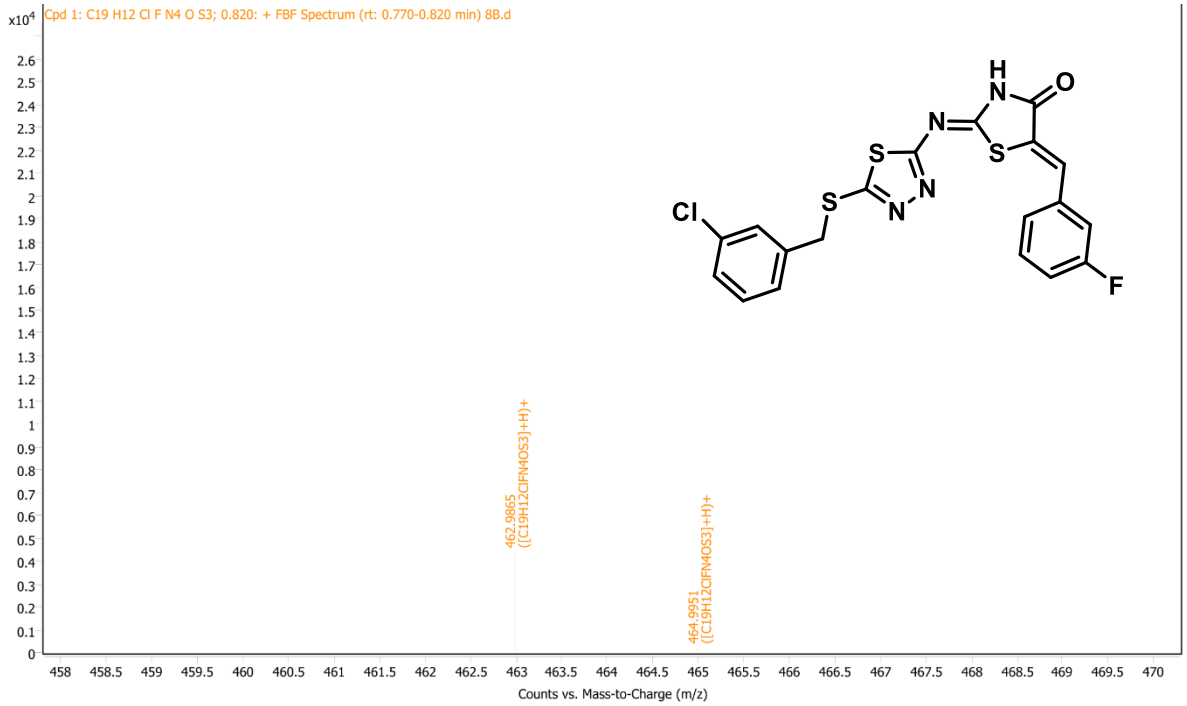

S.F36: HRMS data Compound **8b**

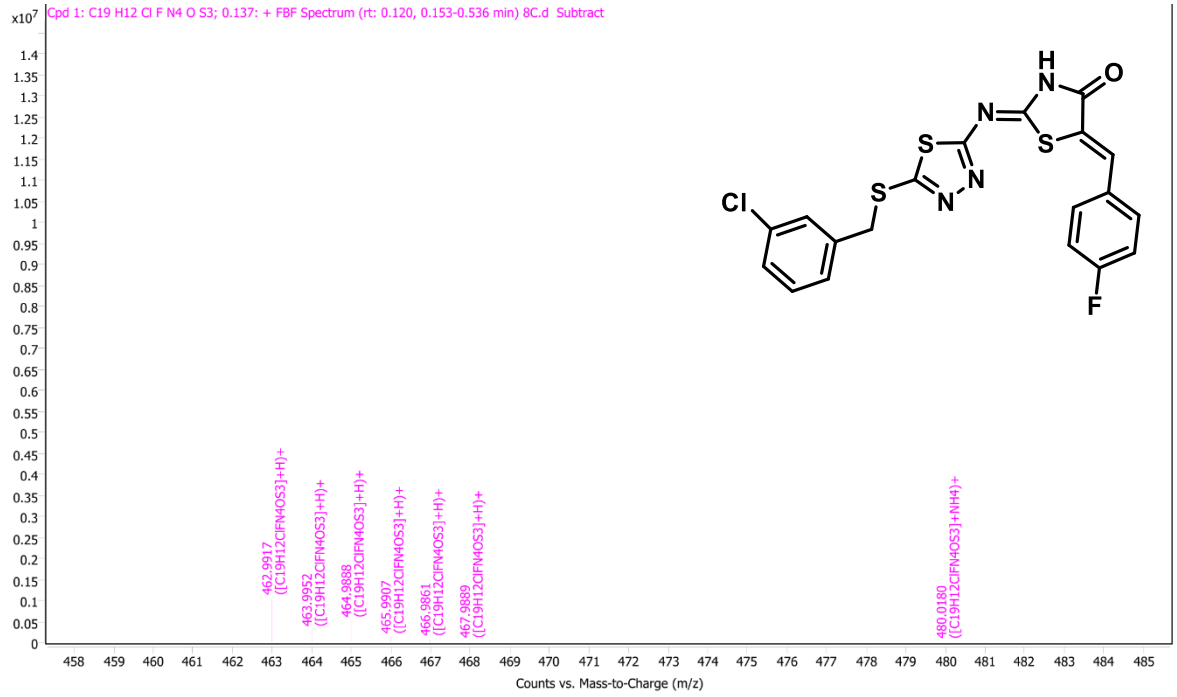

S.F37: HRMS data Compound **8c**

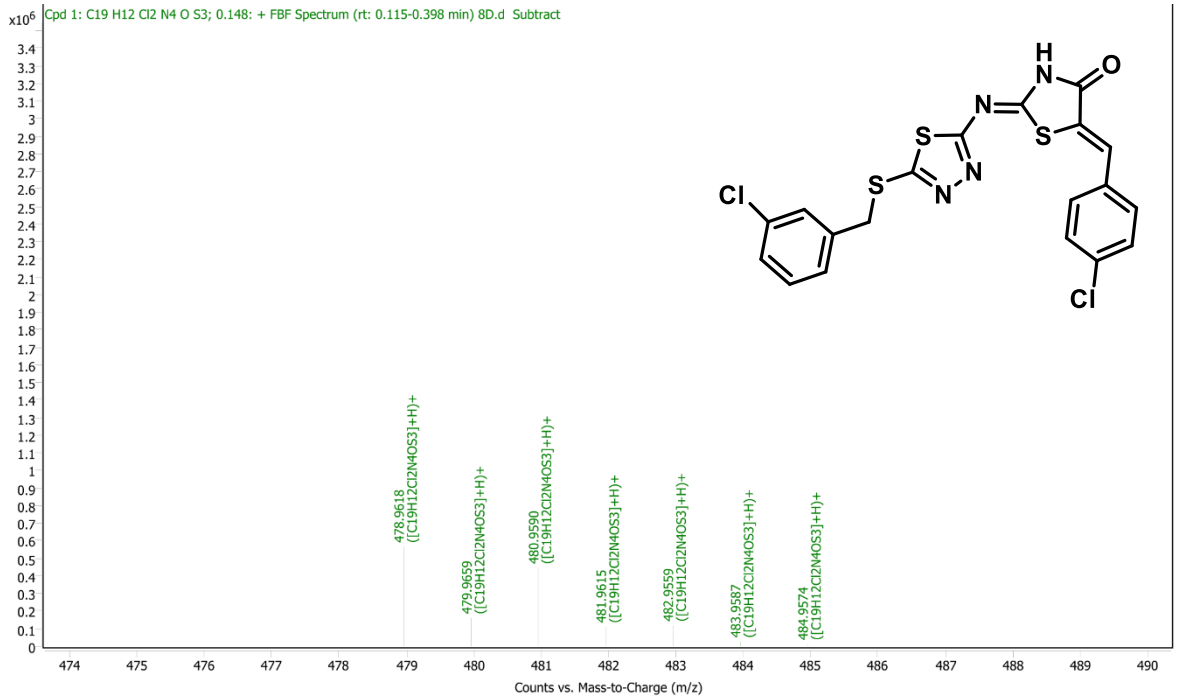

S.F38: HRMS data Compound **8d**

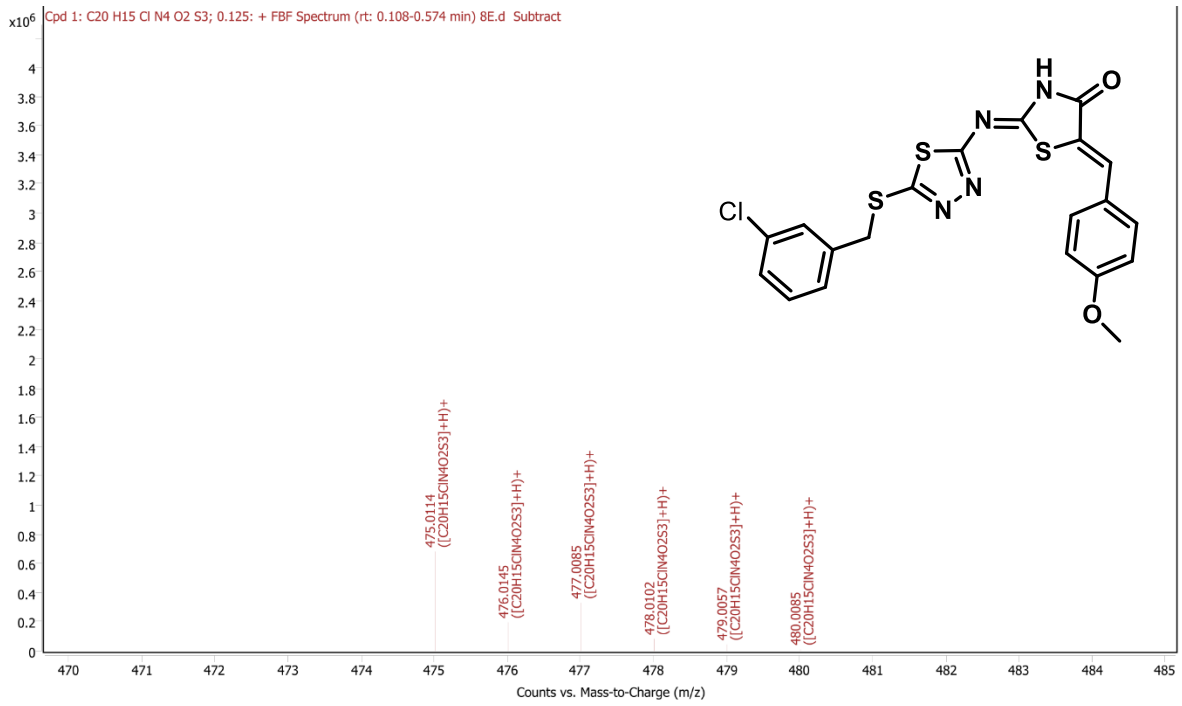

S.F39: HRMS data Compound **8e**

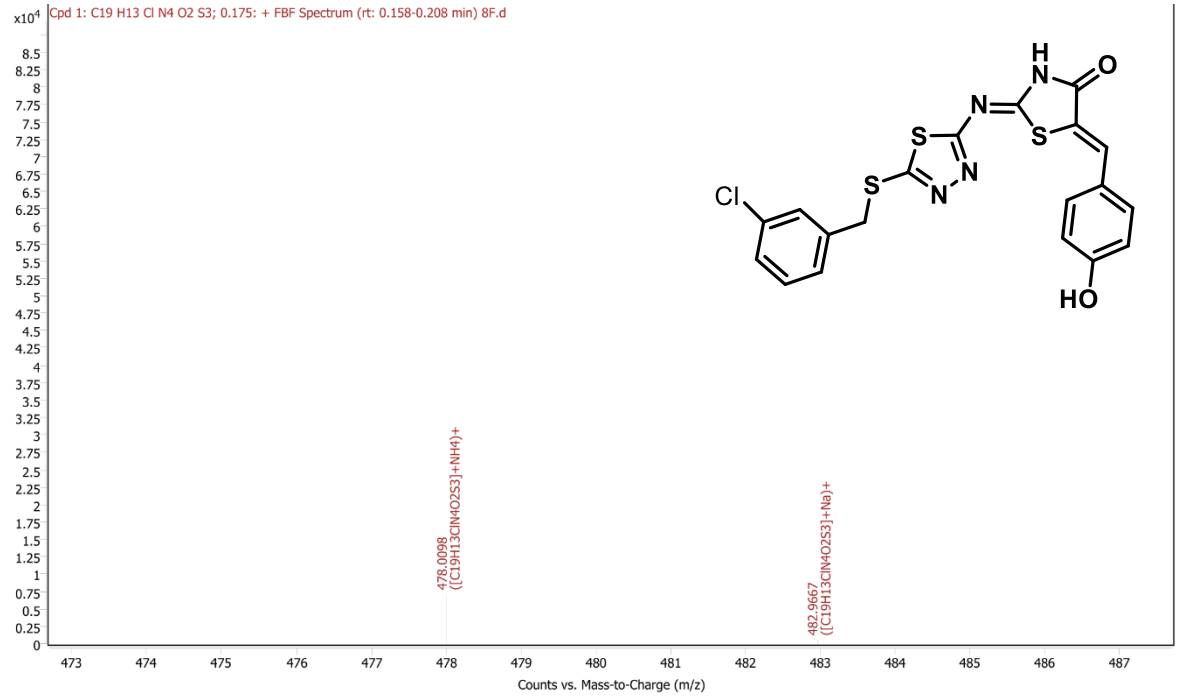

S.F40: HRMS data Compound **8f**

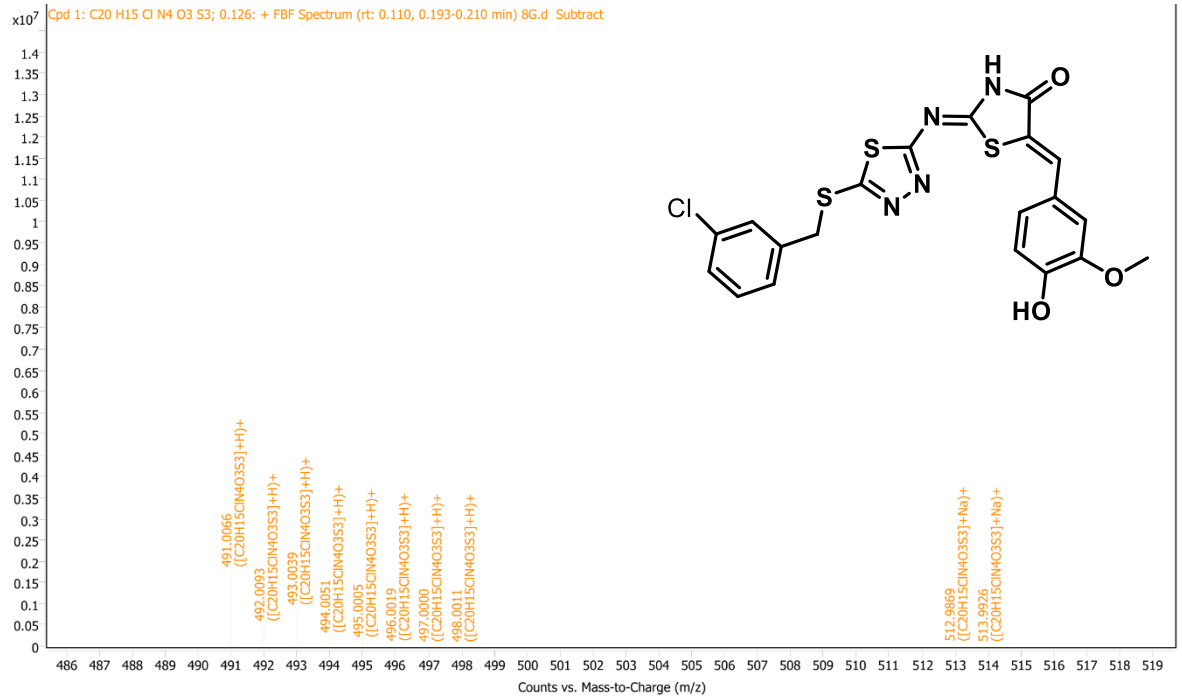

S.F41: HRMS data Compound **8g**

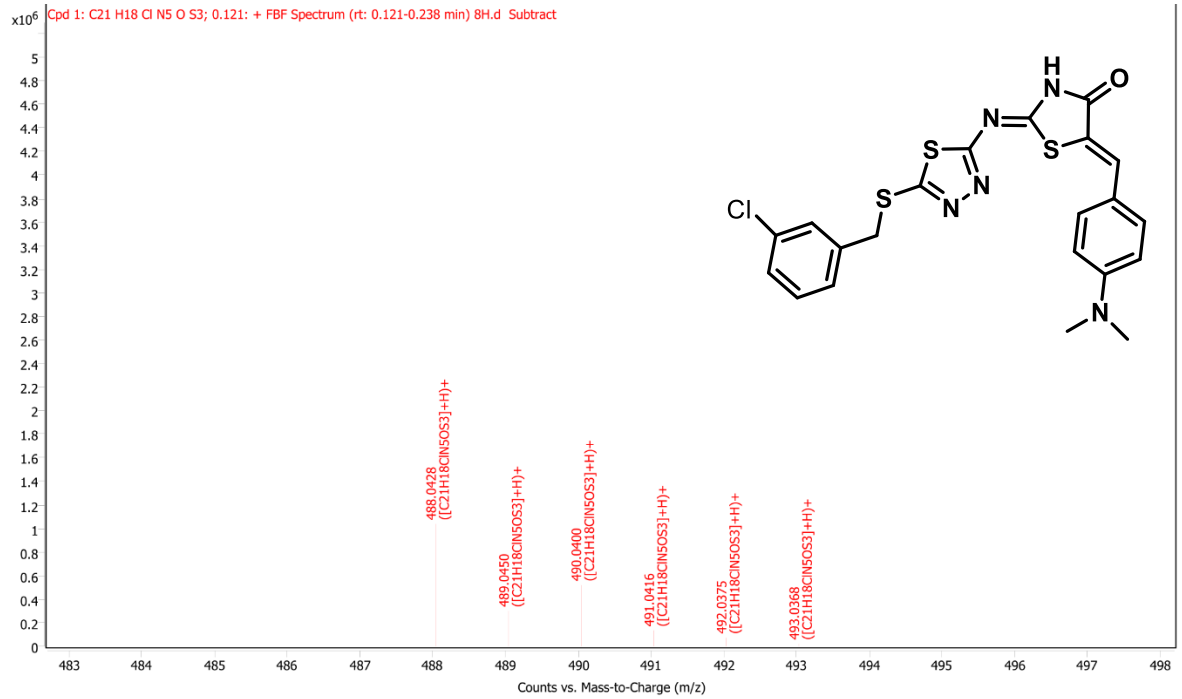

S.F42: HRMS data Compound **8h**

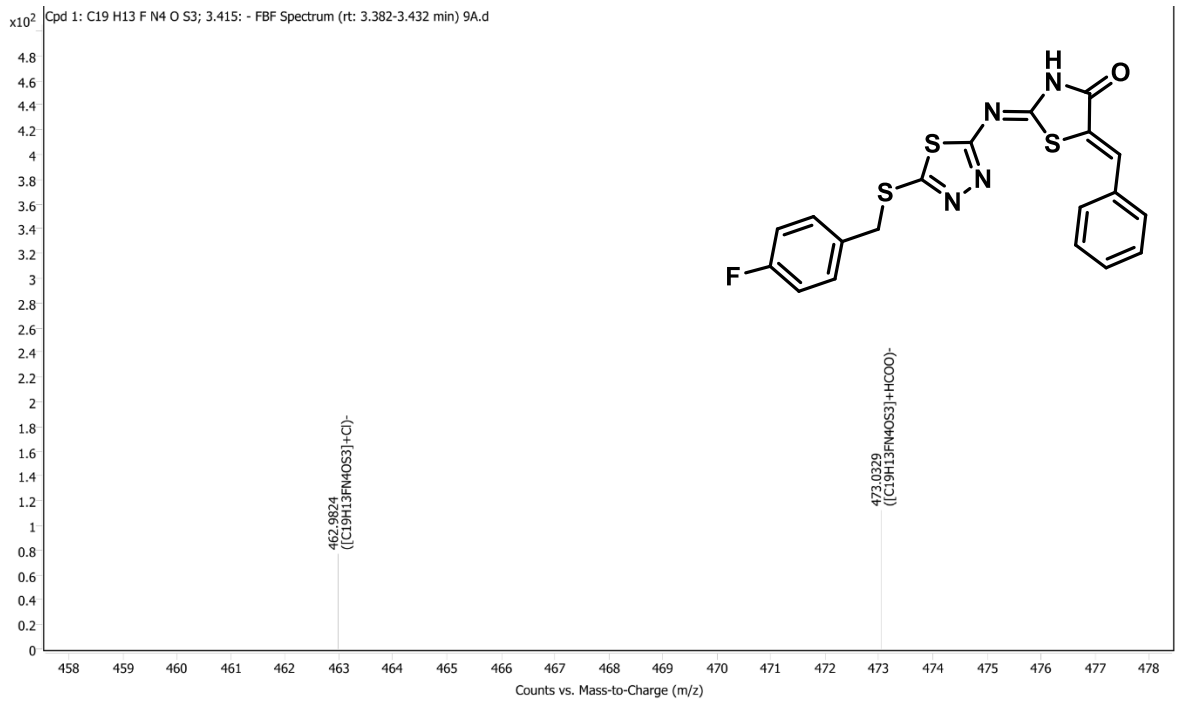

S.F43: HRMS data Compound **9a**

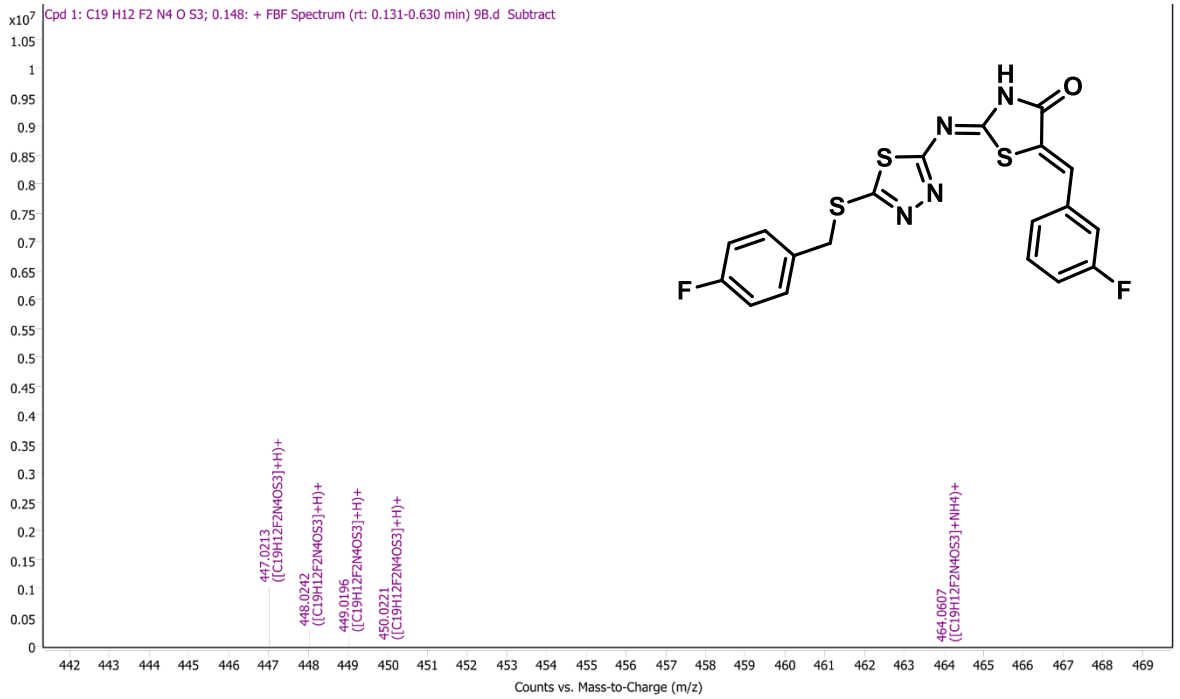

S.F44: HRMS data Compound **9b**

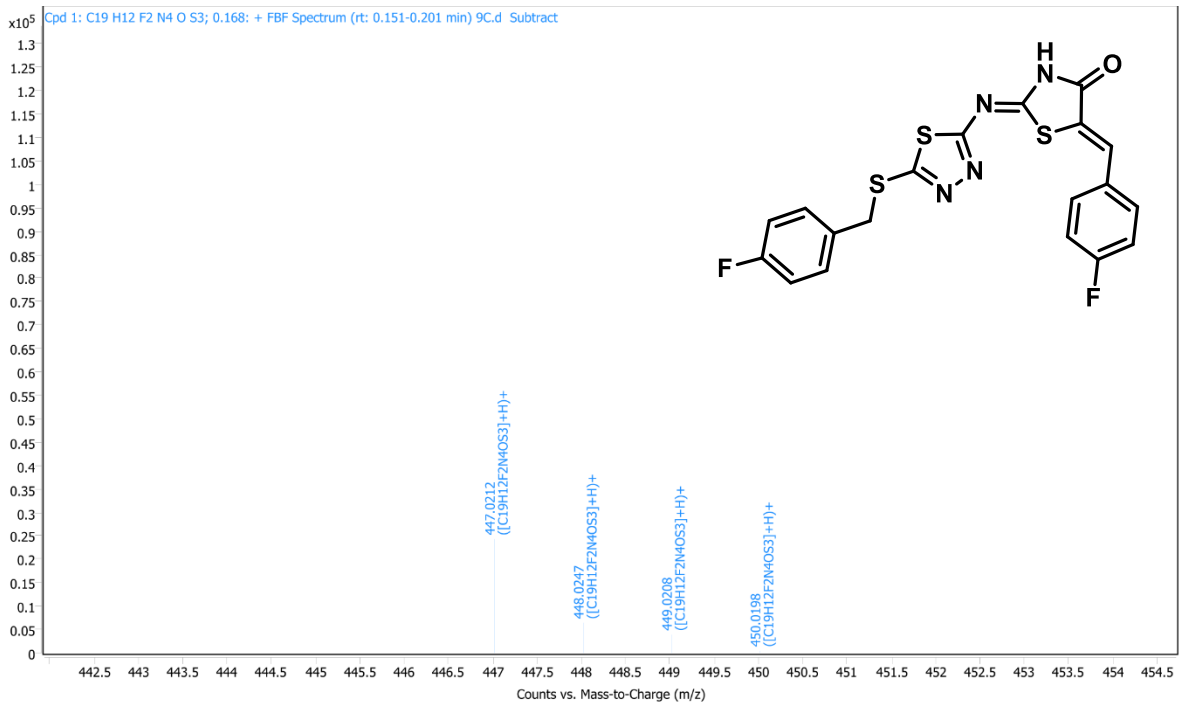

S.F45: HRMS data Compound **9c**

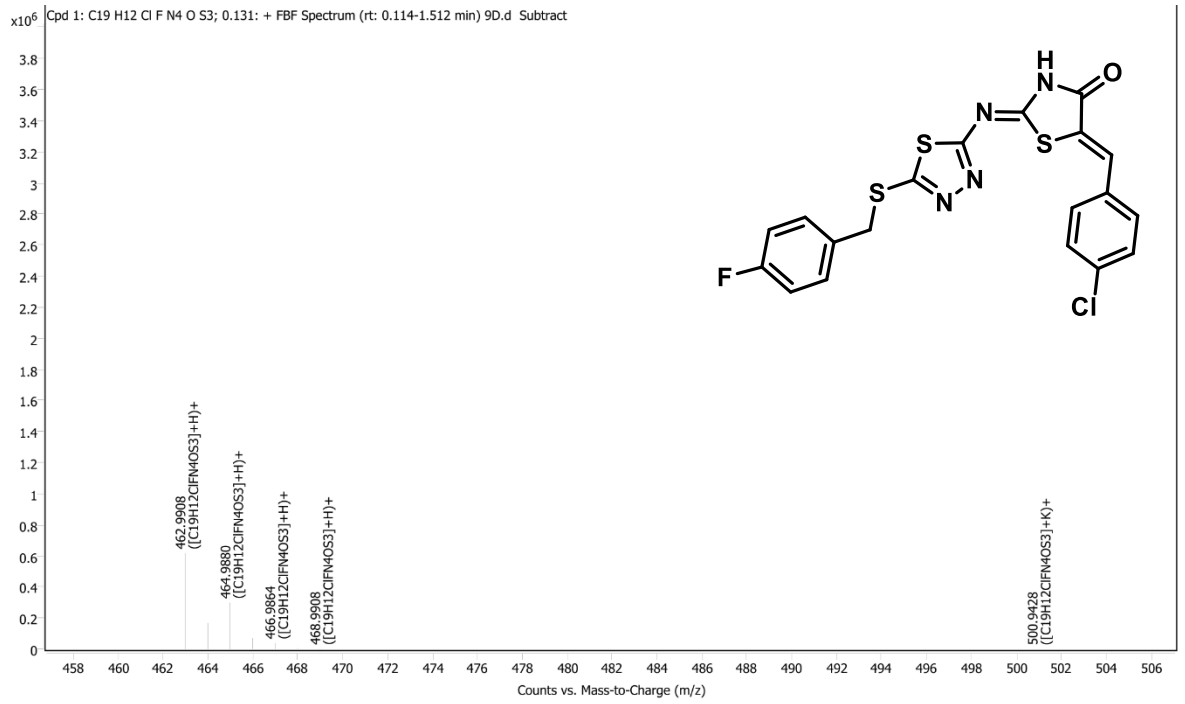

S.F46: HRMS data Compound **9d**

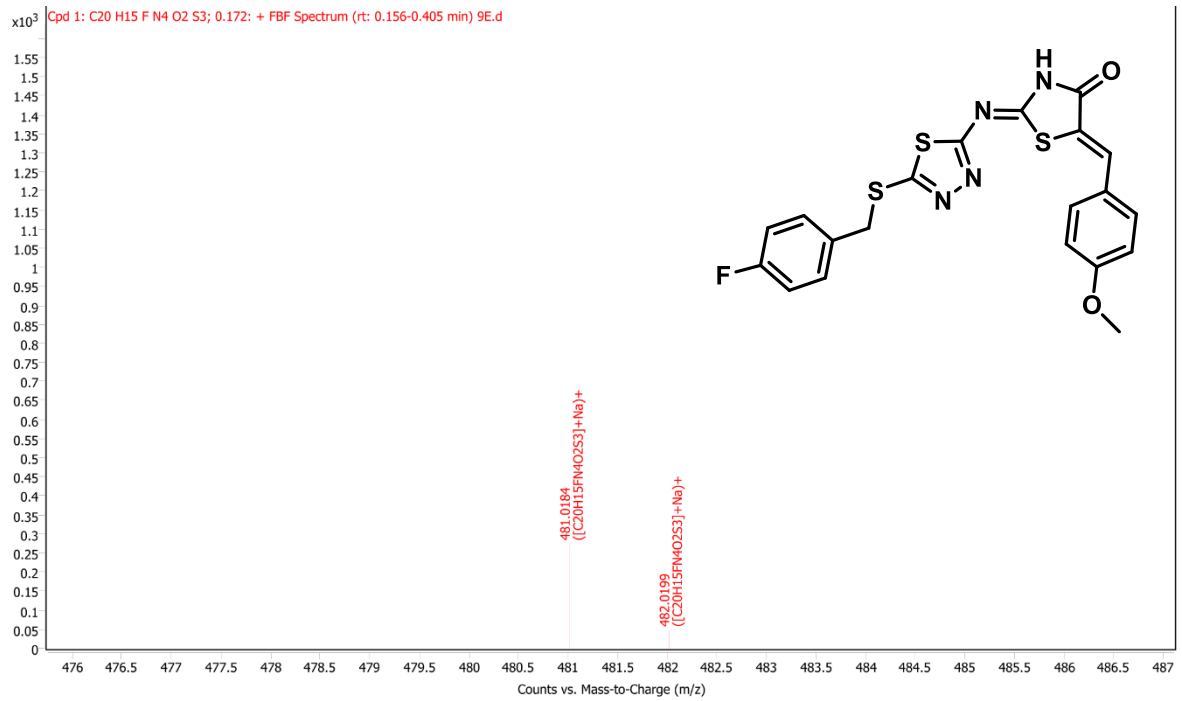

S.F47: HRMS data Compound **9e**

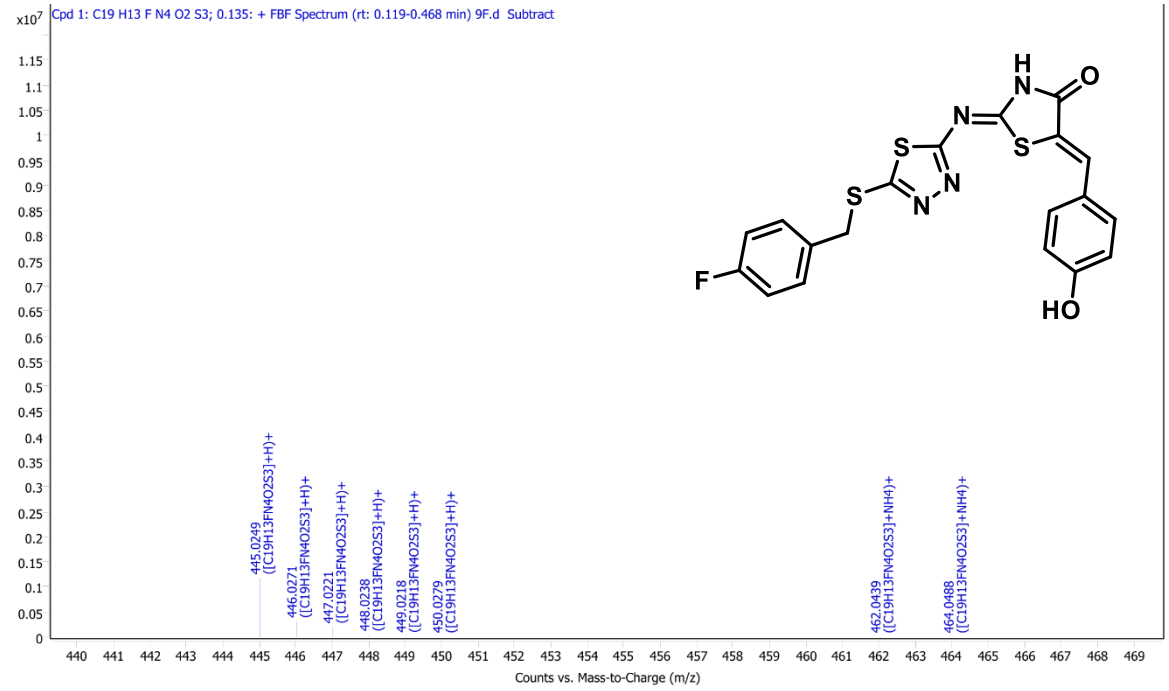

S.F48: HRMS data Compound **9f**

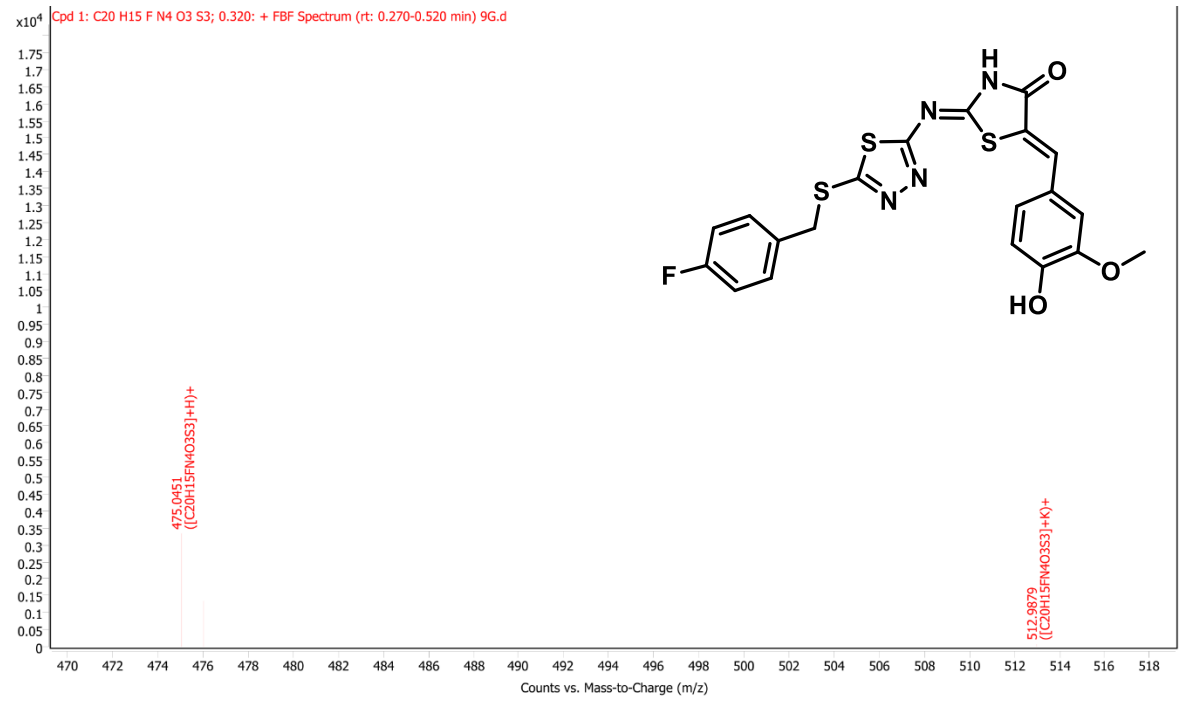

S.F49: HRMS data Compound **9g**

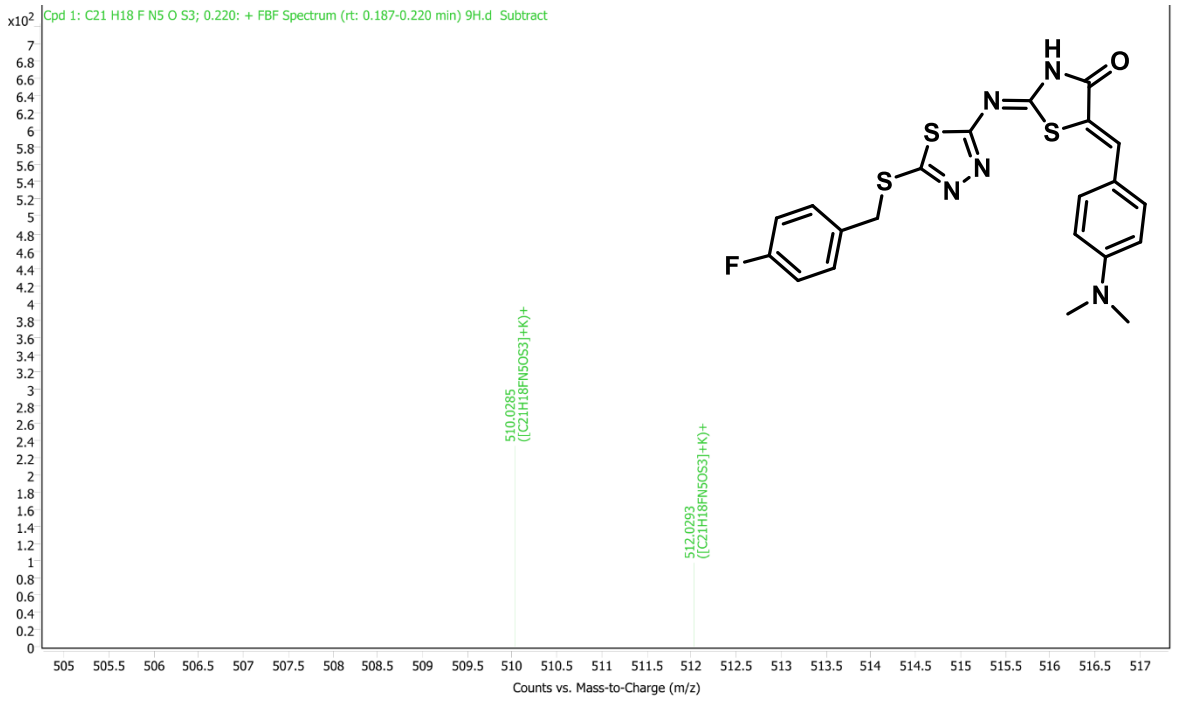

S.F50: HRMS data Compound **9h**

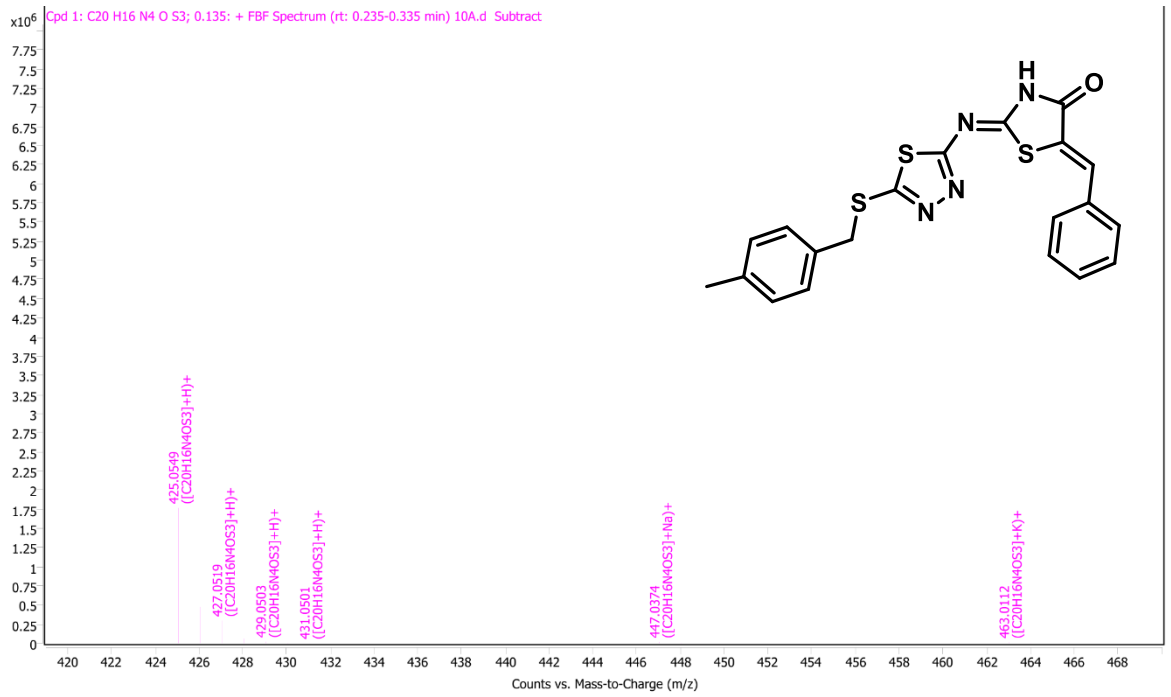

S.F51: HRMS data Compound **10a**

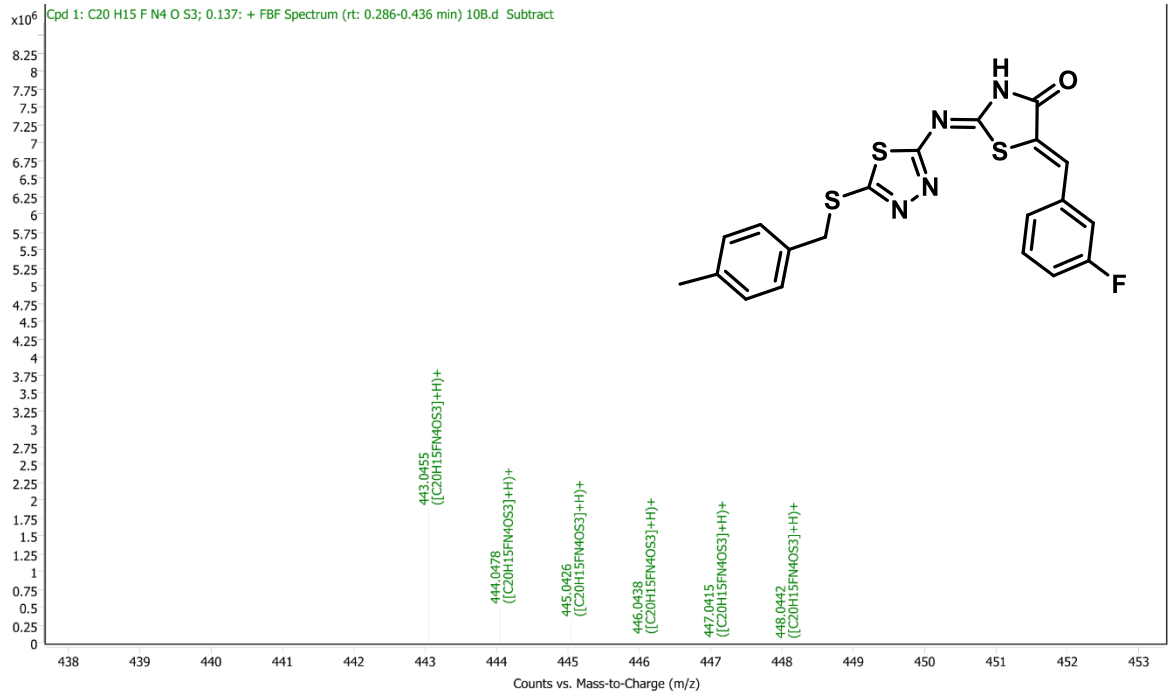

S.F52: HRMS data Compound **10b**

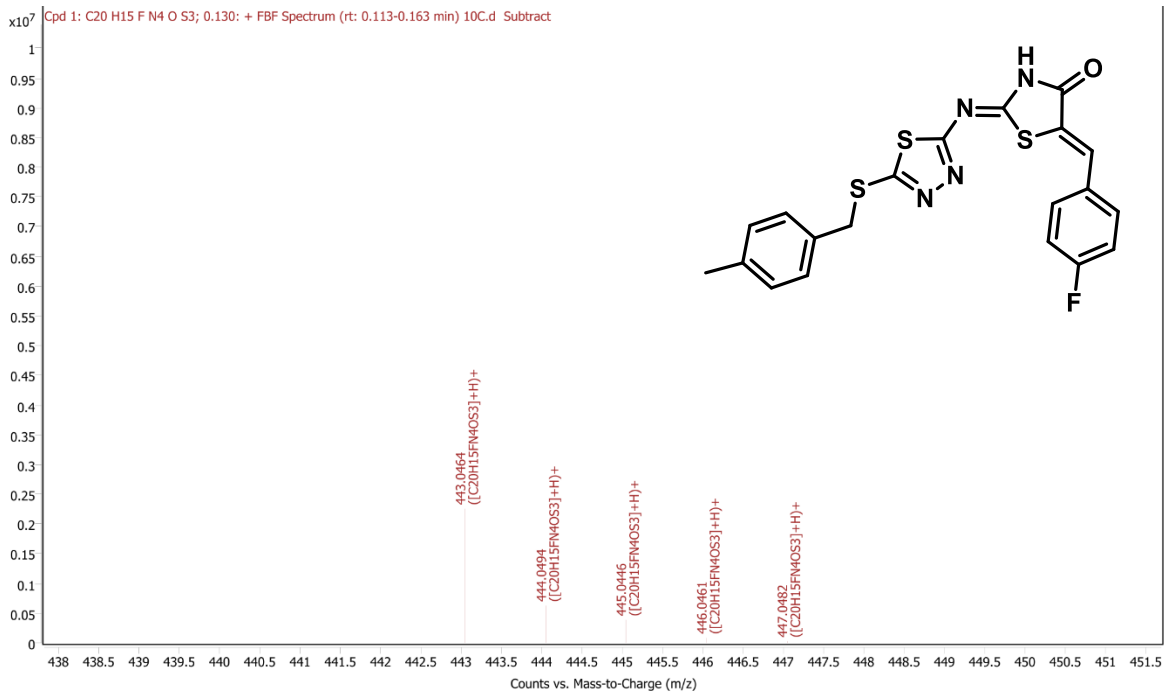

S.F53: HRMS data Compound **10c**

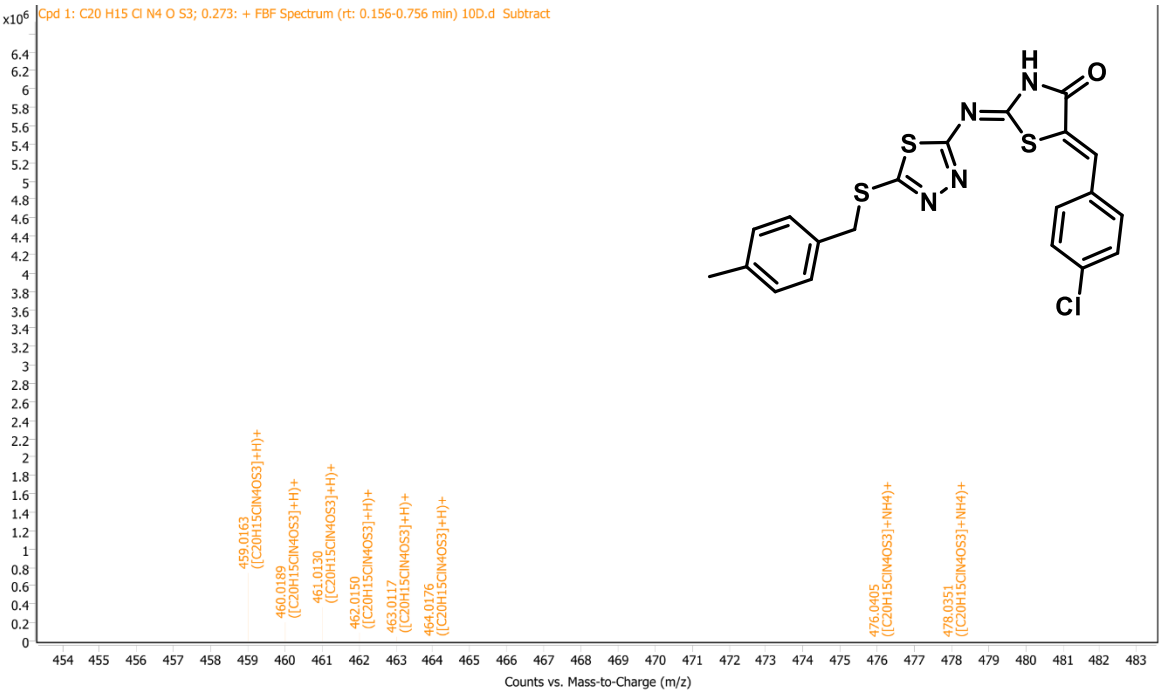

S.F54: HRMS data Compound **10d**

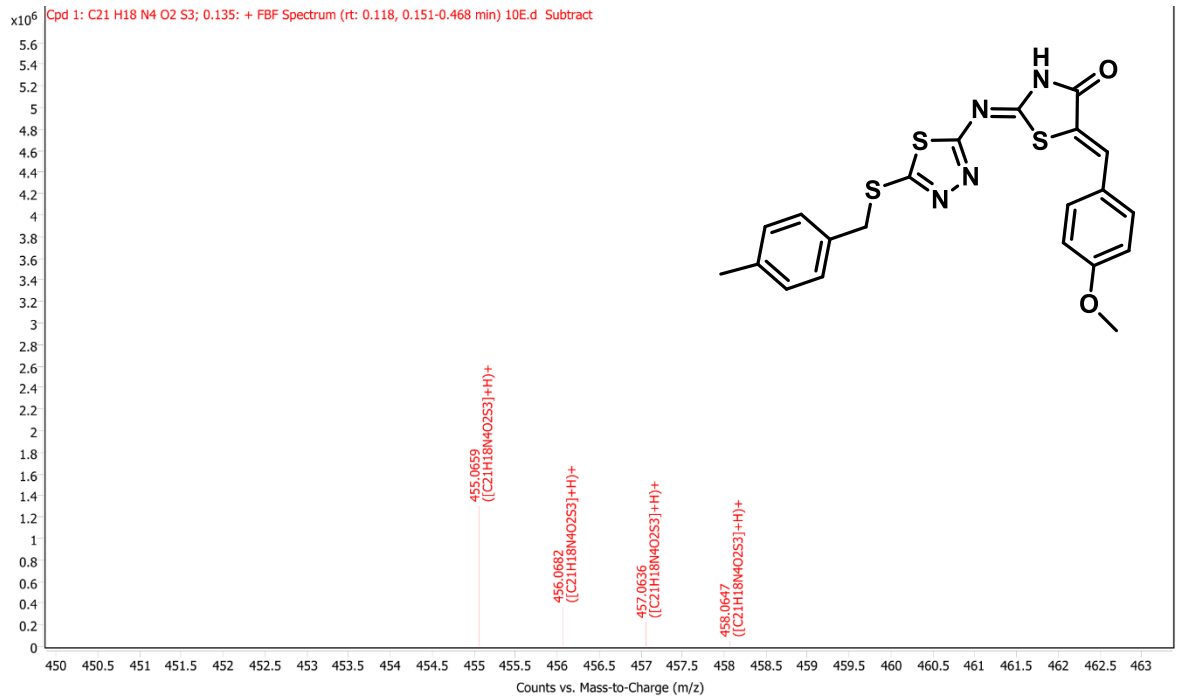

S.F55: HRMS data Compound **10e**

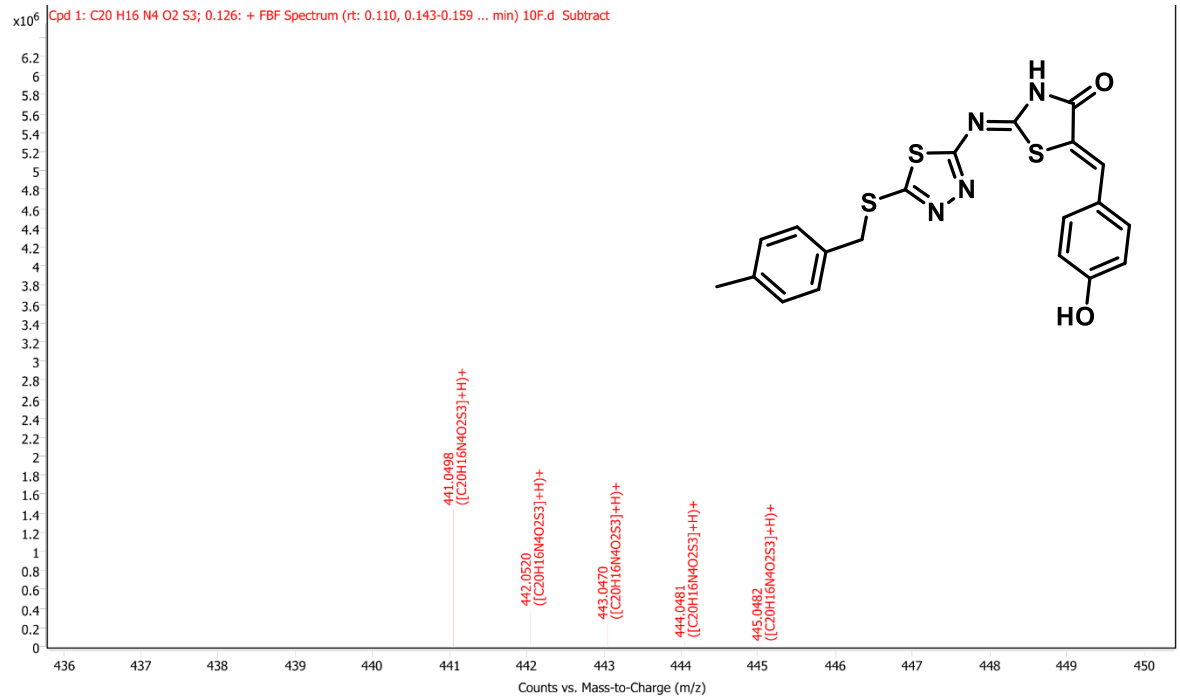

S.F56: HRMS data Compound **10f**

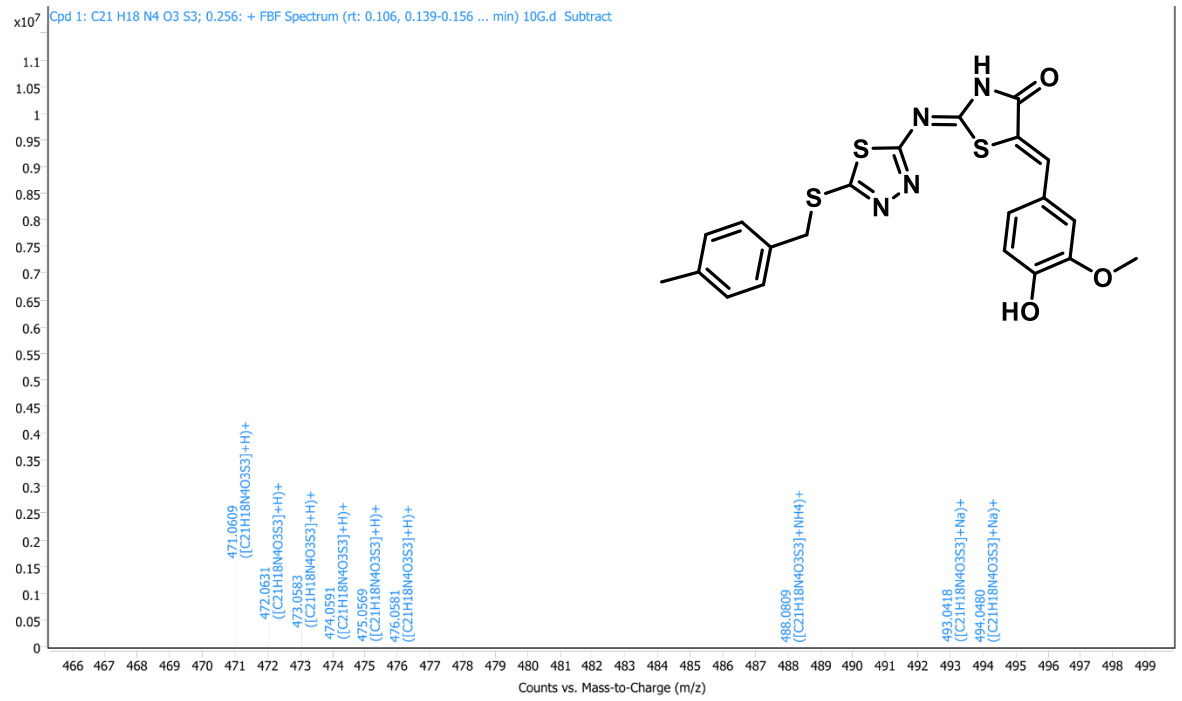

S.F57: HRMS data Compound **10g**

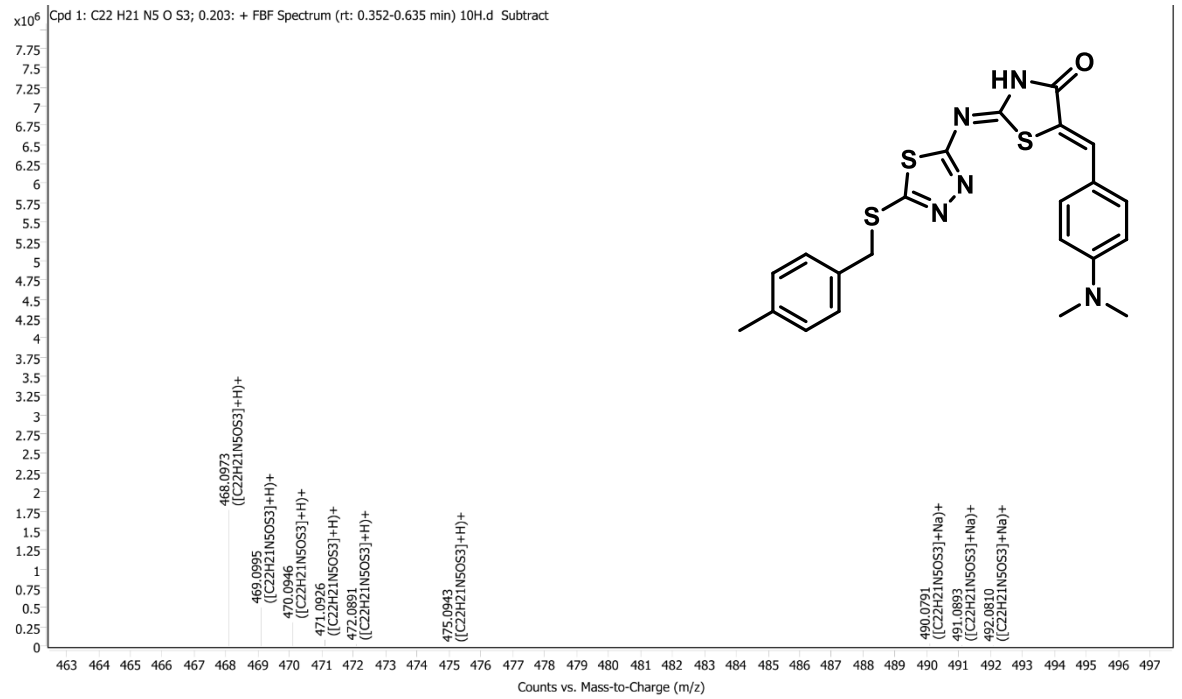

S.F58: HRMS data Compound **10h**

3. Supplementary data of X-ray crystallography:

X-ray crystallography of compound 9e:

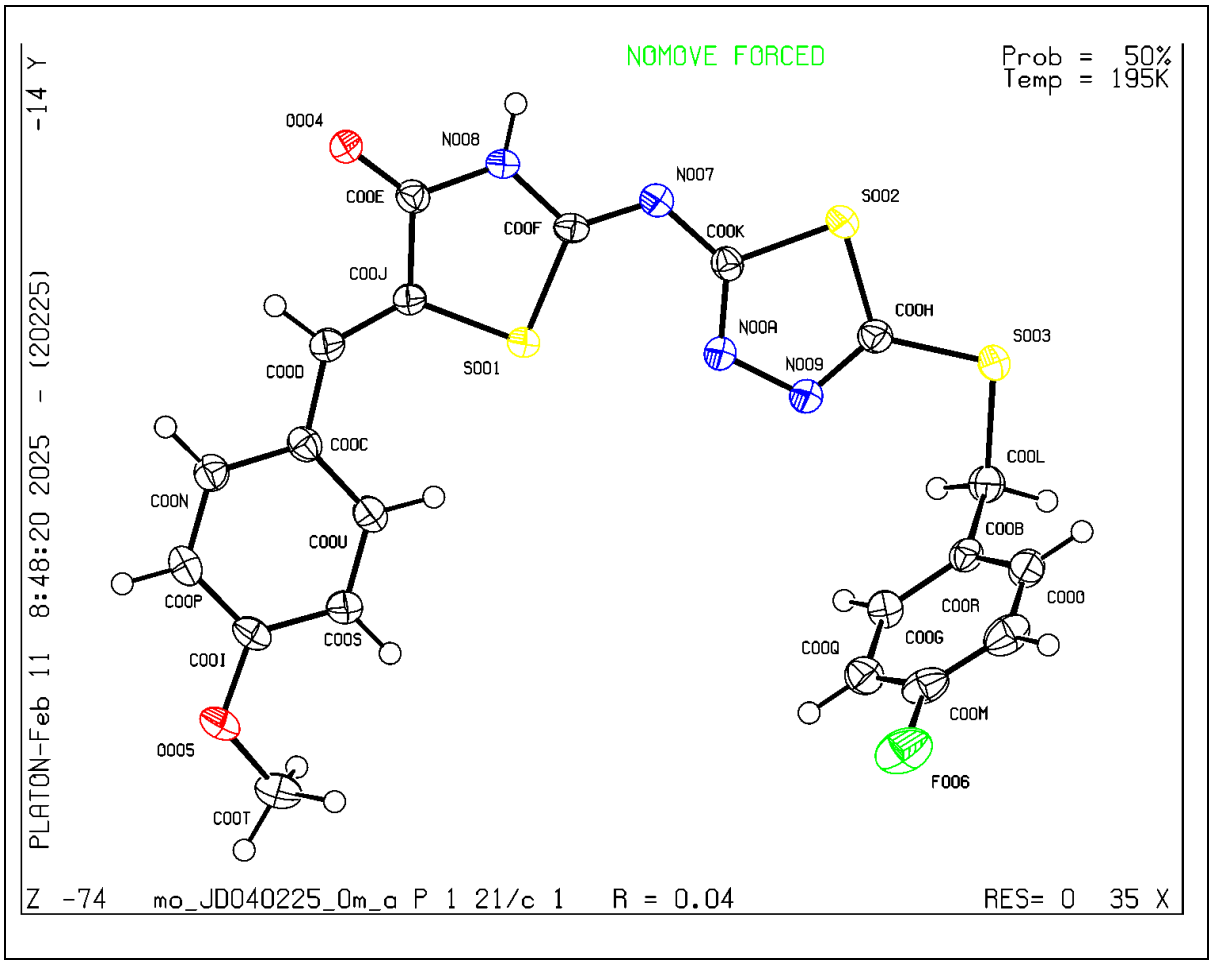

S.F59: Molecular geometries of compound **9e** in crystals.

Table S1: Crystallographic table (compound **9e):**

Complexes	**9e**
CCDC	2422956
Formula	$C_{20}H_{15}FN_4O_2S_3$
FW	458.54
Crystal system	Monoclinic
Space group	P 21/c
a (Å)	9.3081(16)
b (Å)	23.167(4)
c (Å)	9.5777(18)
α (°)	90

β (°)	106.744(6)
γ (°)	90
V (Å^3)	1977.8(6)
Z	4
T (K)	195
Dx, g cm-3	1.540
μ (mm^{-1})	0.411
R1[a][I>2σ(I)]/GOF[b]	0.0438/ 1.076
wR2[c] (I>2σ (I))	0.1291
Observation criterion: [a]R1 = $\Sigma\|\|F_o\|-\|F_c\|\|/\Sigma\|F_o\|$. [b]GOF = $\{\Sigma[w(F_o^2-F_c^2)^2]/(n-p)\}^{1/2}$, [c]$w$R2 = $[\Sigma[w(F_o^2-F_c^2)^2]/\Sigma[w(F_o^2)^2]]^{1/2}$ where $w = 1/[\sigma^2(F_o^2) + (aP)^2+bP]$, $P = (F_o^2+2F_c^2)/3$.	

NB: **S.F**-Spectral Figure

References:

[1] www.who.int/news-room/fact-sheets/detail/cancer, (n.d.).

[2] L.A. Torre, F. Bray, R.L. Siegel, J. Ferlay, J. Lortet-Tieulent, A. Jemal, Global cancer statistics, 2012, CA Cancer J Clin 65 (2015) 87–108. https://doi.org/10.3322/caac.21262.

[3] D.R. Youlden, S.M. Cramb, N.A.M. Dunn, J.M. Muller, C.M. Pyke, P.D. Baade, The descriptive epidemiology of female breast cancer: An international comparison of screening, incidence, survival and mortality, Cancer Epidemiol 36 (2012) 237–248. https://doi.org/10.1016/j.canep.2012.02.007.

[4] T.A. Theodossiou, M. Ali, M. Grigalavicius, B. Grallert, P. Dillard, K.O. Schink, C.E. Olsen, S. Wälchli, E.M. Inderberg, A. Kubin, Q. Peng, K. Berg, Simultaneous defeat of MCF7 and MDA-MB-231 resistances by a hypericin PDT–tamoxifen hybrid therapy, NPJ Breast Cancer 5 (2019) 13. https://doi.org/10.1038/s41523-019-0108-8.

[5] M.G. Salem, D.M.A. El-Maaty, Y.I.M. El-Deen, B.H. Elesawy, A. El Askary, A. Saleh, E.M. Saied, M. El Behery, Novel 1,3-Thiazole Analogues with Potent Activity against Breast Cancer: A Design, Synthesis, In Vitro, and In Silico Study, Molecules 27 (2022) 4898. https://doi.org/10.3390/molecules27154898.

[6] A. Maji, A. Paul, A. Sarkar, S. Nahar, R. Bhowmik, A. Samanta, P. Nahata, B. Ghosh, S. Karmakar, T. Kumar Maity, Significance of TRAIL/Apo-2 ligand and its death receptors in apoptosis and necroptosis signalling: Implications for cancer-targeted therapeutics, Biochem Pharmacol 221 (2024) 116041. https://doi.org/10.1016/j.bcp.2024.116041.

[7] S. Arora, P. Narayan, C.L. Osgood, S. Wedam, T.M. Prowell, J.J. Gao, M. Shah, D. Krol, S. Wahby, M. Royce, S. Ghosh, R. Philip, G. Ison, T. Berman, C. Brus, E.W. Bloomquist, M.H. Fiero, S. Tang, R. Pazdur, A. Ibrahim, L. Amiri-Kordestani, J.A. Beaver, U.S. FDA Drug Approvals for Breast Cancer: A Decade in Review, Clinical Cancer Research 28 (2022) 1072–1086. https://doi.org/10.1158/1078-0432.CCR-21-2600.

[8] J. An, C. Peng, X. Xie, F. Peng, New Advances in Targeted Therapy of HER2-Negative Breast Cancer, Front Oncol 12 (2022). https://doi.org/10.3389/fonc.2022.828438.

[9] W. Cui, A. Aouidate, S. Wang, Q. Yu, Y. Li, S. Yuan, Discovering Anti-Cancer Drugs via Computational Methods, Front Pharmacol 11 (2020). https://doi.org/10.3389/fphar.2020.00733.

[10] C.R. Quijia, M. Chorilli, Piperine for treating breast cancer: A review of molecular mechanisms, combination with anticancer drugs, and nanosystems, Phytotherapy Research 36 (2022) 147–163. https://doi.org/10.1002/ptr.7291.

[11] A. Maji, A. Himaja, S. Nikhitha, S. Rana, A. Paul, A. Samanta, U. Shee, C. Mukhopadhyay, B. Ghosh, T.K. Maity, Synthesis and antiproliferative potency of 1,3,4-thiadiazole and 1,3-thiazolidine-4-one based new binary heterocyclic molecules: *in*

vitro cell-based anticancer studies, RSC Med Chem 15 (2024) 3057–3069. https://doi.org/10.1039/D4MD00279B.

[12] A. Paul, S.S. Mishra, A. Sarkar, R. Bhowmik, A. De, A. Maji, U. Shee, A. Samanta, S. Karmakar, T.K. Maity, Synthesis, single crystal XRD, in vitro evaluation, molecular docking and ADMET studies of cuminaldehyde-thiazolidine-2,4-dione hybrids as potential α-glucosidase inhibitors, J Mol Struct 1331 (2025) 141510. https://doi.org/10.1016/j.molstruc.2025.141510.

[13] M. Fawzi, A. Oubella, A. El Mansouri, A. Bimoussa, E.M. Ketatni, M. Saadi, L. El Ammari, M.Y. Ait Itto, H. Morjani, A. Auhmani, Novel Hydrazono-2-Iminothiazolidin-4-Ones Based on a Monoterpenic Skeleton as Potential Antitumor Agents: Synthesis, DFT Studies, *in Vitro* Cytotoxicity, Apoptosis Inducing Properties and Molecular Docking, Chem Biodivers 19 (2022). https://doi.org/10.1002/cbdv.202100836.

[14] S.M. Gomha, M.M. Edress, Z.A. Muhammad, H.M. Gaber, M.M. Amin, I.K. Matar, Synthesis Under Microwave Irradiation and Molecular Docking of Some Novel Bioactive Thiadiazoles, Mini-Reviews in Medicinal Chemistry 19 (2019) 437–447. https://doi.org/10.2174/1389557518666180329122317.

[15] A. Bimoussa, A. Oubella, F.Z. Bamou, Z.A. Khdar, M. Fawzi, Y. Laamari, M.Y. Ait Itto, H. Morjani, A. Auhmani, New 1,3,4-thiadiazoles Derivatives: Synthesis, Antiproliferative Activity, Molecular Docking and Molecular Dynamics, Future Med Chem 14 (2022) 881–897. https://doi.org/10.4155/fmc-2022-0016.

[16] N.S. El-Gohary, M.I. Shaaban, Synthesis, antimicrobial, antiquorum-sensing, antitumor and cytotoxic activities of new series of fused [1,3,4]thiadiazoles, Eur J Med Chem 63 (2013) 185–195. https://doi.org/10.1016/j.ejmech.2013.02.010.

[17] K.-Y. Jung, S.-K. Kim, Z.-G. Gao, A.S. Gross, N. Melman, K.A. Jacobson, Y.-C. Kim, Structure–activity relationships of thiazole and thiadiazole derivatives as potent and selective human adenosine A3 receptor antagonists, Bioorg Med Chem 12 (2004) 613–623. https://doi.org/10.1016/j.bmc.2003.10.041.

[18] L. Hosseinzadeh, A. Khorand, A. Aliabadi, Discovery of 2- <scp>P</scp> henyl- <scp> *N* </scp> -(5-(trifluoromethyl)-1,3,4-thiadiazol-2-yl)acetamide Derivatives as Apoptosis Inducers via the Caspase Pathway with Potential Anticancer Activity, Arch Pharm (Weinheim) 346 (2013) 812–818. https://doi.org/10.1002/ardp.201300180.

[19] A. Mohammadi-Farani, N. Heidarian, A. Aliabadi, N-(5-Mercapto-1,3,4-Thiadiazol-2-yl)-2-Phenylacetamide Derivatives: Synthesis and In-vitro Cytotoxicity Evaluation as Potential Anticancer Agents., Iran J Pharm Res 13 (2014) 487–92.

[20] X. Li, D. Wang, S. Li, W. Xue, X. Qian, K. Liu, Y. Li, Q. Lin, G. Dong, F. Meng, L. Jian, Discovery of N-(1,3,4-thiadiazol-2-yl)benzamide derivatives containing a 6,7-methoxyquinoline structure as novel EGFR/HER-2 dual-target inhibitors against cancer growth and angiogenesis, Bioorg Chem 119 (2022) 105469. https://doi.org/10.1016/j.bioorg.2021.105469.

[21] M.I. Serag, S.S. Tawfik, H.M. Eisa, S.M.I. Badr, Design, Synthesis, Biological Evaluation and Molecular Docking Study of New 1,3,4-Thiadiazole-Based Compounds as EGFR Inhibitors, Drug Dev Res 86 (2025). https://doi.org/10.1002/ddr.70035.

[22] A. Aghcheli, M. Toolabi, A. Ayati, S. Moghimi, L. Firoozpour, T.O. Bakhshaiesh, E. Nazeri, M. Norouzbahari, R. Esmaeili, A. Foroumadi, Design, synthesis, and biological evaluation of 1-(5-(benzylthio)-1,3,4-thiadiazol-2-yl)-3-phenylurea derivatives as anticancer agents, Medicinal Chemistry Research 29 (2020) 2000–2010. https://doi.org/10.1007/s00044-020-02616-2.

[23] A. Faraji, T. Oghabi Bakhshaiesh, Z. Hasanvand, R. Motahari, E. Nazeri, M.A. Boshagh, L. Firoozpour, H. Mehrabi, A. Khalaj, R. Esmaeili, A. Foroumadi, Design, synthesis and evaluation of novel thienopyrimidine-based agents bearing diaryl urea functionality as potential inhibitors of angiogenesis, Eur J Med Chem 209 (2021) 112942. https://doi.org/10.1016/j.ejmech.2020.112942.

[24] W.-S. Liu, J.-F. Zhao, X.-J. Guo, S.-Z. Lu, W. Li, W.-Z. Li, Design, synthesis, activity and molecular dynamics studies of 1,3,4-thiadiazole derivatives as selective allosteric inhibitors of SHP2 for the treatment of cancer, Eur J Med Chem 258 (2023) 115585. https://doi.org/10.1016/j.ejmech.2023.115585.

[25] T. Yang, Y. Tian, Y. Yang, M. Tang, M. Shi, Y. Chen, Z. Yang, L. Chen, Design, synthesis, and pharmacological evaluation of 2-(1-(1,3,4-thiadiazol-2-yl)piperidin-4-yl)ethan-1-ol analogs as novel glutaminase 1 inhibitors, Eur J Med Chem 243 (2022) 114686. https://doi.org/10.1016/j.ejmech.2022.114686.

[26] A. Ayati, S. Emami, A. Asadipour, A. Shafiee, A. Foroumadi, Recent applications of 1,3-thiazole core structure in the identification of new lead compounds and drug discovery, Eur J Med Chem 97 (2015) 699–718. https://doi.org/10.1016/j.ejmech.2015.04.015.

[27] A.M. Isloor, D. Sunil, P. Shetty, S. Malladi, K.S.R. Pai, N. Maliyakkl, Synthesis, characterization, anticancer, and antioxidant activity of some new thiazolidin-4-ones in MCF-7 cells, Medicinal Chemistry Research 22 (2013) 758–767. https://doi.org/10.1007/s00044-012-0071-5.

[28] S. D Shankara, A.M. Isloor, P.K. Jayaswamy, P. Shetty, D. Chakraborty, P.P. Venugopal, Vetting of New 2,5-Bis (2,2,2-trifluoroethoxy) Phenyl-Linked 1,3-Thiazolidine-4-one Derivatives as AURKA and VEGFR-2 Inhibitor Antiglioma Agents Assisted with In Vitro and In Silico Studies, ACS Omega 8 (2023) 43596–43609. https://doi.org/10.1021/acsomega.3c04662.

[29] H.N. Tawfeek, A.A. Hassan, S. Bräse, M. Nieger, Y.A. Mostafa, H.A.M. Gomaa, B.G.M. Youssif, E.M. El-Shreef, Design, synthesis, crystal structures and biological evaluation of some 1,3-thiazolidin-4-ones as dual CDK2/EGFR potent inhibitors with potential apoptotic antiproliferative effects, Arabian Journal of Chemistry 15 (2022) 104280. https://doi.org/10.1016/j.arabjc.2022.104280.

[30] B. Qi, X. Xu, Y. Yang, Y. Zhou, T. Chen, G. Gong, X. Yue, X. Xu, L. Hu, H. He, Discovery of thiazolidin-4-one urea analogues as novel multikinase inhibitors that potently inhibit FLT3 and VEGFR2, Bioorg Med Chem 27 (2019) 2127–2139. https://doi.org/10.1016/j.bmc.2019.03.049.

[31] N.O. Mahmoodi, M. Mohammadi Zeydi, E. Biazar, Z. Kazeminejad, Synthesis of novel thiazolidine-4-one derivatives and their anticancer activity, Phosphorus Sulfur Silicon Relat Elem 192 (2017) 344–350. https://doi.org/10.1080/10426507.2016.1239197.

[32] Z.Y. Kadhim, H.G.J. Alqaraghuli, M.T. Abd, Synthesis, Characterization, Molecular Docking, In Vitro Biological Evaluation and In Vitro Cytotoxicity Study of Novel Thiazolidine-4-One Derivatives as Anti-Breast Cancer Agents, Anticancer Agents Med Chem 21 (2021) 2397–2406. https://doi.org/10.2174/1871520621666210401100801.

[33] Y.O. Mekhlef, A.M. AboulMagd, A.M. Gouda, Design, Synthesis, Molecular docking, and biological evaluation of novel 2,3-diaryl-1,3-thiazolidine-4-one derivatives as potential anti-inflammatory and cytotoxic agents, Bioorg Chem 133 (2023) 106411. https://doi.org/10.1016/j.bioorg.2023.106411.

[34] S. Shahjahan, L.T. Naraharisetti, A. Begum, P.A. Yakkala, P.S. Lakshmi Soukya, C. Godugu, S.A. Begum, A. Kamal, Oxindoline Containing Thiazolidine-4-one Tethered Triazoles Act as Antimitotic Agents by Targeting Microtubule Dynamics, ChemistrySelect 9 (2024). https://doi.org/10.1002/slct.202400539.

[35] S. Pulya, T. Patel, M. Paul, N. Adhikari, S. Banerjee, G. Routholla, S. Biswas, T. Jha, B. Ghosh, Selective inhibition of histone deacetylase 3 by novel hydrazide based small molecules as therapeutic intervention for the treatment of cancer, Eur J Med Chem 238 (2022) 114470. https://doi.org/10.1016/j.ejmech.2022.114470.

[36] G. Routholla, S. Pulya, T. Patel, N. Adhikari, Sk. Abdul Amin, M. Paul, S. Bhagavatula, S. Biswas, T. Jha, B. Ghosh, Design, synthesis and binding mode of interaction of novel small molecule o-hydroxy benzamides as HDAC3-selective inhibitors with promising antitumor effects in 4T1-Luc breast cancer xenograft model, Bioorg Chem 117 (2021) 105446. https://doi.org/10.1016/j.bioorg.2021.105446.

[37] G. Routholla, S. Pulya, T. Patel, Sk. Abdul Amin, N. Adhikari, S. Biswas, T. Jha, B. Ghosh, Synthesis, biological evaluation, and molecular docking analysis of novel linker-less benzamide based potent and selective HDAC3 inhibitors, Bioorg Chem 114 (2021) 105050. https://doi.org/10.1016/j.bioorg.2021.105050.

[38] P. Trivedi, N. Adhikari, Sk.A. Amin, T. Jha, B. Ghosh, Design, synthesis and biological screening of 2-aminobenzamides as selective HDAC3 inhibitors with promising anticancer effects, European Journal of Pharmaceutical Sciences 124 (2018) 165–181. https://doi.org/10.1016/j.ejps.2018.08.030.

[39] S. Pulya, A. Himaja, M. Paul, N. Adhikari, S. Banerjee, G. Routholla, S. Biswas, T. Jha, B. Ghosh, Selective HDAC3 Inhibitors with Potent In Vivo Antitumor Efficacy against Triple-Negative Breast Cancer, J Med Chem 66 (2023) 12033–12058. https://doi.org/10.1021/acs.jmedchem.3c00614.

[40] R. Aluri, A. Natarajan, T. Patel, D. Begum, J. Kumari, D. Sriram, B. Ghosh, K. Rangan, Synthesis, characterisation, single crystal structure and evaluation of a redox innocent carbazate functionalized phenanthroline for antimycobacterial and anticancer activity, J Mol Struct 1323 (2025) 140729. https://doi.org/10.1016/j.molstruc.2024.140729.

[41] S.K. Baidya, T. Patel, A. Himaja, S. Banerjee, S. Das, B. Ghosh, T. Jha, N. Adhikari, Biphenylsulfonamides as effective MMP-2 inhibitors with promising antileukemic efficacy: Synthesis, in vitro biological evaluation, molecular docking, and MD simulation analysis, Drug Dev Res 85 (2024). https://doi.org/10.1002/ddr.22255.

[42] S. Das, S. Mondal, T. Patel, A. Himaja, N. Adhikari, S. Banerjee, S.K. Baidya, A.K. De, S. Gayen, B. Ghosh, T. Jha, Derivatives of D(−) glutamine-based MMP-2 inhibitors as an effective remedy for the management of chronic myeloid leukemia-Part-I: Synthesis, biological screening and in silico binding interaction analysis, Eur J Med Chem 274 (2024) 116563. https://doi.org/10.1016/j.ejmech.2024.116563.

[43] S. Das, T. Patel, A. Himaja, S. Regula, S. Banerjee, A.K. De, I.A. Qureshi, S. Gayen, B. Ghosh, N. Adhikari, T. Jha, Derivatives of D(−)-glutamine-based MMP-2 inhibitors as an effective remedy for the management of chronic myeloid leukemia-Part-III: Synthesis, biological screening and in silico binding interaction analysis, Bioorg Chem 154 (2025) 108057. https://doi.org/10.1016/j.bioorg.2024.108057.

[44] P.A. Marks, W. -S. Xu, Histone deacetylase inhibitors: Potential in cancer therapy, J Cell Biochem 107 (2009) 600–608. https://doi.org/10.1002/jcb.22185.

[45] J.S. Ungerstedt, Y. Sowa, W.-S. Xu, Y. Shao, M. Dokmanovic, G. Perez, L. Ngo, A. Holmgren, X. Jiang, P.A. Marks, Role of thioredoxin in the response of normal and transformed cells to histone deacetylase inhibitors, Proceedings of the National Academy of Sciences 102 (2005) 673–678. https://doi.org/10.1073/pnas.0408732102.

CHAPTER-V

CONCLUSION AND FUTURE PERSPECTIVE

1. Conclusion and Future Perspective:

This research work reports the synthesis and development of new hybrid molecules featuring a 1,3,4-thiadiazole and 1,3-thiazolidine-4-one heterocyclic moiety, and their structural confirmation through spectral studies and data analysis (^{1}H NMR, ^{13}C NMR, and HRMS). X-ray diffraction (XRD) analysis of the single crystals of compounds **6g**, **7f**, and **9e** also confirmed the exact structure and geometry of the compounds. The cytotoxic properties of the developed molecules were evaluated on *in vitro* tumour cell lines. Most of the compounds exhibited notable anticancer potential against cancer cell lines, with higher selectivity compared to normal cell lines (HEK-293). When considering the anticancer activity of the compound series, we found that compounds displayed the best inhibitory potential toward the proliferation of MCF-7 cell lines. Compounds **6e** and **9e** emerged as potential lead molecules, exhibiting more than 35- and 40-fold selectivity against MCF-7 cancer cells compared to HEK-293 cell lines. Additionally, the *in vitro* exploration of the anticancer mechanism of action revealed that compounds **6e** and **9e** induced cell cycle arrest at the G0/G1 (25.3%) and G1/S (28.2%) phases in MCF-7 cells after treatment with the compounds. In the nuclear staining assay (DAPI and AO), both compounds enhanced fluorescence intensity, indicating chromosomal condensation and nuclear fragmentation, which ultimately suggests an apoptotic mechanism of cancer cell death. Compounds **6e** and **9e** induced intracellular ROS formation, which simultaneously led to cell shrinkage, chromosomal condensation, and damage to nucleic acid contents. Furthermore, in the Western blot experiment, the compound **9e** induced the upregulation of pro-apoptotic proteins caspase-3 and -7, and the downregulation of anti-apoptotic protein BCL-2, further confirming the apoptosis mechanism of the compounds. Additionally, compound **9e** exhibited potential anti-angiogenic properties in an *in vitro* tube formation assay on ACHN cells. In brief, this research work demonstrates that the lead molecule, i.e., compounds **6e** and **9e**, may be subjected to further *in vivo* antitumour

experiments followed by preclinical translation for rigorous assessment of anticancer efficacy. Hence, this research work implied that the design and development of 1,3,4-thiadiazole and 1,3-thiazolidine-4-one scaffold-based hybrid compounds might be effective in anticancer drug discovery and clinical development.

APPENDICES

Publication & Certificates

Publication:

RSC
Medicinal Chemistry

ROYAL SOCIETY OF CHEMISTRY

RESEARCH ARTICLE

View Article Online
View Journal

Check for updates

Cite this: DOI: 10.1039/d4md00279b

Synthesis and antiproliferative potency of 1,3,4-thiadiazole and 1,3-thiazolidine-4-one based new binary heterocyclic molecules: *in vitro* cell-based anticancer studies†

Avik Maji,[a] Ambati Himaja,[b] Sripathi Nikhitha,[b] Soumitra Rana,[c] Abhik Paul,[a] Ajeya Samanta,[a] Uday Shee,[d] Chhanda Mukhopadhyay,[c] Balaram Ghosh*[b] and Tapan Kumar Maity*[a]

Received 19th April 2024,
Accepted 3rd July 2024

DOI: 10.1039/d4md00279b

rsc.li/medchem

Herein, we report the synthesis and anticancer properties of 21 new 1,3,4-thiadiazole-2-yl-imino-thiazolidine-4-one containing binary heterocyclic molecules. Cytotoxicity of the synthesized molecules was evaluated on various *in vitro* cancer cell lines (MCF-7, PC3, 4T1, MDA-MB-231, and MOC2) and normal human embryonic cell lines (HEK-293) *via* MTT assay. The cytotoxicity data of developed compounds was compared with the reference anticancer molecule **BG45**, a selective inhibitor of the HDAC3 enzyme. All compounds showed a significant cytotoxic effect higher than **BG45** on tested cancer cell lines. Moreover, the compounds exhibited better selectivity on cancer cells than on normal cells. Among the molecules, compound **6e** is the most potent in cytotoxic activity on MCF-7 cell lines (IC_{50} value of 3.85 μM). Additional mechanistic investigation revealed that compound **6e** promotes apoptosis (25.3%) and G0/G1 phase cell cycle arrest of MCF-7 cells. Also, compound **6e** induces intracellular ROS accumulation and subsequent nuclear fragmentation. Hence, this research finds new hybrid molecules active against *in vitro* cancer cells.

1. Introduction

The majority of chemist's interests throughout the past few decades have been in heterocyclic compounds, their different derivatives, and their uses in the chemical and pharmaceutical industries. Numerous research studies have been published recently that discuss research on the synthesis and application of a wide variety of heterocyclic compounds, including pyrazole, tetrahydroquinolines, benzotriazole, 1,2,3,4-tetrazine, thiazole, 2-thiazoline, pyrimidine, and so on. 1,3,4-Thiadiazole is a prevalent and important five-membered heterocyclic system containing two nitrogen atoms and a sulfur atom.[1] Thiadiazole occurs in various isomers, such as 1,2,3-, 1,2,4-, 1,2,5-thiadiazole, and the above-mentioned ones. A quick look at the high-quality research articles revealed that 1,3,4-thiadiazole had received more research attention than other isomers.[2] Accordingly, recent research by Yang Li and colleagues developed some quinoline and 1,3,4-thiadiazole molecular hybrids showing potential anti-breast cancer activity in *in vitro* and *in vivo* preclinical settings. Compounds also inhibited EGFR and HER2 protein, as evident from *in vitro* kinase assay and molecular docking studies.[3] One significant resource for identifying new therapeutic possibilities is the growing diversity of small chemical libraries. Heterocycles, specifically 1,3-thiazolidine-4-ones, are among the most studied groups of chemicals in this context. These are heterocyclic nuclei containing a carbonyl group at position four and nitrogen and sulfur atoms at positions 1 and 3, respectively. Research on the production of these compounds and bioactivity has garnered a lot of interest.[4,5] Numerous pharmacological actions, including anticancer activity, have been shown by thiazolidine-4-one and its derivatives.[6] Similarly, a recent research study by Şenol H. and coworkers reported some new thiazolidine-4-one derivatives showing impressive cytotoxicity on MCF-7 breast cancer cell lines in the MTT assay. Potent compounds also exhibited excellent binding interaction with HER2 (PDB; 3PP0) protein, one growth factor for breast

[a] *Synthetic and Natural Products Research Laboratory, Department of Pharmaceutical Technology, Jadavpur University, Kolkata-700032, West Bengal, India. E-mail: tapan.maity@jadavpuruniversity.in*
[b] *Epigenetic Research Laboratory, Department of Pharmacy, Birla Institute of Technology and Science-Pilani, Hyderabad Campus, Hyderabad-500078, India*
[c] *Department of Chemistry, University of Calcutta, Kolkata-700009, West Bengal, India*
[d] *Department of Chemistry, Jadavpur University, Kolkata-700032, West Bengal, India*

† Electronic supplementary information (ESI) available. CCDC 2366716 and 2366780. For ESI and crystallographic data in CIF or other electronic format see DOI: https://doi.org/10.1039/d4md00279b

Certificates:

INTERNATIONAL SEMINAR on
"MODERN MEDICINE AND RATIONAL USE OF MEDICINE-A CHALLENGE"
Dr. Triguna Sen Memorial Hall, Jadavpur University, Kolkata, India
17th January, 2025

Certificate

Prof. / Dr. / Mr. / Mrs. / Miss Avik Maji

has attended the INTERNATIONAL CONFERENCE 2025 on "MODERN MEDICINE AND RATIONAL USE OF MEDICINE-A CHALLENGE" as a STUDENT/RESEARCH SCHOLAR/IAPST MEMBER/DELEGATE/FACULTY/INDUSTRY /ACCOMPANIED PERSON and presented a SCIENTIFIC (ORAL/POSTER) PRESENTATION

Jointly organized by:

INDIAN ASSOCIATION OF PHARMACEUTICAL SCIENTISTS AND TECHNOLOGISTS (IAPST), KOLKATA, INDIA

DR. V. RAVICHANDRAN CENTER FOR ADVANCED RESEARCH IN PHARMACEUTICAL SCIENCES, JADAVPUR UNIVERSITY (CARPS), KOLKATA, INDIA

COMMUNITY DEVELOPMENT MEDICINAL UNIT (CDMU), KOLKATA & ODISHA, INDIA

WEST BENGAL VOLUNTARY HEALTH ASSOCIATION (WBVHA), KOLKATA, INDIA

Prof. N. Udupa
President
IAPST

Prof. Biswajit Mukherjee
Coordinator
CARPS

Dr. Ketaki Das
Secretary
CDMU

Mr. Biswanath Basu
Project Director
WBVHA

INTERNATIONAL SEMINAR on
"MODERN MEDICINE AND RATIONAL USE OF MEDICINE-A CHALLENGE"
Dr. Triguna Sen Memorial Hall, Jadavpur University, Kolkata, India
17th January, 2025

Certificate

Prof. / Dr. / Mr. / Mrs. / Miss *Ashik Maji*

For Participating in the Scientific (~~Oral~~ / Poster) Presentation Competition and Securing 1st / 2nd / 3rd Position.

Jointly organized by:

INDIAN ASSOCIATION OF PHARMACEUTICAL SCIENTISTS AND TECHNOLOGISTS (IAPST), KOLKATA, INDIA

DR. V. RAVICHANDRAN CENTER FOR ADVANCED RESEARCH IN PHARMACEUTICAL SCIENCES, JADAVPUR UNIVERSITY (CARPS), KOLKATA, INDIA

COMMUNITY DEVELOPMENT MEDICINAL UNIT (CDMU), KOLKATA & ODISHA, INDIA

WEST BENGAL VOLUNTARY HEALTH ASSOCIATION (WBVHA), KOLKATA, INDIA

Prof. N. Udupa
President
IAPST

Prof. Biswajit Mukherjee
Coordinator
CARPS

Dr. Ketaki Das
Secretary
CDMU

Mr. Biswanath Basu
Project Director
WBVHA

International Conference on Pharmacy & Healthcare
NATCONPH 2024

A+ NAAC

NSHM KNOWLEDGE CAMPUS KOLKATA

CERTIFICATE

OF APPRECIATION

AWARDED TO

Prof./Dr./Mr./Ms. Avik Maji

FOR HIS/HER ORAL/POSTER PRESENTATION IN THE

14TH INTERNATIONAL CONFERENCE ON

"NAVIGATING THE FUTURE OF HEALTHCARE: Trends, Challenges and Innovations"

ORGANISED BY

NSHM INSTITUTE OF HEALTH SCIENCES

NSHM KNOWLEDGE CAMPUS, KOLKATA ON 27TH AND 28TH SEPTEMBER, 2024

PROF. (DR.) SOUMENDRA NATH BANDYOPADHYAY
CHAIRPERSON,
iNATCONPH 2024

DR. APARNA DATTA
CONVENER,
iNATCONPH 2024

Certificate No.:DDDLO/2024/565

CIPET

CRIKC

CERTIFICATE
OF PARTICIPATION

This is to certify that,

Mr. Avik Maji

has been successfully **PARTICIPATED** in International Online Conference on

"DRUG DISCOVERY, DEVELOPMENT AND LEAD OPTIMIZATION"

Prof. (Dr) Tejvir Singh
Professor Emeritus

Prof. (Dr) V. K. Kapoor
Professor Emeritus

Prof. (Dr) T. R. Bhardwaj
Advisor to Chancellor

Prof. (Dr) Ravinesh Mishra
Chairperson

Organized By
School of Pharmacy and Emerging Sciences,
Baddi University of Emerging Sciences & Technology, Baddi,
Himachal Pradesh, India

05-06 APRIL, 2024

Avik Maji 07.07.2025

Dr. Tapan Kr. Maity 07/07/25
Dr. Tapan Kr. Maity
M. Pharm., Ph.D.
Professor
Dept. of Pharmaceutical Technology
Jadavpur University, Kolkata - 700 032